FORCES IN BIOLOGY - CELL AND DEVELOPMENTAL MECHANOBIOLOGY AND ITS IMPLICATIONS IN DISEASE

EDITED BY: Selwin K. Wu, Michael Smutny, Samantha J. Stehbens and Guillermo A. Gomez

PUBLISHED IN: Frontiers in Cell and Developmental Biology

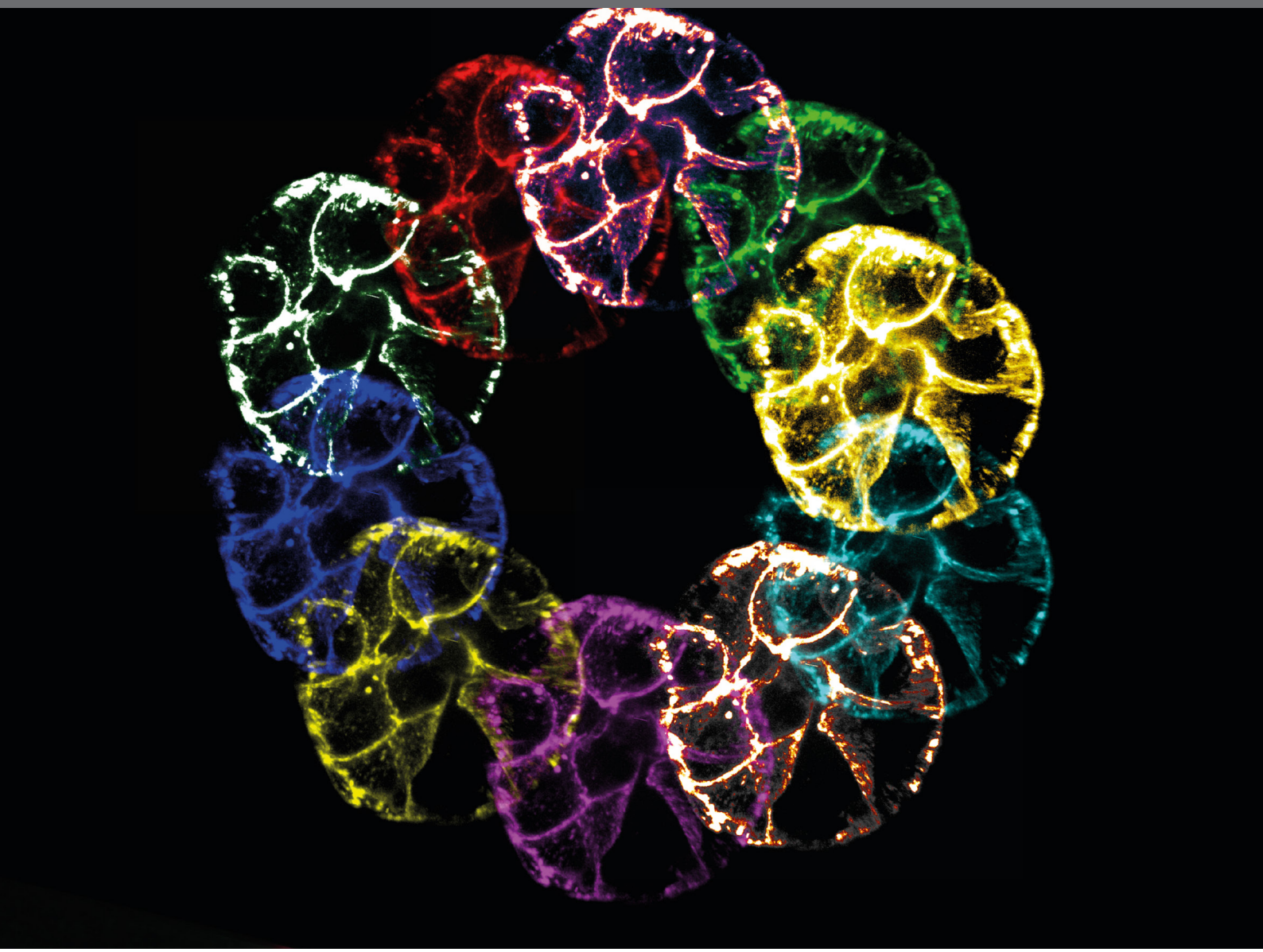

frontiers Research Topics

Frontiers eBook Copyright Statement

The copyright in the text of individual articles in this eBook is the property of their respective authors or their respective institutions or funders. The copyright in graphics and images within each article may be subject to copyright of other parties. In both cases this is subject to a license granted to Frontiers.

The compilation of articles constituting this eBook is the property of Frontiers.

Each article within this eBook, and the eBook itself, are published under the most recent version of the Creative Commons CC-BY licence. The version current at the date of publication of this eBook is CC-BY 4.0. If the CC-BY licence is updated, the licence granted by Frontiers is automatically updated to the new version.

When exercising any right under the CC-BY licence, Frontiers must be attributed as the original publisher of the article or eBook, as applicable.

Authors have the responsibility of ensuring that any graphics or other materials which are the property of others may be included in the CC-BY licence, but this should be checked before relying on the CC-BY licence to reproduce those materials. Any copyright notices relating to those materials must be complied with.

Copyright and source acknowledgement notices may not be removed and must be displayed in any copy, derivative work or partial copy which includes the elements in question.

All copyright, and all rights therein, are protected by national and international copyright laws. The above represents a summary only. For further information please read Frontiers' Conditions for Website Use and Copyright Statement, and the applicable CC-BY licence.

ISSN 1664-8714
ISBN 978-2-88966-217-3
DOI 10.3389/978-2-88966-217-3

About Frontiers

Frontiers is more than just an open-access publisher of scholarly articles: it is a pioneering approach to the world of academia, radically improving the way scholarly research is managed. The grand vision of Frontiers is a world where all people have an equal opportunity to seek, share and generate knowledge. Frontiers provides immediate and permanent online open access to all its publications, but this alone is not enough to realize our grand goals.

Frontiers Journal Series

The Frontiers Journal Series is a multi-tier and interdisciplinary set of open-access, online journals, promising a paradigm shift from the current review, selection and dissemination processes in academic publishing. All Frontiers journals are driven by researchers for researchers; therefore, they constitute a service to the scholarly community. At the same time, the Frontiers Journal Series operates on a revolutionary invention, the tiered publishing system, initially addressing specific communities of scholars, and gradually climbing up to broader public understanding, thus serving the interests of the lay society, too.

Dedication to Quality

Each Frontiers article is a landmark of the highest quality, thanks to genuinely collaborative interactions between authors and review editors, who include some of the world's best academicians. Research must be certified by peers before entering a stream of knowledge that may eventually reach the public - and shape society; therefore, Frontiers only applies the most rigorous and unbiased reviews.
Frontiers revolutionizes research publishing by freely delivering the most outstanding research, evaluated with no bias from both the academic and social point of view. By applying the most advanced information technologies, Frontiers is catapulting scholarly publishing into a new generation.

What are Frontiers Research Topics?

Frontiers Research Topics are very popular trademarks of the Frontiers Journals Series: they are collections of at least ten articles, all centered on a particular subject. With their unique mix of varied contributions from Original Research to Review Articles, Frontiers Research Topics unify the most influential researchers, the latest key findings and historical advances in a hot research area! Find out more on how to host your own Frontiers Research Topic or contribute to one as an author by contacting the Frontiers Editorial Office: frontiersin.org/about/contact

FORCES IN BIOLOGY - CELL AND DEVELOPMENTAL MECHANOBIOLOGY AND ITS IMPLICATIONS IN DISEASE

Topic Editors:
Selwin K. Wu, Harvard Medical School, Boston, MA, United States
Michael Smutny, University of Warwick, United Kingdom
Samantha J. Stehbens, The University of Queensland, Australia
Guillermo A. Gomez, University of South Australia, Australia

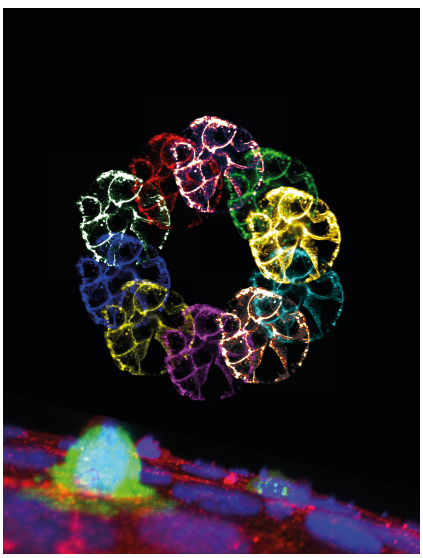

3D and 2D cellular patterns in space. Colorectal adenocarcinoma cells (Caco-2) were grown as 3D spheres with Dr Karen Chambers assistance (top) or as a monolayer (bottom). A single Ras (green) overexpressing cell can be seen extruding from the epithelium (bottom). The Olympus spinning disk confocal microscope (IX81 with a disc scanning unit) was used to image the Caco-2 spheres labelled with E-cadherin-GFP and the point scanning confocal LSM710 was used with Dr Guillermo Gomez guidance to image the epithelium (N-WASP, red; nucleus, blue). These images were obtained in Professor Alpha Yap's laboratory at the University of Queensland by Dr Selwin Wu.
Cover design: Selwin K. Wu.

Citation: Wu, S. K., Smutny, M., Stehbens, S. J., Gomez, G. A., eds. (2020). Forces in Biology - Cell and Developmental Mechanobiology and Its Implications in Disease. Lausanne: Frontiers Media SA. doi: 10.3389/978-2-88966-217-3

Table of Contents

frontiers in Cell and Developmental Biology

EDITORIAL
published: 30 September 2020
doi: 10.3389/fcell.2020.598179

Editorial: Forces in Biology - Cell and Developmental Mechanobiology and Its Implications in Disease

Selwin K. Wu[1,2*†‡], *Guillermo A. Gomez*[3*†], *Samantha J. Stehbens*[4] *and Michael Smutny*[5]

[1] *Department of Cell Biology, Harvard Medical School, Boston, MA, United States,* [2] *Department of Pediatric Oncology, Dana-Farber Cancer Institute, Boston, MA, United States,* [3] *Centre for Cancer Biology, SA Pathology and University of South Australia, Adelaide, SA, Australia,* [4] *Cell Biology and Molecular Medicine Division, Institute for Molecular Bioscience, University of Queensland, Brisbane, QLD, Australia,* [5] *Centre for Mechanochemical Cell Biology & Warwick Medical School, University of Warwick, Coventry, United Kingdom*

Keywords: mechanobiology, cell biology, developmental biology, cardiovascular, signaling, stem cells, neuroscience, bone

OPEN ACCESS

Edited and reviewed by:
Akihiko Ito,
Kindai University, Japan

***Correspondence:**
Selwin K. Wu
selwin_wu@mail.dfci.harvard.edu
Guillermo A. Gomez
guillermo.gomez@unisa.edu.au

†These authors have contributed equally to this work

‡Present address:
Selwin K. Wu,
Department of Biological Sciences, Mechanobiology Institute, National University of Singapore, Singapore, Singapore

Specialty section:
This article was submitted to Cell Adhesion and Migration, a section of the journal Frontiers in Cell and Developmental Biology

Received: *24 August 2020*
Accepted: *26 August 2020*
Published: *30 September 2020*

Citation:
Wu SK, Gomez GA, Stehbens SJ and Smutny M (2020) Editorial: Forces in Biology - Cell and Developmental Mechanobiology and Its Implications in Disease. Front. Cell Dev. Biol. 8:598179. doi: 10.3389/fcell.2020.598179

Editorial on the Research Topic

Forces in Biology - Cell and Developmental Mechanobiology and Its Implications in Disease

Mechanobiology despite widely regarded as an emerging discipline, its concept, is proposed more than a hundred years ago by mathematical biologist D'Arcy Wentworth Thompson. In his 1917's book *On Growth and Form* (Thompson, 1992), life forms were envisioned to reflect physics and mathematical principles. Since then mechanobiologists endeavored to transform cell and developmental biology into a field of quantitative science and technology, accelerated by the development and application of new approaches including virtual power theory (Putra et al.) and random positioning machines (Bradbury et al.).

In the past three decades, the authoritative concept that "phenotype can dominate over genotype" (Nelson and Bissell, 2006) by Mina Bissell and others have further underscored the overarching role of tissue and cellular mechanisms in health and disease. Indeed, an increase of matrix stiffness can promote tissue transformation through abnormal mitosis and signaling from adhesion receptors (Butcher et al., 2009; Knouse et al., 2018). Nevertheless, the quantitative nature of sequence analysis in the field of genomics have almost realized the promise of personalized medicine. In this post-genomic era, we envision that cell, developmental mechanobiology and its pathogenesis could, in principle, drive a new form of personalized medicine; that would emerge from the quantitative description of molecular, cell, and tissue dynamics (Putra et al.). In this issue, we highlight recent developments in six chapters: namely (1) stem cells mechanobiology, (2) bone biomechanics & cellular physiology, (3) Rho GTPases signaling, (4) cardiovascular mechanobiology, (5) mechanobiology of the brain, and (6) molecular mechanisms of mechanobiology.

CHAPTER 1: STEM CELLS MECHANOBIOLOGY

Stem cells and their local microenvironment communicate via mechanical cues to regulate gene expression that influence developmental processes. Domingues et al. showed that Cofilin-1 is a mechanosensitive regulator of transcription in human umbilical cord mesenchymal stem/stromal cells. Cofilin-1 activity is regulated by substrate stiffness and activated cofilin-1 promoted transcription in human umbilical cord mesenchymal stem/stromal cells (Domingues et al.).

With regards to stem cell-based treatment, pluripotent stem cells can revolutionize regenerative medicine as they have the potential to form organs. However, the scaling up of pluripotent stem cells expansion is required to achieve the goal of therapeutic use. Chan et al. reviewed recent

advances in pluripotent stem cell expansion focusing on *in vitro* design of two-dimensional surface modification and three-dimensional encapsulation, which can provide the mechanical cues required for the expansion of pluripotent stem cells.

Besides regenerative medicine, the integration of big data obtained from mechanobiology and stem cell studies remains a challenge. To that end Putra et al. summarize various approaches, including a perfusion chamber platform, to analyse biomechanics. They proposed the study of mechanobiology at the "omics" level, thus termed mechanomics. To integrate "omics" data, various computational modeling approaches are applied for the mapping of the mechanome of biological systems including stem cells, bones and tissues (Putra et al.).

CHAPTER 2: BONE BIOMECHANICS AND CELLULAR PHYSIOLOGY

The osteochondral interface between the bone and cartilage facilitates signaling crosstalk and nutritional molecules exchange, thus enabling an integrated response to mechanical stimuli. Oliveira Silva et al. describe the molecular interactions and transport in the osteochondral interface and discuss the potential of using contrast agents for studying molecular transport and structural changes of the joint.

Cellular physiology and our bones are profoundly influenced by gravitational forces. Bradbury et al. reviewed the impact of simulated microgravity on the cytoskeleton, extracellular matrix synthesis and bone cell signaling.

CHAPTER 3: RHO GTPASES SIGNALING

GTPase signaling is an important aspect of mechanobiology. In particular, RhoGTPases are canonical upstream regulators of actomyosin structure and function controlling cellular mechanics (Wu and Priya). Feedback signaling pathways are found to complete the RhoGTPases signaling loop. Myosin II controls RhoGTPases signaling through multiple mechanisms, namely contractility driven advection (Moore et al., 2014), scaffolding (Priya et al., 2015), and sequestration of signaling molecules. Wu and Priya discuss these mechanisms by which myosin II regulates RhoGTPase signaling in cell adhesion, migration, and tissue morphogenesis.

The genetic regulation of Rho GTPases may also play an important role in pathology such as recurrent miscarriage. The small G-protein Rnd3 (or RhoE) is implicated as a therapeutic target in recurrent miscarriage. Ma et al. suggest that the upregulation of Rnd3 by forkhead box D3 (FOXD3), a key transcription factor that binds to the RND3 core promoter region, regulated trophoblast migration and proliferation via the RhoA-ROCK1 signaling pathway and inhibits apoptosis via ERK1/2 signaling.

CHAPTER 4: CARDIOVASCULAR MECHANOBIOLOGY

Forces emerge from and act on the cardiovascular system during development and from the heart pumping of blood flow. Simpson et al. reviewed the role of biomechanical stress-induced translational control in the heart and vascular cells. Several specific areas were reviewed including protein translation regulation by mechanical stimuli, mTOR signaling, endoplasmic reticulum stress, atherosclerosis, and cardiac hypertrophy.

Next, Gaetani et al. reviewed a combination of theoretical models of cell and tissue mechanics and experimental findings. Tissue engineering and induced pluripotent stem cell (iPSC) technologies were then discussed as potential personalized medicine strategies to treat heart failure.

CHAPTER 5: MECHANOBIOLOGY OF THE BRAIN

Besides the cardiovascular system, the neuronal system is another exciting area covered in this issue including cell interactions and migration of neurons. Veeraval et al. reviewed the role of adherens junctions in cortical brain development. The reciprocal interactions between adherens junctions and the epithelial polarity complexes that promote glial apicobasal polarity are highlighted. Several key processes of cortical brain development are integrated including asymmetric cell division, with a focus on the mechanisms that integrate adherens junctions and the actin cytoskeleton (Wu and Yap, 2013; Wu et al., 2014). Processes underlying cortical malformations are also discussed.

In the brain, neuronal migration is a critical step during the formation of functional neural circuits. Nakazawa and Kengaku reviewed the synergistic role of actomyosin microfilaments and microtubule motor proteins, in generating mechanical forces to translocate the nuclei of newborn neurons through confined space. In addition, the authors concluded that the mechanical properties of the nucleus and surrounding tissues not only contribute to force transmission but also present a physical barrier to nuclear translocation.

CHAPTER 6: MOLECULAR MECHANISMS OF MECHANOBIOLOGY

Following up on cytoskeletal force exertion on the nucleus. Terriac et al. describe and measure the turnover of vimentin intermediate filament rings that deform the nucleus during cell spreading in cells. Indeed, force exertion on nucleus can often lead to transcriptional changes. Accordingly, Martinez et al. highlighted the regulation of Yap/Taz nuclear translocation, transcription and mechanotransduction with the use of atomic force microscopy.

Lastly, with a focus on the epithelium of mammary gland, pancreas, and urinary system. Stewart and Davis review the role of the mechanosensitive ion channel PIEZO1 in the development, function, and dysfunction of epithelia.

In this issue, we presented a broad spectrum of work from fundamental cell biology to articles at the interface of development and disease. We believe that this issue will be of interest to students and researchers studying the molecular and

cellular mechanisms in development and diseases, enabling them to appreciate how clearer understanding of these mechanisms can inspire therapeutics and diagnostics.

AUTHOR CONTRIBUTIONS

SW wrote the manuscript. GG edited the manuscript. All authors provided intellectual input to the editorial.

FUNDING

SW was supported by a Leukemia and Lymphoma Society Fellow Award (5454-17). GG and SS are supported by Australian Research Council Future Fellowships (FT160100366 & FT190100516). MS was supported by the Wellcome Trust ISSF Quantitative Biomedicine Programme and a BBSRC New Investigator grant (BB/T016493/1).

REFERENCES

Butcher, D. T., Alliston, T., and Weaver, V. M. (2009). A tense situation: forcing tumour progression. *Nat. Rev. Cancer* 9, 108–122. doi: 10.1038/nrc2544

Knouse, K. A., Lopez, K. E., Bachofner, M., and Amon, A. (2018). Chromosome segregation fidelity in epithelia requires tissue architecture. *Cell* 175, 200–211. e213. doi: 10.1016/j.cell.2018.07.042

Moore, T., Wu, S. K., Michael, M., Yap, A. S., Gomez, G. A., and Neufeld, Z. (2014). Self-organizing actomyosin patterns on the cell cortex at epithelial cell-cell junctions. *Biophys. J.* 107, 2652–2661. doi: 10.1016/j.bpj.2014.10.045

Nelson, C. M., and Bissell, M. J. (2006). Of extracellular matrix, scaffolds, and signaling: tissue architecture regulates development, homeostasis, and cancer. *Annu. Rev. Cell. Dev. Biol.* 22, 287–309. doi: 10.1146/annurev.cellbio.22.010305.104315

Priya, R., Gomez, G. A., Budnar, S., Verma, S., Cox, H. L., Hamilton, N. A., et al. (2015). Feedback regulation through myosin II confers robustness on RhoA signalling at E-cadherin junctions. *Nat. Cell. Biol.* 17, 1282–1293. doi: 10.1038/ncb3239

Thompson, D. A. W. (1992). *On Growth and Form*. New York: Dover. doi: 10.1017/CBO9781107325852

Wu, S. K., Gomez, G. A., Michael, M., Verma, S., Cox, H. L., Lefevre, J. G., et al. (2014). Cortical F-actin stabilization generates apical-lateral patterns of junctional contractility that integrate cells into epithelia. *Nat. Cell. Biol.* 16, 167–178. doi: 10.1038/ncb2900

Wu, S. K., and Yap, A. S. (2013). Patterns in space: coordinating adhesion and actomyosin contractility at E-cadherin junctions. *Cell Commun. Adhes.* 20, 201–212. doi: 10.3109/15419061.2013.856889

Conflict of Interest: The authors declare that the research was conducted in the absence of any commercial or financial relationships that could be construed as a potential conflict of interest.

Copyright © 2020 Wu, Gomez, Stehbens and Smutny. This is an open-access article distributed under the terms of the Creative Commons Attribution License (CC BY). The use, distribution or reproduction in other forums is permitted, provided the original author(s) and the copyright owner(s) are credited and that the original publication in this journal is cited, in accordance with accepted academic practice. No use, distribution or reproduction is permitted which does not comply with these terms.

frontiers in Cell and Developmental Biology

ORIGINAL RESEARCH
published: 30 July 2020
doi: 10.3389/fcell.2020.00678

Cofilin-1 Is a Mechanosensitive Regulator of Transcription

Catarina Domingues[1,2], A. Margarida Geraldo[1], Sandra Isabel Anjo[1], André Matos[1,3], Cláudio Almeida[1,3], Inês Caramelo[1,2], José A. Lopes-da-Silva[4], Artur Paiva[5,6,7,8], João Carvalho[9], Ricardo Pires das Neves[1,2], Bruno Manadas[1] and Mário Grãos[1,2,10]**

[1] Center for Neuroscience and Cell Biology (CNC), University of Coimbra, Coimbra, Portugal, [2] Institute for Interdisciplinary Research, University of Coimbra (IIIUC), Coimbra, Portugal, [3] Polytechnic Institute of Coimbra, Coimbra College of Agriculture, Coimbra, Portugal, [4] LAQV-REQUIMTE, Department of Chemistry, University of Aveiro, Aveiro, Portugal, [5] Flow Cytometry Unit, Department of Clinical Pathology, Centro Hospitalar e Universitário de Coimbra, Coimbra, Portugal, [6] Coimbra Institute for Clinical and Biomedical Research, Faculty of Medicine, University of Coimbra, Coimbra, Portugal, [7] Center for Innovative Biomedicine and Biotechnology, University of Coimbra, Coimbra, Portugal, [8] Instituto Politécnico de Coimbra, ESTESC-Coimbra Health School, Ciências Biomédicas Laboratoriais, Coimbra, Portugal, [9] Centro de Física da Universidade de Coimbra (CFisUC), Department of Physics, University of Coimbra, Coimbra, Portugal, [10] Biocant, Technology Transfer Association, Cantanhede, Portugal

OPEN ACCESS

Edited by:
Selwin K. Wu, National University of Singapore, Singapore

Reviewed by:
Manoj B. Menon, Indian Institute of Technology Delhi, India
Antoine Jégou, UMR7592 Institut Jacques Monod (IJM), France

***Correspondence:**
Bruno Manadas
bmanadas@cnc.uc.pt
Mário Grãos
mgraos@biocant.pt

Specialty section:
This article was submitted to Signaling, a section of the journal Frontiers in Cell and Developmental Biology

Received: 06 May 2020
Accepted: 06 July 2020
Published: 30 July 2020

Citation:
Domingues C, Geraldo AM, Anjo SI, Matos A, Almeida C, Caramelo I, Lopes-da-Silva JA, Paiva A, Carvalho J, Pires das Neves R, Manadas B and Grãos M (2020) Cofilin-1 Is a Mechanosensitive Regulator of Transcription. Front. Cell Dev. Biol. 8:678. doi: 10.3389/fcell.2020.00678

The mechanical properties of the extracellular environment are interrogated by cells and integrated through mechanotransduction. Many cellular processes depend on actomyosin-dependent contractility, which is influenced by the microenvironment's stiffness. Here, we explored the influence of substrate stiffness on the proteome of proliferating undifferentiated human umbilical cord-matrix mesenchymal stem/stromal cells. The relative abundance of several proteins changed significantly by expanding cells on soft (∼3 kPa) or stiff substrates (GPa). Many such proteins are associated with the regulation of the actin cytoskeleton, a major player of mechanotransduction and cell physiology in response to mechanical cues. Specifically, Cofilin-1 levels were elevated in cells cultured on soft comparing with stiff substrates. Furthermore, Cofilin-1 was de-phosphorylated (active) and present in the nuclei of cells kept on soft substrates, in contrast with phosphorylated (inactive) and widespread distribution in cells on stiff. Soft substrates promoted Cofilin-1-dependent increased RNA transcription and faster RNA polymerase II-mediated transcription elongation. Cofilin-1 is part of a novel mechanism linking mechanotransduction and transcription.

Keywords: mechanotransduction, Cofilin-1, cytoskeleton, transcription, hUCM-MSCs, proteomics

Abbreviations: 5-FUrd, 5-fluorouridine; COL-1, Type-I collagen; CV, coefficient of variation; DMSO, dimethyl sulfoxide; *E*, Young's modulus; ECF, enhanced chemifluorescence; ECM, extracellular matrix; F-actin, filamentous actin; FAK, focal adhesion kinase; FAs, focal adhesions; FBS, foetal bovine serum; FLIP, fluorescence loss in photobleaching; FN, fibronectin; G-actin, globular actin; G', Elastic/Storage modulus; G'', Viscous/Loss modulus; hUCM-MSCs, human umbilical cord matrix mesenchymal stem/stromal cells; ICC, immunocytochemistry; IDA, information-dependent acquisition; LIMK1, LIM Kinase 1; Limki-3, LIM Kinase inhibitor; LINC, Linker of nucleoskeleton and cytoskeleton; LPA, lysophosphatidic acid; mAbs, monoclonal antibodies; MFI, mean of fluorescence intensity; NMM-II, non-muscle myosin-II; ON, overnight; PDMS, polydimethylsiloxane; PFA, paraformaldehyde; PVDF, polyvinylidene fluoride; ROCK, rho-associated protein kinase; ROIs, regions of interest; RT, room temperature; SEM, standard error of the mean; SWATH-MS, sequential window acquisition of all theoretical fragment-ion spectra mass spectrometry; TCPS, tissue culture polystyrene; UCM, umbilical cord matrix; WB, western blot.

INTRODUCTION

Cells sense and respond to the mechanical properties of the extracellular environment. Specifically, mechanotransduction originated at the cell-extracellular matrix (ECM) interface (or cell-substrate interface in case of *in vitro* cell culture) initiates at the focal adhesions (FAs). FAs encompass several proteins like integrins (transmembrane receptors that bind to EMC proteins, constituting anchoring points of adherent cells), adapter proteins like talin and vinculin (bridging integrins with the actin cytoskeleton), as well as signalling proteins like focal adhesion kinase (FAK) (reviewed in Vining and Mooney, 2017). Upon activation of integrins, these proteins interact with each other, leading to the formation of FAs and subsequent recruitment of the actin cytoskeleton (Humphries et al., 2007; Thievessen et al., 2013). The formation of FAs leads to the activation of a wide range of signalling pathways, several of which converge on and activate RhoA, a member of the Rho GTPase family (Lessey et al., 2012). In turn, active RhoA engages its downstream effector Rho-associated protein kinase (ROCK), and subsequently, the motor protein non-muscle myosin-II (NMM-II) (Marjoram et al., 2014; Burridge et al., 2019). Activation of NMM-II leads to the contraction of actin stress fibres, constituted by crosslinked anti-parallel filamentous (*F*)-actin bundles, resulting in the build-up of intracellular tension. Hence, intracellular tension occurs as the result of the contractile forces generated by actomyosin spanning from the plasma membrane (at FAs) to the nucleus (through the linker of nucleoskeleton and cytoskeleton — LINC — complex) (Jaalouk and Lammerding, 2009; Burridge and Guilluy, 2016), which dictates to a great extent the mechanical properties of the cell. If the stiffness of the extracellular matrix (or substrate if *in vitro*) is high, the reinforcement of FAs occurs, resulting in increased intracellular contractility and mechanical stress exerted on the ECM and the nucleus (Moore et al., 2010; Klapholz and Brown, 2017). Hence, cells probe the ECM by exerting forces (intrinsic forces), subsequently responding according to the mechanical properties of the environment. Likewise, cells also sense and respond to forces originating on the ECM/substrate (extrinsic forces). The intrinsic or extrinsic forces occurring as the result of actomyosin contractility as a function of ECM/substrate stiffness, or other mechanical cues provided by the microenvironment influence many aspects of cell biology, including proliferation, differentiation and gene expression (Sun et al., 2012; Discher et al., 2017; Kumar et al., 2017; Uhler and Shivashankar, 2017; Vining and Mooney, 2017).

Another consequence of the activation of RhoA and ROCK is the stabilisation of F-actin by a mechanism involving LIM Kinase 1 (LIMK1), which in turn phosphorylates and inhibits Cofilin-1 (Yang et al., 1998; Maekawa et al., 1999; Mizuno, 2013; Prunier et al., 2017). Cofilin-1 is an essential actin-regulating protein, promoting the severing of actin filaments and disassembly of F-actin into globular actin (G-actin), playing a central role in actin cytoskeleton dynamics (Bamburg and Bernstein, 2010; Ohashi, 2015). Interestingly, both RhoA and ROCK activity and F-actin/G-actin ratio increase with substrate stiffness (Engler et al., 2006; Fu et al., 2010; Trichet et al., 2012; Gupta et al., 2015; Gerardo et al., 2019). The activity and subcellular localisation of Cofilin-1 depend on the phosphorylation state of its Ser3, a target of LIMK1. Phosphorylated Cofilin-1 is inactive and remains in the cytosol, while the non-phosphorylated form is active and able to severe and depolymerise F-actin (Nebl et al., 1996; Yang et al., 1998), adopting a subsequent nuclear localisation (Munsie et al., 2012). Other important cellular functions have been described for Cofilin-1. It is required for the nuclear transport of G-actin (through a mechanism mediated by importin 9) (Dopie et al., 2012; Percipalle, 2013) and together promote transcription elongation mediated by RNA polymerase II (Obrdlik and Percipalle, 2011). More recently, Cofilin-1 was identified as an essential protein for normal nuclear structure and function in distinct cell types (Wiggan et al., 2017).

In this study, we sought to explore how the proteome of human mesenchymal stem/stromal cells obtained from the umbilical cord matrix (hUCM-MSCs) is regulated when cells are cultured on substrates with distinct stiffness. There are two reasons for using this cellular model. First, MSCs are highly mechanosensitive and have been used extensively for studies in the field of mechanobiology (Engler et al., 2006; Fu et al., 2010; Yang et al., 2014; Gerardo et al., 2019). Second, MSCs are very promising for clinical applications, but require extensive *in vitro* expansion before being used. It is known that *in vitro* expansion of MSCs using standard cell-culture conditions leads to the loss of cell potency (Hoch and Leach, 2014; Müller et al., 2015; Galipeau et al., 2016). Increasing evidence suggests that the high stiffness of substrates typically used in standard cell culture conditions (like for example tissue culture polystyrene — TCPS —, with Young's modulus in the GPa range), several orders of magnitude higher than the natural cellular microenvironment, contributes significantly to such loss (Lee et al., 2014; Yang et al., 2014; Kusuma et al., 2017). Interestingly, a recent report indicates that the proliferative and differentiation potential of MSCs (at least toward the adipogenic lineage) is prolonged and senescence is delayed when cells are extensively cultured on a polyacrylamide 5 kPa substrate in comparison with stiff TCPS, while maintaining typical MSC surface markers (Kureel et al., 2019). Although in a distinct context, our studies also indicate that MSC stemness is favoured by soft substrates (Gerardo et al., 2019).

MSCs are a heterogeneous population of stromal cells, including multipotent adult stem cells, that can be isolated from vascularised tissues like bone marrow, adipose tissue and umbilical cord (Wagner et al., 2005). MSCs possess well-known cell-surface markers (positive expression of CD105, CD90, CD73 and negative expression of haematopoietic markers like CD34, CD45, HLA-DR, CD14 or CD11B, CD79α or CD19) and can differentiate *in vitro* into osteoblasts, chondroblasts and adipocytes (Pittenger et al., 1999; Dominici et al., 2006). MSCs can migrate *in vivo* to damaged tissues in response to cytokines/chemokines, growth-factors or adhesion molecules and therein provide potent immunomodulatory and regenerative responses (Kim and Cho, 2013). Also, MSCs have been extensively used for cell-based therapies in clinical trials (Squillaro et al., 2016). Furthermore, it was recently reported that MSCs retain mechanical information from their past physical

extracellular environment, developing mechanical memory that is dependent on the time in culture, or mechanical dosing. This has significant implications in stem cell function and differentiation (Yang et al., 2014; Peng et al., 2017), reinforcing the need to develop new strategies for stem cell maintenance and expansion *in vitro*. Currently, a variety of substrates that mimic distinct aspects of the ECM are available for cell culture, providing cell adhesion and mechanical support (Green and Elisseeff, 2016). The influence of mechanical and biochemical properties of such ECM-like substrates for the differentiation of MSCs into distinct lineages has been studied for a decade now (Engler et al., 2006; Fu et al., 2010). However, the effect of biophysical elements on proliferating undifferentiated MSCs is largely unknown and remains to be studied employing biologically relevant and comprehensive approaches.

This study presents a comparative and quantitative proteomics analysis of hUCM-MSCs cultured on stiff TCPS and soft polydimethylsiloxane (PDMS) substrates, which allowed the identification and characterisation of Cofilin-1 as a mechanosensitive protein involved in the regulation of transcription in response to substrate stiffness. To our knowledge, this is the first report of a quantitative and comprehensive characterisation of the MSC proteome in the mechanobiology field, with an expected impact on future studies evaluating MSCs' therapeutic effectiveness and clinical value. The link between mechanotransduction, Cofilin-1 and transcription is also novel, which will open a new research avenue regarding the regulation of gene expression upon modulation by mechanical factors.

MATERIALS AND METHODS

Cell Culture

Human umbilical cords were obtained after birth from healthy donors upon informed consent from the parent(s) and the study was approved by the Ethics Committee of the Faculty of Medicine, University of Coimbra, Portugal (ref. CE-075/2019). All methods were carried out in accordance with national and European guidelines and regulations. MSCs were isolated from cryopreserved fragments of human umbilical cord matrix (UCM) as described (Leite et al., 2014) with some modifications, as indicated. Briefly, cryopreserved fragments from human UCM were thawed at 37°C and washed with Alpha-MEM medium supplemented with 100 U/ml of Penicillin, 10 μg/ml Streptomycin and 2.5 μg/ml Amphotericin B (all from Life Technologies). Groups of 30 fragments were transferred to 21 cm^2 TCPS (Corning Costar) and left to dry for 30 min. Then, the proliferation medium [Alpha-MEM with 10% (v/v) MSC-qualified foetal bovine serum (FBS) (Hyclone, GE Healthcare) and antibiotics (as above)] was added to the culture plates until the fragments were immersed. Plates were incubated at 37°C with 5% CO_2/95% air and 90% humidity until the formation of well-defined MSC colonies was observed by phase-contrast microscopy. Next, fragments were removed, and adherent cells were detached using Trypsin (500 μg/ml)-EDTA (200 μg/ml) solution (Life Technologies) and re-seeded on a new plate (passage 1 – P1) in order to homogenise the culture. hUCM-MSCs were expanded in TCPS until P1 and then seeded and maintained on the distinct cell culture substrates between P2 and P4. For proliferation kinetics experiments, cells were passaged until P6.

The human foetal lung fibroblast cell line (MRC-5) (Steurer et al., 2018) was cultured in DMEM/F12 with 10% (v/v) FBS (both from Life Technologies) and antibiotics (as above).

Flow Cytometry

Immunophenotypic characterisation of hUCM-MSCs was performed at P4 for four independent samples. Cells were dissociated using Accutase (LifeTechnologies) and then stained with the monoclonal antibodies (mAbs) for surface antigens during 30 min in the dark, at room temperature (RT). The mAb panel used for the characterisation of hUCM-MSCs is detailed in **Supplementary Table S1**. For all mAbs, we used the concentration recommended by the manufacturer. Then, cells were washed and resuspended in PBS, and immediately acquired in a FACSCanto^{TM}II (BD) flow cytometer equipped with the FACSDiva software (v6.1.2; BD). Data analysis was performed using the Infinicyt software (version 1.7; Cytognos SL, Salamanca, Spain).

Proliferation Kinetics

hUCM-MSCs were cultured on TCPS and 40:1 PDMS at 3,000 cell/cm^2 from P2 to P6. Cells were counted once they reached 80% confluence at each passage and the following parameters were calculated (Leite et al., 2014): total numbers of cells, population doubling, cumulative population doubling and generation time. Total numbers of cells was calculated using the formula $TNC = N_H \times B/N_I$, in which N_H represents the number of cells harvested at the end of each passage, B represents the total number of cells from the previous passage and N_I the number of cells plated in each passage. Population doubling rate was calculated using the equation $N_H/N_I = 2^{PD}$ or $PD = [\log_{10}(N_H) - \log_{10}(N_I)]/\log_{10}(2)$. The population doubling for each passage was calculated and added to that of the previous passages to obtain cumulative population doubling. The generation time – average time between two cell doublings – was calculated from P3 to P6 using the following formula: $GT = [\log_{10}(2) \times \Delta t]/[\log_{10}(N_H) - \log_{10}(N_I)]$.

Pharmacological Treatments

For pharmacological treatments, hUCM-MSCs were seeded at 7,000 cells/cm^2 on coated custom-made 40:1 PDMS, glass coverslips or TCPS. Twenty four hour after seeding, cells on soft PDMS were incubated with 25 μM of lysophosphatidic acid (LPA – Enzo, BML-LP100) for 2 h. Cells on glass coverslips or TCPS were incubated with 30 or 50 μM of racemic Blebbistatin (Calbiochem, 203389-5MG), respectively, for 24 h. Cells cultured on TCPS were incubated with 10 or 12 μM of LIM Kinase inhibitor (Limki-3 – Calbiochem, 435930) for 24 h. Stock solutions were prepared in dimethyl sulfoxide (DMSO, Santa Cruz Biotechnology) and the incubations were performed in a serum-free medium. For MRC-5 cells the procedures were similar. Briefly, cells were cultured at 4,000 cells/cm^2 on glass

coverslips or 1.5 kPa PDMS (IBIDI). Cells on glass coverslips were cultured for 32 h and then incubated with 25 μM of Blebbistatin for an additional 40 h. Cells on PDMS were cultured for 70 h and then incubated with 1 μM of LPA for 2 h. In both cases, cells were fixed after 72 h in cultured and immunostained as indicated.

Preparation of Cell Culture Substrates

The substrates used for cell culture included TCPS (Corning Costar), glass coverslips (Thermo Fischer Scientific) and PDMS (1.5 and 15 kPa μ-Dish from IBIDI and ∼3 kPa custom-made substrates).

Custom-made PDMS substrates were prepared by mixing the silicone elastomer base with the curing agent (Sylgard 184; Dow Corning/Dowsil) on a 40:1 proportion. In order to remove air bubbles, the mixture was degassed under vacuum (−5 inHg) at RT for 40 min. Next, a specific volume of that mixture was poured according to the area of each platform used in order to create substrates approximately 300 μm thick (higher than the recommended substrate thickness to avoid cells from sensing the underlying stiff support) (Buxboim et al., 2010). PDMS substrates were then cured at 80°C for 4 h in an incubator (Memmert).

Since PDMS is highly hydrophobic and does not readily bind to cell-adhesion proteins, all PDMS substrates were chemically treated (based on existing literature; Yu et al., 2009; Kuddannaya et al., 2013) in order to become more hydrophilic and receptive to protein coating and cell culture as described before (Gerardo et al., 2019). Solution 1 [double deionised (dd) H_2O, 37% hydrochloric acid (Fluka) and 30% (w/w) hydrogen peroxide (Sigma) in a volumetric proportion of 5:1:1] was added over the PDMS surface for 5 min at RT. Substrates were then washed three times with abundant ddH_2O and treated with Solution 2 [10% (v/v) of 3-aminopropyltrimethoxisilane (3-APTMS, Alfa Aesar) in 96% ethanol (Merck)] for 30 min at RT. Next, the substrates were washed three times with ddH_2O (10 min each) with agitation. Finally, the substrates were incubated with Solution 3 [3% (w/v) glutaraldehyde in PBS] for 20 min at RT followed by three washes with ddH_2O (5 min each) with agitation. Glass coverslips were treated as described for PDMS except that 1M NaOH (Merck) was used (30 min with agitation) instead of Solution 1. After functionalisation, PDMS substrates and glass coverslips were exposed to ultraviolet light for 30 min in an air flow cabinet for sterilisation.

To allow cell adhesion, the surface of PDMS substrates and glass coverslips were coated with human plasma purified fibronectin (FN) (Merck Millipore) and rat tail type-I collagen (COL-I) (BD Biosciences) in PBS at a final concentration of 10 and 17 μg/ml, respectively. The coating solution was used at 143 μl/cm^2, resulting in 1.4 μg/cm^2 of FN and 2.4 μg/cm^2 of COL-I. All substrates were incubated with the coating solution for 4 h at 37°C, and then washed once with sterile PBS before cell seeding. The TCPS dishes used in this study were not coated.

Characterisation of PDMS Substrates

The rheological characterisation of custom-made 40:1 PDMS substrates was performed by small-strain oscillatory shear tests using a Kinexus Pro rheometer and rSpace software (Malvern) fitted with a parallel plate geometry (stainless steel wrinkled plate, 4 cm diameter). Frequency sweeps were performed from 10 to 0.1 Hz (five reads per decade) with 1% strain at 37°C and under a normal force of 0.5 N to guarantee adherence. The Young's modulus (E) was calculated using the values measured for viscoelastic shear modulus and using the formula $E = 2G'(1 + \nu)$, in which G' is the shear storage modulus at 1 Hz and ν the Poisson's ratio, assumed to be 0.5 as for materials whose volume do not change upon stretching.

To measure the thickness of the PDMS substrates, a pre-polymer to curing agent ratio of 10:1 was used, since polymers prepared with this formulation could readily be detached from the dishes in which were cured. After curing (as described above), the substrates were detached from the dishes and sliced across the centre. The thickness of the central zone of the PDMS substrates was measured using a phase-contrast microscope (Axiovert 40C) and the AxioVision software (both from Zeiss).

Subproteome Fractionation

Subproteome fractionation was performed using hUCM-MSCs at the end of P4 after expansion in TCPS or custom-made PDMS from P2 to P4, using the protocol described in Anjo et al. (2017). Briefly, cells were washed once with PBS and then incubated with extraction buffer [50 mM Tris-HCl pH 7.4 supplemented with protease inhibitors – Protease Inhibitor Cocktail tablets, Complete EDTA-free (Roche)]. Next, cells were subjected to ultrasonication in a H_2O-bath (Vibra-Cell 750 watts, Sonics) with 40% amplitude and 30 s cycles. After centrifugation (1,000 × g) for 5 min at 4°C, supernatants were ultracentrifuged (126,000 × g) for 1 h at 4°C (Beckman Coulter), and the pellet corresponding to the membrane-enriched fraction was solubilised in SDS sample buffer [1.7% (w/v) SDS and 100 mM DTT in 50 mM Tris pH 6.8]. Five volumes of cold acetone were added to each supernatant (corresponding to the soluble fraction) and samples were stored at −20°C to precipitate the protein content, which was recovered by centrifugation at 4,000 × g during 30 min at 4°C and then the protein pellets were washed with cold acetone. Next, the pellet corresponding to the soluble fraction was resuspended in SDS sample buffer. Protein quantification was performed using the Direct Detect Spectrometer (Millipore) according to the manufacturer's instructions, and 100 μg of protein (soluble or membrane fraction) were used for sequential windowed data independent acquisition of total high-resolution mass spectra (SWATH-MS) analysis.

SWATH-MS Analysis

After denaturation at 95°C, samples were alkylated with acrylamide and subjected to in-gel digestion using the short-GeLC approach (Anjo et al., 2015). Pooled samples were created for protein identification and the same amount of MBP-GFP was added to all samples to be used as an internal standard. Samples were analysed on a Triple TOF^{TM} 5600 System (AB Sciex®) in two phases: information-dependent acquisition (IDA) of the pooled samples for protein identification and SWATH acquisition of each individual sample for quantification (detailed in the

Supplementary Methods). A specific library of precursor masses and fragment ions was created by combining all files from the IDA experiments, and used for subsequent SWATH processing. Libraries were obtained using ProteinPilot™ software (v5.1, AB Sciex®) searching against a database composed by *Homo sapiens* from Swiss-Prot and the sequence of the recombinant protein MBP-GFP. SWATH data processing was performed using SWATH™ processing plug-in for PeakView™ (v2.0.01, AB Sciex®). Peptides were selected automatically from the library and up to 15 peptides with up to 5 fragment ions were chosen per protein. Quantitation was attempted for all proteins in the library file that were identified below 5% local FDR from ProteinPilot™ searches, by extracting the peak areas of the target fragment ions of those peptides using an extracted-ion chromatogram (XIC) window of 3 and 4 min (for soluble and membrane-enriched fraction, respectively) with 20 ppm XIC width.

All the peptides that met the 1% FDR threshold in at least one sample were retained and the levels of the proteins were estimated by summing the respective transitions and peptides that met the criteria established (an adaptation of Collins et al., 2013). For comparisons between experimental conditions, the protein levels were subjected to two steps of data normalisation: (1) normalised to the internal standard (MBP-GFP) followed by (2) a normalisation using the sample total intensity.

The mass spectrometry proteomics data have been deposited to the ProteomeXchange Consortium via the PRIDE (Vizcaíno et al., 2016) partner repository with the dataset identifier PXD017674.

Bioinformatics and Data Analysis

PANTHER Classification System was executed for Gene Ontology analysis. Gene Ontology enrichment analysis was performed for proteins identified using the web-based application Gene Ontology enrichment analysis and visualisation tool – GOrilla. In order to identify and collect information about the proteins that were found, UniProt was used. Venn graphs were generated using BioVenn web application.

Protein Extracts and Western Blot Analysis

To obtain whole-cell protein extracts from hUCM-MSCs (P2–P4), cells were detached using a cell scraper in the presence of Laemmli buffer [120 mM Tris-HCl pH 6.8, 4% SDS (w/v) and 20% glycerol (v/v)], heated for 5 min at 95°C and passed ten times through a 25G needle. Total protein was quantified using Pierce™ 660 nm Protein Assay (Thermo Fischer Scientific) according to manufacturer's instructions followed by addition of DTT to each protein sample at a final concentration of 0.1 M. Protein extracts (10 or 20 μg) were separated by SDS-PAGE as previously described (Leite et al., 2014) and transferred onto polyvinylidene fluoride (PVDF) membranes (Bio-Rad). The membranes were blocked in TBS- or PBS-0.1% (v/v) Tween 20 containing 5% (w/v) non-fat dried milk for 1 h at RT. Incubations with the antibodies indicated in the **Supplementary Table S2** were performed with gentle agitation overnight (ON) at 4°C followed by 1 h at RT. All membranes were washed with TBS- or PBS-0.1% (v/v) Tween 20 and then incubated for 1 h at RT with gentle agitation with the respective alkaline phosphatase-conjugated secondary antibody (Jackson ImmunoResearch) diluted in blocking solution. Next, membranes were incubated with enhanced chemifluorescence (ECF) kit (GE Healthcare) according to the manufacturer's instructions and detection was performed on a Molecular Imager FX Pro Plus system using the software Quantity One (both from Bio-Rad). To quantify the total protein in each lane, the membranes were stained using SERVA purple (SERVA electrophoresis, Enzo) according to the manufacturer's guidelines. The integrated density of antibody-stained protein bands and total protein content of each lane were measured using Quantity One software (Bio-Rad).

Immunocytochemistry, Fluorescence Microscopy and Image Analyses

hUCM-MSCs between P2–P4 on glass coverslips or custom-made PDMS substrates were fixed with 4% (w/v) paraformaldehyde (PFA, Santa Cruz Biotechnology) in PBS for 20 min at RT. Immunocytochemistry (ICC) was performed as detailed in Leite et al. (2014). Fixed cells were washed three times with PBS and permeabilised with 0.1% Triton X-100 in PBS for 20 min. Cells were blocked with 1% (w/v) BSA (Calbiochem) in PBS for 30 min at RT and then incubated with primary antibodies (**Supplementary Table S2**) diluted in blocking solution ON at 4°C in humidified conditions. Next, cells were washed with PBS and incubated with the appropriate secondary antibodies (**Supplementary Table S2**) in PBS with 1% (w/v) BSA for 1 h at RT. For nuclear staining, cells were incubated with DAPI (**Supplementary Table S2**) for 5 min. To visualise polymerised actin, cells were stained with TRITC-labelled Phalloidin (**Supplementary Table S2**) for 1 h at RT and then washed three times with PBS (5 min each) to remove unbound reagent. Fluorescence microscopy was performed using a Zeiss Axiovert 200M microscope using AxioVision Release 4.8 software (Zeiss). Exposure time was the same for each analysed marker and for each independent experiment. To quantify the mean of fluorescence intensity (MFI) of F-actin, the regions of interest (ROIs) were defined as limiting cells by the edges. DAPI images were used to defined ROIs to measure the MFI of Cofilin-1 in the nucleus. The MFI of Cofilin-1 in the cytoplasm was quantified using ROIs defined by segmented lines within the whole cytoplasm. Image processing and analyses were performed using ImageJ (Fiji) software.

5-FUrd Incorporation

To quantify transcription, hUCM-MSCs were seeded at P2 and 48 h later were incubated with 2 mM of 5-fluorouridine (5-FUrd, Sigma-Aldrich) in proliferation medium during 15, 30, and 45 min at 37°C. Next, cells were washed once with cold PBS, permeabilised with 1% Triton X-100 for 20 min and fixed with 4% (w/v) PFA in PBS for another 20 min. 5-FUrd incorporation was analysed by ICC using an anti-BrdU antibody (**Supplementary Table S2**) previously described to recognise 5-FUrd (Obrdlik and Percipalle, 2011). Quantification of fluorescence levels was performed by calculating the corrected total cell fluorescence

using DAPI to define ROIs and quantify the integrated density and nuclear area using Fiji software. The slopes were calculated by performing linear regression analysis of the corrected total cell fluorescence values of FUrd incorporation considering the time points between 15 and 45 min (GraphPad Prism 8).

Cofilin-1 Gene Silencing

To knockdown Cofilin-1, hUCM-MSCs were transfected at P2 according to the manufacturer's instructions on TCPS or custom-made 40:1 PDMS using lipofectamine 3000 (Thermo Fisher Scientific) with 150 nM of SignalSilence® Cofilin siRNA I or SignalSilence® Control siRNA as control (Cell Signalling Technology). 5-FUrd incorporation experiments were performed 72 h after transfection.

Fluorescence Loss in Photobleaching (FLIP) and Image Analysis

Fluorescence Loss in Photobleaching (FLIP) was performed using a Zeiss LSM 710 confocal microscope with stage heated at 37.5°C and the Zen software was used for image acquisition (Zeiss). For this experiment MRC-5 cells were seeded at 15,000 cells/cm^2 on 1.5 kPa PDMS or μ-slide well glass (both from IBIDI) and maintained in culture for 3 days. The experiment was performed according to Das Neves et al. (2010), Lima et al. (2018), and Steurer et al. (2018). Briefly, to photobleach GFP-RNA POL II in MRC-5 cells, rectangles covering approximately half of each nucleus were selected and 100% laser power was applied to bleach all fluorescent molecules in these areas. The bleaching acquisition cycles were run in a continuous mode during 1,800 s. A set of images were taken and the fluorescence intensity of GFP in the nucleus was quantified at the unbleached area using Fiji software. The fluorescence decay was plotted against the time of photobleaching, fitting data in a three-phase exponential decay curve to obtain half-life values attributed to the elongation time (GraphPad Prism 8).

Statistical Analysis

Proteomics data were presented as the mean fold change of 40:1 PDMS over the respective TCPS sample for three biological replicates (umbilical cord samples from three different donors). Statistical analysis was performed using the SPSS® Statistics V22 (IBM) for all proteins that presented PDMS/TCPS ratio with coefficient of variation (CV) below 30%. Data normality was assessed by Shapiro–Wilk test performed in infernoRDN and the One-Sample *t*-student test against a theoretical value of 1 was used to test the variations. Statistical significance was considered for $p < 0.05$.

Statistical analysis of the remaining data was performed using GraphPad Prism 8 software. Values are expressed as mean ± standard error of the mean (SEM) or median with range (as indicated) for at least three independent experiments. Differences between two groups were tested using Student's *t*-test, One-Sample *t*-test (theoretical mean of 1) or the non-parametric Mann–Whitney test. Parametric analysis of variance (ANOVA) followed by Dunnett's multiple comparisons test was used to compare more than two groups. For all statistical analysis, differences were considered significant for $p < 0.05$.

RESULTS

Characterisation of Human Umbilical Cord Mesenchymal Stem/Stromal Cells (hUCM-MSCs) and 40:1 PDMS Substrates

MSCs are plastic-adherent cells that proliferate readily *in vitro* when maintained in standard culture conditions, being positive for CD105, CD73 and CD90 and negative for CD45, CD34, HLA-DR, CD14 or CD11B, CD79α or CD19 surface markers, as described by the International Society for Cellular Therapy (Dominici et al., 2006). For this study, we isolated hUCM-MSCs as previously described (Leite et al., 2014). The immunophenotypic characterisation of the cells in P4 by flow cytometry confirmed their identity, being positive for CD10, CD13, CD90, and CD105, and negative for CD34, CD45, and HLA-DR (**Figure 1A**).

For this study, polydimethylsiloxane substrates with a pre-polymer to curing agent ratio of 40:1 (40:1 PDMS) were produced for cell culture. The rheological analysis was performed to assess the shear elastic (storage modulus, G') and viscous (loss modulus, G'') properties of the substrates. A frequency sweep between 0.1 and 10 Hz was performed using a rheometer (**Supplementary Figure S1B**). Our results indicate that the elastic properties of the substrate are dominant, since $\tan\delta$ ($\tan\delta = G''/G'$) values were lower than 1 and G' and G'' were essentially independent of the measurement frequency (Rosales and Anseth, 2016) (**Supplementary Figures S1B,C**).

The Young's modulus (E) was determined at 1 Hz as being 2870 ± 625 Pa (∼3 kPa) (**Supplementary Figure S1C**). To guarantee that the custom-made PDMS substrates reached the minimum thickness described to prevent cells from sensing the stiff supporting material underneath the elastomer (>100 μm) (Buxboim et al., 2010), substrate thickness was determined to be 315.5 ± 4.6 μm (**Supplementary Figure S1**), sufficient to allow the cells to sense only the soft material.

In order to evaluate the proliferative capacity of hUCM-MSCs when cultured on stiff (TCPS) or soft (40:1 PDMS) substrates, the total number of cells was determined between P2 and P6 (**Figure 1B**). In general, the total number of cells obtained on TCPS was higher when compared with PDMS, showing that cells cultured on soft substrates exhibit lower proliferative profile in comparison with those cultured on stiff TCPS (**Figure 1B**). Nevertheless, except in P2, no significant differences were found for the total number of cells, indicating some adaptation of the cells to the new soft environment. These results are in agreement with previous studies reporting higher cell proliferation on stiffer substrates (Provenzano and Keely, 2011). Additionally, population doubling, cumulative population doubling, and generation time were evaluated between P2 and P6 (**Supplementary Figure S2**), indicating a trend for

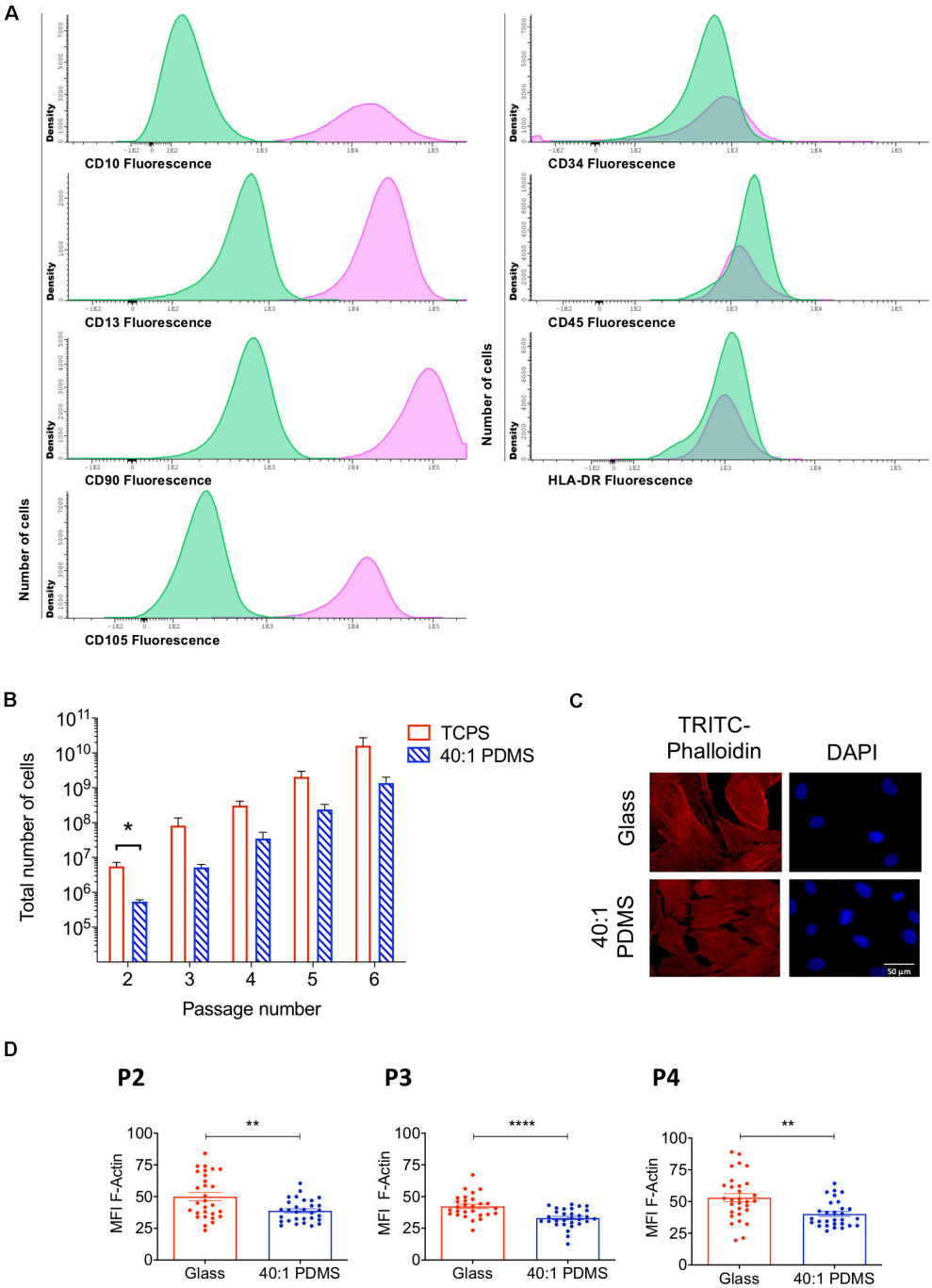

FIGURE 1 | hUCM-MSCs can proliferate on and respond to mechanical cues provided by a soft PDMS substrate. **(A)** Immunophenotypic characterisation of hUCM-MSCs (average of four independent samples at P4). Cells were labelled with antibodies against the indicated antigens and analysed by flow cytometry. In parallel, unlabelled hUCM-MSCs were also acquired in the flow cytometer as negative controls. In the histograms, *y*-axis represents the number of cells (density); and *x*-axis represents the amount of protein expressed per cell, measured as mean fluorescence intensity (MFI). Labelled hUCM-MSCs are represented as pink lines, whereas green lines correspond to unlabelled hUCM-MSCs (negative control). hUCM-MSCs were positive for CD10, CD13, CD90, and CD105, and negative for CD34, CD45 and HLA-DR. **(B)** Total number of cells calculated for hUCM-MSCs on each passage (P2–P6) in culture on TCPS or 40:1 PDMS (as indicated). Bars represent mean ± SEM of at least three independent experiments using cells obtained from different donors. Statistical analysis was performed using the non-parametric Mann–Whitney test with significant differences indicated as $*p < 0.05$. **(C)** Representative fluorescence microscopy images and **(D)**, respective MFI of F-actin of hUCM-MSCs cultured on stiff or soft 40:1 PDMS substrates from P2 to P4 (as indicated). At each of the indicated passages, cells were seeded on stiff glass coverslips or soft 40:1 PDMS substrates for 48 h and then fixed and stained with TRITC-Phalloidin (to stain F-actin, in red) and DAPI (to counterstain nuclei, in blue). Bars represent mean ± SEM of three independent experiments. Statistical analysis was performed using a two-tailed Student's *t*-test with significant differences indicated as $**p < 0.01$ and $****p < 0.0001$.

slower proliferation kinetics of hUCM-MSCs on PDMS, but no significant differences were found.

To confirm that hUCM-MSCs respond to the distinct degrees of stiffness, P1 cells were seeded in parallel on glass coverslips (stiff) and 40:1 PDMS substrates (soft). After reaching P2, P3, or P4 on each substrate, F-actin levels were assessed to evaluate intracellular contractility, which is known to scale with the stiffness of the environment in mechanosensitive cells (Engler et al., 2006; Fu et al., 2010; Gerardo et al., 2019). As expected, F-actin levels were significantly lower in cells cultured on soft PDMS substrates when compared with cells maintained on stiff glass coverslips in all passages tested (**Figures 1C,D**).

Substrate Stiffness Modulates the Proteome of hUCM-MSCs

To explore the influence of mechanical cues, and in particular the effect of substrate stiffness on the proteome of hUCM-MSCs, a SWATH-MS/MS proteomics analysis was performed using cells maintained on stiff TCPS or soft 40:1 PDMS substrates from P2 until P4 (workflow in **Figure 2A**). To obtain samples with less complexity (and to achieve a more comprehensive protein coverage), the intracellular contents were fractionated into soluble and membrane-enriched fractions. 796 proteins were identified in the soluble fraction, 558 of which were detected in cells cultured on both substrates (TCPS and 40:1 PDMS), representing 70% of the total number of proteins identified. On the other hand, 173 and 65 proteins were exclusively detected in the proteome of cells cultured on soft or stiff substrates (**Figure 2B**). Similarly, in the membrane-enriched fraction, 1125 proteins were identified, being 744 common for cells on TCPS and PDMS, representing 66% of the total proteins identified in that fraction. Hundred and thirty seven and 244 proteins were exclusively identified in the proteome of cells cultured on soft or stiff substrates (**Figure 2B**). To further characterize the differences between the cells cultured on the two systems, protein quantification was attempted to all the proteins identified (**Figure 2C**). Through SWATH-MS/MS analysis, 633 proteins were quantified in the soluble fraction obtained from cells cultured on both substrates, and among those 33 showed lower abundance, while 27 displayed higher expression in cells cultured in PDMS in comparison with TCPS (**Figure 2C**). In the membrane fraction, 624 proteins were quantified, with 43 and 19 proteins showing lower and higher expression, respectively, in cells maintained on the soft versus stiff substrate (**Figure 2C**).

Next, we analysed the twenty most statistically significant proteins more abundantly expressed in cells cultured on PDMS when compared with TCPS and vice versa (among both fractions). Data show that several of the identified proteins are involved in the regulation of actin cytoskeleton, hence putative modulators of mechanotransduction (**Figures 2D,E**). Within this category, Filamin-A/B, Lamin-A/C and Actin were more abundant in TCPS in comparison with PDMS, while subunit 4 of the Arp2/3 complex and Cofilin-1 were more expressed in cells in 40:1 PDMS when compared with TCPS (**Figures 2D,E**). Cofilin-1 presented good *p*-value and increased expression of approximately 1.3-fold (PDMS vs. TCPS; **Supplementary Table S3**) in the membrane fraction, being one of the most differentially expressed proteins in the proteome of hUCM-MSCs cultured on the soft when compared with the stiff substrate. Additionally, Cofilin-1 is a pivotal regulator of actin dynamics (Bamburg and Bernstein, 2010; Ohashi, 2015) and in turn the actin cytoskeleton is one the most important players in mechanotransduction (Harris et al., 2018). Hence, Cofilin-1 seemed to be a promising protein to focus on and to characterise further in the context of mechanotransduction and attempt to find implications in other important biological processes regulated by the protein such as transcription (Obrdlik and Percipalle, 2011; Percipalle, 2013).

Cofilin-1 Is More Abundantly Present in Cells Cultured on Soft Versus Stiff Substrates

In order to validate and further explore the results obtained by mass spectrometry regarding Cofilin-1, western blot (WB) analysis was performed to measure the protein's level in whole-cell extracts prepared from cells cultured on stiff (TCPS) or soft (40:1 PDMS) substrates until P2, P3, and P4. The results show that Cofilin-1 levels became gradually higher in cells cultured from P2 to P4 on the soft substrate when compared to those maintained on the stiffer one, achieving statistical significance in P4 (**Figure 3A**). This is consistent with the proteomics data regarding the increased presence of Cofilin-1 on the soft substrate in P4 (**Figures 2D,E**). As a control, we further analysed vinculin (**Supplementary Figure S3**), another protein related to mechanotransduction (Carisey et al., 2013) whose expression levels did not significantly change in the proteomics analysis (**Supplementary Table S3**). As expected, WB analysis confirmed the SWATH-MS/MS results.

To gain further insight into the regulation of the protein, the levels of Cofilin-1 were also assessed specifically in the nucleus and in the cytoplasm of cells cultured on soft and stiff (glass coverslips) substrates until P2, P3, and P4 by immunofluorescence microscopy. Data show a significant increase of the MFI of Cofilin-1 in both subcellular spaces (nucleus and cytoplasm) for all passages tested (**Figures 3B,C**). Taken together, these results strongly indicate that Cofilin-1 levels are higher in cells cultured on soft when compared with stiff substrates.

Substrate Stiffness and Soluble Modulators of Actomyosin Influence Cofilin-1 Subcellular Localisation and Phosphorylation State

The immunofluorescence images of Cofilin-1 in hUCM-MSCs immediately suggested that the protein's subcellular localisation might be influenced by substrate stiffness (**Figure 3B**). Image quantification revealed that the ratio of nuclear/cytoplasmic Cofilin-1 increased significantly in cells cultured on the soft substrates when compared with those on stiff glass coverslips (**Figure 3D** and **Supplementary Figure S4**). Cofilin-1 activity and subcellular localisation (Nebl et al., 1996) were reported to be largely regulated by phosphorylation on Serine 3 by its

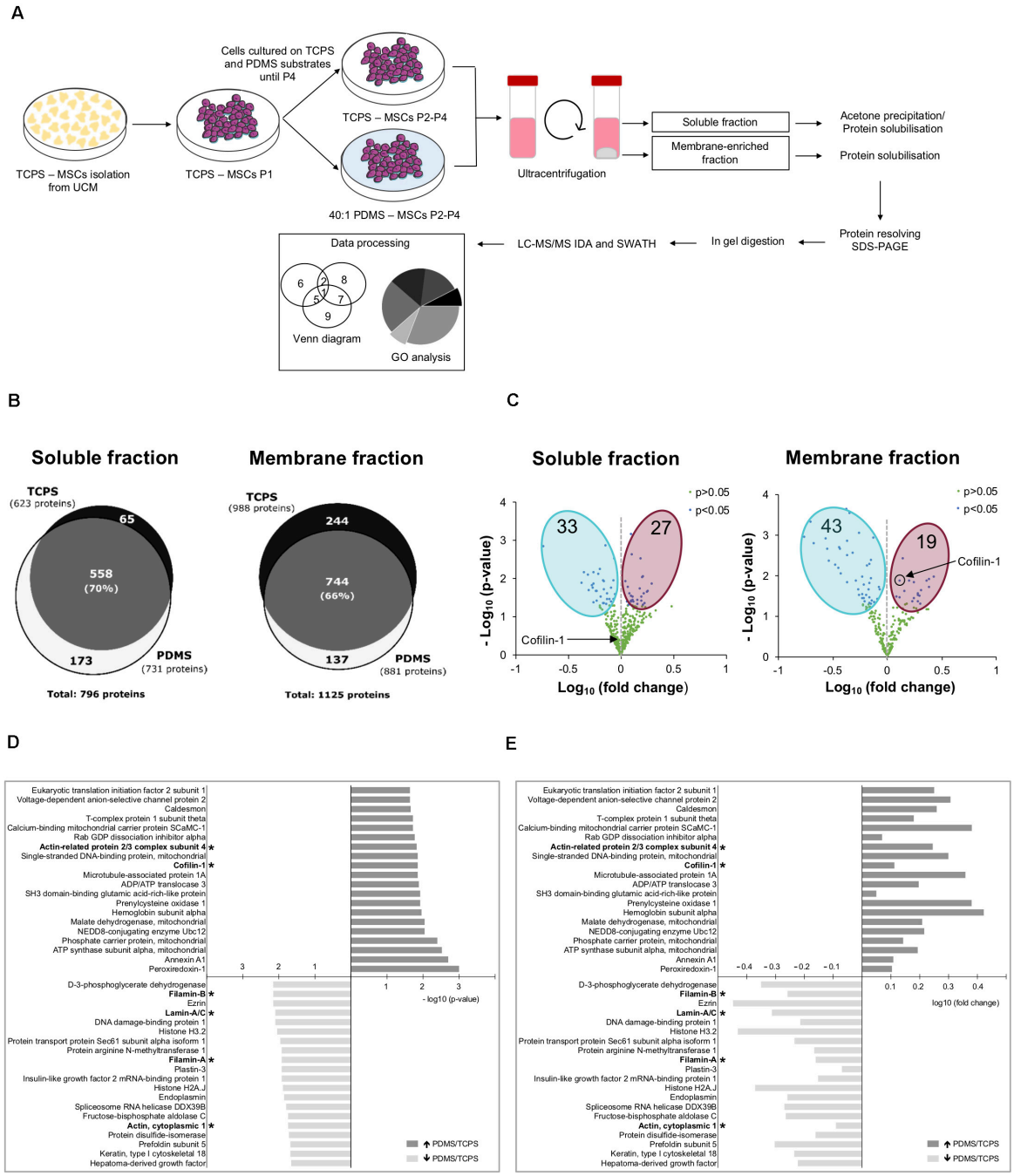

FIGURE 2 | Substrate stiffness influences the proteome of hUCM-MSCs. **(A)** Experimental workflow. hUCM-MSCs were isolated from umbilical cord explants obtained from three distinct donors on TCPS plates and passaged (into P1) when the colonies were well developed. Cells were then maintained in parallel in culture from P2 until P4 on stiff TCPS and soft 40:1 PDMS substrates. Cells were lysed and then the membrane- and soluble-enriched fractions were obtained by ultra-centrifugation. The proteins from the two fractions were precipitated and/or solubilised, resolved by SDS-PAGE and analysed by mass spectrometry. **(B)** Venn diagrams illustrating the total number of proteins and the number of exclusive and common proteins identified in cells cultured on TCPS or 40:1 PDMS present in the soluble (left) or membrane (right) enriched fractions. **(C)** Volcano plots representing proteins with statistically significant differences ($p < 0.05$, blue dots) or non-significant differences ($p > 0.05$, green dots) between proteins found in the proteome of soluble (left) and membrane (right) fractions obtained from cells cultured on soft PDMS substrates relative to stiff TCPS. The blue and magenta areas surround the proteins with statistically significant lower or higher expression in cells cultured on soft PDMS versus stiff TCPS, respectively. Black circle and arrows pinpoint Cofilin-1 found in soluble (left) and membrane (right) fractions of cells cultured on soft PDMS versus stiff TCPS. Statistical analysis was performed using One-Sample *t*-test (theoretical mean of 1.0). **(D)** Bar chart representing the top 20 most significant ($p < 0.05$) and **(E)** differentially abundant proteins (fold change) present in soluble and membrane fractions obtained from cells cultured on 40:1 PDMS versus TCPS substrates. (*) marks proteins involved in mechanotransduction or actin cytoskeleton regulation. Bars represent –log10 of the *p*-value **(D)** or log10 of the fold change **(E)**. All data were collected from three independent experiments using cells obtained from three distinct donors.

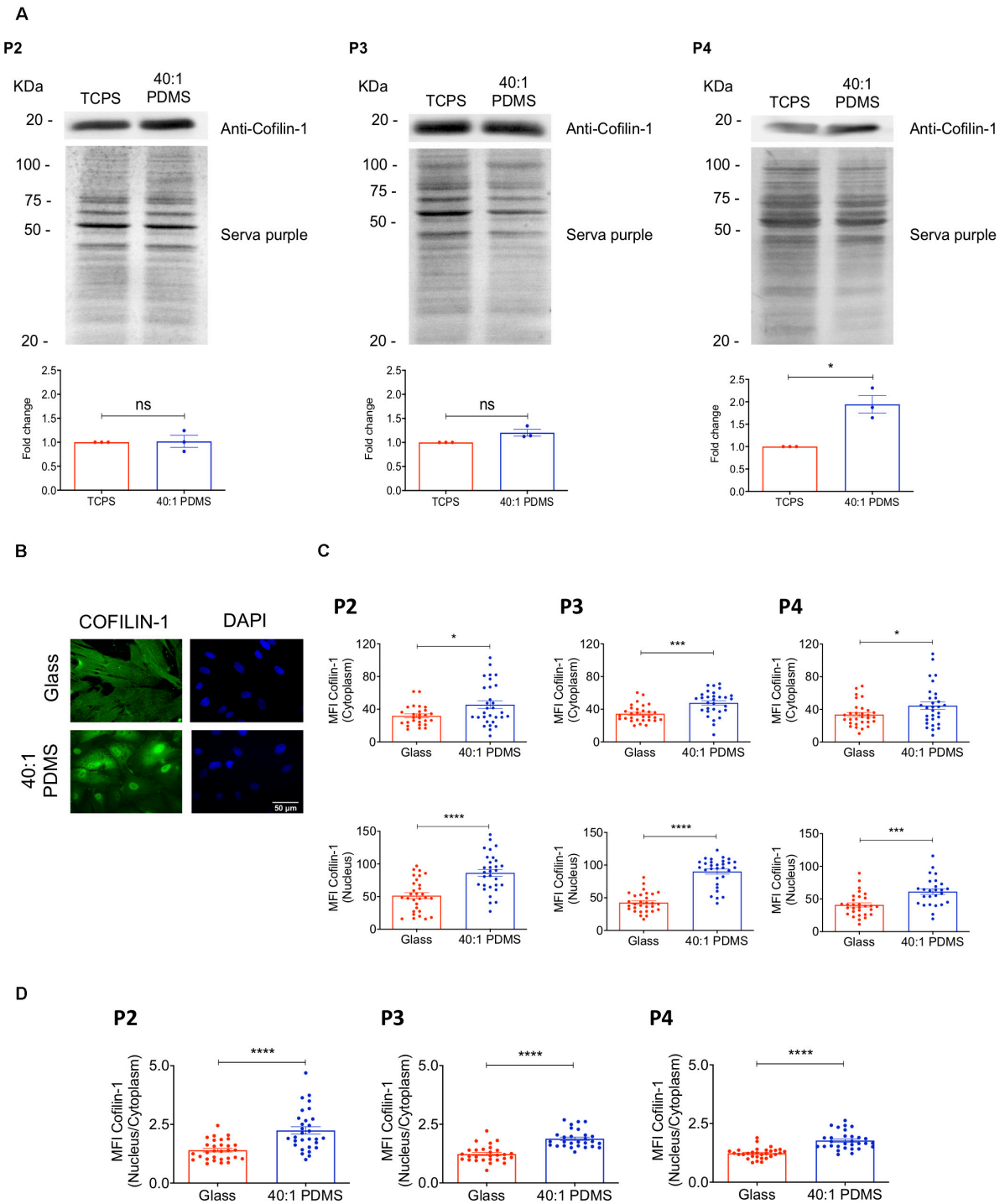

FIGURE 3 | Cofilin-1 is highly present in cells cultured on soft versus stiff substrates. **(A)** Western blot analysis (top) of Cofilin-1 present in whole-cell protein extracts (separated by SDS-PAGE) obtained from hUCM-MSCs isolated and cultured on TCPS until P1 and then cultured on stiff TCPS or soft 40:1 PDMS until P2, P3, or P4 (as indicated). For quantification analysis (bottom), Cofilin-1 expression was normalised using the respective total protein level assessed by staining the WB membrane using SERVA purple (top). Bars (bottom) represent mean ± SEM of three independent experiments. Statistical analysis was performed using One-Sample *t*-test (theoretical mean of 1.0) with significant differences indicated as $*p < 0.05$; ns, non-significant. **(B)** Representative fluorescence microscopy images and **(C)** respective MFI quantification of Cofilin-1 in the nucleus or cytoplasm of cells cultured on glass coverslips or 40:1 PDMS until P2, P3, or P4 (as indicated). **(D)** MFI quantification of Cofilin-1 ratio (nucleus/cytoplasm) present in cells cultured as in **(C).** Cells were fixed and stained with an anti-Cofilin-1 antibody (green) and DAPI for nuclear counterstaining (blue). In **(C,D)** bars represent mean ± SEM of cells analysed from three independent experiments. Statistical analysis was performed using a two-tailed Student's *t*-test, with significant differences indicated as $*p < 0.05$, $***p < 0.001$, and $****p < 0.0001$.

cognate kinase LIMK1 (Yang et al., 1998). Our results showed that after incubating cells with a pharmacological inhibitor of LIMK (LIMKi-3), the phosphorylation levels of Cofilin-1 on Ser3 drastically decreased in a dose-dependent manner (**Supplementary Figure S5**).

It is also described that phospho-Cofilin-1 (p-Cofilin-1) is inactive and remains in the cytosol. When dephosphorylated, Cofilin-1 is active and hence able to severe and depolymerise actin filaments into globular actin, subsequently remaining bound to G-actin (Percipalle, 2013). Then, still bound to G-actin, Cofilin-1 translocates into the nucleus through a mechanism mediated by importin 9 (Dopie et al., 2012; Percipalle, 2013). To assess if the changes in subcellular localisation of Cofilin-1 in response to substrate stiffness correlated with the phosphorylation state of the protein, we measured the levels of *p*-Cofilin-1 on Ser3 and total Cofilin-1 (by western blot analysis) in cells cultured on TCPS and 40:1 PDMS. We observed a significant decrease in the ratio of Cofilin-1 (pSer3)/total Cofilin-1 (**Figure 4A**) in cells cultured on the soft in comparison with those on the stiff substrate. The phosphorylation of Cofilin-1 on Ser3 was also detected by proteomics analysis. The ratio of Cofilin-1 (pSer3)/total Cofilin-1 measured in cells cultured on soft (PDMS) was only about 40% of the value found in cells maintained on stiff (TCPS) until P4 (**Supplementary Figure S6**). Hence, data indicate that the expected correlation between the subcellular localisation and phosphorylation state of Cofilin-1 reported in the abovementioned literature holds true when these changes occur in response to substrate stiffness.

To further understand the response of Cofilin-1 to mechanical stimuli in terms of subcellular localisation and phosphorylation state, we devised an experiment to mimic stiff conditions while cells were cultured on a soft substrate and vice versa. To that end, cells were seeded on stiff glass coverslips or soft 40:1 PDMS substrates and then incubated with Blebbistatin or LPA, respectively. Blebbistatin is a NMM-II inhibitor, causing relaxation of the cellular actin network (typical of cells cultured on a soft condition) (Engler et al., 2006; Lourenco et al., 2016) and LPA leads to activation of RhoA, inducing actomyosin contractility (typical of cells on stiff substrates) (Sun et al., 2014), hence mimicking a soft condition on stiff substrates and vice versa. When cells on glass coverslips were incubated with Blebbistatin, the ratio of nuclear/cytosolic Cofilin-1 increased significantly compared to untreated cells. Conversely, cells incubated with LPA cultured on soft PDMS showed a significant decrease in the nuclear/cytosolic ratio of the protein when compared to the respective control (**Figures 4B,C**). Additionally, we analysed the levels of F-actin upon incubation with Blebbistatin or LPA using TRITC-phalloidin. As expected, a significant decrease or increase of F-actin was observed in cells incubated with Blebbistatin or with LPA (respectively) comparing with their respective controls (**Figures 4B,C**), indicating that the treatments with the actomyosin-modulating soluble-factors tested were indeed effective.

To assess the phosphorylation state of Cofilin-1 in cells incubated with Blebbistatin or LPA, WB analysis was performed. After incubation with Blebbistatin, the ratio of Cofilin-1(pSer3)/total Cofilin-1 in cells cultured on a stiff substrate decreased significantly. Conversely, in cells incubated with LPA while cultured on a soft substrate, this ratio was significantly higher than in control cells (**Figure 4D**).

These results indicate that cells cultured on stiff substrates (or on soft but in the presence of LPA) display high intracellular actomyosin tension (**Figures 1C**, **4B**), which is accompanied by a low nuclear/cytosolic ratio distribution of Cofilin-1 and high phosphorylation of the protein on Ser3 (**Figures 4A,D**). Conversely, MSCs cultured on soft substrates (or on stiff but in the presence of Blebbistatin) present low intracellular contractility (**Figures 1C**, **4B**), which correlates with a high ratio of nuclear/cytosolic distribution of Cofilin-1 and low phosphorylation of the protein on Ser3 (**Figures 4A,D**).

hUCM-MSCs Respond to Soft Substrates With Increased Overall Transcription in a Cofilin-1-Dependent Manner

Knowing that Cofilin-1 (in combination with G-actin) is required for RNA polymerase II-mediated transcription elongation (Obrdlik and Percipalle, 2011; Percipalle, 2013), we sought to elucidate if the increased presence of Cofilin-1 in the nucleus of hUCM-MSCs cultured on soft substrates correlated with increased transcription. Hence, to measure global transcriptional activity, cells (cultured on stiff glass coverslips or soft 40:1 PDMS) were subjected to a FUrd pulse-chase (Obrdlik and Percipalle, 2011). We observed that FUrd incorporation in cells maintained on stiff substrates occurred mostly in discrete nucleolar *foci* for short incubation times, with increasing nucleoplasmic signal with time (**Figure 5A**), as validated by ICC analysis against the nucleolus-associated protein Nucleolin (**Supplementary Figure S7**). On the other hand, for cells cultured on the 40:1 PDMS substrate, data show multiple and more intense nucleoplasmic *foci* (**Figure 5A**) in addition to the nucleolar signal similar to that observed on the stiff condition. This strongly suggests that the increase in FUrd incorporation observed in cells on the soft substrate relies on RNA polymerase II- (with nucleoplasmic localisation) and not on RNA polymerase I- (with nucleolar localisation) mediated transcription (Szentirmay and Sawadogo, 2000). Quantification of FUrd incorporation over time showed that the slope of the curve within a linear range (between 15 and 45 min of incorporation) was significantly higher in cells cultured on the soft substrate when compared to the stiff (**Figure 5B**). Since the slope is proportional to the overall transcription, these results indicate that soft 40:1 PDMS substrates enhance hUCM-MSCs transcriptional activity by favouring the formation of nascent transcripts.

To assess if the increase of transcriptional activity in cells cultured on soft substrates is Cofilin-1-dependent, we performed similar FUrd pulse-chase experiments after performing Cofilin-1 knockdown using siRNA (as confirmed by western blot and fluorescence microscopy in **Supplementary Figure S8**). Data show that in cells in which Cofilin-1 was effectively silenced, the transcriptional activity was drastically decreased, resulting in few to almost non-existent nucleoplasmic *foci* (**Figure 5C**). Quantification analysis of the FUrd incorporation curve slopes

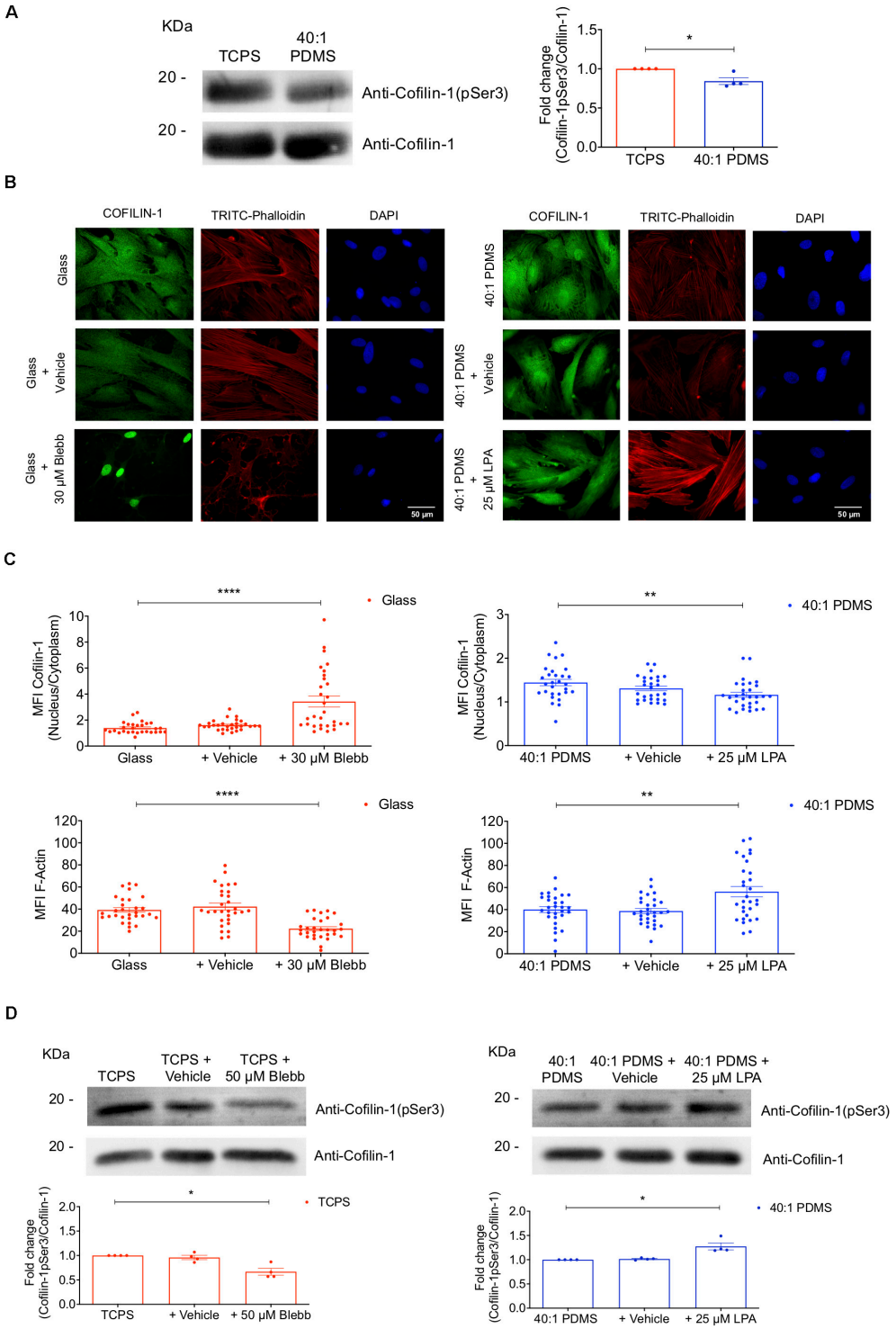

FIGURE 4 | Substrate stiffness and soluble modulators of actomyosin influence Cofilin-1 subcellular localisation and phosphorylation state. **(A)** Cofilin-1 and phospho-Cofilin-1 (pSer3) levels were evaluated by western blot analysis of whole-cell protein extracts separated by SDS-PAGE (left) obtained from cells cultured on TCPS or 40:1 PDMS between P2 and P4. For the quantification (right) values were normalised by the respective total Cofilin-1 protein level in TCPS or PDMS for each independent experiment. Bars represent the mean of the ratio of Cofilin-1 (pSer3)/total Cofilin-1 ± SEM of four independent experiments. Statistical analysis was performed using One-Sample *t*-test (theoretical mean of 1.0) with significant differences indicated as $^{*}p < 0.05$. **(B)** Representative fluorescence microscopy images and **(C)** respective MFI quantification of Cofilin-1 nucleus/cytoplasm ratio and F-actin (TRITC-Phalloidin) for cells cultured on glass coverslips or 40:1 PDMS after treatment or not with Blebbistatin or LPA (as indicated). Cells seeded on stiff glass coverslips (left) were cultured for 24 h and then incubated or not with

(Continued)

FIGURE 4 | Continued
Blebbistatin (30 μM) for an additional 24 h; cells seeded on soft 40:1 PDMS (right) were cultured for 46 h and then incubated or not with LPA (25 μM) for an additional 2 h. In both cases, cells were fixed after 48 h in culture and stained with anti-Cofilin-1 antibody (green), TRITC-Phalloidin for F-actin (red) and DAPI for nuclear counterstaining (blue). Bars represent mean ± SEM of cells analysed from three independent experiments. Statistical analysis was performed using One-Way ANOVA followed by Dunnett's multiple comparisons test between all conditions (**$p < 0.01$; ****$p < 0.0001$). **(D)** Western blot analyses were performed to detect Cofilin-1 and phospho-Cofilin-1 (pSer3) as described in **(A)**, using whole-cell extracts obtained from cells cultured on stiff TCPS and treated or not with Blebbistatin or cultured on soft 40:1 PDMS and treated or not with LPA (as indicated), with seeding and treatment regimens similar to those described in **(B,C)**. For the quantification (bottom) values were normalised by the respective total Cofilin-1 protein level in TCPS (left) or PDMS (right) for each independent experiment. Bars represent the mean of the ratio of Cofilin-1 (pSer3)/total Cofilin-1 ± SEM of four independent experiments. Statistical analysis was performed using One-Sample *t*-test (theoretical mean of 1.0) with significant differences indicated as *$p < 0.05$.

revealed that the transcriptional activity in untreated cells cultured on soft substrates (40:1 PDMS) was not significantly different from those treated with scrambled siRNA, but was statistically higher than in hUCM-MSCs in which Cofilin-1 was effectively silenced (siRNA Cofilin-1), as well as in cells left untreated but maintained on a stiff substrate (glass), which were used as a control (**Figure 5D**). Hence, data indicate that soft substrate-induced increase of transcriptional activity observed in hUCM-MSCs is, at least in part, dependent on Cofilin-1.

RNA Polymerase II Transcription Elongation Is Faster in Cells Cultured on Soft PDMS Substrates

To understand if the enhanced transcriptional activity measured in cells cultured on soft versus stiff substrates was at least in part due to faster RNA polymerase II transcription elongation, the mechanism in which Cofilin-1 is described to be involved in (reviewed by Percipalle, 2013), we performed FLIP assays. To that end, we used human fibroblasts engineered with GFP-RNA polymerase II (MRC-5 cells) (Steurer et al., 2018) cultured for 3 days on stiff glass or soft 1.5 kPa PDMS. This was the time required to verify Cofilin-1 nuclear distribution (**Supplementary Figure S9A**) similar to that observed in hUCM-MSCs on a soft substrate, hence demonstrating that MRC-5 cells were mechanoresponsive. Additionally, similar to hUCM-MSCs, Cofilin-1 in MRC-5 cells also responded to soluble modulators of actomyosin contractility (**Supplementary Figure S9B**), with a significant increase or decrease of the ratio of nuclear/cytosolic Cofilin-1 in cells treated with Blebbistatin or LPA (respectively). Regarding FLIP, data show a faster decay of fluorescence in cells cultured on soft PDMS when compared with those cultured on stiff conditions, indicating that the transcriptional elongation is faster on soft substrates (**Figure 6A**). By quantifying the fluorescence decay in single cells as a function of time during the FLIP assay allowed the creation of three-phase exponential decay curves (**Figure 6B**). By analysing curves parameters attributed to the elongation phase — half-life slow (Das Neves et al., 2010; Lima et al., 2018; Steurer et al., 2018) —, the elongation half-life time of RNA polymerase II in cells cultured on the soft substrate was significantly lower than that in cells maintained on stiff conditions (**Figure 6C**). This indicates that RNA polymerase II transcription elongation speed is higher in cells maintained on soft than on stiff substrates.

The overall results indicate that the increased presence of Cofilin-1 in the nucleus of mechanosensitive cells in response to soft substrates facilitates transcription, through a mechanism that is consistent with enhanced RNA polymerase II transcription elongation speed.

DISCUSSION

This study explores the effects of substrate stiffness in the proteome of proliferating undifferentiated hUCM-MSCs. *In vitro* expansion of MSCs has been associated with the loss of cell potency due to extensive proliferation, which is required for example, to obtain a clinically relevant number of cells for therapeutic purposes (reviewed in Hoch and Leach, 2014; Müller et al., 2015; Galipeau et al., 2016). Recently, there is growing evidence suggesting that such loss of potency may at least in part be related to the mechanical properties of standard cell-culture substrates (Lee et al., 2014; Yang et al., 2014; Kusuma et al., 2017), like TCPS, much stiffer than most tissues present in biological systems.

MSCs are well known for being highly mechanosensitive cells, scaling intracellular contractility according to the stiffness of the surrounding environment (Fu et al., 2010; Swift et al., 2013; Gerardo et al., 2019), which greatly affects their differentiation potential toward distinct lineages (Engler et al., 2006; Fu et al., 2010; Gao et al., 2010), as well as reprogramming into iPSCs (as previously shown by our laboratory (Gerardo et al., 2019). However, the impact of mechanical cues and in particular of substrate stiffness in proliferating undifferentiated MSCs is still largely unknown.

Our results demonstrate that the proteome of hUCM-MSCs presents differences between cells cultured (at least between P2 and P4) on stiff TCPS (standard cell culture conditions) or on soft PDMS substrates. A putative limitation is that the TCPS used for the proteomics approach was not coated with the ECM proteins used on the PDMS substrate, although the glass coverslips used for subsequent experiments were treated in a way similar to the elastomeric surface. In this study, we focussed our attention on proteins that could be identified in both cell culture conditions, but whose relative abundance was significantly different. Among such proteins, many are involved in the regulation and modulation of the actin cytoskeleton, hence being putative good candidates to be involved in mechanotransduction mechanisms. Within this group, Filamin-A/B, Lamin-A/C and Actin were found to be more abundantly present in TCPS in comparison with PDMS. To our knowledge, Filamin-A/B and Actin were not previously reported to change their levels in

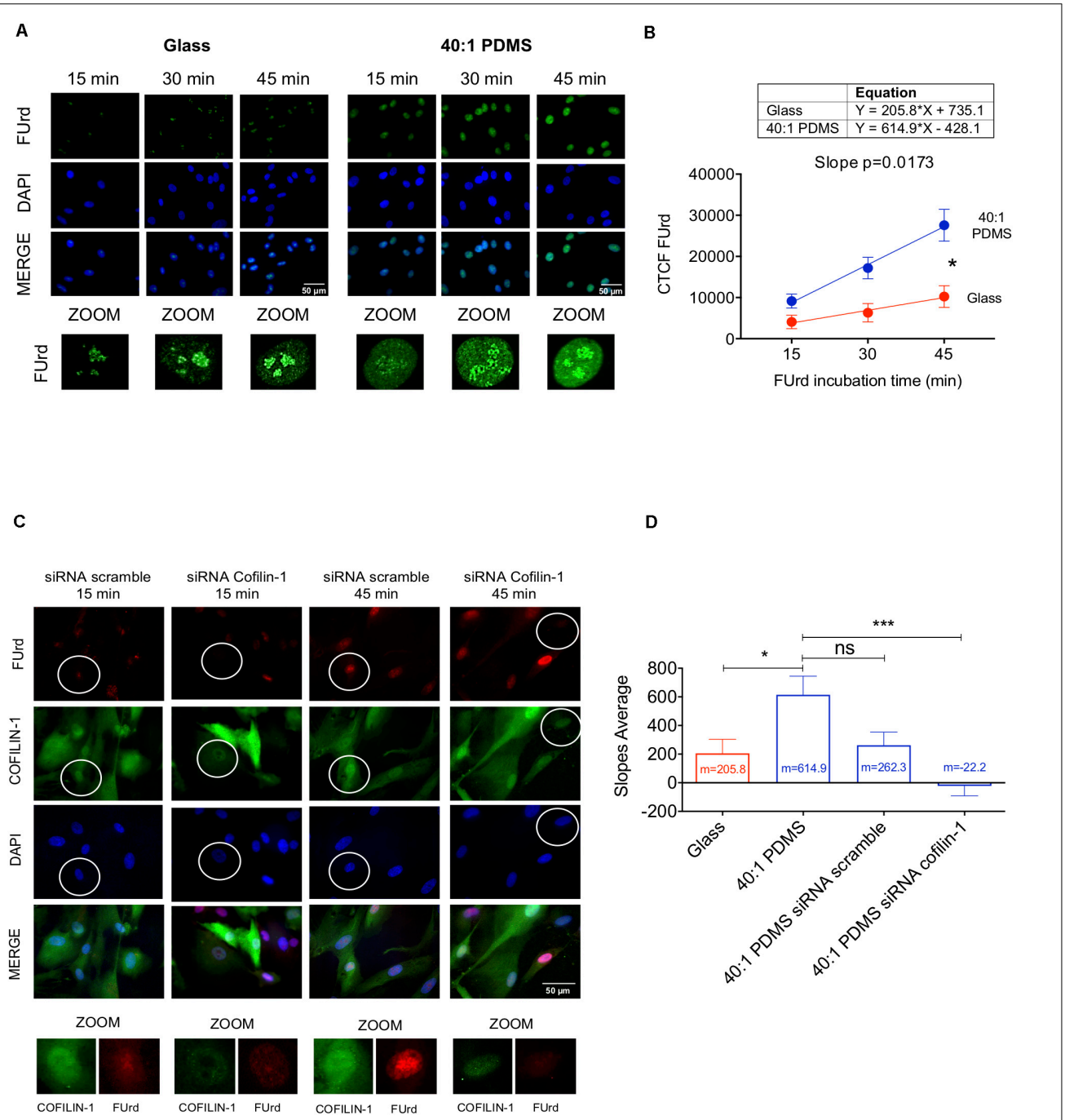

FIGURE 5 | Soft substrates induce overall increased transcription in hUCM-MSCs in a Cofilin-1-dependent manner. **(A)** Representative fluorescence microscopy images of the nuclei of cells cultured on glass coverslips or 40:1 PDMS. After 48 h in culture, hUCM-MSCs were incubated with FUrd during 15, 30, and 45 min, fixed and stained with an anti-BrdU antibody that recognises FUrd (green) to identify the new transcripts and nuclei were counterstained with DAPI (blue). **(B)** Linear regression of FUrd nuclear incorporation (CTCF, corrected total cell fluorescence) as a function of time occurring in cells on each substrate (data represent mean ± SEM of 6 independent experiments). Linear regression analysis (using the linear regression tools of GraphPad Prism 8) shows that the slopes of the two curves are significantly different from each other ($p = 0.0173$), indicating increased transcriptional activity in cells cultured on soft PDMS substrates (blue line) when compared with glass (red). **(C)** Representative fluorescence microscopy images of FUrd incorporation during 15 and 45 min in control and Cofilin-1 knock-down cells (using siRNA). Cells were immunostained with anti-Cofilin-1 (green) and anti-BrdU/FUrd (red) antibodies and nuclei were counterstained with DAPI (blue). **(D)** Bars represent the mean ± SEM of the slope values of FUrd incorporation (as determined in **B**) for each of the indicated conditions. Only cells effectively knocked-down for Cofilin-1 (representative images highlighted with circles) were taken into account during corrected total cell fluorescence quantification of FUrd. Statistical analysis was performed for 6 independent experiments using One-Way ANOVA followed by Dunnett's multiple comparisons test comparing all conditions against 40:1 PDMS (ns, non-significant; *$p < 0.05$; ***$p < 0.001$).

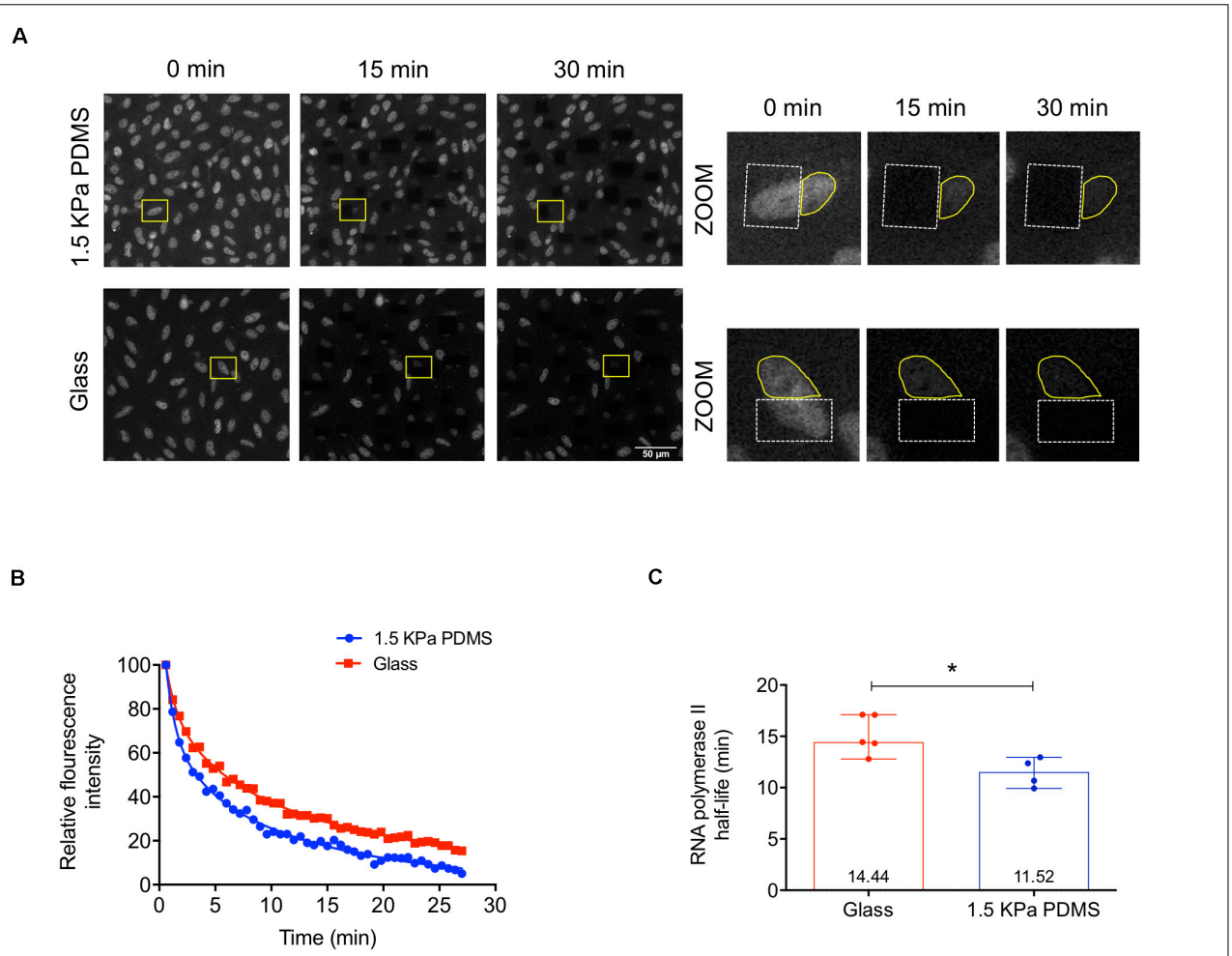

FIGURE 6 | RNA polymerase II transcription elongation is faster in cells cultured on soft PDMS substrates. **(A)** Representative confocal microscopy images of MRC-5 cells (expressing GFP-RNA polymerase II) during fluorescence loss in photobleaching (FLIP) experiments. MRC-5 cells were cultured on stiff µ-slide glass wells or soft 1.5 kPa PDMS and after 72 h in culture cells were subjected to FLIP assay. In the zoomed images on the right panel (from the highlighted regions indicated with the yellow rectangles on the left panel), the dashed white lines circumscribe the bleached areas and the solid yellow lines represent the fluorescence measurement areas. **(B)** Representative three-phase exponential decay curves of GFP-RNA polymerase II signal of two single cells cultured on each substrate (glass or PDMS). **(C)** RNA polymerase II elongation half-life time was calculated based on the half-time slow parameter of the three-phase exponential decay curves obtained from cells cultured on stiff or soft substrates. Bars represent the median with range of at least four independent experiments. For each experiment, at least 10 cells were quantified. Statistical analysis was performed using the non-parametric Mann–Whitney test, with significant differences indicated as $*p < 0.05$.

response to changes in substrate stiffness. Concerning Lamin-A, our data is in line with previous studies showing that the protein is mechanoresponsive and that its levels scale with the stiffness of the microenvironment (Swift et al., 2013; Swift and Discher, 2014; Toh et al., 2015). Similar to subunit 4 of the Arp2/3 complex (involved in the regulation of actin cytoskeleton (May, 2001), Cofilin-1 was one of the proteins whose levels increased mostly in the proteome of hUCM-MSCs cultured on soft PDMS compared to stiff TCPS substrates (as confirmed by western blot and ICC). For that reason and being Cofilin-1 an important actin-regulating protein, together with the lack of information about its role in the context of cellular mechanobiology, our studies became focussed on this protein.

ICC analysis revealed that Cofilin-1 present in hUCM-MSCS cultured on soft substrates exhibited a preferential nuclear localisation, in contrast with cells on stiff substrates, in which Cofilin-1 presented a more widespread distribution. Moreover, the phosphorylation state of Cofilin-1 [by its cognate kinase LIMK1 (Yang et al., 1998)] in hUCM-MSCs cultured in soft versus stiff substrates also changed. WB analysis showed that the ratio of Cofilin-1 (pSer3)/total Cofilin-1 in hUCM-MSCs cultured on soft substrates was significantly lower than when cultured on stiff conditions (which was also supported by the proteomics data). Our results are in line with a report showing that mechanical force applied to cells via integrins caused Rho/ROCK/LIMK-dependent phosphorylation of Cofilin-1 (Zhao et al., 2007). Moreover, as it was previously shown using Cofilin-1 Ser3 phosphorylation mutants, the non-phosphorylated mimetic (Ser3→Ala) tends to accumulate in the nucleus, while the WT is consistent

with a predominantly cytosolic localisation (Nebl et al., 1996). Taken together, our results strongly indicate that Cofilin-1 nuclear localisation increases when cells are cultured on soft substrates, and in these conditions Cofilin-1 is less phosphorylated. On the other hand, on stiff substrates, the protein presents a widespread localisation and is highly phosphorylated on Ser3 by LIMK1. Additionally, Cofilin-1 and other cytoskeletal proteins were recently identified as novel neddylation substrates, suggesting that this post-translational modification could generally modulate cytoskeletal proteins (Vogl et al., 2020). Specifically, Cofilin-1 activity seems to increase when neddylation is inhibited, at least in neurons. Interestingly, NEDD8-conjugating enzyme Ubc12, one of the pivotal proteins for neddylation, was found more abundantly present in the proteome of hUCM-MSCs cultured on the soft 40:1 PDMS substrate (as shown in the proteomics data). This observation prompts us to speculate that regulation of the cytoskeleton by mechanotransduction may involve neddylation of cytoskeletal proteins, and Cofilin-1 in particular, which should be explored in future studies.

The Cofilin-1 localisation data is also consistent with literature indicating that Cofilin-1 is not able to bind to actin filaments which are under tension and/or populated by myosin (Ngo et al., 2016), which would be expected to occur in cells cultured on stiff substrates. We can speculate that, if Cofilin-1 is not able to bind to and depolymerise F-actin filaments into G-actin, the protein should not be able to migrate to the nucleus, since both Cofilin-1 and G-actin seem to migrate together with importin-9 (Pendleton et al., 2003; Dopie et al., 2012).

Knowing that Blebbistatin inhibits NMM-II, promoting the relaxation of the actin cytoskeleton (Engler et al., 2006; Lourenco et al., 2016), and that LPA induces intracellular contractility by activating RhoA and consequently favouring NMM-II activity (Sun et al., 2014), we sought to promote changes in the intracellular tension of hUCM-MSCs to further study the role of Cofilin-1 in mechanotransduction. Hence, by mimicking soft conditions on stiff substrates, and vice versa, using an inhibitor or a stimulator of actomyosin contractility (Blebbistatin or LPA, respectively), we confirmed that hUCM-MSCs respond to these modulators with a significant increase of the nuclear/cytosolic ratio of Cofilin-1 in response to Blebbistatin and a significant decrease in cells incubated with LPA. Moreover, the phosphorylation of Cofilin-1 on Ser3 decreased upon incubation with Blebbistatin and increased in response to LPA. Hence, Cofilin-1 seems to change in terms of intracellular localisation and phosphorylation state in response to low (Blebbistatin or soft substrates) or high (LPA or stiff matrices) intracellular contractility, reinforcing its role as a mechanotransduction player.

It has been reported that Cofilin-1 dephosphorylated on Ser3 is the active form of the protein, becoming capable to severe and depolymerise F-actin (Wioland et al., 2017). As a consequence of F-actin severing or depolymerisation activity, Cofilin-1 remains bound to G-actin, forming a complex that is imported into the nucleus (Dopie et al., 2012; Percipalle, 2013). Hence, our results regarding the increased nuclear presence of Cofilin-1 and its lower phosphorylation on Ser3 (in cells cultured on soft substrates or treated with Blebbistatin) are consistent with the abovementioned literature.

Moreover, our results indicate that soft substrates induce an increase of hUCM-MSCs overall transcriptional activity. In the nucleus, Cofilin-1 (in association with G-actin) was reported to be required for RNA polymerase II transcription elongation (Obrdlik and Percipalle, 2011; Percipalle, 2013). In fact, as a consequence of Cofilin-1 gene silencing, we observed a global decrease of transcription in cells cultured on soft substrates with few to almost non-existent nucleoplasmic foci (which are associated with RNA polymerase II activity) (Szentirmay and Sawadogo, 2000). By performing FLIP assays, we observed that the half-life elongation time of RNA polymerase II was significantly lower in mechanoresponsive fibroblasts (MRC-5 cells expressing GFP-RNA polymerase II) cultured on soft when compared with those cultured on a stiff substrate. This result indicates a higher RNA polymerase II transcription elongation speed in cells cultured on soft comparing to stiff substrates. Therefore, our findings strongly suggest that in soft conditions Cofilin-1 localises preferentially in the nucleus, facilitating transcription through the enhancement of RNA polymerase II transcription elongation.

Overall, our data indicate that Cofilin-1 is a central player of a newly identified mechanism coupling mechanotransduction and regulation of transcription, opening a new avenue for future studies in this field. Other mechanisms involved in the regulation of transcription in response to mechanotransduction stimuli have been reported. Some involve mechanosensitive transcription factors (Mammoto et al., 2012), like YAP/TAZ (Dupont et al., 2011; Morgan et al., 2013), Runx2 (Kanno et al., 2007) or NKX2.5 (Dingal et al., 2015). In fact, the LIMK/Cofilin-1 pathway was shown to modulate the activity of YAP/TAZ by regulating the formation of F-actin and stress fibres. Cofilin-1 depletion leads to high F-actin content and consequent increase in YAP/TAZ nuclear localisation, transcriptional activity, and cell proliferation (Aragona et al., 2013). Other involve changes in nuclear architecture and modulation of chromosome territories. The existence of physical links and bi-directional force transmission between the ECM and the nucleus (namely through the protein-protein interactions existing between integrins and focal adhesion proteins, the cytoskeleton, the LINC complex and the nucleoskeleton) (Jaalouk and Lammerding, 2009; Wang et al., 2009; Yu et al., 2009) influence the nuclear architecture and in turn modulate the genome's organisation and gene expression (Wang et al., 2009; Shivashankar, 2011, 2019). Another example is a group of epigenetic changes occurring in response to mechanical cues, which can be generically encompassed within the concept of mechanoepigenetics (Missirlis, 2016). Some of the best-known mechanisms concerning chromatin epigenetic modifications in response to mechanical stimuli involve changes in histone acetylation and/or methylation (Downing et al., 2013; Hernandez et al., 2016; Roy et al., 2018; Gerardo et al., 2019), although many of the detailed mechanisms involved remain elusive.

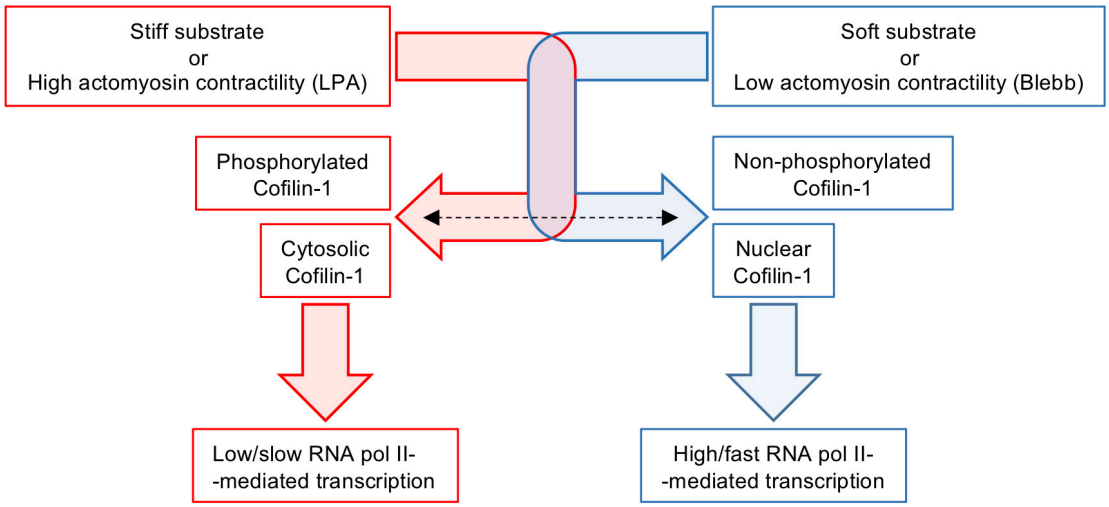

FIGURE 7 | Schematics illustrating the modulation of Cofilin-1 by substrates stiffness or soluble factors affecting intracellular contractility. Stiff substrates or actomyosin tension induced by LPA favour elevated levels of F-actin, Cofilin-1 phosphorylation and Cofilin-1 adopts a mainly cytosolic localisation. On the other hand, soft substrates or low actomyosin tension caused by treatment with Blebbistatin induce low amounts of F-actin, no Cofilin-1 phosphorylation and Cofilin-1 adopts a nuclear localisation. The presence of Cofilin-1 in the nucleus is consistent with enhanced/faster RNA polymerase II-dependent transcription.

We showed that the proteome of proliferating and undifferentiated hUCM-MSCs changes depending on the stiffness of the extracellular environment. As a consequence of such finding, we identified and characterised Cofilin-1 as a new mechanotransduction player that responds (in terms of abundance, intracellular localisation and phosphorylation/activation state) to changes in the extracellular stiffness and intracellular contractility, playing a significant role in transcription mediated by RNA polymerase II (**Figure 7**). This study contributes with new fundamental knowledge in cell biology and in particular in the field of cellular mechanobiology, further establishing hUCM-MSCs as being highly mechanosensitive. It also shows that substrate stiffness is a highly relevant aspect for the expansion of this cell type *in vitro*, with impact in both research and clinical settings.

DATA AVAILABILITY STATEMENT

The datasets presented in this study can be found in online repositories. The names of the repository/repositories and accession number(s) can be found below: http://www.proteomexchange.org/, PXD017674.

ETHICS STATEMENT

The studies involving human participants were reviewed and approved by the Ethics Committee of the Faculty of Medicine, University of Coimbra, Portugal (ref. CE-075/2019). Written informed consent to participate in this study was provided by the participants' legal guardian/next of kin.

AUTHOR CONTRIBUTIONS

CD contributed to the design of the project, performed most of the experiments and data analysis, and prepared the manuscript. AG performed the MSC proliferation experiments and mass spectrometry experiments. SA performed the mass spectrometry experiments, proteomics data analysis and interpretation. AM and CA performed the FLIP experiments. IC and JL-S performed the rheological characterisation of PDMS substrates. JL-S contributed with the interpretation of the data. AP performed the immunophenotypic characterisation of hUCM-MSCs and data interpretation. JC contributed with the design and interpretation of the data. RP designed and performed the FLIP experiments and contributed to transcription-related data analysis and interpretation. BM contributed with the interpretation of the mass spectrometry proteomics data and with financial support. MG conceived and designed the project, interpreted the data, prepared the manuscript, and contributed with financial support. All the authors read and approved the final manuscript.

FUNDING

This work was supported by the European Regional Development Fund (ERDF), through the COMPETE 2020 – Operational Programme for Competitiveness and Internationalisation and Portuguese national funds via FCT – Fundação para a Ciência e a Tecnologia, I.P., under projects: POCI-01-0145-FEDER-029516 (ref.: PTDC/MED-NEU/29516/2017) to MG; POCI-01-0145-FEDER-029311 (ref.: PTDC/BTM-TEC/29311/2017) and POCI-01-0145-FEDER-016428 (ref.: SAICTPAC/0010/2015) to BM; UID/NEU/04539/2019 (CNC.IBILI strategic plan) and UIDB/04539/2020 (CIBB strategic plan). FCT is acknowledged for the Ph.D. fellowships

attributed to Catarina Domingues (SFRH/BD/115527/2016) and Inês Caramelo (SFRH/BD/143442/2019).

ACKNOWLEDGMENTS

Carla Cardoso, Sofia Couceiro, and Ana Cabeleira from Stemlab S.A. (Crioestaminal) are acknowledged for providing umbilical cord samples. Paula Laranjeira is acknowledged for assistance in flow cytometry. We are thankful to Jurgen A. Marteijn, who provided MRC-5 cells.

SUPPLEMENTARY MATERIAL

The Supplementary Material for this article can be found online at: https://www.frontiersin.org/articles/10.3389/fcell.2020.00678/full#supplementary-material

REFERENCES

Anjo, S. I., Santa, C., and Manadas, B. (2015). Short GeLC-SWATH: a fast and reliable quantitative approach for proteomic screenings. *Proteomics* 15, 757–762. doi: 10.1002/pmic.201400221

Anjo, S. I., Santa, C., Saraiva, S. C., Freitas, K., Barah, F., Carreira, B., et al. (2017). "Neuroproteomics using short GeLC-SWATH: from the evaluation of proteome changes to the clarification of protein function," in *Current Proteomic Approaches Applied to Brain Function*, eds E. Santamaría, and J. Fernández-Irigoyen (Cham: Springer), 107–138. doi: 10.1007/978-1-4939-7119-0_8

Aragona, M., Panciera, T., Manfrin, A., Giulitti, S., Michielin, F., Elvassore, N., et al. (2013). A mechanical checkpoint controls multicellular growth through YAP/TAZ regulation by actin-processing factors. *Cell* 154, 1047–1059. doi: 10.1016/j.cell.2013.07.042

Bamburg, J. R., and Bernstein, B. W. (2010). Roles of ADF/cofilin in actin polymerization and beyond. *F1000 Biol. Rep*. 2:62.

Burridge, K., and Guilluy, C. (2016). Focal adhesions, stress fibers and mechanical tension. *Exp. Cell Res.* 343, 14–20. doi: 10.1016/j.yexcr.2015.10.029

Burridge, K., Monaghan-Benson, E., and Graham, D. M. (2019). Mechanotransduction: from the cell surface to the nucleus via RhoA. *Philos. Trans. R Soc. Lond. B Biol. Sci.* 374:20180229. doi: 10.1098/rstb.2018.0229

Buxboim, A., Rajagopal, K., Brown, A. E., and Discher, D. E. (2010). How deeply cells feel: methods for thin gels. *J. Phys. Condens. Matter.* 22:194116. doi: 10.1088/0953-8984/22/19/194116

Carisey, A., Tsang, R., Greiner, A. M., Nijenhuis, N., Heath, N., Nazgiewicz, A., et al. (2013). Vinculin regulates the recruitment and release of core focal adhesion proteins in a force-dependent manner. *Curr. Biol.* 23, 271–281. doi: 10.1016/j.cub.2013.01.009

Collins, B. C., Gillet, L. C., Rosenberger, G., Rost, H. L., Vichalkovski, A., Gstaiger, M., et al. (2013). Quantifying protein interaction dynamics by SWATH mass spectrometry: application to the 14-3-3 system. *Nat. Methods* 10, 1246–1253. doi: 10.1038/nmeth.2703

Das Neves, R. P., Jones, N. S., Andreu, L., Gupta, R., Enver, T., and Iborra, F. J. (2010). Connecting variability in global transcription rate to mitochondrial variability. *PLoS Biol.* 8:e1000560. doi: 10.1371/journal.pbio.1000560

Dingal, P. C., Bradshaw, A. M., Cho, S., Raab, M., Buxboim, A., Swift, J., et al. (2015). Fractal heterogeneity in minimal matrix models of scars modulates stiff-niche stem-cell responses via nuclear exit of a mechanorepressor. *Nat. Mater.* 14, 951–960. doi: 10.1038/nmat4350

Discher, D. E., Smith, L., Cho, S., Colasurdo, M., Garcia, A. J., and Safran, S. (2017). Matrix mechanosensing: from scaling concepts in 'omics data to mechanisms in the nucleus, regeneration, and cancer. *Annu. Rev. Biophys.* 46, 295–315. doi: 10.1146/annurev-biophys-062215-011206

Dominici, M., Le Blanc, K., Mueller, I., Slaper-Cortenbach, I., Marini, F., Krause, D., et al. (2006). Minimal criteria for defining multipotent mesenchymal stromal cells. The international society for cellular therapy position statement. *Cytotherapy* 8, 315–317. doi: 10.1080/14653240600855905

Dopie, J., Skarp, K. P., Rajakyla, E. K., Tanhuanpaa, K., and Vartiainen, M. K. (2012). Active maintenance of nuclear actin by importin 9 supports transcription. *Proc. Natl. Acad. Sci. U.S.A.* 109, E544–E552.

Downing, T. L., Soto, J., Morez, C., Houssin, T., Fritz, A., Yuan, F., et al. (2013). Biophysical regulation of epigenetic state and cell reprogramming. *Nat. Mater.* 12, 1154–1162. doi: 10.1038/nmat3777

Dupont, S., Morsut, L., Aragona, M., Enzo, E., Giulitti, S., Cordenonsi, M., et al. (2011). Role of YAP/TAZ in mechanotransduction. *Nature* 474, 179–183.

Engler, A. J., Sen, S., Sweeney, H. L., and Discher, D. E. (2006). Matrix elasticity directs stem cell lineage specification. *Cell* 126, 677–689. doi: 10.1016/j.cell.2006.06.044

Fu, J., Wang, Y. K., Yang, M. T., Desai, R. A., Yu, X., Liu, Z., et al. (2010). Mechanical regulation of cell function with geometrically modulated elastomeric substrates. *Nat. Methods* 7, 733–736. doi: 10.1038/nmeth.1487

Galipeau, J., Krampera, M., Barrett, J., Dazzi, F., Deans, R. J., Debruijn, J., et al. (2016). International society for cellular therapy perspective on immune functional assays for mesenchymal stromal cells as potency release criterion for advanced phase clinical trials. *Cytotherapy* 18, 151–159. doi: 10.1016/j.jcyt.2015.11.008

Gao, L., Mcbeath, R., and Chen, C. S. (2010). Stem cell shape regulates a chondrogenic versus myogenic fate through Rac1 and N-cadherin. *Stem Cells* 28, 564–572.

Gerardo, H., Lima, A., Carvalho, J., Ramos, J. R. D., Couceiro, S., Travasso, R. D. M., et al. (2019). Soft culture substrates favor stem-like cellular phenotype and facilitate reprogramming of human mesenchymal stem/stromal cells (hMSCs) through mechanotransduction. *Sci. Rep.* 9:9086.

Green, J. J., and Elisseeff, J. H. (2016). Mimicking biological functionality with polymers for biomedical applications. *Nature* 540, 386–394. doi: 10.1038/nature21005

Gupta, M., Sarangi, B. R., Deschamps, J., Nematbakhsh, Y., Callan-Jones, A., Margadant, F., et al. (2015). Adaptive rheology and ordering of cell cytoskeleton govern matrix rigidity sensing. *Nat. Commun.* 6:7525.

Harris, A. R., Jreij, P., and Fletcher, D. A. (2018). Mechanotransduction by the actin cytoskeleton: converting mechanical stimuli into biochemical signals. *Annu. Rev. Biophys.* 47, 617–631. doi: 10.1146/annurev-biophys-070816-033547

Hernandez, M., Patzig, J., Mayoral, S. R., Costa, K. D., Chan, J. R., and Casaccia, P. (2016). Mechanostimulation promotes nuclear and epigenetic changes in oligodendrocytes. *J. Neurosci.* 36, 806–813. doi: 10.1523/jneurosci.2873-15.2016

Hoch, A. I., and Leach, J. K. (2014). Concise review: optimizing expansion of bone marrow mesenchymal stem/stromal cells for clinical applications. *Stem Cells Transl. Med.* 3, 643–652. doi: 10.5966/sctm.2013-0196

Humphries, J. D., Wang, P., Streuli, C., Geiger, B., Humphries, M. J., and Ballestrem, C. (2007). Vinculin controls focal adhesion formation by direct interactions with talin and actin. *J. Cell Biol.* 179, 1043–1057. doi: 10.1083/jcb.200703036

Jaalouk, D. E., and Lammerding, J. (2009). Mechanotransduction gone awry. *Nat. Rev. Mol. Cell Biol.* 10, 63–73. doi: 10.1038/nrm2597

Kanno, T., Takahashi, T., Tsujisawa, T., Ariyoshi, W., and Nishihara, T. (2007). Mechanical stress-mediated Runx2 activation is dependent on Ras/ERK1/2 MAPK signaling in osteoblasts. *J. Cell Biochem.* 101, 1266–1277. doi: 10.1002/jcb.21249

Kim, N., and Cho, S. G. (2013). Clinical applications of mesenchymal stem cells. *Korea. J. Intern. Med.* 28, 387–402.

Klapholz, B., and Brown, N. H. (2017). Talin - the master of integrin adhesions. *J. Cell Sci.* 130, 2435–2446. doi: 10.1242/jcs.190991

Kuddannaya, S., Chuah, Y. J., Lee, M. H., Menon, N. V., Kang, Y., and Zhang, Y. (2013). Surface chemical modification of poly(dimethylsiloxane) for the enhanced adhesion and proliferation of mesenchymal stem cells. *ACS Appl. Mater. Interf.* 5, 9777–9784. doi: 10.1021/am402903e

Kumar, A., Placone, J. K., and Engler, A. J. (2017). Understanding the extracellular forces that determine cell fate and maintenance. *Development* 144, 4261–4270. doi: 10.1242/dev.158469

Kureel, S. K., Mogha, P., Khadpekar, A., Kumar, V., Joshi, R., Das, S., et al. (2019). Soft substrate maintains proliferative and adipogenic differentiation potential of human mesenchymal stem cells on long-term expansion by delaying senescence. *Biol. Open* 8:bio039453. doi: 10.1242/bio.039453

Kusuma, G. D., Carthew, J., Lim, R., and Frith, J. E. (2017). Effect of the microenvironment on mesenchymal stem cell paracrine signaling: opportunities to engineer the therapeutic effect. *Stem Cells Dev.* 26, 617–631. doi: 10.1089/scd.2016.0349

Lee, J., Abdeen, A. A., and Kilian, K. A. (2014). Rewiring mesenchymal stem cell lineage specification by switching the biophysical microenvironment. *Sci. Rep.* 4:5188.

Leite, C., Silva, N. T., Mendes, S., Ribeiro, A., De Faria, J. P., Lourenco, T., et al. (2014). Differentiation of human umbilical cord matrix mesenchymal stem cells into neural-like progenitor cells and maturation into an oligodendroglial-like lineage. *PLoS One* 9:e111059. doi: 10.1371/journal.pbio.1000059

Lessey, E. C., Guilluy, C., and Burridge, K. (2012). From mechanical force to RhoA activation. *Biochemistry* 51, 7420–7432. doi: 10.1021/bi300758e

Lima, A. F., May, G., Diaz-Colunga, J., Pedreiro, S., Paiva, A., Ferreira, L., et al. (2018). Osmotic modulation of chromatin impacts on efficiency and kinetics of cell fate modulation. *Sci. Rep.* 8:7210.

Lourenco, T., Paes De Faria, J., Bippes, C. A., Maia, J., and Lopes-Da-Silva, J. A. (2016). Modulation of oligodendrocyte differentiation and maturation by combined biochemical and mechanical cues. *Sci. Rep.* 6:21563.

Maekawa, M., Ishizaki, T., Boku, S., Watanabe, N., Fujita, A., Iwamatsu, A., et al. (1999). Signaling from Rho to the actin cytoskeleton through protein kinases ROCK and LIM-kinase. *Science* 285, 895–898. doi: 10.1126/science.285.5429.895

Mammoto, A., Mammoto, T., and Ingber, D. E. (2012). Mechanosensitive mechanisms in transcriptional regulation. *J. Cell Sci.* 125, 3061–3073. doi: 10.1242/jcs.093005

Marjoram, R. J., Lessey, E. C., and Burridge, K. (2014). Regulation of RhoA activity by adhesion molecules and mechanotransduction. *Curr. Mol. Med.* 14, 199–208. doi: 10.2174/1566524014666140128104541

May, R. C. (2001). The Arp2/3 complex: a central regulator of the actin cytoskeleton. *Cell. Mol. Life Sci.* 58, 1607–1626. doi: 10.1007/pl00000800

Missirlis, Y. F. (2016). Mechanoepigenetics. *Front. Cell Dev. Biol.* 4:113. doi: 10.3389/fcell.2016.00113

Mizuno, K. (2013). Signaling mechanisms and functional roles of cofilin phosphorylation and dephosphorylation. *Cell Signal.* 25, 457–469. doi: 10.1016/j.cellsig.2012.11.001

Moore, S. W., Roca-Cusachs, P., and Sheetz, M. P. (2010). Stretchy proteins on stretchy substrates: the important elements of integrin-mediated rigidity sensing. *Dev. Cell* 19, 194–206. doi: 10.1016/j.devcel.2010.07.018

Morgan, J. T., Murphy, C. J., and Russell, P. (2013). What do mechanotransduction, Hippo, Wnt, and TGFbeta have in common? YAP and TAZ as key orchestrating molecules in ocular health and disease. *Exp. Eye Res.* 115, 1–12. doi: 10.1016/j.exer.2013.06.012

Munsie, L. N., Desmond, C. R., and Truant, R. (2012). Cofilin nuclear-cytoplasmic shuttling affects cofilin-actin rod formation during stress. *J. Cell Sci.* 125, 3977–3988. doi: 10.1242/jcs.097667

Müller, S., Dalgarno, K., Dickinson, A., Wang, X.-N., and Nicholson, L. (2015). Enhancing the potency of mesenchymal stem cells for tissue regeneration. *Intern. J. Stem Cell Res. Ther.* 2:13.

Nebl, G., Meuer, S. C., and Samstag, Y. (1996). Dephosphorylation of serine 3 regulates nuclear translocation of cofilin. *J. Biol. Chem.* 271, 26276–26280. doi: 10.1074/jbc.271.42.26276

Ngo, K. X., Umeki, N., Kijima, S. T., Kodera, N., Ueno, H., Furutani-Umezu, N., et al. (2016). Allosteric regulation by cooperative conformational changes of actin filaments drives mutually exclusive binding with cofilin and myosin. *Sci. Rep.* 6:35449.

Obrdlik, A., and Percipalle, P. (2011). The F-actin severing protein cofilin-1 is required for RNA polymerase II transcription elongation. *Nucleus* 2, 72–79. doi: 10.4161/nucl.14508

Ohashi, K. (2015). Roles of cofilin in development and its mechanisms of regulation. *Dev. Growth Differ.* 57, 275–290. doi: 10.1111/dgd.12213

Pendleton, A., Pope, B., Weeds, A., and Koffer, A. (2003). Latrunculin B or ATP depletion induces cofilin-dependent translocation of actin into nuclei of mast cells. *J. Biol. Chem.* 278, 14394–14400. doi: 10.1074/jbc.m206393200

Peng, T., Liu, L., Maclean, A. L., Wong, C. W., Zhao, W., and Nie, Q. (2017). A mathematical model of mechanotransduction reveals how mechanical memory regulates mesenchymal stem cell fate decisions. *BMC Syst. Biol.* 11:55. doi: 10.1186/s12918-017-0429-x

Percipalle, P. (2013). Co-transcriptional nuclear actin dynamics. *Nucleus* 4, 43–52. doi: 10.4161/nucl.22798

Pittenger, M. F., Mackay, A. M., Beck, S. C., Jaiswal, R. K., Douglas, R., Mosca, J. D., et al. (1999). Multilineage potential of adult human mesenchymal stem cells. *Science* 284, 143–147. doi: 10.1126/science.284.5411.143

Provenzano, P. P., and Keely, P. J. (2011). Mechanical signaling through the cytoskeleton regulates cell proliferation by coordinated focal adhesion and Rho GTPase signaling. *J. Cell Sci.* 124, 1195–1205. doi: 10.1242/jcs.067009

Prunier, C., Prudent, R., Kapur, R., Sadoul, K., and LafanechèRe, L. (2017). LIM kinases: cofilin and beyond. *Oncotarget* 8, 41749–41763. doi: 10.18632/oncotarget.16978

Rosales, A. M., and Anseth, K. S. (2016). The design of reversible hydrogels to capture extracellular matrix dynamics. *Nat. Rev. Mater.* 1:15012.

Roy, B., Venkatachalapathy, S., Ratna, P., Wang, Y., Jokhun, D. S., Nagarajan, M., et al. (2018). Laterally confined growth of cells induces nuclear reprogramming in the absence of exogenous biochemical factors. *Proc. Natl. Acad. Sci. U.S.A.* 115, E4741–E4750.

Shivashankar, G. V. (2011). Mechanosignaling to the cell nucleus and gene regulation. *Annu. Rev. Biophys.* 40, 361–378. doi: 10.1146/annurev-biophys-042910-155319

Shivashankar, G. V. (2019). Mechanical regulation of genome architecture and cell-fate decisions. *Curr. Opin. Cell Biol.* 56, 115–121. doi: 10.1016/j.ceb.2018.12.001

Squillaro, T., Peluso, G., and Galderisi, U. (2016). Clinical trials with mesenchymal stem cells: an update. *Cell Transpl.* 25, 829–848. doi: 10.3727/096368915x689622

Steurer, B., Janssens, R. C., Geverts, B., Geijer, M. E., Wienholz, F., Theil, A. F., et al. (2018). Live-cell analysis of endogenous GFP-RPB1 uncovers rapid turnover of initiating and promoter-paused RNA polymerase II. *Proc. Natl. Acad. Sci. U.S.A.* 115, E4368–E4376.

Sun, Y., Chen, C. S., and Fu, J. (2012). Forcing stem cells to behave: a biophysical perspective of the cellular microenvironment. *Annu. Rev. Biophys.* 41, 519–542. doi: 10.1146/annurev-biophys-042910-155306

Sun, Y., Yong, K. M., Villa-Diaz, L. G., Zhang, X., Chen, W., Philson, R., et al. (2014). Hippo/YAP-mediated rigidity-dependent motor neuron differentiation of human pluripotent stem cells. *Nat. Mater.* 13, 599–604. doi: 10.1038/nmat3945

Swift, J., and Discher, D. E. (2014). The nuclear lamina is mechano-responsive to ECM elasticity in mature tissue. *J. Cell Sci.* 127, 3005–3015. doi: 10.1242/jcs.149203

Swift, J., Ivanovska, I. L., Buxboim, A., Harada, T., Dingal, P. C., Pinter, J., et al. (2013). Nuclear lamin-A scales with tissue stiffness and enhances matrix-directed differentiation. *Science* 341:1240104. doi: 10.1126/science.1240104

Szentirmay, M. N., and Sawadogo, M. L. (2000). Spatial organization of RNA polymerase II transcription in the nucleus. *Nucleic Acids Res.* 28, 2019–2025. doi: 10.1093/nar/28.10.2019

Thievessen, I., Thompson, P. M., Berlemont, S., Plevock, K. M., Plotnikov, S. V., Zemljic-Harpf, A., et al. (2013). Vinculin-actin interaction couples actin retrograde flow to focal adhesions, but is dispensable for focal adhesion growth. *J. Cell Biol.* 202, 163–177. doi: 10.1083/jcb.201303129

Toh, K. C., Ramdas, N. M., and Shivashankar, G. V. (2015). Actin cytoskeleton differentially alters the dynamics of lamin A, HP1alpha and H2B core histone proteins to remodel chromatin condensation state in living cells. *Integr. Biol.* 7, 1309–1317. doi: 10.1039/c5ib00027k

Trichet, L., Le Digabel, J., Hawkins, R. J., Vedula, S. R., Gupta, M., Ribrault, C., et al. (2012). Evidence of a large-scale mechanosensing mechanism for cellular adaptation to substrate stiffness. *Proc. Natl. Acad. Sci. U.S.A.* 109, 6933–6938. doi: 10.1073/pnas.1117810109

Uhler, C., and Shivashankar, G. V. (2017). Chromosome intermingling: mechanical hotspots for genome regulation. *Trends Cell Biol.* 27, 810–819. doi: 10.1016/j.tcb.2017.06.005

Vining, K. H., and Mooney, D. J. (2017). Mechanical forces direct stem cell behaviour in development and regeneration. *Nat. Rev. Mol. Cell. Biol.* 18, 728–742. doi: 10.1038/nrm.2017.108

Vizcaíno, J. A., Csordas, A., Del-Toro, N., Dianes, J. A., Griss, J., Lavidas, I., et al. (2016). 2016 update of the PRIDE database and its related tools. *Nucleic Acids Res.* 44, D447–D456.

Vogl, A. M., Phu, L., Becerra, R., Giusti, S. A., Verschueren, E., Hinkle, T. B., et al. (2020). Global site-specific neddylation profiling reveals that NEDDylated cofilin regulates actin dynamics. *Nat. Struct. Mol. Biol.* 27, 210–220. doi: 10.1038/s41594-019-0370-3

Wagner, W., Wein, F., Seckinger, A., Frankhauser, M., Wirkner, U., Krause, U., et al. (2005). Comparative characteristics of mesenchymal stem cells from human bone marrow, adipose tissue, and umbilical cord blood. *Exp. Hematol.* 33, 1402–1416. doi: 10.1016/j.exphem.2005.07.003

Wang, N., Tytell, J. D., and Ingber, D. E. (2009). Mechanotransduction at a distance: mechanically coupling the extracellular matrix with the nucleus. *Mol. Cell Biol.* 10, 75–82. doi: 10.1038/nrm2594

Wiggan, O., Schroder, B., Krapf, D., Bamburg, J. R., and Deluca, J. G. (2017). Cofilin regulates nuclear architecture through a myosin-II dependent mechanotransduction module. *Sci. Rep.* 7:40953.

Wioland, H., Guichard, B., Senju, Y., Myram, S., Lappalainen, P., Jegou, A., et al. (2017). ADF/cofilin accelerates actin dynamics by severing filaments and promoting their depolymerization at both ends. *Curr. Biol.* 27, 1956–1967.

Yang, C., Tibbitt, M. W., Basta, L., and Anseth, K. S. (2014). Mechanical memory and dosing influence stem cell fate. *Nat. Mater.* 13, 645–652. doi: 10.1038/nmat3889

Yang, N., Higuchi, O., Ohashi, K., Nagata, K., Wada, A., Kangawa, K., et al. (1998). Cofilin phosphorylation by LIM-kinase 1 and its role in Rac-mediated actin reorganization. *Lett. Nat.* 393, 809–812. doi: 10.1038/31735

Yu, L., Li, C. M., Liu, Y., Gao, J., Wang, W., and Gan, Y. (2009). Flow-through functionalized PDMS microfluidic channels with dextran derivative for ELISAs. *Lab. Chip* 9, 1243–1247.

Zhao, X. H., Laschinger, C., Arora, P., Szaszi, K., Kapus, A., and Mcculloch, C. A. (2007). Force activates smooth muscle alpha-actin promoter activity through the Rho signaling pathway. *J. Cell Sci.* 120, 1801–1809. doi: 10.1242/jcs.001586

Conflict of Interest: The authors declare that the research was conducted in the absence of any commercial or financial relationships that could be construed as a potential conflict of interest.

Copyright © 2020 Domingues, Geraldo, Anjo, Matos, Almeida, Caramelo, Lopes-da-Silva, Paiva, Carvalho, Pires das Neves, Manadas and Grãos. This is an open-access article distributed under the terms of the Creative Commons Attribution License (CC BY). The use, distribution or reproduction in other forums is permitted, provided the original author(s) and the copyright owner(s) are credited and that the original publication in this journal is cited, in accordance with accepted academic practice. No use, distribution or reproduction is permitted which does not comply with these terms.

frontiers in Cell and Developmental Biology

MINI REVIEW
published: 14 February 2020
doi: 10.3389/fcell.2020.00070

Emerging Methods for Enhancing Pluripotent Stem Cell Expansion

*Sarah W. Chan[1‡], Muhammad Rizwan[1†‡] and Evelyn K. F. Yim[1,2,3]**

[1] Department of Chemical Engineering, Faculty of Engineering, University of Waterloo, Waterloo, ON, Canada, [2] Waterloo Institute for Nanotechnology, University of Waterloo, Waterloo, ON, Canada, [3] Centre for Biotechnology and Bioengineering, University of Waterloo, Waterloo, ON, Canada

Pluripotent stem cells (PSCs) have great potential to revolutionize the fields of tissue engineering and regenerative medicine as well as stem cell therapeutics. However, the end goal of using PSCs for therapeutic use remains distant due to limitations in current PSC production. Conventional methods for PSC expansion have limited potential to be scaled up to produce the number of cells required for the end-goal of therapeutic use due to xenogenic components, high cost or low efficiency. In this mini review, we explore novel methods and emerging technologies of improving PSC expansion: the use of the two-dimensional mechanobiological strategies of topography and stiffness and the use of three-dimensional (3D) expansion methods including encapsulation, microcarrier-based culture, and suspension culture. Additionally, we discuss the limitations of conventional PSC expansion methods as well as the challenges in implementing non-conventional methods.

Keywords: pluripotent stem cell culture, mechanobiology, three-dimension (3D) culture methods, topography, stiffness, encapsulation, microcarriers, suspension

OPEN ACCESS

Edited by:
Selwin K. Wu,
National University of Singapore, Singapore

Reviewed by:
David Schaffer,
University of California, Berkeley, United States
Yang Xiao,
Columbia University, United States

***Correspondence:**
Evelyn K. F. Yim
eyim@uwaterloo.ca

†Present address:
Muhammad Rizwan,
Donnelly Center for Cellular & Biomolecular Research, University of Toronto, Toronto, ON, Canada

‡*These authors have contributed equally to this work*

Specialty section:
This article was submitted to Cell Adhesion and Migration, a section of the journal Frontiers in Cell and Developmental Biology

Received: *31 October 2019*
Accepted: *27 January 2020*
Published: *14 February 2020*

Citation:
Chan SW, Rizwan M and Yim EKF (2020) Emerging Methods for Enhancing Pluripotent Stem Cell Expansion. Front. Cell Dev. Biol. 8:70. doi: 10.3389/fcell.2020.00070

INTRODUCTION

Pluripotent stem cells (PSCs), including embryonic and induced pluripotent stem cells (ESCs and iPSCs, respectively), are unique for their unlimited self-renewal and ability to differentiate into any cell of the three germ layers. These potentials could revolutionize the fields of disease modeling and regenerative medicine. Conventional PSC expansion methods, including feeder layers and the addition of growth factors to feeder-free culture, have been shown to maintain the undifferentiated state of PSCs efficiently. However, using feeder layers to expand human PSCs (hPSCs) is limited by concerns of transmission of animal pathogens and immunogens for clinical applications (Villa-Diaz et al., 2013) and are laborious to work with, having to culture two types of cells. Additionally, both methods can be irreproducible due to the poorly defined xenogenic culture conditions. Although xeno-free and defined media for hPSC expansion (Chen G. et al., 2011; Baghbaderani et al., 2016; Yasuda et al., 2018) are available, such media are expensive to scale-up for clinical use (Chen et al., 2014). Thus, much research has gone into novel methods that can improve hPSC expansion such as using mechanobiological principles, including surface topography, stiffness and surface modification. Mechanobiological principles have shown promises in reducing or replacing the need for biochemical growth factors in PSC culture (Ireland and Simmons, 2015; Argentati et al., 2019). For example, the transforming growth factor-beta (TGF-β) pathway, which is essential to maintaining hPSC pluripotency (James et al., 2005), can be activated by mechanotransduction, eliminating the need for supplementing TGF-β (Eyckmans et al., 2011; Rys et al., 2016). Use of the synthetic PSC niche is motivated by their low cost and high availability (Brafman et al., 2010;

Fan et al., 2015). This review will focus on two types of emerging methods for improving PSC expansion: (1) two-dimensional (2D) methods that employ mechanobiological principles (e.g., topography and stiffness) and (2) three-dimensional (3D) methods of expansion including use of encapsulation, microcarriers, and suspension. **Figure 1** summarizes both conventional and emerging strategies for enhancing PSC expansion.

As the field is not yet mature, the majority of studies have used mouse models as groundwork for human PSC studies. It is noteworthy, however, that results are not necessarily consistent between the two species due to differences in pathways associated with maintenance and the state of pluripotency of the cell. Mouse ESCs (mESCs) are in the naïve state of pluripotency, in which there has been no lineage specification (Ying et al., 2008); while hPSCs are in the primed state of pluripotency after isolation from the blastocyte (Huang et al., 2012), though generation of naïve hPSCs has been recently achieved (Zimmerlin et al., 2016; Yang et al., 2017; Lipsitz et al., 2018) with much of the knowledge gained from studying mESCs. Although the overall goal for improvement of PSC expansion, we will discuss mPSC studies in addition to hPSC studies to highlight the importance of mechanobiology in regulating PSC fate as most work in mechanobiology relating to PSC expansion has been done in mouse PSCs (mPSCs). Due to the differences in pluripotency states, the numerous differences in patterns of pluripotency-associated gene expression, morphology, culture requirements, differentiation behavior and molecular profiles will determine different expansion methods for mPSCs and hPSCs (Nichols and Smith, 2009; Davidson et al., 2015). We suggest an excellent review by Davidson et al. (2015) for a comprehensive understanding of the differences and significances of mouse and human pluripotency.

CONVENTIONAL METHODS OF PSC EXPANSION

PSCs are commonly cultured using feeder layers or feeder-free systems (**Table 1**) that require the use of a biological matrix supplemented with chemical growth factors. Feeder layers consist of cells that create and maintain the stem cell niche required for expanding and maintaining the pluripotency of PSCs (Johnson et al., 2008). Feeder cells provide the biochemical factors required by PSCs for self-renewal and proliferation, along with biophysical cues, including topography and stiffness (López-Fagundo et al., 2016). We suggest a comprehensive review on feeder layers by Llames et al. (2015).

The other conventional methods of culturing PSCs involve using ECM components with cell culture media supplemented with growth factors that regulate genes related to pluripotency (Srinivasan et al., 2016) – either to up-regulate promoters of pluripotency or down-regulate inhibitors of pluripotency. The growth factors used depend on the pathways to be regulated, which depend on the cell type. For example, mPSC culture depends on growth factors such as leukemia inhibitory factor (LIF) (Smith et al., 1988; Williams et al., 1988) to maintain pluripotency, while hPSC maintenance depends on fibroblast growth factor 2 (FGF2) (Dvorak et al., 2006) and Activin A (Beattie et al., 2005). Despite containing animal-derived products (bovine serum albumin), the most commonly used feeder-free media for hPSC expansion is mTeSR media and is typically used with the animal-derived Matrigel coating.

Xeno-free and chemically defined systems have been developed for PSC expansion. However, their high cost limits its use in large-scale production of PSCs (Chen G. et al., 2011). The most basic xeno-free medium for hPSC expansion is Essential 8 (E8). These media are used with a vitronectin coated culture vessel to make the expansion system completely defined and xeno-free. However, E8's use in hPSC expansion is limited due to inconsistencies and slower growth rates (Hey et al., 2018). Therefore, it is worth exploring the use of physical and mechanical cues in PSC maintenance and expansion, which could improve the large-scale xeno-free expansion. We recommend a book chapter (Srinivasan et al., 2016) for a comprehensive review of conventional hPSC expansion, a review by Dakhore et al. (2018) that compares hPSC expansion media, and a review by Hayashi and Furue (2016) that summarizes substrates used in hPSC expansion.

NON-CONVENTIONAL METHODS OF PSC EXPANSION

Due to the limitations of conventional methods PSC expansion, new expansion methods that improve PSC expansion are needed to make progress toward therapeutic use of PSCs. Additionally, these non-conventional methods aim to improve efficiency, reproducibility and cost. For clinical use, current Good Manufacturing Practice (GMP) is an important aspect to consider. However, most mechanobiological studies of PSC expansion have not covered this area yet. We recommend the recent review by Bedford et al. (2018) for a comprehensive review of cGMP for cell therapy and the review by De Sousa et al. (2016), which reviews cGMP in hPSC expansion specifically.

Two-Dimensional (2D) Non-conventional Methods

2D methods focus on surface and materials properties of the expansion substrate, which can scale-out expansion in 2D and be implemented into a 3D culture for scaling up expansion. The 2D mechanobiological strategies that have been studied include growth factor immobilization (Alberti et al., 2008; Sohi et al., 2018) and micropatterning with proteins (Mosiewicz et al., 2013; Hammad et al., 2016) or other ECM molecules (Meade et al., 2013), surface chemistry (Saha et al., 2011; Kimura et al., 2018), and nanomaterials including graphene (Chen G.Y. et al., 2012) and carbon nanotubes (Akasaka et al., 2011; Pryzhkova et al., 2014). However, we will only discuss topographical cues and stiffness in this review.

Topographical Cues for PSC Expansion

Topography plays a key role in determining PSC fate (Ankam et al., 2013, 2015, 2018; Chan et al., 2013), including

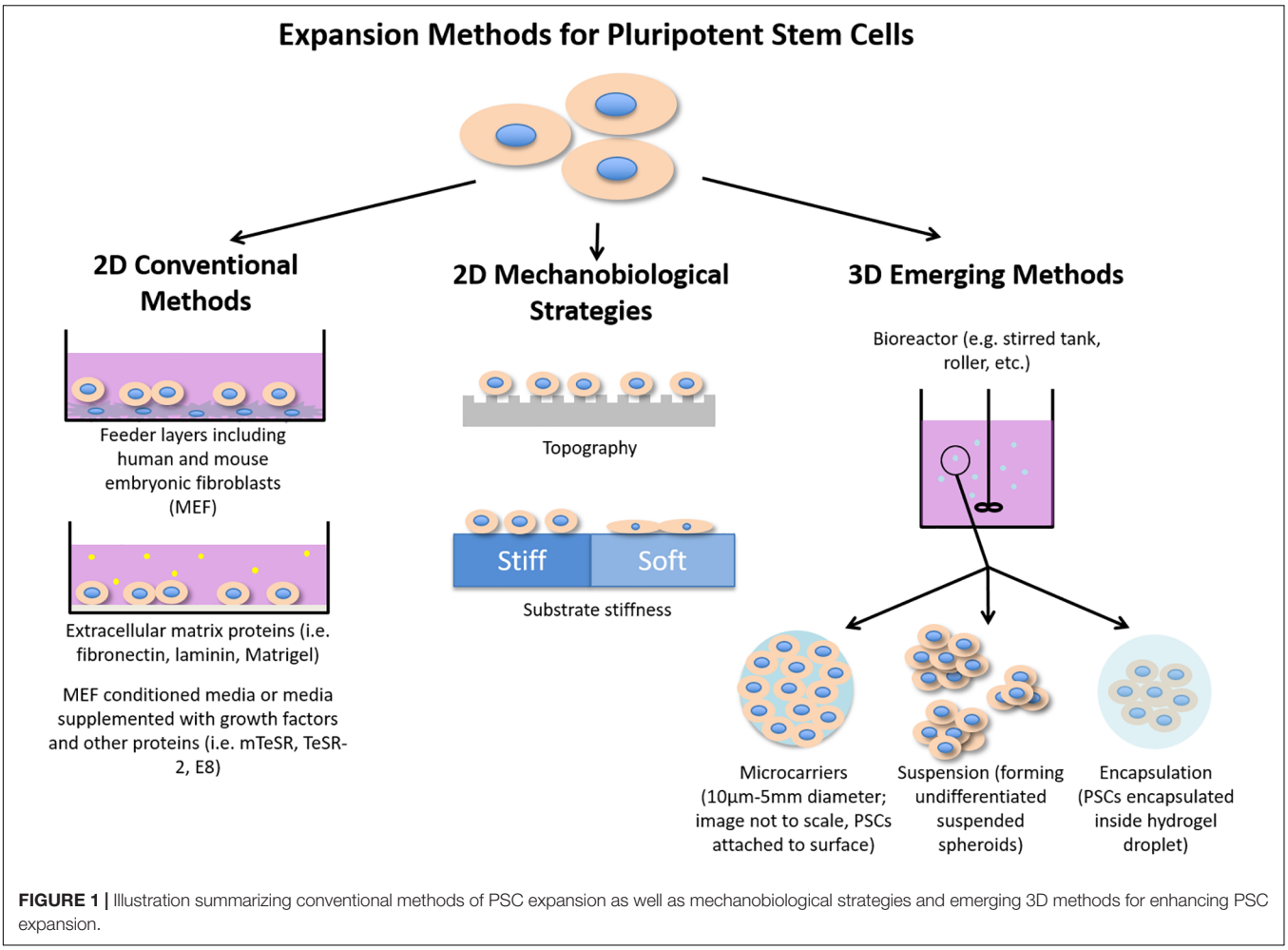

FIGURE 1 | Illustration summarizing conventional methods of PSC expansion as well as mechanobiological strategies and emerging 3D methods for enhancing PSC expansion.

maintaining pluripotency and regulating self-renewal and proliferation. **Table 2** lists examples of studies of micro and nanotopographies on PSC maintenance and expansion. Studies of hPSCs suggest that smaller topographical features promote their undifferentiated state (Bae et al., 2014; Reimer et al., 2016; Ko et al., 2017). Using a TopoChip with over 1000 patterns made of tissue culture polystyrene (T), small feature size with high feature density were found to promote hPSC pluripotency best (Reimer et al., 2016). Comparatively, another study found that nano-pillars and nano-grooves of around 200 nm on polydimethylsiloxane (PDMS) promoted proliferation and maintenance of hiPSCs in feeder-free conditions (Ko et al., 2017). A study using nanopillars of 120–360 nm in diameter, found that pillars with diameters 120–170 nm retained the most pluripotency marker expression and had the least amount of colony spreading (Bae et al., 2014). Meanwhile, hESCs cultured on vitronectin-coated micro-patterns, binary colloidal crystals of 2 and 5 µm, resulted in improved maintenance of pluripotency (Wang et al., 2018), though this study did not involve nano-sized patterns. In contrast, Chen W. et al. (2012) compared hESC expansion on 150 nm rough glass surface to expansion on a smooth glass surface and found that Oct4 expression of hESCs was lower on the nanorough surface compared to the smooth surface.

While topography undoubtedly contributes significantly to PSC maintenance, a common consensus on which topographies are the most important for PSC maintenance has not been reached. Studies have implied that surface topography alone cannot maintain pluripotency (Ankam et al., 2013; Abagnale et al., 2017; Wang et al., 2018). Interestingly, in studies of mPSCs and hPSCs, it was hypothesized that topography affects focal adhesion formation, which affects colony morphology and stem cell fate. Colonies with retained pluripotency and compact, circular morphology on patterned areas showed significantly fewer focal adhesions compared to the colonies that spread out and grew in irregular shapes on flat surfaces (Jeon et al., 2012; Ji et al., 2012; Bae et al., 2014; Ko et al., 2017; Macgregor et al., 2017). Surface topography may prevent focal adhesion formation, which reduces spreading and leads to the compact, circular colonies associated with preserved pluripotency (Hashemi et al., 2011; Jeon et al., 2012; Ji et al., 2012; Kong et al., 2013; Bae et al., 2014; Ko et al., 2017). It has also been hypothesized that topography affects ECM protein adsorption, affecting the cell adhesion, proliferation

TABLE 1 | A summary of conventional methods of PSC expansion with their advantages and limitations.

Method	Description	Advantages	Limitations
Mouse embryonic fibroblast (MEF) Feeder Layer	Uses mitotically inactivated MEF cells, treated with gamma irradiation or mitomycin C (Conner, 2000), such as SNL and STO lines The most traditional method of maintaining and expanding PSC; used by Kaufman and Evans (1981) for the first mouse embryonic stem cell (mESC) culture, and then by Thomson et al. (1998) for the first human embryonic stem cell (hESC) culture as well as in Takahashi and Yamanaka (2006) for the first induced pluripotent stem cell (iPSC) culture and in Takahashi et al. (2007) and Yu et al. (2007) for the first human iPSC (hiPSC) cultures	Commonly used Inexpensive Well-documented	Xenogenic Difficult to scale up expansion into 3D Laborious Two cultures Undefined components Batch to batch variation (Amit and Itskovitz-Eldor, 2006)
Human feeder layer	Uses human cells, such as fetal fibroblasts (Richards et al., 2002), adult fallopian tube epithelial cells (Richards et al., 2002), foreskin fibroblasts (Hovatta et al., 2003; Amit et al., 2004; Yang et al., 2016), and autologous dermal fibroblasts (Takahashi et al., 2009), to create and maintain the stem cell niche by providing the biochemical growth factors and biophysical cues required for expanding and maintaining the pluripotency of PSC	Commonly used Inexpensive Well-documented Xeno-free	Cannot up-scale expansion into 3D Laborious Two cultures Chemically undefined Batch to batch variation (Amit and Itskovitz-Eldor, 2006)
MEF-conditioned media	Produced by incubating hPSC media (DMEM/F12, Knockout Serum Replacement, L-glutamine, non-essential amino acids, and β-mercaptoethanol) with MEF overnight (Tomishima, 2014) or can be purchased commercially Fibroblast growth factor 2 (FGF2) is added to the media before use	Feeder free Well-documented	Chemically undefined Xenogenic components Batch to batch variation
Essential 8 media	Used with a vitronectin coating for a defined culture Only the essential 8 factors for hPSC propagation: DMEM/F12, human insulin, human transferrin, selenium, ascorbic acid, sodium hydrogen carbonate, human recombinant FGF2, and transforming growth factor b (or NODAL) (Chen G. et al., 2011)	Xeno-free Chemically defined Feeder free Less expensive	Inconsistent and less robust than mTeSR (Hey et al., 2018) More laborious Slow growth rates Higher radical oxygen species (ROS) resulting in increased genotoxic stress (Bangalore et al., 2017)
mTeSR media	Currently the most common system used for hPSC expansion Typically used with a Matrigel ECM coating Contains bovine serum albumin	Feeder free Well-documented Easy to use Less laborious Robust and consistent	Xenogenic components Not completely defined Matrigel is undefined and may vary from batch to batch Higher radical oxygen species (ROS) resulting in increased genotoxic stress (Bangalore et al., 2017)
TeSR-2 media	Used with vitronectin or laminin 521 coatings for completely defined, xeno-free culture system	Xeno-free Feeder free Chemically defined Well-documented Easy to use Less laborious	Expensive and costly (Chen G. et al., 2011)

TABLE 2 | Summary of examples of studies of human or mouse pluripotent stem cells (hPSCs and mPSCs, respectively) on topographical features and their results.

Cell type	Feature type	Size	Substrate material and ECM coating	Media used	Characterizations performed	References
Mouse embryonic stem cell (mESC)	Hierarchically structured surfaces Hierarchically structured surfaces N/A	Micro-nano (MN) (9 μm height, 919 ± 22 nm average surface roughness) Nano (68 ± 30 nm average surface roughness) Smooth (2 ± 0.4 nm average surface roughness)	2-hydroxyethyl methacrylate-co-ethylene dimethacrylate (HEMA-EDMA) (no coating) HEMA-EDMA (no coating) HEMA-EDMA (no coating)	Leukemia inhibitory factor (LIF)-containing mESC media LIF-containing mESC media LIF-containing mESC media	Colony circularity increased in MN substrates compared to on feeder layers after 4 passages Western blot showed increased Oct4 and Nanog protein levels after 4 passages Higher percentage of OCT4 + compared to feeder layer control (Immunofluorescent (IF) imaging) Similar number of cells to feeder layer control Higher percentage of OCT4 + compared to feeder layer control (IF imaging) Fewer cells than on feeder layer control Higher percentage of OCT4 + compared to feeder layer control (IF imaging) Fewer cells than on feeder layer control	Jaggy et al., 2015
	Nanotopography	16 nm 38 nm 68 nm	Gold nanoparticles treated with allylamine, acrylic acid or octadiene and coated with fibronectin	mESC media	16 nm topography showed the lowest mean cell area; significantly less spreading and proliferation From IF imaging, all topographies maintained pluripotency gene expression (Oct4 and Nanog) after 72 h, except when treated with acrylic acid	Macgregor et al., 2017
	Roughness	Root-mean square average roughness less than 392 nm	Aminated gold nanoparticle layers	LIF-containing mESC media	Immunocytochemistry (ICC) for Oct4 showed positive in substrates with roughness less than 392 nm ICC for phalloidin and vinculin showed that nanoroughness supported focal adhesion formation while microroughness decreased focal adhesion formation MTT proliferation and viability assay showed higher proliferation rates in substrates with roughness less than 392 nm Alkaline phosphatase (ALP) activity significantly higher in substrates with roughness less than 392 nm than substrates with roughness greater than 573 nm Quantitative (q)-PCR showed no significant decrease in Oct4 expression in substrates with roughness less than 392 nm Reverse transcriptase (RT)-PCR for endoderm, mesoderm and ectoderm markers found in substrates with roughness more than 573 nm	Lyu et al., 2014
	Grooves Hexagonal Square pillar	Ridge 5 μm Ditch 15 μm Depth 5μm Ridge 5 μm side length 15 μm Depth 5μm Side length 10 μm Inter-pillar gap size 10 μm Depth 5 μm	Polyacrylamide hydrogel functionalized with collagen I	Mouse embryonic fibroblast (MEF)-conditioned media	IF images showed increased pluripotency (Nanog and Oct4) on hexagonal substrates compared to the smooth substrates Similar colony area on all substrates	Lü et al., 2014

(Continued)

TABLE 2 | Continued

Cell type	Feature type	Size	Substrate material and ECM coating	Media used	Characterizations performed	References
	Nanofibres	Fiber diameter 550–750 nm	Polyethersulfone (PES) and collagen-grafted PES (PES-COL)	LIF-containing mESC media	RT-PCR for Oct4 and Nanog significantly higher on PES and PES-COL nanofibers compared to gelatin coated plates MTT proliferation assay showed PES-COL fibers had the significantly highest proliferation though PES fibers still had significantly higher proliferation than on gelatin coated plates Immunocytochemistry (ICC) for SSEA-1 and Oct4 showed the highest expression and dome shaped morphology in cells cultured on PES-COL fibers though cells on PES fibers still had significantly higher expression than on gelatin coated plates ALP assay showed the highest percentage of ALP in cells cultured on PES-COL fibers after 7 passages though cells on PES fibers still had significantly higher expression than cells cultured on gelatin coated plates, which spontaneously differentiated after 1–2 passages	Hashemi et al., 2011
	Nanofibers	N/A	Polyamide (Ultra-Web) coated with gelatin	LIF-containing mESC media	Colony sizes and proliferation rates of undifferentiated mESC were significantly larger on Ultra-Web substrates than on glass slides Rac activity was significantly higher in mESC cultured on Ultra-Web while Rho and Cdc42 activity was unchanged; implies that Rac is essential to mESC proliferation on nanofibrous substrates mESC cultured on Ultra-Web in the presence of retinoic acid expressed GFAP and Nestin while mESC cultured on Ultra-Web without retinoic did not express GFAP and Nestin; therefore, mESC cultured on Ultra-Web retain their ability to differentiate	Nur-E-Kamal et al., 2005
	Irregular nanopatterns	7–8 nm	Polydimethyl-siloxane (PDMS) coated with poly-D-lysine (PDL)	LIF-containing mESC media	Nanopatterned PDMS coated with PDL showed cell attachment and proliferation similar to on tissue culture polystyrene (TCPS) while flat PDMS showed low cell attachment ICC and q-RT-PCR showed increased expression of Oct4, Sox2, Nanog and Klf4 in cells cultured on nanopatterned PDMS Flow cytometry showed in cells cultured on nanopatterned PDMS expressed both Oct4 and SSEA-1 Phosphorylation of FAK, Src, JNK, c-Fos, and ERK decreased in cells cultured on nanopatterned PDMS, indicating that LIF and FAK pathways modulate upregulation of self-renewal-associated proteins and the suppression of spontaneous differentiation mESC were differentiated into the three germ cell lineages; the cells cultured on nanopatterned PDMS had a higher percentage of cells differentiated, thus these cells maintained a higher quality undifferentiated state	Jeon et al., 2012
	BioSurface structure assay; 504 different microstructures of square and round pillars	Alternating square and round pillars 1 μm laterally and 2 μm gap spacing	Silicon coated with 100 nm tantalum oxide layer	mESC media with and without LIF	Circular, well-defined compact colonies Cells passaged on this pattern produced 1 chimera with 100% germ line offspring and 4 sterile males, which was similar to the cells passaged on feeder layers Colonies were positive for Oct3/4 and Nanog	Markert et al., 2009

(Continued)

TABLE 2 | Continued

Cell type	Feature type	Size	Substrate material and ECM coating	Media used	Characterizations performed	References
	Spheres	400 nm	Silica coated with collagen I	LIF-containing mESC media	Semi-quantitative PCR showed up-regulation of pluripotency markers and down-regulation of endoderm markers compared to on glass and in embryoid bodies Light interferometry showed reduced cell spreading on the silica spheres compared to on glass Scanning electron microscopy (SEM) formed rounder, more spherical colonies than on cover slips	Ji et al., 2012
Human embryonic stem cell (hESC)	Multi-architectural (MARC) chip; consists of gratings, pillars and holes	2 μm grating, 2 μm height, 2 μm spacing 2 μm grating, 120 nm height, 1 μm spacing 1 μm grating, 80 nm height, 2 μm spacing 250 nm grating, 250 nm height, 250 nm spacing 1 μm pillar, 6.5 μm pitch, 1 μm height 2 μm holes, 12 μm pitch, 2 μm height	PDMS coated with Matrigel PDMS coated with laminin	mTeSR1 medium Unconditioned hESC medium without supplements	ICC for Nanog showed maintained high levels of the pluripotency marker Nanog but low levels of Nestin ICC for Oct4 showed decreased Oct4 expression in 2 μm and 1 μm gratings, while the 250 nm gratings, 1 μm pillars and 2 μm holes had higher levels of Oct4	Ankam et al., 2013
	Binary colloidal crystals	2 μm silica particles and 0.11 μm PMMA 5 μm silica particles and 0.4 μm PMMA	Silica and polymethyl methacrylate (PMMA) with vitronectin coating	Essential 8 (E8) media	ICC showed that both surfaces of interest were positive for pluripotency markers Tra-1-60 and Oct4 Cells culture on the substrates of interest without a vitronectin coating were not maintained	Wang et al., 2018
	Nanopillars	120–360 nm with 400 nm spacing	Polystyrene (PS) coated with gelatin	hESC medium supplemented with 10 mM rho kinase (ROCK) inhibitor (removed after 2 days)	SEM images showed circular colony morphology on all pattern sizes, however, on the area with patterns 120–170 nm in size, there were less focal adhesions formed and less spreading ICC showed that patterns from 120 to 170 nm had the highest population of Oct4 + and SSEA4 + cells (93%) compared to on 170–190 nm patterns (79%) and 290–360 nm patterns (82%), though all were higher than on the flat control (53%) qPCR showed increased pluripotency marker (Oct4, Sox2, Nanog) expression in 120–290 nm sized pillar areas compared to the flat control; however, the 120–70 nm pillars had the significantly highest expression	Bae et al., 2014
	Microfiber	1.3 μm ± 0.25 μm fiber diameter	Polyurethane plasma treated with argon, hydrogen or oxygen	DEF-CS culture system (Cellectis)	ICC showed a large percentage of cells was Oct4 positive, showing retained pluripotency On randomly oriented fibers, all plasma treatments dramatically improved the expansion capability, as compared to the native fibers; increase in expansion was 7-fold for Ar fibers, 5-fold for H_2 fibers and 4-fold for O_2 fibers	Zandén et al., 2014
Human induced pluripotent stem cell (hiPSC)	Nanoroughness Smooth	Root-mean square average roughness 150 nm Root-mean square average roughness 1 nm	Glass coated with vitronectin	Human-Cell-Conditioned Medium (hCCM) with fibroblast growth factor 2 (FGF2)	hESCs adhered better to the smooth surface; a highly branched, filopodia-rich morphology of single hESCs was observed on the smooth surface compared to the more compact cells with few, short cytoplasmic extensions on the nano-rough surface using SEM	

(Continued)

TABLE 2 | Continued

Cell type	Feature type	Size	Substrate material and ECM coating	Media used	Characterizations performed	References
					Oct3/4 expression was significantly better on the smooth surface (93%) compared to the rough surface (41%) On smooth glass focal adhesions formed on the periphery of Oct3/4 + cells with less spreading while on nanorough glass the focal adhesions formed randomly throughout the colony with more spreading	Chen W. et al., 2012
	Groove-ridge structures	200 nm height with 340, 650, and 1400 nm periodicity; height ∼70 nm	PDMS or polyimide (PI) coated with vitronectin	E8	Grooves with periodicity of 650and 1400 nm resulted in significant colony elongation compared to the control qPCR showed a significant decrease in Oct4 expression in cells cultured on the PI 650 nm grooves compared to the flat PI Upon bone morphogenetic protein (BMP) 4 stimulation, YAP reveals nuclear localization at the rim, whereas it is cytoplasmic at the center of differentiating iPSC colonies TAZ (a YAP paralog) strongly co-localizes with actin filaments and cell-material adhesion sites in iPSCs	Abagnale et al., 2017
	TopoChip (2176 patterns made of circles, rectangles and triangles)	Various, 10 μm height for all	TCPS	E8 with ROCK inhibitor	100 topographies were ranked top or bottom on the basis of number of Oct4 + cells at 24 h After 4 days, the top 100 topographies supported formation of extensive colonies of undifferentiated iPSC that expressed Oct4 and Sox2 At 24 h patterns with the greatest number of cells also had the greatest number of EdU + cells and Oct4 + cells, indicating that they supported self-renewal and prevented differentiation of iPSCs Computational analysis showed that small feature size and high feature density were most important in determining pluripotency	Reimer et al., 2016
	Irregular patterned nanofeatures Grooves Pillars	< 1 μm 100 nm width, 300 nm depth, 300 nm separation 300 nm diameter, 100 nm separation	PDMS coated with PLO and fibronectin	mTeSR1 medium supplemented with 10 mM ROCK inhibitor (removed after 2 days)	a-actinin expression was significantly greater in grooves and pillars than in flat and irregularly patterned surfaces at P6 and P10 Gene and protein expression of FAK did not change during passaging, except for an increase on grooves and pillars at P6. Ki67 (cell proliferation marker) significantly increased on grooves and pillars compared to on irregular nanofeatures and smooth surfaces ICC for Nanog and Oct3/4 significantly increased on grooves and pillars compared to PSCs on irregular nanofeatures and smooth surfaces SEM images showed that cells on grooves and pillars had fewer filopedia and more globular appearance than cells on irregular nanopatterns and smooth surfaces	Ko et al., 2017
hESC and hiPSC	Nanofiber	270 nm fiber diameter, density 4.6 μg/cm^2	Gelatin	mTeSR1 medium	After 20 passages, cells grown on nanofibers continued expressed pluripotency markers Oct4, Nanog and Sox2 but not differentiation markers Pax6, Brachyury, and Afp; expression similar to cells cultured on Matrigel Flow cytometry showed high percentage of SSEA-4 + cells after being cultured on nanofibers qPCR of all genes (84) in the integrin family were analyzed; integrin expression did not change between culture conditions – both on nanofibers and on Matrigel – and had high levels of α5, α6, α7, αv, β1, and β5 and low expression of a8, which was high in cells cultured on flat gelatin *In vitro* embryoid body formation and *in vivo* teratoma formation was performed and cells cultured on the nanofibers were able to differentiate into cells of all three germ layers	Liu et al., 2014

and morphology, thus synergistically maintaining PSCs (Zandén et al., 2014; Macgregor et al., 2017).

Stiffness of Substrate on PSC Expansion

Substrate stiffness plays a significant role in controlling cellular behavior and stem cell fate. Synthetic biomaterials, including hydrogels, are useful tools for studying the effects of stiffness. Hydrogels can be modified to have different stiffness, depending on the molecular weight or concentration of polymer, and the crosslinking density (Caliari and Burdick, 2016), which depends on crosslinker concentration and crosslinking time. Polyacrylamide (PA) hydrogels (Pelham and Wang, 1997; Mih et al., 2011) and polydimethylsiloxane (PDMS) (Evans et al., 2009; Sun et al., 2012), with large tunable ranges of stiffness are examples used for studying the impact of stiffness on PSCs.

Mouse ESCs were cultured on PDMS substrates with varying stiffness and showed increased cell spreading and proliferation with increasing substrate stiffness (0.041–2.7 MPa) along with increased differentiation (Evans et al., 2009). Similarly, mESCs cultured on a stiff poly-L-lysine/hyaluronic acid (PLL/HA) hydrogel film showed increased cell adhesion and proliferation, while weak cell adhesion, and round colonies retaining pluripotency were observed on the softer PLL/HA films (Blin et al., 2010). Soft PA substrates maintained mESC pluripotency better than stiff substrates including TCPS (Chowdhury et al., 2010a). When cultured on substrates similar to mESC intrinsic stiffness (0.5–0.6 kPa), mESCs had improved self-renewal and retention of pluripotency, thus proposing stiffness matching as a method for maintaining mESCs (Chowdhury et al., 2010b). Later, mESCs cultured on PA hydrogels of varying stiffness preserved their pluripotency regardless of the surface topography, with increased Oct4 and Nanog expression on all soft substrates compared to the stiff substrates; topography only influenced pluripotency on cells cultured on stiff substrates (Lü et al., 2014).

The effects of stiffness observed in mESCs are not translated to hPSCs. There is limited consensus on the effects of stiffness, with some groups finding little to no influence of stiffness on pluripotency (Keung et al., 2012; Maldonado et al., 2015; Przybyla et al., 2016; Price et al., 2017) and others finding the opposite (Musah et al., 2012; Sun et al., 2012; Kim et al., 2018; Sung et al., 2018). Nonetheless, observations made by several groups imply that stiffer substrates are more suitable for hPSC expansion. Using PDMS with effective moduli of 1.92 kPa (soft), 14.22 kPa (medium rigid), and 1218.4 kPa (rigid), hESC cytoskeleton contractility was found to increase with matrix rigidity along with maintained pluripotency (Sun et al., 2012). Consistent with these findings, hESCs and hiPSCs, cultured on PA hydrogels functionalized with a glucosaminoglycan binding peptide, attached better and formed more spread out and robust colonies on substrates coated with and without a Matrigel coating (Musah et al., 2012). The stiffest substrates (10 kPa) were found to support hESC expansion in five different hESC lines, with high levels of YAP/TAZ nuclear localization, an indicator of pluripotency. Later studies also found that YAP/TAZ nuclear localization decreases in soft substrates (Price et al., 2017; Lee et al., 2019). Although YAP/TAZ nuclear localization decreased in soft substrates, pluripotency marker expression remained similar between soft and stiff substrates with higher proliferation in stiff substrates (Price et al., 2017). Similarly, as substrate stiffness increased, cell proliferation increased, and substrate stiffness has an inverse relationship with spontaneous differentiation (Maldonado et al., 2015). Ligand density also affects how cells respond to their substrate stiffness; with the right number of functional groups, soft materials can support hPSC attachment proliferation and self-renewal similar to that of a stiff hydrogel (Lee et al., 2019). Despite the inconclusiveness of exactly how substrate stiffness affects hPSC behavior, especially as material choice also affects pluripotency and the absolute stiffness required for PSC culture, it is clear that stiffer substrates are more suitable for hPSC expansion in contrast with softer substrates for mPSC expansion.

Three-Dimensional (3D) Methods of PSC Expansion

Recently, 3D methods of stem cell culture have gained traction due to the need for scalable stem cell expansion to obtain therapeutically relevant number of cells. 3D cell culture methods offer the opportunity to significantly scale-up the expansion of hPSCs. The 3D methods of PSC culture are divided into three categories: (i) PSC encapsulation in hydrogels, (ii) microcarrier-based 3D PSC culture, and (iii) PSC suspension culture.

A growing body of literature suggests that 3D cell culture systems recapitulate the *in vivo* microenvironment of cells that could help to improve stem cells expansion. In a landmark study of PSC encapsulation, a defined and scalable 3D cell encapsulation system in a thermo-responsive hydrogel was developed for hPSC expansion and differentiation; it also enabled efficient retrieval of the cells from the hydrogels following expansion, without using the cell dissociation enzymes (Lei and Schaffer, 2013). The cells expanded ∼80-fold in 3D culture compared to ∼9-fold expansion in 2D over 15 days. Cumulatively, 3D cell culture led to 10^{72}-fold expansion over 60 passages (Lei and Schaffer, 2013). PSCs are mechanosensitive as previously discussed; however, the role of biophysical signals and cell-matrix interactions in the context of 3D PSC expansion was not investigated. Scaffolds used for 3D expansion of PSCs should provide a balance between cell–cell contact and cell–matrix interactions (Li et al., 2012). An alginate-based hydrogel with tethered polypeptides comprising of a cell-binding sequence of E-cadherin for 3D PSC expansion has shown to improve the proliferation rate of PSCs without compromising pluripotency marker expression resulting in up to 23-fold higher expansion in HAV10 peptide conjugated gels (Banerjee et al., 2018). Matrix degradability and remodeling by encapsulated PSCs are other parameters that affect PSC fate. Encapsulated PSCs are known to remodel their environment during proliferation and differentiation (Khetan et al., 2013; Madl et al., 2017). However, the capacity of PSCs to remodel the environment and their effect on the pluripotency related markers are poorly understood. This should be studied in greater detail to design more informed and tailor-made 3D scaffolds for enhanced stem cell expansion.

Microcarrier-based systems are another method for PSC expansion, which combine 2D cell adhesion in microcarriers

with a 3D configuration of the bioreactor system to expand the area available for PSC expansion. Microcarriers act as supporting substrates for adherent cell culture with a diameter varying from 10 μm up to 5 mm (Le and Hasegawa, 2019). The major benefit of using microcarriers is their capacity to provide large surface areas for cell growth while being compatible with adherent cell culture systems. Cells can form a confluent layer around the microporous microcarrier; while in macroporous microcarriers, they are entrapped inside the pores of the microcarriers (Badenes et al., 2014). Factors including the type of materials used to fabricate the microcarriers, the shape of the microcarrier, and the type of ECM coating used for cell adhesion influence the yield and pluripotency of the PSC culture in a microcarrier system (Chen A.K.L. et al., 2011). For instance, use of matrigel coating led to up to 18-fold higher PSC expansion compared to uncoated microcarriers (Chen A.K.L. et al., 2011). Recently, dissolvable microcarriers have been developed, which allow the retrieval of cells without using enzymatic dissociation (Badenes et al., 2014; Shekaran et al., 2016; Rodrigues et al., 2019).

By leveraging the self-aggregation property of PSCs, suspension-based cell culture systems are being developed to improve yield. Such systems promote cell-cell interactions while inhibiting the cell-matrix interactions. Usually, such systems consist of single cell culture in the presence of rho kinase (ROCK) inhibitor (Olmer et al., 2010; Abbasalizadeh et al., 2012), which supports long-term PSC survival in an undifferentiated state. PSCs grow in a monoclonal fashion and form suspended spheroids of varying sizes. Microfabrication technology has been used to further improve the homogeneity of PSC colonies (Hsiao and Palecek, 2012; Hookway et al., 2016). Optimization of bioreactor hydrodynamic conditions using combinations of static and stirred culture has enabled size-controlled aggregates of hPSCs (Abbasalizadeh et al., 2012). Traditionally, the yield of hPSCs is lower compared to mPSCs in suspension bioreactor cultures (Lipsitz et al., 2018). Recently, Lipsitz et al. found that the use of naïve hPSCs, as opposed to primed hPSCs, was a critical element for enabling high-yield expansion of PSCs (Over all 25-fold expansion; up to 5.7-fold higher compared to primed hPSCs) in suspension culture (Lipsitz et al., 2018). Despite tremendous progress in suspension-based cell culture, more research is needed in maintaining the homogeneity of cell aggregates in scalable suspension culture. Additionally, cells on the surface of the suspension aggregates experience uncontrolled shear stress, which could also lead to heterogeneous cell populations, as shear stress is known to affect stem cell fate (Toh and Voldman, 2011; Vining and Mooney, 2017).

CONCLUSION AND FUTURE OUTLOOK

Conventional methods of PSC expansion have clear and significant limitations in expansion. For development of large scale, defined and xeno-free PSC expansion systems, research should look toward using approaches with mechanobiological principles and 3D strategies for enhancing cell pluripotency retention and proliferation to improve current xeno-free expansion systems. Despite great progress in these fields, studying each physical cue in isolation is difficult as they are interconnected. It is challenging to draw conclusions regarding the effects of topography and stiffness due to many variations in study parameters, while 3D culture systems have much to be optimized. Nonetheless, these non-conventional methods have shown to improve PSC yield in xeno-free systems and thus should continue to be studied. Additionally, studies suggest that mechanobiological cues used with current PSC culture methods can enhance current PSC culture methods. The knowledge obtained in organoid cultures, mechanobiology, new advances in microfabrication and stimulus-responsive materials could contribute to future development of non-conventional systems for scaling up PSC expansion and revolutionize the field of regenerative medicine.

AUTHOR CONTRIBUTIONS

Literature search was conducted by SC and MR. Manuscript writing and editing were performed by SC, MR, and EY.

FUNDING

The work was generously supported by the Natural Sciences and Engineering Research Council of Canada (NSERC) Discovery (NSERC 2016040; to MR, SC, and EY) and the University of Waterloo start-up fund (to MR, SC, and EY). In addition, SC was supported by the Ontario Graduate Scholarship.

REFERENCES

Abagnale, G., Sechi, A., Steger, M., Zhou, Q., Kuo, C. C., Aydin, G., et al. (2017). Surface topography guides morphology and spatial patterning of induced pluripotent stem cell colonies. *Stem Cell Rep.* 9, 654–666. doi: 10.1016/j.stemcr.2017.06.016

Abbasalizadeh, S., Larijani, M. R., Samadian, A., and Baharvand, H. (2012). Bioprocess development for mass production of size-controlled human pluripotent stem cell aggregates in stirred suspension bioreactor. *Tissue Eng. Part C Methods* 18, 831–851. doi: 10.1089/ten.tec.2012.0161

Akasaka, T., Yokoyama, A., Matsuoka, M., Hashimoto, T., and Watari, F. (2011). Maintenance of hemiround colonies and undifferentiated state of mouse induced pluripotent stem cells on carbon nanotube-coated dishes. *Carbon N. Y.* 49, 2287–2299. doi: 10.1016/j.carbon.2011.01.061

Alberti, K., Davey, R. E., Onishi, K., George, S., Salchert, K., Seib, F. P., et al. (2008). Functional immobilization of signaling proteins enables control of stem cell fate. *Nat. Methods* 5, 645–650. doi: 10.1038/nmeth.1222

Amit, M., and Itskovitz-Eldor, J. (2006). Feeder-free culture of human embryonic stem cells. *Methods Enzymol.* 420, 37–49. doi: 10.1016/S0076-6879(06)20003-X

Amit, M., Margulets, V., Segev, H., Shariki, K., Laevsky, I., Coleman, R., et al. (2004). Human feeder layers for human embryonic stem cells. *Biol. Reprod.* 68, 2150–2156. doi: 10.1095/biolreprod.102.012583

Ankam, S., Lim, C. K., and Yim, E. K. F. (2015). Actomyosin contractility plays a role in MAP2 expression during nanotopography-directed neuronal differentiation of human embryonic stem cells. *Biomaterials* 47, 20–28. doi: 10.1016/j.biomaterials.2015.01.003

Ankam, S., Suryana, M., Chan, L. Y., Moe, A. A. K., Teo, B. K. K., and Law, J. B. K. (2013). Substrate topography and size determine the fate of human

embryonic stem cells to neuronal or glial lineage. *Acta Biomater.* 9, 4535–4545. doi: 10.1016/j.actbio.2012.08.018

Ankam, S., Teo, B. K. K., Pohan, G., Ho, S. W. L., Lim, C. K., and Yim, E. K. F. (2018). Temporal changes in nucleus morphology, Lamin A/C and histone methylation during nanotopography-induced neuronal differentiation of stem cells. *Front. Bioeng. Biotechnol.* 6:69. doi: 10.3389/fbioe.2018.00069

Argentati, C., Morena, F., Tortorella, I., Bazzucchi, M., Porcellati, S., and Emiliani, C. (2019). Insight into mechanobiology: how stem cells feel mechanical forces and orchestrate biological functions. *Int. J. Mol. Sci.* 20:5337. doi: 10.3390/ijms20215337

Badenes, S. M., Fernandes, T. G., Rodrigues, C. A. V., Diogo, M. M., and Cabral Joaquim, M. S. (2014). "Scalable Expansion of Human-Induced Pluripotent Stem Cells in Xeno-Free Microcarriers," in *Stem Cells and Good Manufacturing Practices. Methods in Molecular Biology*, Vol. 1283, ed. K.Turksen, (New York, NY: Humana Press).

Bae, D., Moon, S. H., Park, B. G., Park, S. J., Jung, T., Kim, J. S., et al. (2014). Nanotopographical control for maintaining undifferentiated human embryonic stem cell colonies in feeder free conditions. *Biomaterials* 35, 916–928. doi: 10.1016/j.biomaterials.2013.10.031

Baghbaderani, B. A., Tian, X., Cadet, J. S., Shah, K., Walde, A., Tran, H., et al. (2016). A newly defined and xeno-free culture medium supports every-other-day medium replacement in the generation and long-term cultivation of human pluripotent stem cells. *PLoS One* 11:e0161229. doi: 10.1371/journal.pone.0161229

Banerjee, I., Kumta, P., and Richardson, T. (2018). *Peptide Conjugated Hydrogel Substrate for the Maintenance and Expansion of Human Pluripotent Stem Cells*. U.S. Patent No US 2018/0171286 A1. Washington, DC: United States Patent and Trademark Office.

Bangalore, M. P., Adhikarla, S., Mukherjee, O., and Panicker, M. M. (2017). Genotoxic effects of culture media on human pluripotent stem cells. *Sci. Rep.* 7, 1–12. doi: 10.1038/srep42222

Beattie, G. M., Lopez, A. D., Bucay, N., Hinton, A., Firpo, M. T., King, C. C., et al. (2005). Activin a maintains pluripotency of human embryonic stem cells in the absence of feeder layers. *Stem Cells* 23, 489–495.

Bedford, P., Jy, J., Collins, L., and Keizer, S. (2018). Considering cell therapy product "Good Manufacturing Practice" status. *Front. Med.* 5:118. doi: 10.3389/fmed.2018.00118

Blin, G., Lablack, N., Louis-Tisserand, M., Nicolas, C., Picart, C., and Pucéat, M. (2010). Nano-scale control of cellular environment to drive embryonic stem cells selfrenewal and fate. *Biomaterials* 31, 1742–1750. doi: 10.1016/j.biomaterials.2009.11.055

Brafman, D. A., Chang, C. W., Fernandez, A., Willert, K., Varghese, S., and Chien, S. (2010). Long-term human pluripotent stem cell self-renewal on synthetic polymer surfaces. *Biomaterials* 31, 9135–9144. doi: 10.1016/j.biomaterials.2010.08.007

Caliari, S. R., and Burdick, J. A. (2016). A practical guide to hydrogels for cell culture. *Nat. Methods* 13, 405–414. doi: 10.1038/nmeth.3839

Chan, L. Y., Birch, W. R., Yim, E. K. F., and Choo, A. B. H. (2013). Temporal application of topography to increase the rate of neural differentiation from human pluripotent stem cells. *Biomaterials* 34, 382–392. doi: 10.1016/j.biomaterials.2012.09.033

Chen, A. K. L., Chen, X., Choo, A. B. H., Reuveny, S., and Oh, S. K. W. (2011). Critical microcarrier properties affecting the expansion of undifferentiated human embryonic stem cells. *Stem Cell Res.* 7, 97–111. doi: 10.1016/j.scr.2011.04.007

Chen, G., Gulbranson, D. R., Hou, Z., Bolin, J. M., Probasco, M. D., Smuga-otto, K., et al. (2011). Chemically defined conditions for human iPS cell derivation and culture. *Nat. Methods* 8, 424–429. doi: 10.1038/nmeth.1593

Chen, G. Y., Pang, D. W. P., Hwang, S. M., Tuan, H. Y., and Hu, Y. C. (2012). A graphene-based platform for induced pluripotent stem cells culture and differentiation. *Biomaterials* 33, 418–427. doi: 10.1016/j.biomaterials.2011.09.071

Chen, K. G., Mallon, B. S., McKay, R. D. G., and Robey, P. G. (2014). Human pluripotent stem cell culture: considerations for maintenance, expansion, and therapeutics. *Cell Stem Cell* 14, 13–26. doi: 10.1016/j.stem.2013.12.005

Chen, W., Villa-Diaz, L. G., Sun, Y., Weng, S., Kim, J. K., Lam, R. H. W., et al. (2012). Nanotopography influences adhesion, spreading, and self-renewal of human embryonic stem cells. *ACS Nano* 6, 4094–4103. doi: 10.1021/nn3004923

Chowdhury, F., Li, Y., Poh, Y. C., Yokohama-Tamaki, T., Wang, N., and Tanaka, T. S. (2010a). Soft substrates promote homogeneous self-renewal of embryonic stem cells via downregulating cell-matrix tractions. *PLoS One* 5:e15655. doi: 10.1371/journal.pone.0015655

Chowdhury, F., Na, S., Li, D., Poh, Y., Tanaka, T. S., Wang, F., et al. (2010b). Cell material property dictates stress-induced spreading and differentiation in embryonic stem cells. *Nat. Mater.* 9, 82–88. doi: 10.1038/nmat2563.Cell

Conner, D. A. (2000). Mouse embryo fibroblast (MEF) feeder cell preparation. *Curr. Protoc. Mol. Biol.* 51, 23.2.1–23.2.7. doi: 10.1002/0471142727.mb2302s51

Dakhore, S., Nayer, B., and Hasegawa, K. (2018). Human pluripotent stem cell culture: current status, challenges, and advancement. *Stem Cells Int.* 2018:7396905. doi: 10.1155/2018/7396905

Davidson, K. C., Mason, E. A., and Pera, M. F. (2015). The pluripotent state in mouse and human. *Development* 142, 3090–3099. doi: 10.1242/dev.116061

De Sousa, P. A., Downie, J. M., Tye, B. J., Bruce, K., Dand, P., Dhanjal, S., et al. (2016). Development and production of good manufacturing practice grade human embryonic stem cell lines as source material for clinical application. *Stem Cell Res.* 17, 379–390. doi: 10.1016/j.scr.2016.08.011

Dvorak, P., Dvorakova, D., and Hampl, A. (2006). Fibroblast growth factor signaling in embryonic and cancer stem cells. *FEBS Lett.* 580, 2869–2874. doi: 10.1016/j.febslet.2006.01.095

Evans, N., Minelli, C., Gentleman, E., LaPointe, V., Patankar, S., Kallivretaki, M., et al. (2009). Substrate stiffness affects early differentiation events in embryonic stem cells. *Eur. Cells Mater.* 18, 1–14. doi: 10.22203/ecm.v018a01

Eyckmans, J., Boudou, T., Yu, X., and Chen, C. S. (2011). A Hitchhiker's guide to mechanobiology. *Dev. Cell* 21, 35–47.

Fan, Y., Wu, J., Ashok, P., Hsiung, M., and Tzanakakis, E. S. (2015). Production of human pluripotent stem cell therapeutics under defined xeno-free conditions: progress and challenges. *Stem Cell Rev. Rep.* 11, 96–109. doi: 10.1007/s12015-014-9544-x

Hammad, M., Rao, W., Smith, J. G. W., Anderson, D. G., Langer, R., Young, L. E., et al. (2016). Identification of polymer surface adsorbed proteins implicated in pluripotent human embryonic stem cell expansion. *Biomater. Sci.* 4, 1381–1391. doi: 10.1039/c6bm00214e

Hashemi, S. M., Soudi, S., Shabani, I., Naderi, M., and Soleimani, M. (2011). The promotion of stemness and pluripotency following feeder-free culture of embryonic stem cells on collagen-grafted 3-dimensional nanofibrous scaffold. *Biomaterials* 32, 7363–7374. doi: 10.1016/j.biomaterials.2011.06.048

Hayashi, Y., and Furue, M. K. (2016). Biological effects of culture substrates on human pluripotent stem cells. *Stem Cells Int.* 2016:5380560. doi: 10.1155/2016/5380560

Hey, C. A. B., Saltōkova, K. B., Bisgaard, H. C., and Møller, L. B. (2018). Comparison of two different culture conditions for derivation of early hiPSC. *Cell Biol. Int.* 42, 1467–1473. doi: 10.1002/cbin.10966

Hookway, T. A., Butts, J. C., Lee, E., Tang, H., and McDevitt, T. C. (2016). Aggregate formation and suspension culture of human pluripotent stem cells and differentiated progeny. *Methods* 101, 11–20. doi: 10.1016/j.ymeth.2015.11.027

Hovatta, O., Mikkola, M., Gertow, K., Strömberg, A. M., Inzunza, J., Hreinsson, J., et al. (2003). A culture system using human foreskin fibroblasts as feeder cells allows production of human embryonic stem cells. *Hum. Reprod.* 18, 1404–1409. doi: 10.1093/humrep/deg290

Hsiao, C., and Palecek, S. P. (2012). Microwell regulation of pluripotent stem cell self-renewal and differentiation. *Bionanoscience* 2, 266–276.

Huang, Y., Osorno, R., Tsakiridis, A., and Wilson, V. (2012). In Vivo differentiation potential of epiblast stem cells revealed by chimeric embryo formation. *Cell Rep.* 2, 1571–1578. doi: 10.1016/j.celrep.2012.10.022

Ireland, R. G., and Simmons, C. A. (2015). Human pluripotent stem cell mechanobiology: Manipulating the biophysical microenvironment for regenerative medicine and tissue engineering applications. *Stem Cells* 33, 3187–3196. doi: 10.1002/stem.2105

Jaggy, M., Zhang, P., Greiner, A. M., Autenrieth, T. J., Nedashkivska, V., Efremov, A. N., et al. (2015). Hierarchical micro-nano surface topography promotes long-term maintenance of undifferentiated mouse embryonic stem cells. *Nano Lett.* 15, 7146–7154. doi: 10.1021/acs.nanolett.5b03359

James, D., Levine, A. J., Besser, D., and Hemmati-Brivanlou, A. (2005). TGFβ/activin/nodal signaling is necessary for the maintenance of pluripotency in human embryonic stem cells. *Development* 132, 1273–1282. doi: 10.1242/dev.01706

Jeon, K., Oh, H. J., Lim, H., Kim, J. H., Lee, D. H., Lee, E. R., et al. (2012). Self-renewal of embryonic stem cells through culture on nanopattern polydimethylsiloxane substrate. *Biomaterials* 33, 5206–5220. doi: 10.1016/j.biomaterials.2012.04.011

Ji, L., Lapointe, V. L. S., Evans, N. D., and Stevens, M. M. (2012). Changes in embryonic stem cell colony morphology and early differentiation markers driven by colloidal crystal topographical cues. *Eur. Cells Mater.* 23, 135–146. doi: 10.22203/eCM.v023a10

Johnson, B. V., Shindo, N., Rathjen, P. D., Rathjen, J., and Keough, R. A. (2008). Understanding pluripotency – How embryonic stem cells keep their options open. *Mol. Hum. Reprod.* 14, 513–520. doi: 10.1093/molehr/gan048

Kaufman, M. H., and Evans, M. J. (1981). Establishment in culture of pluripotential cells from mouse embryos. *Nature* 292, 154–156.

Keung, A. J., Asuri, P., Kumar, S., and Schaffer, D. V. (2012). Soft microenvironments promote the early neurogenic differentiation but not self-renewal of human pluripotent stem cells. *Integr. Biol.* 4, 1049–1058. doi: 10.1039/c2ib20083j

Khetan, S., Guvendiren, M., Legant, W. R., Cohen, D. M., Chen, C. S., and Burdick, J. A. (2013). Degradation-mediated cellular traction directs stem cell fate in covalently crosslinked three-dimensional hydrogels. *Nat. Mater.* 12, 458–465. doi: 10.1038/nmat3586

Kim, I. G., Gil, C. H., Seo, J., Park, S. J., Subbiah, R., Jung, T. H., et al. (2018). Mechanotransduction of human pluripotent stem cells cultivated on tunable cell-derived extracellular matrix. *Biomaterials* 150, 100–111. doi: 10.1016/j.biomaterials.2017.10.016

Kimura, Y., Kasai, K., and Miyata, S. (2018). Feeder-free culture for mouse induced pluripotent stem cells by using UV/ozone surface-modified substrates. *Mater. Sci. Eng. C* 92, 280–286. doi: 10.1016/j.msec.2018.06.053

Ko, J.-Y., Oh, H.-J., Lee, J., and Im, G.-I. (2017). Nanotopographic influence on the in vitro behavior of induced pluripotent stem cells. *Tissue Eng. Part A* 24, 595–606. doi: 10.1089/ten.tea.2017.0144

Kong, Y. P., Tu, C. H., Donovan, P. J., and Yee, A. F. (2013). Expression of Oct4 in human embryonic stem cells is dependent on nanotopographical configuration. *Acta Biomater.* 9, 6369–6380. doi: 10.1016/j.actbio.2013.01.036

Le, M. N. T., and Hasegawa, K. (2019). Expansion culture of human pluripotent stem cells and production of cardiomyocytes. *Bioengineering* 6:48. doi: 10.3390/bioengineering6020048

Lee, S., Stanton, A. E., Tong, X., and Yang, F. (2019). Hydrogels with enhanced protein conjugation efficiency reveal stiffness-induced YAP localization in stem cells depends on biochemical cues. *Biomaterials* 202, 26–34. doi: 10.1016/j.biomaterials.2019.02.021

Lei, Y., and Schaffer, D. V. (2013). A fully defined and scalable 3D culture system for human pluripotent stem cell expansion and differentiation. *Proc. Natl. Acad. Sci. U.S.A.* 10, E5039–E5048. doi: 10.1073/pnas.1309408110

Li, L., Bennett, S. A. L., and Wang, L. (2012). Role of E-cadherin and other cell adhesion molecules in survival and differentiation of human pluripotent stem cells. *Cell Adhes. Migr.* 6, 59–70. doi: 10.4161/cam.6.1.19583

Lipsitz, Y. Y., Woodford, C., Yin, T., Hanna, J. H., and Zandstra, P. W. (2018). Modulating cell state to enhance suspension expansion of human pluripotent stem cells. *Proc. Natl. Acad. Sci. U.S.A.* 115, 6369–6374. doi: 10.1073/pnas.1714099115

Liu, L., Yoshioka, M., Nakajima, M., Ogasawara, A., Liu, J., Hasegawa, K., et al. (2014). Nanofibrous gelatin substrates for long-term expansion of human pluripotent stem cells. *Biomaterials* 35, 6259–6267. doi: 10.1016/j.biomaterials.2014.04.024

Llames, S., García-Pérez, E., Meana, Á, Larcher, F., and del Río, M. (2015). Feeder layer cell actions and applications. *Tissue Eng. Part B Rev.* 21, 345–353. doi: 10.1089/ten.teb.2014.0547

López-Fagundo, C., Livi, L. L., Ramchal, T., Darling, E. M., and Hoffman-Kim, D. (2016). A biomimetic synthetic feeder layer supports the proliferation and self-renewal of mouse embryonic stem cells. *Acta Biomater.* 39, 55–64. doi: 10.1016/j.actbio.2016.04.047

Lü, D., Luo, C., Zhang, C., Li, Z., and Long, M. (2014). Differential regulation of morphology and stemness of mouse embryonic stem cells by substrate stiffness and topography. *Biomaterials* 35, 3945–3955. doi: 10.1016/j.biomaterials.2014.01.066

Lyu, Z., Wang, H., Wang, Y., Ding, K., Liu, H., Yuan, L., et al. (2014). Maintaining the pluripotency of mouse embryonic stem cells on gold nanoparticle layers with nanoscale but not microscale surface roughness. *Nanoscale* 6, 6959–6969. doi: 10.1039/c4nr01540a

Macgregor, M., Williams, R., Downes, J., Bachhuka, A., and Vasilev, K. (2017). The role of controlled surface topography and chemistry on mouse embryonic stem cell attachment, growth and self-renewal. *Materials (Basel)* 10:1081. doi: 10.3390/ma10091081

Madl, C. M., Lesavage, B. L., Dewi, R. E., Dinh, C. B., Stowers, R. S., Khariton, M., et al. (2017). Maintenance of neural progenitor cell stemness in 3D hydrogels requires matrix remodelling. *Nat. Mater.* 16, 1233–1242. doi: 10.1038/nmat5020

Maldonado, M., Wong, L. Y., Echeverria, C., Ico, G., Low, K., Fujimoto, T., et al. (2015). The effects of electrospun substrate-mediated cell colony morphology on the self-renewal of human induced pluripotent stem cells. *Biomaterials* 50, 10–19. doi: 10.1016/j.biomaterials.2015.01.037

Markert, L. D., Lovmand, J., Foss, M., Lauridsen, R. H., Lovmand, M., Füchtbauer, E.-M., et al. (2009). Identification of distinct topographical surface microstructures favoring either undifferentiated expansion or differentiation of murine embryonic stem cells. *Stem Cells Dev.* 18, 1331–1342. doi: 10.1089/scd.2009.0114

Meade, K. A., White, K. J., Pickford, C. E., Holley, R. J., Marson, A., Tillotson, D., et al. (2013). Immobilization of heparan sulfate on electrospun meshes to support embryonic stem cell culture and differentiation. *J. Biol. Chem.* 288, 5530–5538. doi: 10.1074/jbc.M112.423012

Mih, J. D., Sharif, A. S., Liu, F., Marinkovic, A., Symer, M. M., and Tschumperlin, D. J. (2011). A multiwell platform for studying stiffness-dependent cell biology. *PLoS One* 6:e19929. doi: 10.1371/journal.pone.0019929

Mosiewicz, K. A., Kolb, L., Van Der Vlies, A. J., Martino, M. M., Lienemann, P. S., Hubbell, J. A., et al. (2013). In situ cell manipulation through enzymatic hydrogel photopatterning. *Nat. Mater.* 12, 1072–1078. doi: 10.1038/nmat3766

Musah, S., Morin, S. A., Wrighton, P. J., Zwick, D. B., Jin, S., and Kiessling, L. L. (2012). Glycosaminoglycan-binding hydrogels enable mechanical control of human pluripotent stem cell self-renewal. *ACS Nano* 6, 10168–10177. doi: 10.1021/nn3039148

Nichols, J., and Smith, A. (2009). Naive and primed pluripotent states. *Cell Stem Cell* 4, 487–492. doi: 10.1016/j.stem.2009.05.015

Nur-E-Kamal, A., Ahmed, I., Kamal, J., Schindler, M., and Meiners, S. (2005). Three-dimensional nanofibrillar surfaces promote self-renewal in mouse embryonic stem cells. *Stem Cells* 24, 426–433.

Olmer, R., Haase, A., Merkert, S., Cui, W., Paleèek, J., Ran, C., et al. (2010). Long term expansion of undifferentiated human iPS and ES cells in suspension culture using a defined medium. *Stem Cell Res.* 5, 51–64. doi: 10.1016/j.scr.2010.03.005

Pelham, R. J., and Wang, Y. L. (1997). Cell locomotion and focal adhesions are regulated by substrate flexibility. *Proc. Natl. Acad. Sci. U.S.A.* 94, 13661–13665. doi: 10.1073/pnas.94.25.13661

Price, A. J., Huang, E. Y., Sebastiano, V., and Dunn, A. R. (2017). A semi-interpenetrating network of polyacrylamide and recombinant basement membrane allows pluripotent cell culture in a soft, ligand-rich microenvironment. *Biomaterials* 121, 179–192. doi: 10.1016/j.biomaterials.2016.12.005

Pryzhkova, M. V., Aria, I., Cheng, Q., Harris, G. M., Zan, X., Gharib, M., et al. (2014). Carbon nanotube-based substrates for modulation of human pluripotent stem cell fate. *Biomaterials* 35, 5098–5109. doi: 10.1016/j.biomaterials.2014.03.011

Przybyla, L., Lakins, J. N., and Weaver, V. M. (2016). Tissue mechanics orchestrate wnt-dependent human embryonic stem cell differentiation. *Cell Stem Cell* 19, 462–475. doi: 10.1016/j.stem.2016.06.018

Reimer, A., Vasilevich, A., Hulshof, F., Viswanathan, P., Van Blitterswijk, C. A., De Boer, J., et al. (2016). Scalable topographies to support proliferation and

Oct4 expression by human induced pluripotent stem cells. *Sci. Rep.* 6:18948. doi: 10.1038/srep18948

Richards, M., Fong, C. Y., Chan, W. K., Wong, P. C., and Bongso, A. (2002). Human feeders support prolonged undifferentiated growth of human inner cell masses and embryonic stem cells. *Nat. Biotechnol.* 20, 933–936. doi: 10.1038/nbt726

Rodrigues, A. L., Rodrigues, C. A. V., Gomes, A. R., Vieira, S. F., Badenes, S. M., Diogo, M. M., et al. (2019). Dissolvable microcarriers allow scalable expansion and harvesting of human induced pluripotent stem cells under xeno-free conditions. *Biotechnol. J.* 14, 1–12. doi: 10.1002/biot.201800461

Rys, J. P., Monteiro, D. A., and Alliston, T. (2016). Mechanobiology of TGFβ signaling in the skeleton. *Matrix Biol.* 5, 413–425. doi: 10.1016/j.matbio.2016.02.002

Saha, K., Mei, Y., Reisterer, C. M., Pyzocha, N. K., Yang, J., Muffat, J., et al. (2011). Surface-engineered substrates for improved human pluripotent stem cell culture under fully defined conditions. *Proc. Natl. Acad. Sci. U.S.A.* 108, 18714–18719. doi: 10.1073/pnas.1114854108

Shekaran, A., Lam, A., Sim, E., Jialing, L., Jian, L., Wen, J. T. P., et al. (2016). Biodegradable ECM-coated PCL microcarriers support scalable human early MSC expansion and in vivo bone formation. *Cytotherapy* 18, 1332–1344. doi: 10.1016/j.jcyt.2016.06.016

Smith, A. G., Heath, J. K., Donaldson, D. D., Wong, G. G., Moreau, J., and Stahl, M. (1988). Inhibition of pluripotential embryonic stem cell differentiation by purified polypeptides. *Nature* 336, 688–690.

Sohi, A. N., Naderi-Manesh, H., Soleimani, M., Yasaghi, E. R., Manjili, H. K., Tavaddod, S., et al. (2018). Synergistic effect of co-immobilized FGF-2 and vitronectin-derived peptide on feeder-free expansion of induced pluripotent stem cells. *Mater. Sci. Eng. C* 93, 157–169. doi: 10.1016/j.msec.2018.07.072

Srinivasan, A., Toh, Y. C., Loh, X. J., and Toh, W. S. (2016). Substrates and surfaces for control of pluripotent stem cell fate and function. *Adv. Surfaces Stem Cell Res.* 343–380. doi: 10.1002/9781119242642.ch12

Sun, Y., Villa-Diaz, L. G., Lam, R. H. W., Chen, W., Krebsbach, P. H., and Fu, J. (2012). Mechanics regulates fate decisions of human embryonic stem cells. *PLoS One* 7:e37178. doi: 10.1371/journal.pone.0037178

Sung, T.-C., Li, H.-F., Higuchi, A., Ling, Q.-D., Yang, J.-S., Tseng, Y.-C.. Pan, C. H. P., et al. (2018). Human pluripotent stem cell culture on polyvinyl alcohol-co-itaconic acid hydrogels with varying stiffness under xeno-free conditions. *J. Vis. Exp.* 132:e57314. doi: 10.3791/57314

Takahashi, K., Narita, M., Yokura, M., Ichisaka, T., and Yamanaka, S. (2009). Human induced pluripotent stem cells on autologous feeders. *PLoS One* 4:e8067. doi: 10.1371/journal.pone.0008067

Takahashi, K., Tanabe, K., Ohnuki, M., Narita, M., Ichisaka, T., Tomoda, K., et al. (2007). Induction of pluripotent stem cells from adult human fibroblasts by defined factors. *Cell* 131, 861–872. doi: 10.1016/j.cell.2007.11.019

Takahashi, K., and Yamanaka, S. (2006). Induction of pluripotent stem cells from mouse embryonic and adult fibroblast cultures by defined factors. *Cell* 126, 663–676. doi: 10.1016/j.cell.2006.07.024

Thomson, J. A., Itskovitz-Eldor, J., Shapiro, S. S., Waknitz, M. A. J., Swiergiel, J. J., and Marshall, V. S. (1998). Embryonic stem cell lines derived from human blastocysts. *Science* 282, 1145–1147. doi: 10.1126/science.282.5391.1145

Toh, Y. C., and Voldman, J. (2011). Fluid shear stress primes mouse embryonic stem cells for differentiation in a self-renewing environment via heparan sulfate proteoglycans transduction. *FASEB J.* 25, 1208–1217. doi: 10.1096/fj.10-168971

Tomishima, M. (2014). Conditioning pluripotent stem cell media with mouse embryonic fibroblasts (MEF-CM). *StemBook* 20:2. doi: 10.3824/stembook.1.68.1

Villa-Diaz, L. G., Ross, A. M., Lahann, J., and Krebsbach, P. H. (2013). The evolution of human pluripotent stem cell culture: from feeder cells to synthetic coatings. *Stem Cells* 31, 1–7. doi: 10.1002/stem.1260.The

Vining, K. H., and Mooney, D. J. (2017). Mechanical forces direct stem cell behaviour in development and regeneration. *Nat. Rev. Mol. Cell Biol.* 18, 728–742. doi: 10.1016/j.bone.2016.06.013

Wang, P. Y., Khan, S., Nguyen, T., Kingshott, P., and Wong, R. C. B. (2018). Topographical modulation of pluripotency and differentiation of human embryonic stem cells. *IEEE Trans. Nanotechnol.* 17, 381–384. doi: 10.1109/TNANO.2017.2763604

Williams, R. L., Hilton, D. J., Pease, S., Willson, T. A., Stewart, C. L., Gearing, D. P., et al. (1988). Myeloid leukaemia inhibitory factor maintains the developmental potential of embryonic stem cells. *Nature* 336, 684–687. doi: 10.1038/336684a0

Yang, H., Qiu, Y., Zeng, X., Ding, Y., Zeng, J., Lu, K., et al. (2016). Effect of a feeder layer composed of mouse embryonic and human foreskin fibroblasts on the proliferation of human embryonic stem cells. *Exp. Ther. Med.* 11, 2321–2328. doi: 10.3892/etm.2016.3204

Yang, Y., Liu, B., Xu, J., Wang, J., Wu, J., and Shi, C. (2017). Derivation of pluripotent stem cells with in vivo embryonic and extraembryonic potency. *Cell* 169, 243.e25–257.e25. doi: 10.1016/j.cell.2017.02.005

Yasuda, S. Y., Ikeda, T., Shahsavarani, H., Yoshida, N., Nayer, B., Hino, M., et al. (2018). Chemically defined and growth-factor-free culture system for the expansion and derivation of human pluripotent stem cells. *Nat. Biomed. Eng.* 2, 173–182. doi: 10.1038/s41551-018-0200-7

Ying, Q. L., Wray, J., Nichols, J., Batlle-Morera, L., Doble, B., Woodgett, J., et al. (2008). The ground state of embryonic stem cell self-renewal. *Nature* 453, 519–523. doi: 10.1038/nature06968

Yu, J., Smuga-Otto, K., Antosiewicz-Bourget, J., Frane, J. L., Thomson, J. A., Vodyanik, M. A., et al. (2007). Induced pluripotent stem cell lines derived from human somatic cells. *Science* 318, 1917–1920. doi: 10.1126/science.1151526

Zandén, C., Hellström Erkenstam, N., Padel, T., Wittgenstein, J., Liu, J., and Kuhn, H. G. (2014). Stem cell responses to plasma surface modified electrospun polyurethane scaffolds. *Nanomedicine* 10, e949–e958. doi: 10.1016/j.nano.2014.01.010

Zimmerlin, L., Park, T. S., Huo, J. S., Verma, K., Pather, S. R., Talbot, C. C., et al. (2016). Tankyrase inhibition promotes a stable human naïve pluripotent state with improved functionality. *Development* 143, 4368–4380. doi: 10.1242/dev.138982

Conflict of Interest: The authors declare that the research was conducted in the absence of any commercial or financial relationships that could be construed as a potential conflict of interest.

Copyright © 2020 Chan, Rizwan and Yim. This is an open-access article distributed under the terms of the Creative Commons Attribution License (CC BY). The use, distribution or reproduction in other forums is permitted, provided the original author(s) and the copyright owner(s) are credited and that the original publication in this journal is cited, in accordance with accepted academic practice. No use, distribution or reproduction is permitted which does not comply with these terms.

frontiers in Cell and Developmental Biology

MINI REVIEW
published: 17 January 2020
doi: 10.3389/fcell.2019.00354

Mechanomics Approaches to Understand Cell Behavior in Context of Tissue Neogenesis, During Prenatal Development and Postnatal Healing

Vina D. L. Putra[1], Min Jae Song[2,3], Sarah McBride-Gagyi[2,4], Hana Chang[2†], Kate Poole[5], Renee Whan[6], David Dean[7], Vittorio Sansalone[8] and Melissa L. Knothe Tate[1,2]*

[1] MechBio Team, Graduate School of Biomedical Engineering, University of New South Wales, Sydney, NSW, Australia, [2] MechBio Team, Departments of Biomedical and Mechanical & Aerospace Engineering, School of Engineering, Case Western Reserve University, Cleveland, OH, United States, [3] 3D Bioprinting Core, Ocular and Stem Cell Translational Research Unit, National Center for Advancing Translational Sciences, National Institutes of Health, Bethesda, MD, United States, [4] Department of Orthopaedic Surgery, Saint Louis University School of Medicine, St. Louis, MO, United States, [5] Cellular Mechanotransduction Group, School of Medical Sciences, University of New South Wales, Sydney, NSW, Australia, [6] Biomedical Imaging Facility, Mark Wainwright Analytical Centre, University of New South Wales, Sydney, NSW, Australia, [7] Department of Plastic and Reconstructive Surgery, The Ohio State University, Columbus, OH, United States, [8] Université Paris-Est Créteil, Laboratoire Modélisation et Simulation Multi Echelle, MSME UMR 8208 CNRS, Créteil Cedex, France

OPEN ACCESS

Edited by:
Guillermo Alberto Gomez, University of South Australia, Australia

Reviewed by:
Zhizhan Gu, Dana–Farber Cancer Institute, United States
Lidija Radenovic, University of Belgrade, Serbia

***Correspondence:**
Melissa L. Knothe Tate
m.knothetate@unsw.edu.au

†Present address:
Hana Chang, Integrity Bio, Newbury Park, CA, United States

Specialty section:
This article was submitted to Cell Adhesion and Migration, a section of the journal Frontiers in Cell and Developmental Biology

Received: *18 July 2019*
Accepted: *05 December 2019*
Published: *17 January 2020*

Citation:
Putra VDL, Song MJ, McBride-Gagyi S, Chang H, Poole K, Whan R, Dean D, Sansalone V and Knothe Tate ML (2020) Mechanomics Approaches to Understand Cell Behavior in Context of Tissue Neogenesis, During Prenatal Development and Postnatal Healing. Front. Cell Dev. Biol. 7:354. doi: 10.3389/fcell.2019.00354

Mechanomics represents the natural progression of knowledge at the intersection of mechanics and biology with the aim to codify the role of mechanical environment on biological adaptation. Compared to the mapping of the human genome, the challenge of mapping the mechanome remains unsolved. Solving this grand challenge will require both top down and bottom up R&D approaches using experimental and computational tools to visualize and measure adaptation as it occurs. Akin to a mechanical test of a smart material that changes its mechanical properties and local environment under load, stem cells adapt their shape, cytoskeletal architecture, intrinsic mechanical properties, as well as their own niche, through cytoskeletal adaptation as well as up- and down-regulation of structural proteins that modulate their mechanical *milieux*. Recent advances in live cell imaging allow for unprecedented study and measurements of displacements, shape and volume changes in stem cells, reconfiguring of cytoskeletal machinery (nucleus, cytoskeleton), in response to controlled mechanical forces and stresses applied at cellular boundaries. Coupled with multiphysics computational and virtual power theoretical approaches, these novel experimental approaches enable mechanical testing of stem cells, multicellular templates, and tissues inhabited by stem cells, *while the stem cells themselves evolve over time*. The novel approach is paving the way to decipher mechanisms of structural and functional adaptation of stem cells in response to controlled mechanical cues. This mini-review outlines integrated

approaches and methodologies implemented to date in a series of studies carried out by our consortium. The consortium's body of work is described in context of current roadblocks in the field and innovative, breakthrough solutions and is designed to encourage discourse and cross disciplinary collaboration in the scientific community.

Keywords: mechanoadaptation, stem cell, live imaging, cell motility, cell adherence, mechanomics

INTRODUCTION

Mechanomics studies the influence of forces on biological structure and function, across length scales, from molecules to cells, to tissues, to organs and organ systems that make up organisms. *Mechanomics* encapsulates the natural progression of knowledge at the intersection of mechanics and biology, from an understanding of biomechanics and mechanobiology, with the aim to codify the role of mechanical environment on biology. Substituting the words "mechanics" and "genetics," *mechanomics* could be considered the mechanics equivalent of *genomics*, which addresses the role of genetics on structure and function in biology. While the genome includes genes or genetic material encoded chemically (base pairs) and structurally (chromosomes) within a cell or organism, the mechanome comprises the genome's environmental equivalent that literally shapes the organism at every length scale, throughout organismal life and evolution of species. The mechanome, like the genome, is unique to each individual. Yet the mechanome is not pre-programed at conception. Indeed, the mechanome is quite the opposite–it is adaptive, making it challenging to codify while also compelling to emulate, as a means to promote well being and to harness for therapeutic purposes throughout life (Anderson and Knothe Tate, 2007a; Knothe Tate et al., 2008, 2016a; Knothe Tate, 2017).

EMERGING CONCEPT

The basic concept that forces intrinsic to life on Earth shape the structure, and thereby modulate function and adaptation of living organisms, from conception and throughout life, has a rich history. Centuries of research and observations recorded in a vast body of scientific literature underpin the concept, e.g., among others, Leonardo Da Vinci (1452–1519), Giovanni Borelli (1608–1679), D'Arcy Thompson (1860–1948), and Friedrich Pauwels (1885–1980) (Anderson et al., 2008; Knothe Tate et al., 2016a). *Mapping the mechanome* is an emerging concept that follows in the progression of the large scale human genome mapping project initiated in 1990 and completed in 2003, where *circa* 3.3 billion base pairs of the human genome were sequenced and identified (Collins et al., 2003).

In contrast to *mapping the human genome*, the challenge of *mapping the mechanome* remains unsolved, likely because it presents further dimensions of complexity, the principal one being the adaptation of living material over time, which itself plays out in development, growth, adaptation and aging of individuals over a lifetime and evolution of species and phyla over generations. Indeed, understanding and mapping the underlying mechanisms of mechanical adaptation of cells and the tissues they create, making up organs and organ systems of living organisms, over time periods ranging from periods of development to lifetimes to evolutionary time periods is a grand challenge of biology (**Figure 1**) (Knothe Tate et al., 2010b, 2016a).

Solving this grand challenge will require both top down and bottom up R&D approaches using experimental and computational tools to visualize and measure adaptation as it occurs (Anderson et al., 2005; Anderson and Knothe Tate, 2008). Top down approaches start with the big picture, in full cognizance of the system complexity, and provide invaluable contextual information regarding the system's building blocks, i.e., cells, in their natural and or model environments. Bottom up approaches piece together units to build complexity (Knothe Tate, 2011). In the context of mechanomics, one could argue that the *most basic unit comprises the totipotent and/or pluripotent stem cell* which itself arises from the fertilized egg, through which the complex organismal system emerges over a lifetime.

Akin to a mechanical test of a smart material that changes its mechanical properties and local environment under load, stem cells adapt their shape, cytoskeletal architecture, intrinsic mechanical properties, as well as their own niche, through cytoskeletal adaptation as well as up- and down-regulation of structural proteins that modulate their mechanical *milieu*. Recent advances in live cell imaging allow for unprecedented study and measurements of displacements, shape and volume changes in stem cells, their cytoskeletal machinery (nucleus, cytoskeleton) and local environment, in response to controlled mechanical forces and stresses applied at cellular boundaries. Together, these enable experimental studies akin to mechanical testing of stem cells, multicellular templates, and tissues inhabited by stem cells, while the stem cells themselves evolve over time. The approaches are paving the way to decipher mechanisms of structural and functional adaptation of stem cells in response to controlled mechanical cues (Anderson et al., 2008; McBride and Knothe Tate, 2008; Song et al., 2010, 2012, 2013; McBride et al., 2011a).

Similarly, new approaches to mechanics of materials enable characterization of the cell's stress state using virtual power theory. This mathematical approach predicts the energy expended over time (power) during a virtual mechanical test of an idealized cell model, where the cell is idealized as a collection of infinitesimally small material elements. Through iterative implementation of the model, mechanoadaptation of a cell can be predicted over time (Knothe Tate et al., 2016b). Displacements and/or stresses and strains measured in the experimental models noted above serve as inputs for the analytical and/or computational

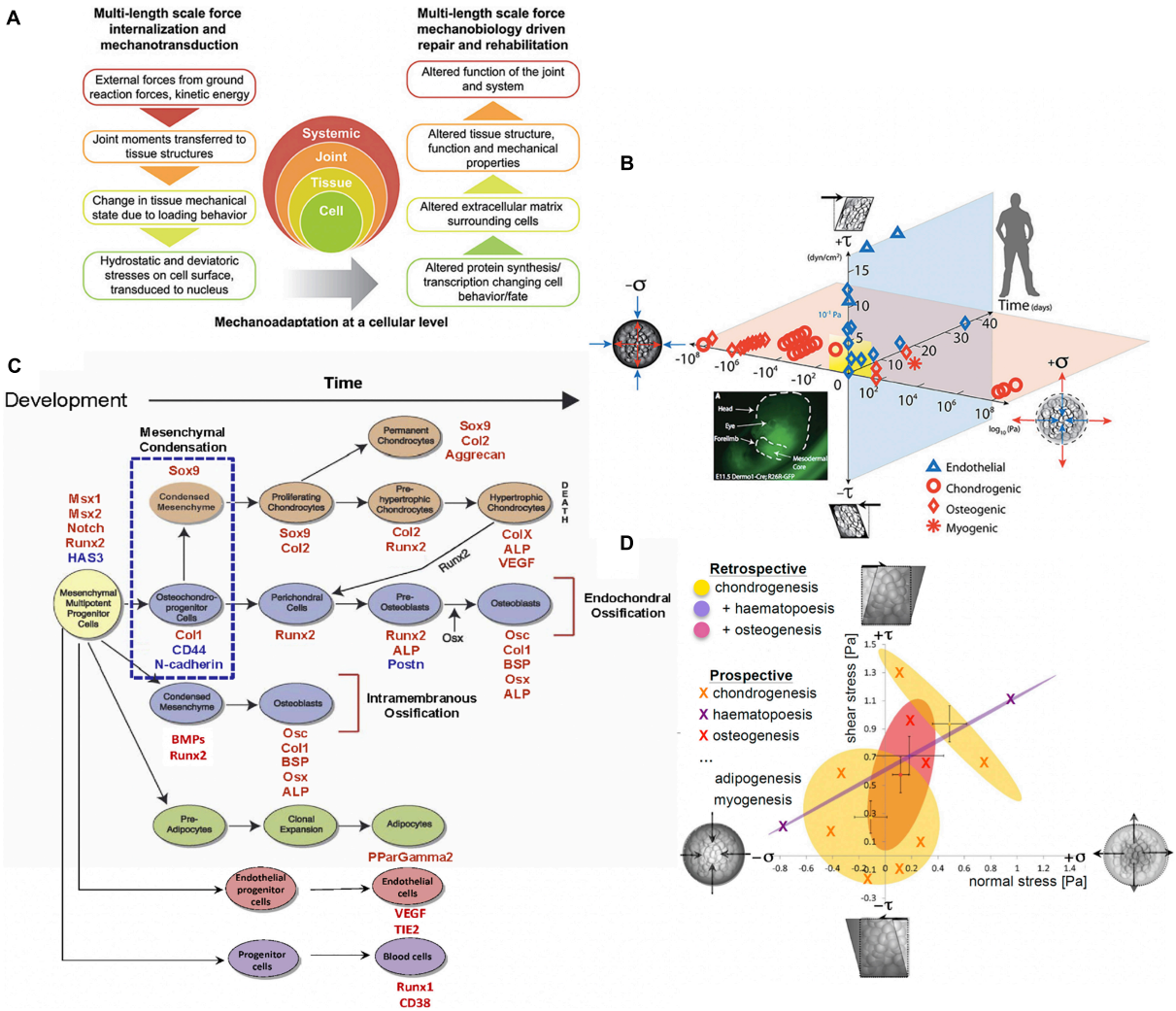

FIGURE 1 | Multiscale and multidisciplinary approaches to mechanomics. **(A)** Mechanoadaptation of tissues and organs aligns closely with mechanoadaptation at a cellular level, since cells manufacture the structural proteins making up the extracellular tissue matrix and the matrix in turn modulates how exogenous mechanical signals are transferred to cells and their nuclei, *after* (Ng et al., 2017), *used with permission*. **(B)** A recently updated first map of the mechanome includes data points from a number of labs in which volume and shape changing stresses were mapped against time and lineage commitment was noted by the shape of the data point, *after* (Anderson and Knothe Tate, 2007a; McBride et al., 2008; Ng et al., 2017), *used with permission*. **(C)** Fate map for mesenchymal stem cells. Mesenchymal condensation (blue dotted box, E11.5 in the mouse), the first step in skeletogenesis, is followed by lineage commitment toward chondrogenic (orange), osteogenic (blue), and adipogenic (green) fates. Transcription levels for factors (red and blue font) at points in time can be used to benchmark stages of development along specific lineages, *after* (Song et al., 2013), *used with permission.* **(D)** Each oval represents a 95% confidence area for specific lineage commitment (indicated by color) associated with areas ranges of shear and normal stress states, some of which overlap, *after* (Song et al., 2013), *used with permission.*

models and enable formation of mechanome maps based on 95% confidence intervals of actual data (**Figure 1**) (Song et al., 2013).

This mini-review outlines integrates different approaches and methodologies implemented to date (provided below section "Different Approaches") in series of studies carried out by our consortium. This body of work is described context of current roadblocks in the field (*Current Research Gaps*) and innovative, breakthrough solutions (*Future Developments in the Field*). While the focus of the mini-review is on presenting for the first time an integrative perspective on studies from our consortium, we aim to raise awareness, encourage discussion and build collective understanding through interactive posting of comments and insights as part of the online *Frontiers* publication.

DIFFERENT APPROACHES

A multitude of models and approaches are necessary to unravel the complexity of multiscale mechanoadaptation via cells (**Figure 2**). Through a breadth of studies modeling prenatal development and postnatal healing, the exquisite mechanosensitivity of stem cells to their mechanical environment

has been documented (McBride et al., 2008). While this mini-review focuses on our consortium's body of work, recent reviews and original articles offer further perspectives, i.a. (Heo et al., 2015; Steward and Kelly, 2015; Le et al., 2016; Ladoux and Mege, 2017; Stumpf et al., 2017; Ni et al., 2019).

Engineering and Culture of Model Tissue *Anlagen* or Templates

Consortium studies from over a decade ago demonstrated the modulatory effect of cell density seeding protocol (either seeded at density or proliferated to density) on baseline gene expression of transcription factors indicative of pre-, peri-, and post-mesenchymal condensation, an event marking the initiation of skeletogenesis in the embryo and occurring at development stage E11.5 in the mouse. Remarkably, through the choice of stem cell seeding protocols or biophysical effects intrinsic to cell density at seeding, it was possible to form model tissue templates and to guide their differentiation toward mesenchymal condensation (McBride and Knothe Tate, 2008; Zimmerman and Knothe Tate, 2011). Through imaging and gene transcription studies it could be shown that increasing density at seeding results in changes to stem cell volume while seeding at density compared to proliferating to density results in changes to stem cell nucleus shape. Hence cell seeding density and protocols for reaching density provide physical mechanisms by which force transmission between cells can translate to conformational and gene transcription changes within the nucleus (Zimmerman and Knothe Tate, 2011).

Development and Implementation of a Testing Platform for Controlled Mechanical Testing of Model Tissue Templates

To study effects of controlled mechanical forces on stem cell lineage commitment, our consortium aimed to identify experimental platforms that mimicked physiological conditions while introducing minimal artifacts and enabling live cell imaging during testing procedures (**Figures 2F,G**) (Sorkin et al., 2004; Anderson et al., 2006; Anderson and Knothe Tate, 2007b). In testing then state-of-the-art, commercialized parallel flow chambers used in mechanotransduction studies, we discovered that none of the commercialized chambers studied delivered the flow regimes predicted by fluid dynamics. The lack of reproducibility of flow regimes between chambers, within and between manufacturers, called into question the comparability of a host of published studies using such chambers. In addition, none of the commercialized chamber manufacturers had tested flows in the presence of cells (Anderson et al., 2006; Anderson and Knothe Tate, 2007b).

Hence we developed an R&D program integrating computational fluid dynamics simulations (computational) and bench top imaging and fluid dynamics studies to study flows in the absence and presence of cells (**Figures 2F,G**). These studies enabled development of a novel perfusion chamber platform, which we provided on an open source, at cost basis (Anderson et al., 2006; Anderson and Knothe Tate, 2007b), and commercialized non-exclusively by Harvard Apparatus for industry. The so-called ProFlow chamber lent itself for studies of cells seeded on coverslips, permeable membranes, PDMA substrates, and tissue templates and subjected to low, laminar flow regimes typical for *in vivo* mechanical environments (Harvard apparatus catalog).

Contrary to contemporary understanding at the time, our consortium's series of studies showed that flow regimes exposed cells and multicellular templates not only to the expected shear (deviatoric) stresses at fluid-cell and cell-cell interfaces but also to normal stresses (dilatational: compression, tension) (**Figure 2G**) (Song et al., 2013). Furthermore, through spatiotemporal control of flow velocities (achieved through chamber geometries and/or flow pumps), changes in fluid viscosity, and template design considerations (seeding density and protocol), the platform proved ideal to deliver controlled shape (deviatoric) and volume (dilatational) stresses to cells within the chamber while imaging volumes within the chamber, using a laser scanning confocal or multiphoton microscope (Anderson et al., 2005, 2006; Anderson and Knothe Tate, 2007b, 2008; McBride et al., 2008).

Using micro-particle image velocimetry (micro-PIV), we calculated the precise flow field in each plane of focus of the microscope by measuring the direction and distance traveled of micron sized fluorescent particles introduced into the fluid, and then visualized the flow field in three dimensions, in the absence and presence of cells (Song et al., 2010; Song et al., 2012) (**Figures 2F,G**). Similarly, we calculated displacements on cell surfaces by tracking displacements of microspheres coated with Concanavalin A, a lectin carbohydrate binding protein that binds covalently to the glycocalyx of the cell (Song et al., 2013). In this way, we measured at subcellular resolution the delivery of forces and the resulting deformation of the cell or cell constructs/tissue templates in near-real time (Song et al., 2010, 2012, 2013) (**Figures 2F,G**).

The spatial and temporal data including the flow fields and cells/tissue templates were used as inputs for a coupled multi-physics computational model (**Figure 2G**), enabling calculation of changes in modulus of elasticity of the cells over time as well as between experimental cohorts of different seeding densities, protocols and substrates/tissue templates. This, together with measurements of changes in baseline gene transcription of factors indicative of lineage commitment (osteogenesis, chondrogenesis, adipogenesis, vasculogenesis, and hematopoiesis) provided thousands of single cell data points that could be depicted as 95% confidence intervals, relating stress and strain to lineage commitment (**Figure 1D**), forming the basis of the first mechanome map of model embryonic murine mesenchymal stem cells (Song et al., 2013).

Role of Cell and Nucleus Shape, Volume as Well as Cytoskeletal Proteins Actin and Tubulin in Mechanoadaptation

In our consortium's earliest studies of mechanoadaptation, we realized that cell fixation itself changed the shape and volume of individual cells, underscoring the importance of live cell imaging in study of mechanoadaptation (Zimmerman and Knothe Tate, 2011). Live imaging required the use of new methods to assess cytoskeletal proteins including compression resisting tubulin

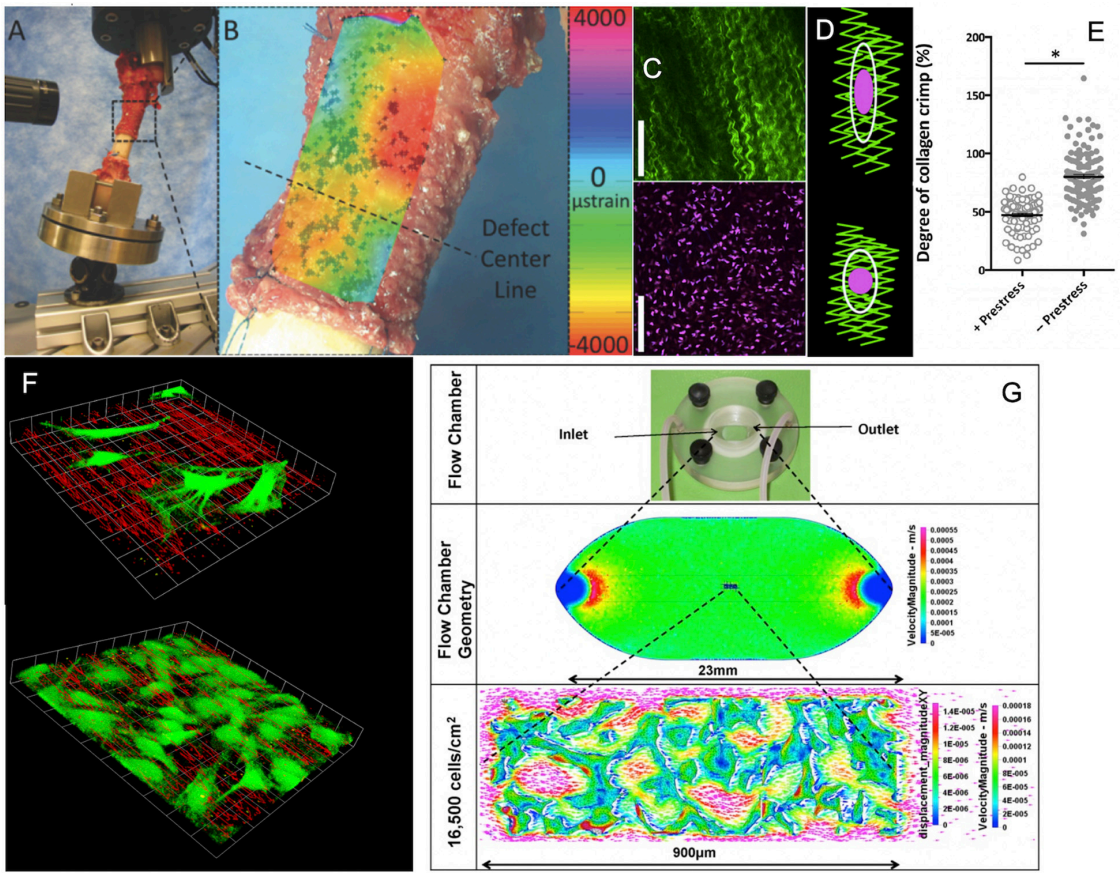

FIGURE 2 | Cross length and time scale experimental and coupled computational approaches to map the mechanome. **(A)** Ultra high resolution digital image correlation and **(B)** strain mapping of the periosteum *milieu* using high definition television lenses and *ex vivo* loading of the sheep femur to mimic stance shift loading after treatment of a critical sized defect with periosteum *in situ. After* (Knothe Tate et al., 2007; McBride et al., 2011a), *used with permission*. **(C)** High resolution imaging of collagen (green) and periosteum derived stem cell nuclei *ex vivo* to visualize hypothesized mechanism of modulating stem cell quiescence via loss of intrinsic prestress with injury. *After* (Yu et al., 2017), *used with permission*. **(D,E)** In its natural, healthy state, periosteum is attached under prestress to every bone surface like Velcro, through a multitude of collagenous Sharpey's fibers. When the Sharpey's fibers become detached, e.g., due to trauma, the pre-tensioned, crimped collagen relaxes and becomes more crimped (less stretched), *after* (Yu et al., 2017), *used with permission*. **(F)** Using computational fluid dynamics predictions and computer-aided design and manufacture, perfusion chambers were manufactured to deliver precise volumetric flow fields to cells and tissue templates cultured within. The system was designed to enable concomitant microscopy, demonstrating the effect of cells themselves on local flow fields, when seeded at low density (top) and at near confluence (bottom), *after* (Song et al., 2010, 2012, 2013), *used with permission*. **(G)** After full computational and experimental validation of the system, including mechanical stresses delivered and resulting deformation on cell/tissue surfaces, tissue templates were tested using the same experimental platform and paired with multiphysics computational methods to enable near-real time mechanical testing of cells and tissue templates as they evolve (change phenotype and/or change their baseline gene expression of transcription markers typifying lineage commitment pathways), *after* (Song et al., 2010, 2012, 2013), *used with permission*. *Indicates a significant differences, as defined by a $p < 0.05$.

and tension resisting actin. Initial work used the BacMam vector to tag fluorescently actin or tubulin monomers during transcription and live imaging to follow the tagged monomers in space and time within cells exposed to forces through seeding density/protocols and/or delivery of forces via flow (Chang and Knothe Tate, 2011; Zimmerman and Knothe Tate, 2011) In addition to exerting dilatational (pressure) forces on cells, increasing seeding densities were observed to result in higher concentrations (fluorescence intensities) of tubulin within the cell (Zimmerman and Knothe Tate, 2011). Exposure to normal and shear stresses via fluid flow, in combination with seeding density resulted in differential expression of actin in the cells (Chang and Knothe Tate, 2011). Hence, the mechanical loading and imaging platform lent itself well for observation and measurement of mechanoadaptation in stem cells via cytoskeletal re-/modeling.

To characterize mechanoadaptation as a function of changes in cell and nucleus shape and volume concomitant to cytoskeletal re-/modeling, new methods were recently developed for cells seeded on substrates and tissue templates as well as cells ingressing into Matrigel-based, tissue templates (Putra et al., 2019 accepted conditional to revision). It is expected that these methods will enable prospective probing of the mechanome, i.e., application of mechanical loads predicted to lead to desired differentiation (from 95% confidence intervals of retrospective plots) and testing of efficacy in achieving target lineages.

Modulation of Mechanoadaptation Through Control of Boundaries via Cell-Cell Adhesion Complexes

To mimic processes of emergent architecture and loss of such architecture in a controlled model of tissue neogenesis our consortium developed novel models using primary mouse and human mesenchymal cells. We first used primary mouse mesoderm stem cells from wild type mice and a mouse model with conditional knockout for beta-catenin, a protein linking cell-cell adhesion proteins (cadherins) to the actin cytoskeleton within the cell (Falls et al., 2008; Knothe Tate et al., 2010b). Mesoderm was resected, dissociated and cultured from embryonic mice at E11.5, the stage when mesenchymal condensation initiates. Cells from conditional knockouts were compared to wild type cells under exposure to low amplitude (1 dyn/cm^2) flow. Exposure of primary murine mesodermal cells to stress via fluid flow significantly up-regulated Col1a1 transcription in the cells lacking β-catenin and down-regulated transcription in cells not lacking β-catenin. Transcription of Sox9 and AGC, Runx2 and Osx, and Ppar-γ (transcriptional markers of chondrogenesis, osteogenesis, and adipogenesis, respectfully) was not significantly affected by exposure to flow. Previous studies showed that cells lacking β-catenin do not reassociate in culture to the same degree as normal cells after dissociation from the mesoderm. Using computer models, we demonstrated that more isolated cells (lacking β-catenin) would be exposed to higher levels of stress than reassociated, normal cells. These data showed, for the first time to our knowledge, that gene transcription activity of primary embryonic mesenchymal cells can be modulated by mechanical cues even in the absence of β-catenin, a protein that links cadherins to the cytoskeleton (Falls et al., 2008; Knothe Tate et al., 2010b).

In a second study we created a biosynthetic platform to mimic processes of cellular self assembly and emergent phenotype at early stages of tissue neogenesis, e.g., during postnatal healing. Using primary mesenchymal stem cells derived from human periosteum (PDCs), our consortium engineered solid-supported lipid bilayers (SSLB) to model large scale cell membranes. PDCs express both N-cadherin, a hallmark of mesenchymal condensation, and ZO-1 proteins which build tight junctions and confer epithelial membrane function. By functionalizing the SSLBs with recombinant N-cadherin and using different cell seeding densities and protocols to probe cell aggregation and emergent tissue architectures it was possible to engineer prospectively cellular contexts similar to mesenchymal condensations and formation of epithelia, two key tissue architectures underpinning tissue and organ development and physiology (Evans et al., 2013).

Coupled Computational – *In vivo* Models of Postnatal Tissue Genesis in Critical Sized Defects

While *in vitro* experimental platforms enable significantly greater control of variables than *in vivo* approaches, it is essential to observe processes in physiologically relevant contexts to maximize translation to human wellbeing and health outcomes. *In vivo* models themselves are also idealized approximations of true system complexity intrinsic to human physiology and, though idealizing true system complexity, are in some cases invaluable for understanding and elucidating mechanisms of adaptation. For example, our consortium carried out a series of *in vivo* ovine experiments to study postnatal healing of critical sized bone defects via stem cells. The series of studies tested the efficacy of periosteum, a niche for stem cells, and/or periosteum substitutes mimicking the natural tissue as a delivery vehicle for stem cells and tissue genesis via the stem cells. Though the study design was relatively simple, the number of variables and their interactions was not trivial (Knothe Tate et al., 2007, 2010a, 2011; Knothe et al., 2010; McBride et al., 2011a,b,c; Moore et al., 2016).

To understand the interplay between mechanics, mechanically modulated transport of cells and molecular factors, tissue genesis via stem cells, and subsequent cell and tissue differentiation in the series of *in vivo* ovine models, we would have had to carry out thousands of experiments to probe each permutation as well as interactions of the respective variables. Instead we developed a mechanistic, mathematical model to predict the dynamics of tissue neogenesis by mesenchymal stem cells deriving from the periosteum or a periosteum substitute implant. By coupling a mechanical finite element model with a cell dynamics model, we simulated the clinical scenario by which a patient's own periosteum or a novel substitute periosteum implant would be used to heal a critical sized bone defect in a human patient. The model predictions, which incorporated mechanical feedback, matched spatial and temporal patterns of tissue neogenesis and differentiation observed in the series of preclinical (ovine) experiments. The model platform incorporating computational, physical and engineering science approaches with an understanding of cell and developmental biology, provides a platform to test new hypotheses *in silico* (Moore et al., 2014, 2016).

In situ Imaging – Mechanical Regulation of Live Progenitor Cell Niche Quiescence *ex vivo*

In the *in vivo* model we observed, from quantitative histological analysis coupled with cellular resolution digital image correlation (live mechanical testing) of tissue strains under stance shift loading, that volumes of maximal tissue genesis in the defect correlated with areas of periosteum which had the greatest shift in baseline strain prior to and after surgery (**Figures 2A,B**) (McBride et al., 2011a,b). Previous *in vitro* studies showed that periosteum is prestressed *in situ*, like curly hair that is stretched and held in place; upon release of the periosteum from bone surfaces, the tissue shrinks (**Figures 2C,D**) (McBride et al., 2011c). We hypothesized that stem cell adherence and motility are regulated mechanically but needed a way to see how changes in stress state of the periosteum were felt by individual cells. We initiated a live cell and second harmonic imaging of collagen study on fresh, *ex vivo* tissue preparations of periosteum. In the natural, prestressed state, collagen was

stretched out and cells were adherent with a flattened shape. Upon release of the prestress, collagen curled up slightly and cells rounded (**Figures 2C–E**), providing evidence for our working hypothesis that the mechanical state of the tissue may regulate stem cell shape and, potentially motility and later lineage commitment (**Figure 2E**) (Yu et al., 2017).

While these studies continue, the concept that injury to a stem cell niche exerts mechanical effects that may modulate cell behavior is new. Of course, these mechanical effects occur simultaneous to release of cytokines and other healing modulatory biochemical factors, the molecular transport of which is modulated by prevailing mechanical stress states. Nonetheless, the concept of a mechanical trigger for regulation of stem cell quiescence is quite exciting in a therapeutic and in an engineering design context (Knothe Tate et al., 2016b).

CURRENT GAPS AND FUTURE DEVELOPMENTS IN THE FIELD

Given the burgeoning body of evidence, at virtually every length and time scale addressed by scientific investigation and discovery to date, an understanding of mechanomics is key to elucidating mechanisms of stem cell behavior in context of tissue neogenesis, both during prenatal development as well as postnatal healing. Integration of top–down and bottom–up approaches, and use of a multivalent toolset including live imaging across length and time scales, computational modeling, creation of benchmarking research tools such as validated flow/imaging chambers and microfluidics platforms, and models that cross species as well as development contexts, enables unraveling of the system complexity in different physiological contexts. Integration of engineering with fundamental biology and chemistry and physics approaches is also key; until educational training catches up with these multidisciplinary needs, research and development teams can aim for diversity across disciplines and cultural contexts to develop, test and probe with new scientific platforms that enable deciphering of emergent behavior underpinning life and living architectures of tissues, organs, and organisms comprising organ systems (Knothe Tate, 2017). Validation of new platforms, from microfluidics to organoid models, is essential, to insure that datasets are comparable between labs and are relatable across length scales and experimental models.

DISCLOSURE

The senior author (MK) and her doctoral trainee E.J. Anderson (currently Chief Fluid Dynamics, U.S. National Oceanic Atmospheric Administration, provided open access to academic researchers for the flow chamber technology described in the mini-review (Anderson et al., 2006; Anderson and Knothe Tate, 2007b). They also licensed the flow chamber technology non-exclusively to Harvard Apparatus, where it has been commercialized for purchase by non-academic researchers and companies.

AUTHOR CONTRIBUTIONS

Postgraduate trainees (VP, MS, SMc-G, and HC) developed and carried out the experimental and computational studies underpinning mechanome mapping as well as developmental (prenatal development) and regenerative medicine (postnatal healing) contexts, going on to lead research programs of their own that focus on regenerative medicine and its translation (HC), for medical conditions as varied as orthopedic (SMc-G), ocular (MS). Mentors and experts in stem cell biology (KP, DD, and MK), imaging (RW, DD, and MK), and computational modeling (VS and MK) formed the original consortium which started approximately 15 years ago. All authors approved the manuscript.

FUNDING

The work was supported through an R01 (DD and MK) and a training (SMc-G, HC, and MK) grant from the U.S. National Institutes of Health, U.S. National Science Foundation (MK and MS), the AO Foundation (Switzerland; MK and SMc-G), the Case Western Reserve University Presidential Initiative (MK), the Paul Trainor Foundation (Australia: MK), a National Health and Medical Research Council Development Grant (Australia: MK), and UNSW's Silver and Gold Star funding programs for "near miss" grants (top tier of unfunded proposals, Australia: MK and KP).

ACKNOWLEDGMENTS

We kindly acknowledge Leica Microsystems for the first in world research contract (MK) enabling development of the imaging and engineering platforms presented herein (that were published in 2013 and before). The Biomedical Imaging Facility of the Mark Wainwright Analytical Centre (Directed by RW) was instrumental in enabling development of more recent live imaging approaches (published after 2013).

REFERENCES

Anderson, E. J., Falls, T. D., Sorkin, A., and Knothe Tate, M. L. (2006). The imperative for controlled mechanical stresses in unraveling cellular mechanisms of mechanotransduction. *BioMed. Eng. OnLine* 5:27.

Anderson, E. J., Kaliyamoorthy, S., Alexander, J. I. D., and Knothe Tate, M. L. (2005). Nano-microscale models of periosteocytic flow show differences in stresses imparted to cell body and processes. *Ann. Biomed. Eng.* 33, 52–62. doi: 10.1007/s10439-005-8962-y

Anderson, E. J., and Knothe Tate, M. L. (2007a). Design of tissue engineering scaffolds as delivery devices for mechanical and mechanically modulated signals. *Tissue Eng.* 13, 2525–2538. doi: 10.1089/ten.2006.0443

Anderson, E. J., and Knothe Tate, M. L. (2007b). Open access to novel flow chamber technology for *in vitro* cell mechanotransduction, toxicity and pharmacokinetic studies. *BioMed. Eng. OnLine* 6:46. doi: 10.1186/1475-925x-6-46

Anderson, E. J., and Knothe Tate, M. L. (2008). Idealization of pericellular fluid space geometry and dimension results in a profound underprediction of

nano-microscale stresses imparted by fluid drag on osteocytes. *J. Biomech.* 41, 1736–1746. doi: 10.1016/j.jbiomech.2008.02.035

Anderson, E. J., Kreuzer, S. M., Small, O., and Knothe Tate, M. L. (2008). Pairing computational and scaled physical models to determine permeability as a measure of cellular communication in micro- and nano-scale pericellular spaces. *Microfluid. Nanofluid.* 4, 193–204. doi: 10.1007/s10404-007-0156-5

Chang, H., and Knothe Tate, M. L. (2011). Structure – function relationships in the stem cell's mechanical world B: emergent anisotropy of the cytoskeleton correlates to volume and shape changing stress exposure. *Mol. Cell. Biomech.* 8, 297–318.

Collins, F. S., Morgan, M., and Patrinos, A. (2003). The human genome project: lessons from large-scale biology. *Science* 300, 286–290. doi: 10.1126/science.1084564

Evans, S. F., Docheva, D., Bernecker, A., Colnot, C., Richter, R., Knothe Tate, M. L. (2013). Solid-supported lipid bilayers as a novel platform to engineer emergence of stem cell fate and tissue architecture using periosteum derived progenitor cells. *Biomaterials* 34, 1878–1887. doi: 10.1016/j.biomaterials.2012.09.024

Falls, T. D., Atit, R., Anderson, E. J., Knothe Tate, M. L. (2008). Beta-catenin's role in the mechanosensitivity of osteochondroprogenitor cells. *Trans. Orthop. Res. Soc.* 33:0156.

Heo, S. J., Thorpe, S. D., Driscoll, T. P., Duncan, R. L., Lee, D. A., and Mauck, R. L. (2015). Biophysical regulation of chromatin architecture instills a mechanical memory in mesenchymal stem cells. *Sci. Rep.* 5:16895. doi: 10.1038/srep16895

Warner Instruments, Available at: https://www.harvardapparatus.com/media/manuals/PFC-1%20(120127).pdf (accessed September 2, 2019).

Knothe, U., Dolejs, S., Miller, R. M., and Knothe Tate, M. L. (2010). Effects of mechanical loading patterns, bone graft, and proximity to periosteum on bone defect healing. *J. Biomech.* 43, 2728–2737. doi: 10.1016/j.jbiomech.2010.06.026 doi: 10.1016/j.jbiomech.2010.06.026

Knothe Tate, M. L. (2011). Top down and bottom up engineering of bone. *J. Biomech.* 44, 304–312. doi: 10.1016/j.jbiomech.2010.10.019

Knothe Tate, M. L. (2017). "Navigation of bee brains to human hips - microscopy and the modern Magellans," in *A New Age in Scanning Electron Microscopy: Applications in the Life Sciences* ed. AAAS, Science (Washington, DC: Science/AAAS), 19–23.

Knothe Tate, M. L., Falls, T., McBride, S. H., Atit, R., and Knothe, U. R. (2008). Mechanical modulation of osteochondroprogenitor cell fate. *Int. J. Biochem. Cell Biol.* 40, 2720–2738. doi: 10.1016/j.biocel.2008.05.011

Knothe Tate, M. L., Dolejs, S., Miller, R. M., and Knothe, U. (2010a). Role of mechanical loading in healing of massive bone autografts. *J. Orthopaedic Res.* 28, 1657–1684. doi: 10.1002/jor.21190

Knothe Tate, M. L., Falls, T., Mishra, S., and Atit, R. (2010b). Engineering an ecosystem: taking cues from nature's paradigm to build tissue in the lab and the body. *Fields Inst. Math. Biol.* 57, 113–134. doi: 10.1090/fic/057/06

Knothe Tate, M. L., Gunning, P., and Sansalone, V. (2016a). Emergence of form from function: role of stem cell mechanoadaptation in sealing of cell fate. *BioArchitecture* 6, 85–103. doi: 10.1080/19490992.2016.1229729

Knothe Tate, M. L., Yu, N. Y. C., Jalilian, I., Pereira, A., and Knothe, U. R. (2016b). Periosteum mechanobiology and mechanistic insights for regenerative medicine. *Nat. Publ. Group BoneKey Rep.* 5:857.

Knothe Tate, M. L., Moore, S., Chang, H., and Knothe, U. (2011). Surgical membranes as directional delivery devices to generate tissue in critical sized defects. *PLoS One* 6:e28702. doi: 10.1371/journal.pone.0028702

Knothe Tate, M. L., Ritzman, T., Schneider, E., and Knothe, U. (2007). Testing of a new one-stage bone-transport surgical procedure exploiting the periosteum and bone transport for repair of long bone defects. *J. Bone Joint Surg. Am.* 89, 307–316. doi: 10.2106/jbjs.e.00512

Ladoux, B., and Mege, R. M. (2017). Mechanobiology of collective cell behaviours. *Nat. Rev. Mol. Cell. Biol.* 18, 743–757. doi: 10.1038/nrm.2017.98

Le, H. Q., Ghatak, S., Yeung, C. Y., Tellkamp, F., Günschmann, C., Dieterich, C., et al. (2016). Mechanical regulation of transcription controls Polycomb-mediated gene silencing during lineage commitment. *Nat. Cell Biol.* 18, 864–875. doi: 10.1038/ncb3387

McBride, S. H., Dolejs, S., Brianza, S., Knothe, U., and Knothe Tate, M. L. (2011a). Net change in periosteal strain correlates to rapid *de novo* bone generation in critical sized defects. *Ann. Biomed. Eng.* 39, 1570–1581. doi: 10.1007/s10439-010-0242-9

McBride, S. H., Dolejs, S., Miller, R. M., Knothe, U., and Knothe Tate, M. L. (2011b). Major and minor centroidal axes serve as absolute reference points to test mechanobiological hypotheses using histomorphometry. *J. Biomech.* 44, 1205–1208. doi: 10.1016/j.jbiomech.2011.01.033

McBride, S. H., Evans, S., and Knothe Tate, M. L. (2011c). Anisotropic mechanical properties of ovine femoral periosteum and the effects of cryopreservation. *J. Biomech.* 44, 1954–1959. doi: 10.1016/j.jbiomech.2011.04.036

McBride, S. H., Falls, T., and Knothe Tate, M. L. (2008). Modulation of stem cell shape and fate, B: mechanical modulation of cell shape and gene expression. *Tissue Eng.* 14, 1573–1580. doi: 10.1089/ten.tea.2008.0113

McBride, S. H., and Knothe Tate, M. L. (2008). Modulation of stem cell shape and fate, a: role of density and seeding protocol on nucleus shape and gene expression. *Tissue Eng.* 14, 1561–1572. doi: 10.1089/ten.tea.2008.0112

Moore, S., Saidel, G., Knothe, U., and Knothe Tate, M. L. (2014). Mechanistic, mathematical model to predict the dynamics of tissue genesis in bone defects via mechanical feedback and mediation of biochemical factors. *PLoS Comp. Biol.* 10:e1003604. doi: 10.1371/journal.pcbi.1003604

Moore, S. R., Heu, C., Yu, N., Whan, R., Knothe, U., Milz, S., et al. (2016). Translating periosteum's regenerative power: insights from quantitative analysis of tissue genesis with a periosteum substitute implant. *Stem Cells Transl. Med.* 5, 1739–1749. doi: 10.5966/sctm.2016-0004

Ng, J., Kilbreath, S., Kersh, M., and Knothe Tate, M. L. (2017). Establishing the basis for mechanobiology-based physical therapy protocols to potentiate cellular healing and tissue regeneration. *Front. Physiol.* 8:303. doi: 10.3389/fphys.2017.00303

Ni, F., Yu, W. M., Wang, X., Fay, M. E., Young, K. M., Qiu, Y., et al. (2019). Ptpn21 controls hematopoietic stem cell homeostasis and biomechanics. *Cell Stem Cell* 24:608-620e.6. doi: 10.1016/j.stem.2019.02.009

Putra, V., Jalilian, I., Campbell, M., Poole, K., Whan, R., Tomasetig, F., et al. (2019). Protocol for live imaging of cytoskeletal mechanoadaptation and cell ingression. *Bio-protocol* 9. doi: 10.21769/BioProtoc.3439

Song, M. J., Brady-Kalnay, S., Phillips-Mason, P., Dean, D., and Knothe Tate, M. L. (2012). Mapping the mechanome of live stem cells: using a novel method to measure local strain fields *in situ* at the fluid-cell interface. *PLoS One* 7:e43601. doi: 10.1371/journal.pone.0043601

Song, M. J., Dean, D., and Knothe Tate, M. L. (2010). In situ spatiotemporal mapping of flow fields around seeded stem cells at the subcellular length scale. *PLoS One* 5:e12796. doi: 10.1371/journal.pone.0012796

Song, M. J., Dean, D., and Knothe Tate, M. L. (2013). Mechanical Modulation of nascent cell lineage commitment in tissue engineering scaffolds. *Biomaterials* 34, 5766–5775. doi: 10.1016/j.biomaterials.2013.04.023

Sorkin, A., Dee, K. C., and Knothe Tate, M. L. (2004). Culture Shock" from the bone cell's perspective: emulating physiologic conditions for mechanobiological investigation. *Am. J. Physiol. Cell Physiol.* 287, C1527–C1536.

Steward, A. J., and Kelly, D. J. (2015). Mechanical regulation of mesenchymal stem cell differentiation. *J. Anat.* 227, 717–731. doi: 10.1111/joa.12243

Stumpf, P. S., Smith, R. C. G., Lenz, M., Schuppert, A., Müller, F. J., Babtie, A., et al. (2017). Stem cell differentiation as a non-Markov stochastic process. *Cell Syst.* 5, 268–282. doi: 10.1016/j.cels.2017.08.009

Yu, N., O'Brien, C. A., Slapetova, I., Whan, R., and Knothe Tate, M. L. (2017). Live tissue imaging to elucidate mechanical modulation of stem cell niche quiescence. *Stem Cells Transl. Med.* 6, 282–292. doi: 10.5966/sctm.2015-0306

Zimmerman J., and Knothe Tate, M. L. (2011). Structure – function relationships in the stem cell's mechanical world A: seeding protocols as a means to control shape and fate of live cells. *Mol. Cell. Biomech.* 8, 275–296.

Conflict of Interest: The authors declare that the research was conducted in the absence of any commercial or financial relationships that could be construed as a potential conflict of interest.

Copyright © 2020 Putra, Song, McBride-Gagyi, Chang, Poole, Whan, Dean, Sansalone and Knothe Tate. This is an open-access article distributed under the terms of the Creative Commons Attribution License (CC BY). The use, distribution or reproduction in other forums is permitted, provided the original author(s) and the copyright owner(s) are credited and that the original publication in this journal is cited, in accordance with accepted academic practice. No use, distribution or reproduction is permitted which does not comply with these terms.

frontiers in Cell and Developmental Biology

REVIEW
published: 19 August 2020
doi: 10.3389/fcell.2020.00750

Molecular Signaling Interactions and Transport at the Osteochondral Interface: A Review

*Mateus Oliveira Silva, Julia L. Gregory, Niloufar Ansari and Kathryn S. Stok**

Department of Biomedical Engineering, University of Melbourne, Parkville, VIC, Australia

Articular joints are comprised of different tissues, including cartilage and bone, with distinctive structural and mechanical properties. Joint homeostasis depends on mechanical and biological integrity of these components and signaling exchanges between them. Chondrocytes and osteocytes actively sense, integrate, and convert mechanical forces into biochemical signals in cartilage and bone, respectively. The osteochondral interface between the bone and cartilage allows these tissues to communicate with each other and exchange signaling and nutritional molecules, and by that ensure an integrated response to mechanical stimuli. It is currently not well known how molecules are transported between these tissues. Measuring molecular transport *in vivo* is highly desirable for tracking cartilage degeneration and osteoarthritis progression. Since transport of contrast agents, which are used for joint imaging, also depend on diffusion through the cartilage extracellular matrix, contrast agent enhanced imaging may provide a high resolution, non-invasive method for investigating molecular transport in the osteochondral unit. Only a few techniques have been developed to track molecular transport at the osteochondral interface, and there appear opportunities for development in this field. This review will describe current knowledge of the molecular interactions and transport in the osteochondral interface and discuss the potential of using contrast agents for investigating molecular transport and structural changes of the joint.

Keywords: joint, articular cartilage, bone, molecular signaling, transport, osteoarthritis

OPEN ACCESS

Edited by:
Samantha Jane Stehbens, The University of Queensland, Australia

Reviewed by:
Indira Prasadam, Queensland University of Technology, Australia
Jens Staal, Ghent University, Belgium

***Correspondence:**
Kathryn S. Stok
kstok@unimelb.edu.au

Specialty section:
This article was submitted to Signaling, a section of the journal Frontiers in Cell and Developmental Biology

Received: *09 May 2020*
Accepted: *17 July 2020*
Published: *19 August 2020*

Citation:
Oliveira Silva M, Gregory JL, Ansari N and Stok KS (2020) Molecular Signaling Interactions and Transport at the Osteochondral Interface: A Review. Front. Cell Dev. Biol. 8:750. doi: 10.3389/fcell.2020.00750

INTRODUCTION

Within a lifetime joints can undergo changes and progressive degeneration as a result of natural ageing or injury. These are the primary risk factors for the development of osteoarthritis (OA), a painful and debilitating condition affecting millions worldwide (Felson et al., 2013; Sanchez-Adams et al., 2014). The joint is a complex structure that relies on mechanical and biological integrity to function properly. To investigate these events, mechanobiology has emerged as a field that can address the dynamic interactions between cells and their mechanical environment. Understanding

the complex interactions of the joint tissues, as well as the cellular, biochemical and mechanical responses at work, may provide insights into joint degeneration and OA (Lepage et al., 2019).

The joint is comprised largely of bone and cartilage, separated by an osteochondral interface that is comprised of deep layers of cartilage and the underlying subchondral bone. These individual components interact cooperatively to make a complex functional unit (Yuan et al., 2014). Due to the proximity of the joint layers, homeostasis is maintained through tightly regulated mechanoregulatory pathways that facilitate communication between tissues and responses to the environment (Li et al., 2013). Among the signaling molecules involved, transforming growth factor-β (TGF-β) and the protein Wnt, are key components in the development, growth, maintenance and repair of cartilage. Alterations in these pathways contribute to OA progression (Finnson et al., 2012).

In response to mechanical or biological stimuli, increased vascular activity and angiogenesis occurs in the subchondral bone. This process is largely mediated by vascular endothelial growth factor (VEGF), expressed by multiple sources within the joint. During OA, new blood vessels invade the deep layers of articular cartilage creating porous channels between the tissues. The newly formed channels increase the capacity for transport across the bone-cartilage interface, suggesting a direct path for the migration of biological factors and nutrients, thus enhancing the overall crosstalk and molecular interactions at the osteochondral interface (Greenwald and Haynes, 1969; Lane et al., 1977). Despite evidence for increased transport via vascular channels from the subchondral bone, the primary route for nutrients to access the extracellular matrix (ECM) and chondrocytes of the articular cartilage is via diffusion (Pan et al., 2009; Sharma et al., 2013; Villalvilla et al., 2013).

Both molecular size and mechanical loading affect diffusion transport rates at the osteochondral interface (Malinin and Ouellette, 2000; Sophia Fox et al., 2009; Di Luca et al., 2015). There is evidence to suggest an increase in molecular transport in OA, however, a lack of understanding of how materials transport to and from the tissues still remains, limiting our ability to develop new treatments for OA (Yuan et al., 2014). Since contrast agents may also be transported via diffusion through the cartilage ECM, contrast agent enhanced imaging modalities such as fluorescence microscopy, magnetic resonance imaging or X-ray computed tomography (CT), may serve as efficient, non-destructive techniques for investigating molecular transport at the osteochondral interface (Joshi et al., 2009; Kulmala et al., 2010; Choi and Gold, 2011; DiDomenico et al., 2018; Pouran et al., 2018). To date, few studies using contrast agent-based imaging have been performed to investigate solute transport through articular cartilage (Kulmala et al., 2010; Silvast et al., 2013; Arbabi et al., 2015; Kokkonen et al., 2017).

This review describes the structure and biological properties of the osteochondral interface, providing background for the reader. Followed by current knowledge on molecular interactions and transport at the osteochondral interface. Finally, we seek to highlight methods for investigating molecular transport, specifically with a view to understanding transport across the osteochondral interface and changes induced by disease progression.

THE OSTEOCHONDRAL INTERFACE IS A KEY STRUCTURE IN JOINT PATHOPHYSIOLOGY

The osteochondral interface is a gradient tissue that consists of articular cartilage ∼90%, calcified cartilage ∼5%, and subchondral bone ∼5% (**Figure 1**). These tissues present different structural, mechanical and biological properties allowing the individual components to interact cooperatively forming an integrated functional unit (Yuan et al., 2014; Longley et al., 2018).

The articular cartilage consists of three zones, beginning at the joint space and finishing at the tidemark: (1) superficial zone (at the articular surface); (2) transition/middle zone, and (3) radial/deep zone (Sophia Fox et al., 2009; Suri and Walsh, 2012). This is followed by the tidemark and adjoining calcified cartilage layer. The subchondral bone layer lies at the bottom and includes the subchondral bone plate (**Figure 1**).

Articular cartilage is an avascular and alymphatic tissue, composed of ECM and embedded chondrocytes. Chondrocytes constitute only 2% of the total volume in cartilage and are responsible for the synthesis of the ECM (Hunziker et al., 2002). As they are the sole cell type present, chondrocytes are essential for maintaining cartilage integrity, by responding to growth factors, mechanical loads, and other physicochemical stimuli (Muir, 1995; Akkiraju and Nohe, 2015).

The ECM is comprised largely of collagen type II and proteoglycans. These components retain water within the cartilage, providing strength and stabilization to the tissue (Sophia Fox et al., 2009). The composition of ECM, its water content, and cell density vary in the different layers. The superficial zone makes up ∼10–20% of articular cartilage thickness, has the highest density of chondrocytes, and collagen fibrils that are tightly packed and aligned parallel to the articular surface. It also has the highest water content (∼80%) and solute transport compared to other zones (Eyre, 2002; Akkiraju and Nohe, 2015).

The transition zone makes up ∼40–60% of cartilage thickness. This layer has a low density of chondrocytes with cells spherical in shape. The collagen fibers are thick and have an oblique orientation (Sophia Fox et al., 2009).

The deep zone makes up ∼30% of cartilage thickness. This layer has the highest level of proteoglycans and the lowest water content (∼60%). The chondrocytes are aligned in typical columns, perpendicular to the articular surface. Collagen fibers are thick and orientated parallel to the cell columns (Sophia Fox et al., 2009).

The layer that interfaces with the subchondral bone is the calcified cartilage, anchoring the articular cartilage to the bone with collagen fibers of the cartilage deep zone (Martel-Pelletier et al., 2008). The calcified layer is split into zones by the tidemark and presents characteristics of both cartilage (the deposition of

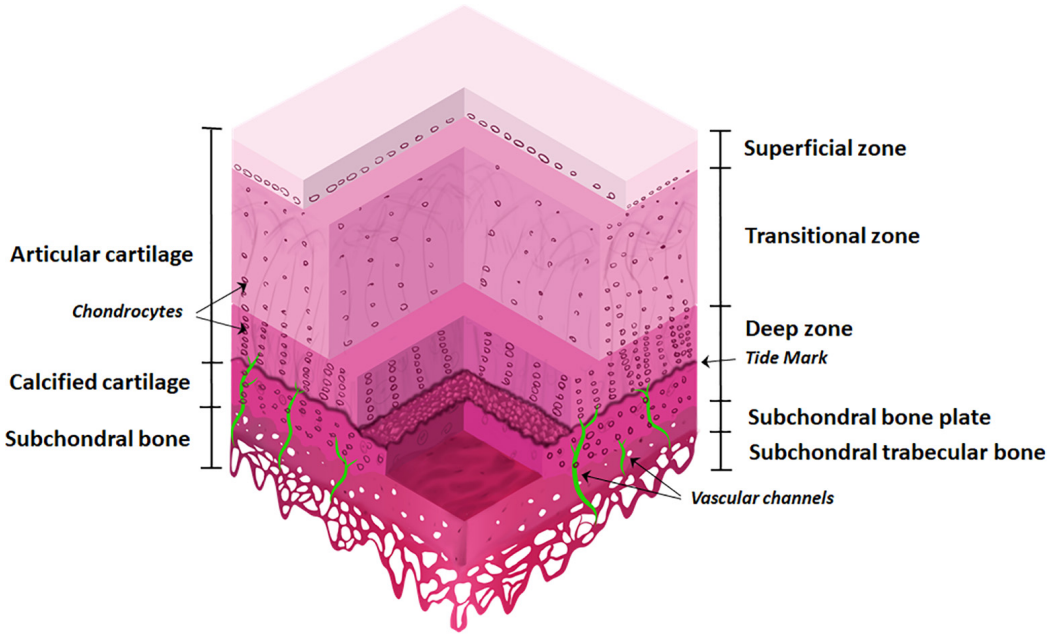

FIGURE 1 | The osteochondral interface and bone and cartilage zones. The osteochondral interface lies between the connecting layers of articular cartilage and subchondral bone. The articular cartilage consists of three zones: superficial zone, transitional zone, and deep zone and finishes at the tidemark. Below this lies the calcified cartilage layer. The subchondral bone is located below the calcified cartilage and consists of the subchondral bone plate and subchondral trabecular bone. Vascular channels lie within the subchondral bone.

collagen type X) and bone (presence of alkaline phosphatase and mineral deposits). It contains a very low density of hydrophobic chondrocytes (Martel-Pelletier et al., 2008).

The subchondral bone is comprised of both inorganic and organic components. Crystalline hydroxyapatite is the most abundant inorganic component of the bone matrix, while calcium, carbonate, phosphate and other inorganic elements are also present at low levels (Feng, 2009). The organic components are collagen type I fibers (90%), and proteins including enzymes, cytokines, and growth factors. The subchondral bone contains vessels and channels which are essential for supplying nutrients to the bone and potentially the deeper layers of cartilage, thus also providing transport pathways for signaling molecules and factors across the osteochondral interface (Robling et al., 2006; Li et al., 2013).

With the onset of OA (**Figure 2**), the subchondral bone plate begins to thicken and perforate. The bone is a poor-quality (low mineral) bone, the trabecular architecture alters, and bone cysts appear. In the cartilage, there is a breakdown in the collagen network, leading to swelling and eventual reduction in proteoglycan content, as well as fissures and cracks across the osteochondral interface. The tidemark becomes irregular. Additionally, bone remodeling stimulates new vascularization and nerve growth from already formed blood vessels and nerves in the subchondral bone (Goldring and Goldring, 2016; Lepage et al., 2019). These structural alterations are tightly linked to molecular signaling interactions at the osteochondral interface.

MOLECULAR SIGNALING INTERACTIONS AT THE OSTEOCHONDRAL INTERFACE

Among the diverse mechanoregulatory pathways involved in joint pathophysiology, TGF-β and Wnt play an integral role in both the maintenance and degradation of cartilage via signaling across the osteochondral interface. Specifically, deregulation of TGF-β and Wnt signaling causes instability in ECM structure and function, and alters chondrocyte development, contributing to OA progression (Finnson et al., 2012).

TGF-β

The TGF-β family are multipurpose growth factors that play a fundamental role in cartilage development, homeostasis and repair. They consist of up to 35 members including TGF-βs, bone morphogenetic proteins (BMPs), growth and differentiation factors (GDFs) and activins (Finnson et al., 2012; Thielen et al., 2019). To initiate signaling (**Figure 3**), growth factors bind to membrane-bound activin-like kinase receptors (ALK5 or ALK1), in turn activating SMAD2/SMAD3 phosphorylation or SMAD1/5/8 signaling pathways, respectively. The availability of TGF-β determines which signaling pathway is activated (Remst et al., 2014; van der Kraan, 2017). During regular physiological loading of healthy joints, readily available TGF-β will signal via the ALK5-SMAD2/3 pathway, thus driving a protective role for cartilage by maintaining chondrocyte metabolism and survival.

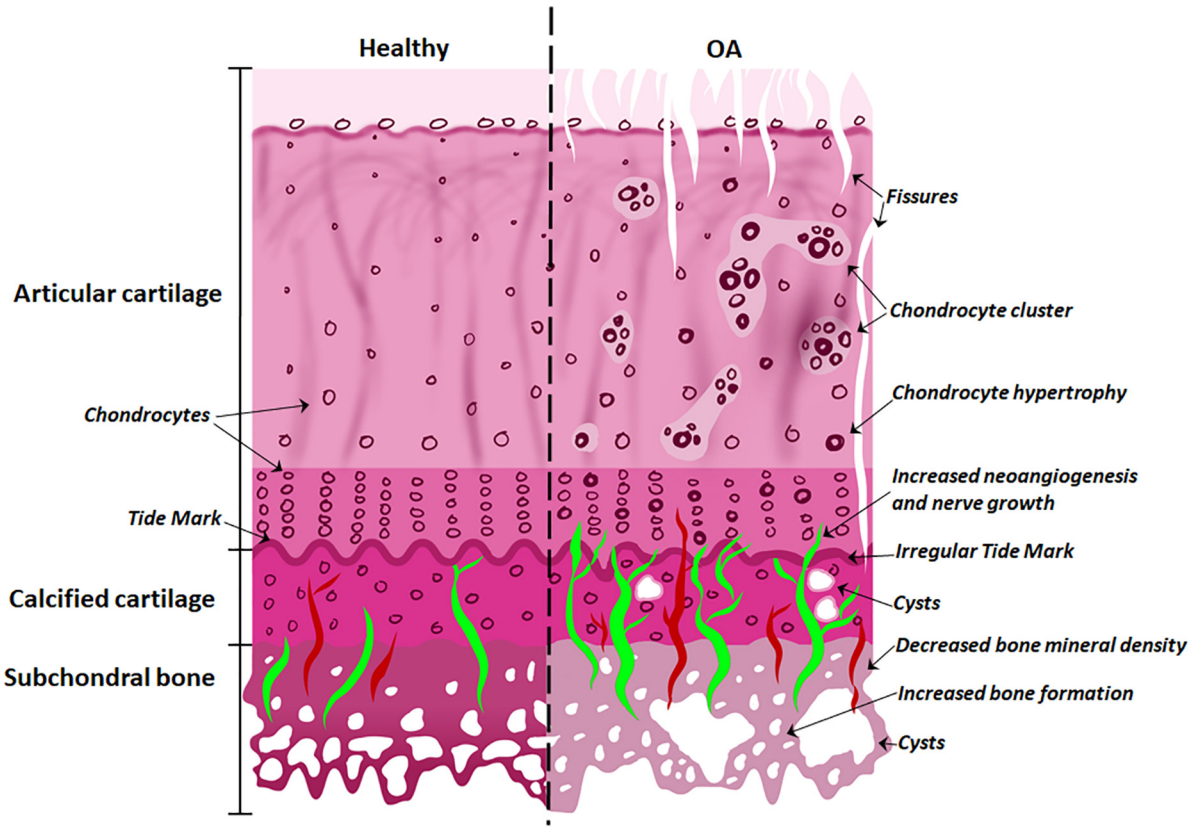

FIGURE 2 | Differences between normal and osteoarthritic osteochondral tissues. The features of the healthy osteochondral interface are homogeneous articular surface, normal chondrocytes and vascularization of the subchondral bone. With the onset of OA, the articular surface exhibits fissures; chondrocyte hypertrophy and clusters; while cysts appear in the calcified cartilage; with increased angiogenesis and nerve growth penetrating the tide mark; and decreased bone mineral density and increased bone formation in the subchondral bone.

In a pathologic setting such as OA or in aging, the role of TGF-β may shift and the ALK1-SMAD1/5/8 pathway dominates. This causes a hypertrophic phenotype in chondrocytes, resulting in an imbalance in ECM turnover (Retting et al., 2009; Li et al., 2010; Chen et al., 2012). The TGF-β/SMAD signaling pathways are essential for maintaining cartilage integrity and importantly, chondrocyte function.

The importance of TGF-β in OA has been well established in numerous studies to date. Animal models with genetic alterations in signaling molecules of the TGF-β pathway including *Smad* gene mutations, ALK5 knock-outs, and overexpression of TGF-β receptor II develop features of OA, including cartilage damage and alterations in chondrocyte differentiation (Serra et al., 1997; Yang et al., 2001; Blaney Davidson et al., 2006; Shen et al., 2013; Wang et al., 2017). Mice with modifications to the *Smad3* gene show a loss of articular cartilage, reduced proteoglycans and increased chondrocyte differentiation (Yang et al., 2001). Conditional knockout mice for TGF-β receptor II in chondrocytes specifically, developed a severe form of OA-like disease with hypertrophic chondrocytes and degraded cartilage (Shen et al., 2013).

TGF-β signaling also contributes to cartilage maintenance and integrity by controlling inflammatory cytokine production. The proinflammatory cytokines, IL-1β and TNF-α are produced by multiple sources in joint tissue including chondrocytes (Wojdasiewicz et al., 2014). They are potent inducers of matrix metalloproteinases (MMPs) that are responsible for cleaving ECM components to maintain normal matrix remodeling and excessive degradation of cartilage during OA (Vincenti and Brinckerhoff, 2001; Burrage et al., 2006; Wojdasiewicz et al., 2014). The proteases MMP-1 and MMP-13 are among the most prevalent in OA cartilage and target collagens I, II, and III, thus contributing directly to disease progression (Mitchell et al., 1996; Vincenti et al., 1998; Martel-Pelletier et al., 2008). Another key activator of MMPs in OA tissue is the Wnt glycoproteins. The Wnt signaling pathway has a key role in maintaining cartilage and bone homeostasis (Zhou et al., 2017).

Wnt Signaling

One of the common pathways that Wnt molecules use to drive their downstream transcriptional events is the canonical signaling pathway (**Figure 3**). Wnt binds to its receptors, Frizzled (Fz) and low-density lipoprotein receptor-related protein 5/6 (LRP5/6), activating β-catenin synthesis which in turn accumulates in the cell nucleus for use in gene transcription. In the absence of Wnt, β-catenin is degraded and prevented from

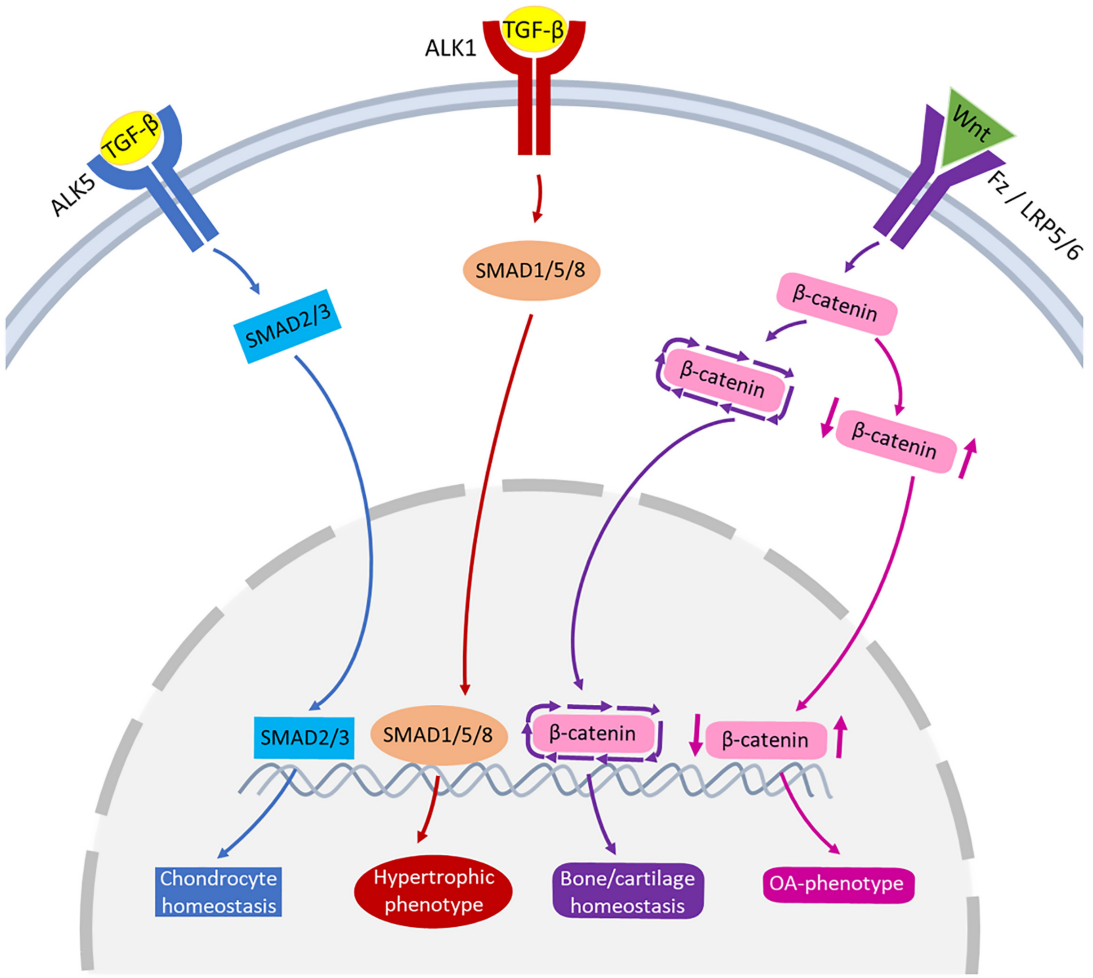

FIGURE 3 | Schematic representation of the signaling pathways of TGF-β and Wnt involved in joint pathophysiology. TGF-β can bind to ALK5, that activates SMAD2/3 leading to chondrocyte homeostasis (blue pathway arrows). TGF-β can also bind to ALK1, activating SMAD1/5/8 that may lead to hypertrophic phenotype of chondrocytes (red pathway arrows). Wnt binds to receptors Fz or LRP5/6 activating β-catenin synthesis. A healthy expression of β-catenin leads to bone/cartilage homeostasis (purple pathway arrows) while imbalanced β-catenin can result in an OA-phenotype (pink pathway arrows).

translocating to the cell nucleus (Krause and Gregory, 2012; Li et al., 2012). There is a fine balance between the level of Wnt-Fz activation and the accumulation of β-catenin in cells that can escalate to an OA-like phenotype. Both excessive and insufficient Wnt activation, as well as increased and reduced β-catenin signaling, can result in cartilage degradation, chondrocyte apoptosis, subchondral bone damage and osteophyte formation (Lories et al., 2007; Zhu et al., 2008, 2009; Zhou et al., 2017).

Mice with a chondrocyte-specific transgene for β-catenin and T cell factor (ICAT) have reduced β-catenin signaling that causes significant articular cartilage damage and high levels of chondrocyte apoptosis (Zhu et al., 2008). Similarly, preventing the natural degradation of β-catenin (which occurs in the absence of Wnt-Fz activation) by inhibiting the kinase, GSK3β, results in reduced β-catenin signaling (Miclea et al., 2011). Mouse cultured metatarsal explants with the GSK3β inhibitor had reduced chondrocyte proliferation, loss of proteoglycans and cartilage degradation. Microarray analysis showed increased MMP expression and down-regulation of cartilage ECM proteins (Miclea et al., 2011). On the contrary, transgenic mice with conditional β-catenin activation have an increase in β-catenin levels in articular chondrocytes. This causes an overall accelerated OA-like phenotype with increased rates of chondrocyte development (Zhu et al., 2009).

TRANSPORT AT THE OSTEOCHONDRAL INTERFACE

The presence of vascular networks in the subchondral bone and, to a lesser extent, the calcified cartilage regions of normal healthy joints has been well established (Bullough and Jagannath, 1983). Early evidence for these transport pathways was observed using electron microscopy in healthy tissue. This included the appearance of holes with vessel-like features in the subchondral bone of human tibias (Duncan et al., 1987). Studies done in the

joints of rabbits and canines further supported these observations showing small vascular canals and capillaries running through the subchondral bone region. Interestingly, the majority of these structures were not present in calcified or deeper layers of the cartilage (Clark, 1990).

In contrast, during the early stages of OA (Botter et al., 2011; Goldring and Goldring, 2016), bone remodeling stimulates new vascularization from already formed blood vessels in the subchondral bone (**Figure 2**). Histological evidence in human knee cartilage has shown porous channel formation and accompanying blood vessels that pass through the calcified cartilage, across the tidemark and into the deep zone of articular cartilage (Suri et al., 2007; Walsh et al., 2007). Models of OA in both rabbits and rats as well as human clinical samples have also shown a positive correlation between increasing angiogenic activity and increased vascular invasion in articular cartilage in the early stages of disease (Franses et al., 2010; Ashraf et al., 2011; Saito et al., 2012; Li et al., 2013).

Despite the evidence for transport across the osteochondral interface via *de novo* vasculature formation penetrating the cartilage tissue during OA, there is currently no functional evidence to support this route of transfer, and thus diffusion of solutes and nutrients is considered the primary method of transport.

Solute transport through the ECM is crucial to chondrocyte physiology and maintenance of biochemical and mechanical integrity (Evans and Quinn, 2005). Solute physicochemical properties (size, shape, charge, and concentration), mechanical environment (such as loading or unloading), and tissue properties (composition and structure) are all factors that contribute to effective molecular transport at the osteochondral interface (Knothe Tate et al., 1998; Knothe Tate and Knothe, 2000; Farnum et al., 2006; Serrat et al., 2009, 2014; Knothe Tate et al., 2012; Ngo et al., 2018). Changes in tissue structures during OA would affect solute diffusion kinetics in the osteochondral interface due to altered subchondral bone porosity, tide mark perforations and cartilage permeability (**Figure 2**).

Solute Physicochemical Effect on Molecular Transport

Molecular size is one of the most important factors determining the nature and rate of transport, affecting the interaction of the molecule and the pores in the cartilage. There is an inverse relationship between the molecular size and its diffusivity (also called mass diffusivity or diffusion coefficient) (Leddy and Guilak, 2003). Diffusivity is the rate of material transport; i.e., quantity of a substance fluxing through a surface per unit of time. Molecular size also has an inverse correlation to partition coefficient, which is the ratio of the concentrations of a solute in two layers after equilibrium (Kokkonen et al., 2017).

Since different layers of articular cartilage have different structures, diffusivity of a single molecule varies as it passes through these zones. An *ex vivo* study of the transport kinetics of different size dextrans showed that small and large dextrans (with radii of ∼2 and 15 nm, respectively) have their highest diffusivity in the superficial zone, however, surprisingly, the middle sizes (with radii of ∼6–7 nm) had the highest diffusivity in the middle and deep zones (Shoga et al., 2017).

In contrast to cartilage, bone tissue has both vascular networks and lacunar-canalicular systems that enable transport of nutrients from blood circulation to osteocytes. To affect osteocytes, it is critical for macromolecules to be able to pass through the canaliculi to reach the cells. In humans, the average canalicular diameter has been shown to be ∼315 nm, while the diameter of the osteocyte dendritic process is ∼145 nm, leaving a pericellular space surrounding each process of ∼85 nm (Dallas et al., 2013). Murine samples with an average ∼260 nm canalicular diameter and ∼100 nm osteocyte dendritic process, have a similar pericellular space (∼80 nm), suggesting that molecules larger than this size cannot pass through the lacunar-canalicular system (Wang, 2018).

Studies have shown that the rate of transport depends on both size and shape of solute (summarized in **Table 1**). This was assessed by using fluorescent tracers between ∼375 and 43,000 Da in size and a range of shapes (linear, spherical and globular). Transport of larger and linear molecules in bone, was slower than smaller molecules of the same shape and also globular molecules of similar molecular weight, respectively (Li et al., 2009).

Due to the close association between bone and articular cartilage, studies have also investigated the solute transport at the osteochondral interface. Solute transport was assessed using sodium fluorescein (376 Da) and fluorescence loss induced by photobleaching (FLIP) methods. The results showed a significantly lower (three to four-fold) diffusivity across the osteochondral interface, compared to that of calcified cartilage (Pan et al., 2009). Calculated average diffusion within bone tissue based on previously published results of diffusion with the same tracer in the lacunar-canalicular system, assuming the porosity of the lacunar-canalicular system in the subchondral bone is 5–10% (Wang et al., 2005). By comparing their result with this average diffusivity in subchondral bone, they suggested that calcified cartilage and subchondral bone both have high permeability.

This provides new insight into diffusion at the osteochondral interface however, since these two studies have used different methods for measuring diffusion, a direct comparison is misleading. In addition, calculations and mathematical models proposed by the authors had many assumptions including a homogeneous matrix, the amount of porosity of the lacunar-canalicular system, and the neglect of the other surrounding cells (Pan et al., 2009). Further research is required to compare the diffusion within the subchondral bone and cartilage to that at the osteochondral interface. Overall, the results suggest that solute transport does occur at the osteochondral interface. Electron microscopy of the calcified cartilage matrix also shows non-mineralized regions (∼22% volume fraction), which contains porous channels that may enable solute transport (Pan et al., 2009).

Molecular transport has also been quantified by injecting different size fluorescent tracers in aged guinea pigs, a natural model for OA (Ngo et al., 2018). After a single intracardiac injection of low (10 kDa) and high (70 kDa) molecular weight tracer, the 70 kDa tracer was abundantly detected in the marrow

TABLE 1 | Overview of studies testing solute diffusion kinetics within bone-cartilage.

References	Technique	Specimen	Tracer	Parameters
Pan et al., 2009	Fluorescence loss induced by photobleaching (FLIP)	Distal femur, C57BL/6J mice, *ex vivo*	Sodium fluorescein 376 Da	Diffusion coefficient
Evans and Quinn, 2005	Confocal microscopy, stage equipped with compression system	Osteochondral cores from bovine humeral heads	TMR 430 Da, Oregon Green 412 Da, AF488 hydrazide 570 Da, Rhodamine Green 10 kDa, Dextran-TMR 10 kDa, Dextran-TMR anionic 10 kDa	Diffusion coefficient
Knothe Tate et al., 1998	Fluorescence microscopy	Metacarpal and tibiae, Sprague–Dawley rats, *ex vivo*	Procion red 300–400 MW, Microperoxidase 1800 MW	Tracer distribution
Ngo et al., 2018	Microtome-blockface episcopic imaging system	Femoral and posterior tibae, Dunkin-Hartley guinea pigs, *ex vivo*	Texas-red 70 kDa, Rhodamine-green 10 kDa	Tracer distribution, cartilage and bone morphology
Serrat et al., 2014	Multiphoton microscopy	Proximal tibia, C57BL/6J mice, *in vivo*	Dextran 10, 40, 70 kDa	Tracer accumulation in growth plate cartilage
Serrat et al., 2009	Multiphoton microscopy	Hindlimbs, Col II/GFP mice, *in vivo*	Fluorescein 332.3 Da	Tracer accumulation in growth plate cartilage
Leddy and Guilak, 2003	Fluorescence recovery after photobleaching (FRAP)	Porcine articular cartilage explants	Dextran 3, 40, 70, 500 kDa	Diffusion coefficient
Shoga et al., 2017	Fluorescence correlation spectroscopy (FCS) and raster image correlation spectroscopy (RICS)	Bovine articular cartilage explants	Dextran 3, 10 kDa	Diffusion coefficient
Li et al., 2009	FRAP	Tibiae, C57BL/6J mice, *in situ*	Sodium fluorescein, Dextran-3, 10 k, Parvalbumin 12 kDa, Ovalbumin 43 kDa	Diffusion coefficient
Arkill and Winlove, 2008	Fluorescence microscopy	Equine cartilage and bone explants	Rhodamine B base (cationic), rhodamine B (neutral polar) Sodium fluorescein Fluorescein (all low MW)	Diffusion coefficient
Pan et al., 2012	FLIP	Knee joints, C57BL/6J mice. Aged, spontaneous OA and DMM, *ex vivo*	Sodium fluorescein 376 Da	Diffusivity

cavity. In contrast, the 10 kDa tracer was detected in meniscus, ligament, and tendon, while none of these tracers were found in articular cartilage. Volumes of tissue containing 10 kDa tracer were significantly lower in older animals compared to younger ones, indicating that molecular transport decreases with age (Ngo et al., 2018).

These studies suggest that tissue sieving properties of the osteochondral interface determine the movement of molecules based on their size. Small molecules can diffuse through the osteochondral interface, however, this transport is altered with age and disease. In contrast, large molecules are unlikely to penetrate some tissues regions in a healthy osteochondral interface, that become available through structural alterations with disease (Ngo et al., 2018). Diffusive transport may also be increased by applying a mechanical load.

Mechanical Loading Effect on Molecular Transport

Mechanical loading can increase the diffusive transport of molecules across the osteochondral interface. For example, mechanical loading of bone increased the transport and velocity of parvalbumin, a low molecular weight protein (12.3 kDa), which has a size similar to signaling molecules such as sclerostin, in the osteocyte-canaliculi network (Wang et al., 2013).

Molecular transport processes and fluid flow within bone under controlled mechanical loading conditions have been studied on sheep metacarpus using an *ex vivo* perfusion model (Knothe Tate and Knothe, 2000). In this study, before applying mechanical loading, a bolus of tracer was introduced intra-arterially. After loading, the concentration of tracer was significantly higher in loaded bone verses unloaded controls, suggesting that loading can increase molecular transport in bones.

The effect of mechanical loading on transport via the ulna radius interosseous membrane ligament was investigated using different molecular weight fluorescent dextrans. Mechanical loading increased penetration of low molecular weight dextrans (3–500 kDa) through the matrix ligament (Knothe Tate et al., 2012). However, high molecular weight dextrans (2,000 kDa) were only observed in vascular and lymphatic spaces of the bone. They were not detected in the matrix ligament, or in the absence of and after mechanical loading (Knothe Tate et al., 2012). This suggests that although loading increases the magnitude of molecular transport, it cannot overcome the size barrier of the lacunar-canalicular system.

These studies suggest that load-induced fluid flow represents a potential mechanism to increase molecular transport at the osteochondral interface. However, static compression reduces fluid volume and increases charge density of cartilage,

resulting in an overall decrease in diffusion, indicating tissue properties also affect diffusive transport of molecules at the osteochondral interface.

Tissue Properties Effect on Molecular Transport

Under physiological conditions, ECM composition can affect the diffusion of large molecules. This is due to the density and orientation of collagen fibres, whereby higher density and orientation opposite to the direction of solute transport, can reduce solute mobility and diffusivity.

Changes in ECM due to mechanical injury of articular cartilage explants saw increased diffusion of a range of fluorescent solutes, including fluorescein isothiocyanate, dextrans, insulin, chondroitin sulfate and the X-ray contrast agent sodium iodide (Chin et al., 2013). Since chondrocytes were not functional in these explants, the results highlight a role for solute-matrix interactions, independent of the role of cells. Although OA is associated with changes in the gene expression and activity of chondrocytes and bone cells, it is also associated with structural changes at the osteochondral interface, such as loss of proteoglycans, increased subchondral bone thickness, increased vascularization, formation of osteophytes and microcracks.

At early stage OA, high bone turnover causes bone loss and structural changes in the subchondral bone. This is followed by a reduction in bone remodeling, which results in sclerosis of subchondral bone (Bellido et al., 2010). These changes are expected to affect the molecular transport of signaling molecules and crosstalk of these tissues during disease. Interestingly, measuring diffusion at the osteochondral interface and in calcified cartilage of two animal models of mild OA (aging mice and surgical destabilization of the medial meniscus, DMM) showed no significant difference between diffusivity of OA mice and controls (Pan et al., 2009). This might be due to the limitation of the FLIP method for studying large-scale structures. Consequently, improved and non-invasive high-resolution techniques are required to address this issue and track the changes in molecular transport at the osteochondral interface *in vivo*.

THE USE OF CONTRAST AGENT ENHANCED IMAGING TECHNIQUES TO STUDY MOLECULAR TRANSPORT IN CARTILAGE

Different techniques have been used to study molecular transport at the osteochondral interface, however, their application has been limited to *ex vivo* studies. This includes the use of fluorescence recovery after photobleaching (FRAP) which allows measurement of diffusion of fluorescently labeled molecules. Although FRAP has been be used to study small areas of cartilage or biofabricated scaffolds, it is not feasible for use in large-scale for cartilage tissue due to its complex structure (Nettles et al., 2004). Diffusion cell experiments and solute absorption/desorption techniques measure the transport across the tissue *ex vivo* and cannot be used *in vivo* since the setup relies on optical microscopy. Moreover, they are not accurate for heterogenous tissues, such as articular cartilage, which is comprised of different layers with different structural properties.

Among the methods that have been proposed so far, CT imaging of articular cartilage can be used *in vivo* and at large scale (Joshi et al., 2009; Kulmala et al., 2010; Choi et al., 2019). Contrast agent-based clinical imaging of articular cartilage, such as CT imaging, relies on the transport of contrast agents to and through the cartilage ECM. This method of studying molecular transport can be used as a diagnostic technique to track changes at the osteochondral interface in degenerative diseases, such as OA. It can also provide useful information to design therapeutic molecules and drug delivery systems for these conditions (DiDomenico et al., 2018). Diffusion through the articular surface is the primary route of transport for contrast agents within cartilage (Bashir et al., 1996; Nelson et al., 2018; Bhattarai et al., 2020; Freedman et al., 2020; Meng et al., 2020). A summary of the relevant studies using contrast agent-based diffusion methods for micro-CT is shown in **Table 2**.

Diffusion of Contrast Agents Within Cartilage

Measuring the diffusion of four contrast agents, ioxaglate, gadopentetate, iodide and gadodiamide in bovine articular cartilage, showed that the diffusion coefficients of these agents were relatively low (142.8–253.7 m^2/s). However, diffusion through the articular surface was faster than deep cartilage (Kulmala et al., 2010). In addition, iodide diffuses into cartilage significantly faster than the other three contrast agents in both surface and deep zones, likely due to its atomic size (Kulmala et al., 2010). This study suggests that the diffusion coefficient correlates with cartilage composition, which may be used as a tool for tracking cartilage structural changes.

Differences in transport of solutes across cartilage zones has also been investigated by combining experimental and modeling approaches (Arbabi et al., 2015). Axial diffusion of the neutral solute, iodixanol into cartilage was monitored using calibrated microCT images for up to 48 h. A biphasic-solute computational model was fitted to the experimental data to determine its diffusion coefficients in cartilage. Cartilage was modeled either using one single diffusion coefficient (single-zone model) or using three diffusion coefficients corresponding to superficial, middle, and deep cartilage zones (multizone model). The results showed that the diffusion coefficient of iodixanol in the superficial zone was at least one order of magnitude higher than that of the middle zone. One of the main differences between these zones is their amount of glycosaminoglycan (GAG) content. By having a negative charge, GAG repel the contrast agents with negative charge (inverse correlation) and bind to the ones with positive charge (direct correlation). However, since iodixanol is neutral, GAG content alone cannot explain the large differences between the diffusion coefficients of the different cartilage zones (Arbabi et al., 2015). This finding suggests that diffusion across different zones of the cartilage is affected not only by the charge of solutes and GAG content of cartilage, but also by ECM composition

TABLE 2 | Overview of studies using contrast agent-based diffusion within cartilage.

References	Technique	Specimen type	Contrast agent	Parameters
Kulmala et al., 2010	Peripheral quantitative computed tomography (pQCT)	Articular cartilage discs from bovine patella	Ioxaglate, Gadopentetate, Iodide, Gadodiamide	Diffusion coefficient
Arbabi et al., 2015	MicroCT	Equine osteochondral explants	Iodixanol	Diffusion coefficient
Kokkonen et al., 2017	MicroCT	Articular cartilage discs from bovine patella	Iodine, Gd-DTPA	Partition coefficient and diffusion fluxes
Silvast et al., 2013	pQCT	Articular cartilage discs from bovine patella	Ioxaglate, iodine	Diffusion and partition coefficient
Freedman et al., 2020	MicroCT	Metacarpophalangeal joint from cadaveric hands	Ioxaglate, CA4+	Contrast agent tissue concentration, time to reach equilibrium
Bhattarai et al., 2020	MicroCT	Osteochondral plugs from human cadaver	CA4+, gadoteridol	Contrast agent tissue concentration and partition
Meng et al., 2020	MicroCT	Osteochondral plugs from human tibial plateaus	Ohexol	Contrast agent tissue concentration, diffusion flux and diffusion coefficients
Nelson et al., 2018	MicroCT	Equine osteochondral plugs from the femoral condyles	CA4+	Diffusion time constant and time to reach equilibrium
Kokkonen et al., 2011	MicroCT	Osteochondral plugs from bovine patella	Ioxaglate (Hexabrix), Sodium iodide (NaI)	Diffusion coefficient, diffusion flux

and/or structure, such as water content and the orientation of collagen fibers. Diffusion across cartilage may also be affected by concentration of the contrast agent.

Alteration of ECM structure and solute-matrix interactions due to cartilage injuries additionally affects solute transport through cartilage (Kokkonen et al., 2011; Chin et al., 2013). Effects of mechanical injury on transport of negatively charged contrast agents in cartilage has been investigated (Kokkonen et al., 2017). Using cartilage plugs injured by mechanical compression protocol, effective partition coefficients and diffusion fluxes of different contrast agents were measured using high resolution microCT imaging. For all contrast agents studied (Sodium iodide, sodium diatrizoate and Gd-DTPA) effective diffusion fluxes increased significantly, particularly at early time points of the diffusion process. Moreover, the results suggest that alterations in contrast agent diffusion flux provides a more sensitive indicator for assessment of cartilage matrix integrity than partition coefficient and the equilibrium distribution of solute.

Effect of Concentration on the Transport of Contrast Agents in Cartilage

The effect of concentration on diffusion of anionic contrast agents like ioxaglate and iodide in cartilage have been investigated *in vitro* (Silvast et al., 2013). Samples were imaged with a clinical peripheral quantitative CT scanner before immersion in contrast agent, and after several time points in the diffusion and partition coefficients of these contrast agents were not affected by concentration at the equilibrium. One possible explanation given by authors for these results is that dependency of diffusion to concentration is only minor in diluted solutions (Silvast et al., 2013). Changes in contrast agent diffusion reflect the changes in composition and structure of articular cartilage (Leddy and Guilak, 2003; Evans and Quinn, 2005; Arkill and Winlove, 2008). However, clinical use of contrast agents for this purpose, requires highly consistent concentration before their administration.

Although these *ex vivo* microCT studies provide insights into the diffusion transport of contrast agents through articular cartilage, it is unknown whether the same mechanisms are relevant in *in vivo* transport of molecules at the osteochondral interface. *In vivo* experiments would enable time-lapse study of changes, and correlation of these changes with OA progression.

CONCLUSION AND PERSPECTIVES

The osteochondral interface plays a critical role in joint function and disease by connecting joint compartments and allowing the exchange of signaling and nutritional molecules between them. Chondrocytes and osteocytes sense and respond to chemical and mechanical stimuli by releasing the signaling molecules that they produce. The exchange of molecules between these two tissues provides an integrated response to environmental stimuli affecting joint homeostasis.

Studies using a novel imaging method based on FLIP have shown intravenous administration of fluorescent molecules can diffuse through the bone-cartilage interface (Knothe Tate et al., 1998; Pan et al., 2009). Using this method, transport capacity was higher in mouse models of OA than normal joints (Pan et al., 2012), however, this approach is not compatible with time-lapse measurement. Capturing transport variations over time is the next step toward expanding the knowledge of OA pathways. Coupling mechanical tests and microCT longitudinal measurement approach may enable measurement of joint remodeling responses at both organ and tissue levels. It may also provide insights into the association between molecular transport alteration and joint disease progress under mechanical loading.

Currently, there is no single preclinical imaging modality available for imaging molecular transport and its correlation

with the structural changes of the osteochondral interface at the onset and during the progression of joint diseases, such as OA. Capturing *in vivo* molecular transport over time in the osteochondral interface is the next step toward expanding the knowledge of OA nutrient pathways.

To achieve this goal, a non-toxic contrast agent for high-resolution molecular transport imaging is desirable for imaging *in vivo* molecular transport changes in the osteochondral interface. MicroCT is used for capturing high resolution structural details of cartilage and bone (Stok et al., 2016). By using a non-toxic contrast agent capable of diffusing through the osteochondral interface, it could be possible to track *in vivo* molecular transport and structural changes of the tissues. The fundamental knowledge provided by this method may be beneficial for designing advance drug delivery systems for joint disorders. This method could be also be used for time-course studies, at the research level, minimizing the number of animals used per study, and providing improved controls for interpreting results. In addition, this method would be non-invasive, and a promising diagnostic tool to track structural changes of cartilage with the progress of disease in subjects, in a longitudinal manner.

AUTHOR CONTRIBUTIONS

KS and MO conceived and designed the review. MO drafted the manuscript. All authors contributed to the manuscript and critically reviewed the manuscript prior to submission.

FUNDING

This work was supported by the Discovery Projects scheme of the Australian Research Council (DP180101838) and a 2018 Selby Research Award.

REFERENCES

Akkiraju, H., and Nohe, A. (2015). Role of chondrocytes in cartilage formation, progression of osteoarthritis and cartilage regeneration. *J. Dev. Biol.* 3, 177–192. doi: 10.3390/jdb3040177

Arbabi, V., Pouran, B., Weinans, H., and Zadpoor, A. A. (2015). Transport of neutral solute across articular cartilage: the role of zonal diffusivities. *J. Biomech. Eng.* 137:071001. doi: 10.1115/1.4030070

Arkill, K., and Winlove, C. (2008). Solute transport in the deep and calcified zones of articular cartilage. *Osteoarthritis Cartilage* 16, 708–714. doi: 10.1016/j.joca.2007.10.001

Ashraf, S., Mapp, I., and Walsh, D. A. (2011). Contributions of angiogenesis to inflammation, joint damage, and pain in a rat model of osteoarthritis. *Arthritis Rheum.* 63, 2700–2710. doi: 10.1002/art.30422

Bashir, A., Gray, M. L., and Burstein, D. (1996). Gd-DTPA2- as a measure of cartilage degradation. *Magn. Reson. Med.* 36, 665–673. doi: 10.1002/mrm.1910360504

Bellido, M., Lugo, L., Roman-Blas, J. A., Castaneda, S., Caeiro, J. R., Dapia, S., et al. (2010). Subchondral bone microstructural damage by increased remodelling aggravates experimental osteoarthritis preceded by osteoporosis. *Arthritis Res. Ther.* 12:R152. doi: 10.1186/ar3103

Bhattarai, A., Pouran, B., Makela, J. T. A., Shaikh, R., Honkanen, M. K. M., Prakash, M., et al. (2020). Dual contrast in computed tomography allows earlier characterization of articular cartilage over single contrast. *J. Orthop. Res.* doi: 10.1002/jor.24774

Blaney Davidson, E. N., Vitters, E. L., van der Kraan, M., and van den Berg, W. B. (2006). Expression of transforming growth factor-beta (TGFbeta) and the TGFbeta signalling molecule SMAD-2P in spontaneous and instability-induced osteoarthritis: role in cartilage degradation, chondrogenesis and osteophyte formation. *Ann. Rheum. Dis.* 65, 1414–1421. doi: 10.1136/ard.2005.045971

Botter, S. M., van Osch, G. J. V. M., Clockaerts, S., Waarsing, J. H., Weinans, H., and van Leeuwen, J. T. M. (2011). Osteoarthritis induction leads to early and temporal subchondral plate porosity in the tibial plateau of mice an in vivo microfocal computed tomography study. *Arthritis Rheum.* 63, 2690–2699. doi: 10.1002/art.30307

Bullough, G., and Jagannath, A. (1983). The morphology of the calcification front in articular cartilage. Its significance in joint function. *J. Bone Joint Surg. Br.* 65, 72–78. doi: 10.1302/0301-620x.65b1.6337169

Burrage, S., Mix, K. S., and Brinckerhoff, C. E. (2006). Matrix metalloproteinases: role in arthritis. *Front. Biosci.* 11, 529–543. doi: 10.2741/1817

Chen, C. G., Thuillier, D., Chin, E. N., and Alliston, T. (2012). Chondrocyte-intrinsic Smad3 represses Runx2-inducible matrix metalloproteinase 13 expression to maintain articular cartilage and prevent osteoarthritis. *Arthritis Rheum.* 64, 3278–3289. doi: 10.1002/art.34566

Chin, H. C., Moeini, M., and Quinn, T. M. (2013). Solute transport across the articular surface of injured cartilage. *Arch. Biochem. Biophys.* 535, 241–247. doi: 10.1016/j.abb.2013.04.011

Choi, D. J., Choi, S. I., Choi, B. R., Lee, Y. S., Lee, D. Y., and Kim, G. S. (2019). Cartilage protective and anti-analgesic effects of ALM16 on monosodium iodoacetate induced osteoarthritis in rats. *BMC Complement Altern. Med.* 19:325. doi: 10.1186/s12906-019-2746-7

Choi, J. A., and Gold, G. E. (2011). MR imaging of articular cartilage physiology. *Magn. Reson. Imaging Clin. N. Am.* 19, 249–282. doi: 10.1016/j.mric.2011.02.010

Clark, J. M. (1990). The structure of vascular channels in the subchondral plate. *J. Anat.* 171, 105–115.

Dallas, S. L., Prideaux, M., and Bonewald, L. F. (2013). The osteocyte: an endocrine cell and more. *Endocrine Rev.* 34, 658–690. doi: 10.1210/er.2012-1026

Di Luca, A., Blitterswijk, C. Van, and Moroni, L. (2015). The osteochondral interface as a gradient tissue: from development to the fabrication of gradient scaffolds for regenerative medicine. *Birth Defects Res. C Embryo Today* 105, 34–52. doi: 10.1002/bdrc.21092

DiDomenico, C. D., Lintz, M., and Bonassar, L. J. (2018). Molecular transport in articular cartilage – what have we learned from the past 50 years? *Nat. Rev. Rheumatol.* 14, 393–403. doi: 10.1038/s41584-018-0033-5

Duncan, H., Jundt, J., Riddle, J. M., Pitchford, W., and Christopherson, T. (1987). The tibial subchondral plate. A scanning electron microscopic study. *J. Bone Joint Surg. Am.* 69, 1212–1220. doi: 10.2106/00004623-198769080-00015

Evans, R. C., and Quinn, T. M. (2005). Solute diffusivity correlates with mechanical properties and matrix density of compressed articular cartilage. *Arch. Biochem. Biophys.* 442, 1–10. doi: 10.1016/j.abb.2005.07.025

Eyre, D. (2002). Collagen of articular cartilage. *Arthritis Res.* 4, 30–35.

Farnum, C. E., Lenox, M., Zipfel, W., Horton, W., and Williams, R. (2006). In vivo delivery of fluoresceinated dextrans to the murine growth plate: imaging of three vascular routes by multiphoton microscopy. *Anat. Rec. A Discov. Mol. Cell. Evol. Biol.* 288, 91–103. doi: 10.1002/ar.a.20272

Felson, D. T., Niu, J., Yang, T., Torner, J., Lewis, C. E., Aliabadi, P., et al. (2013). Physical activity, alignment and knee osteoarthritis: data from MOST and the OAI. *Osteoarthritis Cartilage* 21, 789–795. doi: 10.1016/j.joca.2013.03.001

Feng, X. (2009). Chemical and biochemical basis of cell-bone matrix interaction in health and disease. *Curr. Chem. Biol.* 3, 189–196. doi: 10.2174/187231309788166398

Finnson, K. W., Chi, Y., Bou-Gharios, G., Leask, A., and Philip, A. (2012). TGF-b signaling in cartilage homeostasis and osteoarthritis. *Front. Biosci. (Schol Ed)* 4, 251–268. doi: 10.2741/s266

Franses, R. E., McWilliams, D. F., Mapp, I., and Walsh, D. A. (2010). Osteochondral angiogenesis and increased protease inhibitor expression in OA. *Osteoarthritis Cartilage* 18, 563–571. doi: 10.1016/j.joca.2009.11.015

Freedman, J. D., Ellis, D. J., Lusic, H., Varma, G., Grant, A. K., Lakin, B. A., et al. (2020). dGEMRIC and CECT comparison of cationic and anionic contrast agents in cadaveric human metacarpal cartilage. *J. Orthop. Res.* 38, 719–725. doi: 10.1002/jor.24511

Goldring, S. R., and Goldring, M. B. (2016). Changes in the osteochondral unit during osteoarthritis: structure, function and cartilage-bone crosstalk. *Nat. Rev. Rheum.* 12, 632–644. doi: 10.1038/nrrheum.2016.148

Greenwald, A. S., and Haynes, D. W. (1969). A pathway for nutrients from the medullary cavity to the articular cartilage of the human femoral head. *J. Bone Joint Surg. Br.* 51, 747–753. doi: 10.1302/0301-620x.51b4.747

Hunziker, E. B., Quinn, T. M., and Hauselmann, H. J. (2002). Quantitative structural organization of normal adult human articular cartilage. *Osteoarthritis Cartilage* 10, 564–572. doi: 10.1053/joca.2002.0814

Joshi, N. S., Bansal, N., Stewart, R. C., Snyder, B. D., and Grinstaff, M. W. (2009). Effect of contrast agent charge on visualization of articular cartilage using computed tomography: exploiting electrostatic interactions for improved sensitivity. *J. Am. Chem. Soc.* 131, 13234–13235. doi: 10.1021/ja9053306

Knothe Tate, M. L., and Knothe, U. (2000). An ex vivo model to study transport processes and fluid flow in loaded bone. *J. Biomech.* 33, 247–254. doi: 10.1016/s0021-9290(99)00143-8

Knothe Tate, M. L., Niederer, and Knothe, U. (1998). In vivo tracer transport through the lacunocanalicular system of rat bone in an environment devoid of mechanical loading. *Bone* 22, 107–117. doi: 10.1016/s8756-3282(97)00234-2

Knothe Tate, M. L., Tami, A. E., Netrebko, Milz, S., and Docheva, D. (2012). Multiscale computational and experimental approaches to elucidate bone and ligament mechanobiology using the ulna-radius-interosseous membrane construct as a model system. *Technol. Health Care* 20, 363–378. doi: 10.3233/thc-2012-0686

Kokkonen, H. T., Chin, H. C., Toyras, J., Jurvelin, J. S., and Quinn, T. M. (2017). Solute transport of negatively charged contrast agents across articular surface of injured cartilage. *Ann. Biomed. Eng.* 45, 973–981. doi: 10.1007/s10439-016-1756-6

Kokkonen, H. T., Jurvelin, J. S., Tiitu, V., and Toyras, J. (2011). Detection of mechanical injury of articular cartilage using contrast enhanced computed tomography. *Osteoarthritis Cartilage* 19, 295–301. doi: 10.1016/j.joca.2010.12.012

Krause, U., and Gregory, C. A. (2012). Potential of modulating Wnt signaling pathway toward the development of bone anabolic agent. *Curr. Mol. Pharmacol.* 5, 164–173. doi: 10.2174/1874467211205020164

Kulmala, K. A., Korhonen, R. K., Julkunen, Jurvelin, J. S., Quinn, T. M., Kroger, H., et al. (2010). Diffusion coefficients of articular cartilage for different CT and MRI contrast agents. *Med. Eng. Phys.* 32, 878–882. doi: 10.1016/j.medengphy.2010.06.002

Lane, L. B., Villacin, A., and Bullough, G. (1977). The vascularity and remodelling of subchondrial bone and calcified cartilage in adult human femoral and humeral heads. An age- and stress-related phenomenon. *J. Bone Joint Surg. Br.* 59, 272–278. doi: 10.1302/0301-620x.59b3.893504

Leddy, H. A., and Guilak, F. (2003). Site-specific molecular diffusion in articular cartilage measured using fluorescence recovery after photobleaching. *Ann. Biomed. Eng.* 31, 753–760. doi: 10.1114/1.1581879

Lepage, S. I. M., Robson, N., Gilmore, H., Davis, O., Hooper, A., St John, S., et al. (2019). Beyond cartilage repair: the role of the osteochondral unit in joint health and disease. *Tissue Eng. Part B Rev.* 25, 114–125. doi: 10.1089/ten.teb.2018.0122

Li, G., Yin, J., Gao, J., Cheng, T. S., Pavlos, N. J., Zhang, C., et al. (2013). Subchondral bone in osteoarthritis: insight into risk factors and microstructural changes. *Arthritis Res. Ther.* 15:223. doi: 10.1186/ar4405

Li, T. F., Gao, L., Sheu, T. J., Sampson, E. R., Flick, L. M., Konttinen, Y. T., et al. (2010). Aberrant hypertrophy in Smad3-deficient murine chondrocytes is rescued by restoring transforming growth factor beta-activated kinase 1/activating transcription factor 2 signaling: a potential clinical implication for osteoarthritis. *Arthritis Rheum.* 62, 2359–2369. doi: 10.1002/art.27537

Li, V. S., Ng, S. S., Boersema, J., Low, T. Y., Karthaus, W. R., Gerlach, J., et al. (2012). Wnt signaling through inhibition of beta-catenin degradation in an intact Axin1 complex. *Cell* 149, 1245–1256. doi: 10.1016/j.cell.2012.05.002

Li, W., You, L., Schaffler, M. B., and Wang, L. (2009). The dependency of solute diffusion on molecular weight and shape in intact bone. *Bone* 45, 1017–1023. doi: 10.1016/j.bone.2009.07.076

Longley, R., Ferreira, A. M., and Gentile, P. (2018). Recent approaches to the manufacturing of biomimetic multi-phasic scaffolds for osteochondral regeneration. *Int. J. Mol. Sci.* 19:1755. doi: 10.3390/ijms19061755

Lories, R. J., Peeters, J., Bakker, A., Tylzanowski, Derese, I., Schrooten, J., et al. (2007). Articular cartilage and biomechanical properties of the long bones in Frzb-knockout mice. *Arthritis Rheum.* 56, 4095–4103. doi: 10.1002/art.23137

Malinin, T., and Ouellette, E. A. (2000). Articular cartilage nutrition is mediated by subchondral bone: a long-term autograft study in baboons. *Osteoarthritis Cartilage* 8, 483–491. doi: 10.1053/joca.1999.0324

Martel-Pelletier, J., Boileau, C., Pelletier, J., and Roughley, J. (2008). Cartilage in normal and osteoarthritis conditions. *Best Pract. Res. Clin. Rheumatol.* 22, 351–384.

Meng, H. Y., Quan, Q., Yuan, X. L., Zheng, Y. D., Peng, J., Guo, Q. Y., et al. (2020). Diffusion of neutral solutes within human osteoarthritic cartilage: effect of loading patterns. *J. Orthopaedic Transl.* 22, 58–66. doi: 10.1016/j.jot.2019.10.013

Miclea, R. L., Siebelt, M., Finos, L., Goeman, J. J., Lowik, C. W., Oostdijk, W., et al. (2011). Inhibition of Gsk3beta in cartilage induces osteoarthritic features through activation of the canonical Wnt signaling pathway. *Osteoarthritis Cartilage* 19, 1363–1372. doi: 10.1016/j.joca.2011.07.014

Mitchell, G., Magna, H. A., Reeves, L. M., Lopresti-Morrow, L. L., Yocum, S. A., Rosner, J., et al. (1996). Cloning, expression, and type II collagenolytic activity of matrix metalloproteinase-13 from human osteoarthritic cartilage. *J. Clin. Invest.* 97, 761–768. doi: 10.1172/jci118475

Muir, H. (1995). The chondrocyte, architect of cartilage. Biomechanics, structure, function and molecular biology of cartilage matrix macromolecules. *Bioessays* 17, 1039–1048. doi: 10.1002/bies.950171208

Nelson, B. B., Stewart, R. C., Kawcak, C. E., Freedman, J. D., Patwa, A. N., Snyder, B. D., et al. (2018). Quantitative evaluation of equine articular cartilage using cationic contrast-enhanced computed tomography. *Cartilage*

Nettles, D. L., Vail, T., Morgan, M. T., Grinstaff, M. W., and Setton, L. A. (2004). Photocrosslinkable hyaluronan as a scaffold for articular cartilage repair. *Ann. Biomed. Eng.* 32, 391–397. doi: 10.1023/b:abme.0000017552.65260.94

Ngo, L., Knothe, L. E., and Knothe, M. L. (2018). Tate, knee joint tissues effectively separate mixed sized molecules delivered in a single bolus to the heart. *Sci. Rep.* 8:10254.

Pan, J., Wang, B., Li, W., Zhou, X., Scherr, T., Yang, Y., et al. (2012). Elevated cross-talk between subchondral bone and cartilage in osteoarthritic joints. *Bone* 51, 212–217. doi: 10.1016/j.bone.2011.11.030

Pan, J., Zhou, X., Li, W., Novotny, J. E., Doty, S. B., and Wang, L. (2009). In situ measurement of transport between subchondral bone and articular cartilage. *J. Orthop. Res.* 27, 1347–1352. doi: 10.1002/jor.20883

Pouran, B., Arbabi, V., Bajpayee, A. G., van Tiel, J., Toyras, J., Jurvelin, J. S., et al. (2018). Multi-scale imaging techniques to investigate solute transport across articular cartilage. *J. Biomech.* 78, 10–20. doi: 10.1016/j.jbiomech.2018.06.012

Remst, D. F., Blaney Davidson, E. N., Vitters, E. L., Bank, R. A., van den Berg, W. B., and van der Kraan, M. (2014). TGF-ss induces Lysyl hydroxylase 2b in human synovial osteoarthritic fibroblasts through ALK5 signaling. *Cell Tissue Res.* 355, 163–171. doi: 10.1007/s00441-013-1740-5

Retting, K. N., Song, B., Yoon, B. S., and Lyons, K. M. (2009). BMP canonical Smad signaling through Smad1 and Smad5 is required for endochondral bone formation. *Development* 136, 1093–1104. doi: 10.1242/dev.029926

Robling, A. G., Castillo, A. B., and Turner, C. H. (2006). Biomechanical and molecular regulation of bone remodeling. *Annu. Rev. Biomed. Eng.* 8, 455–498. doi: 10.1146/annurev.bioeng.8.061505.095721

Saito, M., Sasho, T., Yamaguchi, S., Ikegawa, N., Akagi, R., Muramatsu, Y., et al. (2012). Angiogenic activity of subchondral bone during the progression of osteoarthritis in a rabbit anterior cruciate ligament transection model. *Osteoarthritis Cartilage* 20, 1574–1582. doi: 10.1016/j.joca.2012.08.023

Sanchez-Adams, J., Leddy, H. A., McNulty, A. L., O'Conor, C. J., and Guilak, F. (2014). The mechanobiology of articular cartilage: bearing the burden of osteoarthritis. *Curr. Rheumatol. Rep.* 16:451. doi: 10.1007/s11926-014-0451-6

Serra, R., Johnson, M., Filvaroff, E. H., LaBorde, J., Sheehan, D. M., Derynck, R., et al. (1997). Expression of a truncated, kinase-defective TGF-beta type II receptor in mouse skeletal tissue promotes terminal chondrocyte differentiation and osteoarthritis. *J. Cell Biol.* 139, 541–552. doi: 10.1083/jcb.139.2.541

Serrat, M. A., Efaw, M. L., and Williams, R. M. (2014). Hindlimb heating increases vascular access of large molecules to murine tibial growth plates measured

by in vivo multiphoton imaging. *J. Appl. Physiol. (1985)* 116, 425–438. doi: 10.1152/japplphysiol.01212.2013

Serrat, M. A., Williams, R. M., and Farnum, C. E. (2009). Temperature alters solute transport in growth plate cartilage measured by in vivo multiphoton microscopy. *J. Appl. Physiol. (1985)* 106, 2016–2025. doi: 10.1152/japplphysiol.00295.2009

Sharma, A. R., Jagga, S., Lee, S. S., and Nam, J. S. (2013). Interplay between cartilage and subchondral bone contributing to pathogenesis of osteoarthritis. *Int. J. Mol. Sci.* 14, 19805–19830. doi: 10.3390/ijms141019805

Shen, J., Li, J., Wang, B., Jin, H., Wang, M., Zhang, Y., et al. (2013). Deletion of the transforming growth factor beta receptor type II gene in articular chondrocytes leads to a progressive osteoarthritis-like phenotype in mice. *Arthritis Rheum.* 65, 3107–3119. doi: 10.1002/art.38122

Shoga, J. S., Graham, B. T., Wang, L., and Price, C. (2017). Direct quantification of solute diffusivity in agarose and articular cartilage using correlation spectroscopy. *Ann. Biomed. Eng.* 45, 2461–2474. doi: 10.1007/s10439-017-1869-6

Silvast, T. S., Jurvelin, J. S., Tiitu, V., Quinn, T. M., and Toyras, J. (2013). Bath concentration of anionic contrast agents does not affect their diffusion and distribution in articular cartilage in vitro. *Cartilage* 4, 42–51. doi: 10.1177/1947603512451023

Sophia Fox, A. J., Bedi, A., and Rodeo, S. A. (2009). The basic science of articular cartilage: structure, composition, and function. *Sports Health* 1, 461–468. doi: 10.1177/1941738109350438

Stok, K. S., Besler, B. A., Steiner, T. H., Villarreal Escudero, A. V., Zulliger, M. A., Wilke, M., et al. (2016). Three-dimensional quantitative morphometric analysis (QMA) for in situ joint and tissue assessment of osteoarthritis in a preclinical rabbit disease model. *PLoS One* 11:e0147564. doi: 10.1371/journal.pone.0147564

Suri, S., Gill, S. E., Massena de Camin, S., Wilson, D., McWilliams, D. F., and Walsh, D. A. (2007). Neurovascular invasion at the osteochondral junction and in osteophytes in osteoarthritis. *Ann. Rheum. Dis.* 66, 1423–1428. doi: 10.1136/ard.2006.063354

Suri, S., and Walsh, D. A. (2012). Osteochondral alterations in osteoarthritis. *Bone* 51, 204–211. doi: 10.1016/j.bone.2011.10.010

Thielen, N. G. M., van der Kraan, M., and van Caam, A. M. (2019). TGFbeta/BMP signaling pathway in cartilage homeostasis. *Cells* 8:969. doi: 10.3390/cells8090969

van der Kraan, M. (2017). The changing role of TGFbeta in healthy, ageing and osteoarthritic joints. *Nat. Rev. Rheumatol.* 13, 155–163. doi: 10.1038/nrrheum.2016.219

Villalvilla, A., Gomez, R., Largo, R., and Herrero-Beaumont, G. (2013). Lipid transport and metabolism in healthy and osteoarthritic cartilage. *Int. J. Mol. Sci.* 14, 20793–20808. doi: 10.3390/ijms141020793

Vincenti, M., and Brinckerhoff, C. E. (2001). Early response genes induced in chondrocytes stimulated with the inflammatory cytokine interleukin-1beta. *Arthritis Res.* 3, 381–388.

Vincenti, M., Coon, C. I., Mengshol, J. A., Yocum, S., Mitchell, and Brinckerhoff, C. E. (1998). Cloning of the gene for interstitial collagenase-3 (matrix metalloproteinase-13) from rabbit synovial fibroblasts: differential expression with collagenase-1 (matrix metalloproteinase-1). *Biochem. J.* 331(Pt 1), 341–346. doi: 10.1042/bj3310341

Walsh, D. A., Bonnet, C. S., Turner, E. L., Wilson, D., Situ, M., and McWilliams, D. F. (2007). Angiogenesis in the synovium and at the osteochondral junction in osteoarthritis. *Osteoarthritis Cartilage* 15, 743–751. doi: 10.1016/j.joca.2007.01.020

Wang, B., Zhou, X., Price, C., Li, W., Pan, J., and Wang, L. (2013). Quantifying load-induced solute transport and solute-matrix interaction within the osteocyte lacunar-canalicular system. *J. Bone Miner. Res.* 28, 1075–1086. doi: 10.1002/jbmr.1804

Wang, L. (2018). Solute transport in the bone lacunar-canalicular system (LCS). *Curr. Osteoporosis Rep.* 16, 32–41. doi: 10.1007/s11914-018-0414-3

Wang, L., Wang, Y., Han, Y., Henderson, S. C., Majeska, R. J., Weinbaum, S., et al. (2005). In situ measurement of solute transport in the bone lacunar-canalicular system. *Proc. Natl. Acad. Sci. U.S.A.* 102, 11911–11916. doi: 10.1073/pnas.0505193102

Wang, Q., Tan, Q. Y., Xu, W., Qi, H. B., Chen, D., Zhou, S., et al. (2017). Cartilage-specific deletion of Alk5 gene results in a progressive osteoarthritis-like phenotype in mice. *Osteoarthritis Cartilage* 25, 1868–1879. doi: 10.1016/j.joca.2017.07.010

Wojdasiewicz, P., Poniatowski, L. A., and Szukiewicz, D. (2014). The role of inflammatory and anti-inflammatory cytokines in the pathogenesis of osteoarthritis. *Mediators Inflamm.* 2014:561459.

Yang, X., Chen, L., Xu, X., Li, C., Huang, C., and Deng, C. X. (2001). TGF-beta/Smad3 signals repress chondrocyte hypertrophic differentiation and are required for maintaining articular cartilage. *J. Cell Biol.* 153, 35–46. doi: 10.1083/jcb.153.1.35

Yuan, X. L., Meng, H. Y., Wang, Y. C., Peng, J., Guo, Q. Y., Wang, A. Y., et al. (2014). Bone-cartilage interface crosstalk in osteoarthritis: potential pathways and future therapeutic strategies. *Osteoarthritis Cartilage* 22, 1077–1089. doi: 10.1016/j.joca.2014.05.023

Zhou, Y., Wang, T., Hamilton, J. L., and Chen, D. (2017). Wnt/beta-catenin signaling in osteoarthritis and in other forms of arthritis. *Curr. Rheumatol. Rep.* 19:53.

Zhu, M., Chen, M., Zuscik, M., Wu, Q., Wang, Y. J., Rosier, R. N., et al. (2008). Inhibition of beta-catenin signaling in articular chondrocytes results in articular cartilage destruction. *Arthritis Rheum.* 58, 2053–2064. doi: 10.1002/art.23614

Zhu, M., Tang, D., Wu, Q., Hao, S., Chen, M., Xie, C., et al. (2009). Activation of beta-catenin signaling in articular chondrocytes leads to osteoarthritis-like phenotype in adult beta-catenin conditional activation mice. *J. Bone Miner. Res.* 24, 12–21. doi: 10.1359/jbmr.080901

Conflict of Interest: The authors declare that the research was conducted in the absence of any commercial or financial relationships that could be construed as a potential conflict of interest.

Copyright © 2020 Oliveira Silva, Gregory, Ansari and Stok. This is an open-access article distributed under the terms of the Creative Commons Attribution License (CC BY). The use, distribution or reproduction in other forums is permitted, provided the original author(s) and the copyright owner(s) are credited and that the original publication in this journal is cited, in accordance with accepted academic practice. No use, distribution or reproduction is permitted which does not comply with these terms.

frontiers in Cell and Developmental Biology

MINI REVIEW
published: 21 February 2020
doi: 10.3389/fcell.2020.00096

Modeling the Impact of Microgravity at the Cellular Level: Implications for Human Disease

*Peta Bradbury[1], Hanjie Wu[2], Jung Un Choi[3], Alan E. Rowan[3], Hongyu Zhang[4], Kate Poole[5], Jan Lauko[3] and Joshua Chou[2]**

[1] Respiratory Technology, Woolcock Institute of Medical Research, Sydney, NSW, Australia, [2] School of Biomedical Engineering, Faculty of Engineering and Information Technology, University of Technology Sydney, Sydney, NSW, Australia, [3] Australian Institute for Bioengineering and Nanotechnology, The University of Queensland, Brisbane, QLD, Australia, [4] State Key Laboratory of Tribology, Department of Mechanical Engineering, Tsinghua University, Beijing, China, [5] EMBL Australia Node in Single Molecule Science, School of Medical Sciences, University of New South Wales, Sydney, NSW, Australia

A lack of gravity experienced during space flight has been shown to have profound effects on human physiology including muscle atrophy, reductions in bone density and immune function, and endocrine disorders. At present, these physiological changes present major obstacles to long-term space missions. What is not clear is which pathophysiological disruptions reflect changes at the cellular level versus changes that occur due to the impact of weightlessness on the entire body. This review focuses on current research investigating the impact of microgravity at the cellular level including cellular morphology, proliferation, and adhesion. As direct research in space is currently cost prohibitive, we describe here the use of microgravity simulators for studies at the cellular level. Such instruments provide valuable tools for cost-effective research to better discern the impact of weightlessness on cellular function. Despite recent advances in understanding the relationship between extracellular forces and cell behavior, very little is understood about cellular biology and mechanotransduction under microgravity conditions. This review will examine recent insights into the impact of simulated microgravity on cell biology and how this technology may provide new insight into advancing our understanding of mechanically driven biology and disease.

Keywords: microgravity, mechanobiology, mechanotransduction, cytoskeletal, mechanosensing

OPEN ACCESS

Edited by:
Michael Smutny, University of Warwick, United Kingdom

Reviewed by:
Sarah Boyle, Centre for Cancer Biology (CCB), Australia
Ludmila Buravkova, Institute of Biomedical Problems (RAS), Russia

****Correspondence:***
Joshua Chou
Joshua.chou@uts.edu.au

Specialty section:
This article was submitted to Cell Adhesion and Migration, a section of the journal Frontiers in Cell and Developmental Biology

Received: *30 September 2019*
Accepted: *04 February 2020*
Published: *21 February 2020*

Citation:
Bradbury P, Wu H, Choi JU, Rowan AE, Zhang H, Poole K, Lauko J and Chou J (2020) Modeling the Impact of Microgravity at the Cellular Level: Implications for Human Disease. Front. Cell Dev. Biol. 8:96. doi: 10.3389/fcell.2020.00096

INTRODUCTION

Humans are subjected to persistent gravitational force and the importance of gravity for maintaining physiological function has been revealed by the detrimental impacts of space travel on human health. During space flight, astronauts are exposed to a prolonged state of microgravity and develop a myriad of physiological disruptions including a loss of muscle mass and bone density, impaired vision, decreased kidney function, diminished neurological responses, and a compromised immune system (White and Averner, 2001; Horneck et al., 2003; Crucian et al., 2014; White et al., 2016). This review will discuss recent data that highlight the impact of microgravity at the cellular level. Additionally, this review addresses how such research can be conducted on earth by simulating the microgravity state. These studies are not only important for understanding how humans are affected by microgravity but have the potential to elucidate the role of mechanical stimuli on cellular function and the development of mechanically driven disease states.

Mechanobiology is the study of how cells are influenced by their physical environment. This emerging field of research provides an important perspective on understanding

many aspects of cellular function and dysfunction. Cells can convert mechanical inputs into biochemical signals to initiate downstream signaling cascades in process known as mechanotransduction. Gravitational force is presumed to play a crucial role in regulating cell and tissue homeostasis by inducing mechanical stresses experienced at the cellular level. Thus, the concept of mechanical unloading (a decrease in mechanical stress) is associated with the weightlessness of space and can be replicated by simulating microgravity conditions, allowing for investigation of the mechanobiology aspects of cell function. The mechanical unloading of cells under microgravity conditions shifts the balance between physiology and pathophysiology, accelerating the progression and development of some disease states. For example, kidney stone formation is accelerated under microgravity conditions compared to Earth's gravity (1 g) (Pavlakou et al., 2018). Similarly, osteoporosis can take decades to develop under normal gravitational loading, yet this disease can be modeled under microgravity over shorter time scales (Pajevic et al., 2013). The mechanisms by which human physiology are disrupted in microgravity remain unknown, rendering numerous open questions regarding the adaptive changes that occur at the cellular and molecular level in response to microgravity.

SIMULATING MICROGRAVITY

One of the key challenges in using microgravity as an investigative tool is creating a microgravity condition that can be applied at a cellular level, on Earth. The process of conducting space research missions is costly and time consuming, thereby limiting the advancement of microgravity research and widespread application of this approach. Currently, there are a number of microgravity devices available for purchase that are designed to achieve microgravity conditions. Microgravity simulators specific to cellular studies include strong magnetic field-induced levitation (i.e., diamagnetic simulation), as well as two-dimensional and three-dimensional clinostats, rotating wall vessels and random positioning machines (RPMs) (Huijser, 2000; Russomano et al., 2005; Herranz et al., 2012; Ikeda et al., 2017). Each of the simulation techniques has shown advantages and disadvantages however, when chosen correctly for a given experiment, the results obtained are similar to those observed in Space flight studies (Stamenkovic et al., 2010; Herranz et al., 2013; Martinez et al., 2015; Krüger et al., 2019b). For cell culture studies, the use of RPM is common as the system achieves microgravity by continually providing random changes in orientation relative to the gravity vector and thus an averaging of the impact of the gravity vector to zero occurs over time (Beysens and van Loon, 2015). This averaging is achieved by the independent, yet simultaneous, rotation of two axes – with one axis rotating in the *X*-plane, and the second axis rotating in the *Y*-plane. It is important that the cell culture flask/sample be placed at the midpoint of the *x*-axis, cell culture flasks placed at a distance from the center of the *x*-axis will be subjected to a greater rotational force resulting in cells experiencing both centrifugal force and an increased gravity load (Beysens and van Loon, 2015). Furthermore, the RPM is designed to subject the cells to 10^{-3} g (or as close to this value as possible) but cannot achieve complete zero gravity and hence termed microgravity (Huijser, 2000; Beysens and van Loon, 2015).

THE IMPACT OF MICROGRAVITY OF CELL CYTOSKELETON

Cellular response to mechanical loading has been well documented over the decades however, the response that occurs when cells are placed under conditions of mechanical unloading remains in its infancy. The most apparent cellular changes that occur following exposure to a microgravity environment are alterations to cell shape, size, volume, and adherence properties (Buken et al., 2019; Dietz et al., 2019; Thiel et al., 2019b). These microgravity induced changes to cellular morphology reflect modifications to cytoskeletal structures, namely microtubules and actin filaments (F-actin), as cells sense a reduced gravitational load and therefore mechanical unloading (Crawford-Young, 2006; Corydon et al., 2016a; Thiel et al., 2019a). Microgravity, whether in Space or simulated in the laboratory, offers a unique mechanical unloading environment to explore cellular mechanotransduction by providing an unparalleled research environment to investigate the relationship between mechanical unloading and cellular response.

Numerous studies have been conducted on a myriad of cell types highlighting morphological sensitivity to microgravity (Ingber, 1999; Vorselen et al., 2014), with the first documented morphological change reported by Rijken et al. (1991). Morphological changes as a result of microgravity conditions, either real or simulated, have been shown to have altered transcription, translation, and organization of cytoskeletal proteins (Vassy et al., 2001; Infanger et al., 2006b; Tauber et al., 2017). Fundamental work carried out by Tabony, Pochon, and Papaseit showed that while tubulin self-assembly into microtubules occurs independent of gravity, the assembly and organization of the microtubule network is gravity dependent (Papaseit et al., 2000; Tabony et al., 2002). Importantly, this gravity-dependent organization of the microtubule network has since been described in multiple cell lines during both real and simulated microgravity exposures (Vassy et al., 2001; Uva et al., 2002; Hughes-Fulford, 2003; Rosner et al., 2006; Janmaleki et al., 2016) and possibly be the result of a poorly defined microtubule organizing center (MTOC) (Lewis et al., 1998). Taken together these data highlight an important regulatory role for the microtubule network and the MTOC following exposure to a microgravity environment. However, the data surrounding the response of the actin cytoskeleton to microgravity exposure are less clear. Many studies have reported that microgravity exposure had decreased expression of actin and actin-associated proteins, namely Arp2/3 and RhoA, subsequently resulting in the disorganization of the actin cytoskeleton (Carlsson et al., 2003; Higashibata et al., 2006; Corydon et al., 2016a,b; Louis et al., 2017; Tan et al., 2018). However, other studies have showed increased F-actin and stress fiber formation that accompanied the development of lamellipodia protrusions following exposure to microgravity (Gruener et al., 1994; Nassef et al., 2019). Contrary

to this, Rosner et al. (2006) reported no changes to actin structure or organization and further suggested that the actin cytoskeleton is only regulated in a hyper-gravity environment. Thus, the data surrounding cellular morphological changes in response to microgravity and the role of actin is confounding and at times contradictory.

The actin cytoskeleton, its organization and ability to generate force are critical for cellular mechanosensing and importantly any changes to these processes can initiate pathophysiological disruption. Transduction of mechanical forces by integrins requires clustering of these transmembrane receptors and the subsequent formation of focal contacts and adhesions that physically link the extracellular matrix (ECM) to the cytoskeleton (Wang et al., 1993; Ingber, 1997; Maniotis et al., 1997). Binding of integrins to matrix proteins promotes the bundling of F-actin at the cell-matrix adhesion and the subsequent maturation of both the focal adhesion and the actin stress fiber (Zaidel-Bar et al., 2003; Wolfenson et al., 2009, 2011) to generate the tension required for cell adherence, migration, and tissue homeostasis. Exposure to microgravity reduces the formation, number, and total area of focal adhesions per cell (Guignandon et al., 2003; Tan et al., 2018) consequently affecting cellular adherence, migration capacity, and viability (Plett et al., 2004; Nabavi et al., 2011; Shi et al., 2015; Ahn et al., 2019; Dietz et al., 2019), albeit with contradictory results. Mechanical unloading has been shown to significantly reduce gene expression of a number of focal adhesion proteins, including FAK, DOCK1, and PTEN, while caveolin and p130Cas expression were shown to be increased (Grenon et al., 2013; Ratushnyy and Buravkova, 2017). Thus, the activity of the downstream signaling pathways that govern the microgravity-induced cytoskeletal changes are significantly impaired and are at least in part due to the microgravity-triggered inhibition of FAK and/or RhoA signaling (Higashibata et al., 2006; Li et al., 2009; Tan et al., 2018). Furthermore, recent data suggest that changes to the cytoskeleton may also impact signaling via mechanically activated ion channels and contacts in response to both cell-generated (Nourse and Pathak, 2017; Ellefsen et al., 2019) and externally applied mechanical inputs (Bavi et al., 2019). Thus, downstream signaling of the numerous mechanotransduction pathways depend on the concerted interaction of the cytoskeleton, cell adhesion molecules, and force sensing proteins, including mechanically activated ion channels. To date, there is little information regarding the role of mechanically activated ion channels in microgravity environments.

MICROGRAVITY IMPACT BONE CELL SIGNALING RESPONSE AND CARTILAGE ECM SYNTHESIS

The accelerated loss of bone and muscle mass as a result of microgravity has been well documented over the decades (Burger and Klein-Nulend, 1998; Harris et al., 2000; Fitts et al., 2001). Osteocytes and osteoblasts are known mechanosensitive bone cells responsible for maintaining the balance of bone absorption and resorption – a process that is coordinated by both the actin cytoskeleton and microtubule network (Okumura et al., 2006). Bone cell morphology is significantly modified following exposure to microgravity when compared to control cells (Guignandon et al., 1995; Hughes-Fulford, 2003). To adapt to the new mechanical environment the bone cells have reduced transcription and translation of cytoskeletal and cytoskeletal-associated proteins (Xu et al., 2017; Mann et al., 2019), decreased focal adhesion formation, together resulting in the increased formation of osteoclast resorption pits (Nabavi et al., 2011). Furthermore, the actin cytoskeleton of osteoblasts subjected to 4 days of microgravity exposure completely collapsed (Hughes-Fulford, 2003), significantly impacting multiple downstream signaling pathways, most notably, the inhibition of bone morphogenic protein (BMP) signaling axis (Patel et al., 2007; Xu et al., 2017). The BMP family of proteins regulates the expression of an important mechanosensing protein, sclerostin, found exclusively in osteocytes (Poole et al., 2005; Kamiya et al., 2016), whereby mechanical unloading increases sclerostin protein expression to promote bone resorption and cause a loss of bone density (Robling et al., 2008) – a phenotype that closely mimics both osteoporosis and osteonecrosis. Thus by applying the unique mechanical unloading environment offered by both real and simulated-microgravity to bone (specifically, osteoporosis) research has led to the introduction of the FDA approved drug, Evenity, a monoclonal antibody that works as an anabolic agent to increase bone mass via the sclerostin pathway (Scheiber et al., 2019).

While a significant number of studies have identified the importance of mechanical unloading in regulating bone structure and function, the articular cartilage (AC) is also particularly susceptible to the effects of mechanical loading and unloading (Sanchez-Adams et al., 2014). The cells found in AC, chondrocytes, sense and respond to changing mechanical loads in order to maintain the balanced production of ECM molecules ensuring that the tissue maintains the ability to resist tensile and compressive forces. Both mechanical unloading and overloading of chondrocytes can disrupt the homeostatic balance in the cartilage leading to cartilage degradation and osteoarthritis thereby tipping the balance from homeostatic maintenance to pathophysiology, leading to cartilage degradation and osteoarthritis (Vanwanseele et al., 2002; Kurz et al., 2005). To study the effect of extended microgravity on AC specifically on the joint tissue, mice were exposed to 30 days of spaceflight during the Bion-M1 mission (Fitzgerald et al., 2019). Interestingly, tissue degradation was observed only in the AC of load-bearing joints, but not in minimally loaded sternal fibrocartilage highlighting a differential response to mechanical unloading and the predisposition of load bearing joints, but not structural joints, to mechanical stimuli. Additionally, decreased proteoglycan levels were found in the AC of the mice after the 30 days (Vanwanseele et al., 2002) further characterizing a mechanical unloading pathology specific to AC atrophy. Importantly, reduced proteoglycan levels have also been reported in hindlimb unloading and limb immobilization studies in various animals (Salter et al., 1980; Haapala et al., 1996; O'Connor, 1997). The reduced proteoglycan levels paired with

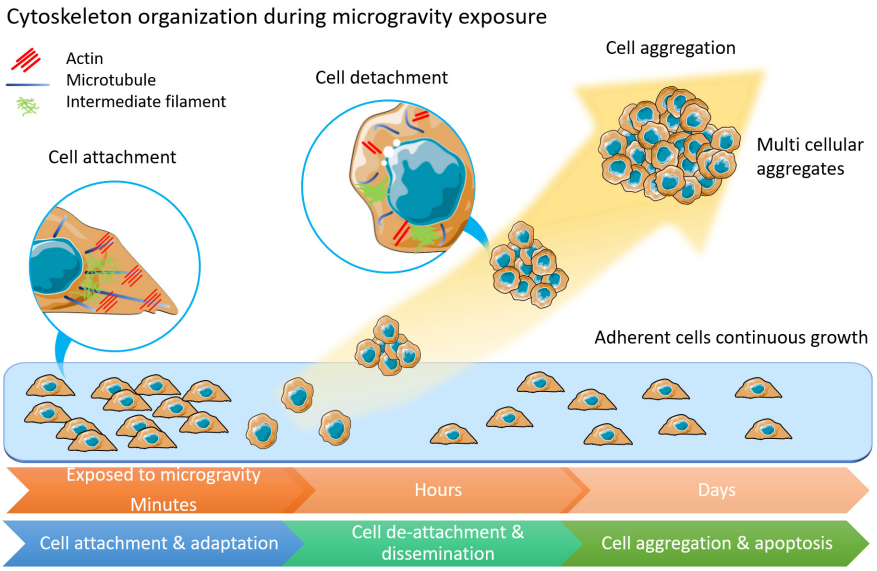

FIGURE 1 | The morphology and physiology alterations of adherently growing cells after microgravity exposure. Cytoskeleton components of actin, microtubules and intermediate filament are displayed in inset circles. In adherent cells, microtubules form radiation arrangement near nuclear. Actin fibers anchor to cell membranes. Intermediate filament forms loose network around nuclear. Among cells under microgravity influence, the microtubules are shortened and curved. Less actin fibers but more condense intermediate filament are observed. This illustration was inspired by long-term thyroid cells culture in simulated microgravity environment (Kopp et al., 2015; Krüger et al., 2019a) .

the augmented regulation of ECM-associated genes and proteins that help protect against osteoarthritic changes, including collagen type I, II, and X, $\beta_1$integrin, vimentin, and chondrocyte sulfate (Ulbrich et al., 2010; Aleshcheva et al., 2013, 2015), suggest that while the microgravity-induced osteoarthritic pathology is observed cartilage recovery of the AC is possible. Further to this, cell-based studies have shown that primary chondrocytes are to adapt to a microgravity environment within 24 h (Aleshcheva et al., 2013). There is a clear need for more research into the response of AC and specifically chondrocytes as elucidation of the molecular mechanism that underpins chondrocytes mechanoadaptation to a microgravity environment, holds great promise for novel osteoarthritic treatments.

MICROGRAVITY-INDUCED CYTOSKELETAL REGULATION OF IMMUNE AND CANCER CELLS

The function of the immune system is strongly impacted (Frippiat et al., 2016; Smith, 2018) with several studies reporting dysregulation or immunosuppression following simulated or real microgravity conditions (Boonyaratanakornkit et al., 2005; Crucian et al., 2015; Martinez et al., 2015; Thiel et al., 2017). Peripheral monocytes collected from astronauts post short-duration Space missions (13–16 days) showed that there was no change in the numbers of circulating monocytes indicating that the change to an immunosuppressive phenotype was not due a reduced cell number (Crucian et al., 2011). However, peripheral monocytes showed a significantly decreased expression of surface markers CD26L and HLA-DR, known regulators of lymphocyte-endothelial cell adhesion and tissue migration (Crucian et al., 2011). *In vitro* studies performed during Space flights have revealed that lymphocytes exhibit important changes in their cytoskeletal properties, suggesting that T cell activation may be compromised at the level of the T cell receptor (TCR) interaction (Sonnenfeld et al., 1992). It has been hypothesized that immunosuppression produced in microgravity is due to impaired TCR activation resulting from cytoskeletal disruption (Bradley et al., 2019); however, the underlying molecular mechanisms remain unknown.

When applied to tumor cells microgravity has been found to impact tumor cell adhesion, proliferation, migration, and viability (Grimm et al., 2002; Plett et al., 2004; Infanger et al., 2006a; Shi et al., 2015; Tan et al., 2018), and to induce cell autophagy (Jeong et al., 2018). Changes in apoptotic rate were also observed in colorectal cancer cells (DLD-1) and a lymphoblast leukemic cell line (MOLT-4), accompanied by reduced transcription of the genes involved in colony formation, oncogenic progression, and metastatic potential (Vidyasekar et al., 2015). The foremost changes to tumor cell following exposure to microgravity are alterations of cell shape, size, and adhesion, indicating changes in cytoskeletal organization (**Figure 1**). Modulation of the cytoskeletal network have been demonstrated to occur after just minutes (Rijken et al., 1992; Sciola et al., 1999) or hours (Lewis et al., 1998; Vassy et al., 2001) in microgravity. Microtubule disorganization was observed in both the breast cancer MCF-7 cells and the thyroid cancer cell line FTC-133 when exposed to real microgravity (Kopp et al., 2018a,b). In contrast, no changes in Rac-controlled F-actin were detected in the neuroblastoma cell line, SH-Y-5Y (Rosner

TABLE 1 | Effects of sub-cellular functions concerning various cell types and exposure duration in microgravity environment.

Cell type	Effects of cells	Microgravity exposure time	References
Osteosarcoma cells (ROS 17/2.8)	Cell morphological change to rounded shape with long cytoplasmic extensions	4 days and 6 days	Guignandon et al., 1997
Osteosarcoma cells (ROS 17/2.8)	Reduction in cell spread area and vinculin spot area, actin and focal adhesion, and stress fibers	12 and 24 h	Guignandon et al., 2003
Breast cancer (MCF-7)	Disoriented microtubule	1.5 h	Vassy et al., 2003
Thyroid cancer (ML-1)	Actin fiber reorganization	Parabola flight	Ulbrich et al., 2011
Human macrophages	No effect on cytoskeletal structure	11 days	Tauber et al., 2017
Human chondrocytes	Effect on cell cytoplasm, microtubule network disruption, loss of stress fibers, actin fiber reorganization.	Parabola flight	Aleshcheva et al., 2015
Osteoblasts (MC3T3-E1)	Reduction in actin cytoskeletal stress fibers and reduction of nuclei size by 30%	4 days	Hughes-Fulford and Lewis, 1996
Primary mouse osteoblasts	Thicker microtubule, smaller focal adhesion spots, reduction in actin stress fibers, and increase in cell spread area	5 days	Nabavi et al., 2011
Osteocytes	Increase in cellular organelles including Golgi complex, vacuoles, and vesicles	14 days	Rodionova et al., 2002

et al., 2006), highlighting the differing responses of distinct cell types to mechanical unloading. The expression of focal adhesion proteins, moesin and ezrin, was found to be significantly down-regulated after 24-h of microgravity exposure (Kopp et al., 2018a). There remains a gap in the understanding of the molecular mechanisms that drive changes in the cytoskeleton in response to mechanical unloading and the physiological systems that will be impacted by microgravity. Thus, there is a dual potential of microgravity studies in both elucidating the underlying importance of mechanical signaling in human physiology and in developing understanding and countermeasures for long-duration space flights.

DISCUSSION

Microgravity research conducted on the International Space Station (ISS) and in simulated microgravity has highlighted the importance of cellular mechanotransduction in human health and disease (**Table 1**). Understanding the molecular mechanisms by which cells respond to mechanical unloading will not only be important for preparing humans for longer-term space exploration but may also contribute to therapeutics for the treatment of diseases that depend on mechanical interactions, highlighting opportunities to manipulate and correct certain disease states. The discovery of sclerostin and the subsequent generation and use of the sclerostin monoclonal antibody to treat both osteoporotic patients has been a major outcome of the field (Martin et al., 2020). Thus, Space and microgravity biological research constitute extreme environments in which novel mechanotransduction molecules and mechanosensing mechanisms can be identified and may prove helpful in better designing immunotherapies or developing better and more targeted anti-cancer therapies. Studies that leverage these low gravity environments have the unique potential to unveil important physiological changes that occur in response to changing mechanical loads and are of considerable importance in expanding our understanding of mechanobiology.

With the privatization and commercialization of the ISS and a global push toward the exploration of space, the gateway for conducting research under simulated and Space microgravity is becoming more accessible. In particular the development of different variations of the RPM device provides a simulated microgravity environment on Earth for investigating the changes in cellular function due to mechanical unloading. Over the last several years, experiments involving the use of microgravity to study cellular mechanobiology and disease mechanisms have continued to rise, reinforcing the importance of this platform. This area of research has highlighted the importance of mechanical cues in maintaining cell and tissue homeostasis. The emergence of Space mechanobiology will continue to rise in the foreseeable future as it is evident that the benefits of such research can catapult survival of astronauts in space for extended duration as well as developing understanding and better treatments for Earth-borne diseases.

AUTHOR CONTRIBUTIONS

PB contributed to the sections "Simulating Microgravity" and "The Impact of Microgravity of Cell Cytoskeleton." JuC and JL contributed to the section "Microgravity Impact Bone Cell Signaling Response and Cartilage ECM Synthesis." HW, HZ, and KP contributed to the section "Microgravity-Induced Cytoskeletal Regulation of Immune and Cancer Cells." AR, KP, and JoC initiated, conceptualized the review, and edited the manuscript.

FUNDING

The author acknowledges the support of the Australian Research Council Discovery Project (ARC DP) (DP190101973), the NHMRC project grant APP1122104, and the University of Technology Sydney FEIT 2019 BlueSky grants FL160100139 (Laureate Fellowship AER) and DP190102230 (DP AER).

REFERENCES

Ahn, C. B., Lee, J. H., Han, D. G., Kang, H. W., Lee, S. H., Lee, J. I., et al. (2019). Simulated microgravity with floating environment promotes migration of non-small cell lung cancers. *Sci. Rep.* 9:14553. doi: 10.1038/s41598-019-50736-6

Aleshcheva, G., Sahana, J., Ma, X., Hauslage, J., Hemmersbach, R., Egli, M., et al. (2013). Changes in morphology, gene expression and protein content in chondrocytes cultured on a random positioning machine. *PLoS One* 8:e79057. doi: 10.1371/journal.pone.0079057

Aleshcheva, G., Wehland, M., Sahana, J., Bauer, J., Corydon, T. J., Hemmersbach, R., et al. (2015). Moderate alterations of the cytoskeleton in human chondrocytes after short-term microgravity produced by parabolic flight maneuvers could be prevented by up-regulation of BMP-2 and SOX-9. *FASEB J.* 29, 2303–2314. doi: 10.1096/fj.14-268151

Bavi, N., Richardson, J., Heu, C., Martinac, B., and Poole, K. (2019). PIEZO1-mediated currents are modulated by substrate mechanics. *ACS Nano* 13, 13545–13559. doi: 10.1021/acsnano.9b07499

Beysens, D. A., and van Loon, J. J. W. A. (2015). *Generation and Applications of Extra-Terrestrial Environments on Earth*. Denmark: River Publishers.

Boonyaratanakornkit, J. B., Cogoli, A., Li, C. F., Schopper, T., Pippia, P., Galleri, G., et al. (2005). Key gravity-sensitive signaling pathways drive T cell activation. *FASEB J.* 19, 2020–2022. doi: 10.1096/fj.05-3778fje

Bradley, J. H., Barwick, S., Horn, G. Q., Ullrich, E., Best, B., Arnold, J. P., et al. (2019). Simulated microgravity-mediated reversion of murine lymphoma immune evasion. *Sci. Rep.* 9:14623. doi: 10.1038/s41598-019-51106-y

Buken, C., Sahana, J., Corydon, T. J., Melnik, D., Bauer, J., Wehland, M., et al. (2019). Morphological and molecular changes in juvenile normal human fibroblasts exposed to simulated microgravity. *Sci. Rep.* 9:11882. doi: 10.1038/s41598-019-48378-9

Burger, E. H., and Klein-Nulend, J. (1998). Microgravity and bone cell mechanosensitivity. *Bone* 22(5 Suppl.), 127S–130S. doi: 10.1016/s8756-3282(98)00010-6

Carlsson, S. I., Bertilaccio, M. T., Ballabio, E., and Maier, J. A. (2003). Endothelial stress by gravitational unloading: effects on cell growth and cytoskeletal organization. *Biochim. Biophys. Acta* 1642, 173–179. doi: 10.1016/j.bbamcr.2003.08.003

Corydon, T. J., Kopp, S., Wehland, M., Braun, M., Schutte, A., Mayer, T., et al. (2016a). Alterations of the cytoskeleton in human cells in space proved by life-cell imaging. *Sci. Rep.* 6:20043. doi: 10.1038/srep20043

Corydon, T. J., Mann, V., Slumstrup, L., Kopp, S., Sahana, J., Askou, A. L., et al. (2016b). Reduced expression of cytoskeletal and extracellular matrix genes in human adult retinal pigment epithelium cells exposed to simulated microgravity. *Cell. Physiol. Biochem.* 40, 1–17. doi: 10.1159/000452520

Crawford-Young, S. J. (2006). Effects of microgravity on cell cytoskeleton and embryogenesis. *Int. J. Dev. Biol.* 50, 183–191. doi: 10.1387/ijdb.052077sc

Crucian, B., Simpson, R. J., Mehta, S., Stowe, R., Chouker, A., Hwang, S. A., et al. (2014). Terrestrial stress analogs for spaceflight associated immune system dysregulation. *Brain Behav. Immun.* 39, 23–32. doi: 10.1016/j.bbi.2014.01.011

Crucian, B., Stowe, R., Quiriarte, H., Pierson, D., and Sams, C. (2011). Monocyte phenotype and cytokine production profiles are dysregulated by short-duration spaceflight. *Aviat. Space Environ. Med.* 82, 857–862. doi: 10.3357/asem.3047.2011

Crucian, B., Stowe, R. P., Mehta, S., Quiriarte, H., Pierson, D., and Sams, C. (2015). Alterations in adaptive immunity persist during long-duration spaceflight. *NPJ Microgravity* 1:15013. doi: 10.1038/npjmgrav.2015.13

Dietz, C., Infanger, M., Romswinkel, A., Strube, F., and Kraus, A. (2019). Apoptosis induction and alteration of cell adherence in human lung cancer cells under simulated microgravity. *Int. J. Mol. Sci.* 20:E3601. doi: 10.3390/ijms20143601

Ellefsen, K. L., Holt, J. R., Chang, A. C., Nourse, J. L., Arulmoli, J., Mekhdjian, A. H., et al. (2019). Myosin-II mediated traction forces evoke localized Piezo1-dependent Ca(2+) flickers. *Commun. Biol.* 2:298.

Fitts, R. H., Riley, D. R., and Widrick, J. J. (2001). Functional and structural adaptations of skeletal muscle to microgravity. *J. Exp. Biol.* 204(Pt 18), 3201–3208.

Fitzgerald, J., Endicott, J., Hansen, U., and Janowitz, C. (2019). Articular cartilage and sternal fibrocartilage respond differently to extended microgravity. *NPJ Microgravity* 5:3. doi: 10.1038/s41526-019-0063-6

Frippiat, J. P., Crucian, B. E., de Quervain, D. J., Grimm, D., Montano, N., Praun, S., et al. (2016). Towards human exploration of space: the THESEUS review series on immunology research priorities. *NPJ Microgravity* 2:16040. doi: 10.1038/npjmgrav.2016.40

Grenon, S. M., Jeanne, M., Aguado-Zuniga, J., Conte, M. S., and Hughes-Fulford, M. (2013). Effects of gravitational mechanical unloading in endothelial cells: association between caveolins, inflammation and adhesion molecules. *Sci. Rep.* 3:1494. doi: 10.1038/srep01494

Grimm, D., Bauer, J., Kossmehl, P., Shakibaei, M., Schoberger, J., Pickenhahn, H., et al. (2002). Simulated microgravity alters differentiation and increases apoptosis in human follicular thyroid carcinoma cells. *FASEB J.* 16, 604–606. doi: 10.1096/fj.01-0673fje

Gruener, R., Roberts, R., Fau-Reitstetter, R., and Reitstetter, R. (1994). Reduced receptor aggregation and altered cytoskeleton in cultured myocytes after spaceflight. *Biol. Sci. Space* 8, 79–93. doi: 10.2187/bss.8.79

Guignandon, A., Akhouayri, O., Usson, Y., Rattner, A., Laroche, N., Lafage-Proust, M. H., et al. (2003). Focal contact clustering in osteoblastic cells under mechanical stresses: microgravity and cyclic deformation. *Cell Commun. Adhes.* 10, 69–83. doi: 10.1080/15419060390260987

Guignandon, A., Genty, C., Vico, L., Lafage-Proust, M. H., Palle, S., and Alexandre, C. (1997). Demonstration of feasibility of automated osteoblastic line culture in space flight. *Bone* 20, 109–116. doi: 10.1016/s8756-3282(96)00337-7

Guignandon, A., Vico, L., Alexandre, C., and Lafage-Proust, M. H. (1995). Shape changes of osteoblastic cells under gravitational variations during parabolic flight–relationship with PGE2 synthesis. *Cell Struct. Funct.* 20, 369–375. doi: 10.1247/csf.20.369

Haapala, J., Lammi, M. J., Inkinen, R., Parkkinen, J. J., Agren, U. M., Arokoski, J., et al. (1996). Coordinated regulation of hyaluronan and aggrecan content in the articular cartilage of immobilized and exercised dogs. *J. Rheumatol.* 23, 1586–1593.

Harris, S. A., Zhang, M., Kidder, L. S., Evans, G. L., Spelsberg, T. C., and Turner, R. T. (2000). Effects of orbital spaceflight on human osteoblastic cell physiology and gene expression. *Bone* 26, 325–331. doi: 10.1016/s8756-3282(00)00234-9

Herranz, R., Anken, R., Boonstra, J., Braun, M., Christianen, P. C., de Geest, M., et al. (2013). Ground-based facilities for simulation of microgravity: organism-specific recommendations for their use, and recommended terminology. *Astrobiology* 13, 1–17. doi: 10.1089/ast.2012.0876

Herranz, R., Larkin, O. J., Dijkstra, C. E., Hill, R. J., Anthony, P., Davey, M. R., et al. (2012). Microgravity simulation by diamagnetic levitation: effects of a strong gradient magnetic field on the transcriptional profile of *Drosophila melanogaster*. *BMC Genomics* 13:52. doi: 10.1186/1471-2164-13-52

Higashibata, A., Imamizo-Sato, M., Seki, M., Yamazaki, T., and Ishioka, N. (2006). Influence of simulated microgravity on the activation of the small GTPase Rho involved in cytoskeletal formation–molecular cloning and sequencing of bovine leukemia-associated guanine nucleotide exchange factor. *BMC Biochem.* 7:19. doi: 10.1186/1471-2091-7-19

Horneck, G., Facius, R., Reichert, M., Rettberg, P., Seboldt, W., Manzey, D., et al. (2003). HUMEX, a study on the survivability and adaptation of humans to long-duration exploratory missions, part I: lunar missions. *Adv. Space Res.* 31, 2389–2401. doi: 10.1016/s0273-1177(03)00568-4

Hughes-Fulford, M. (2003). Function of the cytoskeleton in gravisensing during spaceflight. *Adv. Space Res.* 32, 1585–1593. doi: 10.1016/s0273-1177(03)90399-1

Hughes-Fulford, M., and Lewis, M. L. (1996). Effects of microgravity on osteoblast growth activation. *Exp. Cell Res.* 224, 103–109.

Huijser, R. (2000). *Desktop RPM: New Small Size Microgravity Simulator for the Bioscience Laboratory*. Amsterdam: Fokker Space.

Ikeda, H., Souda, H., Puspitasari, A., Held, K. D., Hidema, J., Nikawa, T., et al. (2017). Development and performance evaluation of a three-dimensional clinostat synchronized heavy-ion irradiation system. *Life Sci. Space Res.* 12, 51–60. doi: 10.1016/j.lssr.2017.01.003

Infanger, M., Kossmehl, P., Shakibaei, M., Baatout, S., Witzing, A., Grosse, J., et al. (2006a). Induction of three-dimensional assembly and increase in apoptosis of human endothelial cells by simulated microgravity: impact of vascular

endothelial growth factor. *Apoptosis* 11, 749–764. doi: 10.1007/s10495-006-5697-7

Infanger, M., Kossmehl, P., Shakibaei, M., Bauer, J., Kossmehl-Zorn, S., Cogoli, A., et al. (2006b). Simulated weightlessness changes the cytoskeleton and extracellular matrix proteins in papillary thyroid carcinoma cells. *Cell Tissue Res.* 324, 267–277. doi: 10.1007/s00441-005-0142-8

Ingber, D. (1999). How cells (might) sense microgravity. *FASEB J.* 13(Suppl.), S3–S15. doi: 10.1096/fasebj.13.9001.s3

Ingber, D. E. (1997). Tensegrity: the architectural basis of cellular mechanotransduction. *Annu. Rev. Physiol.* 59, 575–599. doi: 10.1146/annurev.physiol.59.1.575

Janmaleki, M., Pachenari, M., Seyedpour, S. M., Shahghadami, R., and Sanati-Nezhad, A. (2016). Impact of simulated microgravity on cytoskeleton and viscoelastic properties of endothelial cell. *Sci. Rep.* 6:32418. doi: 10.1038/srep32418

Jeong, A. J., Kim, Y. J., Lim, M. H., Lee, H., Noh, K., Kim, B.-H., et al. (2018). Microgravity induces autophagy via mitochondrial dysfunction in human Hodgkin's lymphoma cells. *Sci. Rep.* 8:14646. doi: 10.1038/s41598-018-32965-3

Kamiya, N., Shuxian, L., Yamaguchi, R., Phipps, M., Aruwajoye, O., Adapala, N. S., et al. (2016). Targeted disruption of BMP signaling through type IA receptor (BMPR1A) in osteocyte suppresses SOST and RANKL, leading to dramatic increase in bone mass, bone mineral density and mechanical strength. *Bone* 91, 53–63. doi: 10.1016/j.bone.2016.07.002

Kopp, S., Krüger, M., Feldmann, S., Oltmann, H., Schütte, A., Schmitz, B., et al. (2018a). Thyroid cancer cells in space during the TEXUS-53 sounding rocket mission – the THYROID project. *Sci. Rep.* 8:10355. doi: 10.1038/s41598-018-28695-1

Kopp, S., Sahana, J., Islam, T., Petersen, A. G., Bauer, J., Corydon, T. J., et al. (2018b). The role of NFκB in spheroid formation of human breast cancer cells cultured on the Random Positioning Machine. *Sci. Rep.* 8:921. doi: 10.1038/s41598-017-18556-8

Kopp, S., Warnke, E., Wehland, M., Aleshcheva, G., Magnusson, N. E., Hemmersbach, R., et al. (2015). Mechanisms of three-dimensional growth of thyroid cells during long-term simulated microgravity. *Sci. Rep.* 5:16691. doi: 10.1038/srep16691

Krüger, M., Melnik, D., Kopp, S., Buken, C., Sahana, J., Bauer, J., et al. (2019a). Fighting thyroid cancer with microgravity research. *Int. J. Mol. Sci.* 20:2553. doi: 10.3390/ijms20102553

Krüger, M., Pietsch, J., Bauer, J., Kopp, S., Carvalho, D. T. O., Baatout, S., et al. (2019b). Growth of endothelial cells in space and in simulated microgravity - a comparison on the secretory level. *Cell Physiol. Biochem.* 52, 1039–1060. doi: 10.33594/000000071

Kurz, B., Lemke, A. K., Fay, J., Pufe, T., Grodzinsky, A. J., and Schunke, M. (2005). Pathomechanisms of cartilage destruction by mechanical injury. *Ann. Anat.* 187, 473–485. doi: 10.1016/j.aanat.2005.07.003

Lewis, M. L., Reynolds, J. L., Cubano, L. A., Hatton, J. P., Lawless, B. D., and Piepmeier, E. H. (1998). Spaceflight alters microtubules and increases apoptosis in human lymphocytes (Jurkat). *FASEB J.* 12, 1007–1018. doi: 10.1096/fasebj.12.11.1007

Li, J., Zhang, S., Chen, J., Du, T., Wang, Y., and Wang, Z. (2009). Modeled microgravity causes changes in the cytoskeleton and focal adhesions, and decreases in migration in malignant human MCF-7 cells. *Protoplasma* 238, 23–33. doi: 10.1007/s00709-009-0068-1

Louis, F., Bouleftour, W., Rattner, A., Linossier, M. T., Vico, L., and Guignandon, A. (2017). RhoGTPase stimulation is associated with strontium chloride treatment to counter simulated microgravity-induced changes in multipotent cell commitment. *NPJ Microgravity* 3:7. doi: 10.1038/s41526-016-0004-6

Maniotis, A. J., Chen, C. S., and Ingber, D. E. (1997). Demonstration of mechanical connections between integrins, cytoskeletal filaments, and nucleoplasm that stabilize nuclear structure. *Proc. Natl. Acad. Sci. U.S.A.* 94, 849–854. doi: 10.1073/pnas.94.3.849

Mann, V., Grimm, D., Corydon, T. J., Kruger, M., Wehland, M., Riwaldt, S., et al. (2019). Changes in human foetal osteoblasts exposed to the random positioning machine and bone construct tissue engineering. *Int. J. Mol. Sci.* 20:1357. doi: 10.3390/ijms20061357

Martin, M., Sansalone, V., Cooper, D. M. L., Forwood, M. R., and Pivonka, P. (2020). Assessment of romosozumab efficacy in the treatment of postmenopausal osteoporosis: results from a mechanistic PK-PD mechanostat model of bone remodeling. *Bone* doi: 10.1016/j.bone.2020.115223 [Epub ahead of print].

Martinez, E. M., Yoshida, M. C., Candelario, T. L., and Hughes-Fulford, M. (2015). Spaceflight and simulated microgravity cause a significant reduction of key gene expression in early T-cell activation. *Am. J. Physiol. Regul. Integr. Comp. Physiol.* 308, R480–R488. doi: 10.1152/ajpregu.00449.2014

Nabavi, N., Khandani, A., Camirand, A., and Harrison, R. E. (2011). Effects of microgravity on osteoclast bone resorption and osteoblast cytoskeletal organization and adhesion. *Bone* 49, 965–974. doi: 10.1016/j.bone.2011.07.036

Nassef, M. Z., Kopp, S., Wehland, M., Melnik, D., Sahana, J., Kruger, M., et al. (2019). Real microgravity influences the cytoskeleton and focal adhesions in human breast cancer cells. *Int. J. Mol. Sci.* 20:3156. doi: 10.3390/ijms20133156

Nourse, J. L., and Pathak, M. M. (2017). How cells channel their stress: interplay between Piezo1 and the cytoskeleton. *Semin. Cell Dev. Biol.* 71, 3–12. doi: 10.1016/j.semcdb.2017.06.018

O'Connor, K. M. (1997). Unweighting accelerates tidemark advancement in articular cartilage at the knee joint of rats. *J. Bone Miner. Res.* 12, 580–589. doi: 10.1359/jbmr.1997.12.4.580

Okumura, S., Mizoguchi, T., Sato, N., Yamaki, M., Kobayashi, Y., Yamauchi, H., et al. (2006). Coordination of microtubules and the actin cytoskeleton is important in osteoclast function, but calcitonin disrupts sealing zones without affecting microtubule networks. *Bone* 39, 684–693. doi: 10.1016/j.bone.2006.04.010

Pajevic, P. D., Spatz, J. M., Garr, J., Adamson, C., and Misener, L. (2013). Osteocyte biology and space flight. *Curr. Biotechnol.* 2, 179–183. doi: 10.2174/22115501113029990017

Papaseit, C., Pochon, N., and Tabony, J. (2000). Microtubule self-organization is gravity-dependent. *Proc. Natl. Acad. Sci. U.S.A.* 97, 8364–8368. doi: 10.1073/pnas.140029597

Patel, M. J., Liu, W., Sykes, M. C., Ward, N. E., Risin, S. A., Risin, D., et al. (2007). Identification of mechanosensitive genes in osteoblasts by comparative microarray studies using the rotating wall vessel and the random positioning machine. *J. Cell Biochem.* 101, 587–599. doi: 10.1002/jcb.21218

Pavlakou, P., Dounousi, E., Roumeliotis, S., Eleftheriadis, T., and Liakopoulos, V. (2018). Oxidative stress and the kidney in the space environment. *Int. J. Mol. Sci.* 19:3176. doi: 10.3390/ijms19103176

Plett, P. A., Abonour, R., Frankovitz, S. M., and Orschell, C. M. (2004). Impact of modeled microgravity on migration, differentiation, and cell cycle control of primitive human hematopoietic progenitor cells. *Exp. Hematol.* 32, 773–781. doi: 10.1016/j.exphem.2004.03.014

Poole, K. E., van Bezooijen, R. L., Loveridge, N., Hamersma, H., Papapoulos, S. E., Lowik, C. W., et al. (2005). Sclerostin is a delayed secreted product of osteocytes that inhibits bone formation. *FASEB J.* 19, 1842–1844. doi: 10.1096/fj.05-4221fje

Ratushnyy, A. Y., and Buravkova, L. B. (2017). Expression of focal adhesion genes in mesenchymal stem cells under simulated microgravity. *Dokl. Biochem. Biophys.* 477, 354–356. doi: 10.1134/s1607672917060035

Rijken, P. J., de Groot, R. P., Briegleb, W., Kruijer, W., Verkleij, A. J., Boonstra, J., et al. (1991). Epidermal growth factor-induced cell rounding is sensitive to simulated microgravity. *Aviat. Space Environ. Med.* 62, 32–36.

Rijken, P. J., de Groot, R. P., Kruijer, W., de Laat, S. W., Verkleij, A. J., and Boonstra, J. (1992). Identification of specific gravity sensitive signal transduction pathways in human A431 carcinoma cells. *Adv. Space Res.* 12, 145–152. doi: 10.1016/0273-1177(92)90277-5

Robling, A. G., Niziolek, P. J., Baldridge, L. A., Condon, K. W., Allen, M. R., Alam, I., et al. (2008). Mechanical stimulation of bone in vivo reduces osteocyte expression of Sost/sclerostin. *J. Biol. Chem.* 283, 5866–5875. doi: 10.1074/jbc.M705092200

Rodionova, N. V., Oganov, V. S., and Zolotova, N. V. (2002). Ultrastructural changes in osteocytes in microgravity conditions. *Adv. Space Res.* 30, 765–770. doi: 10.1016/s0273-1177(02)00393-9

Rosner, H., Wassermann, T., Moller, W., and Hanke, W. (2006). Effects of altered gravity on the actin and microtubule cytoskeleton of human SH-SY5Y neuroblastoma cells. *Protoplasma* 229, 225–234. doi: 10.1007/s00709-006-0202-2

Russomano, T., Cardoso, R., Falcao, F., Dalmarco, G., Santos, C. V. D., Santos, L. F. D., et al. (2005). Development and validation of a 3D clinostat for the study

of cells during microgravity simulation. *Conf. Proc. IEEE Eng. Med. Biol. Soc.* 1, 564–566. doi: 10.1109/iembs.2005.1616474

Salter, R. B., Simmonds, D. F., Malcolm, B. W., Rumble, E. J., MacMichael, D., and Clements, N. D. (1980). The biological effect of continuous passive motion on the healing of full-thickness defects in articular cartilage. An experimental investigation in the rabbit. *J. Bone Joint Surg. Am.* 62, 1232–1251. doi: 10.2106/00004623-198062080-00002

Sanchez-Adams, J., Leddy, H. A., McNulty, A. L., O'Conor, C. J., and Guilak, F. (2014). The mechanobiology of articular cartilage: bearing the burden of osteoarthritis. *Curr. Rheumatol. Rep.* 16:451. doi: 10.1007/s11926-014-0451-6

Scheiber, A. L., Barton, D. K., Khoury, B. M., Marini, J. C., Swiderski, D. L., Caird, M. S., et al. (2019). Sclerostin antibody-induced changes in bone mass are site specific in developing Crania. *J. Bone Miner. Res.* 34, 2301–2310. doi: 10.1002/jbmr.3858

Sciola, L., Cogoli-Greuter, M., Cogoli, A., Spano, A., and Pippia, P. (1999). Influence of microgravity on mitogen binding and cytoskeleton in Jurkat cells. *Adv. Space Res.* 24, 801–805. doi: 10.1016/s0273-1177(99)00078-2

Shi, Z. X., Rao, W., Wang, H., Wang, N. D., Si, J. W., Zhao, J., et al. (2015). Modeled microgravity suppressed invasion and migration of human glioblastoma U87 cells through downregulating store-operated calcium entry. *Biochem. Biophys. Res. Commun.* 457, 378–384. doi: 10.1016/j.bbrc.2014.12.120

Smith, J. K. (2018). IL-6 and the dysregulation of immune, bone, muscle, and metabolic homeostasis during spaceflight. *NPJ Microgravity* 4:24. doi: 10.1038/s41526-018-0057-9

Sonnenfeld, G., Mandel, A. D., Konstantinova, I. V., Berry, W. D., Taylor, G. R., Lesnyak, A. T., et al. (1992). Spaceflight alters immune cell function and distribution. *J. Appl. Physiol.* 73(2 Suppl.), 191S–195S. doi: 10.1152/jappl.1992.73.2.S191

Stamenkovic, V., Keller, G., Nesic, D., Cogoli, A., and Grogan, S. P. (2010). Neocartilage formation in 1 g, simulated, and microgravity environments: implications for tissue engineering. *Tissue Eng. Part A* 16, 1729–1736. doi: 10.1089/ten.tea.2008.0624

Tabony, J., Glade, N., Papaseit, C., and Demongeot, J. (2002). Microtubule self-organisation and its gravity dependence. *Adv. Space Biol. Med.* 8, 19–58. doi: 10.1016/s1569-2574(02)08014-0

Tan, X., Xu, A., Zhao, T., Zhao, Q., Zhang, J., Fan, C., et al. (2018). Simulated microgravity inhibits cell focal adhesions leading to reduced melanoma cell proliferation and metastasis via FAK/RhoA-regulated mTORC1 and AMPK pathways. *Sci. Rep.* 8:3769. doi: 10.1038/s41598-018-20459-1

Tauber, S., Lauber, B. A., Paulsen, K., Layer, L. E., Lehmann, M., Hauschild, S., et al. (2017). Cytoskeletal stability and metabolic alterations in primary human macrophages in long-term microgravity. *PLoS One* 12:e0175599. doi: 10.1371/journal.pone.0175599

Thiel, C. S., Hauschild, S., Huge, A., Tauber, S., Lauber, B. A., Polzer, J., et al. (2017). Dynamic gene expression response to altered gravity in human T cells. *Sci. Rep.* 7:5204. doi: 10.1038/s41598-017-05580-x

Thiel, C. S., Tauber, S., Lauber, B., Polzer, J., Seebacher, C., Uhl, R., et al. (2019a). Rapid morphological and cytoskeletal response to microgravity in human primary macrophages. *Int. J. Mol. Sci.* 20:2402. doi: 10.3390/ijms20102402

Thiel, C. S., Tauber, S., Seebacher, C., Schropp, M., Uhl, R., Lauber, B., et al. (2019b). Real-time 3D high-resolution microscopy of human cells on the international space station. *Int. J. Mol. Sci.* 20:2033. doi: 10.3390/ijms20082033

Ulbrich, C., Westphal, K., Pietsch, J., Winkler, H. D., Leder, A., Bauer, J., et al. (2010). Characterization of human chondrocytes exposed to simulated microgravity. *Cell Physiol. Biochem.* 25, 551–560. doi: 10.1159/000303059

Ulbrich, C., Pietsch, J., Grosse, J., Wehland, M., Schulz, H., Saar, K., et al. (2011). Differential gene regulation under altered gravity conditions in follicular thyroid cancer cells: relationship between the extracellular matrix and the cytoskeleton. *Cell. Physiol. Biochem.* 28, 185–198. doi: 10.1159/000331730

Uva, B. M., Masini, M. A., Sturla, M., Prato, P., Passalacqua, M., Giuliani, M., et al. (2002). Clinorotation-induced weightlessness influences the cytoskeleton of glial cells in culture. *Brain Res.* 934, 132–139. doi: 10.1016/s0006-8993(02)02415-0

Vanwanseele, B., Eckstein, F., Knecht, H., Stussi, E., and Spaepen, A. (2002). Knee cartilage of spinal cord-injured patients displays progressive thinning in the absence of normal joint loading and movement. *Arthritis Rheum.* 46, 2073–2078. doi: 10.1002/art.10462

Vassy, J., Portet, S., Beil, M., Millot, G., Fauvel-Lafeve, F., Karniguian, A., et al. (2001). The effect of weightlessness on cytoskeleton architecture and proliferation of human breast cancer cell line MCF-7. *FASEB J.* 15, 1104–1106. doi: 10.1096/fj.00-0527fje

Vassy, J., Portet, S., Beil, M., Millot, G., Fauvel-Laféve, F., Gasset, G., et al. (2003). Weightlessness acts on human breast cancer cell line MCF-7. *Adv. Space Res.* 32, 1595–1603. doi: 10.1016/S0273-1177(03)90400-5

Vidyasekar, P., Shyamsunder, P., Arun, R., Santhakumar, R., Kapadia, N. K., Kumar, R., et al. (2015). Genome wide expression profiling of cancer cell lines cultured in microgravity reveals significant dysregulation of cell cycle and MicroRNA gene networks. *PLoS One* 10:e0135958. doi: 10.1371/journal.pone.0135958

Vorselen, D., Roos, W. H., MacKintosh, F. C., Wuite, G. J., and van Loon, J. J. (2014). The role of the cytoskeleton in sensing changes in gravity by nonspecialized cells. *FASEB J.* 28, 536–547. doi: 10.1096/fj.13-236356

Wang, N., Butler, J. P., and Ingber, D. E. (1993). Mechanotransduction across the cell surface and through the cytoskeleton. *Science* 260, 1124–1127. doi: 10.1126/science.7684161

White, O., Clement, G., Fortrat, J. O., Pavy-LeTraon, A., Thonnard, J. L., Blanc, S., et al. (2016). Towards human exploration of space: the THESEUS review series on neurophysiology research priorities. *NPJ Microgravity* 2:16023. doi: 10.1038/npjmgrav.2016.23

White, R. J., and Averner, M. (2001). Humans in space. *Nature* 409, 1115–1118. doi: 10.1038/35059243

Wolfenson, H., Bershadsky, A., Henis, Y. I., and Geiger, B. (2011). Actomyosin-generated tension controls the molecular kinetics of focal adhesions. *J. Cell Sci.* 124(Pt 9), 1425–1432. doi: 10.1242/jcs.077388

Wolfenson, H., Lubelski, A., Regev, T., Klafter, J., Henis, Y. I., and Geiger, B. (2009). A role for the juxtamembrane cytoplasm in the molecular dynamics of focal adhesions. *PLoS One* 4:e4304. doi: 10.1371/journal.pone.0004304

Xu, H., Wu, F., Zhang, H., Yang, C., Li, K., Wang, H., et al. (2017). Actin cytoskeleton mediates BMP2-Smad signaling via calponin 1 in preosteoblast under simulated microgravity. *Biochimie* 138, 184–193. doi: 10.1016/j.biochi.2017.04.015

Zaidel-Bar, R., Ballestrem, C., Kam, Z., and Geiger, B. (2003). Early molecular events in the assembly of matrix adhesions at the leading edge of migrating cells. *J. Cell Sci.* 116(Pt 22), 4605–4613. doi: 10.1242/jcs.00792

Conflict of Interest: The authors declare that the research was conducted in the absence of any commercial or financial relationships that could be construed as a potential conflict of interest.

Copyright © 2020 Bradbury, Wu, Choi, Rowan, Zhang, Poole, Lauko and Chou. This is an open-access article distributed under the terms of the Creative Commons Attribution License (CC BY). The use, distribution or reproduction in other forums is permitted, provided the original author(s) and the copyright owner(s) are credited and that the original publication in this journal is cited, in accordance with accepted academic practice. No use, distribution or reproduction is permitted which does not comply with these terms.

frontiers in Cell and Developmental Biology

MINI REVIEW
published: 28 May 2019
doi: 10.3389/fcell.2019.00090

Spatio-Temporal Regulation of RhoGTPases Signaling by Myosin II

Selwin K. Wu[1,2] and Rashmi Priya[3]**

[1] Department of Cell Biology, Harvard Medical School, Boston, MA, United States, [2] Department of Pediatric Oncology, Dana-Farber Cancer Institute, Boston, MA, United States, [3] Department of Developmental Genetics, Max Planck Institute for Heart and Lung Research, Bad Nauheim, Germany

RhoGTPase activation of non-muscle myosin II regulates cell division, extrusion, adhesion, migration, and tissue morphogenesis. However, the regulation of myosin II and mechanotransduction is not straightforward. Increasingly, the role of myosin II on the feedback regulation of RhoGTPase signaling is emerging. Indeed, myosin II controls RhoGTPase signaling through multiple mechanisms, namely contractility driven advection, scaffolding, and sequestration of signaling molecules. Here we discuss these mechanisms by which myosin II regulates RhoGTPase signaling in cell adhesion, migration, and tissue morphogenesis.

Keywords: pulsatility, morphogenesis, GTPase signaling, adhesion and migration, active fluid media, actomyosin

OPEN ACCESS

Edited by:
Vania Braga,
Imperial College London,
United Kingdom

Reviewed by:
René-Marc Mège,
Centre National de la Recherche Scientifique (CNRS), France
Simone Diestel,
University of Bonn, Germany

****Correspondence:***
Selwin K. Wu
selwin_wu@mail.dfci.harvard.edu
Rashmi Priya
rashmi.priya@mpi-bn.mpg.de

Specialty section:
This article was submitted to Cell Adhesion and Migration, a section of the journal Frontiers in Cell and Developmental Biology

Received: *04 December 2018*
Accepted: *13 May 2019*
Published: *28 May 2019*

Citation:
Wu SK and Priya R (2019) Spatio-Temporal Regulation of RhoGTPases Signaling by Myosin II. Front. Cell Dev. Biol. 7:90. doi: 10.3389/fcell.2019.00090

INTRODUCTION

Non-muscle myosin II is a major determinant of cell and tissue morphogenesis (Vicente-Manzanares et al., 2009; Wu and Yap, 2013; Priya and Yap, 2015). Myosin II is best characterized as a cytoskeletal motor-protein, which binds to filamentous actin and generates forces as an actomyosin complex (Even-Ram et al., 2007; Conti and Adelstein, 2008; Vicente-Manzanares et al., 2009; Lee et al., 2010; Gomez et al., 2011; Kuo et al., 2011; Shin et al., 2014; Priya et al., 2015). Myosin II regulates forces in cells by cross-linking the filamentous actin network across the cytoplasmic cortex of a cell (Cai et al., 2006, 2010; Luo et al., 2013). In extension to the well-established pathway of active Rho GTPase activating myosin II, strikingly, myosin II can also feedback to regulate Rho GTP signaling by scaffolding signaling molecules and through generating contractile forces (Priya et al., 2015; Munjal et al., 2015).

ACTOMYOSIN PULSATILITY FEEDBACKS TO RHO SIGNALING

Pulsatile behavior of the medipoapical actomyosin network regulates epithelial elongation changes during morphogenesis (Munjal et al., 2015; **Figure 1**). Pulsatility of actomyosin network induced by lateral cadherin clusters also promotes dissipation of local tensile stress at the junctions of tightly packed cells limiting apical extrusion of cells out of the epithelia (Wu et al., 2014a,b, 2015; **Figure 1**). At the medial apical region of cells during intercalation, myosin II contractility initially amplifies then dampens Rho GTPases signaling (Munjal et al., 2015). First, actomyosin contraction locally concentrates (activators of myosin II) Rho and Rho kinase (**Figure 1B**). Subsequently, this contractility dependent recruitment of actomyosin network and activators then amplifies local RhoGTP activation and tension (Munjal et al., 2015). Second, many

F-actin associated regulators, such as formins and coronin 1B, can also organize actomyosin into tensile cortical networks that are highly contractile and stiff (Priya et al., 2016; Acharya et al., 2017). A stiff and tensile actomyosin network would lead to immobilization of the cell cortex (Wu et al., 2014b; Munjal et al., 2015), slowing down the contractility driven recruitment of Rho and Rho kinase. Thus, instead of recruitment, there will be an overall higher rate of dissociation of these actomyosin components. Consequently, relaxation of the actomyosin network occurs (Munjal et al., 2015) (**Figure 1B**).

Similarly, contractile stress-induced disassembly of tensile actomyosin cables can also relax the actomyosin network (Wu et al., 2014a,b; Jodoin et al., 2015). Actomyosin pulsatility observed at cell-cell junctions (Wu et al., 2014a,b) and medial apical region of cells (Munjal et al., 2015) can be reproduced with computer simulations that model actomyosin as an active fluid, where both extremely dense and low density of simulated actomyosin produces an immobile behavior (Moore et al., 2014). Indeed, overexpression of formins or treatment of cells with jasplakinolide, which increases the density of actomyosin, immobilizes the cortex whereas inhibition of myosin II also leads to an immobile cortex (Munjal et al., 2015; Wu et al., 2014a,b). Only at the intermediate density, cyclical events of contraction and relaxation of a pulsatile network is observed (Moore et al., 2014).

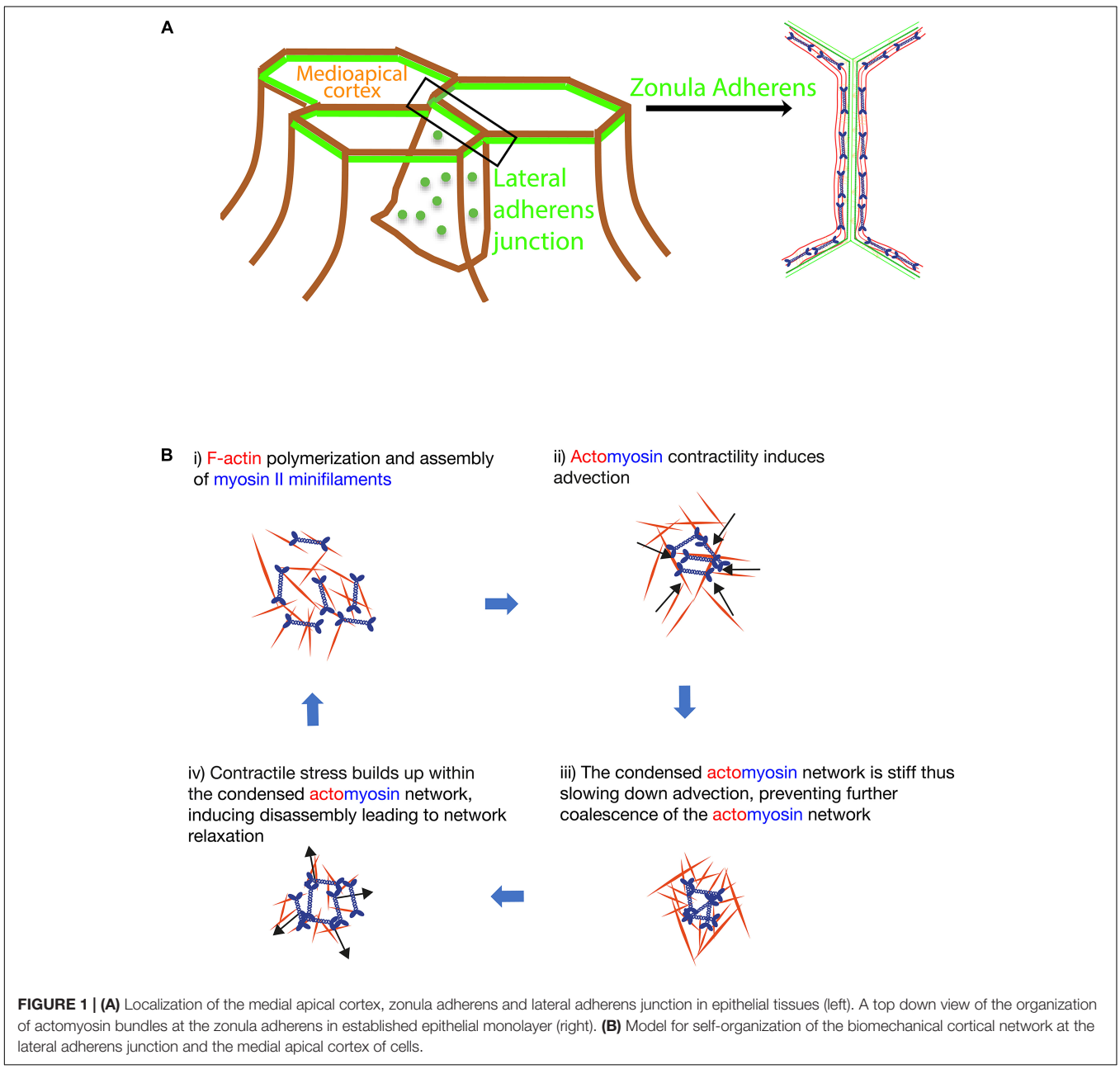

FIGURE 1 | (A) Localization of the medial apical cortex, zonula adherens and lateral adherens junction in epithelial tissues (left). A top down view of the organization of actomyosin bundles at the zonula adherens in established epithelial monolayer (right). **(B)** Model for self-organization of the biomechanical cortical network at the lateral adherens junction and the medial apical cortex of cells.

MYOSIN II PROMOTES STABILITY OF ACTIVE RHOA AT THE ZONULA ADHERENS

In addition, myosin II can scaffold signaling molecules to regulate RhoGTPase activity (Conti and Adelstein, 2008). Myosin II has a head domain that binds and exerts forces on F-actin, and also rod domains which self-associate to form bipolar filaments of Myosin molecules (**Figure 2**). Strikingly, myosin II can regulate signaling via its rod domain. Indeed, we find that myosin II rod domain plays an important role in preventing the inactivation of RhoA at the zonula adherens. The zonula adherens is an apical cell-cell contact zone of concentrated E-cadherin (**Figures 1**, **2**) which is linked to an enrichment of a variety of cytoskeletal proteins (Smutny et al., 2010; Leerberg et al., 2014; Han et al., 2014). We find that the rod domain of myosin II can further reinforce RhoA GTPases activation by preventing the inactivation of RhoA GTPase (Choi et al., 2008; Smutny et al., 2010; Ma et al., 2012; Priya et al., 2015). How does the rod domain of myosin II prevent the inactivation of RhoA GTPase? This is achieved via myosin IIA rod domain regulation of RhoA GAP signaling (Priya et al., 2015; **Figure 2**). Rho GTPase is inhibited by GAP and activated by Guanine Exchange Factors (GEFs) (McCormack et al., 2013). In brief, the rod-domain of myosin II scaffolds Rho kinase (ROCK-1) at the zonula adherens, where ROCK-1 phosphorylates Rnd3 GTPase rendering it inactive. Inactivating Rnd3 GTPase is essential to maintain active RhoA because active Rnd3 inhibits RhoA by recruiting and activating p190B Rho GAP (Priya et al., 2015). Thus, myosin IIA recruitment of ROCK-1 supports RhoA signaling by inhibiting the cortical localization of Rnd3-p190B GAP RhoA complex (Priya et al., 2015).

Myosin IIA supports RhoGTPase signaling by scaffolding ROCK-1 independent of myosin IIB. This is consistent with myosin IIA and myosin IIB responding to distinct upstream signals at zonula adherens; myosin IIA is activated by the RhoA pathway while myosin IIB is primarily regulated by Rap1 signaling (Smutny et al., 2010, 2011; Gomez et al., 2015). The rod domain of myosin II exhibits greater dissimilarity in protein sequence between different paralogs and thus, could potentially explain why these myosin isoforms respond to distinct signaling pathways (Conti and Adelstein, 2008; Vicente-Manzanares et al., 2009; Heissler and Manstein, 2013). For example, the rod domain of myosin II harbors unique regulatory modifications like phosphorylation sites (Rosenberg and Ravid, 2006).

MYOSIN II REGULATES RAC AND CDC42 GTPASES

Myosin II can also affect Rac GTPase signaling. The GEFs that activates Rac-1 includes Tiam-1 and β-pix. GEFs including Tiam-1 and β-pix activates Rac-1 by binding to the inactive Rac-1 GDP, catalyzing the sequential release of GDP and binding of GTP, to activate Rac-1. Rac GTPase signaling regulates cell migration, by stimulating cellular protrusions through inducing Arp2/3 branched actin formation (Ridley, 2015). Interestingly, consistent

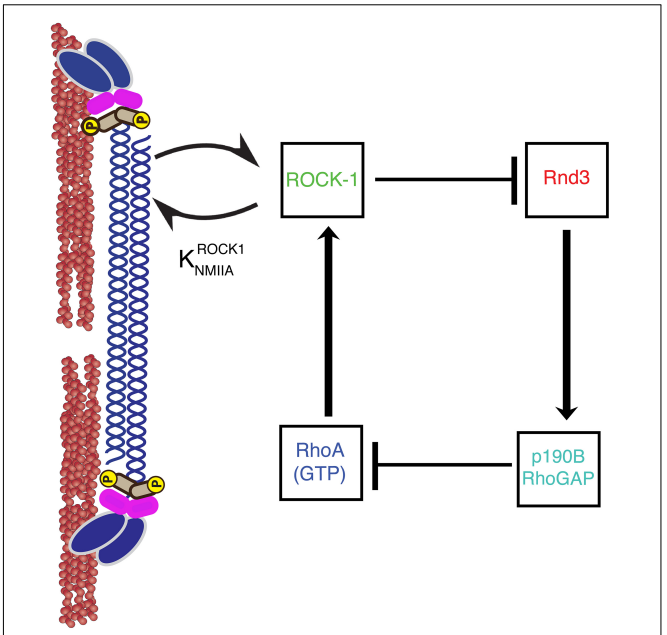

FIGURE 2 | A non-muscle Myosin II minifilament cross linking F-actin filaments (left). ROCK1 binding to myosin II regulates GTP–RhoA, ROCK1, Rnd3, and p190B RhoGAP signaling at the zonula adherens (right). Arrows and T-junctions represent stimulation and repression of junctional recruitment.

with the commonly reported antagonism between Rac1 and RhoA, myosin II can activate RhoA but dampen Rac activation. Indeed, myosin IIA was implicated as negative regulator of Rac GTP dependent cell migration (Even-Ram et al., 2007). Inhibition of myosin IIA stabilized microtubules which then recruited Rac GEF Tiam1 to activate Rac GTPase at the leading edge of cells. Thus, active myosin II can retard cell migration by reducing Tiam-1 mediated Rac activation. Alternatively, active myosin II can also dampen Rac GTPase signaling by sequestering Rac1-GEF β-pix from RacGTPase (Kuo et al., 2011). Inhibiting myosin II by blebbistatin or plating fibroblasts on a compliant substrate to reduce cellular contractility stimulated the localization of Rac1-GEF β-pix to focal-adhesions thus activating Rac-1. Similarly, the gain of function experiments in CHO epithelial cells, by expressing myosin II phosphomimetic regulatory light chain (RLD-DD) reduces the localization of Rac GEFs β-pix to cortical Rac GTPase, thus dampening Rac GTPase activation (Vicente-Manzanares et al., 2011). Taken together, myosin II can retard cell-migration by preventing the colocalization of Rac1 activators such as Tiam-1 and β-pix to Rac GTPase.

Additionally, myosin II is reported to affect the Rho GTPase-CDC42. Myosin II was found to regulate neuronal morphology by modulating CDC42 signaling (Shin et al., 2014). In the growth cone of hippocampal cells, blebbistatin mediated inhibition of myosin II released the β-pix GEFs from myosin II-GEF complex to associate with and activate CDC42. Thus, promoting actin dependent protrusions and filopodia formation from the neurite shaft.

Then, how does myosin II block the recruitment of these activators to Rac and CDC42? Interestingly, myosin II was found

to directly interact with various Dbl family of GEFs including β-pix and Tiam1 (Lee et al., 2010). The ATPase activity and actomyosin filament assembly were necessary for this interaction. Indeed, blebbistatin, ATPase-defective mutants or obliteration of filamentous-actin from the lysates compromised myosin II interaction with these GEFs. Myosin II perturbs the catalytic activity of these bound GEFs. Thus, the contractile actomyosin filament may suppress cell-migration by sequestering Dbl-family of GEFs which activates Rac and CDC42.

In summary, myosin II regulates Rho GTPase signaling in many developmental related processes including cell adhesion, migration and morphogenesis. Since Rho GTPases signaling are commonly misregulated in cancer (Lozano et al., 2003), how myosin II-regulated signaling is regulated in cellular processes related to cancer including cell-contact inhibition of growth (Chiasson-MacKenzie et al., 2015) and epithelial-to-mesenchymal transition (Thiery and Sleeman, 2006; Mangold et al., 2011; Greenlees et al., 2015; Wu et al., 2015) remains to be explored.

AUTHOR CONTRIBUTIONS

SW and RP wrote the manuscript and made figures.

FUNDING

SW is supported by a Leukemia and Lymphoma Society Fellow Award (5454-17). RP is supported by an EMBO Long-Term Fellowship (ALTF 1569-2016) and a post-doctoral fellowship from the Alexander von Humboldt Foundation.

ACKNOWLEDGMENTS

We thank Alpha Yap and Guillermo Gomez for discussions and apologize to all colleagues whose work could not be cited owing to space limitations.

REFERENCES

Acharya, B. R., Wu, S. K., Lieu, Z. Z., Parton, R. G., Grill, S. W., Bershadsky, A. D., et al. (2017). Mammalian diaphanous 1 mediates a pathway for e-cadherin to stabilize epithelial barriers through junctional contractility. *Cell Rep.* 18, 2854–2867. doi: 10.1016/j.celrep.2017.02.078

Cai, Y., Biais, N., Giannone, G., Tanase, M., Jiang, G., Hofman, J. M., et al. (2006). Nonmuscle myosin IIA-dependent force inhibits cell spreading and drives F-actin flow. *Biophys. J.* 91, 3907–3920.

Cai, Y., Rossier, O., Gauthier, N. C., Biais, N., Fardin, M. A., Zhang, X., et al. (2010). Cytoskeletal coherence requires myosin-IIA contractility. *J. Cell. Sci.* 123, 413–423. doi: 10.1242/jcs.058297

Chiasson-MacKenzie, C., Morris, Z. S., Baca, Q., Morris, B., Coker, J. K., Mirchev, R., et al. (2015). NF2/Merlin mediates contact-dependent inhibition of EGFR mobility and internalization via cortical actomyosin. *J. Cell. Biol.* 211, 391–405. doi: 10.1083/jcb.201503081

Choi, C. K., Vicente-Manzanares, M., Zareno, J., Whitmore, L. A., Mogilner, A., and Horwitz, A. R. (2008). Actin and alpha-actinin orchestrate the assembly and maturation of nascent adhesions in a myosin II motor-independent manner. *Nat. Cell. Biol.* 10, 1039–1050. doi: 10.1038/ncb1763

Conti, M. A., and Adelstein, R. S. (2008). Nonmuscle myosin II moves in new directions. *J. Cell. Sci.* 121, 11–18.

Even-Ram, S., Doyle, A. D., Couti, M. A., Matsumoto, K., Adelstein, R. S., Yamada, K. M., et al. (2007). Myosin IIA regulates cell motility and actomyosin-microtubule crosstalk. *Nat. Cell. Biol.* 9, 299–309.

Gomez, G. A., McLachlan, R. W., Wu, S. K., Caldwell, B. J., Moussa, E., Verma, S., et al. (2015). An RPTPalpha/Src family kinase/Rap1 signaling module recruits myosin IIB to support contractile tension at apical E-cadherin junctions. *Mol. Biol. Cell* 26, 1249–1262. doi: 10.1091/mbc.E14-07-1223

Gomez, G. A., McLachlan, R. W., and Yap, A. S. (2011). Productive tension: force-sensing and homeostasis of cell-cell junctions. *Trends Cell. Biol.* 21, 499–505. doi: 10.1016/j.tcb.2011.05.006

Greenlees, R., Mihelec, M., Yousoof, S., Speidel, D., Wu, S. K., Rinkwitz, S., et al. (2015). Mutations in $SIPA_1L_3$ cause eye defects through disruption of cell polarity and cytoskeleton organization. *Hum. Mol. Genet.* 24, 5789–5804. doi: 10.1093/hmg/ddv298

Han, S. P., Gambin, Y., Gomez, G. A., Verma, S., Giles, N., Michael, M., et al. (2014). Cortactin scaffolds Arp2/3 and WAVE2 at the epithelial zonula adherens. *J. Biol. Chem.* 289, 7764–7775. doi: 10.1074/jbc.M113.544478

Heissler, S. M., and Manstein, D. J. (2013). Nonmuscle myosin-2: mix and match. *Cell. Mol. Life Sci.* 70, 1–21. doi: 10.1007/s00018-012-1002-9

Jodoin, J. N., Coravos, J. S., Chanet, S., Vasquez, C. G., Tworoger, M., Kingston, E. R., et al. (2015). Stable force balance between epithelial cells arises from F-Actin turnover. *Dev. Cell* 35, 685–697. doi: 10.1016/j.devcel.2015.11.018

Kuo, J. C., Han, X., Hsiao, C. T., Yates, J. R. III, and Waterman, C. M. (2011). Analysis of the myosin-II-responsive focal adhesion proteome reveals a role for beta-Pix in negative regulation of focal adhesion maturation. *Nat. Cell. Biol.* 13, 383–393. doi: 10.1038/ncb2216

Lee, C. S., Choi, C. K., Shin, E. Y., Schwartz, M. A., and Kim, E. G. (2010). Myosin II directly binds and inhibits Dbl family guanine nucleotide exchange factors: a possible link to Rho family GTPases. *J. Cell. Biol.* 190, 663–674. doi: 10.1083/jcb.201003057

Leerberg, J. M., Gomez, G. A., Verma, S., Moussa, E. J., Wu, S. K., Priya, R., et al. (2014). Tension-sensitive actin assembly supports contractility at the epithelial zonula adherens. *Curr. Biol.* 24, 1689–1699. doi: 10.1016/j.cub.2014.06.028

Lozano, E., Betson, M., and Braga, V. M. (2003). Tumor progression: small GTPases and loss of cell-cell adhesion. *Bioessays* 25, 452–463.

Luo, W., Yu, C. H., Lieu, Z. Z., Allard, J., Mogilner, A., Sheetz, M. P., et al. (2013). Analysis of the local organization and dynamics of cellular actin networks. *J. Cell. Biol.* 202, 1057–1073. doi: 10.1083/jcb.201210123

Ma, X., Kovács, M., Conti, M. A., Wang, A., Zhang, Y., Sellers, J. R., et al. (2012). Nonmuscle myosin II exerts tension but does not translocate actin in vertebrate cytokinesis. *Proc. Natl. Acad. Sci. U.S.A.* 109, 4509–4514. doi: 10.1073/pnas.1116268109

Mangold, S., Wu, S. K., Norwood, S. J., Collins, B. M., Hamilton, N. A., Thorn, P., et al. (2011). Hepatocyte growth factor acutely perturbs actin filament anchorage at the epithelial zonula adherens. *Curr. Biol.* 21, 503–507. doi: 10.1016/j.cub.2011.02.018

McCormack, J., Welsh, N. J., and Braga, V. M. (2013). Cycling around cell-cell adhesion with Rho GTPase regulators. *J. Cell. Sci.* 126, 379–391. doi: 10.1242/jcs.097923

Moore, T., Wu, S. K., Michael, M., Yap, A. S., Gomez, G. A., and Neufeld, Z. (2014). Self-organizing actomyosin patterns on the cell cortex at epithelial cell-cell junctions. *Biophys. J.* 107, 2652–2661. doi: 10.1016/j.bpj.2014.10.045

Munjal, A., Philippe, J. M., Munro, E., and Lecuit, T. A. (2015). Self-organized biomechanical network drives shape changes during tissue morphogenesis. *Nature* 524, 351–355. doi: 10.1038/nature14603

Priya, R., Gomez, G. A., Badnar, S., Verma, S., Cox, H. L., Hamilton, N. A., et al. (2015). Feedback regulation through myosin II confers robustness on RhoA signalling at E-cadherin junctions. *Nat. Cell. Biol.* 17, 1282–1293. doi: 10.1038/ncb3239

Priya, R., Wee, K., Budnar, S., Gomez, G. A., Yap, A. S., and Michael, M. (2016). Coronin 1B supports RhoA signaling at cell-cell junctions through Myosin II. *Cell Cycle* 15, 3033–3041.

Priya, R., and Yap, A. S. (2015). Active tension: the role of cadherin adhesion and signaling in generating junctional contractility. *Curr. Top. Dev. Biol.* 112, 65–102. doi: 10.1016/bs.ctdb.2014.11.016

Ridley, A. J. (2015). Rho GTPase signalling in cell migration. *Curr. Opin. Cell. Biol.* 36, 103–112. doi: 10.1016/j.ceb.2015.08.005

Rosenberg, M., and Ravid, S. (2006). Protein kinase Cgamma regulates myosin IIB phosphorylation, cellular localization, and filament assembly. *Mol. Biol. Cell* 17, 1364–1374.

Shin, E. Y., Lee, C. S., Yun, C. Y., Won, S. Y., Kim, H. K., Lee, Y. H., et al. (2014). Non-muscle myosin II regulates neuronal actin dynamics by interacting with guanine nucleotide exchange factors. *PLoS One* 9:e95212. doi: 10.1371/journal.pone.0095212

Smutny, M., Cox, H. L., Leerberg, J. M., Kovacs, E. M., Conti, M. A., Ferguson, C., et al. (2010). Myosin II isoforms identify distinct functional modules that support integrity of the epithelial zonula adherens. *Nat. Cell. Biol.* 12, 696–702. doi: 10.1038/ncb2072

Smutny, M., Wu, S. K., Gomez, G. A., Mangold, S., Yap, A. S., and Hamilton, N. A. (2011). Multicomponent analysis of junctional movements regulated by myosin II isoforms at the epithelial zonula adherens. *PLoS One* 6:e22458. doi: 10.1371/journal.pone.0022458

Thiery, J. P., and Sleeman, J. P. (2006). Complex networks orchestrate epithelial-mesenchymal transitions. *Nat. Rev. Mol. Cell. Biol.* 7, 131–142.

Vicente-Manzanares, M., Ma, X., Adelstein, R. S., and Horwitz, A. R. (2009). Non-muscle myosin II takes centre stage in cell adhesion and migration. *Nat. Rev. Mol. Cell. Biol.* 10, 778–790. doi: 10.1038/nrm2786

Vicente-Manzanares, M., Newell-Litwa, K., Bachir, A. I., Whitmore, L. A., and Horwitz, A. R. (2011). Myosin IIA/IIB restrict adhesive and protrusive signaling to generate front-back polarity in migrating cells. *J. Cell. Biol.* 193, 381–396. doi: 10.1083/jcb.201012159

Wu, S. K., Budnar, S., Yap, A. S., and Gomez, G. A. (2014a). Pulsatile contractility of actomyosin networks organizes the cellular cortex at lateral cadherin junctions. *Eur. J. Cell. Biol.* 93, 396–404. doi: 10.1016/j.ejcb.2014.09.001

Wu, S. K., Gomez, G. A., Michael, M., Verma, S., Cox, H. L., Lefevre, J. G., et al. (2014b). Cortical F-actin stabilization generates apical-lateral patterns of junctional contractility that integrate cells into epithelia. *Nat. Cell. Biol.* 16, 167–178. doi: 10.1038/ncb2900

Wu, S. K., Lagendijk, A. K., Hogan, B. M., Gomez, G. A., and Yap, A. S. (2015). Active contractility at E-cadherin junctions and its implications for cell extrusion in cancer. *Cell Cycle* 14, 315–322. doi: 10.4161/15384101.2014.989127

Wu, S. K., and Yap, A. S. (2013). Patterns in space: coordinating adhesion and actomyosin contractility at E-cadherin junctions. *Cell. Commun. Adhes.* 20, 201–212. doi: 10.3109/15419061.2013.856889

Conflict of Interest Statement: The authors declare that the research was conducted in the absence of any commercial or financial relationships that could be construed as a potential conflict of interest.

Copyright © 2019 Wu and Priya. This is an open-access article distributed under the terms of the Creative Commons Attribution License (CC BY). The use, distribution or reproduction in other forums is permitted, provided the original author(s) and the copyright owner(s) are credited and that the original publication in this journal is cited, in accordance with accepted academic practice. No use, distribution or reproduction is permitted which does not comply with these terms.

frontiers in Cell and Developmental Biology

ORIGINAL RESEARCH
published: 13 March 2020
doi: 10.3389/fcell.2020.00153

Upregulation of RND3 Affects Trophoblast Proliferation, Apoptosis, and Migration at the Maternal-Fetal Interface

Xiao-Ling Ma[1], Xiao Li[2], Fu-Ju Tian[1], Wei-Hong Zeng[1], Jun Zhang[3], Hui-Qin Mo[1], Shi Qin[1], Li-Qun Sun[1], Yu-Chen Zhang[1], Yan Zhang[3] and Yi Lin[1]**

[1] Shanghai Key Laboratory of Embryo Original Diseases, International Peace Maternity and Child Health Hospital, Shanghai Jiao Tong University School of Medicine, Shanghai, China, [2] Department of Obstetrics and Gynecology, Shanghai Jiao Tong University Affiliated Sixth People's Hospital, Shanghai, China, [3] Department of Obstetrics and Gynecology, Renmin Hospital of Wuhan University, Wuhan, China

OPEN ACCESS

Edited by:
Guillermo Alberto Gomez, University of South Australia, Australia

Reviewed by:
Jiang Chang, Texas A&M University, United States
Melanie D. White, Agency for Science, Technology and Research (A*STAR), Singapore

***Correspondence:**
Yan Zhang
zyan2200@gmail.com
Yi Lin
yilinonline@126.com

Specialty section:
This article was submitted to Cell Adhesion and Migration, a section of the journal Frontiers in Cell and Developmental Biology

Received: 06 November 2019
Accepted: 25 February 2020
Published: 13 March 2020

Citation:
Ma X-L, Li X, Tian F-J, Zeng W-H, Zhang J, Mo H-Q, Qin S, Sun L-Q, Zhang Y-C, Zhang Y and Lin Y (2020) Upregulation of RND3 Affects Trophoblast Proliferation, Apoptosis, and Migration at the Maternal-Fetal Interface. Front. Cell Dev. Biol. 8:153. doi: 10.3389/fcell.2020.00153

Trophoblasts as the particular cells of the placenta play an important role in implantation and formation of the maternal-fetal interface. RND3 (also known as RhoE) is a unique member of the Rnd subfamily of small GTP-binding proteins. However, its function in cytotrophoblasts (CTBs) at the maternal-fetal interface is poorly understood. In the present study, we found that RND3 expression was significantly increased in trophoblasts from the villous tissues of patients with recurrent miscarriage (RM). RND3 inhibited proliferation and migration and promoted apoptosis in HTR-8/SVneo cells. Using dual-luciferase reporter and chromatin immunoprecipitation assays, we found that forkhead box D3 (FOXD3) is a key transcription factor that binds to the RND3 core promoter region and regulates RND3 expression. Here, the level of FOXD3 was upregulated in the first-trimester CTBs of patients with RM, which in turn mediated RND3 function, including inhibition of cell proliferation and migration and promotion of apoptosis. Further, we found that RND3 regulates trophoblast migration and proliferation via the RhoA-ROCK1 signaling pathway and inhibits apoptosis via ERK1/2 signaling. Taken together, our findings suggest that RND3 and FOXD3 may be involved in pathogenesis of RM and may serve as potential therapeutic targets.

Keywords: RND3, FOXD3, recurrent miscarriage, trophoblast, ROCK, ERK1/2

INTRODUCTION

Recurrent miscarriage (RM), defined as two or more consecutive spontaneous abortions, occurs in approximately 1–5% of all couples trying to conceive (Rai and Regan, 2006; Practice Committee of American Society for Reproductive Medicine, 2013). Numerous studies have shown that trophoblasts as the particular cells of the placenta play an important role in implantation and formation of the maternal-fetal interface (Red-Horse et al., 2004). The special structure of maternal-fetal interface is composed of differentiation of villous cytotrophoblast (CTB) cells at the tips of anchoring villi and migrating into the decidual tissue (Yilmaz and Christofori, 2009). Impaired trophoblast function is related to RM, intrauterine growth retardation, preeclampsia (PE),

and many other pregnancy-related complications. Although trophoblast function appears to be tightly regulated, the mechanisms underlying trophoblast migration and apoptosis are complex and unknown.

The members of the Rho family of GTPases as a subfamily of the Ras family are included in the regulation of cellular functions and the basics of cellular biology, such as cell adhesion, proliferation, migration and survival, and play a critical role in tumor and other normal cells (Jaffe and Hall, 2005). There are 22 mammalian genes encoding Rho GTPases and they are divided into eight subgroup (Aspenström and Fransson, 2004). Most members of the Rho family can cycle by the ratio of an active, GTP-bound conformation and an inactive, GDP-bound conformation, and GDP/GTP exchange process is regulated by several classes of regulators, including GDP/GTP exchange factors (GEFs) and GTPase-activating proteins (GAPs) (David et al., 2012). But RND3 (also known as RhoE), a unique member of the Rnd subfamily, is found that it do not hydrolyze GTP, and thus remains constitutively active upon expression without regulation by GEFs/GAPs cycling (Jie et al., 2015).

Foster et al. (1996) firstly cloned RND3 which was shown to display no detectable GTPase activity, similar to RND1 and RND2, indicating that RND3 has a different manner in which to regulate its activity. Data from this study imply that RND3 may be a special small GTPase. The basic role of RND3 is to inhibit signaling downstream of RhoA to cause actin cytoskeleton dynamics, which contributes to migration, invasion of rounded tumor cells and neuron polarity. Besides, RND3 plays multiple roles in arresting cell cycle, inhibiting cell growth, and inducing apoptosis and differentiation (Belgiovine et al., 2010; Lin et al., 2013; Liu et al., 2016). Interestingly, previous research shows that RND proteins have an important function in the human uterus. It has been demonstrated that RND1, RND2, and RND3 proteins are expressed in the human myometrium, and the level of RND2 and RND3 proteins is upregulated during pregnancy (Lartey et al., 2006; Fortier et al., 2008; Lartey and Lopez Bernal, 2009). Moreover, Collett et al. (2012) found that RND3 promotes fusion of BeWo choriocarcinoma cells via cyclic AMP.

Forkhead box D3 (FOXD3) which is presented in human chromosome 1p31 is an important member of the FOX transcription factor family. It is originally shown that FOXD3 binds to DNA by identified with the consensus sequence 5′-A[AT]T[AG]TTTGTTT-3′ to initiate transcription (Sutton et al., 1996). FOXD3 functions in cell development is established as it has reported to be expressed in embryonic stem cells in the late-stage gastrula inner cell mass, in mouse and human embryonic stem cells, and is required in the preimplantation mouse embryo (Hanna et al., 2002; Tompers et al., 2005; Perera et al., 2006). FOXD3 as a tumor suppressor has been reported to affect growth, metastasis, invasion, and angiogenesis of many tumors. FOXD3 silencing in lung cancer cells was shown to promote cell growth and inhibit apoptosis (Yan et al., 2015; Xu et al., 2019).

Together, with evidence of RND3 associated with human diseases and abnormal animal phenotypes, these studies led us to examine its important role in the pathogenesis of diseases. Here, we found that RND3 expression was upregulated in patients with RM. To investigate expression and functional role of RND3 in trophoblasts, a series of experiments were performed in this study. We found that FOXD3 directly binds to the promoter regions of RND3 and enhances its protein expression. Besides, FOXD3 regulated RND3 function, including cell proliferation, apoptosis, and migration. Moreover, we further identified two pathways that regulated RND3 function.

MATERIALS AND METHODS

Human Tissue Samples

Twenty-three patients with RM (age, 26–36 years) and twenty-four healthy pregnant women (HC) (age, 22–38 years) who had been treated at the Department of Obstetrics and Gynecology of the International Peace Maternity and Child Health Hospital of the China Welfare Institute, Shanghai Jiao Tong University School of Medicine, China, between April 2016 and March 2017. Patients were recruited did not have the following features: (1) chromosomal abnormality of parents or embryo, (2) abnormal immune function, (3) endocrine disorders, (4) abnormal uterine anatomy, (5) infectious disease, and (6) other identified causes of miscarriage.

The HC group have had previous pregnancies without spontaneous abortion, preterm labor, or PE and undergone painless induced abortions to terminate their unwanted pregnancies. Unwanted pregnancies refer to unintended pregnancies or unplanned pregnancies due to contraceptive failure. We exclude the patients who are unable to bear pregnancy because of physical condition, or whose fetus was diagnosed as malformation or congenital disease. Pregnancy interruption follows the individual will of women and is legal in China according to the *Chinese Maternal and Child Health Law*, *Women's Rights Protection Law* and the *Population and Family Planning Law*. All villous tissue samples collected at 8–12 weeks of gestation were immediately collected, cleaned the clot with saline, and stored in liquid nitrogen. Two groups patients' demographic information is showed in **Table 1**.

The Medical Ethics Committee of International Peace Maternity and Child Health Hospital of the China Welfare Institute approved this study. Written informed consents were obtained from all patients who participated in the study before enrollment.

Quantitative Real-Time PCR (qRT-PCR)

Total RNA was extracted from the villous tissue using TRIzol reagent (Life Technologies, Grand Island, NY, United States),

TABLE 1 | Demographic information of the study population.

	Number	Age (years)	Number of miscarriages	Gestational age (weeks)
HC	24	30.08 ± 1.22 (22–38)	0.71 ± 0.16	10.74 ± 0.24
RM	23	30.65 ± 0.58 (26–36)	2.65 ± 0.29	10.30 ± 0.41
		$P = 0.6807$	$P < 0.0001$	$P = 0.3661$

and used to generate cDNA with the PrimeScript™ RT reagent Kit with gDNA Eraser (RR047Q, Takara Bio, Kusatsu, Shiga, Japan). SYBR® Premix Ex Taq (RR420A, Takara Bio) was used to perform PCR according to the manufacture's instructions, on an ABI 7900 real-time PCR instrument. The PCR products were quantified using the $2^{-\Delta\Delta Ct}$ method relative to Glyceraldehyde-3-phosphate dehydrogenase (GAPDH) to normalized gene expression levels. The specific primers used are showed in **Supplementary Table S1**.

Western Blot Analysis

Cells or tissue were lysed and analyzed by western blotting as described previously (Ma et al., 2017). Briefly, cells were washed twice with cold phosphate buffered saline (PBS) and harvested. Cell were lysed in radio immunoprecipitation assay buffer containing protease inhibitor on ice for 20 min. Proteins were detected using 10 or 12% polyacrylamide gels and transferred onto polyvinylidene fluoride (PVDF) membranes. 5% non-fat milk were used to block with PVDF membranes. Then they were incubated with primary antibody in 5% non-fat milk at 4°C overnight. The primary antibodies used are listed in **Supplementary Table S2**. After washing three times, membranes were incubated with secondary antibodies (1:5000; Yeasen, Shanghai, China) labeled with horseradish peroxidase (HRP). Signals were detected using an autoradiography film.

Immunohistochemical and Immunofluorescence Staining of Tissues

Immunohistochemical staining was performed as described in our previous work (Li et al., 2019), using the Mouse- and Rabbit-specific HRP/DAB (ABC) Detection IHC Kit (ab64264; Abcam, Cambridge, United Kingdom) following the manufacturer's protocol. Briefly, the tissue sections were deparaffinized and rehydrated. Epitope retrieval was performed in ethylenediaminetetraacetic acid (EDTA). After incubation with primary antibody overnight, HRP conjugated secondary antibody was used. For immunohistochemical detection, tissue was subsequently counterstained with diaminobenzidine, hematoxylin and hydrated. It is replaced the primary antibody with PBS as negative controls. Staining intensity was evaluated by ImageJ-Pro Plus 6.0 software. Pictures were captured under a Leica DMi8 microscope (Wetzlar, Germany).

Immunofluorescence staining of tissues was performed as described previously (Zhang et al., 2018).

Cell Culture

The HTR-8/SVneo cell line (HTR-8, human extravillous trophoblast cell line, EVTs) were a kind gift from Dr PK Lala (University of Western Ontario, ON, Canada). The cells were grown in Dulbecco's modified Eagle's medium (DMEM)/F12 plus 10% fetal bovine serum (FBS, Gibco, Grand Island, NY, United States) at 37°C with 5% CO_2. Cells were cultured in a 10 cm^2 dish, with a medium change every 48 h. For passaging, trypsin (Sigma-Aldrich, St. Louis, MO, United States) were used to detach cells at 37°C for 3 min.

Small Interfering RNA (siRNA), Plasmids, and Transfection

RND3 and FOXD3 ON-TARGET plus SMART pool siRNAs and non-targeting siRNAs (siNC) were purchased from Thermo Scientific (Dharmacon RNAi Technologies, Lafayette, CO, United States; RND3: L-007794-00-0005, FOXD3: L-009152-00-0005, siNC: D-001810-10-15). HTR-8 cells were then transfected with 25 nM siRNA using DharmaFECT™ Transfection reagents (Dharmacon RNAi Technologies) according to the manufacturer's instructions. siROCK1-1 (5′-CCAGCUGCAAGCUAUAUUATT-3′) and siROCK1-2 (5′-GCAGAUGAAACAGGAAAUATT-3′) are purchased from GenePharma (Shanghai, China) and transfected into the cells at a final concentration of 100 nmol/L using oligofectamine reagent (Life Technologies). The RND3 overexpression plasmid was constructed by cloned the coding region sequence (CDS) of human RND3 into vector GV358 (GeneChem, Shanghai, China). JetPRIME® reagent (Polyplus-transfection® SA, Strasbourg, France) was used to perform cell transfection.

Cell Proliferation Assay

After transfection about two thousand HTR-8 cells per well were plated in 96-well plates. Ten microliter per well the cell counting kit-8 (CCK-8) regents (Dojindo, Kumamoto, Japan) were added to cells to assess cell viability at 0, 24, 48, 72, and 96 h. After incubation with CCK-8 reagent for 2 h, the optical density value was detected at 450 nm using the Synergy H1 microplate reader (BioTek, Winooski, VT, United States).

Immunofluorescence Staining of Cells

A suitable size slide was placed into 24-well plate each. HTR-8 cells cultured in a 24-well plate were fixed with 4% formaldehyde. Blocking buffer contained 0.3% Triton X-100 and 5% FBS was used to permeabilize cells for a minimum of 30 min. Then, cells were incubated with primary antibodies overnight (**Supplementary Table S2**). The next day, after washing three times with PBS cells were incubated with the appropriate secondary antibodies (1:1000; Thermo Fisher Scientific, Waltham, MA, United States). Concurrently, it is replaced the primary antibody with PBS alone as negative controls. HTR-8 cells were incubated for 2 h in the dark and washed with PBS. 4′,6-diamidino-2-phenylindole (DAPI; Abcam) was used to stain with the nuclei of HTR-8 cells. Slips which covered with cells were placed on the marked glass slides and images were captured under a microscope.

Flow Cytometry Analysis for Apoptosis and Cell Cycle Assay

After transfection with siRNA or overexpression plasmid for 48 h, cells were detached and apoptosis was detected with the APC Annexin V Apoptosis Detection kit with 7-aminoactinomycin D (7-AAD) (BioLegend, Inc., San Diego, CA, United States) according to the manufacturer's manual. For cell cycle analysis, cells were evaluated using propidium oxide using the Cycle Test Plus DNA Reagent kit (BD Biosciences, Franklin Lakes, NJ, United States) following the instruction manual. The percentage

of apoptosis was analyzed by FlowJo software. And the percentage of cell cycle stage was analyzed by ModFit software. The apoptosis rate of HTR-8 cells in different phase was assessed.

Transwell Assay

Transwell chambers (8 mm pores; Costar Corp., Cambridge, MA, United States) were used to perform cell migration assay as described previously (Tian et al., 2015). Briefly, serum-starved HTR-8 cells were detached and suspended. We loaded the upper chamber with 10^5 cells in 200 μL 1% FBS DMEM/F12 medium and the chamber below with 700 μL medium with 15% FBS. After 24 h, non-migratory cells were removed gently and the migratory cells on the undersurface were fixed with 4% paraformaldehyde for 15 min and washed three times with PBS. 0.1% crystal violet was used to stain HTR-8 cells for 20 min and lastly we counted in 3–4 random fields to analyze.

Explant Culture

Twenty-four-well culture dishes precoated with Matrigel® substrate (Corning Life Sciences, New York, NY, United States) (Zhang et al., 2017) is prepared before one hour. Then first-trimester human placental villi (6–10 weeks) were immediately obtained from healthy patients after curettage surgery and put in cold ice during transport. And then the villi were dissected in small sections and explanted in overnight. About 8–10 tissue sections were placed into a well of a 24-well culture dish (Costar Corp.). The next day, villi that successfully grown in the Matrigel matrix were used for subsequent experiments, and were referred to as 24 h samples. Twenty-five nanometer siRND3 or 1 μg RND3 overexpression plasmid and their negative controls were transfected into the extravillous explants. Pictures were captured using a Leica microscope after 72 h overgrowth. ImageJ-Pro Plus 6.0 software was used to analysis cell migration.

RND3 Promoter Luciferase Construction

A purification kit (Qiagen, Dusseldorf, Germany) was used to extract genomic DNA from HTR-8 cells and then the genomic DNA was used as a template for PCR. The RND3 promoter (nucleotides −1000 to +1, relative to the translation initiation site; GenBank accession number: MN685775, **Supplementary Table S3**) was synthesized by PCR and cloned into the plasmid pGL3-basic (Promega, Madison, WI, United States) with containing firefly luciferase activity by *Kpn*I and *Xho*I cleaved sites (Thermo Fisher Scientific). Following *E. coli* transformation, shaking, plasmid extraction, digestion, and purification steps were performed to successfully generate the RND3 promoter luciferase construct. Lastly, the right digestion fragment was sent to Sangon for sequencing (Shanghai, China). RND3 promoter luciferase report plasmid carrying mutations in the putative FOXD3 binding sites were generated using a QuikChange Lightning Muti Site-Directed Mutagenesis Kit (Stratagene, La Jolla, CA, United States).

For HTR-8 cells, the full-length FOXD3 cDNA was obtained from total RNA using PCR. The FOXD3 primers used were as follows: 5′-ATTGGATCCATGA CCCTCTCCGGCGGCG-3′ (forward) and 5′-AGGCTCGAGC TATTGCGCCGGCCATTTGG-3′ (reverse). The FOXD3 products were cloned into the vector pcDNA3.1 (+) (Invitrogen) to generate pcDNA3.1-FOXD3 overexpression plasmid.

Dual-Luciferase Reporter Assay

HTR-8 cells were transfected with the control vector or FOXD3 overexpression plasmid, the RND3 promoter luciferase reporter plasmids and the Renilla luciferase expression vector pRL-TK (Promega), and using jetPRIME® reagent. At 48 h post transfection, cells were lysed, and detected intracellular luciferase activity with a Dual-Luciferase® Reporter Assay System (E1910; Promega) according to the manufacturer's manual. Luciferase activities were detected with a microplate reader.

Chromatin Immunoprecipitation (ChIP) Assay

The EZ-Magna ChIP™A/G Kit (17-10086; Millipore, Billerica, MA, United States) was used to detect the binding of FOXD3 to RND3 according to the manufacturer's manual. Five million cells were fixed in 1% formaldehyde for 10 min at room temperature. Cells were broken open and the crosslinked DNA was sheared to an average fragment size of 200–2000 bp. Subsequently, FOXD3 antibody (1 μg/10^5 cells; Abcam) was used to immunoprecipitate with chromatin. The purified chromatin was subjected to qualitative PCR analysis using Premix Ex Taq™ Hot Start Version (RR030Q; Takara) and quantified by qRT-PCR using SYBR® Premix Ex Mix (Takara). The primer pairs used are showed in **Supplementary Table S4**. In this text, an input sample, 1% of starting chromatin was obtained from the ChIP assay each as a control for DNA contamination according the manufacturer's protocol.

Evaluation of the Activity of ROCK1

The ROCK1 activity was evaluated by immunoprecipitating ROCK1 and then performing an *in vitro* kinase activity assay (Mong and Wang, 2009; Han et al., 2016). Cells were lysed using a lysis buffer and then incubated for 1 h at 4°C with 2 μg of isotype control IgG, rabbit anti-ROCK1. And then the mixture was incubated with protein A/G agarose (Sigma-Aldrich) at 4°C overnight. Next day, the beads were pelleted, washed and incubated for 30 min at 30°C with a buffer containing 50 μM ATP and 0.5 μg of purified MYPT-1 (Millipore). Examination of phosphorylated MYPT-1 or immunoprecipitated ROCK1 was performed using western blotting.

Statistical Analysis

Data are shown as means ± standard deviation (SD). All *in vitro* experiments were performed at least three times. Statistical analysis was calculated using the SPSS 15.1 (SPSS Inc., Chicago, IL, United States) and GraphPad Prism 5 (GraphPad Software, San Diego, CA, United States). Data were evaluated using Student's *t*-test and two-way analysis of variance (ANOVA). A difference at $P < 0.05$ was considered statistically significant.

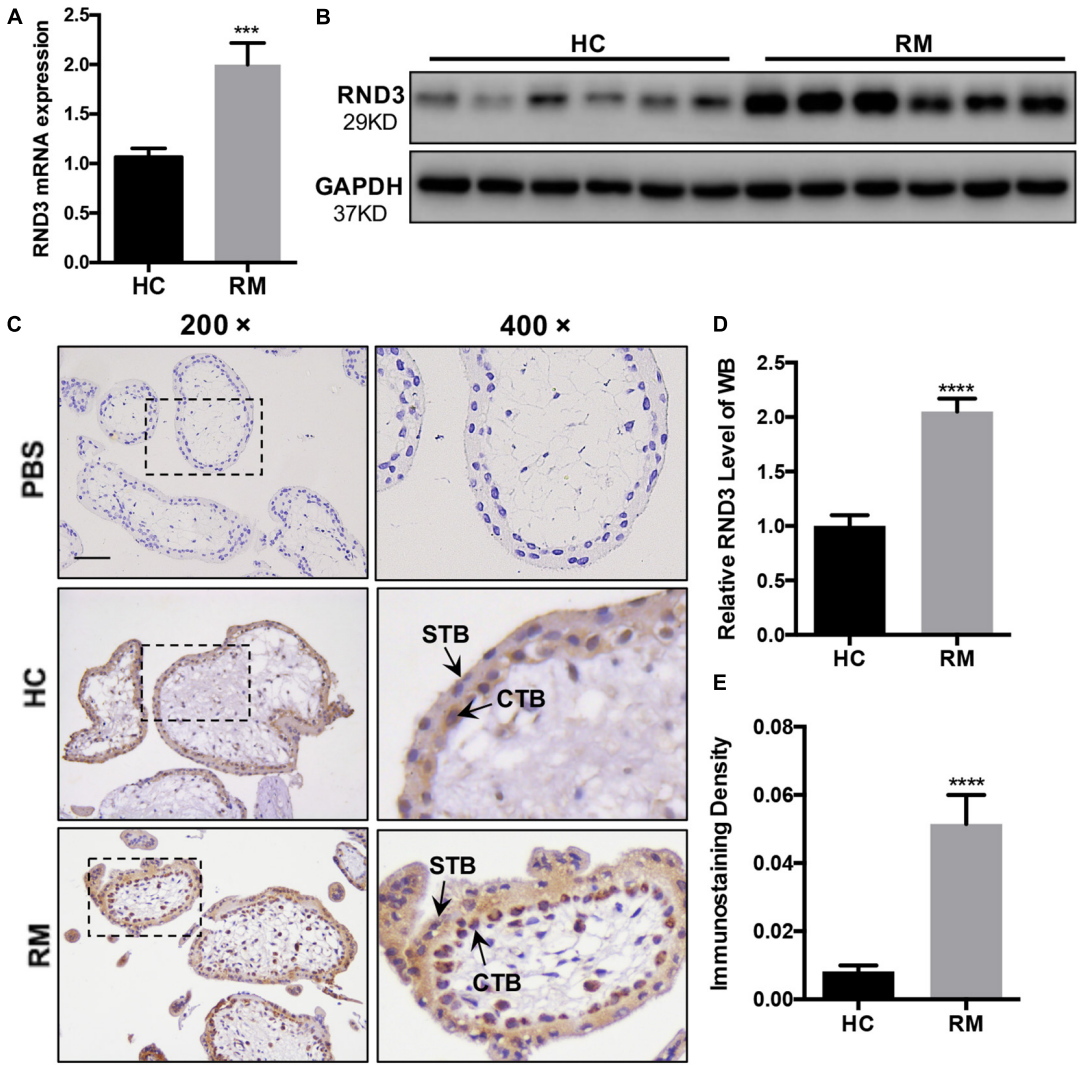

FIGURE 1 | RND3 is upregulated in first-trimester placental CTB in patients with RM. **(A,B,D)** RND3 expression in first-trimester human villi tissues from patients with RM or HC was determined using qRT-PCR (n = 11) and western blot analysis (n = 6). **(C,E)** Immunohistochemical analysis of paraffin-embedded villous tissues showed that RND3 expression was increased in patients with RM compared with that in HC (n = 18). Scale bar = 100 μm. **(D)** Histogram showing the relative expression level of RND3 protein in HTR-8 cells as determined using ImageJ software. **(E)** The staining intensity of RND3 in both CTB and STB in paraffin-embedded villous tissues was quantified using Image-Pro Plus 6.0. CTB, cytotrophoblast; STB, syncytiotrophoblast. ***P < 0.001, ****P < 0.0001 vs. HC.

RESULTS

RND3 Is Upregulated in Trophoblasts From Patients With RM

We first analyzed the RND3 expression at the first-trimester villi in patients with RM. qRT-PCR and western blotting results indicated that RND3 expressions were significantly increased in patients with RM as compared to those in HC (**Figures 1A,B,D** and **Supplementary Figure S1**). Immunohistochemistry results confirmed these findings (**Figures 1C,E**). We also found that the RND3 protein is present in the cytoplasm of CTB and syncytiotrophoblast (STB). According to previous studies, villous CTB cells as progenitor cells with a significantly proliferative ability differentiates into EVT or STB. Further, RND3 has been shown to promote the fusion of BeWo choriocarcinoma cells (Collett et al., 2012). In this text, we mainly explored the function of RND3 in CTB.

RND3 Inhibits Trophoblast Proliferation, Blocks G1 Phase Cell Cycle Progression and Promotes HTR-8 Cell Apoptosis

In our previous study, we demonstrated that the expression of Ki-67 expressed among proliferating cells was significantly decreased in patients with RM compared to those in HC (Li et al., 2019). Here, HTR-8 cells were transfected with siRND3 or RND3 overexpression construct to explore the function of RND3 (**Supplementary Table S5**). The CCK-8 assay revealed

that RND3 knockdown promoted proliferation, whereas RND3 overexpression had the opposite effect (**Figure 2A**). In order to investigate how RND3 inhibits cell proliferation, we performed cell cycle assay. We found that downregulation of RND3 led to reduction in degrees of cells in the G0/G1phase (41.26 ± 0.706 vs. 34.55 ± 2.071) and upregulation of RND3 led to accumulation of cells in the G0/G1 phase (43.41 ± 0.332 vs. 51.23 ± 0.2569). And upregulation of RND3 led to reduction in degrees of cells in S phase (50.5 ± 1.637 vs. 37.32 ± 3.705). There were no differences in the percentage of cells in the G2/M phase (**Figures 2B–D**). Ki-67 which is only expressed in the proliferative phases such as G2/M and S phases was decreased after transfection with GFP-RND3 overexpression plasmid which transfection efficiency is around 50% by using GFP as a report gene (**Figure 2E**). The expression of cyclin D1, a G1-S phase cell cyclic protein, was increased in RND3 knockdown cells and decreased in RND3-overexpressing cells compared with that in their respective control groups (**Figures 2F,G**). Taken together, these experimental results suggest that RND3 inhibits cell proliferation by preventing S-phase entry.

In our previous study, TUNEL staining results showed accumulated apoptosis in the placenta villi from patients with RM (Wu et al., 2017). In this text, we further investigated the effect of RND3 on apoptosis by flow cytometry after Annexin V and 7-AAD staining. Our results showed that RND3 overexpression aggravated cell apoptosis at all stages, but RND3 knockdown attenuated early stage and total apoptosis (**Figures 2H,I**). The expression of BAX and cleaved caspase-3, two key components for cellular induced apoptosis, was increased in RND3-overexpressing cells and decreased in RND3 knockdown cells compared with that in their respective control groups (**Figures 2J,K**).

RND3 Inhibits Trophoblast Migration *in vitro* and Outgrowth in a Villous Explant Culture Model

The migration and invasion potential of trophoblasts play an important role in embryo implantation. Hence, we explored the effect of RND3 on trophoblast migration. Transwell assay results showed that RND3 knockdown increased migration ability, while RND3 overexpression drastically decreased migration ability of HTR-8 cells (**Figures 3A,C**). Matrix metalloproteinase (MMP)-2 and MMP-9 are two vital members of the MMP family that can facilitate trophoblast cell movement by degrading fibronectin. MMP-2 and MMP-9 expression were found to be increased in RND3 knockdown cells and decreased in RND3-overexpressing cells compared with those in their respective control groups (**Figures 3B,D**). The function of RND3 in trophoblast migration *in vitro* was verified by villous explants derived from healthy samples cultured on Matrigel-coated plates. Immunofluorescence staining and western blotting confirmed the effects of knocking down or overexpressing RND3 using cytokeratin 7 (CK7) as trophoblast cell marker to identify trophoblast in the villous plants (**Supplementary Figure S2**). Results showed that RND3 knockdown or RND3-overexpressing enhanced or weakened the migration ability of trophoblasts, respectively (**Figures 3E,F**). To

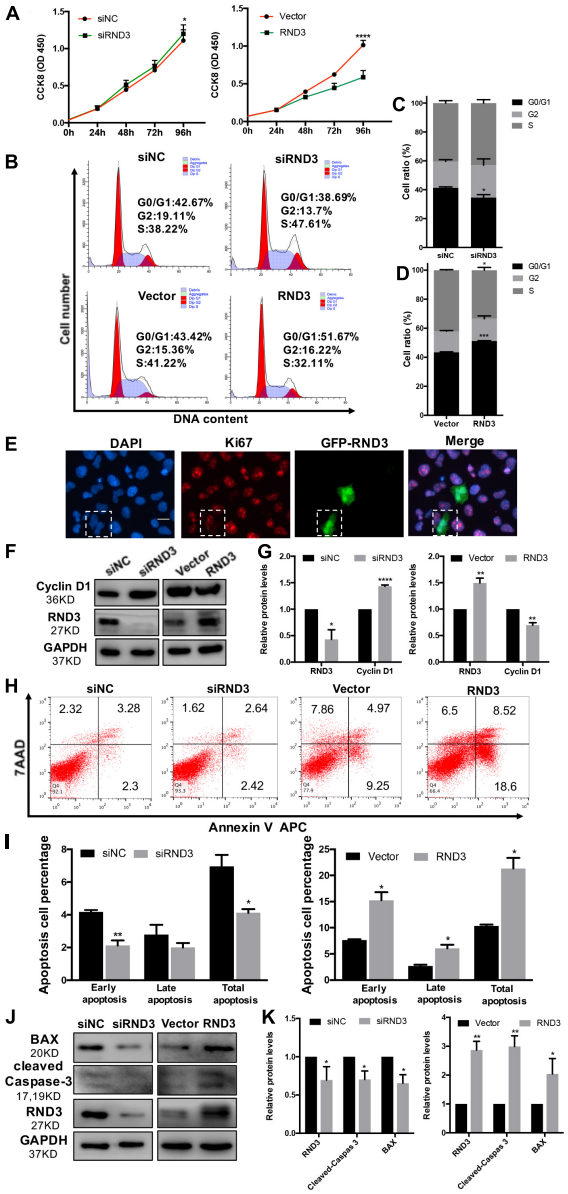

FIGURE 2 | RND3 inhibits trophoblast proliferation, blocks G1 phase cell cycle progression and promotes HTR-8 cell apoptosis. **(A)** CCK-8 cell proliferation assay of RND3 knockdown and RND3-overexpressing HTR-8 cells and their respective control groups. **(B–D)** Cell cycle assay of RND3 knockdown and RND3-overexpressing HTR-8 cells and their respective control groups. The proliferation rate of cells in each phase was assessed. **(E)** Immunofluorescence staining with GFP-RND3 (green), Ki-67 (red), and DAPI (blue). Original magnification: ×200. Scale bar = 25 μm. **(F–G)** Western blot analysis of cyclin D1 levels in RND3 knockdown and RND3-overexpressing HTR-8 cells and their respective control groups. **(H,I)** Flow cytometry analysis of the apoptosis rate of RND3 knockdown and RND3-overexpressing HTR8 cells and their respective control groups. Histogram of Annexin V $APC^+/7\text{-}AAD^-$ represents early apoptotic cells. Histogram of Annexin V $APC^+/7\text{-}AAD^+$ represents late apoptotic cells. The sum of the former two categories equals the total number of apoptotic cells. **(J,K)** Western blot analysis of BAX and cleaved caspase-3 expression in RND3 knockdown and RND3-overexpressing HTR8 cells and their respective control groups. Data represent the means ± SD of three independent experiments. $^*P < 0.05$, $^{**}P < 0.01$, $^{***}P < 0.001$ vs. siNC or Vector group.

further confirm the role of RND3 in trophoblast invasion and migration *in vivo*, explants were obtained from HC and RM and planted into Matrigel. After 24 h of culture, the explants from RM anchored on to the Matrigel were separated into two groups. They were treated with siNC and siRND3. At 72 h of *in vitro* culture, RM group explants showed smaller migration and proliferation capacities than HC group. However, the hindered migration of RM group can be rescued by siRND3 treatment (**Figures 3G,H**). All these results demonstrated that RND3 plays an importance role in trophoblast migration.

Verification of RND3 Core Promoter Region and FOXD3 as a Key Transcriptional Enhancer for RND3

We selected a 1000 bp region (positive −1000 to +1) located upstream of the RND3 initiation codon as the core promoter region. According to the forecasting result, we designed the different length fragments (966, 699, 617, 313, and 126 bp) of RND3 promoter. These fragments were subjected to PCR amplification using total DNA from human trophoblasts (**Supplementary Table S6**). After identifying a series of incomplete promoter fragments by double-enzyme digestion, they were subcloned into the pGL3-basic luciferase reporter vector. The positive samples were subjected to sequencing, and the results were as expected, indicating that the vectors were successfully constructed and named F1–F5 (**Figures 4A,B**). HTR-8 cells were transfected with the reporter plasmids and pRL-TK plasmids. After 48 h, reporter activity was measured by dual-luciferase reporter assay. Results showed that the activity of F4 plasmid was significantly higher than that of F5 plasmid or basic plasmid, while that of F3 plasmid was significantly increased. The activity of F2 plasmid was higher than that of F3 plasmid (**Figure 4C**). These results indicated the presence of important regulatory elements at the promoter region of −125 to −698 bp.

Next, we attempted to identify the transcription factor at −125 to −698 bp region that regulates RND3 expression using the TRANSFAC tool (ALGGEN-PROMO and JASPAR). According to the candidate transcription factor score, relative score, dissimilarity, matching degree, and some other standards, we identified FOXD3 as the highest scoring transcription factor in the −125 to −698 bp region (**Supplementary Tables S7, S8**). We focused on the sequence with a candidate transcription factor score greater than 6.5, a relative score greater than 0.8, relatively smaller dissimilarity and positive strand. At the same time, we removed some repetitive sequences in one method and chose the same segments in two tools. To determine binds to this genomic locus, ChIP assay was performed in HTR-8 cells. Four pairs of RND3 primers were designed for standard end-point PCR and qRT-PCR using the DNA obtained from the ChIP assay. ChIP results indicated that FOXD3 binds directly to the identified promoter region of RND3 (−649 to −239 bp) (**Figures 4D,E**). The reporter plasmids F2–F4 were transfected into HTR-8 cells in conjunction with the control plasmid or FOXD3 expression plasmid. Dual-luciferase reporter assay showed that the activity of F2 and F3 plasmids increased after transfection with FOXD3 overexpression plasmid compared with that after transfection with control vector (**Figure 4F**). Based on the above results, we predicted two FOXD3 binding sites in the RND3 core promoter region (−663 to −572). Furthermore, two luciferase reporters were constructed with control of either the wild-type RND3 reporter plasmid (WT, also F1 plasmids) or two mutants in which two putative FOXD3 binding sites had been mutated (Mut-1 and Mut-2 reporter, respectively) (**Figure 4G**). As expected, the activity of the reporter plasmid was decreased in HTR-8 cells which were transfected with Mut-1 or Mut-2 reporter as compared with transfection in WT reporter (**Figure 4H**). These results suggest that FOXD3 acts as a transcriptional enhancer for RND3 in HTR-8 cells.

FOXD3 Is Upregulated in Trophoblasts From Patients With RM

Next, we explored the FOXD3 level at the first-trimester villi in patients with RM. qRT-PCR and western blotting results indicated that FOXD3 expression was increased in patients with RM as compared to those in HC (**Figures 5A,B,D**). Immunohistochemical and immunofluorescence staining results further confirmed these findings (**Figures 5C,E,F**). Our results also demonstrated that the FOXD3 protein was present in the cytoplasm of CTB, with almost no expression in STB.

FOXD3 Regulates RND3 Expression, Inhibits Proliferation and Migration, and Promotes Apoptosis in HTR-8 Cells

As FOXD3 directly regulates RND3 expression, we examined whether FOXD3 influences the biological behavior of trophoblasts. The results of CCK-8 assay showed that knockdown of FOXD3 promoted HTR-8 cell proliferation, while overexpression of FOXD3 inhibited HTR-8 cell proliferation (**Figure 6A**). In order to claim that FOXD3 regulates RND3 function, we transfected FOXD3-overexpressing cells with siRND3 or FOXD3 knockdown cells with RND3 overexpression plasmid, respectively. Transwell assay results showed that FOXD3 overexpression inhibited HTR-8 cell migration and RND3 knockdown can reverse the effect. In addition, FOXD3 knockdown-promoted HTR-8 migration was weakened by RND3 overexpression (**Figures 6B,D**). Flow cytometry analysis showed that FOXD3 knockdown decreased the ratio of early apoptotic and total apoptotic cells but did not alter the proportion of late apoptotic cells, while RND3 overexpression can reverse the effects. FOXD3 overexpression increased the ratio of early apoptotic and late apoptotic cells, and RND3 knockdown can suppress the effect (**Figure 6C**). RND3 and FOXD3 mRNA expression in first-trimester villi in patients with RM and HC was analyzed by qRT-PCR. Results showed that RND3 mRNA expression was correlated positively with FOXD3 mRNA expression in the first-trimester villi (**Figure 6E**). Western blot analysis showed that Cyclin D1, MMP2 level was upregulated and BAX level was downregulated in HTR-8 cells transfected with siFOXD3 as compared with that in their respective control groups (**Figures 6F,H**). In

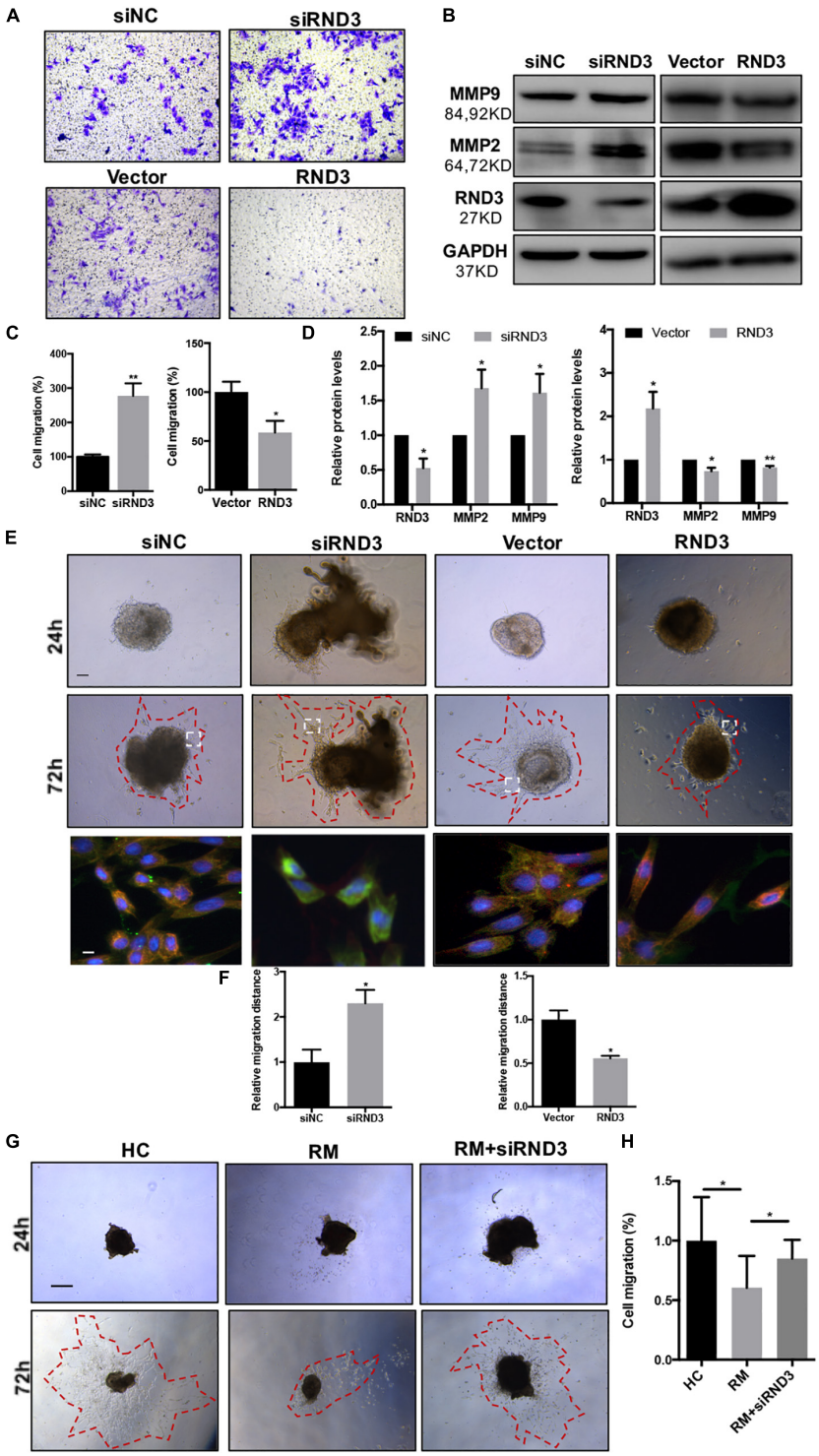

FIGURE 3 | RND3 promotes trophoblast migration *in vitro*. **(A,C)** Transwell migration assay of RND3 knockdown and RND3-overexpressing HTR-8 cells and their respective control groups. Original magnification: ×100. Scale bar = 50 μm. **(B,D)** Western blot analysis of MMP-2 and MMP-9 expression in HTR-8 cells at 48 h after transfection with siNC, siRND3, control vector, or RND3 overexpression vector. **(E,F)** Villous explants were obtained from HC at 8–10 weeks of gestation and cultured on Matrigel. Tissues were then transfected with siRND3 or RND3 overexpression vector. Images were acquired after *in vitro* culture for 24 and 72 h. Original magnification: ×100. Scale bar = 100 μm. Immunofluorescence staining images of trophoblasts expressing RND3 (red) and CK7 (green). Original magnification: ×200. Scale bar = 25 μm. **(G,H)** Villous explants were obtained from HC and RM at 8–12 weeks of gestation and cultured on Matrigel. RM tissues were then transfected with siRND3. Images were acquired after *in vitro* culture for 24 and 72 h. Original magnification: ×40. Scale bar = 200 μm. Data represent the means ± SD of three independent experiments. $^{*}P < 0.05$, $^{**}P < 0.01$ vs. siNC, Vector, HC or RM group.

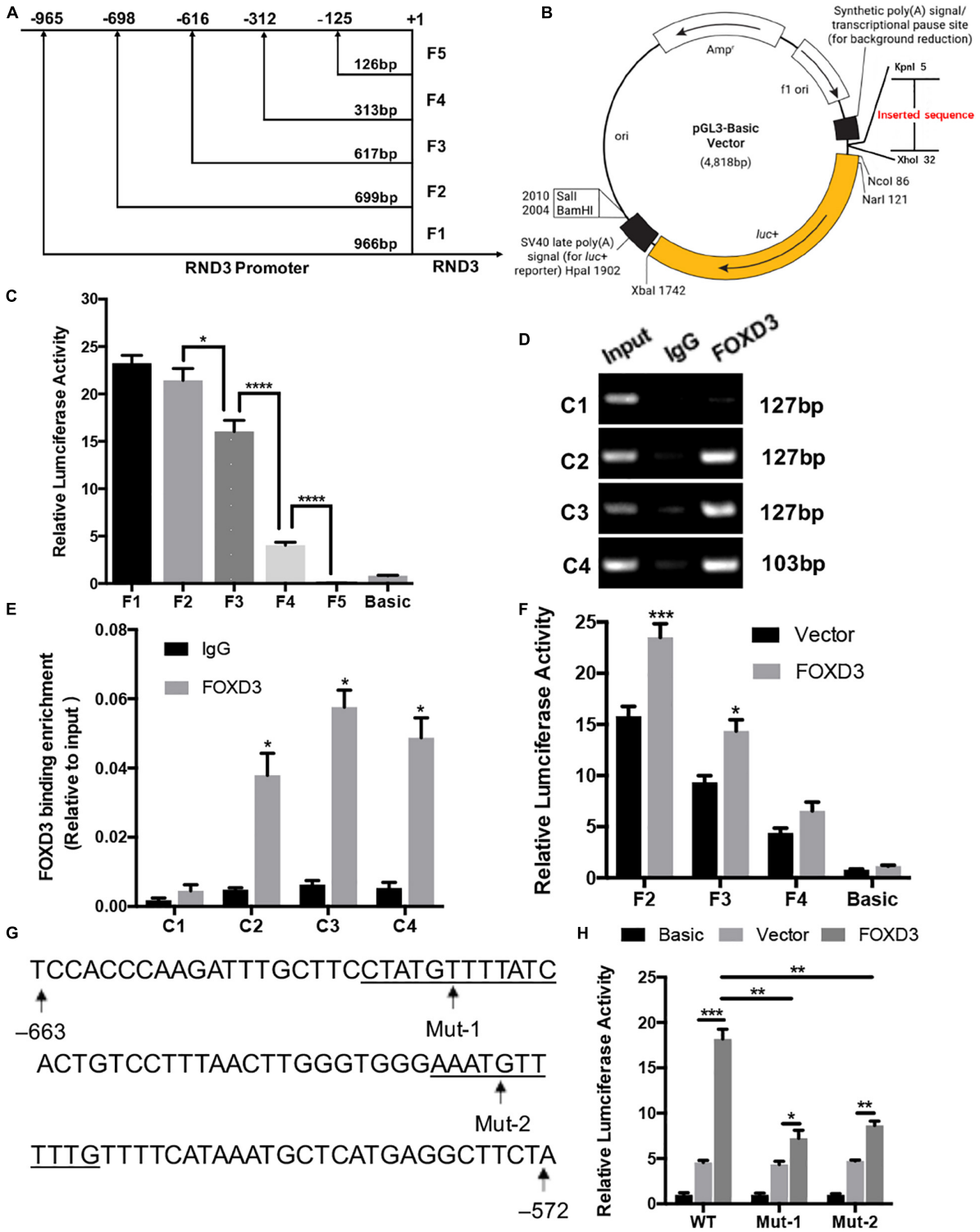

FIGURE 4 | Identification of RND3 core promoter region and FOXD3 as a transcriptional enhancer for RND3 in HTR-8 cells. **(A)** Specific primers for sequences upstream of the RND3 transcription initiation site were designed and **(B)** cloned into pGL3-basic vector. **(C)** Relative luciferase activity of F1–F5 and basic plasmids. $^{*}P < 0.05$, $^{****}P < 0.0001$. **(D,E)** ChIP assay of the combination of RND3 promoter. $^{*}P < 0.05$ vs. the IgG group. **(F)** Relative luciferase activity of F2–F4 and basic plasmids in HTR-8 cells at 48 h after transfection with control vector or RND3 overexpression vector. $^{*}P < 0.05$ vs. Vector group. **(G)** Prediction of two FOXD3 binding sites in the RND3 core promoter region (–663 to –572) (underlined) and construction of the FOXD3 binding site mutant reporters. **(H)** Relative luciferase activity of RND3 reporter plasmids (WT) and FOXD3 binding site mutant reporters (Mut-1 and Mut-2). Data represent the means ± SD of three independent experiments. $^{*}P < 0.05$, $^{**}P < 0.01$, $^{***}P < 0.001$ vs. Vector group or FOXD3 group.

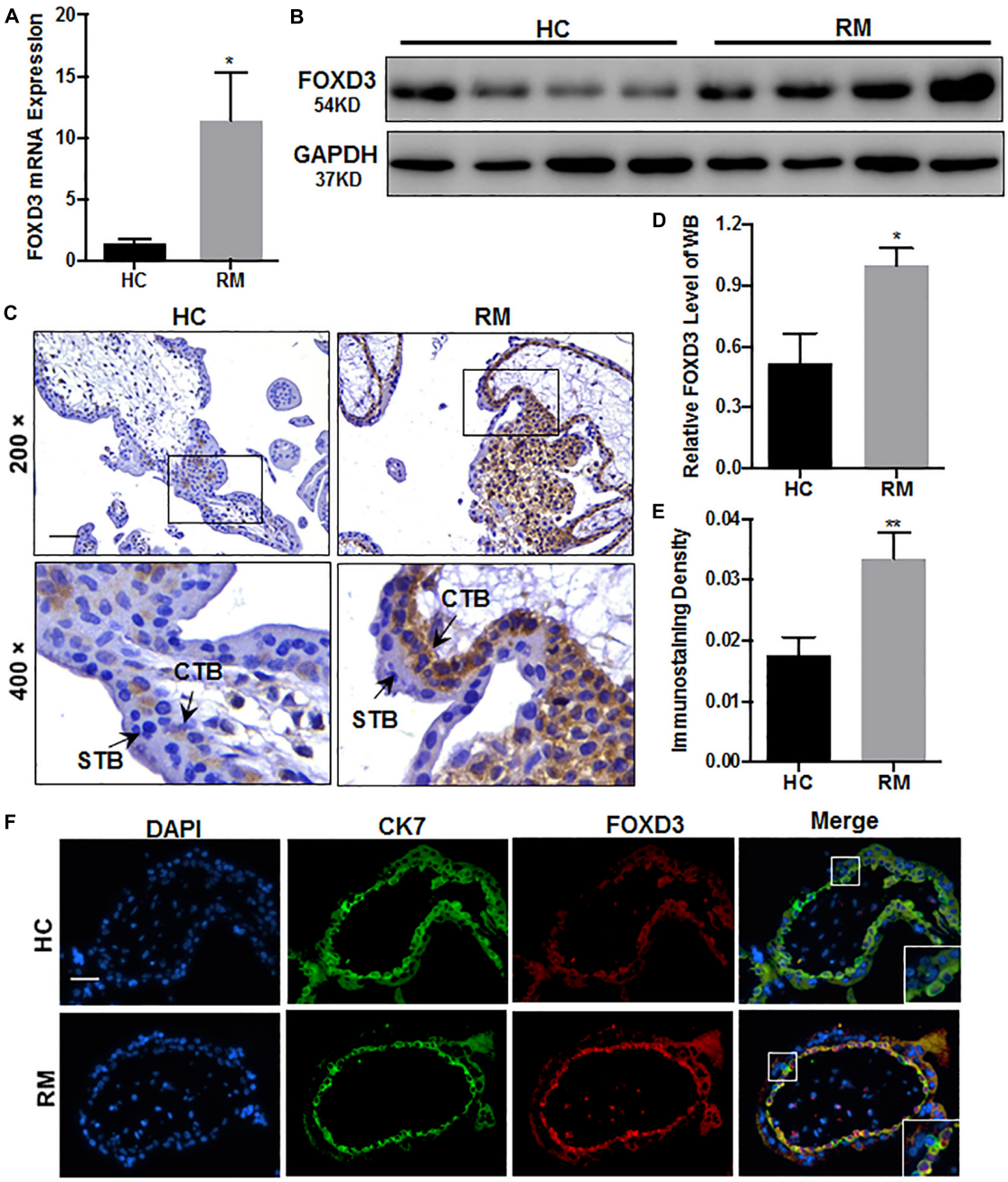

FIGURE 5 | FOXD3 is upregulated in first-trimester placental CTB in patients with RM. **(A,B,D)** FOXD3 expression in first-trimester human villi tissues from patients with RM or HC was determined using qRT-PCR (n = 10) and western blot analysis (n = 6). **(C,E)** Immunohistochemical analyses of paraffin-embedded villous tissue showed that FOXD3 expression was increased in patients with RM compared with that in HC (n = 17). Original magnification: ×200. Scale bar = 100 μm. **(D)** Histogram showing the relative expression level of FOXD3 protein in HTR-8 cells as determined using ImageJ software. **(E)** The staining intensity of FOXD3 in paraffin-embedded villous tissues was quantified using Image-Pro Plus 6.0. **(F)** Two-color immunofluorescence staining analyses of paraffin-embedded villous tissues revealed expression of FOXD3 (red) and CK7 (green), and counterstaining with DAPI (blue). Original magnification: ×200. Scale bar = 50 μm. CTB, cytotrophoblast; STB, syncytiotrophoblast. *P < 0.05, **P < 0.01 vs. HC.

contrast, Cyclin D1, MMP2 level was downregulated and BAX level was upregulated in cells transfected with FOXD3 overexpression plasmid (**Figures 6G,I**). In addition, RND3 overexpression or RND3 knockdown can partly rescue the change in FOXD3 knockdown cells or in FOXD3-overexpressing cells (**Figures 6F–I**). These results confirmed that FOXD3 acts as a transcriptional enhancer for RND3 in HTR-8 cells and regulates RND3 function.

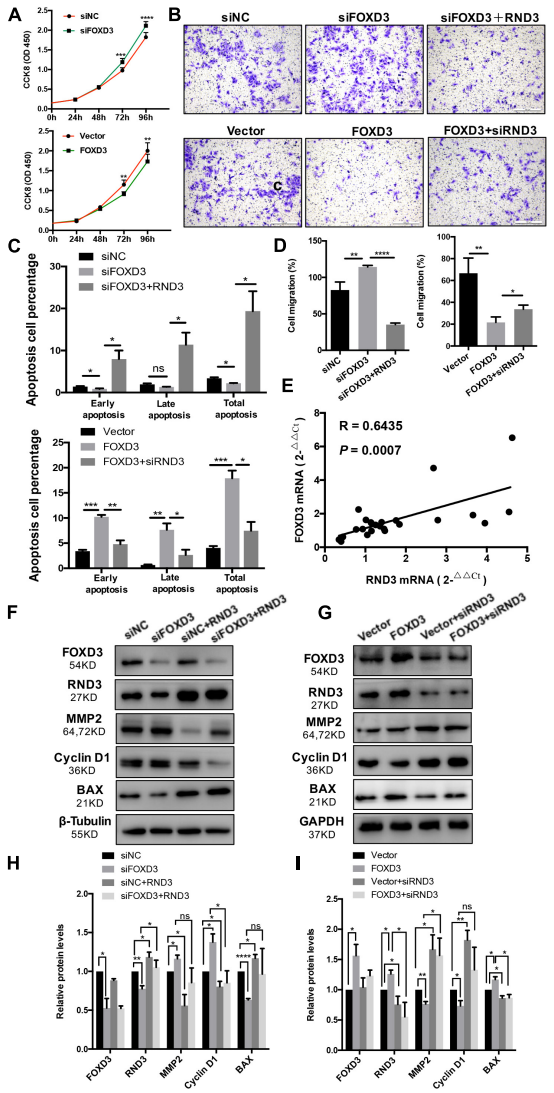

FIGURE 6 | FOXD3 regulates RND3 expression, inhibits proliferation and migration, and promotes apoptosis in HTR-8 cells *in vitro*. **(A)** CCK-8 assay of FOXD3 knockdown and FOXD3-overexpressing HTR8 cells and their respective control groups. **(B,D)** Transwell migration assay of FOXD3 knockdown without or with RND3 overexpression and FOXD3-overexpressing without or with siRND3 HTR-8 cells and their respective control groups. Original magnification: × 100. Scale bar = 100 μm. **(C)** Flow cytometry analysis of the apoptosis rate of siNC, siFOXD3, siFOXD3 + RND3 and Vector, FOXD3, FOXD3 + siRND3 group. Histogram of Annexin V $APC^+/7\text{-}AAD^-$ represents early apoptotic cells. Histogram of Annexin $VAPC^+/7\text{-}AAD^+$ cells represents late apoptotic cells. The sum of the former two categories equals the total number of apoptotic cells. **(E)** The mRNA expression level of RND3 and FOXD3 in the villous tissues of patients with RM and HC was determined using qRT-PCR (n = 24). RND3 mRNA expression was correlated with FOXD3 mRNA expression in villous tissues. Correlation analysis was performed using Spearman's rank correlation test. **(F–I)** Western blot analysis of FOXD3, RND3, MMP2, Cyclin D1, and BAX expression in HTR-8 cells at 48 h after transfection with siNC and siFOXD3 or control vector and FOXD3 overexpression vector. AT 24 h after transfection with siFOXD3 or FOXD3 overexpression vector, HTR-8 cells were transfected RND3 overexpression vector or siRND3 again. Data represent the means ± SD of three independent experiments. $^*P < 0.05$, $^{**}P < 0.01$, $^{***}P < 0.001$, $^{****}P < 0.0001$ vs. siNC, Vector, siFOXD3 or FOXD3 group.

RND3 Regulates Trophoblast Migration and Proliferation via the RhoA-Rho-Associated Coiled-Coil Containing Kinase 1 (ROCK1) Signaling Pathway

Previous findings have suggested that RND3 is closely related to the RhoA-ROCK pathway (Riento et al., 2005; Riento and Ridley, 2006). Hence, we analyzed ROCK1/2 and RhoA expression in HTR-8 cells after RND3 interference. Results showed that ROCK1 and RhoA expression was increased in RND3 knockdown cells and decreased in RND3-overexpressing cells (**Figures 7A,B**). However, no significant difference in ROCK2 expression between both these groups was observed. Besides, ROCK1 activity was examined by measuring the phosphorylation state of a major ROCK1 substrate, MYPT-1, at Thr853 by western blotting. We found that p-MYPT1 was upregulated in RND3 knockdown cells consistent with the change of total ROCK1 level (**Supplementary Figure S3C**). siROCK1 and Y-27632 (Selleck Chemicals), a specific inhibitor of ROCK, was used to inhibit ROCK expression. Western blot analysis revealed that Y-27632 can inhibit ROCK1 expression at concentrations ranging from 5 to 25 μM. Hence, we chose 10 μM as a working concentration for following experiments (**Supplementary Figure S3A**). CCK-8 and transwell assay results showed that Y-27632 and siROCK1 treatment inhibited proliferation and migration in RND3 knockdown HTR-8 cells (**Figures 7C–F**). However, flow cytometry results showed no differences in migration and proliferation in the presence or absence of Y-27632 or siROCK1 in RND3 knockdown HTR-8 cells (**Supplementary Figure S4**). These findings indicate that RND3 regulates trophoblast migration and proliferation via the RhoA-ROCK1 signaling pathway, but ROCK1 is not involved in RND3-induced apoptosis in HTR-8 cells.

RND3 Regulates Trophoblast Apoptosis via the Extracellular Signal-Regulated Protein Kinases 1 and 2 (ERK1/2) Signaling Pathway

In order to identify the unknown pathways or key molecules involved in trophoblast apoptosis, we explored various signaling pathways, including the p53, phosphatidylinositol-3 kinase-protein kinase B, JAK (Janus kinase)/STAT, and ERK1/2 pathways. We discovered that the expression of phosphorylated ERK1/2 (p-ERK) was decreased in RND3 knockdown HTR-8 cells and increased in RND3-overexpressing cells (**Figures 7G,H**). In order to determine the part of the ERK1/2 pathway in RND3 function, U0126 (Sigma-Aldrich), an inhibitor of mitogen-activated protein kinase (MAPK), was used to inhibit the ERK1/2 pathway. Western blot analysis revealed that U0126 can inhibit phosphorylated ERK1/2 expression at concentrations ranging from 5 to 25 μM. Hence, we chose 5 μM as a working concentration for following experiments (**Supplementary Figure S3B**). Flow cytometry results showed that although treatment with U0126 increased the percentage of apoptotic cells, U0126 can rescue some percentage of apoptosis caused by overexpression-RND3 in HTR-8 cells (**Figures 7I,K**).

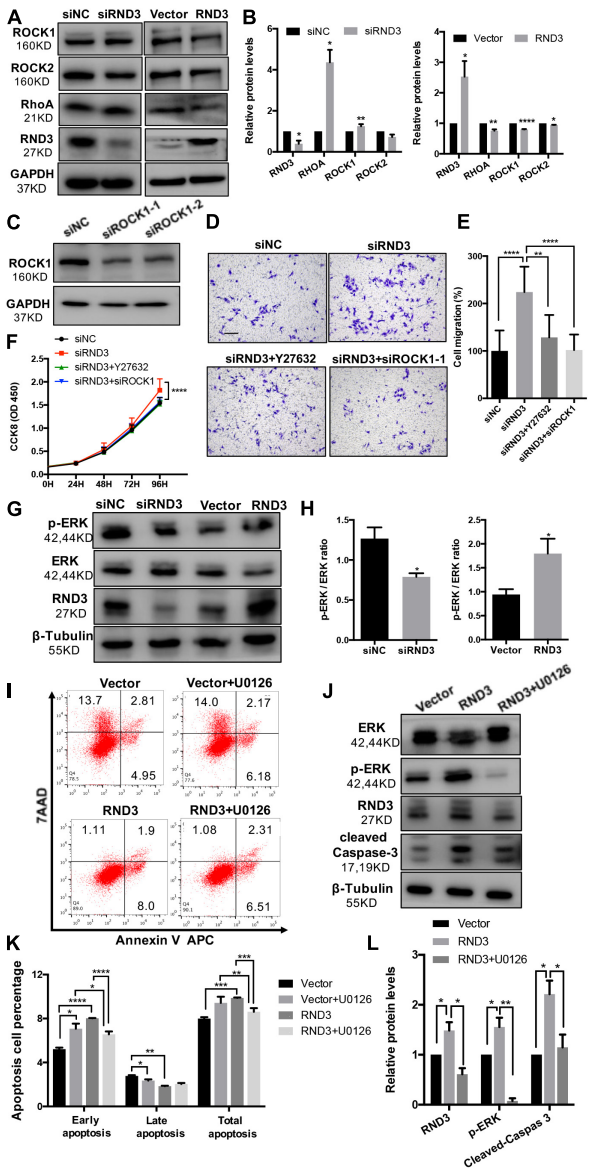

FIGURE 7 | RND3 regulates trophoblast proliferation and migration via the RhoA-ROCK1 signaling pathway and regulates trophoblast apoptosis via the ERK1/2 signaling pathway. **(A,B)** Western blot analysis of ROCK1, ROCK2, and RhoA expression in HTR-8 cells at 48 h after transfection with siNC and siRND3 or control vector and RND3 overexpression vector. **(C)** Western blot showing ROCK1 levels in HTR-8 cells transfected with siROCK1. **(D,E)** HTR-8 cells were transfected with siNC, siRND3, siROCK1 for 36 h, and then treated with Y-27632 for 12 h. Trophoblast migration was assessed by crystal violet staining. Original magnification: ×100. Scale bar = 100 μm. **(F)** CCK-8 assay of siNC- and siRND3-transfected HTR-8 cells in the presence or absence of Y-27632 or siROCK1. **(G,H)** Western blot analysis of p-ERK and ERK expression in HTR-8 cells at 48 h after transfection with siNC and siRND3 or control vector and RND3 overexpression vector. **(I,K)** HTR-8 cells were transfected with control vector or RND3 overexpression vector for 36 h, and then treated with U0126 for 12 h. The apoptosis rate was assessed by flow cytometry. **(J,L)** Western blot analysis of p-ERK, ERK, cleaved caspase-3, and RND3 expression in HTR-8 cells at 48 h after transfection with control vector or RND3 overexpression vector in the presence or absence of U0126. Data represent the means ± SD of three independent experiments. $^{*}P < 0.05$, $^{**}P < 0.01$, $^{***}P < 0.001$, $^{****}P < 0.0001$ vs. siNC, Vector or RND3 group.

Besides, western blotting results revealed that cleaved caspase-3 expression was decreased in RND3-overexpressing HTR-8 cells in the presence U0126 compared with that in the absence of U0126 (**Figures 7J,L**). Interesting, we found that p-ERK level in first-trimester human villi tissues from patients with RM or HC was upregulated by western blot analysis (**Supplementary Figures S5A,B**). Immunohistochemical analyses of paraffin-embedded villous tissue showed that p-ERK protein is present in cytoplasm of CTB (**Supplementary Figure S5C**). These results suggest that RND3 regulates HTR-8 cell apoptosis via the ERK1/2 pathway.

In order to further understand the regulatory mechanism of RND3, we explored the relation between the RhoA/ROCK1 and ERK1/2 pathways. Interestingly, western blot analysis showed that Y-27632 treatment increased p-ERK expression and U0126 treatment increased ROCK1 expression (**Supplementary Figure S6**). These findings indicate that ROCK1 and ERK1/2 act as antagonists in HTR-8 cells.

DISCUSSION

An in depth understanding of the molecular mechanisms and functions of RND3 in different tissues is required to identify novel therapeutic targets for the diagnosis and treatment of human diseases (Jie et al., 2015). RND3 plays a complex role in cells. It can regulate cell proliferation and plays a key role in regulating metastasis and invasion in tumor cells (Paysan et al., 2016). Accumulating evidence has shown that RND3 plays an important role in the regulation of trophoblast function (Collett et al., 2012; Xu et al., 2017; Li et al., 2018); however, there are no studies reporting its function in RM and little is known about its underlying regulatory mechanism in trophoblasts.

Our study provides the first insight into the function of RND3 in CTB proliferation, apoptosis, and migration and its potential character in RM (**Figure 8**). Our results showed that RND3 was expressed in CTB and STB in first-trimester human placental villous tissues, and its expression in patients with RM was significantly higher than that in normal villi (**Figure 1**). Further, we found that overexpression of RND3 suppressed HTR-8 cell proliferation and blocked G1 phase cell cycle progression. In addition, overexpression of RND3 promoted HTR-8 cell apoptosis (**Figure 2**). These data are consistent with the results that trophoblasts of RM exhibit a low percentage of proliferation and a high percentage of apoptosis. Normal CTB function play a vital role for embryo implantation, spiral artery remodeling and maternal-fetal communication. Abnormal CTB proliferation and apoptosis show a connection with RM and many other pregnancy-associated disease, such as PE and fetal growth restriction (Wu et al., 2016). Besides, our study demonstrated that overexpression of RND3 suppressed HTR-8 cell migration (**Figure 3**). RM is related with the dysfunction of proliferative and migratory capacities of trophoblasts. Thus, RND3-targeted strategies may provide a new choice for the diagnosis and treatment of RM patients with trophoblasts dysfunction in early pregnancy.

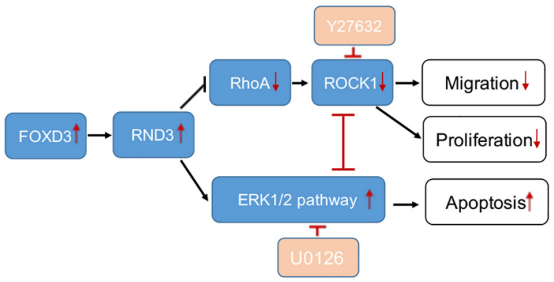

FIGURE 8 | A schematic illustration of the role of RND3 in trophoblast function. RND3 regulates trophoblast migration, proliferation, and apoptosis through different but related pathways. The red arrows show the changes in patients with RM compared with HC. The red T sign indicates the inhibitor effect.

We systemically investigated the transcriptional regulation of RND3 in HTR-8 cells using ChIP and dual-luciferase reporter assays. We found that FOXD3 functioned as a transcriptional enhancer for RND3 and predicted two FOXD3 binding sites in the RND3 core promoter region (**Figure 4**). So far, little is known about the function of FOXD3 compared to other members of the FOX family in adult cells. Many experimental evidences suggest that FOXD3 is a transcriptional repressor in adult cells. However, in our study, we found that FOXD3 directly binds to the promoter regions of RND3 to regulate RND3 function, including inhibition of proliferation and migration and promotion of apoptosis in HTR-8 cells (**Figure 6**), thus suggesting a novel mechanism underlying the regulatory effect of FOXD3 in RM. Moreover, our results demonstrated that FOXD3 and RND3 were highly expressed in the CTB of patients with RM and a positive correlation between their transcript levels was observed (**Figure 6E**).

Rho GTPases which can regulate cell migration, cell cycle and cell morphogenesis are regarded as vital downstream targets of G protein-coupled receptors (Sah et al., 2000). ROCK activity has been involved in the function of migration of tumor cells, particularly in amoeboid cell motility (Hu et al., 2019; Steurer et al., 2019). Many evidences suggested that RhoA and ROCK play important role in the migration of first-trimester EVT cells (Shiokawa et al., 2002). In our study, we demonstrated that RND3 suppressed RhoA-ROCK activates and expression and the pathway mediated HTR-8 cells migration and proliferation of RND3 (**Figures 7A–F**). Next, we found that the level of p-ERK was decreased in RND3 knockdown HTR-8 cells and increased in RND3-overexpressing cells (**Figures 7G,H**). ERK1/2, as members of the MAPK superfamily, mainly regulate cell proliferation and apoptosis. Some studies have suggested that the balance between the intensity and duration of pro-apoptotic or anti-apoptotic signals conveyed by ERK1/2 determines the proliferation or apoptosis of cells (Mebratu and Tesfaigzi, 2009). Sinha et al. (2004) found that withdrawal of soluble survival factors from mouse renal proximal tubular cells lead to apoptosis which was induced by ERK1/2 activity and U0126 or PD98059 can inhibit the activity. The stimuli type and the cell type which provide sufficient ERK1/2 substrates determine that ERK1/2-induced signaling lead to proliferation or apoptosis (Sinha et al., 2004). In the present study, we found that knockdown of RND3 increased ERK1/2 activation-induced apoptosis. However, inhibition of ERK1/2 phosphorylation in RND3-overexpressing HTR-8 cells by U0126 treatment decreased ERK1/2-induced apoptosis. Moreover, previous findings have indicated that ERK1/2 and ROCK1 correlate in a signaling network. Hensel et al. (2014) found that there was a two-way stream of information between ROCK and ERK, with inter-suppression of both molecules in NSC34 cells. But, this process became an unidirectional crosstalk, ultimately leading to dysregulation of neurite outgrowth in a model of spinal muscular atrophy (Hensel et al., 2014). Using western blot analysis, we demonstrated that ROCK and ERK were mutual inhibited in HTR-8 cells (**Supplementary Figure S6**). These data indicate that RND3 function is regulated by these two pathways (**Figure 8**).

CONCLUSION

In conclusion, our study showed that RND3 and FOXD3 expression was significantly increased in the CTB of patients with RM. FOXD3 is a key transcription factor that binds to the RND3 core promoter region and regulates RND3 expression, inhibits proliferation and migration, and promotes apoptosis in HTR-8 cells. Besides, RND3 regulates CTB migration and proliferation via the RhoA-ROCK1 signaling pathway and inhibits apoptosis via the ERK1/2 pathway in HTR-8 cells. Our findings emphasize the importance of RND3 to human pregnancy and provide the basis for the development of molecular therapies for RM. Nevertheless, further research is required for the application of theory to clinical practice.

DATA AVAILABILITY STATEMENT

The nucleotide sequence has been deposited to GenBank, accession number: MN685775. Other raw data supporting the conclusion of this article will be made available by the authors, without undue reservation, to any qualified researcher.

ETHICS STATEMENT

The studies involving human participants were reviewed and approved by the Medical Ethics Committee of International Peace Maternity and Child Health Hospital of the China Welfare Institute, Shanghai Jiao Tong University School of Medicine. The patients/participants provided their written informed consent to participate in this study.

AUTHOR CONTRIBUTIONS

X-LM and XL performed the experiments. X-LM and H-QM contributed to the statistical analyses. SQ and Y-CZ provided the material support. F-JT, W-HZ, L-QS, YZ, and YL provided funding support. JZ, YZ and YL contributed valuable advice to the development of the manuscript. X-LM and YL wrote the manuscript.

FUNDING

Funding sources include the National Key Research and Development Program of China (2018YFC1002802 to W-HZ and 2018YFC1002803 to YL), the National Natural Science Foundation of China (81401218 to F-JT, 81501333 to W-HZ, 81601291 to L-QS, and 31671567, 81971403 to YL), the Special Funds for Local Science and Technology Development Guided by the Central Committee (2018ZYYD014 to YZ), the Interdisciplinary Program of Shanghai Jiao Tong University (YG2017MS38 to F-JT, YG2017ZD09 and YG2017MS40 to YL), and the Clinical Research Fund of the International Peace Maternity and Child Health Hospital, Shanghai Jiao Tong University School of Medicine (GFY5816 to YL and GFY5820 to W-HZ).

SUPPLEMENTARY MATERIAL

The Supplementary Material for this article can be found online at: https://www.frontiersin.org/articles/10.3389/fcell.2020.00153/full#supplementary-material

REFERENCES

Aspenström, P., and Fransson, A. S. J. (2004). Rho GTPases have diverse effects on the organization of the actin filament system. *Biochem. J.* 377, 327–338.

Belgiovine, C., Frapolli, R., Bonezzi, K., Chiodi, I., Favero, F., Mello-Grand, M., et al. (2010). Reduced expression of the ROCK inhibitor Rnd3 is associated with increased invasiveness and metastatic potential in mesenchymal tumor cells. *PLoS One* 5:e14154. doi: 10.1371/journal.pone.0014154

Collett, G. P., Goh, X. F., Linton, E. A., Redman, C. W., and Sargent, I. L. (2012). RhoE is regulated by cyclic AMP and promotes fusion of human BeWo choriocarcinoma cells. *PLoS One* 7:e30453. doi: 10.1371/journal.pone.0030453

David, M., Petit, D., and Bertoglio, J. (2012). Cell cycle regulation of Rho signaling pathways. *Cell Cycle* 11, 3003–3010. doi: 10.4161/cc.21088

Fortier, M., Comunale, F., Kucharczak, J., Blangy, A., Charrasse, S., and Gauthier-Rouviere, C. (2008). RhoE controls myoblast alignment prior fusion through RhoA and ROCK. *Cell Death. Differ.* 15, 1221–1231. doi: 10.1038/cdd.2008.34

Foster, R., Hu, K. Q., Lu, Y., Nolan, K. M., and Thissen, J. S. (1996). Identification of a novel human rho protein with unusual properties: GTPase deficiency and in vivo farnesylation. *Mol Cell Biol.* 16, 2689–2699. doi: 10.1128/mcb.16.6.2689

Han, J., Yang, B. P., Li, Y. L., Li, H. M., Zheng, X. H., Yu, L. L., et al. (2016). RhoB/ROCK mediates oxygen-glucose deprivation-stimulated syncytiotrophoblast microparticle shedding in preeclampsia. *Cell Tissue Res.* 366, 411–425. doi: 10.1007/s00441-016-2436-4

Hanna, H. A., Foreman, R. K., Tarasenko, I. A., Kessler, D. S., and Labosky, P. A. (2002). Requirement for Foxd3 in maintaining pluripotent cells of the early mouse embryo. *Genome Res.* 12, 47–56. doi: 10.1101/gad.1020502

Hensel, N., Stockbrugger, I., Rademacher, S., Broughton, N., Brinkmann, H., Grothe, C., et al. (2014). Bilateral crosstalk of rho- and extracellular-signal-regulated-kinase (ERK) pathways is confined to an unidirectional mode in spinal muscular atrophy (SMA). *Cell. Signal.* 26, 540–548. doi: 10.1016/j.cellsig.2013.11.027

Hu, C., Zhou, H., Liu, Y., Huang, J., Liu, W., Zhang, Q., et al. (2019). ROCK1 promotes migration and invasion of nonsmallcell lung cancer cells through the PTEN/PI3K/FAK pathway. *Int. J. Oncol.* 55, 833–844. doi: 10.3892/ijo.2019.4864

Jaffe, A. B., and Hall, A. (2005). Rho GTPases: biochemistry and biology. *Annu. Rev. Cell Dev. Biol.* 21, 247–269.

Jie, W., Andrade, K. C., Lin, X., Yang, X., Yue, X., and Chang, J. (2015). Pathophysiological functions of Rnd3/RhoE. *Compr. Physiol.* 6, 169–186. doi: 10.1002/cphy.c150018

Lartey, J., Gampel, A., Pawade, J., Mellor, H., and Bernal, A. L. (2006). Expression of RND proteins in human myometrium. *Biol. Reprod.* 75, 452–461. doi: 10.1095/biolreprod.105.049130

Lartey, J., and Lopez Bernal, A. (2009). RHO protein regulation of contraction in the human uterus. *Reproduction* 138, 407–424. doi: 10.1530/REP-09-0160

Li, L., Zhang, X., Hong, S. L., Chen, Y., and Ren, G. H. (2018). Long non-coding HOTTIP regulates preeclampsia by inhibiting RND3. *Eur. Rev. Med. Pharmacol. Sci.* 2018, 3277–3296. doi: 10.26355/eurrev_201806_15146

Li, X., Ma, X. L., Tian, F. J., Wu, F., Zhang, J., Zeng, W. H., et al. (2019). Downregulation of CCNA2 disturbs trophoblast migration, proliferation, and apoptosis during the pathogenesis of recurrent miscarriage. *Am. J. Reprod. Immunol.* 82:e13144. doi: 10.1111/aji.13144

Lin, X., Liu, B. Y., Yue, X., Diao, L., Wang, J., Chang, J., et al. (2013). Genetic deletion of Rnd3 results in aqueductal stenosis leading to hydrocephalus through up-regulation of Notch signaling. *PNAS* 110, 8236–8240. doi: 10.1073/pnas.1219995110

Liu, B., Dong, H., Lin, X., Yang, X., Yue, X., Yang, J., et al. (2016). RND3 promotes Snail 1 protein degradation and inhibits glioblastoma cell migration and invasion. *Oncotarget* 7, 82411–82423. doi: 10.18632/oncotarget.12396

Ma, X. L., Li, X. C., Tian, F. J., Zhang, S. M., Liu, X. R., Zhang, Y., et al. (2017). Effect of the p53-tristetraprolin-stathmin-1 pathway on trophoblasts at maternal-fetal interface. *PLoS One* 12:e0179852. doi: 10.1371/journal.pone.0179852

Mebratu, Y., and Tesfaigzi, Y. (2009). How ERK1/2 activation controls cell proliferation and cell death: Is subcellular localization the answer? *Cell Cycle* 8, 1168–1175. doi: 10.4161/cc.8.8.8147

Mong, P. Y., and Wang, Q. (2009). Activation of Rho kinase isoforms in lung endothelial cells during inflammation. *J. Immunol.* 182, 2385–2394. doi: 10.4049/jimmunol.0802811

Paysan, L., Piquet, L., Saltel, F., and Moreau, V. (2016). Rnd3 in cancer: a review of the evidence for tumor promoter or suppressor. *Mol. Cancer Res.* 14, 1033–1044. doi: 10.1158/1541-7786.MCR-16-0164

Perera, H. K., Caldwell, M. E., Hayes-Patterson, D., Teng, L., Peshavaria, M., Jetton, T. L., et al. (2006). Expression and shifting subcellular localization of the transcription factor, Foxd3, in embryonic and adult pancreas. *Gene Expr. Patter.* 6, 971–977. doi: 10.1016/j.modgep.2006.04.001

Practice Committee of American Society for Reproductive Medicine, (2013). Definitions of infertility and recurrent pregnancy loss: a committee opinion. *Fertil. Steril.* 99:63. doi: 10.1016/j.fertnstert.2012.09.023

Rai, R., and Regan, L. (2006). Recurrent miscarriage. *Lancet* 368, 601–611. doi: 10.1016/s0140-6736(06)69204-0

Red-Horse, K., Zhou, Y., Genbacev, O., Prakobphol, A., Foulk, R., McMaster, M., et al. (2004). Trophoblast differentiation during embryo implantation and formation of the maternal-fetal interface. *J. Clin. Invest.* 114, 744–754. doi: 10.1172/JCI22991

Riento, K., and Ridley, A. J. (2006). Inhibition of ROCK by RhoE. *Methods Enzymol.* 406, 533–541. doi: 10.1016/s0076-6879(06)06041-1

Riento, K., Totty, N., Villalonga, P., Garg, R., Guasch, R., and Ridley, A. (2005). RhoE function is regulated by ROCK I-mediated phosphorylation. *EMBO J.* 24:11. doi: 10.1038/

Sah, V. P., Seasholtz, T. M., and Sagi, S. A. (2000). The role of Rho in G protein-coupled receptor signal transduction. *Annu. Rev. Pharmacol. Taxicol.* 40, 459–490.

Shiokawa, S., Iwashita, M., Akimoto, Y., Nagamatsu, S., Sakai, K., Hanashi, H., et al. (2002). Small guanosine triphospatase RhoA and Rho-associated kinase as regulators of trophoblast migration. *J. Clin. Endocrinol. Metab.* 87, 5808–5816. doi: 10.1210/jc.2002-020376

Sinha, D., Bannergee, S., Schwartz, J. H., Lieberthal, W., and Levine, J. S. (2004). Inhibition of ligand-independent ERK1/2 activity in kidney proximal tubular cells deprived of soluble survival factors up-regulates Akt and prevents apoptosis. *J. Biol. Chem.* 279, 10962–10972. doi: 10.1074/jbc.M312048200

Steurer, S., Hager, B. B., Hoflmayer, D., Tsourlakis, M. C., Minner, S., Clauditz, T. S., et al. (2019). Up regulation of Rho-associated coiled-coil containing kinase1 (ROCK1) is associated with genetic instability and poor prognosis in prostate cancer. *Aging* 11, 7859–7880. doi: 10.18632/aging.102294

Sutton, J., Costa, R., Klug, M., Field, L., Xu, D. L., Largaespada, D. A., et al. (1996). Genesis, a winged helix transcriptional repressor with expression restricted to embryonic stem cells. *J. Biol. Chem.* 271, 23126–23134.

Tian, F. J., Qin, C. M., Li, X. C., Wu, F., Liu, X. R., Xu, W. M., et al. (2015). Decreased stathmin-1 expression inhibits trophoblast proliferation and invasion and is associated with recurrent miscarriage. *Am. J. Pathol.* 185, 2709–2721. doi: 10.1016/j.ajpath.2015.06.010

Tompers, D. M., Foreman, R. K., Wang, Q., Kumanova, M., and Labosky, P. A. (2005). Foxd3 is required in the trophoblast progenitor cell lineage of the mouse embryo. *Dev. Biol.* 285, 126–137. doi: 10.1016/j.ydbio.2005.06.008

Wu, F., Tian, F., Zeng, W., Liu, X., Fan, J., Lin, Y., et al. (2017). Role of peroxiredoxin2 downregulation in recurrent miscarriage through regulation of trophoblast proliferation and apoptosis. *Cell Death Dis.* 8:e2908. doi: 10.1038/cddis.2017.301

Wu, F., Tian, F. J., Lin, Y., and Xu, W. M. (2016). Oxidative stress: placenta function and dysfunction. *Am. J. Reprod. Immunol.* 76, 258–271. doi: 10.1111/aji.12454

Xu, W., Li, J., Li, L., Hou, T., Cai, X., Liu, T., et al. (2019). FOXD3 suppresses tumor-initiating features in lung cancer via transcriptional repression of WDR5. *Stem Cells* 37, 582–592. doi: 10.1002/stem.2984

Xu, Y., Ge, Z., Zhang, E., Zuo, Q., Huang, S., Yang, N., et al. (2017). The lncRNA TUG1 modulates proliferation in trophoblast cells via epigenetic suppression of RND3. *Cell Death Dis.* 8:e3104. doi: 10.1038/cddis.2017.503

Yan, J. H., Zhao, C. L., Ding, L. B., and Zhou, X. (2015). FOXD3 suppresses tumor growth and angiogenesis in non-small cell lung cancer. *Biochem. Biophys. Res. Commun.* 466, 111–116. doi: 10.1016/j.bbrc.2015.08.116

Yilmaz, M., and Christofori, G. (2009). EMT, the cytoskeleton, and cancer cell invasion. *Cancer Metast. Rev.* 28, 15–33. doi: 10.1007/s10555-008-9169-0

Zhang, J., Mo, H. Q., Tian, F. J., Zeng, W. H., Liu, X. R., Ma, X. L., et al. (2018). EIF5A1 promotes trophoblast migration and invasion via ARAF-mediated activation of the integrin/ERK signaling pathway. *Cell Death Dis.* 9:926. doi: 10.1038/s41419-018-0971-5

Zhang, Y., Jin, F., Li, X. C., Shen, F. J., Ma, X. L., Wu, F., et al. (2017). The YY1-HOTAIR-MMP2 signaling axis controls trophoblast invasion at the maternal-fetal interface. *Mol. Ther.* 25, 2394–2403. doi: 10.1016/j.ymthe.2017.06.028

Conflict of Interest: The authors declare that the research was conducted in the absence of any commercial or financial relationships that could be construed as a potential conflict of interest.

Copyright © 2020 Ma, Li, Tian, Zeng, Zhang, Mo, Qin, Sun, Zhang, Zhang and Lin. This is an open-access article distributed under the terms of the Creative Commons Attribution License (CC BY). The use, distribution or reproduction in other forums is permitted, provided the original author(s) and the copyright owner(s) are credited and that the original publication in this journal is cited, in accordance with accepted academic practice. No use, distribution or reproduction is permitted which does not comply with these terms.

frontiers in Cell and Developmental Biology

REVIEW
published: 31 January 2020
doi: 10.3389/fcell.2020.00034

Mechanical Regulation of Protein Translation in the Cardiovascular System

*Lisa J. Simpson, John S. Reader and Ellie Tzima**

Division of Cardiovascular Medicine, Radcliffe Department of Medicine, Wellcome Centre for Human Genetics, University of Oxford, Oxford, United Kingdom

The cardiovascular system can sense and adapt to changes in mechanical stimuli by remodeling the physical properties of the heart and blood vessels in order to maintain homeostasis. Imbalances in mechanical forces and/or impaired sensing are now not only implicated but are, in some cases, considered to be drivers for the development and progression of cardiovascular disease. There is now growing evidence to highlight the role of mechanical forces in the regulation of protein translation pathways. The canonical mechanism of protein synthesis typically involves transcription and translation. Protein translation occurs globally throughout the cell to maintain general function but localized protein synthesis allows for precise spatiotemporal control of protein translation. This Review will cover studies on the role of biomechanical stress -induced translational control in the heart (often in the context of physiological and pathological hypertrophy). We will also discuss the much less studied effects of mechanical forces in regulating protein translation in the vasculature. Understanding how the mechanical environment influences protein translational mechanisms in the cardiovascular system, will help to inform disease pathogenesis and potential areas of therapeutic intervention.

Keywords: mechanotransduction, protein translation, cardiac, endothelial, shear stress, pressure overload

OPEN ACCESS

Edited by:
Guillermo Alberto Gomez, University of South Australia, Australia

Reviewed by:
Srikala Raghavan, Institute for Stem Cell Biology and Regenerative Medicine, India
Elena P. Moiseeva, Retired, Leicester, United Kingdom

***Correspondence:**
Ellie Tzima
ellie@well.ox.ac.uk

Specialty section:
This article was submitted to Cell Adhesion and Migration, a section of the journal Frontiers in Cell and Developmental Biology

Received: *11 October 2019*
Accepted: *15 January 2020*
Published: *31 January 2020*

Citation:
Simpson LJ, Reader JS and Tzima E (2020) Mechanical Regulation of Protein Translation in the Cardiovascular System. Front. Cell Dev. Biol. 8:34. doi: 10.3389/fcell.2020.00034

FORCES IN BIOLOGY

Mechanical forces can occur on the whole body to microscopic scale. During development, mechanical forces govern cell shape and migration and hence orchestrate the growth of multicellular biological tissues (Mammoto and Ingber, 2010; LeGoff and Lecuit, 2016). Mechanical signals drive organogenesis in the late stages of embryonic development in nearly every system. Force drives the formation of the vasculature (Lucitti et al., 2007), lungs (Gutierrez et al., 2003), brain (Anava et al., 2009), musculoskeletal system (Stokes et al., 2002; Kahn et al., 2009) hematopoietic system (Adamo et al., 2009; North et al., 2009) and the heart (Hove et al., 2003; Forouhar et al., 2006). Impaired force sensing or altered mechanotransduction signaling is linked to defects in development of tissues and organs in addition to disease in later life such as cardiovascular diseases and cancer (Jaalouk and Lammerding, 2009).

External forces such as those imposed by gravity and exercise influence musculoskeletal growth and strength. Skeletal muscle requires mechanical load which acts to upregulate protein synthesis and promote myocyte growth and maintenance. Bone growth and metabolism requires frequent pressure and tensile forces generated through skeletal muscle contractions and gravity (Kohrt et al., 2009). Mechanical loading is essential for musculoskeletal homeostasis as withdrawal of force leads to regression and atrophy of these tissues (reviewed well by Felsenthal and Zelzer, 2017). Atrophy is often observed with aging but also in environments such as microgravity in space where force bearing on the skeleton is lower than on Earth (LeBlanc et al., 2007; Amin, 2010). These changes involve alterations in protein synthesis mechanisms, which, in the absence of mechanical stimuli, contribute to reduced growth and cell turnover.

Respiration is another highly mechanical process requiring repeated expansion and subsequent deflation of the lungs in order to oxygenate blood and remove gaseous waste from the body. This vital continual loop generates an array of mechanical forces within the pulmonary system, such as longitudinal or circumferential stretch, surface tension on the alveoli cells of the lungs or fluid shear stress within the pulmonary vasculature caused by blood flow (Breen et al., 1999). Increased ventilation is associated with remodeling of the lungs that involves increases in both protein and DNA as a result of mechanical force (Gutierrez et al., 2003). Mechanical forces are also implicated in lung diseases, for example, force imbalances arising from pulmonary hypertension can remodel the pulmonary vasculature and induce smooth muscle and fibroblast proliferation in conjunction with increased collagen and elastin protein synthesis and gene expression (Wirtz and Dobbs, 2000). Disturbed mechanical forces exerted on pulmonary vascular endothelial cells induces changes in protein synthesis and expression of pro-inflammatory molecules such as IL-8, TNF-α and CXCL5 (Tang et al., 2016).

MECHANICS IN THE CARDIOVASCULAR SYSTEM

Atherosclerosis is characterized as a chronic inflammatory disorder resulting from the accumulation of fatty deposits in the arterial intima which can form plaques occluding blood flow. This disease is highly focal in nature as a result of differential mechanical forces exerted by blood flow in different regions of the vascular network. Briefly, disturbed and complex blood flow profiles arise where blood vessels branch or curve sharply and this primes these areas to have low but chronic inflammation, leaving them more vulnerable to plaque accumulation (Davies, 1995; Hahn and Schwartz, 2009). Conversely, straight regions of the vasculature experience smooth, uniform blood flow which promotes anti-inflammatory pathways and thus keeps them relatively protected from atherosclerotic plaques. Atherosclerotic lesions leave arteries thicker and less compliant therefore they cannot modulate or adapt to changes in blood flow. Rapid changes in shear stress gradients at lesion sites has been shown to be the primary driver of platelet aggregation and activation which increases plaque accumulation (Nesbitt et al., 2009). Disturbed blood flow at injury sites can increase risk of plaque rupture and thrombotic complications downstream. This can be fatal if it occurs in the coronary vessels of the heart. In addition to atherosclerosis, changes to blood flow parameters in the aorta can promote abnormal swelling and weakening of the vessel wall known as aortic aneurysms. Under mechanical strain, these bulges will eventually rupture, leading to potentially fatal complications (Bäck et al., 2013).

The organ that is perhaps the most influenced by biomechanical forces is the heart. The heart beats continuously to transport oxygenated blood and nutrients to the rest of the body to maintain normal organ function. The activity and integrity of the heart itself is highly influenced by biomechanics and mechanical stress is a critical mediator of cardiomyocyte function and extracellular matrix composition (Voorhees and Han, 2015). Biomechanical forces regulate the activity and function of the cells of the heart: cardiomyocytes, fibroblasts, and the vascular cells of the coronary blood vessels (Hahn and Schwartz, 2009; Voorhees and Han, 2015; van Putten et al., 2016; Herum et al., 2017). In response to biomechanical stress, cardiomyocytes undergo hypertrophic growth (Hannan et al., 2003). Hypertrophic adaptive remodeling can occur under physiological settings such as exercise or during pregnancy where the heart undergoes compensatory hypertrophy to deal with increased mechanical load in order to maintain cardiac function and output (Heineke and Molkentin, 2006). In response to chronic endurance exercise undertaken by elite athletes, the heart must remodel to handle the considerable increase in mechanical load (George et al., 2012). Physiological hypertrophy seen in the athlete's heart is typically not associated with myocyte damage, although some studies have shown myocardial death during intense exercise as well as fibrosis in long-term endurance athletes (La Gerche et al., 2012; Galderisi et al., 2015). Nevertheless, most elite athletes will present a healthy physiological adaptation to prolonged bouts of intense exercise that can be distinguished from pathological hypertrophy to pressure overload. Under pathological settings, such as hypertension, the heart deals with sustained, chronic levels of mechanical strain and this can lead to persistent activation of protein synthesis pathways such as mammalian target of rapamycin (mTOR) which regulate cardiomyocyte growth (Heineke and Molkentin, 2006). This hypertrophic remodeling response is chronic and can ultimately result in heart failure (Lyon et al., 2015).

PROTEIN TRANSLATION AND CARDIOVASCULAR FUNCTION

Protein translation is a highly conserved and tightly regulated process which is fundamental for cellular homeostasis. The canonical mechanism of protein synthesis typically involves two major steps: transcription of a messenger RNA (mRNA) transcript in the nucleus and translation of this mRNA into a protein by the translational machinery in the cytoplasm (Clancy and Brown, 2008). Protein translation occurs globally throughout the cell to maintain general function but localized

or polarized protein synthesis occurring for example at the leading edge of migrating cells (Katz et al., 2012), allows for efficient translation of specific proteins required for cell motility in the correct location. It is important to emphasize that mRNA levels do not always correlate to protein expression levels and this disconnect is a result of post transcriptional mechanisms (Spriggs et al., 2010). Having this additional level of translational control enables cells to rapidly respond and adapt to changing micro-environmental conditions.

Translation is segmented into four stages: initiation, elongation, termination and ribosome recycling. Modulation of translation typically occurs at the initiation stage which requires the co-ordination of many translational factors and ribosomal subunits (Sonenberg and Hinnebusch, 2009). Eukaryotic initiation factors (eIFs) are involved in mediating the start of translation through assembly of initiation complex on the 40S ribosomal subunit and chaperoning of the 60S subunit to join the 40S (Sonenberg and Hinnebusch, 2009). The activity of eIFs are controlled via phosphorylation and the most common mechanism for switching off global translation is through phosphorylation of eIF2α subunit at its Serine 51 (Jackson et al., 2010). This highlights the importance of translation modulation under conditions of cell stress or when the cell needs to conserve energy. Having the ability to switch off global translation and shift the proteomic landscape to synthesize specific proteins required to maintain cellular function is critical for cell survival.

The highly conserved regulatory pathway, mTOR plays a crucial role in many processes including transcription and protein translation, ribosomal and mitochondrial biogenesis, and cell growth and division (Sciarretta et al., 2014). mTOR is a serine/threonine protein kinase, part of the phosphoinositide 3-kinase (PI3K) family, which interacts with many adaptor proteins to form two distinct signaling complexes, namely mTORC1 and mTORC2. These complexes were distinguished by their relative sensitivity to Rapamycin, which inhibits mTORC1 signaling without disrupting mTORC2 signaling. Broadly, mTORC1 regulates protein synthesis, cell growth and proliferation, cell metabolism and stress responses, whereas mTORC2 regulates cell survival, cytoskeletal organization and polarity (**Figure 1**). Both complexes are relatively large with multiple adaptor proteins which give them their unique signaling identity. Of the two complexes, mTORC1 has been more extensively studied and its upstream inputs and downstream targets are better understood than that of mTORC2, in the cardiovascular system and the rest of the body (Sciarretta et al., 2018).

The major downstream substrates of mTORC1 related to protein synthesis are S6 kinase 1 (S6K1) and eukaryotic ignition factor 4E (eIF4E)-binding protein (4E-BP1) and these have been thoroughly studied (Shin et al., 2011). Once activated, mTORC1 phosphorylates and in turn activates S6K1 which stimulates mRNA biogenesis and the protein translation machinery. mTORC1 negatively regulates 4E-BP1 and in doing so this allows for the formation of the eIF4F initiation complex that promotes the canonical cap-dependent pathway of protein translation. Protein kinase B, or Akt, can directly activate mTOR through phosphorylation whilst also repressing the endogenous mTORC1 inhibitor, PRAS40, and thereby augment mTOR downstream effects. The 5′ adenosine monophosphate-activated protein kinase (AMPK) pathway is a well-established negative regulator of mTORC1 activity. AMPK is normally activated in times of cellular stress e.g., when nutrients, amino acids and energy are scarce. Under stressed conditions, AMPK will stimulate the tuberous sclerosis protein (TSC) 1/TSC2 complex which can inhibit mTORC1 signaling indirectly by converting mTORC1 activator Ras homolog enriched in brain (Rheb) into its inactive GDP-bound form. The active GTP-bound state of Rheb normally directly interacts with and promotes mTORC1's kinase functions (Laplante and Sabatini, 2012). In addition to AMPK, glycogen synthase kinase (GSK) 3β is a potent activator of the TSC1/TSC2 complex and so can also contribute to dampening of mTORC1 activity during times of cellular stress (see **Figure 1** for summary of signaling). It is well established that mTOR signaling can be activated by amino acids, stress, oxygen, energy status and growth factors such as insulin (Laplante and Sabatini, 2012). There is also evidence indicating mechanical force can stimulate mTOR signaling (Kraiss et al., 2000; Guo et al., 2007; Hornberger, 2011; Philip et al., 2011; Jacobs et al., 2017; Vion et al., 2017) and this will be discussed in more detail below.

PROTEIN TRANSLATION IN RESPONSE TO BIOMECHANICAL FORCES IN THE HEART

Force-derived signaling regulates the development of cardiomyopathy and left ventricular remodeling following an infarct by contributing to tissue fibrosis and scarring. Elevated stress and pressure overload on the heart in conditions such as hypertension and valvular disease can promote ventricular hypertrophy and diastolic heart failure (Merino et al., 2018). The most common model used to mimic human cardiovascular disease and elucidate mechanisms of cardiac hypertrophy and heart failure is the transverse aortic constriction (TAC) model in the mouse (Rockman et al., 1991; Merino et al., 2018). In this model, pressure overload is produced by aortic ligation and provides a reproducible model of cardiac hypertrophy and gradual heart failure. Several studies have used this model to evaluate protein synthesis pathways and investigate the therapeutic benefit of their modulation.

The mTOR pathway plays an essential regulatory role in cardiovascular physiology and pathology. Both mTORC1 and mTORC2 signaling are crucial for embryonic cardiovascular development and preserving function in the adult (Sciarretta et al., 2018). Specific cardiac ablation of *mTOR* is embryonic lethal and disruption of mTORC1 components postnatally is associated with increased cardiac dysfunction, apoptosis, metabolic changes and heart failure (Sciarretta et al., 2014). It is widely accepted that mTORC1 activation and signaling is required for the development of adaptive hypertrophy and maintenance of heart function in response to pressure overload (Sciarretta et al., 2018). In the absence of mTOR signaling, inadequate remodeling of the heart under increased mechanical strain leads to dilated cardiomyopathy (Zhang et al., 2010). Rapamycin, a potent mTORC1 inhibitor, alleviates established hypertrophy

and improves cardiac function following TAC-induced pressure overload in murine models (Shioi et al., 2003; McMullen et al., 2004; Gao et al., 2006). Cardiac hypertrophy promoted by increasing systolic blood pressure in the spontaneously hypertensive rat model could also be attenuated with application of rapamycin (Soesanto et al., 2009). It is important to note, however, that while mTORC1/2 signaling is necessary for cardiomyocyte survival and adaptive hypertrophy in response to mechanical or ischemic trauma, persistent activation of mTOR in a disease setting contributes to pathological hypertrophic remodeling, accumulation of misfolded proteins, energy stress and impaired ventricular and overall heart function (Buss et al., 2009). It has been demonstrated that partial mTORC1 inhibitors are effective in reducing an exaggerated hypertrophic response under pressure overload or chronic myocardial infarction and thereby alleviate tissue damage and heart failure (Shioi et al., 2003). On its own, mTOR signaling is not enough to induce hypertrophy but it is a major contributor and hence has become an attractive target for therapeutic intervention under settings of sustained mechanical stress on the heart (Shen et al., 2008). Partial inhibition of mTORC1 during cardiac stress has been under intense investigation in order to achieve dampening of the maladaptive effects of sustained mTORC1 signaling without disrupting its normal physiological actions. Other studies have investigated the role of components of the mTORC1 complex in the heart under physiological and pathological conditions, such as the adaptor protein Raptor. Mice deficient in myocardial *raptor* display cardiac dysfunction leading to heart failure in response to pressure overload induced by TAC; this is associated with a lack of adaptive cardiomyocyte growth due to reduced protein synthesis (Shende et al., 2011). It has also been demonstrated that cardiac specific overexpression of the gene encoding the mTORC1 endogenous inhibitor, PRAS40, is associated with blunted pathological remodeling after pressure overload and preservation of cardiac function (Völkers et al., 2013a,b).

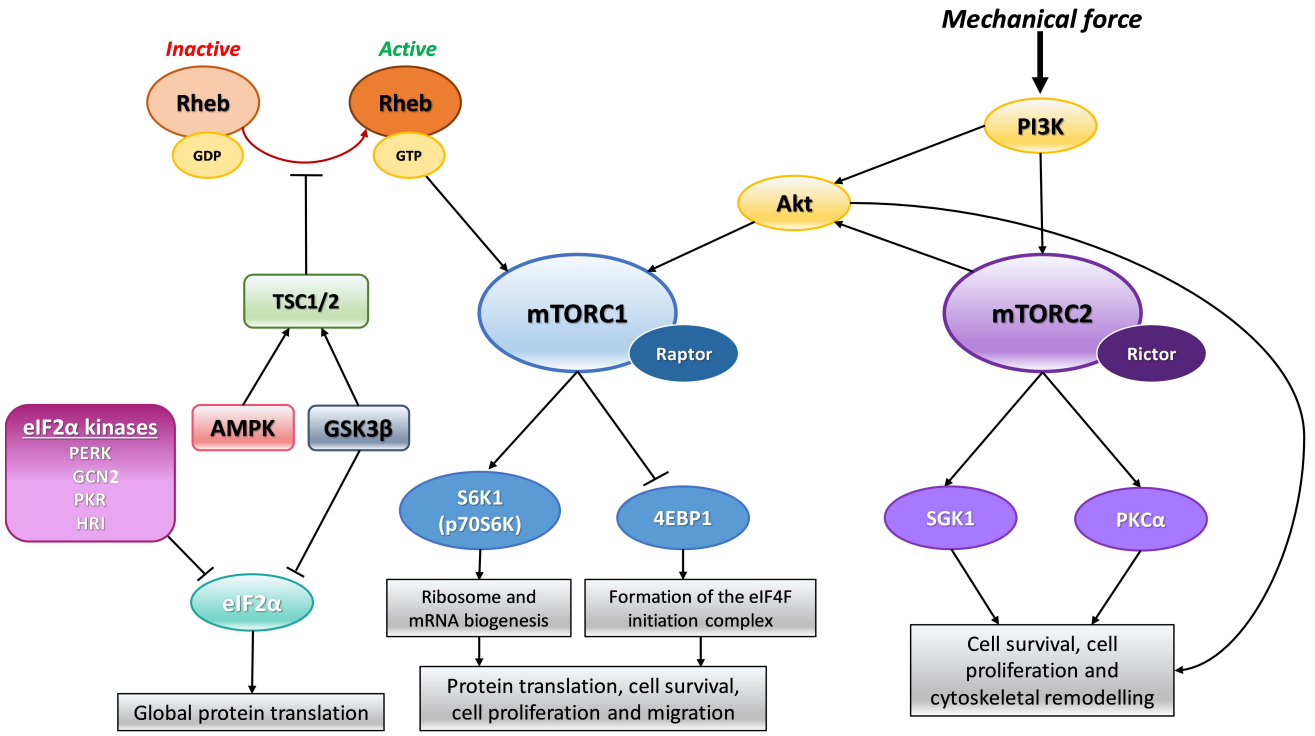

FIGURE 1 | Schematic representation of mTOR signaling. In response to mechanical force, PI3K activates Akt and mTORC2 directly. mTORC2 can further activate Akt which can also directly activate mTORC1. Rheb can directly activate mTORC1 when in its active GTP bound form. Activation of mTORC1 positively regulates S6K1/p70S6K leading to downstream ribosome and mRNA biogenesis. In addition, activation of mTORC1 also negatively regulates 4EBP1 allowing for the formation of the eIF4F translation initiation complex. This combined signaling promotes protein synthesis and cell growth. When mTORC2 is activated it also promotes cell growth and survival through its downstream effectors SGK1 and PKCα. Adaptor proteins, Raptor and Rictor, are specific to mTORC1 and mTORC2, respectively, and are required for active signal transduction. The TSC1/2 complex can prevent mTORC1 activation by Rheb by keeping Rheb in its inactive GDP form. The TSC1/2 complex can be activated by both AMPK and GSK3β signaling to dampen mTORC1 activity in times of cellular stress. GSK3β can also inhibit eIF2α mediated protein translation again to reduce global protein synthesis during cellular stress. In addition, there are four kinases which can phosphorylate and inactivate eIF2α mediated protein translation under distinct stress conditions: PERK, GCN2, PKR and HRI. Phosphoinositide-3-kinase–protein kinase B/Akt (PI3K-PKB/Akt), Mammalian target of rapamycin (mTOR), Tuberous sclerosis protein (TSC), 5′ adenosine monophosphate-activated protein kinase (AMPK), Glycogen synthase kinase 3β (GSK3β), Ras homolog enriched in brain (Rheb), Eukaryotic initiation factor 2α (eIF2α), Protein kinase R (PKR)-like endoplasmic reticulum kinase (PERK), General control non-derepressible 2 (GCN2), Protein kinase RNA-activated (PKR), Heme-regulated inhibitor kinase (HRI), Ribosomal protein S6 kinase beta-1 (S6K1) or p70S6 kinase (p70S6K), Eukaryotic translation initiation factor 4E (eIF4E)-binding protein 1 (4EBP1), Serine/threonine-protein kinase Sgk1 also known as serum and glucocorticoid-regulated kinase 1 (SGK1), Protein kinase C alpha (PKCα).

The role of mTORC2 in cardiac pathology has received considerably less attention. Bénard et al. showed that stromal interaction molecule 1 (STIM1) is required for the initiation of compensatory hypertrophy in response to TAC-induced overload. STIM1 directly activates mTORC2/Akt signaling in order to preserve cardiac function (Bénard et al., 2016). The adaptor protein rictor is unique to and critical for mTORC2 signaling. Cardiomyocyte specific inducible deletion of *RICTOR* leads to cardiac dysfunction in response to pressure overload, again reinforcing the importance of mTOR signaling in the short term, adaptive response to increased mechanical strain (Shende et al., 2016). A similar observation of cardiac dysfunction was seen by Völkers et al. in their *RICTOR* knockdown model which was tested under chronic infarction induced by permanent ligation. In addition to mTOR, the Hippo pathway is another major regulator of cell growth, division and apoptosis. While mTOR signaling promotes growth, the Hippo pathway exerts the opposite effect through negative regulation of its downstream effectors; transcriptional co-activators, yes-associated protein (YAP) and transcriptional coactivator with a PDZ-binding domain (TAZ) (Hansen et al., 2015). The Hippo kinases, MST1/2 in mammals, when active phosphorylate and activate the kinases LATS1/2 which in turn phosphorylate and inactivate YAP and TAZ. When inactive, YAP/TAZ are retained in the cytoplasm where they undergo degradation. When not repressed and in their active form, YAP/TAZ translocate to the nucleus where they predominantly interact with transcription factors from the TEA domain members (TEADs) to promote activation of genes linked with growth (Meng et al., 2016). There has been some research highlighting the cross-talk between Hippo and mTOR signaling during disease states of increased cell growth and proliferation such as cancer (Artinian et al., 2015), however, very little is known with regards to cardiac hypertrophy. One key study has demonstrated that mTORC2 signaling preserves cardiac function following pressure overload induced by TAC by inhibiting the Hippo kinase, MST1 (Sciarretta et al., 2015).

GSK-3β is a negative regulator of protein synthesis and plays a critical role in the cardiomyocyte hypertrophic response to increased mechanical strain. The mechanical stimulus of aortic banding results in a significant decrease in GSK-3β activity which allows for the classic cardiomyocyte hypertrophic response – increased protein accumulation as a result of enhanced protein synthesis, enhanced sarcomere organization and re-expression of the fetal gene program (Haq et al., 2000). Constitutive activation or increased expression of the active form of GSK-3β attenuates pressure overload-induced cardiac hypertrophy *in vivo*, in part due to inactivation of NFAT target genes (Haq et al., 2000; Antos et al., 2001). Active GSK-3β represses eIF2α-mediated protein translation (Antos et al., 2001) and GSK-3β is the primary kinase that phosphorylates eIF2Bε at Serine 535 in rat cardiomyocytes thereby impeding the initiation of translation and resulting in decreased cardiomyocyte hypertrophy (Hardt et al., 2004).

Protein translation rates in the adult heart are generally one of the lowest in the body because cardiomyocytes terminally differentiate soon after birth and therefore show little growth potential and have low cell turnover (Garlick et al., 1980; Paradis et al., 2014). It is only once the heart is mechanically stimulated in an intense and/or prolonged manner e.g., endurance exercise or heart failure, that protein synthesis rates increase, and cardiomyocytes become hypertrophic. One possible mechanism by which biomechanical forces can alter translational control in the heart is via a poly(A) tail based modulatory mechanism. All mature mRNA transcripts in mammalian cells possess a long tail sequence at one end composed of adenosine nucleotide repeats referred to as the poly(A) tail (Hocine et al., 2010). Certain factors can bind onto the poly(A)tail and influence the fate of the mRNA i.e., how efficiently it is translated or degraded (Burgess and Gray, 2010). PABPC1 is a poly(A)tail binding protein known to facilitate mRNA translation (Kini et al., 2016). A recent study by Chorghade, Seimetz and colleagues investigated how PABPC1 mediates protein translation using mouse and human cells. They highlight that PABPC1 is highly expressed in the heart before birth but is downregulated to almost undetectable levels in the adult heart. They found that this decrease in PABPC1 expression was not a result of lower transcription levels but due to changes in translation of the mRNA transcript. The mRNA for PABPC1 has a much shorter poly(A) tail in the adult heart and this affects its translational efficiency causing low protein expression in the adult vs. neonatal heart. This study highlighted that the length of the PABPC1 mRNA poly(A) tail can be extended, and therefore, protein production can be re-established in the adult heart when it has been subjected to hypertrophic conditions triggered by endurance exercise or cardiovascular disease. Experimental re-introduction of PABPC1 in adult hearts allowed for an interaction with pre-initiation factor, eIF4G, which promotes the recruitment of ribosomes and the activation of protein translation (Chorghade et al., 2017).

Impaired force sensing or changes to mechanical signaling that regulates protein translation are clearly linked to cardiac remodeling. Further investigation is required into the mechanical regulation of components of the translational machinery and factors that govern the initiation of protein translation in the context of increased mechanical strain, in both physiological and pathological contexts.

ER STRESS AND BIOMECHANICAL STRESS

The endoplasmic reticulum (ER) plays a crucial role in protein synthesis, folding and quality control to maintain cellular and tissue function (Walter and Ron, 2011). Under pathological mechanical stress such as pressure overload, the tight balance of protein expression and quality control is disrupted, leading to changes in post-translational modifications, increased protein aggregates and misfolding, decreased protein stability and ultimately an ER stress response (Doroudgar et al., 2015). The ER stress response can activate the unfolded protein response (UPR), thus promoting an acute decrease in protein synthesis, increased protein degradation of defective or misfolded proteins and increased synthesis of protective proteins (Glembotski, 2007). These acute mechanisms are cardioprotective in response to

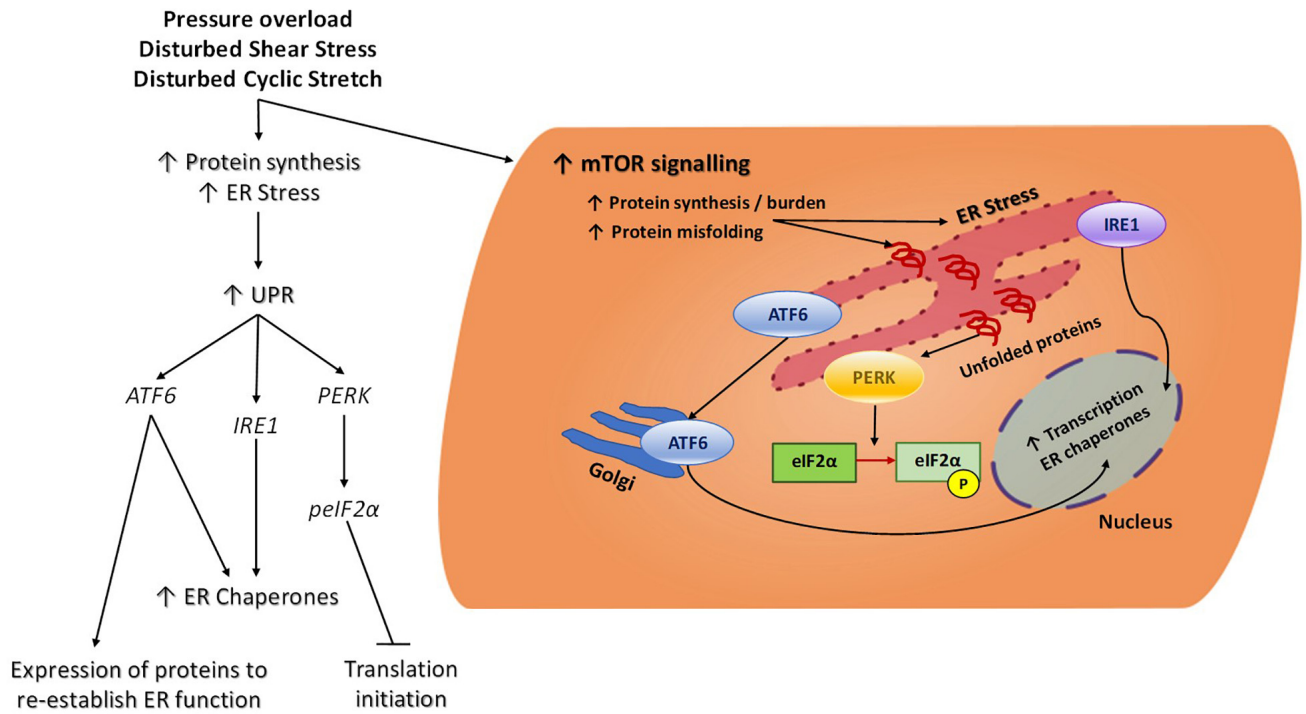

FIGURE 2 | Cellular ER Stress signaling in response to mechanical force. Increased protein synthesis results from chronic mechanical activation of pathways such as mTOR. This results in an increase in protein burden, accumulation of misfolded proteins and ER stress. In an attempt to re-establish ER homeostasis, the UPR is triggered and this consists of three main branches. The eIF2α kinase PERK is an ER transmembrane protein which acts as a sensor to increased protein load and accumulation of unfolded proteins in the ER. Once stimulated, PERK will phosphorylate eIF2α and thereby block global translation initiation to help reduce protein burden in the ER. Phosphorylation of eIF2α also leads to translation of a specific subset of mRNA which will help maintain cellular function and promote cell survival during stress conditions. In times of ER stress, ATF6 will translocate from the ER to the Golgi where it will become cleaved and function as an active transcription factor, promoting the transcription of ER chaperones. IRE1catalyses the splicing of key mRNAs that will become functional transcriptions factors and similar to ATF6, these will promote the transcription and ultimate translation of ER chaperones which will facilitate proper protein folding and degradation to alleviate ER burden. Endoplasmic reticulum (ER), Mammalian target of rapamycin (mTOR), Unfolded protein response (UPR), Eukaryotic translation initiation factor 2-alpha kinase 3, also known as protein kinase R (PKR)-like endoplasmic reticulum kinase (PERK), Activating transcription factor 6 (ATF6), Serine/threonine-protein kinase/endoribonuclease inositol-requiring enzyme 1 (IRE1), Eukaryotic initiation factor 2α (eIF2α).

dynamic and physiological changes in pressure stimuli, however, their prolonged activation is associated with cardiac cell death (Sun et al., 2015).

In response to biomechanical stress, phosphorylation of eIF2α blocks initiation of translation and, as such, helps relieve the excess burden of increased protein synthesis and accumulated unfolded proteins in the ER (see **Figure 2**) (Doroudgar et al., 2015). Attenuation of eIF2α phosphorylation by cardiomyocyte-specific gene deletion of one of its kinases (PERK) resulted in disruption of the cardiac stress response and exacerbated cardiomyocyte hypertrophy, fibrosis and apoptosis (Liu et al., 2014). While deletion of the gene encoding PERK (*EIF2AK3*) appears to be detrimental in the overloaded heart, gene deletion of other eIFα kinases such as GCN2 (*EIF2AK4*) and PKR (*EIF2AK2*) appears to confer some benefit in pressure overload mouse models. When compared to wildtype mice, GCN2 gene deletion did not reduce the degree of cardiac hypertrophy but did protect against ventricular dysfunction, cardiac fibrosis and apoptosis following pressure overload (Lu et al., 2014). Similarly, PKR gene knockout mice are less prone to pressure overload-induced cardiac fibrosis and have preserved left ventricular function despite displaying similar cardiac hypertrophy to their wildtype littermates (Wang et al., 2014). The molecular mechanisms responsible for the different phenotypes of eIF2α kinase gene knockout mouse models following pressure overload remain incompletely understood, but there is increased appreciation for roles of GCN2, PERK and PKR independent of eIF2α phosphorylation. For instance, PERK is a transmembrane protein spanning the ER membrane and not only reduces protein burden via eIF2α-mediated translation block but has been linked to sensing protein folding interactions in the ER during the unfolded protein response (Donnelly et al., 2013). Therefore, cardiac deletion of the gene encoding PERK would ablate ER homeostasis which the other cytoplasmic eIF2α kinases may not be able to fully compensate for and hence cause a more severe reaction to pressure overload.

Reperfusion of the ischemic heart is essential in order to salvage the myocardium, however, it also imposes mechanical stress and injury to the heart. Ischemia-reperfusion (IR) injury induces marked oxidative stress and intracellular calcium overload, leading to ER stress and activation of the UPR.

An important regulator of the UPR in the cardiomyocyte in response to hypertrophy is Activating Transcription Factor 6 (ATF6) (Glembotski, 2014). Upon ER stress, ATF6 is activated and triggers expression of key proteins which will re-establish normal ER function and folding capacity (**Figure 2**; Martindale et al., 2006). Acute activation of ATF6 protects the heart following I/R injury by reducing necrosis and apoptosis (Jin et al., 2017), however, sustained activation of ATF6 and its pro-apoptotic target genes could have detrimental effects on the heart under pathological mechanical stress (Choi et al., 2016). A possible mechanism by which ATF6 regulates cardiac function in response to biomechanical stress is via Rheb-dependent activation of the mTORC1 signaling pathway and downstream protein synthesis (Blackwood et al., 2019). Rheb regulates mTORC1's kinase functions and activity such that when Rheb is in its active GTP-bound state it will directly interact with and activate mTORC1. Another mechanism is via regulation of ubiquitination in the stressed myocardium during compensatory and pathological hypertrophy via the ATF6 target gene *Hrd1* (Sun et al., 2015). Targeted suppression of *Hrd1 in vivo* was associated with pronounced pathological hypertrophic remodeling in response to pressure overload, whereas overexpression of *Hrd1* in the heart led to a significant repression in hypertrophy and preserved heart function under pressure overload.

Heat shock proteins and chaperones protect the heart against pathogenic misfolded and accumulated proteins occurring under biomechanical stress (Ranek et al., 2017). Heat shock protein 70 and its protein homolog, heat shock cognate 70 (HSP70 and HSC70, respectively) defend against cardiomyocyte damage by facilitating folding and transport of new proteins and protein degradation at the proteasome. In response to biomechanical stress, HSP70 expression increases in order to alleviate the increased misfolded protein burden. Animal models of inducible HSP70 expression have indicated a cardioprotective role for HSP70 in response to acute cardiac mechanical stress (Bernardo et al., 2016). Interestingly, increased HSP70 expression may only provide protection under acute mechanical stress, such as exercise or I/R, as studies using mice exposed to chronic pressure overload- induced hypertrophy demonstrated no benefit having increased expression of HSP70 (Weeks et al., 2012; Sapra et al., 2014).

Carboxyl terminus of HSC70-interacting protein (CHIP) is expressed in cardiac muscle and functions as a co-chaperone, facilitating the refolding of misfolded proteins either by itself or by mediating its co-chaperones (heat shock proteins HSP70, HS70 and HSP90) (Kettem et al., 2010). CHIP also plays a critical role in protein degradation through its ubiquitin ligase activity therefore it has an essential role in myocardial protein quality control and expression (McClellan and Frydman, 2001). While overexpression or loss of the gene encoding CHIP (*ATCHIP*) does not affect steady state heart function, manipulation of CHIP gene expression levels has profound effects on myocardial function following an increased mechanical load emphasizing the importance of cardiac CHIP levels in preserving heart function under stress (Zhang et al., 2005). CHIP gene KO mouse models exhibit adverse cardiac hypertrophy in response to either exercise or pressure overload as measured by increased cardiomyocyte size, heart weights and wall thickness (Schisler et al., 2013; Willis et al., 2013). Mice with suppressed CHIP expression and subjected to pressure overload had increased mortality rate associated with severe cardiac hypertrophy and fibrosis (Schisler et al., 2013), impaired HSP70 expression (Zhang et al., 2005) and increased mTOR signaling (Dickey et al., 2008), while mechanical stress from MI or I/R injury in CHIP KO mice causes considerably larger, more damaging infarcts and decreased survival.

MECHANICAL FORCES AND PROTEIN TRANSLATION IN VASCULAR CELLS

Vascular Smooth Muscle Cells (VSMCs)

VSMCs are the major contractile component of blood vessel walls and experience cyclic strain but are generally shielded from shear stress under physiological conditions (Wang et al., 2018). Endothelial cells (ECs) respond to their mechanical environment and crosstalk with VSMCs in order to maintain vascular tone and mediate vascular remodeling. Under stressed or pathological states where there is vessel injury, the endothelial layer is compromised or endothelial signaling is dysfunctional, such as in hypertension or atherosclerosis. Under such conditions, VSMCs are vulnerable to exposure of shear stress from blood flow or their signaling and function can change as a result of inappropriate EC activation (Scott et al., 2012; Kim et al., 2017). Pathological mechanical trauma and changes to cyclic stretch triggers VSMCs to undergo gene, protein expression and phenotypic changes. Examples of this are decreases in contractile genes such as *SM22*α and those encoding myosin light chain, and increases in cell hypertrophy, proliferation and migration (Huang et al., 1999; Feil et al., 2004; Chiu et al., 2013; Wang et al., 2018). The dysregulated proliferative VSMC phenotype is associated with cardiovascular states where the mechanical environment is perturbed such as pulmonary hypertension and atherosclerosis (Morrell et al., 2009; Bennett et al., 2016).

The mTOR signaling pathway has been shown to be activated in VSMCs in response to cyclic strain (Li et al., 2003) and has since been investigated both *in vitro* and *in vivo* in pathological hypertensive settings. Houssaini et al. induced pulmonary hypertension in rats and observed both mTORC1 and mTORC2 activation which contributed to increased pulmonary artery SMC (PASMC) growth compared to control rats. When they treated the hypertensive rats with rapamycin to inhibit mTORC1 signaling, they observed a decrease in SMC proliferation and reduced vessel remodeling (Houssaini et al., 2013). A more recent study by Tang and colleagues evaluated the contribution of mTORC1 and mTORC2 in the development and progression of pulmonary hypertension in mouse models. They functionally disrupted mTORC1 and mTORC2 specifically in SMCs by knocking out genes encoding the adaptor proteins raptor or rictor, respectively (**Figure 1**). When they disrupted mTORC1 signaling, in agreement with previous studies, they observed amelioration of SMC proliferation and therefore reduced development of

hypertension. In contrast, when they knocked out *RICTOR* and therefore interfered with mTORC2 signaling, this caused spontaneous pulmonary hypertension as a result of upregulation of platelet derived growth factor receptors (Tang et al., 2018). This therefore suggests that mTORC2 confers some protective benefit to the SMC phenotype and vascular remodeling, however, the mechanisms and signaling involved require further clarification especially as other studies have shown mTORC2 plays a key role in proliferation and survival of pulmonary artery SMCs in pulmonary arterial hypertension (Goncharov et al., 2014).

Mechanical forces can stimulate ER stress signaling in VSMCs and chronic activation of this response mediates vascular disease progression such as in atherosclerosis, hypertension and aneurysms (reviewed in Shanahan and Furmanik, 2017). Cheng et al. subjected rat aortic SMCs to cyclic stretch to mimic the hemodynamic environment found in arterial vessels. They found that the downstream target of ER stress transmembrane protein PERK, C/EBP homologous protein (CHOP), was upregulated by cyclic stretch suggesting ER stress activation (**Figure 2**; Cheng et al., 2008). Another study by Wan et al. suggested that under mechanical stress induced by hypertension, a positive feedback loop is triggered in aortic SMCs whereby increased mechanical trauma activates the ER stress response and this further exacerbates hypertension. The mechanism by which this occurs is increased splicing of the conductance Ca^{2+} voltage activated K^{+} channels which are essential for maintaining vascular tone and contractility (Wan et al., 2015). A complementary study by Liang et al. demonstrated that aberrant ER stress in VSMCs increases their contractility and as such promotes elevated blood pressure; activation of AMPK counteracted high blood pressure by reducing the effects of ER stress *in vivo* and is therefore essential for vascular homeostasis (Liang et al., 2013).

It has been established for some time that ribosomal proteins have extra-ribosomal functions beyond that of the classical biochemistry of protein translation (Wool, 1996; Graifer et al., 2014; Zhou et al., 2015). Ribosomal protein L17 (RpL17) is a component of the large 60S ribosomal subunit but has also been shown to act as a VSMC growth inhibitor. Smolock et al. were first to show that RpL17 expression is inversely correlated with VSMC growth and that *RPL17* depletion promotes VSMC proliferation using a mouse model of partial carotid ligation. This study suggested that RpL17 could therefore represent a potential therapeutic candidate for limiting VSMC proliferation during carotid intima-media thickening (Smolock et al., 2012). It remains to be further investigated how the ribosome-free ribosomal proteins are balanced or coordinated with their traditional roles in protein synthesis and ribosome biogenesis during normal cell growth and proliferation.

Endothelial Cells (ECs)

There is little study on how mechanical forces from blood flow influence EC function with regards to protein synthesis mechanisms and components of the translational machinery (ribosomes, polysomes, elongation and initiation factors, aminoacyl-tRNA synthetases) and how they could mediate general EC-shear stress responses aside from ER stress in disturbed flow settings. ECs reside in a highly dynamic mechanical microenvironment, and as such, need to be able to adapt quickly changing mechanical stimuli. Translation can occur independently of transcription, suggesting a rationale for specific force-dependent mechanisms that can regulate translation of proteins to bring about rapid cellular responses to force (Brant-Zawadzki et al., 2007). ECs are at the frontline in responding to mechanical cues which alter their activity and phenotype and influence the biologic behavior of the vessel wall i.e., contraction-dilation of blood vessels to mediate changes in blood pressure and re-direct blood flow under exercise training or times of stress (Givens and Tzima, 2016). ECs can also respond to various agonists in the circulation but mechanotransduction, the sensing of a biophysical signal which is converted into an intracellular biochemical response, is more rapid than ligand-receptor signaling (Na et al., 2008). Mechanotransduction responses in ECs involves the dynamic modification of proteins via phosphorylation/de-phosphorylation which will ultimately influence transcriptional and translational control mechanisms. While transcriptional control mechanisms require a longer timeframe to employ, separate translation-only control mechanisms allow ECs to mount a more immediate response to a change in mechanical stimuli, ensuring cell homeostasis while longer term transcriptional changes to gene expression can be put in place.

There is limited study on how fluid shear stress influences protein translation in ECs independent of changes at the transcriptome level. Kraiss et al. were first to demonstrate that fluid shear stress, in the absence of growth factors or hormones, independently activates the mTOR pathway in ECs through phosphorylation of mTOR downstream target, p70S6K (**Figure 1**). In this same study, the investigators highlighted that FSS can modulate protein expression without changing mRNA levels, again revisiting this idea of the disconnect between mRNA and protein levels as a result of translational control. The activation of p70S6K controls translation of a specific set of mRNA transcripts into protein. One of these is the protooncogene, Bcl-3, which was used in this study to detect changes in protein expression following p70S6K activation by shear stress. They found that Bcl-3 expression was rapidly induced following short-term shear stress and its upregulation was attenuated in the presence of Rapamycin but not in response to actinomycin D, suggesting that upregulation is due to translation and not transcription (Kraiss et al., 2000).

An additional study by Kraiss et al. demonstrated that fluid shear stress can modulate the protein expression of adhesion molecule, E-selectin, on the EC cell surface independent of changes to E-selectin mRNA levels. To further investigate this post-transcriptional mechanism, they recovered the polysome fractions of ECs which had been stimulated to express E-selectin and compared them with pre-stimulated ECs which had then been subjected to shear stress. Fluid shear stress markedly reduced the amount of E-selectin mRNA bound to active polysomes compared to the stimulated only ECs, which had a high level of mRNA associated with actively translating polysomes. To ensure this result was not attributed to a general

overall decrease in protein translation following shear stress, they used a radiolabeled methionine incorporation assay to measure relative global protein synthesis occurring in the flowed vs. non-flowed samples. The predominant response of ECs exposed to fluid shear stress shifted toward an overall increase in global protein synthesis compared to their static counterparts therefore indicating a specific downregulation of E-selectin expression. This suggests that the mechanical stimulus of shear stress can influence translational control and specifically control a subset of mRNAs. Interestingly, unlike with Bcl-3, the application of Rapamycin did not affect the flow-mediated response of E-selectin expression suggesting its translation is mTOR/p70S6K independent (Kraiss et al., 2003).

Other studies have examined the effects of different types of shear stress on protein translation mechanisms. Both laminar and disturbed fluid shear stress induce rapid phosphorylation of mTOR at its Serine 2448 and its downstream target p70S6K which is important for protein translation and cell growth. Activation of p70S6K persists under oscillatory shear stress but shows a transient activation following sustained exposure to laminar shear stress (Guo et al., 2007). This highlights the differential actions of different mechanical forces on protein translational signaling. Additionally, mTOR can be also be activated in response to low shear stress as shown by increased phosphorylation of downstream target 4EBP1 (Vion et al., 2017).

In addition to shear stress, pressure also regulates protein translation signaling. Rice et al. investigated pressure-induced activation of p70S6K and other protein synthesis regulators, Akt and GSK3β, in rat aortae from young and aged rats. P70S6K mediates the translation of mRNA transcripts related to cell cycle progression and the translational machinery. They found that pressure-induced phosphorylation of p70S6K and Akt-dependent GSK3β (Serine 9) was attenuated in the aged rat aorta compared to the young adult group suggesting that physiological aging elicits changes to protein synthesis and cell growth pathways (Rice et al., 2005). This study also showed that aged vessels are less compliant as aortic wall thickness increased in the aged animals. More studies are required to highlight the differential mechanisms that occur with normal aging to mechanotransduction pathways in the vasculature which may have different signaling pathways to that which occurs in vascular disease or with age.

The ER stress response, also referred to as the unfolded protein response (UPR), promotes an acute decrease in protein synthesis to ensure ER capacity can match demands of protein load (Walter and Ron, 2011). Activation of the ER stress response also leads to increased protein degradation of defective or misfolded proteins whilst augmenting synthesis of protective proteins (Glembotski, 2007). Protein misfolding is a result of increased protein synthesis, changes in protein oxidation, post-translational modifications and decreased proteasome capacity (Sun et al., 2015). In regions of disturbed flow, such as the inner curvature of the aortic arch, ER stress activates adaptive UPR signaling (see **Figure 2**; Davies et al., 2013). A study by Civelek et al., 2009 observed upregulated gene expression of *ERN1* (IRE-1) and *ATF6*, both transducers of the UPR response, in the aortic arch compared to the descending aorta. This stress response in the aortic arch could be persistently active in order to mitigate the effects of the imbalanced mechanical environment which promotes sustained protein translation and contributes to the accumulation of pathological levels of misfolded proteins. Further analysis of differential effects of shear stress on the EC ER stress response was performed by Bailey and colleagues. They subjected human aortic ECs to low and high shear stress and examined the levels of key factors involved in the ER stress response. They found that low shear stress (2 dynes/cm^2) induced high expression of eIF2α and Xbp1 and high shear stress (12 dynes/cm^2) was associated with low Xbp1 expression (Bailey et al., 2017). This data coincides with Zeng et al. who found that Xbp1 was highly expressed in areas of the vasculature which are susceptible to disturbed flow patterns e.g., branch points. In addition, there were similar high and low expression patterns in their *in vitro* studies when analyzing disturbed and laminar flow, respectively (Zeng et al., 2009).

Perspectives

The control of protein expression in the cardiovascular system is incredibly sensitive to the effects of mechanical forces. Protein translation in the heart is relatively low unless mechanical signaling increases substantially and/or is sustained which can be of a physiological or pathological nature. Endurance exercise causes increases in hemodynamic forces which, if sustained, will trigger protein synthesis mechanisms and adaptive cardiac hypertrophy to cope with increased mechanical demands. In conditions where hemodynamic forces are perturbed, such as hypertension, atherosclerosis and heart failure, dysregulated protein synthesis can contribute to worse outcomes in heart and vessel function and disease progression. These can include dysregulation of mTOR signaling or components which modulate protein translation initiation, such as eIF2α. Signaling systems such as those involved in the ER stress response are highly mechanosensitive and help to regulate protein burden in conditions of mechanical disturbance. Pharmacologic and/or genetic inhibition of protein translation pathways has been shown to extend life span in mammals and reduce cardiac remodeling and heart failure in response to increased biomechanical stress. These studies suggest that targeting of protein translation pathways, especially when they are aberrantly activated in conditions of mechanical disturbance, may represent a novel therapeutic strategy to confer cardioprotection and vessel homeostasis.

AUTHOR CONTRIBUTIONS

LS, JR, and ET wrote the review.

ACKNOWLEDGMENTS

The researchers are funded by grants from Wellcome Senior Research Fellowship 100980/C/13Z, British Heart Foundation (BHF) grant PG/16/29/32128, John Fell Fund and BBSRC (BB/T003553/1) and BHF studentship award number FS/16/59/32735.

REFERENCES

Adamo, L., Naveiras, O., Wenzel, P. L., McKinney-Freeman, S., Mack, P. J., Gracia-Sancho, J., et al. (2009). Biomechanical forces promote embryonic haematopoiesis. *Nature* 459, 1131–1135. doi: 10.1038/nature08073

Amin, S. (2010). Mechanical factors and bone health: effects of weightlessness and neurologic injury. *Curr. Rheumatol. Rep.* 12, 170–176. doi: 10.1007/s11926-010-0096-z

Anava, S., Greenbaum, A., Ben Jacob, E., Hanein, Y., and Ayali, A. (2009). The regulative role of neurite mechanical tension in network development. *Biophys. J.* 96, 1661–1670. doi: 10.1016/j.bpj.2008.10.058

Antos, C. L., McKinsey, T. A., Frey, N., Kutschke, W., McAnally, J., Shelton, J. M., et al. (2001). Activated glycogen synthase-3b suppresses cardiac hypertrophy in vivo. *Proc. Natl. Acad. Sci. U.S.A.* 99, 907–912. doi: 10.1073/pnas.231619298

Artinian, N., Cloninger, C., Holmes, B., Benavides-Serrato, A., Bashir, T., and Gera, J. (2015). Phosphorylation of the hippo pathway component AMOTL2 by the mTORC2 kinase promotes YAP signaling, resulting in enhanced glioblastoma growth and invasiveness. *J. Biol. Chem.* 290, 19387–19401. doi: 10.1074/jbc.M115.656587

Bäck, M., Gasser, T. C., Michel, J. B., and Caligiuri, G. (2013). Biomechanical factors in the biology of aortic wall and aortic valve diseases. *Cardiovasc. Res.* 99, 232–241. doi: 10.1093/cvr/cvt040

Bailey, K. A., Haj, F. G., Simon, S. I., and Passerini, A. G. (2017). Atherosusceptible shear stress activates endoplasmic reticulum stress to promote endothelial inflammation. *Sci. Rep.* 7:8196. doi: 10.1038/s41598-017-084179

Bénard, L., Oh, J. G., Cacheux, M., Lee, A., Nonmenmacher, M., Matasic, D. S., et al. (2016). Cardiac Stim1 silencing impairs adaptive hypertrophy and promotes heart failure through inactivation of mTORC2/Akt signaling. *Circulation* 133, 1458–1471. doi: 10.1161/CIRCULATIONAHA.115.020678

Bennett, M. R., Sinha, S., and Owens, G. K. (2016). Vascular smooth muscle cells in atherosclerosis. *Circ. Res.* 118, 692–702. doi: 10.1161/CIRCRESAHA.115.306361

Bernardo, B. C., Weeks, K. L., Patterson, N. L., and McMullen, J. R. (2016). HSP70: therapeutic potential in acute and chronic cardiac disease settings. *Fut. Med. Chem.* 8, 2177–2183. doi: 10.4155/fmc-2016-0192

Blackwood, E. A., Hofmann, C., Santo Domingo, M., Bilal, A. S., Sarakki, A., Stauffer, W., et al. (2019). ATF6 regulates cardiac hypertrophy by transcriptional induction of the mTORC1 activator. *Rheb. Circ. Res.* 124, 79–93. doi: 10.1161/CIRCRESAHA.118.313854

Brant-Zawadzki, P. B., Schmid, D. I., Jiang, H., Weyrich, A. S., Zimmerman, G. A., and Kraiss, L. W. (2007). Translational control in endothelial cells. *J. Vasc. Surg.* 45, A8–A14. doi: 10.1016/j.jvs.2007.02.033

Breen, E. C., Fu, Z., and Normand, H. (1999). Calcyclin gene expression is increased by mechanical strain in fibroblasts and lung. *Am. J. Respir. Cell Mol. Biol.* 21, 746–752. doi: 10.1165/ajrcmb.21.6.3312

Burgess, H. M., and Gray, N. K. (2010). mRNA-specific regulation of translation by poly(A)-binding proteins. *Biochem. Soc. Trans.* 38, 1517–1522. doi: 10.1042/BST0381517

Buss, S. J., Muenz, S., Riffel, J. H., Malekar, P., Hagenmueller, M., Weiss, C. S., et al. (2009). Beneficial effects of mammalian target of rapamycin inhibition on left ventricular remodeling after myocardial infarction. *J. Am. Coll. Cardiol.* 54, 2435–2446. doi: 10.1016/j.jacc.2009.08.031

Cheng, W. P., Hung, H. F., Wang, B. W., and Shyu, K. G. (2008). The molecular regulation of GADD153 in apoptosis of cultured vascular smooth muscle cells by cyclic mechanical stretch. *Cardiovasc. Res.* 77, 551–559. doi: 10.1093/cvr/cvm057

Chiu, C. Z., Wang, B. W., and Shyu, K. G. (2013). Effects of cyclic stretch on the molecular regulation of myocardin in rat aortic vascular smooth muscle cells. *J. Biomed. Sci.* 20:50. doi: 10.1186/1423-0127-20-50

Choi, S. K., Lim, M., Byeon, S. H., and Lee, Y. H. (2016). Inhibition of endoplasmic reticulum stress improves coronary artery function in the spontaneously hypertensive rats. *Sci. Rep.* 6:31925. doi: 10.1038/srep31925

Chorghade, S., Seimetz, J., Emmons, R., Yang, J., Bresson, S. M., Lisio, M., et al. (2017). Poly(A) tail length regulates PABPC1 expression to tune translation in the heart. *eLife* 6:e24139. doi: 10.7554/eLife.24139

Civelek, M., Manduchi, E., Riley, R. J., Stoeckert, C. J. Jr., and Davies, P. F. (2009). Chronic endoplasmic reticulum stress activates unfolded protein response in arterial endothelium in regions of susceptibility to atherosclerosis. *Circ. Res.* 105, 453–461. doi: 10.1161/CIRCRESAHA.109.203711

Clancy, S., and Brown, W. (2008). Translation: DNA to mRNA to protein. *Nat. Educ.* 1:101.

Davies, P. F. (1995). Flow-mediated endothelial mechanotransduction. *Physiol. Rev.* 75, 519–560. doi: 10.1152/physrev.1995.75.3.519

Davies, P. F., Civelek, M., Fang, Y., and Fleming, I. (2013). The atherosusceptible endothelium: endothelial phenotypes in complex haemodynamic shear stress regions in vivo. *Cardiovasc. Res.* 99, 315–327. doi: 10.1093/cvr/cvt101

Dickey, C. A., Koren, J., Zhang, Y. J., Xu, Y. F., Jinwal, U. K., Birnbaum, M. J., et al. (2008). Akt and CHIP coregulate tau degradation through coordinated interactions. *Proc. Natl. Acad. Sci. U.S.A.* 105, 3622–3627. doi: 10.1073/pnas.0709180105

Donnelly, N., Gorman, A. M., Gupta, S., and Samali, A. (2013). The eIF2α kinases: their structures and functions. *Cell Mol. Life Sci.* 70, 3493–3511. doi: 10.1007/s00018-012-1252-1256

Doroudgar, S., Völkers, M., Thuerauf, D. J., Khan, M., Mohsin, S., Respress, J. L., et al. (2015). Hrd1 and ER-associated protein degradation, ERAD, are critical elements of the adaptive ER stress response in cardiac myocytes. *Circ. Res.* 117, 536–546. doi: 10.1161/CIRCRESAHA.115.306993

Feil, S., Hofmann, F., and Feil, R. (2004). SM22alpha modulates vascular smooth muscle cell phenotype during atherogenesis. *Circ. Res.* 94, 863–865. doi: 10.1161/01.RES.0000126417.38728.F6

Felsenthal, N., and Zelzer, E. (2017). Mechanical regulation of musculoskeletal system development. *Development* 144, 4271–4283. doi: 10.1242/dev.151266

Forouhar, A. S., Liebling, M., Hickerson, A., Nasiraei-Moghaddam, A., Tsai, H. J., Hove, J. R., et al. (2006). The embryonic vertebrate heart tube is a dynamic suction pump. *Science* 312, 751–753. doi: 10.1126/science.1123775

Galderisi, M., Cardim, N., D'Andrea, A., Bruder, O., Cosyns, B., Davin, L., et al. (2015). The multi-modality cardiac imaging approach to the Athlete's heart: an expert consensus of the european association of cardiovascular imaging. *Eur. Heart J. Cardiovasc. Imaging* 16:353. doi: 10.1093/ehjci/jeu323

Gao, X. M., Wong, G., Wang, B., Kiriazis, H., Moore, X. L., Su, Y. D., et al. (2006). Inhibition of mTOR reduces chronic pressure-overload cardiac hypertrophy and fibrosis. *J. Hypertens.* 24, 1663–1670. doi: 10.1097/01.hjh.0000239304.01496.83

Garlick, P. J., McNurlan, M. A., and Preedy, V. R. (1980). A rapid and convenient technique for measuring the rate of protein synthesis in tissues by injection of [3H]phenylalanine. *Biochem. J.* 192, 719–723. doi: 10.1042/bj1920719

George, K., Whyte, G. P., Green, D. J., Oxborough, D., Shave, R. E., Gaze, D., et al. (2012). The endurance athletes heart: acute stress and chronic adaptation. *Br. J. Sports Med.* 46, i29–i36. doi: 10.1136/bjsports-2012-091141

Givens, C., and Tzima, E. (2016). Endothelial mechanosignaling: does one sensor fit all? *Antioxid. Redox Signal.* 25, 373–388. doi: 10.1089/ars.2015.6493

Glembotski, C. C. (2007). Endoplasmic reticulum stress in the heart. *Circ. Res.* 101, 975–984. doi: 10.1161/CIRCRESAHA.107.161273

Glembotski, C. C. (2014). Roles for ATF6 and the sarco/endoplasmic reticulum protein quality control system in the heart. *J. Mol. Cell Cardiol.* 71, 11–15. doi: 10.1016/j.yjmcc.2013.09.018

Goncharov, D. A., Kudryashova, T. V., Ziai, H., Ihida-Stansbury, K., DeLisser, H., Krymskaya, V. P., et al. (2014). Mammalian target of rapamycin complex 2 (mTORC2) coordinates pulmonary artery smooth muscle cell metabolism, proliferation, and survival in pulmonary arterial hypertension. *Circulation* 129, 864–874. doi: 10.1161/CIRCULATIONAHA.113.004581

Graifer, D., Malygin, A., Zharkov, D. O., and Karpova, G. (2014). Eukaryotic ribosomal protein S3: a constituent of translational machinery and an extraribosomal player in various cellular processes. *Biochimistry* 99, 8–18. doi: 10.1016/j.biochi.2013.11.001

Guo, D., Chien, S., and Shyy, J. Y. (2007). Regulation of endothelial cell cycle by laminar versus oscillatory flow - distinct modes of interactions of AMP-activated protein kinase and Akt Pathways. *Circ. Res.* 100, 564–571. doi: 10.1161/01.RES.0000259561.23876.c5

Gutierrez, J. A., Suzara, V. V., and Dobbs, L. G. (2003). Continuous mechanical contraction modulates expression of alveolar epithelial cell phenotype. *Am. J. Respir. Cell Mol. Biol.* 29, 81–87. doi: 10.1165/rcmb.2002-0135OC

Hahn, C., and Schwartz, M. A. (2009). Mechanotransduction in vascular physiology and atherogenesis. *Nat. Rev. Mol. Cell Biol.* 10, 53–62. doi: 10.1038/nrm2596

Hannan, R. D., Jenkins, A., Jenkins, A. K., and Brandenburger, Y. (2003). Cardiac hypertrophy: a matter of translation. *Clin. Exp. Pharmacol. Physiol.* 30, 517–527. doi: 10.1046/j.1440-1681.2003.03873.x

Hansen, C. G., Ng, Y. L., Lam, W. L., Plouffe, S. W., and Guan, K. L. (2015). The Hippo pathway effectors YAP and TAZ promote cell growth by modulating amino acid signaling to mTORC1. *Cell Res.* 25, 1299–1313. doi: 10.1038/cr.2015

Haq, S., Choukroun, G., Kang, Z. B., Ranu, H., Matsui, T., Rosenzweig, A., et al. (2000). Glycogen synthase kinase-3beta is a negative regulator of cardiomyocyte hypertrophy. *J. Cell Biol.* 151, 117–130. doi: 10.1083/jcb.151.1.117

Hardt, S. E., Tomita, H., Katus, H. A., and Sadoshima, J. (2004). Phosphorylation of eukaryotic translation initiation factor 2Bepsilon by glycogen synthase kinase-3beta regulates beta-adrenergic cardiac myocyte hypertrophy. *Circ. Res.* 94, 926–935. doi: 10.1161/01.RES.0000124977.59827.80

Heineke, J., and Molkentin, J. D. (2006). Regulation of cardiac hypertrophy by intracellular signalling pathways. *Nat. Rev. Mol. Cell Biol.* 7, 589–600. doi: 10.1038/nrm1983

Herum, K. M., Lunde, I. G., McCulloch, A. D., and Christensen, G. (2017). The soft- and hard-heartedness of cardiac fibroblasts: mechanotransduction signaling pathways in fibrosis of the heart. *J. Clin. Med.* 6, 53. doi: 10.3390/jcm6050053

Hocine, S., Singer, R. H., and Grunwald, D. (2010). RNA processing and export. *Cold Spring Harb. Perspect. Biol.* 2:a000752. doi: 10.1101/cshperspect.a000752

Hornberger, T. A. (2011). Mechanotransduction and the regulation of mTORC1 signaling in skeletal muscle. *Int. J. Biochem. Cell Biol.* 43, 1267–1276. doi: 10.1016/j.biocel.2011.05.007

Houssaini, A., Abid, S., Mouraret, N., Wan, F., Rideau, D., Saker, M., et al. (2013). Rapamycin reverses pulmonary artery smooth muscle cell proliferation in pulmonary hypertension. *Am. J. Respir. Cell Mol. Biol.* 48, 568–577. doi: 10.1165/rcmb.2012-0429OC

Hove, J. R., Köster, R. W., Forouhar, A. S., Acevedo-Bolton, G., Fraser, S. E., and Gharib, M. (2003). Intracardiac fluid forces are an essential epigenetic factor for embryonic cardiogenesis. *Nature* 421, 172–177. doi: 10.1038/nature01282

Huang, Q. Q., Fisher, S. A., and Brozovich, F. V. (1999). Forced expression of essential myosin light chain isoforms demonstrates their role in smooth muscle force production. *J. Biol. Chem.* 274, 35095–35098. doi: 10.1074/jbc.274.49.35095

Jaalouk, D. E., and Lammerding, J. (2009). Mechanotransduction gone awry. *Nat. Rev. Mol. Cell Biol.* 10, 63–73. doi: 10.1038/nrm2597

Jackson, R. J., Hellen, C. U., and Pestova, T. V. (2010). The mechanism of eukaryotic translation initiation and principles of its regulation. *Nat. Rev. Mol. Cell Biol.* 11, 113–127. doi: 10.1038/nrm2838

Jacobs, B. L., McNally, R. M., Kim, K. J., Blanco, R., Privett, R. E., You, J. S., et al. (2017). Identification of mechanically regulated phosphorylation sites on tuberin (TSC2) that control mechanistic target of rapamycin (mTOR) signalling. *J. Cell Biol.* 292, 6987–6997. doi: 10.1074/jbc.M117.777805

Jin, J. K., Blackwood, E. A., Azizi, K., Thuerauf, D. J., Fahem, A. G., Hofmann, C., et al. (2017). ATF6 decreases myocardial ischemia/reperfusion damage and links ER stress and oxidative stress signaling pathways in the heart. *Circ. Res.* 120, 862–875. doi: 10.1161/CIRCRESAHA.116.310266

Kahn, J., Shwartz, Y., Blitz, E., Krief, S., Sharir, A., Breitel, D. A., et al. (2009). Muscle contraction is necessary to maintain joint progenitor cell fate. *Dev. Cell.* 16, 734–743. doi: 10.1016/j.devcel.2009.04.013

Katz, Z. B., Wells, A. L., Park, H. Y., Wu, B., Shenoy, S. M., and Singer, R. H. (2012). β-Actin mRNA compartmentalization enhances focal adhesion stability and directs cell migration. *Genes Dev.* 26, 1885–1890. doi: 10.1101/gad.190413.112

Kettem, N., Dreiseidler, M., Tawo, R., and Höhfeld, J. (2010). Chaperone-assisted degradation: multiple paths to destruction. *Biol. Chem.* 391, 481–489. doi: 10.1515/BC.2010.058

Kim, S. A., Sung, J. Y., Woo, C. H., and Choi, H. C. (2017). Laminar shear stress suppresses vascular smooth muscle cell proliferation through nitric oxide-AMPK pathway. *Biochem. Biophys. Res. Commun.* 490, 1369–1374. doi: 10.1016/j.bbrc.2017.07.033

Kini, H. K., Silverman, I. M., Ji, X., Gregory, B. D., and Liebhaber, S. A. (2016). Cytoplasmic poly(A) binding protein-1 binds to genomically encoded sequences within mammalian mRNAs. *RNA* 22, 61–74. doi: 10.1261/rna.053447.115

Kohrt, W. M., Barry, D. W., and Schwartz, R. S. (2009). Muscle forces or gravity: what predominates mechanical loading on bone? *Med. Sci. Sports Exerc.* 41, 2050–2055. doi: 10.1249/MSS.0b013e3181a8c717

Kraiss, L. W., Alto, N. M., Dixon, D. A., McIntyre, T. M., Weyrich, A. S., and Zimmerman, G. A. (2003). Fluid flow regulates E-selectin protein levels in human endothelial cells by inhibiting translation. *J. Vasc. Surg.* 37, 161–168. doi: 10.1067/mva.2003.67

Kraiss, L. W., Weyrich, A. S., Alto, N. M., Dixon, D. A., Ennis, T. M., Modur, V., et al. (2000). Fluid flow activates a regulator of translation, p70/p85 S6 kinase, in human endothelial cells. *Am. J. Physiol. Heart Circ. Physiol.* 278, H1537–H1544. doi: 10.1152/ajpheart.2000.278.5.H1537

La Gerche, A., Burns, A. T., Mooney, D. J., Inder, W. J., Taylor, A. J., Bogaert, J., et al. (2012). Exercise-induced right ventricular dysfunction and structural remodelling in endurance athletes. *Eur. Heart J.* 33, 998–1006. doi: 10.1093/eurheartj/ehr397

Laplante, M., and Sabatini, D. M. (2012). mTOR signaling in growth control and disease. *Cell* 149, 274–293. doi: 10.1016/j.cell.2012.03.017

LeBlanc, A. D., Spector, E. R., Evans, H. J., and Sibonga, J. D. (2007). Skeletal responses to space flight and the bed rest analog: a review. *J. Musculoskelet. Neuronal. Interact.* 7, 33–47.

LeGoff, L., and Lecuit, T. (2016). Mechanical forces and growth in animal tissues. *Cold Spring Harb. Perspect. Biol.* 8:a019232. doi: 10.1101/cshperspect.a019232

Li, W., Chen, Q., Mills, I., and Sumpio, B. E. (2003). Involvement of S6 kinase and p38 mitogen activated protein kinase pathways in strain-induced alignment and proliferation of bovine aortic smooth muscle cells. *J. Cell Physiol.* 195, 202–209. doi: 10.1002/jcp.10230

Liang, B., Wang, S., Wang, Q., Zhang, W., Viollet, B., Zhu, Y., et al. (2013). Aberrant endoplasmic reticulum stress in vascular smooth muscle increases vascular contractility and blood pressure in mice deficient of AMP-activated protein kinase-α2 in vivo. *Arterioscler. Thromb. Vasc. Biol.* 33, 595–604. doi: 10.1161/ATVBAHA.112.300606

Liu, X., Kwak, D., Lu, Z., Xu, X., Fassett, J., Wang, H., et al. (2014). Endoplasmic reticulum stress sensor PERK protects against pressure overload induced heart failure and lung remodelling. *Hypertension* 64, 738–744. doi: 10.1161/HYPERTENSIONAHA.114.03811

Lu, Z., Xu, X., Fassett, J., Kwak, D., Liu, X., Hu, X., et al. (2014). Loss of the eukaryotic initiation factor 2α kinase general control nonderepressible 2 protects mice from pressure overload–induced congestive heart failure without affecting ventricular hypertrophy. *Hypertension* 63, 128–135. doi: 10.1161/HYPERTENSIONAHA.113.02313

Lucitti, J. L., Jones, E. A., Huang, C., Chen, J., Fraser, S. E., and Dickinson, M. E. (2007). Vascular remodeling of the mouse yolk sac requires hemodynamic force. *Development* 134, 3317–3326. doi: 10.1242/dev.02883

Lyon, R. C., Zanella, F., Omens, J. H., and Sheikh, F. (2015). Mechanotransduction in cardiac hypertrophy and failure. *Circ. Res.* 116, 1462–1476. doi: 10.1161/CIRCRESAHA.116.304937

Mammoto, T., and Ingber, D. E. (2010). Mechanical control of tissue and organ development. *Development* 137, 1407–1420. doi: 10.1242/dev.024166

Martindale, J. J., Fernandez, R., Thuerauf, D., Whittaker, R., Gude, N., Sussman, M. A., et al. (2006). Endoplasmic reticulum stress gene induction and protection from ischemia/reperfusion injury in the hearts of transgenic mice with a tamoxifen-regulated form of ATF6. *Circ. Res.* 98, 1186–1193. doi: 10.1161/01.RES.0000220643.65941.8d

McClellan, A. J., and Frydman, J. (2001). Molecular chaperones and the art of recognizing a lost cause. *Nat. Cell Biol.* 3, E51–E53. doi: 10.1038/35055162

McMullen, J. R., Sherwood, M. C., Tarnavski, O., Zhang, L., Dorfman, A. L., Shioi, T., et al. (2004). Inhibition of mTOR signaling with rapamycin regresses established cardiac hypertrophy induced by pressure overload. *Circulation* 109, 3050–3055. doi: 10.1161/01.CIR.0000130641.08705.45

Meng, Z., Moroishi, T., and Guan, K. L. (2016). Mechanisms of hippo pathway regulation. *Genes Dev.* 30, 1–17. doi: 10.1101/gad.274027.115

Merino, D., Gil, A., Gómez, J., Ruiz, L., Llano, M., García, R., et al. (2018). Experimental modelling of cardiac pressure overload hypertrophy: modified technique for precise, reproducible, safe and easy aortic arch banding-debanding in mice. *Sci. Rep.* 8:3167. doi: 10.1038/s41598-018-21548-x

Morrell, N. W., Adnot, S., Archer, S. L., Dupuis, J., Jones, P. L., MacLean, M. R., et al. (2009). Cellular and molecular basis of pulmonary arterial hypertension. *J. Am. Coll. Cardiol.* 54, S20–S31. doi: 10.1016/j.jacc.2009.04.018

Na, S., Collin, O., Chowdhury, F., Tay, B., Ouyang, M., Wang, Y., et al. (2008). Rapid signal transduction in living cells is a unique feature of

mechanotransduction. *Proc. Natl. Acad. Sci. U.S.A.* 105, 6626–6631. doi: 10.1073/pnas.0711704105

Nesbitt, W. S., Westein, E., Tovar-Lopez, F. J., Tolouei, E., Mitchell, A., Fu, J., et al. (2009). A shear gradient–dependent platelet aggregation mechanism drives thrombus formation. *Nat. Med.* 15, 665–673. doi: 10.1038/nm.1955

North, T. E., Goessling, W., Peeters, M., Li, P., Ceol, C., Lord, A. M., et al. (2009). Hematopoietic stem cell development is dependent on blood flow. *Cell* 137, 736–748. doi: 10.1016/j.cell.2009.04.023

Paradis, A. N., Gay, M. S., and Zhang, L. (2014). Binucleation of cardiomyocytes: the transition from a proliferative to a terminally differentiated state. *Drug Discov. Today.* 19, 602–609. doi: 10.1016/j.drudis.2013.10.019

Philip, A., Hamilton, D. L., and Baar, K. (2011). Signals mediating skeletal muscle remodeling by resistance exercise: PI3-kinase independent activation of mTORC1. *J. Appl. Physiol.* 110, 561–568. doi: 10.1152/japplphysiol.00941.2010

Ranek, M. J., Stachowski, M. J., Kirk, J. A., and Willis, M. S. (2017). The role of heat shock proteins and co-chaperones in heart failure. *Philos. Trans. R. Soc. Lond. B Biol. Sci.* 373:20160530. doi: 10.1098/rstb.2016.0530

Rice, K. M., Kinnard, R. S., Wright, G. L., and Blough, E. R. (2005). Aging alters vascular mechanotransduction: pressure-induced regulation of p70S6k in the rat aorta. *Mech. Age. Dev.* 126, 1213–1222. doi: 10.1016/j.mad.2005.07.001

Rockman, H. A., Ross, R. S., Harris, A. N., Knowlton, K. U., Steinhelper, M. E., Field, L. J., et al. (1991). Segregation of atrial-specific and inducible expression of an atrial natriuretic factor transgene in an in vivo murine model of cardiac hypertrophy. *Proc. Natl. Acad. Sci. U.S.A.* 88, 8277–8281. doi: 10.1073/pnas.88.18.8277

Sapra, G., Tham, Y. K., Cemerlang, N., Matsumoto, A., Kiriazis, H., Bernardo, B. C., et al. (2014). The small-molecule BGP-15 protects against heart failure and atrial fibrillation in mice. *Nat. Commun.* 5:5705. doi: 10.1038/ncomms6705

Schisler, J. C., Rubel, C. E., Zhang, C., Lockyer, P., Cyr, D. M., and Patterson, C. (2013). CHIP protects against cardiac pressure overload through regulation of AMPK. *J. Clin. Invest.* 123, 3588–3599. doi: 10.1172/JCI69080

Sciarretta, S., Forte, M., Frati, G., and Sadoshima, J. (2018). New insights into the role of mTOR signaling in the cardiovascular system. *Circ. Res.* 122, 489–505. doi: 10.1161/CIRCRESAHA.117.311147

Sciarretta, S., Volpe, M., and Sadoshima, J. (2014). Mammalian target of rapamycin signaling in cardiac physiology and disease. *Circ. Res.* 114, 549–564. doi: 10.1161/CIRCRESAHA.114.302022

Sciarretta, S., Zhai, P., Maejima, Y., Del Re, D. P., Nagarajan, N., Yee, D., et al. (2015). mTORC2 regulates cardiac response to stress by inhibiting MST1. *Cell Rep.* 11, 125–136. doi: 10.1016/j.celrep.2015.03.010

Scott, D., Tan, Y., Shandas, R., Stenmark, K. R., and Tan, W. (2012). High pulsatility flow stimulates smooth muscle cell hypertrophy and contractile protein expression. *Am. J. Physiol. Lung Cell Mol. Physiol.* 304, L70–L81. doi: 10.1152/ajplung.00342.2012

Shanahan, C. M., and Furmanik, M. (2017). Endoplasmic reticulum stress in arterial smooth muscle cells: a novel regulator of vascular disease. *Curr. Cardiol. Rev.* 13, 94–105. doi: 10.2174/1573403X12666161014094738

Shen, W. H., Chen, Z., Shi, S., Chen, H., Zhu, W., Penner, A., et al. (2008). Cardiac restricted overexpression of kinase-dead mammalian target of rapamycin (mTOR) mutant impairs the mTOR-mediated signaling and cardiac function. *J. Biol. Chem.* 283, 13842–13849. doi: 10.1074/jbc.M801510200

Shende, P., Plaisance, I., Morandi, C., Pellieux, C., Berthonneche, C., Zorzato, F., et al. (2011). Cardiac raptor ablation impairs adaptive hypertrophy, alters metabolic gene expression, and causes heart failure in mice. *Circulation* 123, 1073–1082. doi: 10.1161/CIRCULATIONAHA.110.977066

Shende, P., Xu, L., Morandi, C., Pentassuglia, L., Heim, P., Lebboukh, S., et al. (2016). Cardiac mTOR complex 2 preserves ventricular function in pressure-overload hypertrophy. *Cardiovasc. Res.* 109, 103–114. doi: 10.1093/cvr/cvv252

Shin, S., Wolgamott, L., Yu, Y., Blenis, J., and Toon, S. O. (2011). Glycogen synthase kinase (GSK)-3 promotes p70 ribosomal protein S6 kinase (p70S6K) activity and cell proliferation. *Proc. Natl. Acad. Sci. U.S.A.* 108, E1204–E1213. doi: 10.1073/pnas.1110195108

Shioi, T., McMullen, J. R., Tarnavski, O., Converso, K., Sherwood, M. C., Manning, W. J., et al. (2003). Rapamycin attenuates load-induced cardiac hypertrophy in mice. *Circulation* 107, 1664–1670. doi: 10.1161/01.CIR.0000057979.36322.88

Smolock, E. M., Korshunov, V. A., Glazko, G., Qiu, X., Gerloff, J., and Berk, B. C. (2012). Ribosomal protein L17, RpL17, is an inhibitor of vascular smooth muscle growth and carotid intima formation. *Circulation* 126, 2418–2427. doi: 10.1161/CIRCULATIONAHA.112.125971

Soesanto, W., Lin, H. Y., Hu, E., Lefler, S., Litwin, S. E., Sena, S., et al. (2009). Mammalian target of rapamycin is a critical regulator of cardiac hypertrophy in spontaneously hypertensive rats. *Hypertension* 54, 1321–1327. doi: 10.1161/HYPERTENSIONAHA

Sonenberg, N., and Hinnebusch, A. G. (2009). Regulation of translation initiation in eukaryotes: mechanisms and biological targets. *Cell*136, 731–745. doi: 10.1016/j.cell.2009.01.042

Spriggs, K. A., Bushell, M., and Willis, A. E. (2010). Translational regulation of gene expression during conditions of cell stress. *Mol. Cell* 40, 228–237. doi: 10.1016/j.molcel.2010.09.028

Stokes, I. A., Mente, P. L., Iatridis, J. C., Farnum, C. E., and Aronsson, D. D. (2002). Enlargement of growth plate chondrocytes modulated by sustained mechanical loading. *J. Bone Joint Surg. Am.* 84, 1842–1848. doi: 10.2106/00004623-200210000-200210016

Sun, H., Gao, C., and Wang, Y. (2015). A h(a)rd way to adapt in cardiac hypertrophy. *Circ. Res.* 117, 484–486. doi: 10.1161/CIRCRESAHA.115.307164

Tang, H., Wu, K., Wang, J., Vinjamuri, S., Gu, Y., Song, S., et al. (2018). Pathogenic role of mTORC1 and mTORC2 in pulmonary hypertension. *JACC Basic Transl. Sci.* 3, 744–762. doi: 10.1016/j.jacbts.2018.08.009

Tang, Z., Wang, X., Huang, J., Zhou, X., Xie, H., Zhu, Q., et al. (2016). Gene expression profiling of pulmonary artery in a rabbit model of pulmonary thromboembolism. *PLoS One* 11:e0164530. doi: 10.1371/journal.pone.0164530

van Putten, S., Shafieyan, Y., and Hinz, B. (2016). Mechanical control of cardiac myofibroblasts. *J. Mol. Cell Cardiol.* 93, 133–142. doi: 10.1016/j.yjmcc.2015.11.025

Vion, A. C., Kheloufi, M., Hammoutene, A., Poisson, J., Lasselin, J., Devue, C., et al. (2017). Autophagy is required for endothelial cell alignment and atheroprotection under physiological blood flow. *Proc. Natl. Acad. Sci. U.S.A.* 114, E8675–E8684. doi: 10.1073/pnas.1702223114

Völkers, M., Konstandin, M. H., Doroudgar, S., Toko, H., Quijada, P., Din, S., et al. (2013a). Mechanistic target of rapamycin complex 2 protects the heart from ischemic damage. *Circulation* 128, 2132–2144. doi: 10.1161/CIRCULATIONAHA.113.003638

Völkers, M., Toko, H., Doroudgar, S., Din, S., Quijada, P., Joyo, A. Y., et al. (2013b). Pathological hypertrophy amelioration by PRAS40-mediated inhibition of mTORC1. *Proc. Natl. Acad. Sci. U.S.A.* 110, 12661–12666. doi: 10.1073/pnas.1301455110

Voorhees, A. P., and Han, H. C. (2015). Biomechanics of cardiac function. *Compr. Physiol.* 5, 1623–1644. doi: 10.1002/cphy.c140070

Walter, P., and Ron, D. (2011). The unfolded protein response: from stress pathway to homeostatic regulation. *Science* 334, 1081–1086. doi: 10.1126/science.1209038

Wan, X. J., Zhao, H. C., Zhang, P., Huo, B., Shen, B. R., Yan, Z. Q., et al. (2015). Involvement of BK channel in differentiation of vascular smooth muscle cells induced by mechanical stretch. *Int. J. Biochem. Cell Biol.* 59, 21–29. doi: 10.1016/j.biocel.2014.11.011

Wang, H., Xu, X., Fassett, J., Kwak, D., Liu, X., Hu, X., et al. (2014). Double-stranded rna–dependent protein kinase deficiency protects the heart from systolic overload-induced congestive heart failure. *Circulation* 129, 1397–1406. doi: 10.1161/CIRCULATIONAHA.113.002209

Wang, Y., Cao, W., Cui, J., Yu, Y., Zhao, Y., Shi, J., et al. (2018). Arterial wall stress induces phenotypic switching of arterial smooth muscle cells in vascular remodeling by activating the YAP/TAZ signaling pathway. *Cell Physiol. Biochem.* 51, 842–853. doi: 10.1159/000495376

Weeks, K. L., Gao, X., Du, X. J., Boey, E. J., Matsumoto, A., Bernardo, B. C., et al. (2012). Phosphoinositide 3-kinase p110a is a master regulator of exercise induced cardioprotection and PI3K gene therapy rescues cardiac dysfunction. *Circ. Heart Fail.* 5, 523–534. doi: 10.1161/CIRCHEARTFAILURE.112.966622

Willis, M. S., Min, J. N., Wang, S., McDonough, H., Lockyer, P., Wadosky, K. M., et al. (2013). Carboxyl terminus of Hsp70-interacting protein (CHIP) is required to modulate cardiac hypertrophy and attenuate autophagy during exercise. *Cell Biochem. Funct.* 31, 724–735. doi: 10.1002/cbf.2962

Wirtz, H. R., and Dobbs, L. G. (2000). The effects of mechanical forces on lung functions. *Respir. Physiol.* 119, 1–17. doi: 10.1016/s0034-5687(99)00092-94

Wool, I. G. (1996). Extraribosomal functions of ribosomal proteins. *Trends Biochem. Sci.* 21, 164–165. doi: 10.1016/s0968-0004(96)20011-8

Zeng, L., Zampetaki, A., Margariti, A., Pepe, A. E., Alam, S., Martin, D., et al. (2009). Sustained activation of XBP1 splicing leads to endothelial apoptosis and atherosclerosis development in response to disturbed flow. *Proc. Natl. Acad. Sci. U.S.A.* 106, 8326–8331. doi: 10.1073/pnas.0903197106

Zhang, C., Xu, Z., He, X. R., Michael, L. H., and Patterson, C. (2005). CHIP, a cochaperone/ubiquitin ligase that regulates protein quality control, is required for maximal cardioprotection after myocardial infarction in mice. *Am. J. Physiol. Heart Circ. Physiol.* 288, H2836–H8342. doi: 10.1152/ajpheart.01122.2004

Zhang, D., Contu, R., Latronico, M. V., Zhang, J., Rizzi, R., Catalucci, D., et al. (2010). MTORC1 regulates cardiac function and myocyte survival through 4E-BP1 inhibition in mice. *J. Clin Invest.* 120, 2805–2816. doi: 10.1172/JCI43008

Zhou, X., Liao, W. J., Liao, J. M., Liao, P., and Lu, H. (2015). Ribosomal proteins: functions beyond the ribosome. *J. Mol. Cell Biol.* 7, 92–104. doi: 10.1093/jmcb/mjv014

Conflict of Interest: The authors declare that the research was conducted in the absence of any commercial or financial relationships that could be construed as a potential conflict of interest.

Copyright © 2020 Simpson, Reader and Tzima. This is an open-access article distributed under the terms of the Creative Commons Attribution License (CC BY). The use, distribution or reproduction in other forums is permitted, provided the original author(s) and the copyright owner(s) are credited and that the original publication in this journal is cited, in accordance with accepted academic practice. No use, distribution or reproduction is permitted which does not comply with these terms.

frontiers in Cell and Developmental Biology

REVIEW
published: 25 May 2020
doi: 10.3389/fcell.2020.00334

When Stiffness Matters: Mechanosensing in Heart Development and Disease

Roberto Gaetani[1,2], Eric Adriano Zizzi[3], Marco Agostino Deriu[3], Umberto Morbiducci[3], Maurizio Pesce[4] and Elisa Messina[5]**

[1] Department of Molecular Medicine, Faculty of Pharmacy and Medicine, Sapienza University of Rome, Rome, Italy, [2] Department of Bioengineering, Sanford Consortium for Regenerative Medicine, University of California, San Diego, San Diego, CA, United States, [3] PolitoBIOMed Lab, Department of Mechanical and Aerospace Engineering, Politecnico di Torino, Turin, Italy, [4] Tissue Engineering Research Unit, "Centro Cardiologico Monzino," IRCCS, Milan, Italy, [5] Department of Maternal, Infantile, and Urological Sciences, "Umberto I" Hospital, Sapienza University of Rome, Rome, Italy

During embryonic morphogenesis, the heart undergoes a complex series of cellular phenotypic maturations (e.g., transition of myocytes from proliferative to quiescent or maturation of the contractile apparatus), and this involves stiffening of the extracellular matrix (ECM) acting in concert with morphogenetic signals. The maladaptive remodeling of the myocardium, one of the processes involved in determination of heart failure, also involves mechanical cues, with a progressive stiffening of the tissue that produces cellular mechanical damage, inflammation, and ultimately myocardial fibrosis. The assessment of the biomechanical dependence of the molecular machinery (in myocardial and non-myocardial cells) is therefore essential to contextualize the maturation of the cardiac tissue at early stages and understand its pathologic evolution in aging. Because systems to perform multiscale modeling of cellular and tissue mechanics have been developed, it appears particularly novel to design integrated mechano-molecular models of heart development and disease to be tested in *ex vivo* reconstituted cells/tissue-mimicking conditions. In the present contribution, we will discuss the latest implication of mechanosensing in heart development and pathology, describe the most recent models of cell/tissue mechanics, and delineate novel strategies to target the consequences of heart failure with personalized approaches based on tissue engineering and induced pluripotent stem cell (iPSC) technologies.

Keywords: cardiac regeneration, mechanosensing and regulation, cardiac tissue engineering, tissue modeling, stiffness

OPEN ACCESS

Edited by:
Selwin K. Wu, National University of Singapore, Singapore

Reviewed by:
Adam Keen, University of Oxford, United Kingdom
Miguel Angel Del Pozo, Spanish National Centre for Cardiovascular Research, Spain

****Correspondence:***
Roberto Gaetani
roberto.gaetani@uniroma1.it
Elisa Messina
elisa.messina@uniroma1.it

Specialty section:
This article was submitted to Signaling, a section of the journal Frontiers in Cell and Developmental Biology

Received: *24 December 2019*
Accepted: *16 April 2020*
Published: *25 May 2020*

Citation:
Gaetani R, Zizzi EA, Deriu MA, Morbiducci U, Pesce M and Messina E (2020) When Stiffness Matters: Mechanosensing in Heart Development and Disease. Front. Cell Dev. Biol. 8:334. doi: 10.3389/fcell.2020.00334

INTRODUCTION

In recent years, the assessment of biomechanical-dependent molecular machinery has become a new insightful approach to decipher cellular dynamics inside tissues, with implications in morphogenesis, tissue renewal, and pathology progression. For example, mechanical-dependent coordination of tissue growth is one of the major determinants in either preimplantation or postimplantation embryonic patterning (Bredov and Volodyaev, 2018), as well as in pathologic evolution such as cancer (Papalazarou et al., 2018). Moreover, progenitor cells differentiation has been directly linked to compliance of the extracellular matrix (ECM) (Engler et al., 2006) or

to the topography and characteristics of the substrate in which they are cultured. Similarly, when cells are confined onto geometrically defined adhesions surfaces (McBeath et al., 2004; Nelson et al., 2005), aligned in specific patterns onto microgrooved structures (Downing et al., 2013), or exposed to cyclic strain (Ugolini et al., 2016), mechanical stress sensed by the cytoskeleton results in a broad variety of cellular responses such as differentiation, proliferation, or maturation. However, what links mechanical stimuli to cell biology and how mechanical pathways are transduced inside the cell to activate proliferation and/or alternative differentiation pathways are still not fully understood. A greater discernment of these mechanisms is of fundamental importance in order to better understand the development and progression of various cardiac diseases in which a dysregulation of the mechanosensing-mediated pathways are involved. Similarly, it is now evident that the same molecular mechanisms are also involved in the maturation of a functional tissue, both *in vitro* and *in vivo*. They should be further considered when trying to engineer and develop *in vitro* new cardiac tissue, for both regenerative medicine and research applications. In this review, we will address the latest implication of mechanosensing in heart development and pathology, describe the most recent models of cell/tissue mechanics, and delineate novel strategies to target the consequences of heart failure with personalized approaches based on tissue engineering and induced pluripotent stem cell (iPSC) technologies.

CELL MECHANICS AND HEART DEVELOPMENT/DISEASE

From Cytoskeleton Tensioning to Mechanical Sensing and Gene Expression Programming

Mechanical cues are converted into biochemical stimuli by connections established between the cytoskeleton [a network of protein filaments composed of microtubules (MTs), microfilaments (MFs), and intermediate filaments (IFs) involved in many cellular functions because of their role in, e.g., cell shaping, migration, and intracellular architecture conditioning] and the external ECM through focal adhesion contacts and multi-protein structures connecting the actin bundles to the ECM. Among all the proteins present in focal adhesions, integrins are transmembrane heterodimeric receptors, composed of α and β subunits, which bind to the ECM and activate different signal transduction within the cells. Similar to receptor–ligand interactions, mechanical signaling originates from receptor-mediated nucleation of adhesions structures, and further organization of intracellular cytoskeleton with consequent force generation (from intracellular or external stimuli) and intracellular mechanical transduction (Burridge and Wittchen, 2013; Brouhard and Rice, 2018). Downstream of mechanical activation (e.g., increasing force generation by cells attached to substrates with increasing stiffness) is the activation of gene transcription signaling that may have consequences for alternative differentiation of cells with progenitor characteristics. Typical is the example of mesenchymal cells that were shown to differentiate into adipose or osteogenic cells depending on the compliance of the ECM (Engler et al., 2006). This differentiation process occurs by engaging signaling cascades, for example, the so-called Hippo pathway (Piccolo et al., 2014), whose activity is directly dependent on the tension of the cytoskeleton, determining the reversible nuclear translocation of the Yes-associated protein and transcriptional activator with PDZ-binding motif (YAP/TAZ) transcription complex (Dobrokhotov et al., 2018; Dasgupta and McCollum, 2019; Pocaterra et al., 2020).

Mechanical signaling may also determine longer time effects and permanent programming of cell phenotype through specific setting of the epigenome. For example, experiments performed with hydrogels with defined compliance showed that exposure to a stiff three-dimensional (3D) environment modifies permanently gene expression with permanently established "mechanical memory" effects (Yang et al., 2014) that cannot be reversed even by shifting cells into an environment with higher compliance. In line with these evidences, it was observed that forcing cells to acquire specific geometries determines permanent changes in epigenetic marks that likely translate in long-term gene activation/repression at the chromatin level (Downing et al., 2013).

The link between intracellular mechanical signaling and permanent epigenetic changes may depend on the direct effects that generation of intracellular forces has on the opening and closing of the nuclear pores and the accessibility of the chromatin to transcriptional machineries due to long-range interactions with proteins of the nuclear envelope. For example, it was recently observed that connection of the contractile cytoskeleton to the nuclear lamina is important to promote nuclear straining and translocation of the YAP/TAZ complex by physical opening of the nuclear pores independently of the Hippo signaling (Elosegui-Artola et al., 2017; Lomakin et al., 2017). The structure of the chromatin may itself result from generation of intracellular forces due to peculiar conformation of the surrounding environment. For example, confinement of cells into specific geometric patterns resulted in topological chromatin rearrangement due to force-dependent distribution of epigenetically active enzymes [e.g., histone deacetylases (HDACs)], and this may cause permanent opening/compaction of the chromatin in specific gene loci (Jain et al., 2013). This intriguing possibility seems to be linked to the association existing between chromatin and components of the nuclear envelope (e.g., lamins), which, other than a structural function in the nucleus, may also have mechanical transduction and topological insulation functions (Stephens et al., 2018). Recently, Cho et al. (2019) demonstrated that nuclear lamina regulates and reduces the nuclear rupture and leak of DNA repair factors, suggesting a role of the nuclear lamina as a "cushion" potentially protecting from cytoskeleton-dependent nuclear mechanical stress. Together, these evidences support an integration of mechanical forces into the wider control mechanism of cell identity and function and establish

spatial and mechanical criteria for correct tissue development and homeostasis.

Mechanosensitive Control of Heart Development and Growth

Biophysical regulation of chromatin organization appears to be important also in lineage specification and pathway activation from the earliest stages of embryonic development. For example, it has been hypothesized that nuclear translocation of the YAP/TAZ transcriptional complex in response to straining of the cells outside the forming blastocysts may establish the first separation between the embryonic and extraembryonic lineages in preimplantation mammalian embryos (Nishioka et al., 2009; Biggins et al., 2015). On the other hand, cell-to-cell contacts in the inner cells activate the Hippo pathway resulting in the phosphorylation and inactivation of the YAP/TAZ, thus preventing the translocation into the nuclei and allowing pluripotency markers to be expressed (Nishioka et al., 2009; Biggins et al., 2015). This straining effect is likely related to the establishment of the apical domain of the presumptive trophectodermal cells, resulting in molecular determination of the first extraembryonic lineage by cell positioning outside the forming blastocyst and induction of pluripotency in its interior domain (Korotkevich et al., 2017).

Development of the heart is one of the first morphogenetic events occurring in the developing embryos with a complex series of cell migrations and phenotypic transformations also involving mechanical cues. Although we redirect to more specific reports describing the various lineages contributing to the formation of the heart (Meilhac and Buckingham, 2018), it is important to highlight that the origin of the coordinated heartbeat arising in the cardiac tube before its primary looping may have a pure mechanical basis rather than an electromechanical basis. This hypothesis emerges from studies showing that perturbations of mechanosensitive Ca^{2+} channels expressed by cardiac progenitors (Tyser et al., 2016) are determined by a progressive increase in the matrix stiffness leading to a coordinated beating of the newly differentiated myocardial cells (Majkut et al., 2013, Majkut et al., 2014; Chiou et al., 2016) before the onset of electromechanical coupling.

Mechanical cues seem to be profoundly involved in controlling myocyte proliferation and hypertrophy after birth. At this stage, a dramatic increase in the pumping efficiency of the heart is necessary to compensate cessation of the embryonic shunts redirecting circulation of the oxygenated blood from the placenta to the lungs, and the transition from a quasi-zero to a normal gravity level (Kennedy-Lydon and Rosenthal, 2017). The increase in mechanical performance requires a structural and functional maturation of the myocytes, with the conversion from the fetal to the adult structure of the sarcomeres (Ehler, 2016), a change in shape from polygonal to rod-like, and a sudden reduction of their proliferation with an increase in their volume. In parallel, sequestering of YAP by the dystrophin/dystroglycan complex (DGC) due to Hippo pathway-dependent phosphorylation acts as a negative feedback loop preventing further myocyte proliferation (Morikawa et al., 2017). Mechanical maturation of the heart, finally, does not only involve maturation of the contractile cell mass. In fact, the cardiac matrix undergoes a significant stiffening from a value <0.2 kPa (Young modulus) of the cardiac tube, to a value >20 kPa at birth (Majkut et al., 2013, Majkut et al., 2014; Chiou et al., 2016), when it reaches its physiological stiffness. Interestingly, a coordinated control of cardiac myosin expression in myocytes and collagen I deposition by cardiac fibroblasts (CFs) orchestrates maturation of the tissue, preparing it for the increase in mechanical load occurring at birth (Majkut et al., 2014). The connection of myocytes to the surrounding matrix through costameres establish a very sensitive feedback mechanism controlling mitotic block other than cellular mechanical integrity (Sessions and Engler, 2016), and perturbation of this system could be amenable to induce cardiac regeneration. In line with this hypothesis, it was observed that administration of Agrin, a specific component, in the neonatal cardiac matrix promotes dissociation of YAP from the DGC complex and myocyte cell cycle re-entry (Bassat et al., 2017). Because administration of drugs with a matrix softening activity prolongs the cardiac regeneration period in neonatal mice (Notari et al., 2018), it is tempting to speculate that modulating mechanical properties of the myocardial matrix could be a viable strategy to promote heart regeneration in adulthood.

CELL AND TISSUE LEVEL MECHANICAL MODELING: MOLECULAR AND SUBCELLULAR LEVEL MODELING

The pathways of mechanotransduction, that is, the cascade of events originating from mechanical cues eventually leading to biological responses, are known to differ considerably both between different cellular phenotypes and between distinct mechanical stimuli (Omens, 1998; Humphrey, 2001). Historically, the molecular players of mechanotransduction were categorized into the following groups (Ingber, 1997): (1) mechanical-signal-responding ion channels, (2) integrin receptors, (3) protein complexes linking the integrin receptors to the cytoskeleton, and (4) cytoskeleton components, that is, MTs, IFs, and actin MFs. Each one of these players, synergistically and sequentially involved in transmitting mechanical signals from the ECM to the inside of the cell, has benefited from new insights provided by computational theories at various length scales and timescales. Among these theories, computational molecular modeling has gained great momentum in the past 20 years, as a theoretical set of methodologies able to predict conformational and thermodynamic properties of biological building blocks and macromolecular super-assemblies by means of models characterized by atomic or quasi-atomic resolution. In this context, molecular dynamics (MD) simulations have been widely used in the last decades to obtain new insights into biological functions of proteins by studying such molecular systems at the atomistic level (Soncini et al., 2007; Lepre et al., 2017; Grasso et al., 2018, 2019a,b). After McCammon et al. (1977) investigated the dynamic behavior of small proteins on the basis of MD simulations, the method was widely employed for helping experimental design and data rationalization, with

the drawback of an accessible timescale in the order of several hundreds of nanoseconds up to a microsecond (Abraham et al., 2015; Hollingsworth and Dror, 2018), in contrast with the generally much larger timescale encompassing protein function (nanoseconds up to seconds). As a matter of fact, the choice of the proper computational simulation approach is usually related to the timescale to be investigated, the size of the molecular system, and also the properties under investigation. The mechanics of large protein structures is still computationally inaccessible by all-atom MD (AAMD), which, as the name suggests, is based on the explicit modeling of all atoms of the simulated system and all the bonded and non-bonded interactions thereof. Thus, researchers working in the field tried to develop simulation approaches requiring less computational power (Chu and Voth, 2005, 2006, 2007; Marrink et al., 2007; Monticelli et al., 2008; Pfaendtner et al., 2010; Deriu et al., 2012; Bidone et al., 2015). Some of these methods are based on simplified models for describing the protein structure, such as normal mode analysis (NMA) of elastic network models (ENMs) used as a coarse-grained (CG) approach for protein dynamics (Tama et al., 2000; Tama and Sanejouand, 2001; Li and Cui, 2002; Eom et al., 2007; Tatke et al., 2008; Yang and Chng, 2008; Deriu et al., 2010; Cifra et al., 2015). These techniques represent a valid computational alternative to atomistic simulations for understanding the mechanics of large proteins. All these approaches, both atomistic and non-atomistic (**Figure 1**) will be discussed for each of the aforementioned biological players of mechanotransduction, starting from the cell–ECM contact and conceptually moving downstream the mechanotransduction pathway toward the cytoskeleton.

Mechanosensitive Ion Channels

From a cellular perspective, effective translation of mechanical cues from the environment into appropriate biological responses requires a competent transduction pathway connecting the ECM to subcellular structures. For this reason, contacts between the cell and the ECM are being increasingly investigated both *in vitro* and through the application of the tools provided by computational molecular modeling, given the intimate link between mechanotransduction and protein conformational changes (Hoffman et al., 2011). Mechanosensitive ion channels (MSCs), sometimes referred to as stretch-activated channels (SACs), being located at the interface between the cell membrane and the surrounding environment, are a first candidate for the transduction of mechanical stimuli, with functional implications on a variety of biological processes including, for example, the mechano-electric feedback loop in cardiovascular physiology, where force is known to significantly alter ion conductance (Teng et al., 2014). SAC opening and closing dynamics in response to mechanical stress have been investigated both *in vitro* and *in silico* (Kizer et al., 1997; Sachs, 2010) for a variety of cellular phenotypes, and in this context, computational molecular modeling is providing valuable insights into the molecular mechanisms behind the response to mechanical stimuli. Examples of this include computational studies of the bacterial mechanosensitive channels, which are commonly categorized into mechanosensitive channels of small conductance (MscS) and mechanosensitive channels of large conductance (MscL). Sotomayor and Schulten (2004) investigated the dynamics of MscS through MD simulations both restrained to its crystallographic state and unrestrained: in the former case, the open conformation was preserved, and intermittent permeation of water was observed, whereas in the latter, unrestrained case, the presence of local surface tension was shown to mechanically induce widening of the pore. Elmore and Dougherty (2003) computationally investigated the effect of lipid membrane composition on MscL dynamics, highlighting a conformational change in the channel's C-terminal region depending on membrane lipid composition and structural rearrangements following the thinning of the bilayer in response to mechanical tension. The gating mechanism of MscL has been further evaluated computationally by Gullingsrud et al. (2001) through the use of steered MD (SMD), where the application of lateral tension mimicking the bilayer environment subjected to mechanical stress allowed for the characterization of the dynamics of the single molecular events leading to the transition from the closed state to the first open state, in good agreement with experimental data (Sukharev et al., 1999; Kloda and Martinac, 2001). More recently, Sawada et al. (2012) identified a single residue as the main responsible for transmitting the force from the membrane bilayer to the rest of the channel, thereby characterizing the chain of events eventually leading to the first stage of channel opening, with the calculated energy difference between the closed and first conductance states in agreement with experimental data. Overall, the last two decades saw the increasing application of computational modeling techniques to MSCs, effectively shedding light on those molecular events that from the application of mechanical stimuli lead to structural rearrangements of the channels and eventually to the conformational switch to the open state. Given the crucial role of ion-channel mechanics and dynamics in the regulation of cardiovascular function, this approach is promising and expected to provide insights into the causative relationships between the cell's mechanical environment and functional consequences in healthy and pathological myocardial conditions.

Integrin Receptors

Integrins are cell adhesion heterodimers composed of two glycoprotein subunits named α and β, each consisting of an extracellular portion terminating with a globular shaped head, a multidomain "leg," a transmembrane helix, and a cytoplasmic tail region. A total of nine types of β subunits and 24 types of α subunits exist, combining to form functionally distinct heterodimers (Moreno-Layseca et al., 2019). They constitute a well-known contact point between the cell and both the ECM and adjacent cells, and they have been extensively studied in terms of their mechanical properties in the context of transmitting mechanical signals downstream of focal adhesions, which are supramolecular contact points between the cell and ECM enabled by the clustering of adhesion-mediating proteins. Integrins generally bind to specific components of the ECM, which bear a distinct integrin-binding domain consisting in an Arg-Gly-Asp (RGD) triplet. The most common substrates for human integrins are laminins (α3β1 α6β1 α7β1, α6β4, α1β1, and α2β1), collagens

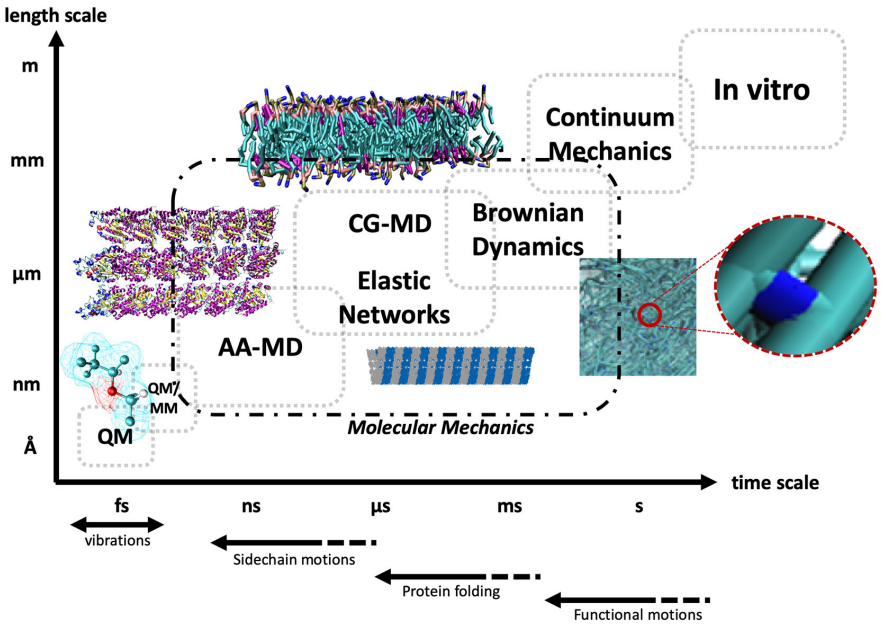

FIGURE 1 | Schematic representation of the different timescales and length scales typically accessible to different computational and experimental techniques, starting from quantum mechanics (QM) and hybrid quantum mechanics/molecular mechanics (QM/MM), and progressively moving up the scales to all-atom molecular dynamics (AA-MD), coarse-grained MD (CG-MD), and elastic networks, up to Brownian dynamics and continuum mechanics, and at the top right *in vitro* approaches. The dashed line encompasses techniques deploying the principles of molecular mechanics. The bottom arrows highlight the typical timescales of different types of biological motions.

(α1β1, α2β1, α10β1, α11β1, αvβ8, and α9β1), and fibronectin (α5β1 α8β1 αvβ1, αvβ3, αIIbβ3, αvβ6, αvβ8, α4β1, and α4β7) (Moreno-Layseca et al., 2019). The location and accessibility of RGD domains thus play a pivotal role in integrin binding, and the exposure of buried RGD triplets as a result of mechanical stress arguably constitutes a first path for mechanotransduction. Different models of the integrin activation process have been proposed. A first model postulates that inactive integrins are in a bent state, with the heads facing the cell membrane. Events such as talin binding in the intracellular region are then thought to lead to a switchblade-like motion, in which the head swings outward toward the extracellular space, thus activating the integrin (Takagi et al., 2002). A second model explained integrin activation as a consequence of the vertical sliding of the stalks in response to the same intracellular binding events (Xiong et al., 2003). Perhaps most importantly, both models explained integrin activation as a function of conformational changes enhancing the affinity of the globular heads for their extracellular ligands. Molecular modeling methods have been deployed to investigate the dynamics of integrin conformational change and activation, for example, the swing-out motion of the hybrid domain in β3 integrins. Indeed, MD and SMD simulations allowed to describe the allosteric pathway leading to hinge-angle opening in α5β3 integrins at the atomistic scale (Puklin-Faucher et al., 2006), also highlighting how RGD-sequence-containing ligand binding and ligand-dependent force application accelerate the conformational alterations (Puklin-Faucher and Vogel, 2009). The conformational dynamics of the β3 integrin headpiece hybrid domains have also been investigated by Gaillard et al. (2009) through MD and NMA, (1) underlining the low-frequency nature of the conformational transition involving the I-like and hybrid domains, (2) detailing the role of the α1 and α7 helices in the conformational transition, and (3) linking local conformational alterations of the identified regions to wider-scale structural rearrangements, allowing for integrin activation. Further studies hinted, again using targeted MD and ENMs, at common structural changes of the I-like domain essential for β3 integrin activation (Matsumoto et al., 2008; Provasi et al., 2009) and detailed the nature of the transition from inactive to active state (Chen et al., 2011). In summary, given the central role of integrins in mediating cell–cell and cell–ECM contacts and their potential as pharmacological targets (Paulhe et al., 2005), and because physiological cardiovascular function is intrinsically liked to correct mechanical coupling between its cellular and extracellular components, computational molecular modeling applied with specific methodological endpoints to the characterization of integrin-receptor mechanics and dynamics shall prove a valuable approach for the investigation of mechanotransduction, also in the context of cardiovascular function.

The Integrin–Cytoskeleton Coupling

The coupling between integrin receptors and the cytoskeleton sees the involvement, among others, of talin and vinculin (**Figure 2**). Moving further downstream of the mechanical chain connecting the cell environment to the inside of the cell, computational modeling has again proven to be a valuable tool in synergy with experimental approaches to unveil the causative

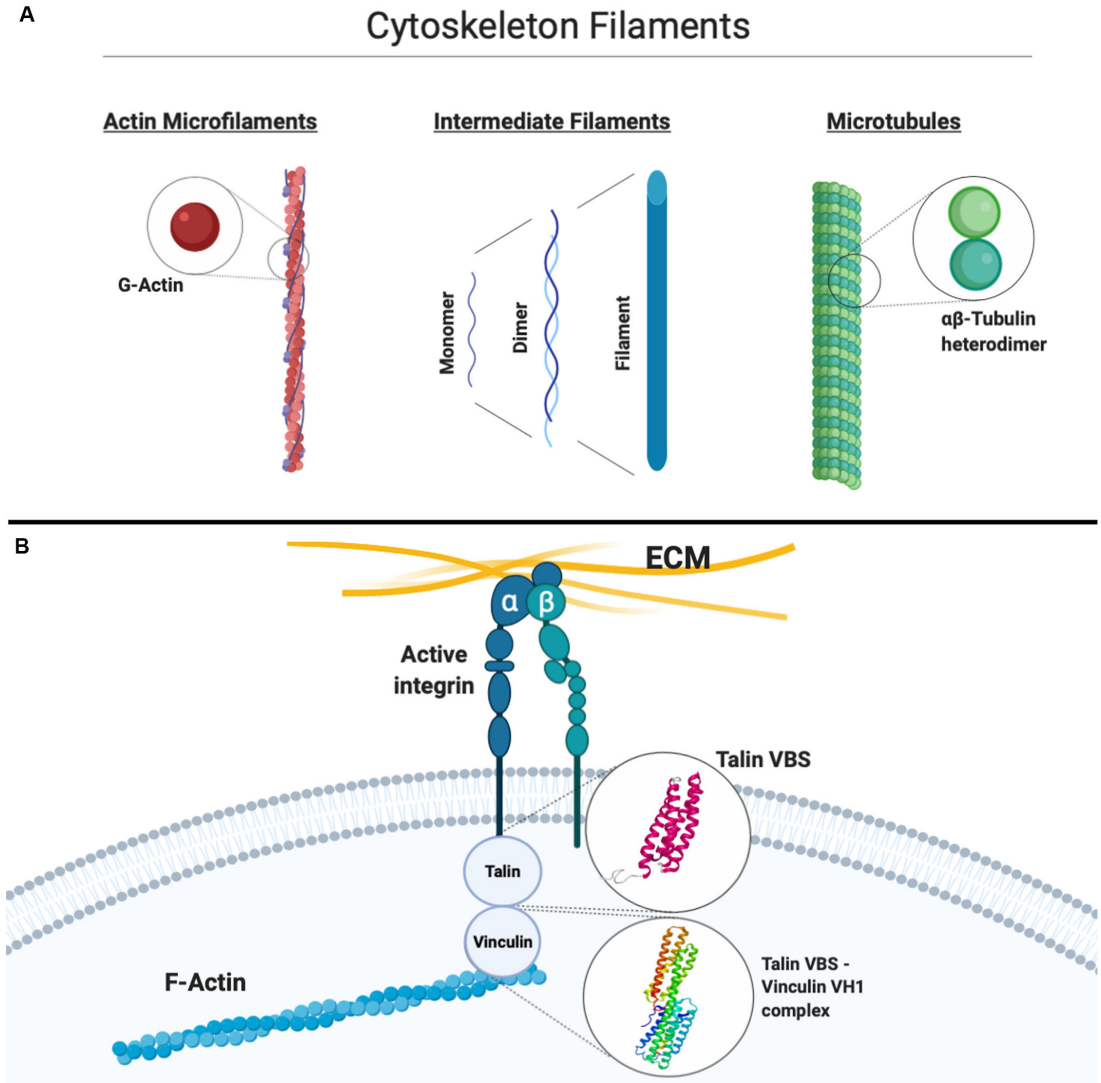

FIGURE 2 | (A) Simplified schematic of the three main constituents of the cytoskeleton, that is, actin microfilaments, intermediate filaments, and microtubules, with their basic constitutive units highlighted. **(B)** Schematic representation of the connection between the extracellular matrix (ECM) and the actin cytoskeleton through integrins. Atomistic models available for the vinculin-binding site (VBS) of talin and the vinculin Vh1–talin VBS complex are shown. Created with Biorender.com.

factors of the translation of mechanical stimuli into competent or aberrant cellular responses. Talin, a globular protein crucial for linking integrins to the actin cytoskeleton, has been suggested through MD simulations to undergo a conformational change of its helical bundles when force is applied at the focal adhesion, effectively exposing cryptic binding residues crucial for vinculin binding (Lee et al., 2007), leading to the strengthening of focal adhesions, as shown by more recent works (del Rio et al., 2009; Yao et al., 2014). Vinculin, simultaneously binding to talin and F-actin, is also known to be essential for the maturation of stable focal adhesions. As Lee and co-workers suggested (Lee et al., 2007), the requirement of an external force to induce vinculin recruitment might be a crucial component in the overall mechanotransduction pathway. In their study, MD simulations were employed and a binding mechanism between the vinculin head subdomain (Vh1) and the talin vinculin-binding site (VBS) was proposed as characterized at the atomic scale in terms of consecutive structural events from hydrophobic insertion on VBS into Vh1 to a conformational rotation of the former (Lee et al., 2007). The predominantly hydrophobic nature of the VBS–vinculin interaction has been later confirmed again through MD simulations by Golji et al. (2011), further confirming the hypothesis of the insertion of the VBS of talin into the hydrophobic vinculin domain 1 core. Interestingly, the more general validity of the proposed mechanism suggested by Lee et al. (2008) constitutes a first example of how the understanding of molecular mechanisms in this context through computational models constitutes an important piece of knowledge, which might eventually lead, in tandem with experimental validation, to a broader multiscale model of mechanotransduction. Moreover,

in the light of studies highlighting the importance of vinculin and in general of the cytoskeleton-binding proteome in heart contractility, cytoskeletal stiffening, and cardiac aging and disease (Heling et al., 2000; Kaushik et al., 2015), it is legitimate to expect that progress in the understanding of cardiac biomechanics can be effectively aided by computational, multiscale molecular models able to explain the functional and causative link between proper mechanotransduction and physiological function.

Computational Investigation of Cytoskeleton Mechanics and Dynamics

Mechanotransduction involves a continuous dynamic rearrangement of the cytoskeleton as an instantaneous response to mechanical stimuli on the cell. Molecular mechanisms driving its activity are still not completely understood, but in the last decades, many experimental studies have been carried out in order to better understand how the cytoskeleton filaments behave under different stress conditions. Specifically, several studies in the past were purposed to shed light on mechanical properties of single cytoskeleton filaments (**Figure 2**), that is, MTs, which are polymers of hierarchically assembled tubulin heterodimers, actin MFs, which are polymers of G-actin, and IFs, which are polymers of intermediate diameter of around 10 nm, commonly divided into six classes on the basis of their composition (Cooper, 2007): computational approaches allowed to add valuable information to the experimental studies aimed at characterizing the biological cytoskeleton filament building blocks. These will be briefly described below.

Microtubules have been widely investigated by modeling approaches spanning from atomic level to continuum, with the common aim to shed light on the causative elements of their peculiar mechanical and electrical properties. To this regard, intracellular processes in the cell are thought to involve electric fields and, because MTs are polar structures and vibrate with frequencies of the order of MHz to GHz (Cifra et al., 2011, 2015), it has been hypothesized that MT charge motion produces electric fields that can interact with subcellular structures and organelles in such processes. In more detail, MTs have been suggested to be excellent conductors of electrical signals and able to amplify an electrical current and axial ionic movements (Priel et al., 2006) in virtue of pores in their lattice structure (Freedman et al., 2010). The latter's proximity to negative-charge-bearing C-terminal tails further enables the interaction with ions, causing conduction through the lumen. Considering the essential role of electrical signal propagation for the cardiovascular function, the exploration of ionic currents through the MT might also be of interest in heart biomechanics. In terms of vibrational properties, the analysis of molecular reasons beneath MT mechanics and vibrations has been a highly considered research field in the scientific community. Molecular modeling has provided much information regarding this topic by synergistically coupling with classical continuum theories. There have been a number of computational studies dealing with MT elasticity, starting from one-dimensional models of the protofilament chain (Pokorný et al., 1997) to the development of hollow cylinders consisting of parallel beams, up to a two-dimensional lattice structure for the MT (Kis et al., 2002; Kasas et al., 2004a,b). A series of studies addressed the characterization of MT longitudinal vibrations (Pokorný et al., 1997; Kis et al., 2002; Kasas et al., 2004a,b; Deriu et al., 2010; Cifra et al., 2011; Barzanjeh et al., 2017). These models allowed to elucidate relationships between tubulin molecular structure and arrangement in the MT lattice and filament principal modes of motion. Vibration dispersion relations accounting for the geometrical architecture of MT as well as insights on protein–protein interactions were predicted in detail. Also, a strong dependence of the microscopic vibration properties of the MTs on the number of the MT protofilaments and MT lattice type has been found (Portet et al., 2005). By analyzing the normal modes of motion, it has been found that circumferential bending, controlled by circumferential bending stiffness, is dominant in circumferential vibrations. Therefore, the excitation of the vibrations could lead to a large deformation of the MT section, thus influencing both the mechanical performances and the structural integrity (Wang and Zhang, 2008; Zhang and Wang, 2014). Several theoretical models have been developed in order to justify experimental evidence demonstrating that the mechanical behavior of the MT could be better described by using the elasticity theory for transversally anisotropic structures (Kis et al., 2002; Kasas et al., 2004b). New insights about MT mechanical properties have been obtained by inspecting the MT mechanical characteristics starting from the atomic level, using a bottom-up approach. For example, anisotropic network model approaches have been able to shed light on the global dynamics of the tubulin dimer (Keskin et al., 2002) and even to predict vibration modes of entire MTs still maintaining an atomic resolution (Deriu et al., 2010).

Just as for MTs, computational investigations of the mechanical properties of actin were initially performed by considering actin filaments as homogeneous and isotropic rods (Yoshimura et al., 1984). However, soon, it has been understood that a potentially vast range of motions and flexibilities of the filaments remained elusive in this approach and that the isotropic rod model does not account for the hierarchical structure of actin filaments, composed of a double helix of G-actin polymers. This was corroborated by the observation of the peculiar 3D atomic models of the actin filament with its unique structural features (ben-Avraham and Tirion, 1995), again showing how the atomistic-scale bottom-up approach yields enhanced insights into mechanical characteristics. At the same time, owing to the huge computational cost of modeling cytoskeleton filaments while keeping their atomic structure into account, CG approaches have been introduced for the same purpose (Deriu et al., 2011, 2012; Bidone et al., 2015). One of the first MD simulations of G-actin in explicit solvent was performed by Wriggers and Schulten (1997), providing an understanding of actin dynamics and functional activity and revealing a propensity of G-actin to alter its structural conformation through a modification of the nucleotide binding cleft. It was soon understood that the application of mechanical stress does indeed play a role in the kinetics of G-actin and thus in the transduction of mechanical stimuli to the cytoskeleton. Lee and colleagues (Lee et al., 2019) recently determined experimentally how the history of the applied forces, especially

cyclic mechanical stress, conditions the G-actin–G-actin and G-actin–F-actin association and dissociation kinetics and strengthens the inter-dimer contacts between G-actin dimers, leading to a mechanical reinforcement, thus acting as a possible mechanotransduction mechanism that allows for the formation of stable cytoskeletal networks as a result of a form of mechanical conditioning. Moreover, SMD studies provided an insight on how the application of force can induce the formation of salt bridges between G-actin subunits, hence significatively altering G-actin dynamics (Lee et al., 2013). Studies employing a CG approach (Chu and Voth, 2005, 2006) allowed to understand how protein conformational changes may significantly modify the inter-monomer interactions of actin assemblies, leading to wider, shorter, and more disordered filaments. Other computational approaches coupled microscopic- and macroscopic-scale levels to predict actin polymerization-related phenomena such as protrusive forces for the directional motion of a virtual lamellipodium. Modeling approaches also allowed to highlight how very stiff MFs are able to generate protrusive force also with a low concentration of G-actin monomer, whereas non-stiff MFs can only generate a protrusive force when enough G-actin monomers are supplied for actin polymerization. Collective long-range deformations of a filament, such as bending, twisting, and stretching, were investigated by NMA-based approaches useful to get information on principal components of the filament motion (ben-Avraham and Tirion, 1995).

Lastly, properties of IFs and IF-associated proteins were investigated by molecular modeling and often by SMD simulations, a powerful technique to characterize protein mechanics. The transition of the spectrin α-helix domain from a folded to an unfolded arrangement in response to the application of a tensile load was discussed in several computational works (Paramore and Voth, 2006). Moreover, in the light of study findings on the capability of IFs (especially keratin, vimentin, and desmin), to sustain large deformations above 250% (Herrmann et al., 2007; Kreplak et al., 2008), the tensile properties of IFs were investigated through computational models specifically on the vimentin dimer using SMD to evaluate the mechanical response to strain and link the macroscopic mechanical properties to structural and geometrical changes in the dimer (i.e., its unfolding state) with atomic resolution (Qin et al., 2009). This is but one example of how computational models can elucidate the key structural features responsible for the final mechanical behavior, with good agreement with experimental data.

MECHANOSENSING IN CARDIAC DISEASE

As mentioned above, the mechanosensing machinery plays a fundamental role in the development and maturation of the heart as well as its physiological function. In the healthy heart, cardiomyocytes (CMs) are exposed to the passive stiffness of the cardiac muscle (independent of the muscle activity) and to the active force of the heart contractile apparatus. In cardiac disease, the active force of the heart changes owing to the loss of CMs or the expression of motor proteins together with changes in the cardiac load and output (Roca-Cusachs et al., 2012; Andres-Delgado and Mercader, 2016). Two different modeling strategies for CMs mechanotransduction have been proposed. The "localized" model involves the generation of a stretch signal in close proximity to the plasma membrane, whereas the decentralized model involves forces generated at the cell surface, which are transmitted via the cytoskeleton to other part of the cells (Tavi et al., 2001; Knoll et al., 2003). The generation of a stretch signal near the cell may involve non-selective ion channels that can be activated by longitudinal stretch of the cell. These channels induce an increase in cations (Na^+ and Ca^{2+}), which cause a release of Ca^{2+} from the sarcoplasmic reticulum, thereby acting as a transducer of a mechanical force into a biochemical signal. Another, and probably the most known, stretch sensor in CMs involves the cytoskeleton and allows the process of mechanotransduction to occur at a different site from where the strain is applied (Ingber, 2003a,b). These models are supported by *in vitro* studies where it has been shown that the application of a mechanical stimulus to isolated CMs or stem cells results in changes in gene and protein expression that are indicative of a (patho)physiological response or cell maturation and differentiation (Vining and Mooney, 2017; Kim et al., 2018; Wong et al., 2018). A possible mechanism for this involves many different proteins ranging from the ECM molecules to membrane and intracellular proteins that bind to the cytoskeleton and orchestrate the cellular response to different microenvironments. The ECM is fundamental in providing mechanical signals to the cells through different integrin receptors, which bind to the focal adhesion complex (FAC) and connect integrin receptors to the cytoskeleton (Belkin and Koteliansky, 1987; Bois et al., 2006; Ye et al., 2014). During development, the expression of the ECM in the developing cardiac tissue is tightly regulated, and several studies, using different animal models, have highlighted the ECM dynamics during embryonic development and in the adult heart. Briefly, collagen I is predominant in both developing and adult tissue, but in the latter, its density and cross-linking are upregulated, and the ratio between collagen I and collagen III decreases (Thompson et al., 1979; Borg, 1982; Hanson et al., 2013; Gonzalez et al., 2019). Fibronectin is highly expressed during embryonic development and is downregulated in the adult tissue (Kim et al., 1999; Lockhart et al., 2011). Conversely, elastin expression has been found to increase in the adult heart (Kim et al., 1999). These changes are generally associated with an increase in cardiac stiffness, with the heart tissue becoming less compliant during heart development, and CM differentiation. In CMs, the cytoskeleton is also anchored to the sarcomeric Z-disk and the myosin protein is stabilized by titin and other structural proteins, suggesting that the sarcomeric proteins also play an important role in CM mechanotransduction (Frank and Frey, 2011; Buyandelger et al., 2014). Several cardiac diseases are characterized by altered mechanical load and are characterized by morphological changes of the ventricular tissue and myocyte shape (Gerdes and Capasso, 1995). Dilated cardiomyopathies are characterized by volume overload and eccentric hypertrophy in which the sarcomere proteins are added in series, resulting in elongated myocytes. These changes ultimately lead to dilation of the ventricular chamber and

thinning of the ventricular wall (Grossman et al., 1975; Beltrami et al., 1995). Conversely, hypertrophic cardiomyopathies are characterized by a pressure overload and concentric myocyte hypertrophy in which sarcomeric proteins are added in parallel, causing an increase in cross-sectional area of the myocytes. These changes lead to reduction in the volume of the ventricular chamber, thickening of the ventricular wall, and diastolic dysfunction (Zierhut et al., 1991; Katz, 2002). Both changes in myocytes shape are ultimately associated with impaired contractility and heart failure due to the altered force produced by CMs, indicating the importance of the mechanosensory machinery in the development and progression of cardiac disease (Gjesdal et al., 2011; Wilson et al., 2014; Janssen, 2019). The maladaptive response of the myocytes are also associated with several genetic mutations in sarcomeric proteins (β-myosin heavy chain, troponin T, and troponin I) (Kamisago et al., 2000) or protein associated with force transmission to the ECM, such as dystrophin (Lapidos et al., 2004). Mutations in these proteins suggest that the proper interaction of the contractile apparatus or the mechanosensing machinery with the cytoskeleton could be altered, thus resulting in a maladaptive response of the myocytes to mechanical loading. Another important feature of most of the cardiomyopathies is ECM remodeling. This is evidenced by numerous studies reporting that both the composition of the ECM and the expression of different integrin receptors are altered in many cardiomyopathies, with ischemic or non-ischemic origins. The remodeling phase associated with myocardial infarction is characterized by an increase in fibronectin and collagen deposition, which ultimately leads to fibrosis (Frangogiannis, 2017) and to an increase in myocardial stiffness (Berry et al., 2006), and it is also associated with a differential expression of α1, α3, and α5 integrins in both acute and chronic stages of myocardial infarction (Nawata et al., 1999). Similar to ischemic cardiomyopathies, pressure overload and genetic-based cardiomyopathies are also characterized by fibrosis and altered expression of integrin levels (Samuel et al., 1991; Schaper and Speiser, 1992; Ross and Borg, 2001; Ross, 2002). Integrin receptors are important in many cellular physiological processes, including cytoskeletal remodeling, and are the main receptors associated with mechanical signaling interacting with various adhesion complex proteins. Their changes in response to the diseased environment affect the mechanical signaling pathway and can ultimately lead to disease progression. An important player in all the previously mentioned pathological features is the cytoskeleton. In consequence of altered mechanical stimuli, genetic mutation, or ECM remodeling, the cytoskeleton responds in different ways ranging from a diminished affinity of the cytoskeletal elements to their binding proteins, thus impairing a physiological response to the mechanical stress, to structural changes in the cytoskeleton following an increase mechanical stress resulting in changes in cell phenotype and reorganization of the sarcomeric apparatus (Sequeira et al., 2014). The understanding of the cytoskeletal remodeling and its adaptation to physiological/pathological stimuli is therefore of fundamental importance in order to better understand the contribution of the mechanosensing machinery to the development and progression of most cardiomyopathies, and it may open new potential therapeutic targets in numerous cardiac diseases.

MECHANOSENSING IN TISSUE REGENERATION AND MODELING

With the development of new emerging technologies in tissue generation and the use of iPSC-derived CMs, the *in vitro* generation of cardiac tissue has become a valid option to re-create *in vitro* different models of healthy and pathologic cardiac tissue to use both for regenerative medicine application and for research purposes. In order to generate *in vitro* cardiac-like tissue, either in the form of 3D construct or in the form of organoids, a combination of soluble (e.g., growth factors) and physical cues is necessary to form a fully mature and functional tissue. The soluble cues have been extensively studied (Paige et al., 2015; Denning et al., 2016; van den Berg et al., 2016; Leitolis et al., 2019), whereas the role of the physical cues is only recently been explored as a valuable approach to induce fully the maturation of the generated tissue (Lindsey et al., 2014). Despite great improvements in the differentiation of human pluripotent stem cell-derived CMs (hPSC-CMs) using a variety of approaches, the main limitation for the experimental use of these cells still remains their immature phenotype (Lieu et al., 2013). As we mentioned previously, mechanical stretch and electrical activity are important factors in the development, maturation, hypertrophy, and disease progression of the heart and should be considered in order to generate a functionally mature phenotype of the hPSC-CMs. Among the physical factors that should be taken into consideration for the development of a fully mature cardiac tissue are the ECM or scaffold in which the cells are cultivated, its rigidity and topography, mechanical loading and stretch, shear stress, and electrical stimulation. The ECM plays a fundamental role in presenting both biochemical and physical signals. When the cells are cultured in a 3D environment, the scaffold in which they are cultivated provides both biochemical and physical signal as the cells feel their environment and pull it. We have previously mentioned that MSCs respond to the substrate stiffness and differentiate according to the compliance of the different tissues (Engler et al., 2006). Similarly, it has been shown that also embryonic stem cell (ESC) differentiation could be driven by the rigidity of the substrate in which they are cultivated (Evans et al., 2009), and it should be taken into consideration in the development of *in vitro* cardiac-like tissue. Another important aspect of the ECM component is the biochemical composition. A decellularized cardiac matrix has been shown to be advantageous in culturing progenitor cells as well as ESC-CMs (Williams et al., 2014, 2015; Gaetani et al., 2016; Bejleri et al., 2018), probably due to its complex biochemical composition. Similarly, Jung et al. (2015) identified fibronectin, laminin-111, and collagen type 1 signaling to be very important in driving the differentiation of murine-derived iPSC-CMs. In the human body, the ECM is mainly synthetized by the fibroblast in response to different stimuli. It has been shown that the differentiation of ESC or iPSCs-CMs in a 3D culture is enhanced when the cells are co-cultured with fibroblast

(Liau et al., 2011; Ou et al., 2011; Valls-Margarit et al., 2019). The fibroblast plays an important role in maintaining and influencing CM function by secreting growth factors (Ottaviano and Yee, 2011), propagating the electrical impulse (Gaudesius et al., 2003; Ogle et al., 2016), and secreting ECM (Zhang et al., 2012; Ogle et al., 2016). In a 3D scaffold, mainly, if it is a hydrogel or soft gel with poor compliance than the heart tissue, the fibroblast can act by remodeling the ECM and allowing a more robust gel compaction and remodeling, which results in a better cell-to-cell contact and likely an increase in tissue mechanical properties, thereby enabling the mechanosensing-mediated signaling, which is fundamental for tissue maturation. Interestingly, in a recently published work, the authors reveal a unique gene signature defining specific quiescent CF and showed that co-culture of hPSC-CFs with hPSC-CMs alter the electrophysiological properties of the CMs, as compared with co-culture with dermal fibroblasts, indicating the importance of tissue specificity, and could be used not only to improve the maturation of cultured cells but also to reveal the specific molecular signaling that regulates, and is regulated by, mechanosensing (Zhang et al., 2019). Another important aspect in the generation of functionally 3D cardiac tissue is the perfusion, which allows enough nutrient supply to the cultured cells, and it overall results in better cell survival, cell organization, and tissue compaction (Carrier et al., 2002; Radisic et al., 2008). Several systems have also integrated electrical stimulation into a perfusion bioreactor showing that the electrical stimulation is important in driving cell maturation and allows synchronous contraction of the perfused construct (Radisic et al., 2008). Nunes et al. (2013) generated a platform named biowire by 3D culturing human iPSC (hiPSC) or ESC-CMs together with supporting cells into a template of polydimethylsiloxane (PDMS) channel, around a sterile surgical suture in type I collagen gels. After 1 week, the cells organized along the suture and were electrically stimulated with increasing intensity over time. The authors demonstrated that the combination of geometric control and electrical stimulation resulted in improved electrical and ultrastructural properties of human cardiac tissue, resulting in cell maturation (Nunes et al., 2013). Similar results were observed in another recent work. Ronaldson-Bouchard et al. (2018) used early stage iPSC-derived CMs, soon after the initiation of spontaneous contractions, and electrically stimulate them with increasing intensity over time. This approach allowed increased maturation of the iPSC-CMs, which showed a gene expression profile and cell ultrastructure, including sarcomeres, T-tubules, and mitochondria, similar to the adult myocytes (Ronaldson-Bouchard et al., 2018, 2019). Another physical stimulus that has been frequently used in cardiac tissue engineering application is mechanical stimulation that consists in the external application of a mechanical stretching apparatus. The applied tension can be static or cyclic, and the stretching can be uniaxial, biaxial, or multiaxial (Cao et al., 2015). The approach of mechanical stretch to induce myocyte maturation has been used for the first time almost two decades ago (Zimmermann et al., 2000) using neonatal rat ventricular myocytes, and the advantages of this pioneering work have been further confirmed by numerous other studies. More recently, when human ESC and iPSC-CMs were 3D cultured in collagen gels and subjected to static or cyclic mechanical stress; the 3D culture promoted a better differentiation of the seeded progenitors, and mechanical stretch influenced maturation and structure of the differentiated tissue (Ruan et al., 2015). In another recently published work, the authors combined mechanical stimulation with electrical stimulation showing that the mechanical stimulation increases cell morphology, alignment, and contractility, whereas additional electric pacing resulted in an additional increase in force production (Ruan et al., 2016).

As of now, we know very little about the molecular mechanisms involved in the maturation of the 3D tissue, as most of the studies aimed at the generation of functional tissue and their characterization. However, it is likely that the same mechanosensing pathways described previously allow also the maturation of the different cultured 3D tissues. Recently, it has been shown that following mechanical stretch, Piezo1, phosphorylated-Ak transforming serine473 (P-AKTS473), and phosphorylated-glycogen synthase kinase-3 beta serine9 (P-GSK3) expression was downregulated in the human CM cell line AC16 (Wong et al., 2018). In another study, the mechanical stretch induces endothelial nitric oxide synthase gene expression in neonatal rat CMs (Cheng et al., 2009). Understanding the molecular pathways associated with mechanical stimuli-mediated maturation of the tissue could be important not only in the generation of functional cardiac *in vitro* tissues but also in the generation of pathological models that resemble the human pathology and could be important in our understanding of the diseased tissue but also in finding a new molecular target for clinical applications.

CONCLUSION AND FUTURE PERSPECTIVE

Independently from the etiology, heart failure is the funnel neck of the balance between genetic and epigenetic (inflammatory and fibrogenic) specific factors involved in the tissue damage and the constant variables to which these factors need to match, that is, mechanosensing and mechanotransduction. With the development of new technologies and a better understanding of the different biochemical and physical stimuli that allow the development, growth, and physiological function of a tissue, it is becoming more realistic to re-create *in vitro* healthy or pathological tissue that can be used for regenerative medicine or drug screening purposes.

The investigation of the mechanics of proteins involved in cell–cell and cell–ECM contacts, from integrins and stretch-sensing ion channels to cytoskeleton filaments, has been a very widely investigated topic by both experimental and computational studies, given the high importance of shedding light on the ability of cells to respond to external stimuli and given the importance thereof in a variety of physiological functions, including in particular the biomechanics of cardiac tissue. Consequently, molecular and multiscale simulations can help experimental studies to shed light on the many debated issues concerning cell mechanics and the broader phenomenon of mechanotransduction. It is also clear that modeling shall not

be a substitute of experimental studies but rather a valuable tool to add complementary information, ultimately helping the interpretation or rationalization of experimental results. The possibility to simulate a fraction of the cytoskeleton, for example, a network of interconnected MTs, MFs, and IFs, maybe even connected to transmembrane transducers such as integrins, seems now to be an explorable possibility. The refinement of methodologies combined with the fast growth of computational capabilities might leave us astonished in the upcoming future.

On the other hand, the discovery of iPSCs has represented a major development in the generation of healthy and diseased functional cells or tissue. The possibility to generate CMs from healthy and diseased patients allows us to generate tissue that can be used for replacement therapy or for drug screening or validation. hIPSC-CMs have been generated from numerous patients with inherited cardiomyopathies and have allowed us to better understand the molecular pathways responsible in the development of the pathological phenotype (Hoes et al., 2019). However, as mentioned previously, the canonical 2D culture and differentiation of these cells still has major limitations, most notably their immature phenotype, which lacks to fully represent developed tissue. The development of new biomaterials (Reis et al., 2016; Wissing et al., 2017; Kuraitis et al., 2019) and the emerging of new technologies such as tissue printing (Charbe et al., 2019; Tomov et al., 2019), organ on a chip (Marsano et al., 2016; Ugolini et al., 2018; Wan et al., 2018), and different types of bioreactors that allow mechanical, perfusion, or electrical stimulation (Freed et al., 2006; Lei and Ferdous, 2016; Paez-Mayorga et al., 2019) allow us to generate cardiac tissue that more closely recapitulate the (patho)physiological features of the developed myocardium. Moreover, these models represent an optimal tool not only to test and validate new drugs or to re-create tissue substitute for regenerative medicine application but also to allow a better understanding of the molecular mechanisms behind disease development and progression. This is particularly important for the mechanosensing machinery and the generation of biochemical signals from physical cues, which are very difficult to recapitulate in static 2D culture conditions. As mentioned previously, these mechanisms are at the basis of many, if not all, cardiomyopathies, whether inherited or not, and could potentially open up new approaches and discover potential new targets for the cure of these pathologies. However, numerous challenges still remain to be addressed, such as the differentiation state of the CMs, the proper stimuli, when and how apply them, and how to coordinate *in vitro* the plethora of the different biochemical and physical signals that are responsible *in vivo* for the development and physiology of the functional tissue.

AUTHOR CONTRIBUTIONS

All authors listed have made a substantial, direct and intellectual contribution to the work, and approved it for publication.

FUNDING

This research has been funded by the Horizon 2020 initiative program, grant agreement number 755523-MEDIRAD. The Virtuous project, funded by the European Union's Horizon 2020 Research and Innovation Programme under the Maria Skłodowska-Curie—RISE Grant Agreement No. 872181.

REFERENCES

Abraham, M. J., Murtola, T., Schulz, R., Páll, S., Smith, J. C., Hess, B., et al. (2015). GROMACS: high performance molecular simulations through multi-level parallelism from laptops to supercomputers. *SoftwareX* 1–2, 19–25. doi: 10.1016/j.softx.2015.06.001

Andres-Delgado, L., and Mercader, N. (2016). Interplay between cardiac function and heart development. *Biochim. Biophys. Acta* 1863(7 Pt B), 1707–1716. doi: 10.1016/j.bbamcr.2016.03.004

Barzanjeh, S., Salari, V., Tuszynski, J. A., Cifra, M., and Simon, C. (2017). Optomechanical proposal for monitoring microtubule mechanical vibrations. *Phys. Rev. E* 96:012404. doi: 10.1103/PhysRevE.96.012404

Bassat, E., Mutlak, Y. E., Genzelinakh, A., Shadrin, I. Y., Baruch Umansky, K., Yifa, O., et al. (2017). The extracellular matrix protein agrin promotes heart regeneration in mice. *Nature* 547, 179–184. doi: 10.1038/nature22978

Bejleri, D., Streeter, B. W., Nachlas, A. L. Y., Brown, M. E., Gaetani, R., Christman, K. L., et al. (2018). A bioprinted cardiac patch composed of cardiac-specific extracellular matrix and progenitor cells for heart repair. *Adv. Healthc. Mater.* 7:e1800672. doi: 10.1002/adhm.201800672

Belkin, A. M., and Koteliansky, V. E. (1987). Interaction of iodinated vinculin, metavinculin and alpha-actinin with cytoskeletal proteins. *FEBS Lett.* 220, 291–294. doi: 10.1016/0014-5793(87)80832-3

Beltrami, C. A., Finato, N., Rocco, M., Feruglio, G. A., Puricelli, C., Cigola, E., et al. (1995). The cellular basis of dilated cardiomyopathy in humans. *J. Mol. Cell Cardiol.* 27, 291–305. doi: 10.1016/s0022-2828(08)80028-4

ben-Avraham, D., and Tirion, M. M. (1995). Dynamic and elastic properties of F-actin: a normal-modes analysis. *Biophys. J.* 68, 1231–1245. doi: 10.1016/s0006-3495(95)80299-7

Berry, M. F., Engler, A. J., Woo, Y. J., Pirolli, T. J., Bish, L. T., Jayasankar, V., et al. (2006). Mesenchymal stem cell injection after myocardial infarction improves myocardial compliance. *Am. J. Physiol. Heart. Circ. Physiol.* 290, H2196–H2203. doi: 10.1152/ajpheart.01017.2005

Bidone, T. C., Kim, T., Deriu, M. A., Morbiducci, U., and Kamm, R. D. (2015). Multiscale impact of nucleotides and cations on the conformational equilibrium, elasticity and rheology of actin filaments and crosslinked networks. *Biomech. Model. Mechanobiol.* 14, 1143–1155. doi: 10.1007/s10237-015-0660-6

Biggins, J. S., Royer, C., Watanabe, T., and Srinivas, S. (2015). Towards understanding the roles of position and geometry on cell fate decisions during preimplantation development. *Semin. Cell Dev. Biol.* 47–48, 74–79. doi: 10.1016/j.semcdb.2015.09.006

Bois, P. R., O'Hara, B. P., Nietlispach, D., Kirkpatrick, J., and Izard, T. (2006). The vinculin binding sites of talin and alpha-actinin are sufficient to activate vinculin. *J. Biol. Chem.* 281, 7228–7236. doi: 10.1074/jbc.M510397200

Borg, T. K. (1982). Development of the connective tissue network in the neonatal hamster heart. *Am. J. Anat.* 165, 435–443. doi: 10.1002/aja.1001650407

Bredov, D., and Volodyaev, I. (2018). Increasing complexity: mechanical guidance and feedback loops as a basis for self-organization in morphogenesis. *Biosystems* 173, 133–156. doi: 10.1016/j.biosystems.2018.10.001

Brouhard, G. J., and Rice, L. M. (2018). Microtubule dynamics: an interplay of biochemistry and mechanics. *Nat. Rev. Mol. Cell Biol.* 19, 451–463. doi: 10.1038/s41580-018-0009-y

Burridge, K., and Wittchen, E. S. (2013). The tension mounts: stress fibers as force-generating mechanotransducers. *J. Cell Biol.* 200, 9–19. doi: 10.1083/jcb.201210090

Buyandelger, B., Mansfield, C., and Knoll, R. (2014). Mechano-signaling in heart failure. *Pflugers Arch.* 466, 1093–1099. doi: 10.1007/s00424-014-1468-4

Cao, H., Kang, B. J., Lee, C. A., Shung, K. K., and Hsiai, T. K. (2015). Electrical and mechanical strategies to enable cardiac repair and regeneration. *IEEE Rev. Biomed. Eng.* 8, 114–124. doi: 10.1109/RBME.2015.2431681

Carrier, R. L., Rupnick, M., Langer, R., Schoen, F. J., Freed, L. E., and Vunjak-Novakovic, G. (2002). Perfusion improves tissue architecture of engineered cardiac muscle. *Tissue Eng.* 8, 175–188. doi: 10.1089/107632702753724950

Charbe, N. B., Zacconi, F. C., Amnerkar, N., Pardhi, D., Shukla, P., Mukattash, T. L., et al. (2019). Emergence of three dimensional printed cardiac tissue: opportunities and challenges in cardiovascular diseases. *Curr. Cardiol. Rev.* 15, 188–204. doi: 10.2174/1573403x15666190112154710

Chen, W., Lou, J., Hsin, J., Schulten, K., Harvey, S. C., and Zhu, C. (2011). Molecular dynamics simulations of forced unbending of integrin alpha(v)beta(3). *PLoS Comput. Biol.* 7:e1001086. doi: 10.1371/journal.pcbi.1001086

Cheng, T. H., Chen, J. J., Shih, N. L., Lin, J. W., Liu, J. C., Chen, Y. L., et al. (2009). Mechanical stretch induces endothelial nitric oxide synthase gene expression in neonatal rat cardiomyocytes. *Clin. Exp. Pharmacol. Physiol.* 36, 559–566. doi: 10.1111/j.1440-1681.2008.05100.x

Chiou, K. K., Rocks, J. W., Chen, C. Y., Cho, S., Merkus, K. E., Rajaratnam, A., et al. (2016). Mechanical signaling coordinates the embryonic heartbeat. *Proc. Natl. Acad. Sci. U.S.A.* 113, 8939–8944. doi: 10.1073/pnas.1520428113

Cho, S., Vashisth, M., Abbas, A., Majkut, S., Vogel, K., Xia, Y., et al. (2019). Mechanosensing by the lamina protects against nuclear rupture, DNA damage, and cell-cycle arrest. *Dev. Cell* 49, 920–935. doi: 10.1016/j.devcel.2019.04.020

Chu, J. W., and Voth, G. A. (2005). Allostery of actin filaments: molecular dynamics simulations and coarse-grained analysis. *Proc. Natl. Acad. Sci. U.S.A.* 102, 13111–13116. doi: 10.1073/pnas.0503732102

Chu, J. W., and Voth, G. A. (2006). Coarse-grained modeling of the actin filament derived from atomistic-scale simulations. *Biophys. J.* 90, 1572–1582. doi: 10.1529/biophysj.105.073924

Chu, J. W., and Voth, G. A. (2007). Coarse-grained free energy functions for studying protein conformational changes: a double-well network model. *Biophys. J.* 93, 3860–3871. doi: 10.1529/biophysj.107.112060

Cifra, M., Havelka, D., and Deriu, M. A. (2011). Electric field generated by longitudinal axial microtubule vibration modes with high spatial resolution microtubule model. *J. Phys. Conf. Ser.* 329:12013. doi: 10.1088/1742-6596/329/1/012013

Cifra, M., Havelka, D., Deriu, M. A., and Kuèera, O. (2015). Microtubule electrodynamics associated with vibrational normal modes. *Biophys. J.* 108(2, Suppl. 1):449a. doi: 10.1016/j.bpj.2014.11.2450

Cooper, G. (2007). *The Cell: A Molecular Approach*. Washington, DC: ASM Press.

Dasgupta, I., and McCollum, D. (2019). Control of cellular responses to mechanical cues through YAP/TAZ regulation. *J. Biol. Chem.* 294, 17693–17706. doi: 10.1074/jbc.REV119.007963

del Rio, A., Perez-Jimenez, R., Liu, R., Roca-Cusachs, P., Fernandez, J. M., and Sheetz, M. P. (2009). Stretching single talin rod molecules activates vinculin binding. *Science* 323, 638–641. doi: 10.1126/science.1162912

Denning, C., Borgdorff, V., Crutchley, J., Firth, K. S., George, V., Kalra, S., et al. (2016). Cardiomyocytes from human pluripotent stem cells: from laboratory curiosity to industrial biomedical platform. *Biochim. Biophys. Acta* 1863(7 Pt B), 1728–1748. doi: 10.1016/j.bbamcr.2015.10.014

Deriu, M. A., Bidone, T. C., Mastrangelo, F., Di Benedetto, G., Soncini, M., Montevecchi, F. M., et al. (2011). Biomechanics of actin filaments: a computational multi-level study. *J. Biomech.* 44, 630–636. doi: 10.1016/j.jbiomech.2010.11.014

Deriu, M. A., Shkurti, A., Paciello, G., Bidone, T. C., Morbiducci, U., Ficarra, E., et al. (2012). Multiscale modeling of cellular actin filaments: from atomistic molecular to coarse-grained dynamics. *Proteins* 80, 1598–1609. doi: 10.1002/prot.24053

Deriu, M. A., Soncini, M., Orsi, M., Patel, M., Essex, J. W., Montevecchi, F. M., et al. (2010). Anisotropic elastic network modeling of entire microtubules. *Biophys. J.* 99, 2190–2199. doi: 10.1016/j.bpj.2010.06.070

Dobrokhotov, O., Samsonov, M., Sokabe, M., and Hirata, H. (2018). Mechanoregulation and pathology of YAP/TAZ via hippo and non-hippo mechanisms. *Clin. Transl. Med.* 7:23. doi: 10.1186/s40169-018-0202-9

Downing, T. L., Soto, J., Morez, C., Houssin, T., Fritz, A., Yuan, F., et al. (2013). Biophysical regulation of epigenetic state and cell reprogramming. *Nat. Mater.* 12, 1154–1162.

Ehler, E. (2016). Cardiac cytoarchitecture — why the "hardware" is important for heart function! *Biochim. Biophys. Acta Mol.Cell Res.* 1863(7, Part B), 1857–1863. doi: 10.1016/j.bbamcr.2015.11.006

Elmore, D. E., and Dougherty, D. A. (2003). Investigating lipid composition effects on the mechanosensitive channel of large conductance (MscL) using molecular dynamics simulations. *Biophys. J.* 85, 1512–1524. doi: 10.1016/s0006-3495(03)74584-6

Elosegui-Artola, A., Andreu, I., Beedle, A. E. M., Lezamiz, A., Uroz, M., Kosmalska, A. J., et al. (2017). Force triggers YAP nuclear entry by regulating transport across nuclear pores. *Cell* 171, 1397–1410. doi: 10.1016/j.cell.2017.10.008

Engler, A. J., Sen, S., Sweeney, H. L., and Discher, D. E. (2006). Matrix elasticity directs stem cell lineage specification. *Cell* 126, 677–689.

Eom, K., Baek, S. C., Ahn, J. H., and Na, S. (2007). Coarse-graining of protein structures for the normal mode studies. *J. Comput. Chem.* 28, 1400–1410. doi: 10.1002/jcc.20672

Evans, N. D., Minelli, C., Gentleman, E., LaPointe, V., Patankar, S. N., Kallivretaki, M., et al. (2009). Substrate stiffness affects early differentiation events in embryonic stem cells. *Eur. Cell Mater.* 18, 1–13. doi: 10.22203/ecm.v018a01

Frangogiannis, N. G. (2017). The extracellular matrix in myocardial injury, repair, and remodeling. *J. Clin. Invest.* 127, 1600–1612. doi: 10.1172/jci87491

Frank, D., and Frey, N. (2011). Cardiac Z-disc signaling network. *J. Biol. Chem.* 286, 9897–9904. doi: 10.1074/jbc.R110.174268

Freed, L. E., Guilak, F., Guo, X. E., Gray, M. L., Tranquillo, R., Holmes, J. W., et al. (2006). Advanced tools for tissue engineering: scaffolds, bioreactors, and signaling. *Tissue Eng.* 12, 3285–3305. doi: 10.1089/ten.2006.12.3285

Freedman, H., Rezania, V., Priel, A., Carpenter, E., Noskov, S. Y., and Tuszynski, J. A. (2010). Model of ionic currents through microtubule nanopores and the lumen. *Phys. Rev. E Stat. Nonlin. Soft Matter. Phys.* 81(5 Pt 1):051912. doi: 10.1103/PhysRevE.81.051912

Gaetani, R., Yin, C., Srikumar, N., Braden, R., Doevendans, P. A., Sluijter, J. P., et al. (2016). Cardiac-derived extracellular matrix enhances cardiogenic properties of human cardiac progenitor cells. *Cell Transplant* 25, 1653–1663. doi: 10.3727/096368915x689794

Gaillard, T., Dejaegere, A., and Stote, R. H. (2009). Dynamics of beta3 integrin I-like and hybrid domains: insight from simulations on the mechanism of transition between open and closed forms. *Proteins* 76, 977–994. doi: 10.1002/prot.22404

Gaudesius, G., Miragoli, M., Thomas, S. P., and Rohr, S. (2003). Coupling of cardiac electrical activity over extended distances by fibroblasts of cardiac origin. *Circ. Res.* 93, 421–428. doi: 10.1161/01.res.0000089258.40661.0c

Gerdes, A. M., and Capasso, J. M. (1995). Structural remodeling and mechanical dysfunction of cardiac myocytes in heart failure. *J. Mol. Cell Cardiol.* 27, 849–856. doi: 10.1016/0022-2828(95)90000-4

Gjesdal, O., Bluemke, D., and Lima, J. (2011). Cardiac remodeling at the population level-risk factors, screening, and outcomes. *Nat. Rev. Cardiol.* 8, 673–685. doi: 10.1038/nrcardio.2011.154

Golji, J., Lam, J., and Mofrad, M. R. (2011). Vinculin activation is necessary for complete talin binding. *Biophys. J.* 100, 332–340. doi: 10.1016/j.bpj.2010.11.024

Gonzalez, A., Lopez, B., Ravassa, S., San Jose, G., and Diez, J. (2019). The complex dynamics of myocardial interstitial fibrosis in heart failure. Focus on collagen cross-linking. *Biochim. Biophys. Acta Mol. Cell Res.* 1866, 1421–1432. doi: 10.1016/j.bbamcr.2019.06.001

Grasso, G., Leanza, L., Morbiducci, U., Danani, A., and Deriu, M. A. (2019a). Aminoacid substitutions in the glycine zipper affect the conformational stability of amyloid beta fibrils. *J. Biomol. Struct. Dyn.* 2019, 1–8. doi: 10.1080/07391102.2019.1671224

Grasso, G., Rebella, M., Morbiducci, U., Tuszynski, J. A., Danani, A., and Deriu, M. A. (2019b). The role of structural polymorphism in driving the mechanical performance of the alzheimer's beta amyloid fibrils. *Front. Bioeng. Biotechnol.* 7:83. doi: 10.3389/fbioe.2019.00083

Grasso, G., Rebella, M., Muscat, S., Morbiducci, U., Tuszynski, J., Danani, A., et al. (2018). Conformational dynamics and stability of u-shaped and s-shaped amyloid beta assemblies. *Int. J. Mol. Sci.* 19:571. doi: 10.3390/ijms19020571

Grossman, W., Jones, D., and McLaurin, L. P. (1975). Wall stress and patterns of hypertrophy in the human left ventricle. *J. Clin. Invest.* 56, 56–64. doi: 10.1172/jci108079

Gullingsrud, J., Kosztin, D., and Schulten, K. (2001). Structural determinants of MscL gating studied by molecular dynamics simulations. *Biophys. J.* 80, 2074–2081. doi: 10.1016/s0006-3495(01)76181-4

Hanson, K. P., Jung, J. P., Tran, Q. A., Hsu, S. P., Iida, R., Ajeti, V., et al. (2013). Spatial and temporal analysis of extracellular matrix proteins in the developing murine heart: a blueprint for regeneration. *Tissue Eng. Part A* 19, 1132–1143. doi: 10.1089/ten.TEA.2012.0316

Heling, A., Zimmermann, R., Kostin, S., Maeno, Y., Hein, S., Devaux, B., et al. (2000). Increased expression of cytoskeletal, linkage, and extracellular proteins in failing human myocardium. *Circ. Res.* 86, 846–853. doi: 10.1161/01.res.86.8.846

Herrmann, H., Bar, H., Kreplak, L., Strelkov, S. V., and Aebi, U. (2007). Intermediate filaments: from cell architecture to nanomechanics. *Nat. Rev. Mol. Cell Biol.* 8, 562–573. doi: 10.1038/nrm2197

Hoes, M. F., Bomer, N., and van der Meer, P. (2019). Concise review: the current state of human in vitro cardiac disease modeling: a focus on gene editing and tissue engineering. *Stem Cells Transl. Med.* 8, 66–74. doi: 10.1002/sctm.18-0052

Hoffman, B. D., Grashoff, C., and Schwartz, M. A. (2011). Dynamic molecular processes mediate cellular mechanotransduction. *Nature* 475, 316–323. doi: 10.1038/nature10316

Hollingsworth, S. A., and Dror, R. O. (2018). Molecular dynamics simulation for all. *Neuron* 99, 1129–1143. doi: 10.1016/j.neuron.2018.08.011

Humphrey, J. D. (2001). Stress, strain, and mechanotransduction in cells. *J. Biomech. Eng.* 123, 638–641. doi: 10.1115/1.1406131

Ingber, D. E. (1997). Tensegrity: the architectural basis of cellular mechanotransduction. *Annu. Rev. Physiol.* 59, 575–599. doi: 10.1146/annurev.physiol.59.1.575

Ingber, D. E. (2003a). Tensegrity I. Cell structure and hierarchical systems biology. *J. Cell Sci.* 116(Pt 7), 1157–1173. doi: 10.1242/jcs.00359

Ingber, D. E. (2003b). Tensegrity II. How structural networks influence cellular information processing networks. *J. Cell Sci.* 116(Pt 8), 1397–1408. doi: 10.1242/jcs.00360

Jain, N., Iyer, K. V., Kumar, A., and Shivashankar, G. V. (2013). Cell geometric constraints induce modular gene-expression patterns via redistribution of HDAC3 regulated by actomyosin contractility. *Proc. Natl. Acad. Sci. U.S.A.* 110, 11349–11354. doi: 10.1073/pnas.1300801110

Janssen, P. M. L. (2019). Myocardial relaxation in human heart failure: why sarcomere kinetics should be center-stage. *Arch. Biochem. Biophys.* 661, 145–148. doi: 10.1016/j.abb.2018.11.011

Jung, J. P., Hu, D., Domian, I. J., and Ogle, B. M. (2015). An integrated statistical model for enhanced murine cardiomyocyte differentiation via optimized engagement of 3D extracellular matrices. *Sci. Rep.* 5:18705. doi: 10.1038/srep18705

Kamisago, M., Sharma, S. D., DePalma, S. R., Solomon, S., Sharma, P., McDonough, B., et al. (2000). Mutations in sarcomere protein genes as a cause of dilated cardiomyopathy. *N. Engl. J Med.* 343, 1688–1696. doi: 10.1056/nejm200012073432304

Kasas, S., Cibert, C., Kis, A., De Rios, P. L., Riederer, B. M., Forró, L., et al. (2004a). Oscillation modes of microtubules. *Biol. Cell* 96, 697–700. doi: 10.1016/j.biolcel.2004.09.002

Kasas, S., Kis, A., Riederer, B. M., Forró, L., Dietler, G., and Catsicas, S. (2004b). Mechanical properties of microtubules explored using the finite elements method. *Chem. Phys. Chem.* 5, 252–257. doi: 10.1002/cphc.200300799

Katz, A. M. (2002). Maladaptive growth in the failing heart: the cardiomyopathy of overload. *Cardiovasc. Drugs Ther.* 16, 245–249. doi: 10.1023/a:1020604623427

Kaushik, G., Spenlehauer, A., Sessions, A. O., Trujillo, A. S., Fuhrmann, A., Fu, Z., et al. (2015). Vinculin network-mediated cytoskeletal remodeling regulates contractile function in the aging heart. *Sci. Transl. Med.* 7:292ra299. doi: 10.1126/scitranslmed.aaa5843

Kennedy-Lydon, T., and Rosenthal, N. (2017). Cardiac regeneration: all work and no repair? *Sci. Transl. Med.* 9:eaad9019. doi: 10.1126/scitranslmed.aad9019

Keskin, O., Durell, S. R., Bahar, I., Jernigan, R. L., and Covell, D. G. (2002). Relating molecular flexibility to function: a case study of tubulin. *Biophys. J.* 83, 663–680. doi: 10.1016/s0006-3495(02)75199-0

Kim, H., Yoon, C. S., Kim, H., and Rah, B. (1999). Expression of extracellular matrix components fibronectin and laminin in the human fetal heart. *Cell Struct. Funct.* 24, 19–26. doi: 10.1247/csf.24.19

Kim, H. K., Kang, Y. G., Jeong, S. H., Park, N., Marquez, J., Ko, K. S., et al. (2018). Cyclic stretch increases mitochondrial biogenesis in a cardiac cell line. *Biochem. Biophys. Res. Commun.* 505, 768–774. doi: 10.1016/j.bbrc.2018.10.003

Kis, A., Kasas, S., Babiæ, B., Kulik, A. J., Benoît, W., Briggs, G. A. D., et al. (2002). Nanomechanics of microtubules. *Phys. Rev. Lett.* 89:248101. doi: 10.1103/PhysRevLett.89.248101

Kizer, N., Guo, X. L., and Hruska, K. (1997). Reconstitution of stretch-activated cation channels by expression of the alpha-subunit of the epithelial sodium channel cloned from osteoblasts. *Proc. Natl. Acad. Sci. U.S.A.* 94, 1013–1018. doi: 10.1073/pnas.94.3.1013

Kloda, A., and Martinac, B. (2001). Mechanosensitive channel of Thermoplasma, the cell wall-less archaea: cloning and molecular characterization. *Cell Biochem. Biophys.* 34, 321–347. doi: 10.1385/cbb:34:3, 321

Knoll, R., Hoshijima, M., and Chien, K. (2003). Cardiac mechanotransduction and implications for heart disease. *J. Mol. Med.* 81, 750–756. doi: 10.1007/s00109-003-0488-x

Korotkevich, E., Niwayama, R., Courtois, A., Friese, S., Berger, N., Buchholz, F., et al. (2017). The apical domain is required and sufficient for the first lineage segregation in the mouse embryo. *Dev. Cell* 40, 235–247. doi: 10.1016/j.devcel.2017.01.006

Kreplak, L., Herrmann, H., and Aebi, U. (2008). Tensile properties of single desmin intermediate filaments. *Biophys. J.* 94, 2790–2799. doi: 10.1529/biophysj.107.119826

Kuraitis, D., Hosoyama, K., Blackburn, N. J. R., Deng, C., Zhong, Z., and Suuronen, E. J. (2019). Functionalization of soft materials for cardiac repair and regeneration. *Crit. Rev. Biotechnol.* 39, 451–468. doi: 10.1080/07388551.2019.1572587

Lapidos, K. A., Kakkar, R., and McNally, E. M. (2004). The dystrophin glycoprotein complex: signaling strength and integrity for the sarcolemma. *Circ. Res.* 94, 1023–1031. doi: 10.1161/01.res.0000126574.61061.25

Lee, C. Y., Lou, J., Wen, K. K., McKane, M., Eskin, S. G., Ono, S., et al. (2013). Actin depolymerization under force is governed by lysine 113:glutamic acid 195-mediated catch-slip bonds. *Proc. Natl. Acad. Sci. U.S.A.* 110, 5022–5027. doi: 10.1073/pnas.1218407110

Lee, H., Eskin, S. G., Ono, S., Zhu, C., and McIntire, L. V. (2019). Force-history dependence and cyclic mechanical reinforcement of actin filaments at the single molecular level. *J. Cell Sci.* 132:e0216911. doi: 10.1242/jcs.216911

Lee, S. E., Chunsrivirot, S., Kamm, R. D., and Mofrad, M. R. (2008). Molecular dynamics study of talin-vinculin binding. *Biophys. J.* 95, 2027–2036. doi: 10.1529/biophysj.107.124487

Lee, S. E., Kamm, R. D., and Mofrad, M. R. (2007). Force-induced activation of talin and its possible role in focal adhesion mechanotransduction. *J. Biomech.* 40, 2096–2106. doi: 10.1016/j.jbiomech.2007.04.006

Lei, Y., and Ferdous, Z. (2016). Design considerations and challenges for mechanical stretch bioreactors in tissue engineering. *Biotechnol. Prog.* 32, 543–553. doi: 10.1002/btpr.2256

Leitolis, A., Robert, A. W., Pereira, I. T., Correa, A., and Stimamiglio, M. A. (2019). Cardiomyogenesis modeling using pluripotent stem cells: the role of microenvironmental signaling. *Front. Cell. Dev. Biol.* 7:164. doi: 10.3389/fcell.2019.00164

Lepre, M. G., Omar, S. I., Grasso, G., Morbiducci, U., Deriu, M. A., and Tuszynski, J. A. (2017). Insights into the effect of the G245S single point mutation on the structure of p53 and the binding of the protein to DNA. *Molecules* 22:58. doi: 10.3390/molecules22081358

Li, G., and Cui, Q. (2002). A coarse-grained normal mode approach for macromolecules: an efficient implementation and application to Ca(2+)-ATPase. *Biophys. J.* 83, 2457–2474. doi: 10.1016/s0006-3495(02)75257-0

Liau, B., Christoforou, N., Leong, K. W., and Bursac, N. (2011). Pluripotent stem cell-derived cardiac tissue patch with advanced structure and function. *Biomaterials* 32, 9180–9187. doi: 10.1016/j.biomaterials.2011.08.050

Lieu, D. K., Fu, J. D., Chiamvimonvat, N., Tung, K. C., McNerney, G. P., Huser, T., et al. (2013). Mechanism-based facilitated maturation of human pluripotent

stem cell-derived cardiomyocytes. *Circ. Arrhythm. Electrophysiol.* 6, 191–201. doi: 10.1161/circep.111.973420

Lindsey, S. E., Butcher, J. T., and Yalcin, H. C. (2014). Mechanical regulation of cardiac development. *Front. Physiol.* 5:318. doi: 10.3389/fphys.2014.00318

Lockhart, M., Wirrig, E., Phelps, A., and Wessels, A. (2011). Extracellular matrix and heart development. *Birth Defects Res. A Clin. Mol. Teratol.* 91, 535–550. doi: 10.1002/bdra.20810

Lomakin, A., Nader, G., and Piel, M. (2017). Forcing entry into the nucleus. *Dev. Cell* 43, 547–548. doi: 10.1016/j.devcel.2017.11.015

Majkut, S., Dingal, P. C., Dave, P., Discher, and Dennis, E. (2014). Stress sensitivity and mechanotransduction during heart development. *Curr. Biol.* 24, R495–R501. doi: 10.1016/j.cub.2014.04.027

Majkut, S., Idema, T., Swift, J., Krieger, C., Liu, A., Discher, et al. (2013). Heart-specific stiffening in early embryos parallels matrix and myosin expression to optimize beating. *Curr. Biol.* 23, 2434–2439. doi: 10.1016/j.cub.2013.10.057

Marrink, S. J., Risselada, H. J., Yefimov, S., Tieleman, D. P., and de Vries, A. H. (2007). The MARTINI force field: coarse grained model for biomolecular simulations. *J. Phys. Chem. B* 111, 7812–7824. doi: 10.1021/jp071097f

Marsano, A., Conficconi, C., Lemme, M., Occhetta, P., Gaudiello, E., Votta, E., et al. (2016). Beating heart on a chip: a novel microfluidic platform to generate functional 3D cardiac microtissues. *Lab. Chip.* 16, 599–610. doi: 10.1039/c5lc01356a

Matsumoto, A., Kamata, T., Takagi, J., Iwasaki, K., and Yura, K. (2008). Key interactions in integrin ectodomain responsible for global conformational change detected by elastic network normal-mode analysis. *Biophys. J.* 95, 2895–2908. doi: 10.1529/biophysj.108.131045

McBeath, R., Pirone, D. M., Nelson, C. M., Bhadriraju, K., and Chen, C. S. (2004). Cell Shape, cytoskeletal tension, and RhoA regulate stem cell lineage commitment. *Dev. Cell* 6, 483–495.

McCammon, J. A., Gelin, B. R., and Karplus, M. (1977). Dynamics of folded proteins. *Nature* 267, 585–590. doi: 10.1038/267585a0

Meilhac, S. M., and Buckingham, M. E. (2018). The deployment of cell lineages that form the mammalian heart. *Nat. Rev. Cardiol.* 15, 705–724. doi: 10.1038/s41569-018-0086-9

Monticelli, L., Kandasamy, S. K., Periole, X., Larson, R. G., Tieleman, D. P., and Marrink, S. J. (2008). The MARTINI coarse-grained force field: extension to proteins. *J. Chem. Theory Comput.* 4, 819–834. doi: 10.1021/ct700324x

Moreno-Layseca, P., Icha, J., Hamidi, H., and Ivaska, J. (2019). Integrin trafficking in cells and tissues. *Nat. Cell Biol.* 21, 122–132. doi: 10.1038/s41556-018-0223-z

Morikawa, Y., Heallen, T., Leach, J., Xiao, Y., and Martin, J. F. (2017). Dystrophin-glycoprotein complex sequesters Yap to inhibit cardiomyocyte proliferation. *Nature* 547, 227–231. doi: 10.1038/nature22979

Nawata, J., Ohno, I., Isoyama, S., Suzuki, J., Miura, S., Ikeda, J., et al. (1999). Differential expression of alpha 1, alpha 3 and alpha 5 integrin subunits in acute and chronic stages of myocardial infarction in rats. *Cardiovasc. Res.* 43, 371–381. doi: 10.1016/s0008-6363(99)00117-0

Nelson, C. M., Jean, R. P., Tan, J. L., Liu, W. F., Sniadecki, N. J., Spector, A. A., et al. (2005). Emergent patterns of growth controlled by multicellular form and mechanics. *Proc. Natl. Acad. Sci. U.S.A.* 102, 11594–11599.

Nishioka, N., Inoue, K.-I., Adachi, K., Kiyonari, H., Ota, M., Ralston, A., et al. (2009). The Hippo signaling pathway components lats and yap pattern tead4 activity to distinguish mouse trophectoderm from inner cell mass. *Dev. Cell* 16, 398–410. doi: 10.1016/j.devcel.2009.02.003

Notari, M., Ventura-Rubio, A., Bedford-Guaus, S. J., Jorba, I., Mulero, L., Navajas, D., et al. (2018). The local microenvironment limits the regenerative potential of the mouse neonatal heart. *Sci. Adv.* 4:eaao5553. doi: 10.1126/sciadv.aao5553

Nunes, S. S., Miklas, J. W., Liu, J., Aschar-Sobbi, R., Xiao, Y., Zhang, B., et al. (2013). Biowire: a platform for maturation of human pluripotent stem cell-derived cardiomyocytes. *Nat. Methods* 10, 781–787. doi: 10.1038/nmeth.2524

Ogle, B. M., Bursac, N., Domian, I., Huang, N. F., Menasche, P., Murry, C. E., et al. (2016). Distilling complexity to advance cardiac tissue engineering. *Sci. Transl. Med.* 8:342s313. doi: 10.1126/scitranslmed.aad2304

Omens, J. H. (1998). Stress and strain as regulators of myocardial growth. *Prog. Biophys. Mol. Biol.* 69, 559–572. doi: 10.1016/s0079-6107(98)00025-x

Ottaviano, F. G., and Yee, K. O. (2011). Communication signals between cardiac fibroblasts and cardiac myocytes. *J. Cardiovasc. Pharmacol.* 57, 513–521. doi: 10.1097/FJC.0b013e31821209ee

Ou, D. B., He, Y., Chen, R., Teng, J. W., Wang, H. T., Zeng, D., et al. (2011). Three-dimensional co-culture facilitates the differentiation of embryonic stem cells into mature cardiomyocytes. *J. Cell Biochem.* 112, 3555–3562. doi: 10.1002/jcb.23283

Paez-Mayorga, J., Hernandez-Vargas, G., Ruiz-Esparza, G. U., Iqbal, H. M. N., Wang, X., Zhang, Y. S., et al. (2019). Bioreactors for cardiac tissue engineering. *Adv. Healthc. Mater.* 8:e1701504. doi: 10.1002/adhm.201701504

Paige, S. L., Plonowska, K., Xu, A., and Wu, S. M. (2015). Molecular regulation of cardiomyocyte differentiation. *Circ. Res.* 116, 341–353. doi: 10.1161/circresaha.116.302752

Papalazarou, V., Salmeron-Sanchez, M., and Machesky, L. M. (2018). Tissue engineering the cancer microenvironment—challenges and opportunities. *Biophys. Rev.* 10, 1695–1711. doi: 10.1007/s12551-018-0466-8

Paramore, S., and Voth, G. A. (2006). Examining the influence of linkers and tertiary structure in the forced unfolding of multiple-repeat spectrin molecules. *Biophys. J.* 91, 3436–3445. doi: 10.1529/biophysj.106.091108

Paulhe, F., Manenti, S., Ysebaert, L., Betous, R., Sultan, P., and Racaud-Sultan, C. (2005). Integrin function and signaling as pharmacological targets in cardiovascular diseases and in cancer. *Curr. Pharm. Des.* 11, 2119–2134. doi: 10.2174/1381612054065765

Pfaendtner, J., Lyman, E., Pollard, T. D., and Voth, G. A. (2010). Structure and dynamics of the actin filament. *J. Mol. Biol.* 396, 252–263. doi: 10.1016/j.jmb.2009.11.034

Piccolo, S., Dupont, S., and Cordenonsi, M. (2014). The biology of YAP/TAZ: hippo signaling and beyond. *Physiol. Rev.* 94, 1287–1312. doi: 10.1152/physrev.00005.2014

Pocaterra, A., Romani, P., and Dupont, S. (2020). YAP/TAZ functions and their regulation at a glance. *J. Cell Sci.* 133:425. doi: 10.1242/jcs.230425

Pokorný, J., Jelínek, F., Trkal, V., Lamprecht, I., and Hölzel, R. (1997). Vibrations in microtubules. *J. Biol. Phys.* 23, 171–179. doi: 10.1023/A:1005092601078

Portet, S., Tuszynski, J. A., Hogue, C. W., and Dixon, J. M. (2005). Elastic vibrations in seamless microtubules. *Eur. Biophys. J.* 34, 912–920. doi: 10.1007/s00249-005-0461-4

Priel, A., Ramos, A. J., Tuszynski, J. A., and Cantiello, H. F. (2006). A biopolymer transistor: electrical amplification by microtubules. *Biophys. J.* 90, 4639–4643. doi: 10.1529/biophysj.105.078915

Provasi, D., Murcia, M., Coller, B. S., and Filizola, M. (2009). Targeted molecular dynamics reveals overall common conformational changes upon hybrid domain swing-out in beta3 integrins. *Proteins* 77, 477–489. doi: 10.1002/prot.22463

Puklin-Faucher, E., Gao, M., Schulten, K., and Vogel, V. (2006). How the headpiece hinge angle is opened: new insights into the dynamics of integrin activation. *J. Cell Biol.* 175, 349–360. doi: 10.1083/jcb.200602071

Puklin-Faucher, E., and Vogel, V. (2009). Integrin activation dynamics between the RGD-binding site and the headpiece hinge. *J. Biol. Chem.* 284, 36557–36568. doi: 10.1074/jbc.M109.041194

Qin, Z., Kreplak, L., and Buehler, M. J. (2009). Nanomechanical properties of vimentin intermediate filament dimers. *Nanotechnology* 20:425101. doi: 10.1088/0957-4484/20/42/425101

Radisic, M., Marsano, A., Maidhof, R., Wang, Y., and Vunjak-Novakovic, G. (2008). Cardiac tissue engineering using perfusion bioreactor systems. *Nat. Protoc.* 3, 719–738. doi: 10.1038/nprot.2008.40

Reis, L. A., Chiu, L. L., Feric, N., Fu, L., and Radisic, M. (2016). Biomaterials in myocardial tissue engineering. *J. Tissue Eng. Regen. Med.* 10, 11–28. doi: 10.1002/term.1944

Roca-Cusachs, P., Iskratsch, T., and Sheetz, M. P. (2012). Finding the weakest link: exploring integrin-mediated mechanical molecular pathways. *J. Cell Sci.* 125(Pt 13), 3025–3038. doi: 10.1242/jcs.095794

Ronaldson-Bouchard, K., Ma, S. P., Yeager, K., Chen, T., Song, L., Sirabella, D., et al. (2018). Advanced maturation of human cardiac tissue grown from pluripotent stem cells. *Nature* 556, 239–243. doi: 10.1038/s41586-018-0016-3

Ronaldson-Bouchard, K., Yeager, K., Teles, D., Chen, T., Ma, S., Song, L., et al. (2019). Engineering of human cardiac muscle electromechanically matured to an adult-like phenotype. *Nat. Protoc.* 14, 2781–2817. doi: 10.1038/s41596-019-0189-8

Ross, R. S. (2002). The extracellular connections: the role of integrins in myocardial remodeling. *J. Card. Fail.* 8(6 Suppl.), S326–S331. doi: 10.1054/jcaf.2002.129263

Ross, R. S., and Borg, T. K. (2001). Integrins and the myocardium. *Circ. Res.* 88, 1112–1119. doi: 10.1161/hh1101.091862

Ruan, J. L., Tulloch, N. L., Razumova, M. V., Saiget, M., Muskheli, V., Pabon, L., et al. (2016). Mechanical stress conditioning and electrical stimulation promote contractility and force maturation of induced pluripotent stem cell-derived human cardiac tissue. *Circulation* 134, 1557–1567. doi: 10.1161/circulationaha.114.014998

Ruan, J. L., Tulloch, N. L., Saiget, M., Paige, S. L., Razumova, M. V., Regnier, M., et al. (2015). Mechanical stress promotes maturation of human myocardium from pluripotent stem cell-derived progenitors. *Stem Cells* 33, 2148–2157. doi: 10.1002/stem.2036

Sachs, F. (2010). Stretch-activated ion channels: what are they? *Physiology* 25, 50–56. doi: 10.1152/physiol.00042.2009

Samuel, J. L., Barrieux, A., Dufour, S., Dubus, I., Contard, F., Koteliansky, V., et al. (1991). Accumulation of fetal fibronectin mRNAs during the development of rat cardiac hypertrophy induced by pressure overload. *J. Clin. Invest.* 88, 1737–1746. doi: 10.1172/jci115492

Sawada, Y., Murase, M., and Sokabe, M. (2012). The gating mechanism of the bacterial mechanosensitive channel MscL revealed by molecular dynamics simulations: from tension sensing to channel opening. *Channels* 6, 317–331. doi: 10.4161/chan.21895

Schaper, J., and Speiser, B. (1992). The extracellular matrix in the failing human heart. *Basic Res. Cardiol.* 87(Suppl. 1), 303–309. doi: 10.1007/978-3-642-72474-9_26

Sequeira, V., Nijenkamp, L. L. A. M., Regan, J. A., and van der Velden, J. (2014). The physiological role of cardiac cytoskeleton and its alterations in heart failure. *Biochim. Biophys. Acta Biomemb.*1838, 700–722. doi: 10.1016/j.bbamem.2013.07.011

Sessions, A. O., and Engler, A. J. (2016). Mechanical regulation of cardiac aging in model systems. *Circ. Res.* 118, 1553–1562. doi: 10.1161/circresaha.116.307472

Soncini, M., Vesentini, S., Ruffoni, D., Orsi, M., Deriu, M. A., and Redaelli, A. (2007). Mechanical response and conformational changes of alpha-actinin domains during unfolding: a molecular dynamics study. *Biomech. Model. Mechanobiol.* 6, 399–407. doi: 10.1007/s10237-006-0060-z

Sotomayor, M., and Schulten, K. (2004). Molecular dynamics study of gating in the mechanosensitive channel of small conductance MscS. *Biophys. J.* 87, 3050–3065. doi: 10.1529/biophysj.104.046045

Stephens, A. D., Banigan, E. J., and Marko, J. F. (2018). Separate roles for chromatin and lamins in nuclear mechanics. *Nucleus* 9, 119–124. doi: 10.1080/19491034.2017.1414118

Sukharev, S. I., Sigurdson, W. J., Kung, C., and Sachs, F. (1999). Energetic and spatial parameters for gating of the bacterial large conductance mechanosensitive channel, MscL. *J. Gen. Physiol.* 113, 525–540. doi: 10.1085/jgp.113.4.525

Takagi, J., Petre, B. M., Walz, T., and Springer, T. A. (2002). Global conformational rearrangements in integrin extracellular domains in outside-in and inside-out signaling. *Cell* 110, 599–511. doi: 10.1016/s0092-8674(02)00935-2

Tama, F., Gadea, F. X., Marques, O., and Sanejouand, Y. H. (2000). Building-block approach for determining low-frequency normal modes of macromolecules. *Proteins* 41, 1–7.

Tama, F., and Sanejouand, Y. H. (2001). Conformational change of proteins arising from normal mode calculations. *Protein Eng.* 14, 1–6. doi: 10.1093/protein/14.1.1

Tatke, S. S., Loong, C. K., D'Souza, N., Schoephoerster, R. T., and Prabhakaran, M. (2008). Large scale motions in a biosensor protein glucose oxidase: a combined approach by QENS, normal mode analysis, and molecular dynamics studies. *Biopolymers* 89, 582–594. doi: 10.1002/bip.20956

Tavi, P., Laine, M., Weckstrom, M., and Ruskoaho, H. (2001). Cardiac mechanotransduction: from sensing to disease and treatment. *Trends Pharmacol. Sci.* 22, 254–260. doi: 10.1016/s0165-6147(00)01679-5

Teng, J., Loukin, S., and Kung, C. (2014). Mechanosensitive ion channels in cardiovascular physiology. *Exp. Clin. Cardiol.* 20, 6550–6560.

Thompson, R. P., Fitzharris, T. P., Denslow, S., and LeRoy, E. C. (1979). Collagen synthesis in the developing chick heart. *Tex. Rep. Biol. Med.* 39, 305–319.

Tomov, M. L., Gil, C. J., Cetnar, A., Theus, A. S., Lima, B. J., Nish, J. E., et al. (2019). Engineering functional cardiac tissues for regenerative medicine applications. *Curr. Cardiol. Rep.* 21:105. doi: 10.1007/s11886-019-1178-9

Tyser, R. C. V., Miranda, A. M. A., Chen, C. M., Davidson, S. M., Srinivas, S., and Riley, P. R. (2016). Calcium handling precedes cardiac differentiation to initiate the first heartbeat. *eLife* 5:e17113. doi: 10.7554/eLife.17113

Ugolini, G. S., Rasponi, M., Pavesi, A., Santoro, R., Kamm, R., Fiore, G. B., et al. (2016). On-chip assessment of human primary cardiac fibroblasts proliferative responses to uniaxial cyclic mechanical strain. *Biotechnol. Bioeng.* 113, 859–869. doi: 10.1002/bit.25847

Ugolini, G. S., Visone, R., Cruz-Moreira, D., Mainardi, A., and Rasponi, M. (2018). Generation of functional cardiac microtissues in a beating heart-on-a-chip. *Methods Cell Biol.* 146, 69–84. doi: 10.1016/bs.mcb.2018.05.005

Valls-Margarit, M., Iglesias-García, O., Di Guglielmo, C., Sarlabous, L., Tadevosyan, K., Paoli, R., et al. (2019). Engineered macroscale cardiac constructs elicit human myocardial tissue-like functionality. *Stem Cell Rep.* 13, 207–220. doi: 10.1016/j.stemcr.2019.05.024

van den Berg, C. W., Elliott, D. A., Braam, S. R., Mummery, C. L., and Davis, R. P. (2016). Differentiation of human pluripotent stem cells to cardiomyocytes under defined conditions. *Methods Mol. Biol.* 1353, 163–180. doi: 10.1007/7651_2014_178

Vining, K. H., and Mooney, D. J. (2017). Mechanical forces direct stem cell behaviour in development and regeneration. *Nat. Rev. Mol. Cell Biol.* 18, 728–742. doi: 10.1038/nrm.2017.108

Wan, H., Gu, C., Gan, Y., Wei, X., Zhu, K., Hu, N., et al. (2018). Sensor-free and sensor-based heart-on-a-chip platform: a review of design and applications. *Curr. Pharm. Des.* 24, 5375–5385. doi: 10.2174/1381612825666190207170004

Wang, C. Y., and Zhang, L. C. (2008). Circumferential vibration of microtubules with long axial wavelength. *J. Biomech.* 41, 1892–1896. doi: 10.1016/j.jbiomech.2008.03.029

Williams, C., Quinn, K. P., Georgakoudi, I., and Black, L. D. (2014). Young developmental age cardiac extracellular matrix promotes the expansion of neonatal cardiomyocytes in vitro. *Acta Biomater.* 10, 194–204. doi: 10.1016/j.actbio.2013.08.037

Williams, C., Sullivan, K., and Black, L. D. (2015). Partially digested adult cardiac extracellular matrix promotes cardiomyocyte proliferation in vitro. *Adv. Healthc. Mater.* 4, 1545–1554. doi: 10.1002/adhm.201500035

Wilson, A. J., Schoenauer, R., Ehler, E., Agarkova, I., and Bennett, P. M. (2014). Cardiomyocyte growth and sarcomerogenesis at the intercalated disc. *Cell Mol. Life Sci.* 71, 165–181. doi: 10.1007/s00018-013-1374-5

Wissing, T. B., Bonito, V., Bouten, C. V. C., and Smits, A. (2017). Biomaterial-driven in situ cardiovascular tissue engineering-a multi-disciplinary perspective. *NPJ Regen. Med.* 2:18. doi: 10.1038/s41536-017-0023-2

Wong, T. Y., Juang, W. C., Tsai, C. T., Tseng, C. J., Lee, W. H., Chang, S. N., et al. (2018). Mechanical stretching simulates cardiac physiology and pathology through mechanosensor piezo1. *J. Clin. Med.* 7:410. doi: 10.3390/jcm7110410

Wriggers, W., and Schulten, K. (1997). Stability and dynamics of G-actin: back-door water diffusion and behavior of a subdomain 3/4 loop. *Biophys. J.* 73, 624–639. doi: 10.1016/s0006-3495(97)78098-6

Xiong, J. P., Stehle, T., Goodman, S. L., and Arnaout, M. A. (2003). New insights into the structural basis of integrin activation. *Blood* 102, 1155–1159. doi: 10.1182/blood-2003-01-0334

Yang, C., Tibbitt, M. W., Basta, L., and Anseth, K. S. (2014). Mechanical memory and dosing influence stem cell fate. *Nat. Mater.* 13, 645–652.

Yang, L. W., and Chng, C. P. (2008). Coarse-grained models reveal functional dynamics–I. Elastic network models–theories, comparisons and perspectives. *Bioinform. Biol. Insights* 2, 25–45. doi: 10.4137/bbi.s460

Yao, M., Goult, B. T., Chen, H., Cong, P., Sheetz, M. P., and Yan, J. (2014). Mechanical activation of vinculin binding to talin locks talin in an unfolded conformation. *Sci. Rep.* 4:4610. doi: 10.1038/srep04610

Ye, N., Verma, D., Meng, F., Davidson, M. W., Suffoletto, K., and Hua, S. Z. (2014). Direct observation of alpha-actinin tension and recruitment at focal adhesions during contact growth. *Exp. Cell Res.* 327, 57–67. doi: 10.1016/j.yexcr.2014.07.026

Yoshimura, H., Nishio, T., Mihashi, K., Kinosita, K. Jr., and Ikegami, A. (1984). Torsional motion of eosin-labeled F-actin as detected in the time-resolved anisotropy decay of the probe in the sub-millisecond time range. *J. Mol. Biol.* 179, 453–467. doi: 10.1016/0022-2836(84)90075-5

Zhang, J., Tao, R., Campbell, K. F., Carvalho, J. L., Ruiz, E. C., Kim, G. C., et al. (2019). Functional cardiac fibroblasts derived from human pluripotent stem

cells via second heart field progenitors. *Nat. Commun.* 10:2238. doi: 10.1038/s41467-019-09831-5

Zhang, J., and Wang, C. (2014). Molecular structural mechanics model for the mechanical properties of microtubules. *Biomech. Model. Mechanobiol.* 13, 1175–1184. doi: 10.1007/s10237-014-0564-x

Zhang, P., Su, J., and Mende, U. (2012). Cross talk between cardiac myocytes and fibroblasts: from multiscale investigative approaches to mechanisms and functional consequences. *Am. J. Physiol. Heart Circ. Physiol.* 303, H1385–H1396. doi: 10.1152/ajpheart.01167.2011

Zierhut, W., Zimmer, H. G., and Gerdes, A. M. (1991). Effect of angiotensin converting enzyme inhibition on pressure-induced left ventricular hypertrophy in rats. *Circ. Res.* 69, 609–617. doi: 10.1161/01.res.69.3.609

Zimmermann, W. H., Fink, C., Kralisch, D., Remmers, U., Weil, J., and Eschenhagen, T. (2000). Three-dimensional engineered heart tissue from neonatal rat cardiac myocytes. *Biotechnol. Bioeng.* 68, 106–114.

Conflict of Interest: The authors declare that the research was conducted in the absence of any commercial or financial relationships that could be construed as a potential conflict of interest.

Copyright © 2020 Gaetani, Zizzi, Deriu, Morbiducci, Pesce and Messina. This is an open-access article distributed under the terms of the Creative Commons Attribution License (CC BY). The use, distribution or reproduction in other forums is permitted, provided the original author(s) and the copyright owner(s) are credited and that the original publication in this journal is cited, in accordance with accepted academic practice. No use, distribution or reproduction is permitted which does not comply with these terms.

frontiers in Cell and Developmental Biology

REVIEW
published: 28 January 2020
doi: 10.3389/fcell.2020.00006

Adherens Junctions: Guardians of Cortical Development

*Lenin Veeraval, Conor J. O'Leary and Helen M. Cooper**

Queensland Brain Institute, The University of Queensland, Brisbane, QLD, Australia

Apical radial glia comprise the pseudostratified neuroepithelium lining the embryonic lateral ventricles and give rise to the extensive repertoire of pyramidal neuronal subtypes of the neocortex. The establishment of a highly apicobasally polarized radial glial morphology is a mandatory prerequisite for cortical development as it governs neurogenesis, neural migration and the integrity of the ventricular wall. As in all epithelia, cadherin-based adherens junctions (AJs) play an obligate role in the maintenance of radial glial apicobasal polarity and neuroepithelial cohesion. In addition, the assembly of resilient AJs is critical to the integrity of the neuroepithelium which must resist the tensile forces arising from increasing CSF volume and other mechanical stresses associated with the expansion of the ventricles in the embryo and neonate. Junctional instability leads to the collapse of radial glial morphology, disruption of the ventricular surface and cortical lamination defects due to failed neuronal migration. The fidelity of cortical development is therefore dependent on AJ assembly and stability. Mutations in genes known to control radial glial junction formation are causative for a subset of inherited cortical malformations (neuronal heterotopias) as well as perinatal hydrocephalus, reinforcing the concept that radial glial junctions are pivotal determinants of successful corticogenesis. In this review we explore the key animal studies that have revealed important insights into the role of AJs in maintaining apical radial glial morphology and function, and as such, have provided a deeper understanding of the aberrant molecular and cellular processes contributing to debilitating cortical malformations. We highlight the reciprocal interactions between AJs and the epithelial polarity complexes that impose radial glial apicobasal polarity. We also discuss the critical molecular networks promoting AJ assembly in apical radial glia and emphasize the role of the actin cytoskeleton in the stabilization of cadherin adhesion – a crucial factor in buffering the mechanical forces exerted as a consequence of cortical expansion.

Keywords: cortical development, radial glia, adherens junctions, cortical malformation, ependymal cell, apicobasal polarity, actin cytoskeleton, cadherin

OPEN ACCESS

Edited by:
Selwin K. Wu,
National University of Singapore, Singapore

Reviewed by:
Guillermo Alberto Gomez, University of South Australia, Australia
Orest William Blaschuk, McGill University, Canada
Lin Deng, Harvard Medical School, United States

***Correspondence:**
Helen M. Cooper
h.cooper@uq.edu.au

Specialty section:
This article was submitted to Cell Adhesion and Migration, a section of the journal Frontiers in Cell and Developmental Biology

Received: *31 October 2019*
Accepted: *10 January 2020*
Published: *28 January 2020*

Citation:
Veeraval L, O'Leary CJ and Cooper HM (2020) Adherens Junctions: Guardians of Cortical Development. Front. Cell Dev. Biol. 8:6. doi: 10.3389/fcell.2020.00006

INTRODUCTION

Uniquely human attributes such as consciousness, creativity and language as well as other higher order functions, including sensory perception, learning and memory arise as a consequence of the enormous array of excitatory pyramidal neurons that populate the six-layered neocortex. As a general principle, neurons of a given subtype are associated with a specific cortical layer (Molyneaux et al., 2007; Fame et al., 2011). For example, the corticospinal motor neurons which

project their axons subcerebrally to the spinal cord are the principal pyramidal subtype of layer 5. In contrast, cortical projection neurons predominantly populate layers 2/3 and send their axons across the corpus callosum to the contralateral hemisphere. However, in reality, cortical architecture is considerably more complex as a variety of subtypes exist within each layer, and conversely, one subtype can be found in multiple layers (O'Leary and Koester, 1993; Kasper et al., 1994; Molyneaux et al., 2007; Fame et al., 2011). This elaborate cytoarchitecture is fundamental to the establishment of the neuronal circuitry which dictates the extent and quality of information flow across the cortex and between the cortex and subcortical regions. Our ability to effectively interact with the world is therefore dependent on the fundamental cell biological processes regulating the birth of new neurons and their subsequent migration to their predetermined cortical layer.

The neural progenitors that give rise directly or indirectly to all pyramidal neurons in the neocortex are classified as apical radial glia (apical RGs) and comprise the pseudostratified neuroepithelium lining the embryonic ventricles (**Figure 1A**) (Kriegstein and Alvarez-Buylla, 2009; Paridaen and Huttner, 2014; Taverna et al., 2014). The highly apicobasally polarized morphology of apical RGs is a mandatory requirement for successful cortical development as it governs the mode of cell division, neuronal production, specification and migration, and the integrity of the ventricular wall. Adherens junctions (AJs), the sites of cadherin-mediated cell–cell adhesion, play an obligate role in the induction and maintenance of apical RG polarity and are thus pivotal determinants of progenitor function and the establishment of a functional neocortex (Stocker and Chenn, 2015; Bustamante et al., 2019). Throughout the developmental period AJs undergo constant remodeling as RGs divide, new progenitors re-establish adhesion and their progeny detach from the neuroepithelium. Concomitantly, it is essential that RG junctions resist the mechanical stresses exerted as a consequence of these cellular behaviors as well as the forces incurred from increasing cerebrospinal fluid (CSF) volume and flow.

Junctional instability leads to the collapse of apical RG morphology, disruption of the ventricular surface and cortical lamination defects due to failed neuronal migration (Kadowaki et al., 2007; Cappello et al., 2012; Gil-Sanz et al., 2014; O'Leary et al., 2017). As in all epithelia, adhesive strength is determined by reciprocal interactions between the cadherins and the actin cytoskeleton which also regulates junctional tension through actomyosin contractility (Priya and Yap, 2015; Yap et al., 2017). It is now clear that junctional failure underpins the etiology of cortical malformations where the inability to assemble AJs leads to reduced neuronal production, the accumulation of neurons in ectopic positions (neuronal heterotopias), incorrect cortical layering and disruption of the ventricular wall. Mutations responsible for inherited cortical malformations have been identified in genes known to control junction formation (Fox et al., 1998; Sheen et al., 2003; Ferland et al., 2009; Lian and Sheen, 2015). These cortical malformations have profound consequences for survival and the individual's quality of life. Therefore, the molecular pathways that promote cadherin adhesion and actin remodeling are crucial factors safeguarding the fidelity of cortical development.

During late embryonic and early postnatal life apical RGs transform into ependymal cells which line the ventricles throughout the adult central nervous system. Ependymal cells form an apicobasally polarized, multi-ciliated epithelium that acts as a bidirectional barrier to transport CSF components between the ventricle and the brain parenchyma (Del Bigio, 2010). The establishment of cadherin-based AJs and a polarized ependymal morphology is essential for barrier function. Hydrocephalus, a prevalent neurodevelopmental disorder associated with neonatal lethality, severe intellectual impairment and motor dysfunction, is characterized by the dilation of the lateral ventricles and reduction in cortical tissue volume (ventromegaly) resulting from excessive CSF (Kousi and Katsanis, 2016). Failure to establish a cohesive ependymal layer in the neonatal telencephalon due to the disruption of AJs in ependymal cells and their predecessors, the apical RGs, is causal for hydrocephalus (Dominguez-Pinos et al., 2005; Rodriguez et al., 2012; Guerra et al., 2015). Moreover, the occurrence of hydrocephalus is often coincident with neuronal heterotopias, indicating that these cortical malformations share a common etiology – the loss of AJs (Sheen et al., 2004; Rodriguez et al., 2012; Jimenez et al., 2014; Guerra et al., 2015).

In this review, we focus on the mechanisms by which AJs ensure successful cortical development and reflect on how our knowledge of apical RG and ependymal junction biology has led to a deeper understanding of the aberrant molecular and cellular processes contributing to devastating cortical malformations. We will explore the pivotal animal studies that have revealed important insights into the role of AJs in maintaining apical RG and ependymal morphology and function, and discuss the important molecular interactions underpinning AJ assembly. We highlight the reciprocal interactions between junctions and the epithelial polarity complexes which govern the establishment of RG apicobasal polarity. In addition, we discuss the role of the actin cytoskeleton in the stabilization of cadherin adhesion – a crucial factor in buffering the mechanical forces exerted as a consequence of cortical expansion. We begin, however, with a brief summary of the key features of cortical development. For more in-depth reviews on this topic see Paridaen and Huttner (2014), Taverna et al. (2014), Lodato and Arlotta (2015), Hansen et al. (2017), and Huttner and Wieland (2019).

A Brief Summary of Cortical Development

In the early vertebrate embryo the brain and spinal cord arise from the pseudostratified neuroepithelial stem cells of the neural tube. Corticogenesis begins in the dorsal telencephalon when these cells transform into apical RGs which retain their apicobasal polarity throughout development by anchoring their basal end feet to the pial extracellular matrix and their apical end feet to the ventricular surface (**Figure 1A**) (Kriegstein and Alvarez-Buylla, 2009; Paridaen and Huttner, 2014). Production of cortical neurons is temporally restricted, with deep layer 5/6 neurons born in the early phase of corticogenesis and upper layer 2/3

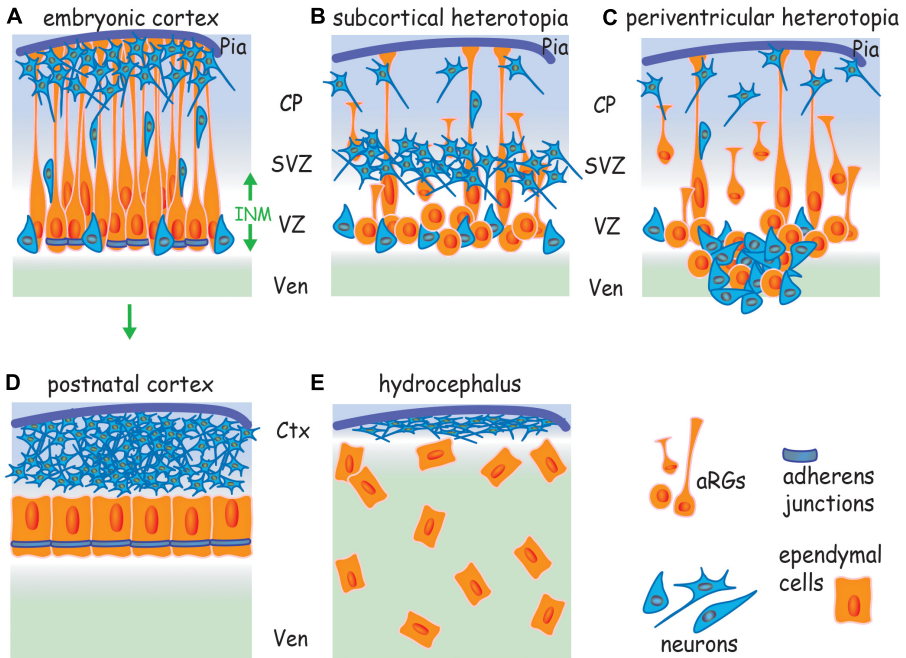

FIGURE 1 | Cortical malformations arise from a failure to assemble AJs. **(A)** Apicobasally polarized RGs undergo symmetric divisions to expand the progenitor pool and then switch to asymmetric division, generating a new apical RG and a neuron or intermediate progenitor. Neurons undergo radial migration along basal processes to populate the cortical plate. AJs encircle the apical RG at the border of the apical and lateral membranes. Failure to assemble AJs and the subsequent loss of RG polarity leads to **(B)** subcortical band heterotopia due to the retraction of basal processes, and **(C)** periventricular heterotopia due to the retraction of basal processes and disruption of the ventricular wall. **(D)** Ependymal cells derive from apical RGs (arrow) and form an apicobasally polarized epithelium. **(E)** Hydrocephalus arises from a failure to establish a cohesive ependymal layer due to the disruption of AJs in apical RGs and ependymal cells. Ctx, cortex; CP, cortical plate; INM, interkinetic nuclear migration; SVZ, subventricular zone; Ven, ventricle; VZ, ventricular zone.

neurons generated in the later developmental period (Molyneaux et al., 2007; Fame et al., 2011). Initially, apical RGs undergo symmetric self-renewing divisions to expand the progenitor pool and then switch to asymmetric neurogenic divisions, generating a progenitor and a neuron which is destined to populate deep layers 5/6 (Miyata et al., 2004; Huttner and Kosodo, 2005; Konno et al., 2008; Paridaen and Huttner, 2014; Oberst et al., 2019). As corticogenesis proceeds the generation of neurons directly from asymmetric RG division ceases, and instead, an array of diverse intermediate progenitor populations are produced (Farkas and Huttner, 2008; Kowalczyk et al., 2009; Postiglione et al., 2011). These secondary progenitors then undergo neurogenic division above the ventricular zone (i.e., in the subventricular zone; **Figure 1A**) to give rise predominantly to upper layer pyramidal neurons. It is the evolutionary expansion of these apical RG-derived intermediate progenitor populations that is responsible for the extensive production of pyramidal neurons that gives rise to the gyrencephalic architecture of the human neocortex. The evolution and cell biology of these fascinating progenitor populations have been comprehensively reviewed by others (Smart et al., 2002; Reillo et al., 2011; Betizeau et al., 2013; Kelava et al., 2013; Huttner and Wieland, 2019). It should be further noted that the mechanical gradients generated in the embryonic cortical tissue and the biomechanics of cortical folding associated with the expansion of the gyrencephalic cortex do not involve apical RGs. Instead, cortical folding arises as a consequence of the massive accumulation of neurons within the cortical plate. The vast majority of these neurons are generated from the basal radial glia (intermediate progenitors) within in the subventricular zone (Striedter et al., 2015; Llinares-Benadero and Borrell, 2019).

Due to the requirement to accommodate large numbers of progenitors within a confined space apical RGs undergo a specialized form of cell division, interkinetic nuclear migration, in which their nuclei migrate toward the pial surface during the G1 phase of the cell cycle (**Figure 1A**) (Sauer, 1935; Murciano et al., 2002; Taverna and Huttner, 2010). S-phase is completed at the ventricular-subventricular interface before the nucleus returns to the ventricular surface to undergo mitosis. During interkinetic nuclear migration the apical RG maintains its attachment to the ventricular surface, thereby ensuring that the primary cilium and associated centrosomes are retained at the apical membrane throughout the cell cycle (Taverna and Huttner, 2010; Das and Storey, 2014). This distinctive mode of cell division demarcates the proliferative ventricular zone, endows the neuroepithelium with its pseudostratified cytoarchitecture and is a prerequisite for the expansion of the progenitor pool.

As new-born neurons populate the emerging cortical plate, the basal processes of the apical RGs increase in length (**Figure 1A**) (Miyata et al., 2001; Noctor et al., 2002). It has been estimated that the lateral membrane of the basal process comprises the vast majority of the RG plasma membrane, whereas the apical (ventricular) membrane encompasses only 2% of the total surface

area (Kosodo et al., 2004). Attachment of the basal end feet to the pial extracellular matrix is dependent on the $\alpha_6\beta_1$, $\alpha_3\beta_1$ and $\alpha_V\beta_3$ integrins and their deletion leads to the detachment of RG basal processes (Haubst et al., 2006; Jeong et al., 2013). Laminin/β_1 integrin interactions are also required to anchor the apical end feet to the ventricular surface (Loulier et al., 2009). Blocking these interactions induces RG detachment, retraction of the basal process and cortical layering defects.

Retention of the highly polarized RG morphology is essential for the expansion and lamination of the six-layered cortex (Nadarajah et al., 2001; Farkas and Huttner, 2008; Kriegstein and Alvarez-Buylla, 2009). Each layer of the cortex is sequentially generated as waves of neurons migrate along the basal processes (radial migration, **Figure 1A**) to populate their predetermined cortical layer. In the early phase of corticogenesis the deep layer pyramidal neurons arising from RG asymmetric neurogenic divisions dissociate from the ventricular surface, attach to the basal processes and undergo radial migration to establish layers 5/6. Subsequently, the upper layer neurons, generated by intermediate progenitor neurogenic divisions, also employ radial migration along the basal processes in order to migrate through the pre-established deep layer neurons.

In summary, the highly polarized morphology of apical RGs is a mandatory prerequisite for cortical development as it directly influences the expansion of the RG progenitor pool, the decision to exit the cell cycle, acquisition of neuronal identity and cortical lamination, all of which are tightly synchronized in space and time. As in all epithelia, cadherin-based AJs play an obligate role in the induction and maintenance of RG apicobasal polarity and are therefore essential to the fidelity of cortical development.

Adherens Junctions Preserve Cortical Architecture

Adherens junctions encircle the RG at the border of the apical and lateral membranes within the apical end feet (**Figure 1A**). In contrast to other epithelia, apical RGs do not have tight junctions and thus rely on cadherin-based AJs to maintain polarity and tissue cohesion (Aaku-Saraste et al., 1996). Cortical malformations such as subcortical band heterotopia in which neurons accumulate below the cortical plate and periventricular heterotopia, characterized by ectopic neuron-containing nodules protruding into the lateral ventricle (**Figures 1B,C**) have previously been attributed to defects in neuronal motility. However, recent studies in rodents and humans have recognized that the principal mechanism contributing to the etiology of these malformations is the disruption of apical RG morphology as a consequence of the inability to assemble AJs (Rodriguez et al., 2012; Lian and Sheen, 2015). Moreover, mutations in genes known to control junction formation have been shown to be causative for inherited forms of these cortical malformations (Fox et al., 1998; Sheen et al., 2003; Ferland et al., 2009), reinforcing the concept that apical RG junctions are critical determinants of successful corticogenesis.

This concept is best illustrated in the cortices of mice lacking N-cadherin or other key junctional proteins, including Afadin, αE-catenin, Neogenin, and RhoA (**Table 1**) (Lien et al., 2006; Kadowaki et al., 2007; Katayama et al., 2011; Cappello et al., 2012; Yamamoto et al., 2013; Gil-Sanz et al., 2014; Schmid et al., 2014; O'Leary et al., 2017; Rakotomamonjy et al., 2017). In these mutants failure of AJ assembly triggers apical RG deadhesion, the collapse of RG morphology and detachment from the ventricular wall. As a consequence, mitotic RGs are no longer restricted to the ventricular surface, but instead redistribute throughout the cortical plate. In addition, retraction of the basal processes prevents radial migration, resulting in neuronal heterotopias.

Cadherin density at the AJ is regulated by vesicular trafficking from the Golgi complex (the biosynthetic pathway) and recycling between internal and plasma membrane pools (Mary et al., 2002; Lock and Stow, 2005; Linford et al., 2012). Disruption of the endosomal system phenocopies loss of N-cadherin. Mutations in the human *FILAMIN-A* (*FLNA*) gene have been identified in inherited and sporadic periventricular heterotopia (Fox et al., 1998; Sheen and Sheen, 2014), whereas periventricular heterotopia can occur with or without microcephaly in patients carrying mutations in the *ARFGEF2* gene which encodes BIG2, a guanine nucleotide exchange factor (Sheen et al., 2003). Both FLNA, an actin binding protein, and BIG2 regulate cadherin trafficking between the Golgi complex and the cell surface. Depletion of FLNA or mutations in *Arfgef2* inhibit AJ assembly and RG polarization in the rodent embryonic cortex resulting in severe disruption of the ventricular surface and the protrusion of nodules into the ventricle (**Table 1**) (Sheen et al., 2003; Ferland et al., 2009; Carabalona et al., 2012; Sheen and Sheen, 2014). These studies emphasize the importance of maintaining steady-state levels of cadherin at the apical RG junction. In addition, FLNA is known to directly affect the actin cytoskeleton and cytokinesis, and as such, may operate at multiple levels in apical RGs (Sheen and Sheen, 2014).

AJ Assembly and Disassembly Govern Corticogenesis

Successful corticogenesis relies on the balance between AJ assembly and disassembly. During symmetric and asymmetric division the acquisition of junctional components allows AJs to reassemble in RG-fated daughters, thereby maintaining polarity and ensuring that they remain integrated into the neuroepithelium. Conversely, commitment to the neural fate is tightly coordinated with the down-regulation of junctional components, allowing detachment from the ventricular surface. For example, at the completion of asymmetric division delamination of the new-born neuron or intermediate progenitor from its RG sister is mandatory for the initiation of radial migration. Upon activation of proneural genes in the neurally-fated daughter, the Scratch transcription factors repress cadherin expression, inducing delamination from the ventricular surface and triggering radial migration (Itoh et al., 2013). When Scratch activity is suppressed cells committed to the neural fate fail to detach and instead accumulate at the ventricular surface. A similar delamination process has evolved in higher order mammals to produce the array of diverse neuronal subtypes underpinning the complexity of the gyrencephalic neocortex. In the ferret the generation of neuronally committed intermediate progenitors, major contributors to cortical expansion, is under

TABLE 1 | Apical RG junctional proteins and associated cortical malformations.

Protein	Function at AJs	Apical RG phenotype	Malformation
Junctional proteins			
N-cadherin	Homophilic cell–cell adhesion, core AJ protein	*Depletion:* loss of AJs and RG morphology, RG detachment from ventricular wall, ectopic RG division, increased RG proliferation, failure of radial migration	SBH[1] Hydrocephalus
αE-catenin	Tension-sensing molecule, couples N-cadherin/β-catenin to actomyosin		SBH
Afadin	Recruits α-catenin to cadherin at AJs, actin-binding protein		SBH Hydrocephalus
β-Catenin	Required for N-cadherin homophilic adhesion and Wnt signaling, transcriptional activator	*Overexpression*: increased RG proliferation and neuronal production	Macrocephaly
		Depletion: loss of AJs, premature RG cell cycle exit and neurogenesis	Heterotopia[2]
Polarity proteins			
Par3, aPKC Cdc42	Par3/Par6/aPKC/Cdc42 complex: GTPase, required for AJ formation, establishes RG polarity and identity Par3: stabilizes nascent adhesion sites, promotes symmetric RG division	*Depletion:* loss of AJs and RG morphology, RG detachment from ventricular wall, ectopic RG division, failure of radial migration, premature neurogenesis	aPKC: PVH[3] Cdc42: heterotopia
Pals	Pals/Crumbs/PatJ complex: maintains RG apicobasal polarity, apical membrane identity, required for AJ formation	*Depletion:* loss of AJs and RG morphology, increased intermediate progenitor production, premature neurogenesis, induction of neuronal cell death	Microcephaly
Lgl, Dlg5	Lgl/Dlg/Scribble complex: maintains RG apicobasal polarity by conferring lateral membrane identity, required for AJ formation, regulates N-cadherin recycling and membrane localization	*Depletion:* loss of AJs and RG morphology, disruption of ventricular wall, ectopic RG division, increased RG proliferation and intermediate progenitor production	Lgl: SBH, PVH Dlg5: hydrocephalus
Actin regulators			
RhoA	GTPase, regulator of actomyosin contractility in response to tension, promotes F-actin elongation	*Depletion:* loss of AJs and RG morphology, RG detachment from ventricular wall, ectopic RG division, failure of radial migration	SBH Hydrocephalus
mDia	Promotes F-actin elongation, downstream of RhoA		PVH Hydrocephalus
Cdc42	GTPase, polarity protein, promotes linear actin polymerization, required for AJ formation, establishes RG polarity and identity	*Depletion:* loss of AJs and RG morphology, ectopic RG division, increased RG proliferation and neuronal production	Heterotopia
Myo II	Drives actomyosin contractility and conduction of force across AJs	*Depletion:* loss of AJs and RG morphology, disruption of ventricular wall, failure of radial migration	PVH Hydrocephalus
Arp2/3	Branched actin nucleation at AJs, required for AJ formation and stability	*Arp2, Cyfip1, Abi1 depletion:* depletion of actin cytoskeleton, loss of N-cadherin and other junctional proteins, disassembly of AJs, detachment from ventricular wall, ectopic RG division, premature neurogenesis, attenuation of junctional tension	Heterotopia
WRC	Activates Arp2/3 at AJs, promotes branched actin nucleation		
Neogenin	Recruits WRC and Arp2/3 to AJs, promotes Arp2/3 branched actin nucleation at AJs and actin stability and tension	*Depletion/inhibition of WRC binding:* loss of WRC, Arp2/3 from AJs, depletion of actin and tension at AJs, loss of AJs and RG morphology, disruption of ventricular wall, failure of radial migration, ectopic RG division	SBH, PVH Hydrocephalus
N-WASP	Activates Arp2/3 at AJs, stabilizes F-actin	*Depletion:* inability to form AJs in postnatal ependyma, loss of cilia	Hydrocephalus

(Continued)

TABLE 1 | Continued

Protein	Function at AJs	Apical RG phenotype	Malformation
Trafficking proteins			
FLNA	Regulates N-cadherin trafficking to AJs, actin binding protein	*Depletion/mutations:* loss of AJs and RG morphology, disruption of ventricular wall, failure of radial migration	Human: PVH, hydrocephalus Rodent: PVH
BIG2 *(ARFGEF2)*	Guanine nucleotide exchange factor, regulates N-cadherin trafficking to AJs	*Mutations:* loss of AJs and RG morphology, disruption of ventricular wall, failure of radial migration	Human: PVH, microcephaly Mouse: PVH
αSnap	Regulator of SNARE-mediated vesicular fusion, regulates N-cadherin trafficking to AJs	*Mutations:* failure to deliver N-cadherin to membrane, loss of AJs and RG morphology, disruption of ventricular wall, failure of radial migration	PVH Hydrocephalus
Numb	Localizes N-cadherin-positive recycling endocytic vesicles to AJs, antagonizes Notch to promote neurogenesis	*Depletion:* mislocalization of N-cadherin to apical membrane, loss of AJs and RG morphology, ectopic RG division, failure of radial migration	PVH, Heterotopia Hydrocephalus

(1) SBH, Subcortical band heterotopia. (2) Heterotopia, abnormal distribution of neurons within cortex. (3) PVH, periventricular heterotopia.

precise temporal control (Martínez-Martínez et al., 2016). Within a 2 day embryonic period delamination of the intermediate progenitors is initiated by cadherin down-regulation during asymmetric division. However, increasing cadherin levels prevent intermediate progenitor detachment, a situation which would be predicted to have a profound effect on the development of the gyrencephalic cortex.

Adherens junction assembly is also important for preserving the balance between proliferation and neuronal differentiation. Failure to exit the cell cycle and sustained RG proliferation is a prevalent phenotype observed after genetic deletion of junctional components in apical RGs throughout the embryonic neuroepithelium (Klezovitch et al., 2004; Lien et al., 2006; Katayama et al., 2011; Cappello et al., 2012; Rakotomamonjy et al., 2017; Zhang et al., 2019). The decision to remain an apical RG or exit the cell cycle and adopt a neural fate is under the strict control of environmental proliferative and neurogenic factors that are spatially restricted within the neuroepithelium or present within the CSF (Lehtinen et al., 2011; Vitali et al., 2018; Oberst et al., 2019). In these mutants extensive junctional loss results in the widespread collapse of apical RG morphology. The concomitant withdrawal of the apical end feet and primary cilium from the ventricular surface precludes access to environmental regulatory cues, leading to unrestrained proliferation. This is exemplified by the occurrence of highly proliferative apical RG populations ectopically positioned in the mutant cortical plate which lacks the appropriate regulatory cues.

In addition to their non-cell autonomous adhesion function, AJs also influence cell cycle exit in a cell autonomous manner. Stable AJ assembly is dictated by the formation of the core cytoplasmic cadherin-catenin complex comprising β-catenin and α-catenin which link the cadherin to the actin cytoskeleton in a tension-dependent manner (**Figure 2**) (Drees et al., 2005; Buckley et al., 2014). The interaction between β-catenin and the cadherin intracellular domain is essential for maintaining effective homophilic cadherin binding. β-Catenin is also a key effector of the canonical Wnt pathway that regulates cell cycle exit and cell fate determination throughout the embryo by modulating gene expression. In the absence of Wnt activation, cytoplasmic β-catenin is targeted for degradation by the proteasome. Upon Wnt binding to the Frizzled receptor complex, β-catenin is rescued from degradation and is free to translocate into the nucleus where it activates the transcription of target genes involved in cell fate specification and progenitor proliferation (for detailed reviews see Stocker and Chenn, 2015; Nusse and Clevers, 2017).

During corticogenesis, canonical Wnts are concentrated adjacent to the ventricular surface and thus are perfectly positioned to control the decision to exit the cell cycle. Moreover, β-catenin is expressed highly in apical RGs and is suppressed upon neural commitment (Woodhead et al., 2006; Stocker and Chenn, 2015). Overexpression in RGs of a stabilized form of β-catenin which is able to bind cadherins, but lacks the degradation targeting sites, produces a substantial enlargement of cortical volume due the extensive expansion of the progenitor pool and subsequently excessive neuronal production (Chenn and Walsh, 2002). This dramatic phenotype has been attributed to the inability to exit the cell cycle as a consequence of persistent β-catenin transcriptional activity (Chenn and Walsh, 2002; Stocker and Chenn, 2015). Conversely, depletion of β-catenin triggers early exit from the cell cycle and premature acquisition of neural fate (Machon et al., 2003; Woodhead et al., 2006). In these mutants, AJs fail to form and the proliferative Wnt transcriptional program is silenced. Thus the ability of cadherins to sequester β-catenin at the membrane is likely to be an important modulator of β-catenin transcriptional activity. AJs therefore influence the decision to re-enter the cell cycle by acting as integration sites for cell adhesion and the signaling networks relaying environmental information.

Adherens junctions also influence RG cell fate acquisition through their ability to preserve polarized apical RG morphology. Many studies have demonstrated that multiple interconnected

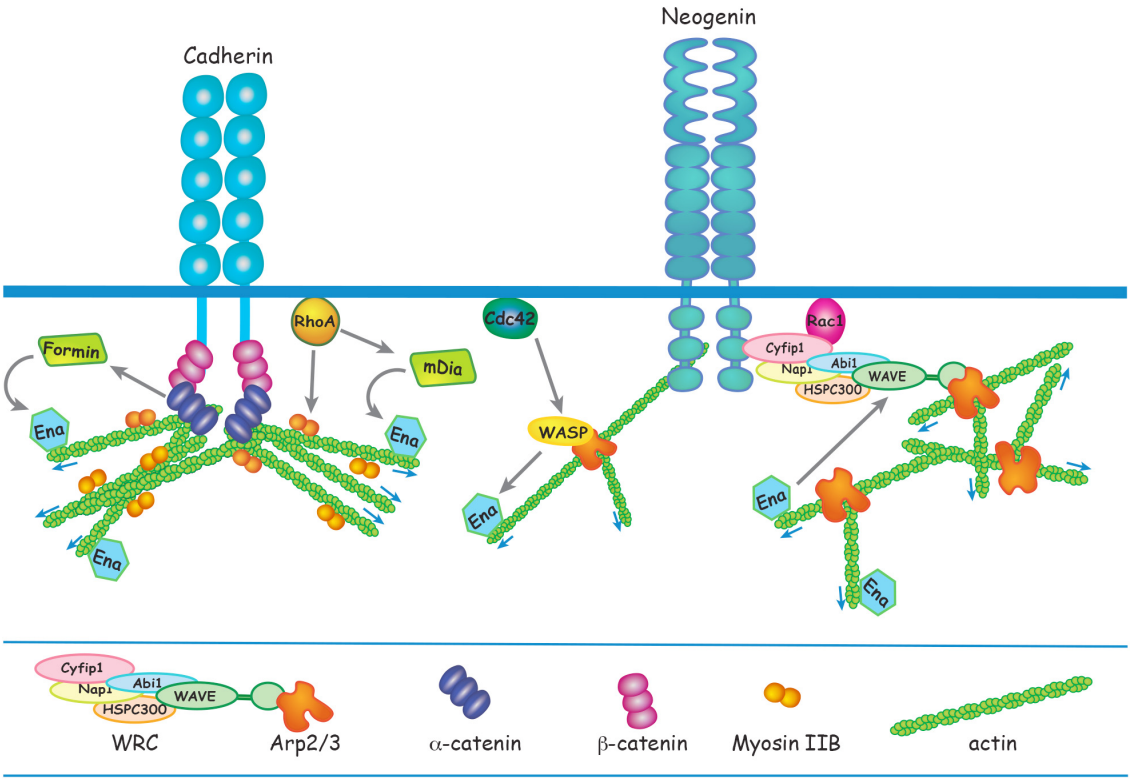

FIGURE 2 | Apical RG AJ assembly is dependent on the reciprocal interactions between cadherins and the actin cytoskeleton. α-catenin links cadherin to F-actin via β-catenin in a tension-dependent manner and also recruits Formin-1 to catalyze linear actin polymerization. RhoA regulates junctional contractility in response to acute tension by promoting phosphorylation of the Myosin regulatory subunit. Ena/VASP adds G-actin to the barbed end of the growing actin filament. N-WASP and mDia act downstream of Cdc42 and RhoA, respectively, to induce Ena/VASP actin polymerization. Branched actin nucleation is initiated at the cadherin adhesion complex by Arp2/3 which is activated by N-WASP or the WRC. Neogenin recruits the WRC and Arp2/3 to cadherin ensuring that branched actin nucleation is confined to the junctional membrane. Ena/VASP binds to WAVE to enhance Arp2/3-mediated branched actin nucleation.

structural factors contribute to apical RG identity, including the retention of the basal process and primary cilium, and the centrosome containing the mother centriole (Konno et al., 2008; Wang et al., 2009; Shitamukai et al., 2011; Wilsch-Brauninger et al., 2012; Paridaen et al., 2013). Establishment of apicobasal polarity, a process dependent on junctional reassembly during cytokinesis, is a prerequisite for retention of these structures. The primary cilium is inherited by the RG-fated daughter and is required for re-entry into the cell cycle, due to its ability to transduce proliferative and morphogenic signals (Eggenschwiler and Anderson, 2007; Oberst et al., 2019). Retention of the primary cilium in the RG-fated cell is dependent on high levels of N-cadherin (Das and Storey, 2014). Conversely, suppression of N-cadherin in the neural daughter by the proneural transcription factor Neurogenin2 prevents the reconstruction of the primary cilium. AJ assembly, therefore, lies upstream of the acquisition of apicobasal polarity and RG cell fate. Induction of RG polarity is governed by multiple polarity complexes whose primary role is to segregate the apical and basolateral membranes. Establishment and maintenance of the polarized state is reliant on the bidirectional interaction between polarity proteins and AJ components.

Interplay Between AJs and Polarity Complexes Impose RG Apicobasal Polarity

The defining attribute of all epithelia is their apicobasally polarized morphology which is characterized by compartmentalized apical and basolateral domains comprising distinct repertoires of proteins and organelles. The apicobasally polarized state emerges as a consequence of the synchronized interplay between networks of polarity complexes which act to break symmetry and magnify asymmetry (reviewed in Peglion and Goehring, 2019). A major outcome of polarity network activity is the establishment of AJs which demarcate the border between the apical and lateral membranes. The Par3/Par6/aPKC/Cdc42 polarity complex delineates the apical membrane and opposes Lgl/Dlg/Scribble activity to maintain apical identity (Betschinger et al., 2003; Dollar et al., 2005). Conversely, the Lgl/Dlg/Scribble complex maintains lateral identity by overriding Par complex activity (Yamanaka et al., 2003). Studies in invertebrates and in *in vitro* models (Peglion and Goehring, 2019) have shown that Par3 is localized to nascent sites of cell–cell adhesion and recruits Par6 and aPKC to the adjacent apical membrane. As the epithelial cell matures Par3 dissociates from Par6/aPCK in response to Cdc42-mediated

aPKC phosphorylation and relocates to the cadherin adhesion complex, thereby stabilizing the apical domain and emerging AJs (Tanentzapf and Tepass, 2003; Yamanaka et al., 2003). In parallel, exclusion of the Lgl/Dlg/Scribble polarity complex from the apical membrane is achieved through localized deactivation of Lgl by phosphorylated aPKC. Lgl/Dlg/Scribble activity, however, is maintained in the lateral membrane by the pool of non-phosphorylated Lgl which acts to exclude the Par3/Par6 complex from this domain. These spatially restricted interactions reinforce AJ stability and partition the apical and lateral membranes (Betschinger et al., 2003, 2005; Plant et al., 2003; Jossin et al., 2017). During the establishment of polarity the Par3 complex also interacts with Crumbs/Pals/PatJ to reinforce apical identity (Morais-de-Sa et al., 2010; Walther and Pichaud, 2010). Concomitant with the recruitment of Par3 to the AJ, dissociated Par6/aPKC recombine with Pals and Crumbs, a membrane bound receptor confined to the apicolateral membrane. Blocking the Par6-Pals interaction inhibits the redistribution of Par6/aPKC to the apical domain (Hurd et al., 2003).

As in all epithelia, the relationship between RG polarity proteins and AJs is bidirectional. Initiation of junction assembly is dependent on polarity protein signaling, and consolidation of the polarized state requires that AJ components confine polarity proteins to the appropriate membrane compartment. The Par3/Par6/aPKC/Cdc42, Lgl/Dlg/Scribble, and Crumbs/Pals/PatJ polarity complexes play pivotal roles in promoting RG apicobasal polarity and AJ formation (**Figure 3** and **Table 1**), and as a consequence, are key factors in determining progenitor fate. However, whether AJs play an instructive role in regulating cell fate commitment and cell cycle exit independently of their role in adhesion remains an open question.

Direct evidence that the Par complex and AJs collaborate in imposing the apical RG phenotype is patently demonstrated by deletion of the polarity determinants aPKC, Par3 or the small GTPase Cdc42, a Par complex activator (Cappello et al., 2006; Imai et al., 2006; Bultje et al., 2009). Loss of these polarity proteins promotes AJ failure, the retraction of the RG basal process and the withdrawal of the apical end feet from the ventricular surface

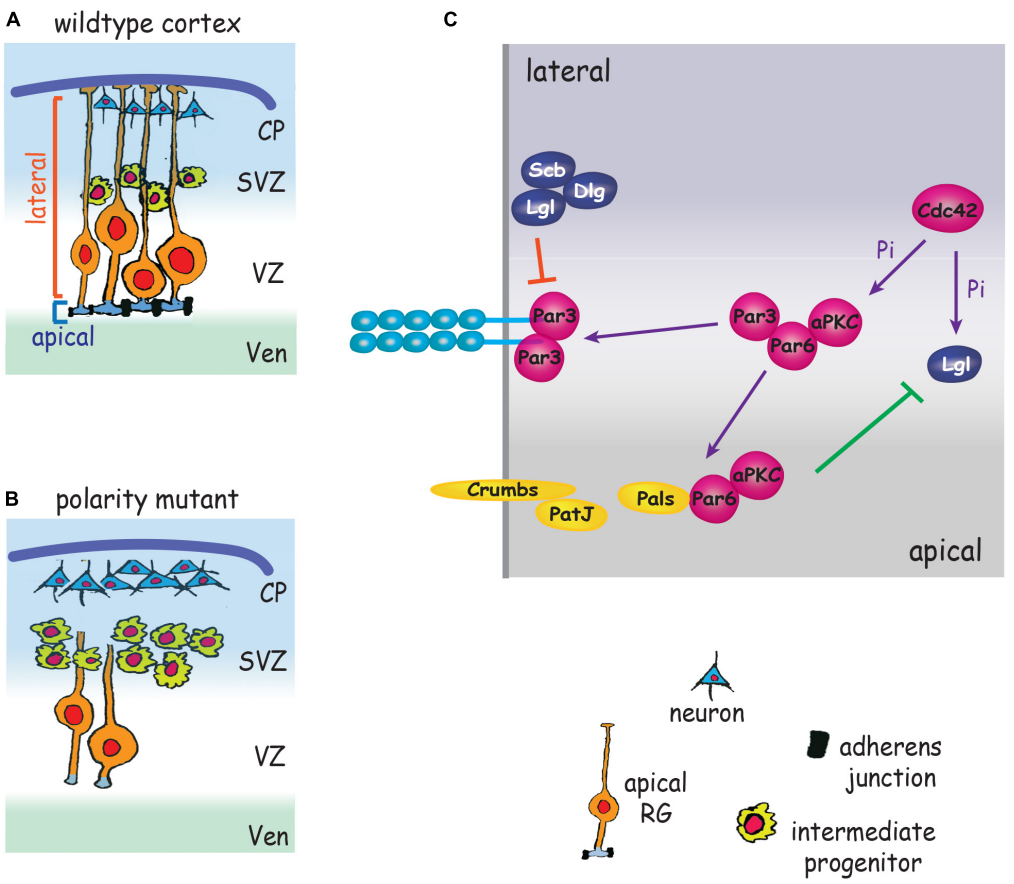

FIGURE 3 | Polarity proteins promote AJ formation and impose RG cell fate. **(A)** Polarity complexes stabilize AJs, promote symmetric RG division and maintain RG polarity by partitioning the apical and lateral membranes. **(B)** Depletion of polarity proteins leads to loss of AJs and RG morphology, RG detachment from the ventricular wall, increased intermediate progenitor production and premature neurogenesis. **(C)** Par3/Par6/aPKC localize adjacent to nascent AJs. Cdc42 induces phosphorylation (Pi) of aPKC. Par3 dissociates from Par6/aPCK and relocates to the cadherin adhesion complex, stabilizing the apical domain and emerging AJs. Par6/aPKC recombine with Pals/Crumbs/PatJ to define the apical membrane. aPKC also phosphorylates Lgl, leading to exclusion of Lgl/Dlg/Scribble from the apical membrane (green line). Non-phosphorylated Lgl excludes Par3/Par6/aPKC from the lateral membrane (red line). CP, cortical plate; SVZ, subventricular zone; Ven, ventricle; VZ, ventricular zone.

(**Figure 3**). As a result RGs undergo precocious differentiation into intermediate progenitors and neurons (Cappello et al., 2006; Bultje et al., 2009). The inhibition of AJ-Par complex interactions therefore promotes the adoption of the neurogenic fate at the expense of the proliferative RG fate, leading to premature neurogenesis. As a consequence of the imbalance in cell fate specification, inadequate numbers of progenitors are generated early in corticogenesis, resulting in long-term depletion of neuronal populations, a phenotype underpinning the etiology of microcephaly (Pinson et al., 2019). This also appears to be the *modus operandi* of Zika virus which causes microcephaly by preferentially infecting apical RGs (Yoon et al., 2017). Zika proteins interact with multiple AJ components resulting in impaired AJ assembly, suppression of RG proliferation and premature neurogenesis in the mouse cortex and in human iPSC-derived organoids.

The Pals polarity protein links Crumbs/PatJ to the Par3/Par6/aPKC complex which act together to define the apical membrane domain. Therefore, it is not surprising that genetic deletion of *Pals* in apical RGs also has devastating consequences for cortical development (Kim et al., 2010). As seen in the *Par3* mutant, apical RGs lacking Pals undergo premature cell cycle exit and extensive neuronal differentiation early in corticogenesis. In the absence of Pals, Crumbs and aPKC no longer associate with the junctional complex, leading to AJ disassembly or a basal shift in AJ location, and the abrogation of RG apicobasal polarity. However, in contrast, to the *Par3* mutant, a rapid induction of neuronal cell death was observed in late cortical development due to the inhibition of the mTOR cell survival pathway.

Inhibition of the Lgl/Dlg/Scribble polarity complex also has profound effects on cortical development. Genetic depletion of Lgl prevents AJ formation and RG polarization and disrupts the ventricular wall (Klezovitch et al., 2004; Beattie et al., 2017; Jossin et al., 2017; Zhang et al., 2019). Both periventricular and subcortical heterotopias are observed in these mutants. Failure to exit the cell cycle translated into excessive RG proliferation and increased neurogenesis, further exacerbating the subcortical heterotopia phenotype. In the absence of Lgl a substantial decrease in N-cadherin endocytosis was observed (Jossin et al., 2017). *In vitro* and *in vivo* experiments revealed that N-cadherin internalization and AJ stabilization require a direct interaction between Lgl and N-cadherin, and that this interaction is inhibited by aPKC-mediated phosphorylation of Lgl. Together, these findings suggest a model whereby Lgl triggers N-cadherin endocytosis at the lateral membrane, but is prevented from doing so at the AJ due to inhibition by junctionally localized aPKC. As a result, high levels of N-cadherin are confined to the junction. This hypothesis is bolstered by a previous study demonstrating that the deletion of aPKC in the embryonic cortex also prevents AJ formation and the establishment of polarized RG morphology (Imai et al., 2006). The central role of the Lgl/Dlg/Scribble complex in the regulation of cadherin recycling at RG junctions is further supported by *Dlg5* loss-of-function embryos which exhibit reduced membrane N-cadherin and phenocopy the *Lgl* mutants (Nechiporuk et al., 2007). *In vitro* studies show that the efficient delivery of cadherin containing vesicles to the membrane relies on the interaction between Dlg5 and Syntaxin4, a member of the q-SNARE membrane fusion complex as well as between Dlg5 and the junctional component, β-catenin (Nechiporuk et al., 2007). These data lead to the hypothesis that Dlg5 anchors the vesicular fusion machinery to AJs to reinforce apical RG junctional integrity.

Adherens junctions also influence the decision to re-enter the cell cycle by spatially coordinating extrinsic signals with polarity complex activity. The stem cell determinant Notch is localized to the apical RG junctional membrane where it associates with the cadherin adhesion complex. AJ assembly is required for Notch activation and retention of the RG fate by sequestering Par3 during asymmetric division (Del Bene et al., 2008; Bultje et al., 2009; Ohata et al., 2011; Hatakeyama et al., 2014). Notch functions downstream of Par3 to specify progenitor identity, whereby the daughter cell inheriting the greatest proportion of Par3 exhibits high Notch activity. Overexpression of Par3 forces cells to adopt the apical RG fate due to the enrichment of Par3 and Notch activity in both daughter cells, whereas Par3 suppression deactivates Notch and confers neuronal identity to both cells. Intriguingly, several studies have revealed an explicit link between Notch signaling and cadherin-mediated adhesion. Numb, a known regulator of Notch clathrin-mediated endocytosis, promotes the acquisition of neuronal cell fate during RG asymmetric division by antagonizing Notch signaling (Rasin et al., 2007; Bultje et al., 2009). Moreover, Numb is found in the apical end feet at interphase where it specifically localizes to cadherin-positive recycling endocytic vesicles and directly interacts with cadherins (Rasin et al., 2007). Silencing Numb activity results in mislocalization of cadherin to the RG apical membrane and prevents junctional assembly, leading to loss of RG morphology, ectopic positioning of neurally fated cells and aberrant cortical lamination. Conversely, overexpression of Numb provokes persistent apical RG anchoring to the ventricular surface, sustained apicobasal polarity and retention of progenitor identity in both siblings. These observations provide persuasive evidence that junction assembly and cell fate determination are tightly coordinated.

Do AJs Influence the Mode of Cell Division?

During symmetrical proliferative divisions retention of junctions and the associated polarity proteins promotes re-establishment of apicobasal polarity and confers RG progenitor identity, whereas depletion of these factors after asymmetric division bestows neural fate. Pioneering studies have revealed that the inheritance of the Par complex and junctional components is dependent on the position of the cleavage plane during cytokinesis (Huttner and Kosodo, 2005; Konno et al., 2008; Marthiens and Ffrench-Constant, 2009; Paridaen et al., 2013). In the early phase of corticogenesis when progenitors are undergoing symmetric self-renewing divisions, mitotic spindles are orientated in the planar orientation (vertical cleavage plane). Cleavage along the vertical plane bisects the apical membrane resulting in the equal distribution of junctional and polarity proteins between the daughters, thereby promoting the proliferative RG fate. As apical RGs switch to asymmetric neurogenic divisions, the mitotic spindle re-orientates such that the cleavage plane becomes

horizontal or oblique, favoring the production of neurons or intermediate progenitors (Huttner and Kosodo, 2005; Konno et al., 2008; Postiglione et al., 2011; Paridaen and Huttner, 2014). In this situation retention of the RG fate is associated with the acquisition of the greater fraction of AJ components and polarity proteins. Conversely, the exclusion of these factors promotes commitment to the neurogenic fate. Whether or not AJs directly influence spindle orientation remains controversial. However, increased oblique divisions and a subsequent increase in intermediate progenitors and their neuronal offspring have been reported after deletion of the junctional component Afadin (Rakotomamonjy et al., 2017), suggesting that AJ component inheritance favors the apical RG fate and inhibits asymmetric division. This premise is supported by studies in other epithelia where Afadin binding to F-actin and LGN, a microtubule motor regulator of spindle orientation, promotes symmetric proliferative division (Carminati et al., 2016). Thus, junctional stability, apicobasal polarity and the direction of cytokinesis are intimately linked.

The Actin Cytoskeleton Fortifies Apical RG Adherens Junctions

In the embryonic brain AJs must resist the mechanical stresses exerted by dynamic cellular behaviors and increased CSF pressure. As in other epithelial tissues the maintenance of apical RG morphology and neuroepithelial integrity relies on the adhesive strength dictated by reciprocal interactions between the cadherins and the circumferential actin ring which runs parallel to the AJ within the RG apical end feet (**Figure 1**). Adhesive strength is dependent on the continual turnover of the actin cytoskeleton, and actomyosin contractility regulates junctional tension and thus resilience to stress (Maître et al., 2012; Priya and Yap, 2015; Yap et al., 2017). Failure to remodel the actin cytoskeleton in apical RGs leads to AJ disassembly, loss of polarized morphology and perturbation of the neuroepithelial cytoarchitecture. The fundamental role of actin remodeling in maintaining polarized RG morphology and neuroepithelial integrity is reinforced by the emergence of cortical malformations in mice lacking actin regulators (**Table 1**).

Spatiotemporal regulation of actin polymerization is coordinated through the Rho GTPases RhoA, Rac1, and Cdc42 which govern actin remodeling by directly linking a diverse array of actin modulators to cell surface receptors and downstream effectors (**Figure 2**) (Priya and Yap, 2015; Lee et al., 2016; Braga, 2017; Acharya et al., 2018; Schaks et al., 2018). RhoA is a major regulator of junctional actomyosin contractility and is also recruited to AJs in response to acute tension, thereby reinforcing the actin cytoskeleton (Priya and Yap, 2015; Acharya et al., 2018). Conditional deletion of RhoA in apical RGs inhibits incorporation of G-actin into the F-actin filament, leading to the destabilization of the actin cytoskeleton and AJ disassembly (Cappello et al., 2006; Katayama et al., 2011). Subsequent RG detachment from the ventricular surface leads to ectopic positioning above the ventricular zone. In addition, although loss of RhoA was found not to affect neuronal motility *per se*, neurons were unable to undergo radial migration due to the retraction of the RG basal processes. Instead, neurons accumulated under the cortical plate forming subcortical band heterotopias. RhoA activation of formins such as mDia promotes F-actin elongation (**Figure 2**). Therefore, it is not surprising that the ablation of the RhoA effector mDia in RGs phenocopies the RhoA mutants, whereby junctional disruption provokes neuronal heterotopias (Thumkeo et al., 2011).

The importance of a direct link between cadherin and the RG actin cytoskeleton is further demonstrated by the conditional deletion of αE-catenin (Lien et al., 2006; Schmid et al., 2014). In epithelial tissues the assembly of functional AJs is dependent on the interaction between cadherin and the cytoplasmic effector, α-catenin which couples the cadherin cytoplasmic domain (via β-catenin) to the actin cytoskeleton (**Figure 2**) (Drees et al., 2005; Buckley et al., 2014). Loss of αE-catenin in apical RGs induces AJ disassembly due to the inability to generate a stable actin cytoskeleton, leading to the retraction of the basal process which in turn severely affects radial migration. Here clusters of neurons accumulate below the cortical plate forming a second neuronal layer equivalent to that seen in subcortical band heterotopia. Insight into the mechanisms underpinning αE-catenin function at RG junctions comes from *in vitro* experiments using optical trap-based assays to quantify α-catenin-actin binding under applied force (Buckley et al., 2014). These experiments revealed that α-catenin is a tension-sensing molecule as it is only able to couple F-actin to cadherins when force is applied (Buckley et al., 2014). It is likely, therefore, that αE-catenin acts in a similar manner at RG junctions, thereby providing a sensitive mechanism with which to detect and modulate junctional tension at the ventricular surface.

Actomyosin activity is dynamic and responds to forces experienced at the junction by modulating cadherin adhesion and promoting actin remodeling, thereby ensuring AJ stability (Smutny et al., 2011; Borghi et al., 2012; Priya and Yap, 2015; Yap et al., 2017). Myosin II drives actomyosin contractility at AJs and therefore plays a central role in the regulation of junctional tension. Upon myosin binding to the actin filament, RhoA-dependent phosphorylation of the myosin regulatory subunit triggers contractility (**Figure 2**). Coupling of myosin to the cadherin cytoplasmic domain enables conduction of force across the junction and facilitates the transmission of actomyosin-induced tension across cell ensembles (Smutny et al., 2011; Borghi et al., 2012; Priya and Yap, 2015). Early pioneering studies using genetic deletion of Myosin IIB provide compelling evidence that actomyosin activity plays an essential role in maintaining apical RG junctional integrity and neuroepithelial cohesion (Tullio et al., 2001; Ma et al., 2007). As seen in N-cadherin loss-of-function mutants, deletion of Myosin IIB leads to AJ failure, collapse of apical RG morphology and disruption of the ventricular surface throughout the neuraxis. Within the forebrain, aggregations of neurons and progenitors protrude into the ventricular space, a phenotype reminiscent of the periventricular heterotopias seen in humans. Furthermore, actomyosin contractility has been shown to play a central role in promoting the abscission of new-born neurons from the ventricular surface during asymmetric RG division, a process required for the initiation of radial migration (Das and Storey,

2014). This activity lies downstream of N-cadherin as increased N-cadherin or inhibition of myosin activity prevents abscission of the prospective neuron.

A common feature of mutants lacking key actin regulators (αE-catenin, RhoA, Myosin IIB, Arp2/3), is the occurrence of apical RG rosettes within the cortical plate where clusters of polarized progenitors assemble around a central lumen (Tullio et al., 2001; Lien et al., 2006; Kadowaki et al., 2007; Katayama et al., 2011; Cappello et al., 2012; Schmid et al., 2014; Wang et al., 2016). The subapical membrane localization of cadherin, catenin, and Par3 preserves cohesion despite the depletion of junctional actin. This is in stark contrast to the ventricular wall where AJ stability in the RG apical end feet is clearly diminished, indicating that in the absence of the actin regulators junctional adhesive strength is manifestly attenuated and unable to buffer the forces exerted at the ventricular surface. The mechanical stresses experienced within the cortical plate, however, would be substantially lower, allowing the compromised junctions to support adhesion. These observations highlight the critical role played by the actin cytoskeleton and its network of regulatory proteins in reinforcing tissue cohesion while preserving junctional flexibility in the embryonic neuroepithelium.

Branched Actin – The Epicenter of the Junctional Cytoskeleton

Investigations using *in vitro* epithelial cell models have revealed that the junctional actin cytoskeleton consists of a dense network of branched actin which seeds the growth of the linear F-actin filaments comprising the actin ring (Verma et al., 2012; Brieher and Yap, 2013; Han et al., 2014; Lee et al., 2016). Branched actin nucleation is initiated at the cadherin adhesion complex and is mediated by the Arp2/3 enzymatic complex, an inefficient actin nucleator (Pizarro-Cerda et al., 2017). Arp2/3 is activated by the pentameric WAVE regulatory complex (WRC), a pivotal branched actin regulator composed of five subunits organized into the Cyfip/Nap and WAVE/Abi/HSPC300 subcomplexes (**Figure 2**) (Chen et al., 2010, 2014). Arp2/3 activity is triggered upon binding to the WAVE subunit, and this interaction is dependent on activated Rac1 binding to Cyfip1 within the holocomplex (Chen et al., 2014; Schaks et al., 2018). Both Arp2/3 and the WRC are tightly associated with AJs and play an important role in the epithelial response to mechanical stress as their dissociation from the cadherin adhesion complex induces junctional disassembly and the attenuation of junctional tension (Verma et al., 2012; Han et al., 2014; Lee et al., 2016).

In RG junctions branched actin nucleation is also dependent on Arp2/3 and the WRC, both of which are concentrated within the RG apical end feet (Yoon et al., 2014; Wang et al., 2016; O'Leary et al., 2017). Conditional deletion of the obligatory Arp2 subunit in the mouse embryonic cortex results in depletion of the actin cytoskeleton from the subapical membrane, loss of N-cadherin and other key junctional proteins and disassembly of AJs (Yoon et al., 2014; Wang et al., 2016). As a consequence of junctional failure, RGs detach from the ventricular surface and form ectopic rosettes in the cortical plate. Moreover, those RGs remaining at the ventricular surface undergo premature commitment to the neuronal fate, which ultimately leads to a decrease in mature pyramidal populations. Similarly, depletion of the WRC subunits Abi1 or Cyfip1 results in the loss of AJs and polarized RG morphology with concomitant ectopic RG redistribution to the upper cortical layers and marked perturbation of the neuroepithelium (Yoon et al., 2014).

Branched actin nucleation precisely at the AJ requires that the WRC and Arp2/3 is spatially restricted to the cadherin complex. A critical molecular mechanism responsible for the recruitment of Arp2/3 and the WRC to cadherins has recently been discovered. Neogenin, a multi-functional receptor for Netrin and the Repulsive Guidance Molecules (Rajagopalan et al., 2004; De Vries and Cooper, 2008; Kee et al., 2008; O'Leary et al., 2015; Siebold et al., 2017), has been identified as a pivotal component of the branched actin nucleation machinery governing junctional stability and tension (Lee et al., 2016; O'Leary et al., 2017). The WRC interacting receptor sequence (WIRS), found in the intracellular domain of Neogenin, binds to a highly conserved binding pocket within the WRC composed of the Cyfip1 and Abi subunits (**Figure 2**) (Chen et al., 2014; Lee et al., 2016). Using an *in vitro* epithelial model it was demonstrated that Neogenin recruitment of the WRC to the cadherin adhesion complex ensures that Arp2/3 actin nucleation is confined precisely to the junctional membrane, thereby promoting actin ring stability and junctional integrity. Loss of Neogenin severely perturbs AJ integrity due to the attenuation of junctional tension resulting from fragmentation of the actin ring (Lee et al., 2016). As would be predicted, blocking the interaction between Neogenin and the WRC subunits Cyfip1 and Abi in RGs prevents Arp2/3-mediated actin nucleation, leading to the loss of F-actin, disintegration of the actin ring and AJ destabilization (O'Leary et al., 2017). The ensuing retraction of RG basal processes and disruption of the ventricular wall prevents radial migration into the cortical plate, resulting in the emergence of periventricular and subcortical band heterotopias.

The activity of the branched actin nucleation machinery and tension-sensing factors are coordinated to ensure that actin remodeling is responsive to local forces generated within the epithelium. Biallelic mutations in the human αN-catenin gene *CTNNA2* is causative for a recessive form of pachygyria (reduction in gyrus formation) (Schaffer et al., 2018). This study and an earlier biochemical study (Drees et al., 2005) revealed that in addition to its role in coupling linear actin to the cadherin complex, α-catenin is able to regulate branched actin polymerization by competing with Arp2/3 for G-actin binding in migrating pyramidal neurons. This competitive behavior is dependent on high concentrations of free cytoplasmic α-catenin, a situation that is likely to arise as AJs mature and cadherin-α-catenin interactions become saturated. As α-catenin also recruits formins to catalyze the polymerization of linear actin filaments at AJs (Kobielak et al., 2004), this suggests that α-catenin may modulate junctional tension by balancing the synthesis of branched and linear actin and that perturbation of this regulatory mechanism is likely to impact junctional stability. We would therefore speculate that αE-catenin functions in a similar manner to stabilize RG junctions.

Branched actin nucleation and linear elongation factors work in unison to reinforce the bidirectional interplay between the cadherin adhesion complex and the actin cytoskeleton. Actin nucleation is the rate-limiting step for polymerization of both branched and linear actin. N-WASP, like its close relative WAVE, is an Arp2/3 activator (**Figure 2**) (Rohatgi et al., 1999). It also functions to stabilize linear actin filaments at AJs and in doing so sustains contractile tension (Kovacs et al., 2011; Wu et al., 2014). The elongation factor Ena/VASP promotes the addition of G-actin to the barbed end of the growing actin filament (Siton-Mendelson and Bernheim-Groswasser, 2017). N-WASP and the formin mDia act downstream of Cdc42 and RhoA, respectively, to induce Ena/VASP-mediated growth of linear actin from branched nodes (**Figure 2**). Silencing this signaling pathway in the neuroepithelium by deleting N-WASP, mDia, RhoA or Cdc42 interferes with junctional integrity, leading to cortical malformations (Symons et al., 1996; Cappello et al., 2006; Katayama et al., 2011; Thumkeo et al., 2011; Cappello et al., 2012; Jain et al., 2014). In addition, Ena/VASP has been shown *in vitro* to bind to WAVE and potentiate Arp2/3-mediated branched actin nucleation (Havrylenko et al., 2015). Together, these observations implicate the WAVE/WASP proteins as a central signaling hub at RG junctions that acts to ensure synergistic linear and branched actin polymerization in order to modulate junctional tension and maintain tissue cohesion.

Adherens Junctions, the Ependymal Epithelium and Hydrocephalus

Ependymal cells form a multi-ciliated cuboidal epithelial monolayer that acts as a bidirectional barrier between the ventricle and the brain parenchyma, and the establishment of an apicobasally polarized ependyma is essential for the maintenance of brain homeostasis (**Figure 1D**) (Del Bigio, 2010; Jimenez et al., 2014). The vectoral transport of proteins, nutrients and waste products across the ependymal epithelium is driven by transporters and channel proteins which are asymmetrically distributed at the apical membrane facing the CSF or the basal membrane adjacent to the parenchyma. In addition, a polarized epithelium is necessary for the elaboration of the motile cilia on the apical surface which propel CSF through the ventricular system. Loss of ependymal integrity resulting from progressive ventricular denudation beginning early in fetal life is the underlying pathology in some forms of perinatal hydrocephalus (Dominguez-Pinos et al., 2005; Rodriguez et al., 2012; Guerra et al., 2015). Denudation of the ependymal epithelium severely hampers nutrient and toxin exchange, and the absence of a multi-ciliated epithelium directly impacts CSF flow further exacerbating ventricle dilation.

Ependymal cells are derived from the apical RGs of the embryonic neuroepithelium (Ortiz-Álvarez et al., 2019; Redmond et al., 2019). In the human embryo, RG expansion and neurogenesis occur between gestational weeks 12 and 22 (Jimenez et al., 2014; Guerra et al., 2015). In parallel, a subpopulation of RGs differentiate into ependymal cells with the mature ependyma being established by gestational week 28. The assembly of resilient AJs is critical to the integrity of the ependymal epithelium which must resist the tensile forces arising from increasing CSF volume and other mechanical stresses associated with the expansion of the ventricles in the embryo and neonate. Evidence is now accumulating that denudation and thus hydrocephalus originate in the embryonic neuroepithelium prior to the onset of ependymal maturation due to the failure of junctional assembly in apical RGs and subsequently ependymal cells (**Figure 1E**) (Jiménez et al., 2009; Rodriguez et al., 2012; Guerra et al., 2015). Moreover, the occurrence of hydrocephalus is often coincident with neuronal heterotopias. For example, periventricular heterotopias are accompanied by the disruption of the ependymal epithelium in postmortem brains of patients carrying *FLNA* mutations (Sheen et al., 2004; Ferland et al., 2009; Jimenez et al., 2014; Lian and Sheen, 2015). Thus hydrocephalus and some forms of cortical malformations share a common etiology – the loss of AJs.

This hypothesis is unequivocally supported in mouse models in which the molecular pathways governing AJ assembly have been disrupted. In the embryonic mouse cortex apical RGs are specified as ependymal cells between embryonic days 14 and 16 (Ortiz-Álvarez et al., 2019; Redmond et al., 2019). However, in contrast to the human, committed apical RGs do not transform into a cuboidal ependymal epithelium until the first week of postnatal life (Tramontin et al., 2003; Spassky et al., 2005). By the end of the second postnatal week all RGs have terminally differentiated into ependymal cells. Hydrocephalus occurs in mice lacking AJ-associated proteins, such as N-cadherin, Yap, Afadin, mDia, Dlg5, Numb, or Plekha7 (Nechiporuk et al., 2007; Rasin et al., 2007; Thumkeo et al., 2011; Oliver et al., 2013; Yamamoto et al., 2013; Park et al., 2016; Tavano et al., 2018), all of which control cadherin adhesion in the apical RG end feet. In addition, disruption of cadherin trafficking has profound effects on both neuroepithelial and ependymal integrity. A mutation in α*SNAP*, a regulator of SNARE-mediated vesicular fusion, has been identified in the hydrocephalus mouse model, *hyh* which also exhibits periventricular heterotopia (Chae et al., 2004; Paez et al., 2007; Ferland et al., 2009; Jiménez et al., 2009). In these mice the failure to deliver cadherin to the plasma membrane prevents AJ formation, leading to severe ventricular disruption from early corticogenesis onwards.

As described above, depletion of the branched actin regulators Neogenin, the WRC and Arp2/3 induces cortical heterotopias due to the inability to establish stable RG junctions. In addition, genetic depletion of Neogenin results in extensive denudation of the ventricular wall by postnatal day 3 and ongoing loss of mature ependymal cells throughout the adult ventricular system, resulting in severe hydrocephalus (O'Leary et al., 2017). *In vitro* and *in vivo* studies confirmed that blocking Neogenin-WRC interactions prohibits the formation of both RG and ependymal junctions. These studies highlight the pivotal role played by the Neogenin-WRC-Arp2/3 actin regulatory network in promoting actin remodeling, AJ stability and the integrity of the embryonic neuroepithelium and the postnatal ependymal epithelium. The fundamental role of actin in maintaining the fidelity of both these epithelia is further reinforced by the emergence of neuronal heterotopias and hydrocephalus in mice lacking actin modulators, including RhoA, Myosin IIB,

mDia, and N-WASP (Tullio et al., 2001; Ma et al., 2007; Thumkeo et al., 2011; Jain et al., 2014).

CONCLUSION

We now have a robust understanding of the key interactions between junctional components and the epithelial polarity complexes which govern RG apicobasal polarity as well as the essential molecular networks promoting AJ assembly and stability (e.g., actin regulators). Nonetheless, we have a limited understanding of how the activity of these many AJ interactors are spatiotemporally coordinated at the junctional interface in the steady state and in response to environmental stresses. Clearly there is a large number of proteins competing for binding sites at the RG junction. However, we currently have little insight into the nanodomain organization of these protein complexes. Do the cadherins form large multi-protein complexes or do they form discrete nanodomains comprising one or a few proteins? Is the mobility of these nanodomains coordinated in time and space? How are these protein–protein interactions synchronized at the nanoscale level in response to regulatory signals and what are the kinetic principles driving these interactions? With the advent of powerful super-resolution microscopic technologies such as dSTORM (stochastic optical reconstruction microscopy) and sptPALM (single-particle tracking photoactivated localization super-resolution microscopy) we are now in a position to address these intriguing and important questions.

It was not until the late 1980s and early 1990s that apical RGs were recognized as the neural stem cells responsible for the generation of all pyramidal neurons of the mammalian cortex (Misson et al., 1988; Malatesta et al., 2000; Hartfuss et al., 2001). Prior to this, RGs were thought to be a fully committed, non-dividing astroglial cell type derived from a lineage distinct from that giving rise to neurons. As such, apical RGs were believed to play only a supportive role in the developing cortex. This review provides a glimpse into the tremendous progress that has been made over the past 30 years in unraveling the fundamental, multifaceted role of apical RGs in the development of the neocortex. As underscored here, AJs play an obligate role in the establishment of RG apicobasal polarity and hence function. The fidelity of cortical development is therefore critically dependent on AJ assembly and stability. This is overwhelmingly illustrated by the occurrence of debilitating cortical malformations, including perinatal hydrocephalus, arising as a consequence of junctional failure.

AUTHOR CONTRIBUTIONS

LV: this review is part of LV's Ph.D. thesis Introduction. He contributed to the intellectual content, selection of review content, interpretation of the literature, and manuscript preparation. CO: contributor to the intellectual content, interpretation of the literature, and manuscript preparation. He also provided content for the figures. HC: senior author and major contributor to the intellectual content, including selection of review content and interpretation of the literature. She also contributed to manuscript preparation.

FUNDING

This work was supported by the National Health and Medical Research Council of Australia (Grant number 1141928). LV was supported by an Australian International Postgraduate Research Scholarship. We are grateful to Frank and Patsy Youngleson for their generous support through a private donation.

ACKNOWLEDGMENTS

We thank Mr. Kiran Asplett for critical reading of the manuscript.

REFERENCES

Aaku-Saraste, E., Hellwig, A., and Huttner, W. B. (1996). Loss of occludin and functional tight junctions, but not ZO-1, during neural tube closure remodeling of the neuroepithelium prior to neurogenesis. *Dev. Biol.* 180, 664–679. doi: 10.1006/dbio.1996.0336

Acharya, B. R., Nestor-Bergmann, A., Liang, X., Gupta, S., Duszyc, K., Gauquelin, E., et al. (2018). A mechanosensitive RhoA pathway that protects epithelia against acute tensile stress. *Dev. Cell* 47, 439–452. doi: 10.1016/j.devcel.2018.09.016

Beattie, R., Postiglione, M. P., Burnett, L. E., Laukoter, S., Streicher, C., Pauler, F. M., et al. (2017). Mosaic analysis with double markers reveals distinct sequential functions of Lgl1 in neural stem cells. *Neuron* 94, 517–533. doi: 10.1016/j.neuron.2017.04.012

Betizeau, M., Cortay, V., Patti, D., Pfister, S., Gautier, E., Bellemin-Ménard, A., et al. (2013). Precursor diversity and complexity of lineage relationships in the outer subventricular zone of the primate. *Neuron* 80, 442–457. doi: 10.1016/j.neuron.2013.09.032

Betschinger, J., Eisenhaber, F., and Knoblich, J. A. (2005). Phosphorylation-induced autoinhibition regulates the cytoskeletal protein Lethal (2) giant larvae. *Curr. Biol.* 15, 276–282. doi: 10.1016/j.cub.2005.01.012

Betschinger, J., Mechtler, K., and Knoblich, J. A. (2003). The Par complex directs asymmetric cell division by phosphorylating the cytoskeletal protein Lgl. *Nature* 422, 326–330. doi: 10.1038/nature01486

Borghi, N., Sorokina, M., Shcherbakova, O. G., Weis, W. I., Pruitt, B. L., Nelson, W. J., et al. (2012). E-cadherin is under constitutive actomyosin-generated tension that is increased at cell-cell contacts upon externally applied stretch. *Proc. Natl. Acad. Sci. U.S.A.* 109, 12568–12573. doi: 10.1073/pnas.1204390109

Braga, V. (2017). Signaling by small GTPases at cell-cell junctions: protein interactions building control and networks. *Cold Spring Harb. Perspect. Biol.* 10:a028746. doi: 10.1101/cshperspect.a028746

Brieher, W. M., and Yap, A. S. (2013). Cadherin junctions and their cytoskeleton(s). *Curr. Opin. Cell Biol.* 25, 39–46. doi: 10.1016/j.ceb.2012.10.010

Buckley, C. D., Tan, J., Anderson, K. L., Hanein, D., Volkmann, N., Weis, W. I., et al. (2014). The minimal cadherin-catenin complex binds to actin filaments under force. *Science* 346:1254211. doi: 10.1126/science.1254211

Bultje, R. S., Castaneda-Castellanos, D. R., Jan, L. Y., Jan, Y. N., Kriegstein, A. R., and Shi, S.-H. (2009). Mammalian Par3 regulates progenitor cell asymmetric division via notch signaling in the developing neocortex. *Neuron* 63, 189–202. doi: 10.1016/j.neuron.2009.07.004

Bustamante, F. A., Miró, M. P., Velásquez, Z. D., Molina, L., Ehrenfeld, P., Rivera, F. J., et al. (2019). Role of adherens junctions and apical-basal polarity of neural stem/progenitor cells in the pathogenesis of neurodevelopmental disorders: a novel perspective on congenital Zika syndrome. *Trans. Res.* 210, 57–79. doi: 10.1016/j.trsl.2019.02.014

Cappello, S., Attardo, A., Wu, X., Iwasato, T., Itohara, S., Wilsch-Bräuninger, M., et al. (2006). The Rho-GTPase Cdc42 regulates neural progenitor fate at the apical surface. *Nat. Neurosci.* 9, 1099–1107. doi: 10.1038/nn1744

Cappello, S., Böhringer, C. R. J., Bergami, M., Conzelmann, K.-K., Ghanem, A., Tomassy, G. S., et al. (2012). A radial glia-specific role of RhoA in double cortex formation. *Neuron* 73, 911–924. doi: 10.1016/j.neuron.2011.12.030

Carabalona, A., Beguin, S., Pallesi-Pocachard, E., Buhler, E., Pellegrino, C., Arnaud, K., et al. (2012). A glial origin for periventricular nodular heterotopia caused by impaired expression of Filamin-A. *Hum. Mol. Genet.* 21, 1004–1017. doi: 10.1093/hmg/ddr531

Carminati, M., Gallini, S., Pirovano, L., Alfieri, A., Bisi, S., and Mapelli, M. (2016). Concomitant binding of Afadin to LGN and F-actin directs planar spindle orientation. *Nat. Struct. Mol. Biol.* 23, 155–163. doi: 10.1038/nsmb.3152

Chae, T. H., Kim, S., Marz, K. E., Hanson, P. I., and Walsh, C. A. (2004). The *hyh* mutation uncovers roles for alpha Snap in apical protein localization and control of neural cell fate. *Nat. Genet.* 36, 264–270. doi: 10.1038/ng1302

Chen, B., Brinkmann, K., Chen, Z., Pak, C. W., Liao, Y., Shi, S., et al. (2014). The WAVE regulatory complex links diverse receptors to the actin cytoskeleton. *Cell* 156, 195–207. doi: 10.1016/j.cell.2013.11.048

Chen, Z., Borek, D., Padrick, S. B., Gomez, T. S., Metlagel, Z., Ismail, A. M., et al. (2010). Structure and control of the actin regulatory WAVE complex. *Nature* 468, 533–538. doi: 10.1038/nature09623

Chenn, A., and Walsh, C. A. (2002). Regulation of cerebral cortical size by control of cell cycle exit in neural precursors. *Science* 297, 365–369. doi: 10.1126/science.1074192

Das, R. M., and Storey, K. G. (2014). Apical abscission alters cell polarity and dismantles the primary cilium during neurogenesis. *Science* 343, 200–204. doi: 10.1126/science.1247521

De Vries, M., and Cooper, H. M. (2008). Emerging roles for neogenin and its ligands in CNS development. *J. Neurochem.* 106, 1483–1492. doi: 10.1111/j.1471-4159.2008.05485.x

Del Bene, F., Wehman, A. M., Link, B. A., and Baier, H. (2008). Regulation of neurogenesis by interkinetic nuclear migration through an apical-basal notch gradient. *Cell* 134, 1055–1065. doi: 10.1016/j.cell.2008.07.017

Del Bigio, M. R. (2010). Ependymal cells: biology and pathology. *Acta Neuropathol.* 119, 55–73. doi: 10.1007/s00401-009-0624-y

Dollar, G. L., Weber, U., Mlodzik, M., and Sokol, S. Y. (2005). Regulation of Lethal giant larvae by Dishevelled. *Nature* 437, 1376–1380. doi: 10.1038/nature04116

Dominguez-Pinos, M. D., Paez, P., Jimenez, A. J., Weil, B., Arraez, M. A., Perez-Figares, J. M., et al. (2005). Ependymal denudation and alterations of the subventricular zone occur in human fetuses with a moderate communicating hydrocephalus. *J. Neuropathol. Exp. Neurol.* 64, 595–604. doi: 10.1097/01.jnen.0000171648.86718.bb

Drees, F., Pokutta, S., Yamada, S., Nelson, W. J., and Weis, W. I. (2005). Alpha-catenin is a molecular switch that binds E-cadherin-beta-catenin and regulates actin-filament assembly. *Cell* 123, 903–915. doi: 10.1016/j.cell.2005.09.021

Eggenschwiler, J. T., and Anderson, K. V. (2007). Cilia and developmental signaling. *Annu. Rev. Cell Dev. Biol.* 23, 345–373. doi: 10.1146/annurev.cellbio.23.090506.123249

Fame, R. M., Macdonald, J. L., and Macklis, J. D. (2011). Development, specification, and diversity of callosal projection neurons. *Trends Neurosci.* 34, 41–50. doi: 10.1016/j.tins.2010.10.002

Farkas, L. M., and Huttner, W. B. (2008). The cell biology of neural stem and progenitor cells and its significance for their proliferation versus differentiation during mammalian brain development. *Curr. Opin. Cell Biol.* 20, 707–715. doi: 10.1016/j.ceb.2008.09.008

Ferland, R. J., Batiz, L. F., Neal, J., Lian, G., Bundock, E., Lu, J., et al. (2009). Disruption of neural progenitors along the ventricular and subventricular zones in periventricular heterotopia. *Hum. Mol. Genet.* 18, 497–516. doi: 10.1093/hmg/ddn377

Fox, J. W., Lamperti, E. D., Eksioglu, Y. Z., Hong, S. E., Feng, Y., Graham, D. A., et al. (1998). Mutations in Filamin 1 prevent migration of cerebral cortical neurons in human periventricular heterotopia. *Neuron* 21, 1315–1325. doi: 10.1016/s0896-6273(00)80651-0

Gil-Sanz, C., Landeira, B., Ramos, C., Costa, M. R., and Müller, U. (2014). Proliferative defects and formation of a double cortex in mice lacking Mltt4 and Cdh2 in the dorsal telencephalon. *J. Neurosci.* 34, 10475–10487. doi: 10.1523/JNEUROSCI.1793-14.2014

Guerra, M. M., Henzi, R., Ortloff, A., Lichtin, N., Vío, K., Jiménez, A. J., et al. (2015). Cell junction pathology of neural stem cells is associated with ventricular zone disruption, hydrocephalus, and abnormal neurogenesis. *J. Neuropathol. Exp. Neurol.* 74, 653–671. doi: 10.1097/NEN.0000000000000203

Han, S. P., Gambin, Y., Gomez, G. A., Verma, S., Giles, N., Michael, M., et al. (2014). Cortactin scaffolds Arp2/3 and WAVE2 at the epithelial zonula adherens. *J. Biol. Chem.* 289, 7764–7775. doi: 10.1074/jbc.M113.544478

Hansen, A. H., Duellberg, C., Mieck, C., Loose, M., and Hippenmeyer, S. (2017). Cell polarity in cerebral cortex development - cellular architecture shaped by biochemical networks. *Front. Cell. Neurosci.* 11:176. doi: 10.3389/fncel.2017.00176

Hartfuss, E., Galli, R., Heins, N., and Gotz, M. (2001). Characterization of CNS precursor subtypes and radial glia. *Dev. Biol.* 229, 15–30. doi: 10.1006/dbio.2000.9962

Hatakeyama, J., Wakamatsu, Y., Nagafuchi, A., Kageyama, R., Shigemoto, R., and Shimamura, K. (2014). Cadherin-based adhesions in the apical endfoot are required for active Notch signaling to control neurogenesis in vertebrates. *Development* 141, 1671–1682. doi: 10.1242/dev.102988

Haubst, N., Georges-Labouesse, E., De Arcangelis, A., Mayer, U., and Götz, M. (2006). Basement membrane attachment is dispensable for radial glial cell fate and for proliferation, but affects positioning of neuronal subtypes. *Development* 133, 3245–3254. doi: 10.1242/dev.02486

Havrylenko, S., Noguera, P., Abou-Ghali, M., Manzi, J., Faqir, F., Lamora, A., et al. (2015). WAVE binds Ena/VASP for enhanced Arp2/3 complex-based actin assembly. *Mol. Biol. Cell* 26, 55–65. doi: 10.1091/mbc.E14-07-1200

Hurd, T. W., Gao, L., Roh, M. H., Macara, I. G., and Margolis, B. (2003). Direct interaction of two polarity complexes implicated in epithelial tight junction assembly. *Nat. Cell Biol.* 5, 137–142. doi: 10.1038/ncb923

Huttner, T. N., and Wieland, B. (2019). Malformations of human neocortex in development – their progenitor cell basis and experimental model systems. *Front. Cell. Neurosci.* 13:305. doi: 10.3389/fncel.2019.00305

Huttner, W. B., and Kosodo, Y. (2005). Symmetric versus asymmetric cell division during neurogenesis in the developing vertebrate central nervous system. *Curr. Opin. Cell Biol.* 17, 648–657. doi: 10.1016/j.ceb.2005.10.005

Imai, F., Hirai, S.-I., Akimoto, K., Koyama, H., Miyata, T., Ogawa, M., et al. (2006). Inactivation of aPKC lambda results in the loss of adherens junctions in neuroepithelial cells without affecting neurogenesis in mouse neocortex. *Development* 133, 1735–1744. doi: 10.1242/dev.02330

Itoh, Y., Moriyama, Y., Hasegawa, T., Endo, T. A., Toyoda, T., and Gotoh, Y. (2013). Scratch regulates neuronal migration onset via an epithelial-mesenchymal transition like mechanism. *Nat. Neurosci.* 16, 416–425. doi: 10.1038/nn.3336

Jain, N., Lim, L. W., Tan, W. T., George, B., Makeyev, E., and Thanabalu, T. (2014). Conditional N-WASP knockout in mouse brain implicates actin cytoskeleton regulation in hydrocephalus pathology. *Exp. Neurol.* 254, 29–40. doi: 10.1016/j.expneurol.2014.01.011

Jeong, S.-J., Luo, R., Singer, K., Giera, S., Kiyozumi, D., Shimono, C., et al. (2013). GPR56 functions together with α3β1 integrin in regulating cerebral cortical development. *PLoS One* 8:e68781. doi: 10.1371/journal.pone.0068781

Jimenez, A. J., Dominguez-Pinos, M. D., Guerra, M. M., Fernandez-Llebrez, P., and Perez-Figares, J. M. (2014). Structure and function of the ependymal barrier and diseases associated with ependyma disruption. *Tissue Barriers* 2:e28426. doi: 10.4161/tisb.28426

Jiménez, A. J., García-Verdugo, J. M., González, C. A., Batiz, L. F., Rodríguez-Pérez, L. M., Páez, P., et al. (2009). Disruption of the neurogenic niche in the subventricular zone of postnatal hydrocephalic *hyh* mice. *J. Neuropathol. Exp. Neurol.* 68, 1006–1020. doi: 10.1097/NEN.0b013e3181b44a5a

Jossin, Y., Lee, M., Klezovitch, O., Kon, E., Cossard, A., Lien, W.-H., et al. (2017). Llgl1 connects cell polarity with cell-cell adhesion in embryonic neural stem cells. *Dev. Cell* 41, 481–495. doi: 10.1016/j.devcel.2017.05.002

Kadowaki, M., Nakamura, S., Machon, O., Krauss, S., Radice, G. L., and Takeichi, M. (2007). N-cadherin mediates cortical organization in the mouse brain. *Dev. Biol.* 304, 22–33. doi: 10.1016/j.ydbio.2006.12.014

Kasper, E. M., Larkman, A. U., Lubke, J., and Blakemore, C. (1994). Pyramidal neurons in layer 5 of the rat visual cortex. I. Correlation among cell morphology, intrinsic electrophysiological properties, and axon targets. *J. Comp. Neurol.* 339, 459–474. doi: 10.1002/cne.903390402

Katayama, K.-I., Melendez, J., Baumann, J. M., Leslie, J. R., Chauhan, B. K., Nemkul, N., et al. (2011). Loss of RhoA in neural progenitor cells causes the disruption of adherens junctions and hyperproliferation. *Proc. Natl. Acad. Sci. U.S.A.* 108, 7607–7612. doi: 10.1073/pnas.1101347108

Kee, N., Wilson, N., De Vries, M., Bradford, D., Key, B., and Cooper, H. M. (2008). Neogenin and RGMa control neural tube closure and neuroepithelial morphology by regulating cell polarity. *J. Neurosci.* 28, 12643–12653. doi: 10.1523/JNEUROSCI.4265-08.2008

Kelava, I., Lewitus, E., and Huttner, W. B. (2013). The secondary loss of gyrencephaly as an example of evolutionary phenotypical reversal. *Front. Neuroanat.* 7:16. doi: 10.3389/fnana.2013.00016

Kim, S., Lehtinen, M. K., Sessa, A., Zappaterra, M. W., Cho, S. H., Gonzalez, D., et al. (2010). The apical complex couples cell fate and cell survival to cerebral cortical development. *Neuron* 66, 69–84. doi: 10.1016/j.neuron.2010.03.019

Klezovitch, O., Fernandez, T. E., Tapscott, S. J., and Vasioukhin, V. (2004). Loss of cell polarity causes severe brain dysplasia in Lgl1 knockout mice. *Genes Dev.* 18, 559–571. doi: 10.1101/gad.1178004

Kobielak, A., Pasolli, H. A., and Fuchs, E. (2004). Mammalian formin-1 participates in adherens junctions and polymerization of linear actin cables. *Nat. Cell Biol.* 6, 21–30. doi: 10.1038/ncb1075

Konno, D., Shioi, G., Shitamukai, A., Mori, A., Kiyonari, H., Miyata, T., et al. (2008). Neuroepithelial progenitors undergo LGN-dependent planar divisions to maintain self-renewability during mammalian neurogenesis. *Nat. Cell Biol.* 10, 93–101. doi: 10.1038/ncb1673

Kosodo, Y., Röper, K., Haubensak, W., Marzesco, A.-M., Corbeil, D., and Huttner, W. B. (2004). Asymmetric distribution of the apical plasma membrane during neurogenic divisions of mammalian neuroepithelial cells. *EMBO J.* 23, 2314–2324. doi: 10.1038/sj.emboj.7600223

Kousi, M., and Katsanis, N. (2016). The genetic basis of hydrocephalus. *Ann. Rev. Neurosci.* 39, 409–435. doi: 10.1146/annurev-neuro-070815-014023

Kovacs, E. M., Verma, S., Ali, R. G., Ratheesh, A., Hamilton, N. A., Akhmanova, A., et al. (2011). N-WASP regulates the epithelial junctional actin cytoskeleton through a non-canonical post-nucleation pathway. *Nat. Cell Biol.* 13, 934–943. doi: 10.1038/ncb2290

Kowalczyk, T., Pontious, A., Englund, C., Daza, R. A. M., Bedogni, F., Hodge, R., et al. (2009). Intermediate neuronal progenitors (basal progenitors) produce pyramidal-projection neurons for all layers of cerebral cortex. *Cereb. Cortex* 19, 2439–2450. doi: 10.1093/cercor/bhn260

Kriegstein, A., and Alvarez-Buylla, A. (2009). The glial nature of embryonic and adult neural stem cells. *Ann. Rev. Neurosci.* 32, 149–184. doi: 10.1146/annurev.neuro.051508.135600

Lee, N., Fok, K., White, A., Wilson, N., O'Leary, C., Cox, H., et al. (2016). Neogenin recruitment of the WAVE Regulatory Complex maintains adherens junction stability and tension. *Nat. Commun.* 7:11082. doi: 10.1038/ncomms11082

Lehtinen, M. K., Zappaterra, M. W., Chen, X., Yang, Y. J., Hill, A. D., Lun, M., et al. (2011). The cerebrospinal fluid provides a proliferative niche for neural progenitor cells. *Neuron* 69, 893–905. doi: 10.1016/j.neuron.2011.01.023

Lian, G., and Sheen, V. L. (2015). Cytoskeletal proteins in cortical development and disease: actin associated proteins in periventricular heterotopia. *Front. Cell. Neurosci.* 9:99. doi: 10.3389/fncel.2015.00099

Lien, W. H., Klezovitch, O., Fernandez, T. E., Delrow, J., and Vasioukhin, V. (2006). Alpha E-catenin controls cerebral cortical size by regulating the hedgehog signaling pathway. *Science* 311, 1609–1612. doi: 10.1126/science.1121449

Linford, A., Yoshimura, S.-I., Nunes Bastos, R., Langemeyer, L., Gerondopoulos, A., Rigden, D. J., et al. (2012). Rab14 and its exchange factor FAM116 link endocytic recycling and adherens junction stability in migrating cells. *Dev. Cell* 22, 952–966. doi: 10.1016/j.devcel.2012.04.010

Llinares-Benadero, C., and Borrell, V. (2019). Deconstructing cortical folding: genetic, cellular and mechanical determinants. *Nat. Rev. Neurosci.* 20, 161–176. doi: 10.1038/s41583-018-0112-2

Lock, J. G., and Stow, J. L. (2005). Rab11 in recycling endosomes regulates the sorting and basolateral transport of E-cadherin. *Mol. Biol. Cell* 16, 1744–1755. doi: 10.1091/mbc.e04-10-0867

Lodato, S., and Arlotta, P. (2015). Generating neuronal diversity in the mammalian cerebral cortex. *Ann. Rev. Cell Dev. Biol.* 31, 699–720. doi: 10.1146/annurev-cellbio-100814-125353

Loulier, K., Lathia, J. D., Marthiens, V., Relucio, J., Mughal, M. R., Tang, S.-C., et al. (2009). β1 integrin maintains integrity of the embryonic neocortical stem cell niche. *PLoS Biol.* 7:e1000176. doi: 10.1371/journal.pbio.1000176

Ma, X., Bao, J., and Adelstein, R. S. (2007). Loss of cell adhesion causes hydrocephalus in nonmuscle myosin II-B-ablated and mutated mice. *Mol. Biol. Cell* 18, 2305–2312. doi: 10.1091/mbc.e07-01-0073

Machon, O., Van Den Bout, C. J., Backman, M., Kemler, R., and Krauss, S. (2003). Role of beta-catenin in the developing cortical and hippocampal neuroepithelium. *Neuroscience* 122, 129–143. doi: 10.1016/s0306-4522(03)00519-0

Maître, J.-L., Berthoumieux, H., Krens, S. F. G., Salbreux, G., Jülicher, F., Paluch, E., et al. (2012). Adhesion functions in cell sorting by mechanically coupling the cortices of adhering cells. *Science* 338, 253–256. doi: 10.1126/science.1225399

Malatesta, P., Hartfuss, E., and Gotz, M. (2000). Isolation of radial glial cells by fluorescent-activated cell sorting reveals a neuronal lineage. *Development* 127, 5253–5263.

Marthiens, V., and Ffrench-Constant, C. (2009). Adherens junction domains are split by asymmetric division of embryonic neural stem cells. *EMBO Rep.* 10, 515–520. doi: 10.1038/embor.2009.36

Martínez-Martínez, M. Á., De Juan Romero, C., Fernández, V., Cárdenas, A., Götz, M., and Borrell, V. (2016). A restricted period for formation of outer subventricular zone defined by Cdh1 and Trnp1 levels. *Nat. Commun.* 7:11812. doi: 10.1038/ncomms11812

Mary, S., Charrasse, S., Meriane, M., Comunale, F., Travo, P., Blangy, A., et al. (2002). Biogenesis of N-cadherin-dependent cell-cell contacts in living fibroblasts is a microtubule-dependent kinesin-driven mechanism. *Mol. Biol. Cell* 13, 285–301. doi: 10.1091/mbc.01-07-0337

Misson, J. P., Edwards, M. A., Yamamoto, M., and Caviness, V. S. Jr. (1988). Mitotic cycling of radial glial cells of the fetal murine cerebral wall: a combined autoradiographic and immunohistochemical study. *Brain Res.* 466, 183–190. doi: 10.1016/0165-3806(88)90043-0

Miyata, T., Kawaguchi, A., Okano, H., and Ogawa, M. (2001). Asymmetric inheritance of radial glial fibers by cortical neurons. *Neuron* 31, 727–741. doi: 10.1016/s0896-6273(01)00420-2

Miyata, T., Kawaguchi, A., Saito, K., Kawano, M., Muto, T., and Ogawa, M. (2004). Asymmetric production of surface-dividing and non-surface dividing cortical progenitor cells. *Development* 131, 3133–3145. doi: 10.1242/dev.01173

Molyneaux, B. J., Arlotta, P., Menezes, J. R. L., and Macklis, J. D. (2007). Neuronal subtype specification in the cerebral cortex. *Nat. Rev. Neurosci.* 8, 427–437. doi: 10.1038/nrn2151

Morais-de-Sa, E., Mirouse, V., and St Johnston, D. (2010). aPKC phosphorylation of Bazooka defines the apical/lateral border in *Drosophila* epithelial cells. *Cell* 141, 509–523. doi: 10.1016/j.cell.2010.02.040

Murciano, A., Zamora, J., Lopez-Sanchez, J., and Frade, J. M. (2002). Interkinetic nuclear movement may provide spatial clues to the regulation of neurogenesis. *Mol. Cell. Neurosci.* 21, 285–300. doi: 10.1006/mcne.2002.1174

Nadarajah, B., Brunstrom, J. E., Grutzendler, J., Wong, R. O., and Pearlman, A. L. (2001). Two modes of radial migration in early development of the cerebral cortex. *Nat. Neurosci.* 4, 143–150. doi: 10.1038/83967

Nechiporuk, T., Fernandez, T. E., and Vasioukhin, V. (2007). Failure of epithelial tube maintenance causes hydrocephalus and renal cysts in Dlg5-/- mice. *Dev. Cell* 13, 338–350. doi: 10.1016/j.devcel.2007.07.017

Noctor, S. C., Flint, A. C., Weissman, T. A., Wong, W. S., Clinton, B. K., and Kriegstein, A. R. (2002). Dividing precursor cells of the embryonic cortical ventricular zone have morphological and molecular characteristics of radial glia. *J. Neurosci.* 22, 3161–3173. doi: 10.1523/jneurosci.22-08-03161.2002

Nusse, R., and Clevers, H. (2017). Wnt/β-catenin signaling, disease, and emerging therapeutic modalities. *Cell* 169, 985–999. doi: 10.1016/j.cell.2017.05.016

Oberst, P., Fièvre, S., Baumann, N., Concetti, C., Bartolini, G., and Jabaudon, D. (2019). Temporal plasticity of apical progenitors in the developing mouse neocortex. *Nature* 573, 370–374. doi: 10.1038/s41586-019-1515-6

Ohata, S., Aoki, R., Kinoshita, S., Yamaguchi, M., Tsuruoka-Kinoshita, S., Tanaka, H., et al. (2011). Dual roles of Notch in regulation of apically restricted mitosis and apicobasal polarity of neuroepithelial cells. *Neuron* 69, 215–230. doi: 10.1016/j.neuron.2010.12.026

O'Leary, C. J., Bradford, D., Chen, M., White, A., Blackmore, D. G., and Cooper, H. M. (2015). The Netrin/RGM receptor, Neogenin, controls adult neurogenesis by promoting neuroblast migration and cell cycle exit. *Stem Cells* 33, 503–514. doi: 10.1002/stem.1861

O'Leary, C. J., Nourse, C. C., Lee, N. K., White, A., Langford, M., Sempert, K., et al. (2017). Neogenin recruitment of the WAVE Regulatory Complex to ependymal and radial progenitor adherens junctions prevents hydrocephalus. *Cell Rep.* 20, 370–383. doi: 10.1016/j.celrep.2017.06.051

O'Leary, D. D., and Koester, S. E. (1993). Development of projection neuron types, axon pathways, and patterned connections of the mammalian cortex. *Neuron* 10, 991–1006. doi: 10.1016/0896-6273(93)90049-w

Oliver, C., Gonzalez, C. A., Alvial, G., Flores, C. A., Rodriguez, E. M., and Batiz, L. F. (2013). Disruption of CDH2/N-cadherin-based adherens junctions leads to apoptosis of ependymal cells and denudation of brain ventricular walls. *J. Neuropathol. Exp. Neurol.* 72, 846–860. doi: 10.1097/NEN.0b013e3182a2d5fe

Ortiz-Álvarez, G., Daclin, M., Shihavuddin, A., Lansade, P., Fortoul, A., Faucourt, M., et al. (2019). Adult neural stem cells and multiciliated ependymal cells share a common lineage regulated by the geminin family members. *Neuron* 102, 159–172. doi: 10.1016/j.neuron.2019.01.051

Paez, P., Batiz, L. F., Roales-Bujan, R., Rodriguez-Perez, L. M., Rodriguez, S., Jimenez, A. J., et al. (2007). Patterned neuropathologic events occurring in *hyh* congenital hydrocephalic mutant mice. *J. Neuropathol. Exp. Neurol.* 66, 1082–1092. doi: 10.1097/nen.0b013e31815c1952

Paridaen, J. T., and Huttner, W. B. (2014). Neurogenesis during development of the vertebrate central nervous system. *EMBO Rep.* 15, 351–364. doi: 10.1002/embr.201438447

Paridaen, J. T., Wilsch-Brauninger, M., and Huttner, W. B. (2013). Asymmetric inheritance of centrosome-associated primary cilium membrane directs ciliogenesis after cell division. *Cell* 155, 333–344. doi: 10.1016/j.cell.2013.08.060

Park, R., Moon, U. Y., Park, J. Y., Hughes, L. J., Johnson, R. L., Cho, S.-H., et al. (2016). Yap is required for ependymal integrity and is suppressed in LPA-induced hydrocephalus. *Nat. Commun.* 7:10329. doi: 10.1038/ncomms10329

Peglion, F., and Goehring, N. W. (2019). Switching states: dynamic remodelling of polarity complexes as a toolkit for cell polarization. *Curr. Opin. Cell Biol.* 60, 121–130. doi: 10.1016/j.ceb.2019.05.002

Pinson, A., Namba, T., and Huttner, W. B. (2019). Malformations of human neocortex in development - their progenitor cell basis and experimental model systems. *Front. Cell. Neurosci.* 13:305. doi: 10.3389/fncel.2019.00305

Pizarro-Cerda, J., Chorev, D. S., Geiger, B., and Cossart, P. (2017). The diverse family of Arp2/3 complexes. *Trends Cell Biol.* 27, 93–100. doi: 10.1016/j.tcb.2016.08.001

Plant, P. J., Fawcett, J. P., Lin, D. C. C., Holdorf, A. D., Binns, K., Kulkarn, S., et al. (2003). A polarity complex of mPar-6 and atypical PKC binds, phosphorylates and regulates mammalian Lgl. *Nat. Cell Biol.* 5, 301–308. doi: 10.1038/ncb948

Postiglione, M. P., Jüschke, C., Xie, Y., Haas, G. A., Charalambous, C., and Knoblich, J. A. (2011). Mouse inscuteable induces apical-basal spindle orientation to facilitate intermediate progenitor generation in the developing neocortex. *Neuron* 72, 269–284. doi: 10.1016/j.neuron.2011.09.022

Priya, R., and Yap, A. S. (2015). Active tension: the role of cadherin adhesion and signaling in generating junctional contractility. *Curr. Top. Dev. Biol.* 112, 65–102. doi: 10.1016/bs.ctdb.2014.11.016

Rajagopalan, S., Deitinghoff, L., Davis, D., Conrad, S., Skutella, T., Chédotal, A., et al. (2004). Neogenin mediates the action of repulsive guidance molecule. *Nat. Cell Biol.* 6, 756–762. doi: 10.1038/ncb1156

Rakotomamonjy, J., Brunner, M., Jüschke, C., Zang, K., Huang, E. J., Reichardt, L. F., et al. (2017). Afadin controls cell polarization and mitotic spindle orientation in developing cortical radial glia. *Neural Dev.* 12:7. doi: 10.1186/s13064-017-0085-2

Rasin, M.-R., Gazula, V.-R., Breunig, J. J., Kwan, K. Y., Johnson, M. B., Liu-Chen, S., et al. (2007). Numb and Numbl are required for maintenance of cadherin-based adhesion and polarity of neural progenitors. *Nat. Neurosci.* 10, 819–827. doi: 10.1038/nn1924

Redmond, S. A., Figueres-Oñate, M., Obernier, K., Nascimento, M. A., Parraguez, J. I., López-Mascaraque, L., et al. (2019). Development of ependymal and postnatal neural stem cells and their origin from a common embryonic progenitor. *Cell Rep.* 27, 429–441. doi: 10.1016/j.celrep.2019.01.088

Reillo, I., De Juan Romero, C., García-Cabezas, M. Á., and Borrell, V. (2011). A role for intermediate radial glia in the tangential expansion of the mammalian cerebral cortex. *Cereb. Cortex* 21, 1674–1694. doi: 10.1093/cercor/bhq238

Rodriguez, E. M., Guerra, M. M., Vío, K., González, C., Ortloff, A., Bátiz, L. F., et al. (2012). A cell junction pathology of neural stem cells leads to abnormal neurogenesis and hydrocephalus. *Biol. Res.* 45, 231–241. doi: 10.4067/S0716-97602012000300005

Rohatgi, R., Ma, L., Miki, H., Lopez, M., Kirchhausen, T., Takenawa, T., et al. (1999). The interaction between N-WASP and the Arp2/3 complex links Cdc42-dependent signals to actin assembly. *Cell* 97, 221–231. doi: 10.1016/s0092-8674(00)80732-1

Sauer, F. C. (1935). Mitosis in the neural tube. *J. Comp. Neurol.* 62, 377–405. doi: 10.1002/cne.900620207

Schaffer, A. E., Breuss, M. W., Caðlayan, A. O., Al-Sanaa, N., Al-Abdulwahed, H. Y., Kaymakçalan, H., et al. (2018). Biallelic loss of human *CTNNA2*, encoding αN-catenin, leads to ARP2/3 complex overactivity and disordered cortical neuronal migration. *Nat. Genet.* 50, 1093–1101. doi: 10.1038/s41588-018-0166-0

Schaks, M., Singh, S. P., Kage, F., Thomason, P., Klunemann, T., Steffen, A., et al. (2018). Distinct interaction sites of Rac GTPase with WAVE regulatory complex have non-redundant functions *in vivo*. *Curr. Biol.* 28, 3674–3684. doi: 10.1016/j.cub.2018.10.002

Schmid, M.-T., Weinandy, F., Wilsch-Bräuninger, M., Huttner, W. B., Cappello, S., and Götz, M. (2014). The role of α-E-catenin in cerebral cortex development: radial glia specific effect on neuronal migration. *Front. Cell. Neurosci.* 8:215. doi: 10.3389/fncel.2014.00215

Sheen, V. L., Basel-Vanagaite, L., Goodman, J. R., Scheffer, I. E., Bodell, A., Ganesh, V. S., et al. (2004). Etiological heterogeneity of familial periventricular heterotopia and hydrocephalus. *Brain Dev.* 26, 326–334. doi: 10.1016/j.braindev.2003.09.004

Sheen, V. L., Ganesh, V. S., Topçu, M., Sebire, G., Bodell, A., Hill, R. S., et al. (2003). Mutations in *ARFGEF2* implicate vesicle trafficking in neural progenitor proliferation and migration in the human cerebral cortex. *Nat. Genet.* 36, 69–76. doi: 10.1038/ng1276

Sheen, V. L., and Sheen, V. (2014). Filamin A mediated Big2 dependent endocytosis: from apical abscission to periventricular heterotopia. *Tissue Barriers* 2:e29431. doi: 10.4161/tisb.29431

Shitamukai, A., Konno, D., and Matsuzaki, F. (2011). Oblique radial glial divisions in the developing mouse neocortex induce self-renewing progenitors outside the germinal zone that resemble primate outer subventricular zone progenitors. *J. Neurosci.* 31, 3683–3695. doi: 10.1523/JNEUROSCI.4773-10.2011

Siebold, C., Yamashita, T., Monnier, P. P., Mueller, B. K., and Pasterkamp, R. J. (2017). RGMs: structural insights, molecular regulation, and downstream signaling. *Trends Cell Biol.* 27, 365–378. doi: 10.1016/j.tcb.2016.11.009

Siton-Mendelson, O., and Bernheim-Groswasser, A. (2017). Functional actin networks under construction: the cooperative action of actin nucleation and elongation factors. *Trends Biochem. Sci.* 42, 414–430. doi: 10.1016/j.tibs.2017.03.002

Smart, I. H. M., Dehay, C., Giroud, P., Berland, M., and Kennedy, H. (2002). Unique morphological features of the proliferative zones and postmitotic compartments of the neural epithelium giving rise to striate and extrastriate cortex in the monkey. *Cereb. Cortex* 12, 37–53. doi: 10.1093/cercor/12.1.37

Smutny, M., Wu, S. K., Gomez, G. A., Mangold, S., Yap, A. S., and Hamilton, N. A. (2011). Multicomponent analysis of junctional movements regulated by myosin II isoforms at the epithelial zonula adherens. *PLoS One* 6:e22458. doi: 10.1371/journal.pone.0022458

Spassky, N., Merkle, F. T., Flames, N., Tramontin, A. D., García-Verdugo, J. M., and Alvarez-Buylla, A. (2005). Adult ependymal cells are postmitotic and are derived from radial glial cells during embryogenesis. *J. Neurosci.* 25, 10–18. doi: 10.1523/jneurosci.1108-04.2005

Stocker, A. M., and Chenn, A. (2015). The role of adherens junctions in the developing neocortex. *Cell Adh. Migr.* 9, 167–174. doi: 10.1080/19336918.2015.1027478

Striedter, G. F., Srinivasan, S., and Monuki, E. S. (2015). Cortical folding: when, where, how and why? *Ann. Rev. Neurosci.* 38, 291–307. doi: 10.1146/annurev-neuro-071714-034128

Symons, M., Derry, J. M., Karlak, B., Jiang, S., Lemahieu, V., Mccormick, F., et al. (1996). Wiskott-Aldrich syndrome protein, a novel effector for the GTPase CDC42Hs, is implicated in actin polymerization. *Cell* 84, 723–734. doi: 10.1016/s0092-8674(00)81050-8

Tanentzapf, G., and Tepass, U. (2003). Interactions between the crumbs, lethal giant larvae and bazooka pathways in epithelial polarization. *Nat. Cell Biol.* 5, 46–52. doi: 10.1038/ncb896

Tavano, S., Taverna, E., Kalebic, N., Haffner, C., Namba, T., Dahl, A., et al. (2018). Insm1 induces neural progenitor delamination in developing neocortex via downregulation of the adherens junction belt-specific protein Plekha7. *Neuron* 97, 1299–1314. doi: 10.1016/j.neuron.2018.01.052

Taverna, E., Götz, M., and Huttner, W. B. (2014). The cell biology of neurogenesis: toward an understanding of the development and evolution of the neocortex. *Ann. Rev. Cell Dev. Biol.* 30, 465–502. doi: 10.1146/annurev-cellbio-101011-155801

Taverna, E., and Huttner, W. B. (2010). Neural progenitor nuclei IN motion. *Neuron* 67, 906–914. doi: 10.1016/j.neuron.2010.08.027

Thumkeo, D., Shinohara, R., Watanabe, K., Takebayashi, H., Toyoda, Y., Tohyama, K., et al. (2011). Deficiency of mDia, an actin nucleator, disrupts integrity of neuroepithelium and causes periventricular dysplasia. *PLoS One* 6:e25465. doi: 10.1371/journal.pone.0025465

Tramontin, A. D., Garcia-Verdugo, J. M., Lim, D. A., and Alvarez-Buylla, A. (2003). Postnatal development of radial glia and the ventricular zone (VZ): a continuum of the neural stem cell compartment. *Cereb. Cortex* 13, 580–587. doi: 10.1093/cercor/13.6.580

Tullio, A. N., Bridgman, P. C., Tresser, N. J., Chan, C. C., Conti, M. A., Adelstein, R. S., et al. (2001). Structural abnormalities develop in the brain after ablation of the gene encoding nonmuscle myosin II-B heavy chain. *J. Comp. Neurol.* 433, 62–74. doi: 10.1002/cne.1125

Verma, S., Han, S. P., Michael, M., Gomez, G. A., Yang, Z., Teasdale, R. D., et al. (2012). A WAVE2-Arp2/3 actin nucleator apparatus supports junctional tension at the epithelial zonula adherens. *Mol. Biol. Cell* 23, 4601–4610. doi: 10.1091/mbc.E12-08-0574

Vitali, I., Fievre, S., Telley, L., Oberst, P., Bariselli, S., Frangeul, L., et al. (2018). Progenitor hyperpolarization regulates the sequential generation of neuronal subtypes in the developing neocortex. *Cell* 174, 1264–1276. doi: 10.1016/j.cell.2018.06.036

Walther, R. F., and Pichaud, F. (2010). Crumbs/DaPKC-dependent apical exclusion of Bazooka promotes photoreceptor polarity remodeling. *Curr. Biol.* 20, 1065–1074. doi: 10.1016/j.cub.2010.04.049

Wang, P.-S., Chou, F.-S., Ramachandran, S., Xia, S., Chen, H.-Y., Guo, F., et al. (2016). Crucial roles of the Arp2/3 complex during mammalian corticogenesis. *Development* 143, 2741–2751. doi: 10.1242/dev.130542

Wang, X., Tsai, J.-W., Imai, J. H., Lian, W.-N., Vallee, R. B., and Shi, S.-H. (2009). Asymmetric centrosome inheritance maintains neural progenitors in the neocortex. *Nature* 461, 947–955. doi: 10.1038/nature08435

Wilsch-Brauninger, M., Peters, J., Paridaen, J. T., and Huttner, W. B. (2012). Basolateral rather than apical primary cilia on neuroepithelial cells committed to delamination. *Development* 139, 95–105. doi: 10.1242/dev.069294

Woodhead, G. J., Mutch, C. A., Olson, E. C., and Chenn, A. (2006). Cell-autonomous beta-catenin signaling regulates cortical precursor proliferation. *J. Neurosci.* 26, 12620–12630. doi: 10.1523/jneurosci.3180-06.2006

Wu, S. K., Gomez, G. A., Michael, M., Verma, S., Cox, H. L., Lefevre, J. G., et al. (2014). Cortical F-actin stabilization generates apical-lateral patterns of junctional contractility that integrate cells into epithelia. *Nat. Cell Biol.* 16, 167–178. doi: 10.1038/ncb2900

Yamamoto, H., Maruo, T., Majima, T., Ishizaki, H., Tanaka-Okamoto, M., Miyoshi, J., et al. (2013). Genetic deletion of afadin causes hydrocephalus by destruction of adherens junctions in radial glial and ependymal cells in the midbrain. *PLoS One* 8:e80356. doi: 10.1371/journal.pone.0080356

Yamanaka, T., Horikoshi, Y., Sugiyama, Y., Ishiyama, C., Suzuki, A., Hirose, T., et al. (2003). Mammalian Lgl forms a protein complex with PAR-6 and aPKC independently of PAR-3 to regulate epithelial cell polarity. *Curr. Biol.* 13, 734–743. doi: 10.1016/s0960-9822(03)00244-6

Yap, A. S., Duszyc, K., and Viasnoff, V. (2017). Mechanosensing and mechanotransduction at cell-cell junctions. *Cold Spring Harb. Perspect. Biol.* 10:a028761. doi: 10.1101/cshperspect.a028761

Yoon, K.-J., Nguyen, H. N., Ursini, G., Zhang, F., Kim, N.-S., Wen, Z., et al. (2014). Modeling a genetic risk for schizophrenia in iPSCs and mice reveals neural stem cell deficits associated with adherens junctions and polarity. *Cell Stem Cell* 15, 79–91. doi: 10.1016/j.stem.2014.05.003

Yoon, K.-J., Song, G., Qian, X., Pan, J., Xu, D., Rho, H. S., et al. (2017). Zika virus-encoded NS2a disrupts mammalian cortical neurogenesis by degrading adherens junction proteins. *Cell Stem Cell* 21, 349–358. doi: 10.1016/j.stem.2017.07.014

Zhang, T., Sen, Z., Song, X., Zhao, X., Hou, C., Li, Z., et al. (2019). Loss of Lgl1 disrupts the radial glial fiber-guided cortical neuronal migration and causes subcortical band heterotopia in mice. *Neuroscience* 400, 132–145. doi: 10.1016/j.neuroscience.2018.12.039

Conflict of Interest: The authors declare that the research was conducted in the absence of any commercial or financial relationships that could be construed as a potential conflict of interest.

Copyright © 2020 Veeraval, O'Leary and Cooper. This is an open-access article distributed under the terms of the Creative Commons Attribution License (CC BY). The use, distribution or reproduction in other forums is permitted, provided the original author(s) and the copyright owner(s) are credited and that the original publication in this journal is cited, in accordance with accepted academic practice. No use, distribution or reproduction is permitted which does not comply with these terms.

frontiers in Cell and Developmental Biology

REVIEW
published: 12 March 2020
doi: 10.3389/fcell.2020.00150

Mechanical Regulation of Nuclear Translocation in Migratory Neurons

Naotaka Nakazawa[1]* *and Mineko Kengaku*[1,2]

[1] *Institute for Integrated Cell-Material Sciences (WPI-iCeMS), Kyoto University Institute for Advanced Study, Kyoto University, Kyoto, Japan,* [2] *Graduate School of Biostudies, Kyoto University, Kyoto, Japan*

Neuronal migration is a critical step during the formation of functional neural circuits in the brain. Newborn neurons need to move across long distances from the germinal zone to their individual sites of function; during their migration, they must often squeeze their large, stiff nuclei, against strong mechanical stresses, through narrow spaces in developing brain tissue. Recent studies have clarified how actomyosin and microtubule motors generate mechanical forces in specific subcellular compartments and synergistically drive nuclear translocation in neurons. On the other hand, the mechanical properties of the surrounding tissues also contribute to their function as an adhesive support for cytoskeletal force transmission, while they also serve as a physical barrier to nuclear translocation. In this review, we discuss recent studies on nuclear migration in developing neurons, from both cell and mechanobiological viewpoints.

Keywords: neuronal migration, nuclear translocation, cytoskeleton, cellular mechanics, actomyosin, microtubule motors

OPEN ACCESS

Edited by:
Selwin K. Wu,
National University of Singapore, Singapore

Reviewed by:
Shenshen Wang,
University of California, Los Angeles, United States
Shiwei Liu,
Harvard University, United States

***Correspondence:**
Naotaka Nakazawa
nakazawa.naotaka.4e@kyoto-u.ac.jp

Specialty section:
This article was submitted to Cell Adhesion and Migration, a section of the journal Frontiers in Cell and Developmental Biology

Received: *01 November 2019*
Accepted: *24 February 2020*
Published: *12 March 2020*

Citation:
Nakazawa N and Kengaku M (2020) Mechanical Regulation of Nuclear Translocation in Migratory Neurons. Front. Cell Dev. Biol. 8:150. doi: 10.3389/fcell.2020.00150

INTRODUCTION

Over a 100 years ago, Wilhelm His and Santiago Ramón y Cajal recognized that neurons were generated in specific germinal zones and migrated to their individual sites of function in the developing brain. Today researchers have caught up to their visionary studies and visualized neuronal migration through live imaging studies. Neuronal migration in earlier stages is critical for neuronal network formation in the later stages of brain development (Stiles and Jernigan, 2010; Silva et al., 2019). Disruption of neuronal migration thus causes brain malformations such as lissencephaly, which is accompanied by defects in neural network organization, manifesting as epilepsy, intellectual disability, and mental disorders. Previous studies have identified mutations in several genes encoding cytoskeletal motors and their associated molecules as the causes of these disorders (Manzini and Walsh, 2011; Cooper, 2013; Moon and Wynshaw-Boris, 2013; Buchsbaum and Cappello, 2019). These studies have expanded our knowledge of the roles of cellular signaling, including post-translational modifications of cytoskeletal molecules, in neuronal migration (Silva et al., 2018, 2019).

Migratory cells move long distances, frequently through confined spaces between other cells and extracellular matrices (ECMs) in tissues. Delivery of the nucleus, the largest and stiffest cargo, presents the biggest physical challenge for the cell to penetrate such confined environments. The nucleus is either pulled or pushed by the mechanical force generated by cytoskeletal motors, which are regulated by intracellular signals governing motor protein activity and cell polarity formation (Li and Gundersen, 2008; Fletcher and Mullins, 2010; Gundersen and Worman, 2013). In many migratory cells, the nucleus is harnessed to adhesions via actin cables and pulled

forward by actomyosin contractility and integrin-mediated traction at the leading edge (Wolf et al., 2013; Wu et al., 2014). In contrast, other migratory cells including leucocytes in confined spaces require actomyosin contraction at the back in order to squeeze the nucleus through narrow pores (Lämmermann et al., 2008; Thomas et al., 2015). Rapid advances in mechanobiology have revealed how mechanical strains generated by physical confinement affect cytoskeletal dynamics in migrating cells (Stroka et al., 2014; Liu et al., 2015; Ruprecht et al., 2015).

However, our understanding of how the mechanical forces generated and sensed by cytoskeletal molecules drive nuclear translocation in migrating neurons lags behind that of other mesenchymal cells (Kengaku, 2018). In addition to intracellular signaling regulating cytoskeletal dynamics, one should consider the impact of mechanical properties of the nucleus, which is physically coupled to the cytoskeleton, in order to understand the mechanics of nuclear migration.

In this review, we summarize recent work on the role of mechanics in nuclear translocation in migrating neurons. First, we describe characteristic features of nuclear translocation and related nuclear machinery in neurons (see sections "Nuclear Migration in Neurons" and "The Machinery of the Nucleus: Its Mechanical Properties and Force Transmission"). Next, we illustrate how cytoskeletal motors drive nuclear translocation during neuronal migration in the brain with examples (see Section "Active Nuclear Translocation by Cytoskeletal Molecules in Neuronal Cells"). Finally, we discuss how the mechanical properties of the nucleus and extracellular environment impact nuclear translocation (see section "Cellular and Extracellular Mechanical Properties Affecting Nuclear Translocation in Neuronal Cells").

NUCLEAR MIGRATION IN NEURONS

Migrating neurons have a clear cell polarity and are subdivided into distinct compartments such as the growth cone, leading process, and cell body (Fletcher and Mullins, 2010; Cooper, 2013). These compartments are propelled independently by differential subsets of cytoskeletal systems, which coordinately regulate overall cell movement. Generally, neuronal migration is driven by two steps (**Figure 1**). The first step is the elongation of the leading process, where the plasma membrane at the growth cone is pushed by polymerizing *F*-actin. *F*-actin filaments are coupled by a molecular clutch to adhesions, thereby converting the myosin II-driven retrograde flow to a driving force for growth cone extension (Lin and Forscher, 1995; Lin et al., 1996; Bard et al., 2008; Lowery and Van Vactor, 2009; Kerstein et al., 2015). The second step is nuclear translocation, which is regulated differently from growth cone extension because of the physical separation of the nucleus from the growth cone. Differential regulation of these two steps causes a unique saltatory movement of the nucleus into the leading process (Edmondson and Hatten, 1987; Komuro and Rakic, 1995; Schaar and McConnell, 2005; Umeshima et al., 2007). This is in contrast to mesenchymal migration where the leading edge extension and nuclear translocation are regulated as sequential events.

THE MACHINERY OF THE NUCLEUS: ITS MECHANICAL PROPERTIES AND FORCE TRANSMISSION

The nucleus is the largest and stiffest cargo in migrating cells. The nucleus is demarcated by the nuclear envelope (NE), a double membrane barrier that separates the chromosomes from the cytoplasm. The inner nuclear membrane is underlined by the nuclear lamina, a meshwork of lamin intermediate filaments, which are critical for structural support of the nucleus (Aebi et al., 1986; Burke and Stewart, 2013; Gruenbaum and Foisner, 2015; Turgay et al., 2017; Ungricht and Kutay, 2017). Lamins are associated with the NE via the LINC (linker of nucleoskeleton and cytoskeleton) complexes formed by SUN (Sad1 and UNC-84) proteins and KASH (Klarsicht, ANC-1, and Syne Homology) proteins (Crisp et al., 2006; Sosa et al., 2013). SUN proteins are embedded in the inner nuclear membrane and bind to lamins in the nucleoplasm, whereas KASH proteins are in the NE lumen (Padmakumar et al., 2005; Sosa et al., 2013) and span the outer nuclear membrane, binding to actin and microtubule motors dynein and kinesin in the cytoplasm (Starr and Han, 2002; Zhen et al., 2002; Zhang et al., 2009). The nucleus inevitably receives significant mechanical strains during its active translocation into the tapering leading process. The driving forces for nuclear translocation are generated by actomyosin contraction and microtubule motor activity, which are transmitted to the NE via the LINC complex (**Figure 1**).

ACTIVE NUCLEAR TRANSLOCATION BY CYTOSKELETAL MOLECULES IN NEURONAL CELLS

Actin-Myosin Based Nuclear Translocation

Of central importance to nuclear translocation are actomyosin-generated forces, yet previous studies have revealed a diversity in the sites of force generation, depending on cell types and assay systems. Granule cells and periglomerular cells, inhibitory interneurons in the olfactory bulb, arise in the anterior subventricular zone (SVZa) in the telencephalon and migrate rostrally to the olfactory bulb during development and throughout adult life. Dynamics of the rostral migration of SVZa neural precursor cells can be recapitulated in a culture of small SVZa explants embedded in a 3D Matrigel (Schaar and McConnell, 2005) (**Figure 2A**). The nucleus shows a characteristic saltatory movement toward a dilation formed in the leading process. Nuclear translocation is preceded by localization of non-muscle myosin IIB and membrane blebbing at the rear of the nucleus. Inhibition of myosin II activity at the nuclear rear by local application of blebbistatin suppresses nuclear translocation, suggesting that actomyosin generates a pushing force behind the nucleus. Accumulation of actomyosin at the nuclear rear is also observed during migration of cortical inhibitory interneurons from the medial ganglionic eminence (MGE) in the ventral telencephalon (Bellion et al., 2005;

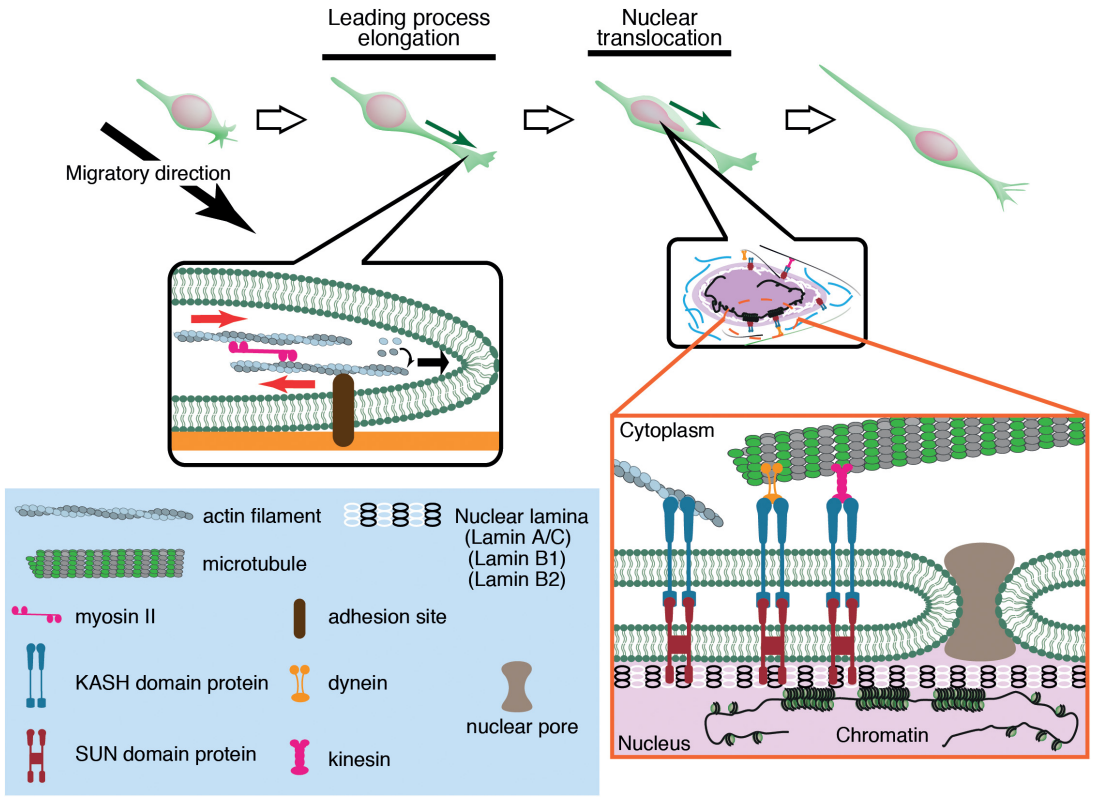

FIGURE 1 | Neuronal migration is driven by leading process elongation and nuclear translocation independently. Leading process elongation is accompanied by growth cone extension driven by actin filament elongation and myosin II-dependent contraction. Nuclear translocation is driven by microtubule motor activities (dynein and kinesin) and actomyosin contraction.

Martini and Valdeolmillos, 2010) (**Figure 2A**). Nuclear migration in MGE neurons is similarly inhibited by blebbistatin treatment, suggesting that myosin activation at the rear is critical for nuclear translocation. How does actomyosin contractility at the rear of the cell drive nuclear transport in these cells? Adhesion sites in the rear need to be detached for cell migration. A possible mechanism for detachment at the rear of the cell could be the mechanical disruption of integrin-ECM bonds by the actomyosin force behind the nucleus. Previous studies using keratocytes and cancer cell lines have demonstrated that actomyosin generates a traction force on focal adhesions which readily break integrin-ECM bonds (Jurchenko et al., 2014; Zhao et al., 2018). However, adhesions and stress fibers are less prominent in migrating neurons than in fibroblasts, seemingly downplaying the importance of de-adhesion at the cell posterior for neuronal migration (Jiang et al., 2015). Another possibility is that actomyosin contraction at the cell cortex constricts the cytoplasm at the rear and squeezes the nucleus to the front (Schaar and McConnell, 2005).

In contrast to the above mentioned inhibitory interneurons, dissociated cerebellar granule cells cultured on laminin-coated glass exhibit myosin IIB localization at the front of the nucleus prior to its saltatory movement (Solecki et al., 2009). Further studies using traction force microscopy (TFM) have demonstrated the generation of a force dipole at the site of myosin IIB accumulation in the leading process during neuronal migration (Jiang et al., 2015; Umeshima et al., 2019). These studies suggest that actomyosin is anchored to cell adhesions in the leading process and it exerts a pulling force to the nucleus in cerebellar granule cells cultured on a flat surface (**Figure 2B**). However, it remains elusive how the actomyosin force is transmitted to the nucleus during neuronal migration. It has been shown that F-actin is connected to the NE through the N-terminal CHD (Calponin Homology Domain) of nesprin-1/2 (Zhen et al., 2002; Padmakumar et al., 2004; Rajgor and Shanahan, 2013). Although the loss of nesprin-1 and 2 causes morphological defects in the mouse brain, an interaction between F-actin and nesprin-1/2 has not been detected in migrating neurons (Zhang et al., 2009). Recent studies have demonstrated that actomyosin in the leading process is anchored to perinuclear microtubules via an adaptor protein drebrin, rather than directly interacting with NE proteins (Trivedi et al., 2017).

The apparent diversity in actomyosin dynamics either in front or behind the nucleus has been attributed to differences among neuron types and/or diversity in migration substrates in different migration models (Trivedi and Solecki, 2011). Recent cell migration assays using rat and human mesenchymal cells and zebrafish germ layer progenitor cells have revealed that the subcellular localization of actomyosin in these cells is dramatically altered in 2D free surface and 3D confined space

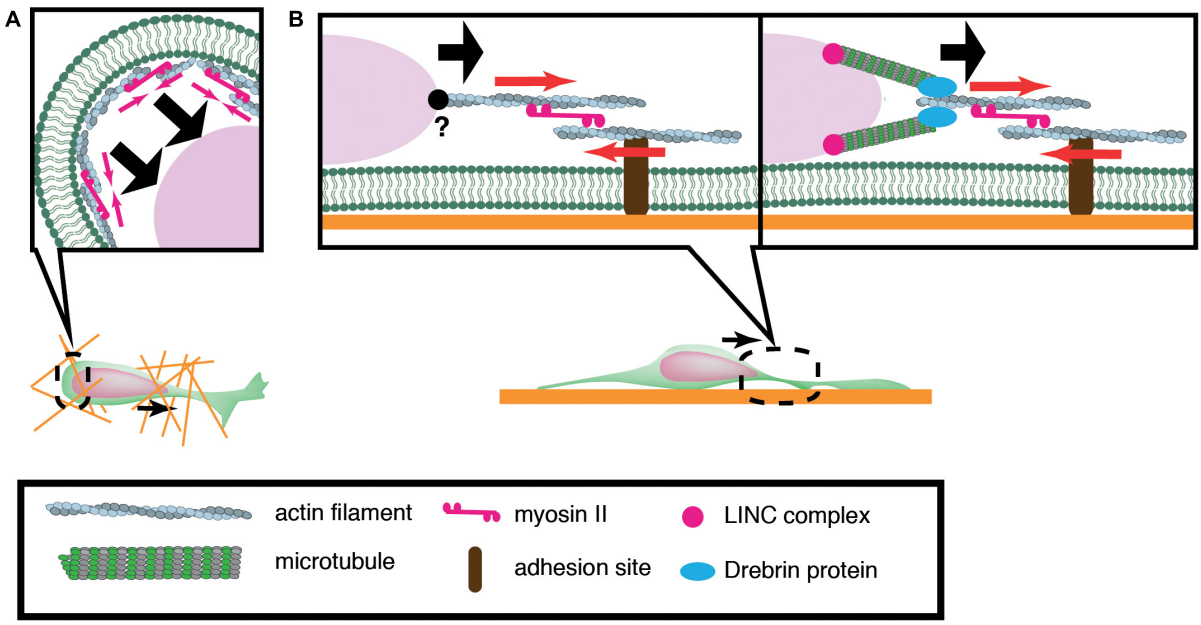

FIGURE 2 | Schematic overview of actomyosin-based nuclear translocation in neurons. **(A)** Myosin II-dependent contraction of cortical actin (red arrows) at the rear of the nucleus might push the nucleus forward in a 3D environment. **(B)** On a 2D substrate, actomyosin contraction between the nucleus and adhesions (red arrows) in the leading process generates a traction force that pulls the nucleus. Direct interaction between actin filaments and the nucleus has not been confirmed in migratory neurons (Left). Actin filaments in the proximal leading process may transmit traction force to the nucleus via the perinuclear microtubules that are associated by microtubule-actomyosin coupling proteins such as drebrin (Right).

(Bergert et al., 2015; Liu et al., 2015; Ruprecht et al., 2015). Similarly, neuroepithelial cells alter the subcellular distribution of actomyosin and adopt different force mechanisms during nuclear translocation depending on cell shape and tissue morphology (Yanakieva et al., 2019). It is thus possible that neurons might also adopt differential cytoskeletal dynamics depending on the extracellular mechanical environment.

Microtubule Based Nuclear Translocation

Previous studies have implicated microtubule motors as important regulators of nuclear translocation in the developing brain. Migrating neurons are polarized along the direction of migration, with the centrosome typically positioned in front of the nucleus. During neuronal migration, the centrosome and Golgi apparatus first move to a distal dilation that emerges in the leading process, and the nucleus then translocates toward the centrosome in the dilation (Bellion et al., 2005; Nishimura et al., 2017). Here, microtubules are thought to uniformly orient their plus-ends to the nucleus, harnessing the NE to the centrosome via the LINC complex. It is widely accepted that the nucleus is pulled forward to the centrosome by the minus-end-directed motor activity of cytoplasmic dynein, as the inhibition of dynein or its regulator LIS1 attenuates nuclear displacement (Hirotsune et al., 1998; Shu et al., 2004; Tanaka et al., 2004; Tsai et al., 2007). In this scenario, the centrosome has to be anchored to the cell cortex of the leading process in order to generate a traction force against the cell membrane or ECM, which pulls the nucleus forward (Aumais et al., 2001; De Simone et al., 2018). However, previous live imaging studies have revealed dynamic movement of the centrosome around the nucleus, raising doubts about whether the centrosome is tightly associated to the cell cortex (Umeshima et al., 2007; Wu et al., 2018) (**Figure 3**). More recent studies using cerebellar granule cells have suggested that the actin- and microtubule tip-binding protein drebrin links the perinuclear microtubules to F-actin in the leading process and mediates a strong actomyosin traction force at the integrin-ECM bonds to the nucleus (Ong and Solecki, 2017; Trivedi et al., 2017) (**Figure 2**). Other studies have indicated that perinuclear microtubules are associated with non-centrosomal microtubules in the leading process, which may be anchored to actomyosin and/or the cell cortex (Rao et al., 2016).

We have recently demonstrated that the nucleus undergoes frequent rotation during migration of cerebellar granule cells (Wu et al., 2018). Live-cell imaging suggests that microtubules around the nucleus are of mixed polarity and dynamically attach to and detach from the nucleus (**Figure 3**). This evidence supports the idea that kinesin and dynein motors exert transient forces to multiple small points on the NE, and thereby induce forward translocation when the net force acts on the center, which otherwise generates torque and drives rotation (Wu and Kengaku, 2018).

As another example, neuroepithelial cells in the developing neural tube show cyclic nuclear translocation between the apical and basal surface of the ventricular zone (VZ) in concert with the cell cycle, in a process known as interkinetic nuclear migration (**Figure 4**) (Spear and Erickson, 2012b; Lee and Norden, 2013;

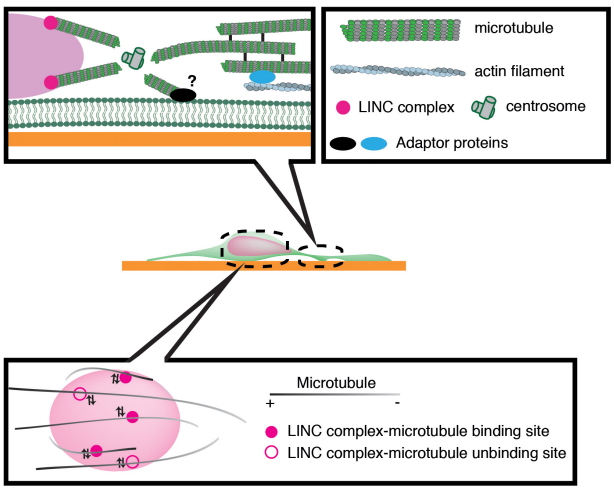

FIGURE 3 | Schematic overview of microtubule-based nuclear translocation in neurons. The centrosome mostly locates in the front of the nucleus and emanates perinuclear microtubules. The centrosome may be anchored to the cell cortex via microtubule networks and actin filaments in the leading process or unknown membrane-associated adaptors. During neuronal migration, microtubules appear to repeat attachment and detachment to the nucleus via interactions of their associated motors with the LINC complex.

Miyata et al., 2015). The centrosome is anchored to the apical endfoot and emanates microtubules along the cell longitudinal axis with their plus-ends toward the basal side (Spear and Erickson, 2012a). Thus, dynein motor activity drives nuclear translocation from the basal side to the centrosome, which is anchored to the apical surface (Tsai et al., 2007; Hu et al., 2013). In contrast, the plus-end-motor activity of KIF1A has been implicated in nuclear translocation from the apical to basal surface away from the centrosome, although the anchor point at the basal side remains unclear (Tsai et al., 2007). An alternative mechanism for apical-to-basal migration involves actomyosin behind the nucleus, constricting the plasma membrane around the apical surface. In this case, the nucleus is squeezed toward the basal side, similarly to SVZa neurons (Norden et al., 2009; Schenk et al., 2009). Thus, synergistic transactions between microtubules and actomyosin are important for the generation and transmission of the force driving nuclear translocation in various contexts.

CELLULAR AND EXTRACELLULAR MECHANICAL PROPERTIES AFFECTING NUCLEAR TRANSLOCATION IN NEURONAL CELLS

The nucleus is exposed to high shear stress from the surrounding tissue during migration in confined interstitial spaces. Besides cytoskeletal forces generated within the cell, the mechanical properties of the nucleus and extracellular microenvironment are important determinants of nuclear translocation.

Nuclear Stiffness and Lamins

The nucleus shows extensive deformation when it passes through constrictions in the interstitial spaces in brain tissue (Wu et al., 2018). Accordingly, the nucleus should have an optimal viscoelastic property that allows flexible deformation and tolerance against shear stress during migration. A critical determinant of nuclear stiffness is the set of type V intermediate filament proteins, called lamins, which underlie the inner nuclear membrane. Lamins are composed of four major isoforms: lamins A and C (products of the LMNA gene by alternative splicing), lamin B1 (encoded by LMNB1) and lamin B2 (encoded by LMNB2). The stoichiometry of lamin A/C and lamin B1/B2 determines the viscoelastic properties of the NE and provides mechanical strength to the nucleus against various physical strains from the cytoplasm and extracellular environment (Swift et al., 2013; Harada et al., 2014).

Lamin A/C levels vary greatly among cell types, with strong correlations to tissue stiffness (Swift et al., 2013). Importantly, the laminA/C level is determined by both transcriptional and post-transcriptional regulation. Transcription of lamin A/C is activated by a transcription factor RARG that is translocated to the nucleus when cells are cultured on stiff substrate. The level of lamin A/C transcripts is thus low in soft tissues, including the brain (Swift et al., 2013). Additionally, lamin A/C proteins are phosphorylated at specific sites, and are thereby subjected to proteolysis under low mechanical stress in soft tissues (Buxboim et al., 2014). It has also been shown that lamin A abundance in the brain is further reduced by a brain-specific micro RNA miR-9 which specifically suppresses the 3′ UTR of the lamin A splice form (Jung et al., 2012, 2013). Generally, lamin A expression in migratory cells, such as immune cells and metastatic cancer cells, is lower than in adherent cells (Shin et al., 2013; Matsumoto et al., 2015; Irianto et al., 2016). Migrating neurons in the developing brain also express very low levels of lamin A/C (Coffinier et al., 2011). Nuclei containing low levels of lamin A are softer, and might be adept at deforming and passing through tiny interstitial spaces during migration.

A very low abundance of lamin A/C has been observed in embryonic cells, and LMNA knockout mice show little or no pathology during development, although postnatal mice develop cardiomyopathy or muscular dystrophy (Sullivan et al., 1999). In contrast, genetic ablation of B-type lamins causes abnormal neuronal migration and malformation of the brain cortex (Coffinier et al., 2011; Young et al., 2012, 2014). In experiments that specifically depleted lamin B1 in the forebrain of mice, the nucleus of migrating cortical neurons showed blebbing and/or fragmentation at the nuclear front (Jung et al., 2013). On the other hand, lamin B2 ablation causes abnormal elongation of the front of the nucleus in migratory neurons (Coffinier et al., 2010). These observations suggest that loss of B-type lamins impairs nuclear lamina integrity and tolerance to cytoskeletal pulling forces during neuronal migration.

It has been shown that the mechanical properties of the nucleus are also affected by the positioning and structure of chromatin (Pajerowski et al., 2007; Mazumder et al., 2008; Furusawa et al., 2015; Shimamoto et al., 2017). In most eukaryotic

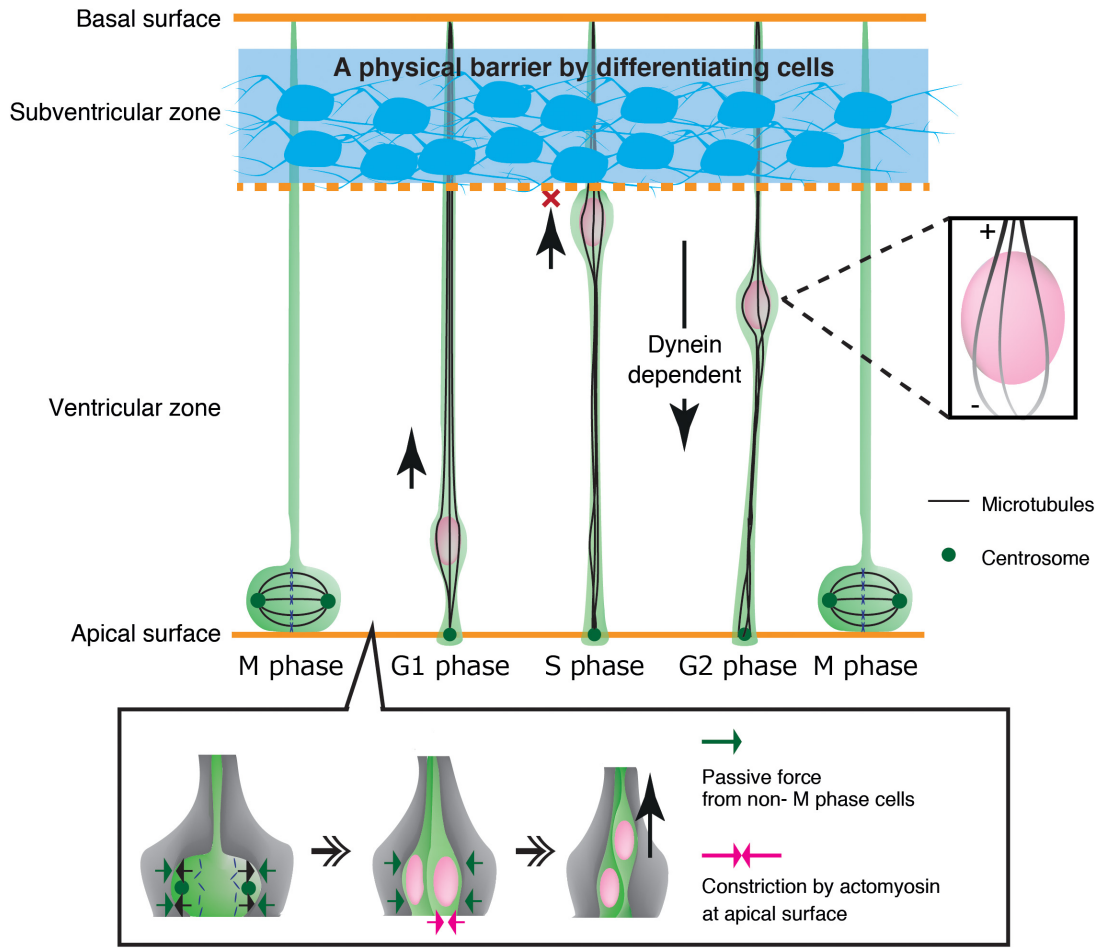

FIGURE 4 | Mechanical regulation of nuclear translocation in neuroepithelial cells. Differentiating cells in the subventricular zone work as a physical fence which prevents invasion of the S phase nuclei in the upper ventricular zone (**Top**, blue region). On the apical surface, lateral expansion of mitotic cells is suppressed by the reactive force of surrounding non-M phase cells. Apical constriction by actomyosin further assists basal translocation of the dividing nuclei **(Bottom)**.

nuclei, heterochromatin regions primarily associate with nuclear lamina via lamins, forming lamina associated domains (LAD) which contribute to nuclear stiffness. In neuronal cells with low expression of lamin A, the inner nuclear membrane protein lamin B receptor plays important roles in LAD formation (Clowney et al., 2012; Solovei et al., 2013). Thus, lamin B receptor might have complementary roles with lamin A in neurons.

Nuclear lamins might have an important role for protection of the genomic architecture and DNA from mechanical stress. Recent studies have shown that knockdown of lamin A increases nuclear rupture and DNA damage in cancer cell lines (Xia et al., 2018). Similarly, mechanical stress in confined spaces induces excessive nuclear deformation and nuclear rupture, followed by DNA repair responses in bone marrow derived dendritic cells and cancer cell lines with low lamin A expression (Denais et al., 2016; Raab et al., 2016). In contrast, it has never been reported that young neurons with very low lamin A are susceptible to nuclear rupture during migration (Chen et al., 2019). Instead, disruption of lamin B1or lamin B2 has been shown to cause nuclear rupture and precocious cell death in migrating neurons, supporting that B-type lamins are more critical for brain development (Jung et al., 2013; Chen et al., 2019). It is unknown how the nuclear envelope with low lamin A maintains structural integrity, but other lamins such as lamin B and lamin B receptor may possibly substitute for lamin A in organizing the nuclear lamina structure in young neurons. Further studies are required to understand the relationships of lamin subtypes and their precise contributions to nuclear stiffness and durability.

Mechanical Properties of the Extracellular Environment

Mechanical properties of surrounding tissues also contribute to interkinetic nuclear migration in neuroepithelial cells in the ventricular zone (Miyata et al., 2015). These cells undergo mitosis that causes cell crowding and increased pressure at the apical surface, contributing to pushing the nucleus up to the basal side (Kosodo et al., 2011; Okamoto et al., 2013). Further studies have demonstrated that the apical surface of the ventricular zone undergoes actomyosin-dependent contraction,

further crowding the apical surface with elastic processes of surrounding progenitor cells. These dense processes exert a centripetal force on the dividing nuclei, thereby enhancing their dorsal displacement (Shinoda et al., 2018) (**Figure 4**). Recent studies have also demonstrated that apical-to-basal migration stops at the boundary of the ventricular zone and the SVZ by the physical fence made by differentiated SVZ neurons (Watanabe et al., 2018) (**Figure 4**).

The ECM is a scaffolding architecture for cells, which binds to integrins and promotes the formation of adhesions, thereby regulating various cellular functions including migration (Hynes, 2009; Bonnans et al., 2014). It has been shown that the mechanical properties of the ECM affect integrin signaling in migrating fibroblasts, so that cell migration is directed toward more rigid substrates in a process known as durotaxis (Choquet et al., 1997; Wang et al., 2002; Plotnikov et al., 2012; Sunyer et al., 2016). In developing neurons, growth cone extension also depends strongly on local mechanical properties (Kostic et al., 2007; Suter and Miller, 2011; Koser et al., 2016). However, whether and how substrate stiffness might affect nuclear translocation is not well understood.

Mechanical stresses to the nucleus influence the interior genome architecture and may affect cellular responses, including gene expression (Uhler and Shivashankar, 2017). It has been demonstrated that the rigidity of the extracellular environment is sensed and transmitted to biochemical signals that induce cytoskeletal remodeling and cytoplasmic-to-nuclear translocation of transcription factors including YAP/TAZ, and thereby affect cell differentiation, morphology, and survival (Engler et al., 2006; Dupont et al., 2011; Nakazawa et al., 2016; Smith et al., 2018; Wolfenson et al., 2018; Yang et al., 2019). Recent studies have also demonstrated that brain stiffness exhibits sharp gradients across layers and regions, which may affect multiple steps of neuronal differentiation including cell fate determination and circuit pathfinding (Iwashita et al., 2014; Koser et al., 2016; Barnes et al., 2017). In fact, the culture substrate with the stiffness of living brain tissue promotes production of dorsal cortical neurons from neural stem cells, suggesting a deep impact of mechanical properties of extracellular environment on gene expression in differentiating neurons (Iwashita et al., 2019). It remains of great interest to clarify if mechanical properties of surrounding tissues affect genome architecture and/or gene expression during neuronal migration.

CONCLUSION

In this review, we summarized recent studies on the mechanical regulation of nuclear translocation in neurons. It is clear that the nucleus is translocated by both actomyosin traction forces and microtubule motors walking along rigid microtubule cables. However, it remains unclear how these cytoskeletal elements are stabilized on the substrate (anchor points) to transmit the force to the nucleus (application points). The research field is awaiting further improvements of emerging techniques for quantification of small mechanical forces in soft and complex tissues (Campàs et al., 2014; Roca-Cusachs et al., 2017; Mongera et al., 2018). For instance, a nesprin tension biosensor is a promising new tool for the quantification of the local, transient force applied to the nucleus in live cells (Arsenovic et al., 2016).

Additionally, increasing evidence highlights the need to carefully consider the impact of mechanical properties of the nucleus and the extracellular environment, and perhaps those of the cytoskeleton and the cell membrane, on nuclear translocation in 3D confined tissue. Recent studies using leukocytes and cancer cell lines suggest that the nucleus serves as a mechanical guide to choose paths of a proper width during confined space migration (Lautscham et al., 2015; Renkawitz et al., 2019). Manipulation of the mechanical properties of the extracellular environment in 3D tissue is required to demonstrate the physiological significance of these findings *in vitro*. A combination of organoid culture and mechanobiology is becoming a powerful system to overcome some of the limitations of *in vivo* experiments (Okuda et al., 2018; Garreta et al., 2019). Similarly, further improvement of micro/nanofabrication techniques to design 3D patterned substrates with various mechanical properties is needed to study the interplay between migrating cells and the surrounding tissue.

DNA damages by mechanical stress during confined migration may cause heterogeneity in cancer cells. It has been shown that nuclear deformation by confined migration induces prolonged DNA breaks due to mislocalization of DNA repair factors in the cytosol, which causes accumulation of chromosomal aberrations (Irianto et al., 2017). Extrapolating from this notion, an interesting hypothesis is that the nuclear deformation under mechanical stress during confined migration might influence the genome architecture and gene expression, and thereby affect the final fate and destination of migrating neurons. Emerging techniques for visualization of genome architecture in live cells in combination with high throughput genome sequencing analyses will offer greater opportunities to answer these questions (Miyanari et al., 2013; Natale et al., 2017; Conic et al., 2018).

AUTHOR CONTRIBUTIONS

All authors listed have made a substantial, direct and intellectual contribution to the work, and approved it for publication.

FUNDING

This work was supported by KAKENHI from JSPS (Grant numbers: 18K14819 to NN, 18KK0212 to NN and MK, and 16H06484 to MK).

ACKNOWLEDGMENTS

We thank Dr. James Hejna and Ms. Rebecca Jimenez for critical reading.

REFERENCES

Aebi, U., Cohn, J., Buhle, L., and Gerace, L. (1986). The nuclear lamina is a meshwork of intermediate-type filaments. *Nature* 323, 560–564. doi: 10.1038/323560a0

Arsenovic, P. T., Ramachandran, I., Bathula, K., Zhu, R., Narang, J. D., Noll, N. A., et al. (2016). Nesprin-2G, a component of the nuclear LINC complex. Is subject to myosin-dependent tension. *Biophys. J.* 110, 34–43. doi: 10.1016/j.bpj.2015.11.014

Aumais, J. P., Tunstead, J. R., McNeil, R. S., Schaar, B. T., McConnell, S. K., Lin, S. H., et al. (2001). NudC associates with Lis1 and the dynein motor at the leading pole of neurons. *J. Neurosci.* 21, 1–7.

Bard, L., Boscher, C., Lambert, M., Mège, R. M., Choquet, D., and Thoumine, O. (2008). A molecular clutch between the actin flow and N-cadherin adhesions drives growth cone migration. *J. Neurosci.* 28, 5879–5890. doi: 10.1523/JNEUROSCI.5331-07.2008

Barnes, J. M., Przybyla, L., and Weaver, V. M. (2017). Tissue mechanics regulate brain development, homeostasis and disease. *J. Cell Sci.* 130, 71–82. doi: 10.1242/jcs.191742

Bellion, A., Baudoin, J. P., Alvarez, C., Bornens, M., and Métin C. (2005). Nucleokinesis in tangentially migrating neurons comprises two alternating phases: forward migration of the golgi/centrosome associated with centrosome splitting and myosin contraction at the rear. *J. Neurosci.* 25, 5691–5699. doi: 10.1523/jneurosci.1030-05.2005

Bergert, M., Erzberger, A., Desai, R. A., Aspalter, I. M., Oates, A. C., Charras, G., et al. (2015). Force transmission during adhesion-independent migration. *Nat. Cell Biol.* 17, 524–529. doi: 10.1038/ncb3134

Bonnans, C., Chou, J., and Werb, Z. (2014). Remodelling the extracellular matrix in development and disease. *Nat. Rev. Mol. Cell Biol.* 15, 786–801. doi: 10.1038/nrm3904

Buchsbaum, I. Y., and Cappello, S. (2019). Neuronal migration in the CNS during development and disease: insights from in vivo and in vitro models. *Development* 146:dev163766. doi: 10.1242/dev.163766

Burke, B., and Stewart, C. L. (2013). The nuclear lamins: flexibility in function. *Nat. Rev. Mol. Cell Biol.* 14, 13–24. doi: 10.1038/nrm3488

Buxboim, A., Swift, J., Irianto, J., Spinler, K. R., Dingal, P. C. D. P., Athirasala, A., et al. (2014). Matrix elasticity regulates lamin-A,C phosphorylation and turnover with feedback to actomyosin. *Curr. Biol.* 24, 1909–1917. doi: 10.1016/j.cub.2014.07.001

Campàs, O., Mammoto, T., Hasso, S., Sperling, R. A., O'connell, D., Bischof, A. G., et al. (2014). Quantifying cell-generated mechanical forces within living embryonic tissues. *Nat. Methods* 11, 183–189. doi: 10.1038/nmeth.2761

Chen, N. Y., Yang, Y., Weston, T. A., Belling, J. N., Heizer, P., Tu, Y., et al. (2019). An absence of lamin B1 in migrating neurons causes nuclear membrane ruptures and cell death. *Proc. Natl. Acad. Sci. U.S.A* 116, 25870–25879. doi: 10.1073/pnas.1917225116

Choquet, D., Felsenfeld, D. P., and Sheetz, M. P. (1997). Extracellular matrix rigidity causes strengthening of integrin- cytoskeleton linkages. *Cell* 88, 39–48. doi: 10.1016/S0092-8674(00)81856-5

Clowney, E. J., Legros, M. A., Mosley, C. P., Clowney, F. G., Markenskoff-Papadimitriou, E. C., Myllys, M., et al. (2012). Nuclear aggregation of olfactory receptor genes governs their monogenic expression. *Cell* 151, 724–737. doi: 10.1016/j.cell.2012.09.043

Coffinier, C., Chang, S. Y., Nobumori, C., Tu, Y., Farber, E. A., Toth, J. I., et al. (2010). Abnormal development of the cerebral cortex and cerebellum in the setting of lamin B2 deficiency. *Proc. Natl. Acad. Sci. U.S.A.* 107, 5076–5081. doi: 10.1073/pnas.0908790107

Coffinier, C., Jung, H. J., Nobumori, C., Chang, S., Tu, Y., Barnes, R. H., et al. (2011). Deficiencies in lamin B1 and lamin B2 cause neurodevelopmental defects and distinct nuclear shape abnormalities in neurons. *Mol. Biol. Cell* 22, 4683–4693. doi: 10.1091/mbc.E11-06-0504

Conic, S., Desplancq, D., Ferrand, A., Fischer, V., Heyer, V., Martin, B. R. S., et al. (2018). Imaging of native transcription factors and histone phosphorylation at high resolution in live cells. *J. Cell Biol.* 217, 1537–1552. doi: 10.1083/jcb.201709153

Cooper, J. A. (2013). Mechanisms of cell migration in the nervous system. *J. Cell Biol.* 202, 725–734. doi: 10.1083/jcb.201305021

Crisp, M., Liu, Q., Roux, K., Rattner, J. B., Shanahan, C., Burke, B., et al. (2006). Coupling of the nucleus and cytoplasm: role of the LINC complex. *J. Cell Biol.* 172, 41–53. doi: 10.1083/jcb.200509124

De Simone, A., Spahr, A., Busso, C., and Gönczy, P. (2018). Uncovering the balance of forces driving microtubule aster migration in C. *Elegans zygotes. Nat. Commun.* 9, 38. doi: 10.1038/s41467-018-03118-x

Denais, C. M., Gilbert, R. M., Isermann, P., McGregor, A. L., Te Lindert, M., Weigelin, B., et al. (2016). Nuclear envelope rupture and repair during cancer cell migration. *Science* 352, 353–358. doi: 10.1126/science.aad7297

Dupont, S., Morsut, L., Aragona, M., Enzo, E., Giulitti, S., Cordenonsi, M., et al. (2011). Role of YAP/TAZ in mechanotransduction. *Nature* 474, 179–184. doi: 10.1038/nature10137

Edmondson, J., and Hatten, M. (1987). Glial-guided granule neuron migration in vitro: a high-resolution time- lapse video microscopic study. *J. Neurosci.* 7, 1928–1934. doi: 10.1523/jneurosci.07-06-01928.1987

Engler, A. J., Sen, S., Sweeney, H. L., and Discher, D. E. (2006). Matrix Elasticity Directs Stem Cell Lineage Specification. *Cell* 126, 677–689. doi: 10.1016/j.cell.2006.06.044

Fletcher, D. A., and Mullins, R. D. (2010). Cell mechanics and the cytoskeleton. *Nature* 463, 485–492. doi: 10.1038/nature08908

Furusawa, T., Rochman, M., Taher, L., Dimitriadis, E. K., Nagashima, K., Anderson, S., et al. (2015). Chromatin decompaction by the nucleosomal binding protein HMGN5 impairs nuclear sturdiness. *Nat. Commun.* 6, 1–10. doi: 10.1038/ncomms7138

Garreta, E., Prado, P., Tarantino, C., Oria, R., Fanlo, L., Martí, E., et al. (2019). Fine tuning the extracellular environment accelerates the derivation of kidney organoids from human pluripotent stem cells. *Nat. Mater.* 18, 397–405. doi: 10.1038/s41563-019-0287-6

Gruenbaum, Y., and Foisner, R. (2015). Lamins: nuclear intermediate filament proteins with fundamental functions in nuclear mechanics and genome regulation. *Annu. Rev. Biochem.* 84, 131–164. doi: 10.1146/annurev-biochem-060614-034115

Gundersen, G. G., and Worman, H. J. (2013). Nuclear positioning. *Cell* 152, 1376–1389. doi: 10.1016/j.cell.2013.02.031

Harada, T., Swift, J., Irianto, J., Shin, J. W., Spinler, K. R., Athirasala, A., et al. (2014). Nuclear lamin stiffness is a barrier to 3D migration, but softness can limit survival. *J. Cell Biol.* 204, 669–682. doi: 10.1083/jcb.201308029

Hirotsune, S., Fleck, M. W., Gambello, M. J., Bix, G. J., Chen, A., Clark, G. D., et al. (1998). Graded reduction of Pafah1b1 (Lis1) activity results in neuronal migration defects and early embryonic lethality. *Nat. Genet.* 19, 333–339. doi: 10.1038/1221

Hu, D. J., Baffet, A. D., Nayak, T., Akhmanova, A., Doye, V., and Vallee, R. B. (2013). Dynein recruitment to nuclear pores activates apical nuclear migration and mitotic entry in brain progenitor cells. *Cell* 154, 1300. doi: 10.1016/j.cell.2013.08.024

Hynes, R. O. (2009). The extracellular matrix: not just pretty fibrils. *Science* 326, 1216–1219. doi: 10.1126/science.1176009

Irianto, J., Pfeifer, C. R., Ivanovska, I. L., Swift, J., and Discher, D. E. (2016). Nuclear lamins in cancer. *Cell. Mol. Bioeng.* 9, 258–267. doi: 10.1007/s12195-016-0437-8

Irianto, J., Xia, Y., Pfeifer, C. R., Athirasala, A., Ji, J., Alvey, C., et al. (2017). DNA damage follows repair factor depletion and portends genome variation in cancer cells after pore migration. *Curr. Biol.* 27, 210–223. doi: 10.1016/j.cub.2016.11.049

Iwashita, M., Kataoka, N., Toida, K., and Kosodo, Y. (2014). Systematic profiling of spatiotemporal tissue and cellular stiffness in the developing brain. *Development* 141, 3793–3798. doi: 10.1242/dev.109637

Iwashita, M., Ohta, H., Fujisawa, T., Cho, M., Ikeya, M., Kidoaki, S., et al. (2019). Brain-stiffness-mimicking tilapia collagen gel promotes the induction of dorsal cortical neurons from human pluripotent stem cells. *Sci. Rep.* 9, 1–17. doi: 10.1038/s41598-018-38395-5

Jiang, J., Zhang, Z. H., Yuan, X. B., and Poo, M. M. (2015). Spatiotemporal dynamics of traction forces show three contraction centers in migratory neurons. *J. Cell Biol.* 209, 759–774. doi: 10.1083/jcb.201410068

Jung, H. J., Coffinier, C., Choe, Y., Beigneux, A. P., Davies, B. S. J., Yang, S. H., et al. (2012). Regulation of prelamin A but not lamin C by miR-9, a brain-specific

microRNA. *Proc. Natl. Acad. Sci. U.S.A.* 109, 423–431. doi: 10.1073/pnas.1111780109

Jung, H.-J., Nobumori, C., Goulbourne, C. N., Tu, Y., Lee, J. M., Tatar, A., et al. (2013). Farnesylation of lamin B1 is important for retention of nuclear chromatin during neuronal migration. *Proc. Natl. Acad. Sci. U.S.A.* 110, E1923–E1932. doi: 10.1073/pnas.1303916110

Jurchenko, C., Chang, Y., Narui, Y., Zhang, Y., and Salaita, K. S. (2014). Integrin-generated forces lead to streptavidin-biotin unbinding in cellular adhesions. *Biophys. J.* 106, 1436–1446. doi: 10.1016/j.bpj.2014.01.049

Kengaku, M. (2018). Cytoskeletal control of nuclear migration in neurons and non-neuronal cells. *Proc. Japan Acad. Ser. B* 94, 337–349. doi: 10.2183/pjab.94.022

Kerstein, P. C., Nichol, R. H., and Gomez, T. M. (2015). Mechanochemical regulation of growth cone motility. *Front. Cell. Neurosci.* 9:244. doi: 10.3389/fncel.2015.00244

Komuro, H., and Rakic, P. (1995). Dynamics of granule cell migration: a confocal microscopic study in acute cerebellar slice preparations. *J. Neurosci.* 15, 1110–1120. doi: 10.1523/jneurosci.15-02-01110.1995

Koser, D. E., Thompson, A. J., Foster, S. K., Dwivedy, A., Pillai, E. K., Sheridan, G. K., et al. (2016). Mechanosensing is critical for axon growth in the developing brain. *Nat. Neurosci.* 19, 1592–1598. doi: 10.1038/nn.4394

Kosodo, Y., Suetsugu, T., Suda, M., Mimori-Kiyosue, Y., Toida, K., Baba, S. A., et al. (2011). Regulation of interkinetic nuclear migration by cell cycle-coupled active and passive mechanisms in the developing brain. *EMBO J.* 30, 1690–1704. doi: 10.1038/emboj.2011.81

Kostic, A., Sap, J., and Sheetz, M. P. (2007). RPTPα is required for rigidity-dependent inhibition of extension and differentiation of hippocampal neurons. *J. Cell Sci.* 120, 3895–3904. doi: 10.1242/jcs.009852

Lämmermann, T., Bader, B. L., Monkley, S. J., Worbs, T., Wedlich-Söldner, R., Hirsch, K., et al. (2008). Rapid leukocyte migration by integrin-independent flowing and squeezing. *Nature* 453, 51–55. doi: 10.1038/nature06887

Lautscham, L. A., Kämmerer, C., Lange, J. R., Kolb, T., Mark, C., Schilling, A., et al. (2015). Migration in confined 3D environments is determined by a combination of adhesiveness, nuclear volume, contractility, and cell stiffness. *Biophys. J.* 109, 900–913. doi: 10.1016/j.bpj.2015.07.025

Lee, H. O., and Norden, C. (2013). Mechanisms controlling arrangements and movements of nuclei in pseudostratified epithelia. *Trends Cell Biol.* 23, 141–150. doi: 10.1016/j.tcb.2012.11.001

Li, R., and Gundersen, G. G. (2008). Beyond polymer polarity: how the cytoskeleton builds a polarized cell. *Nat. Rev. Mol. Cell Biol.* 9, 860–873. doi: 10.1038/nrm2522

Lin, C. H., Espreafico, E. M., Mooseker, M. S., and Forscher, P. (1996). Myosin drives retrograde F-actin flow in neuronal growth cones. *Neuron* 16, 769–782. doi: 10.1016/s0896-6273(00)80097-5

Lin, C. H., and Forscher, P. (1995). Growth cone advance is inversely proportional to retrograde F-actin flow. *Neuron* 14, 763–771. doi: 10.1016/0896-6273(95)90220-1

Liu, Y. J., Le Berre, M., Lautenschlaeger, F., Maiuri, P., Callan-Jones, A., Heuzé, M., et al. (2015). Confinement and low adhesion induce fast amoeboid migration of slow mesenchymal cells. *Cell* 160, 659–672. doi: 10.1016/j.cell.2015.01.007

Lowery, L. A., and Van Vactor, D. (2009). The trip of the tip: understanding the growth cone machinery. *Nat. Rev. Mol. Cell Biol.* 10, 332–343. doi: 10.1038/nrm2679

Manzini, M. C., and Walsh, C. A. (2011). What disorders of cortical development tell us about the cortex: one plus one does not always make two. *Curr. Opin. Genet. Dev.* 21, 333–339. doi: 10.1016/j.gde.2011.01.006

Martini, F. J., and Valdeolmillos, M. (2010). Actomyosin contraction at the cell rear drives nuclear translocation in migrating cortical interneurons. *J. Neurosci.* 30, 8660–8670. doi: 10.1523/jneurosci.1962-10.2010

Matsumoto, A., Hieda, M., Yokoyama, Y., Nishioka, Y., Yoshidome, K., Tsujimoto, M., et al. (2015). Global loss of a nuclear lamina component, lamin A/C, and LINC complex components SUN1, SUN2, and nesprin-2 in breast cancer. *Cancer Med.* 4, 1547–1557. doi: 10.1002/cam4.495

Mazumder, A., Roopa, T., Basu, A., Mahadevan, L., and Shivashankar, G. V. (2008). Dynamics of chromatin decondensation reveals the structural integrity of a mechanically prestressed nucleus. *Biophys. J.* 95, 3028–3035. doi: 10.1529/biophysj.108.132274

Miyanari, Y., Ziegler-Birling, C., and Torres-Padilla, M. E. (2013). Live visualization of chromatin dynamics with fluorescent TALEs. *Nat. Struct. Mol. Biol.* 20, 1321–1324. doi: 10.1038/nsmb.2680

Miyata, T., Okamoto, M., Shinoda, T., and Kawaguchi, A. (2015). Interkinetic nuclear migration generates and opposes ventricular-zone crowding: insight into tissue mechanics. *Front. Cell. Neurosci.* 8:473. doi: 10.3389/fncel.2014.00473

Mongera, A., Rowghanian, P., Gustafson, H. J., Shelton, E., Kealhofer, D. A., Carn, E. K., et al. (2018). A fluid-to-solid jamming transition underlies vertebrate body axis elongation. *Nature* 561, 401–405. doi: 10.1038/s41586-018-0479-2

Moon, H. M., and Wynshaw-Boris, A. (2013). Cytoskeleton in action: lissencephaly, a neuronal migration disorder. *Wiley Interdiscip. Rev. Dev. Biol.* 2, 229–245. doi: 10.1002/wdev.67

Nakazawa, N., Sathe, A. R., Shivashankar, G. V., and Sheetz, M. P. (2016). Matrix mechanics controls FHL2 movement to the nucleus to activate p21 expression. *Proc. Natl. Acad. Sci. U.S.A.* 113, E6813–E6822. doi: 10.1073/pnas.1608210113

Natale, F., Rapp, A., Yu, W., Maiser, A., Harz, H., Scholl, A., et al. (2017). Identification of the elementary structural units of the DNA damage response. *Nat. Commun.* 8:15760. doi: 10.1038/ncomms15760

Nishimura, Y. V., Nabeshima, Y. I., and Kawauchi, T. (2017). Morphological and molecular basis of cytoplasmic dilation and swelling in cortical migrating neurons. *Brain Sci.* 7, 1–12. doi: 10.3390/brainsci7070087

Norden, C., Young, S., Link, B. A., and Harris, W. A. (2009). Actomyosin is the main driver of interkinetic nuclear migration in the retina. *Cell* 138, 1195–1208. doi: 10.1016/j.cell.2009.06.032

Okamoto, M., Namba, T., Shinoda, T., Kondo, T., Watanabe, T., Inoue, Y., et al. (2013). TAG-1-assisted progenitor elongation streamlines nuclear migration to optimize subapical crowding. *Nat. Neurosci.* 16, 1556–1566. doi: 10.1038/nn.3525

Okuda, S., Takata, N., Hasegawa, Y., Kawada, M., Inoue, Y., Adachi, T., et al. (2018). Strain-triggered mechanical feedback in self-organizing optic-cup morphogenesis. *Sci. Adv.* 4, 1–13. doi: 10.1126/sciadv.aau1354

Ong, T., and Solecki, D. J. (2017). Seven in absentia E3 ubiquitin ligases: central regulators of neural cell fate and neuronal polarity. *Front. Cell. Neurosci.* 11:322. doi: 10.3389/fncel.2017.00322

Padmakumar, V. C., Abraham, S., Braune, S., Noegel, A. A., Tunggal, B., Karakesisoglou, I., et al. (2004). Enaptin, a giant actin-binding protein, is an element of the nuclear membrane and the actin cytoskeleton. *Exp. Cell Res.* 295, 330–339. doi: 10.1016/j.yexcr.2004.01.014

Padmakumar, V. C., Libotte, T., Lu, W., Zaim, H., Abraham, S., Noegel, A. A., et al. (2005). The inner nuclear membrane protein Sun1 mediates the anchorage of Nesprin-2 to the nuclear envelope. *J. Cell Sci.* 118, 3419–3430. doi: 10.1242/jcs.02471

Pajerowski, J. D., Dahl, K. N., Zhong, F. L., Sammak, P. J., and Discher, D. E. (2007). Physical plasticity of the nucleus in stem cell differentiation. *Proc. Natl. Acad. Sci. U.S.A.* 104, 15619–15624. doi: 10.1073/pnas.0702576104

Plotnikov, S. V., Pasapera, A. M., Sabass, B., and Waterman, C. M. (2012). Force fluctuations within focal adhesions mediate ECM-rigidity sensing to guide directed cell migration. *Cell* 151, 1513–1527. doi: 10.1016/j.cell.2012.11.034

Raab, M., Gentili, M., De Belly, H., Thiam, H. R., Vargas, P., Jimenez, A. J., et al. (2016). ESCRT III repairs nuclear envelope ruptures during cell migration to limit DNA damage and cell death. *Science* 352, 359–362. doi: 10.1126/science.aad7611

Rajgor, D., and Shanahan, C. M. (2013). Nesprins: from the nuclear envelope and beyond. *Expert Rev. Mol. Med.* 15, 1–17. doi: 10.1017/erm.2013.6

Rao, A. N., Falnikar, A., O'Toole, E. T., Morphew, M. K., Hoenger, A., Davidson, M. W., et al. (2016). Sliding of centrosome-unattached microtubules defines key features of neuronal phenotype. *J. Cell Biol.* 213, 329–341. doi: 10.1083/jcb.201506140

Renkawitz, J., Kopf, A., Stopp, J., de Vries, I., Driscoll, M. K., Merrin, J., et al. (2019). Nuclear positioning facilitates amoeboid migration along the path of least resistance. *Nature* 568, 546–550. doi: 10.1038/s41586-019-1087-5

Roca-Cusachs, P., Conte, V., and Trepat, X. (2017). Quantifying forces in cell biology. *Nat. Cell Biol.* 19, 742–751. doi: 10.1038/ncb3564

Ruprecht, V., Wieser, S., Callan-Jones, A., Smutny, M., Morita, H., Sako, K., et al. (2015). Cortical contractility triggers a stochastic switch to fast amoeboid cell motility. *Cell* 160, 673–685. doi: 10.1016/j.cell.2015.01.008

Schaar, B. T., and McConnell, S. K. (2005). Cytoskeletal coordination during neuronal migration. *Proc. Natl. Acad. Sci. U.S.A.* 102, 13652–13657. doi: 10.1073/pnas.0506008102

Schenk, J., Wilsch-Brauninger, M., Calegari, F., and Huttner, W. B. (2009). Myosin II is required for interkinetic nuclear migration of neural progenitors. *Proc. Natl. Acad. Sci. U.S.A.* 106, 16487–16492. doi: 10.1073/pnas.0908928106

Shimamoto, Y., Tamura, S., Masumoto, H., and Maeshima, K. (2017). Nucleosome-nucleosome interactions via histone tails and linker DNA regulate nuclear rigidity. *Mol. Biol. Cell* 28, 1580–1589. doi: 10.1091/mbc.E16-11-0783

Shin, J. W., Spinler, K. R., Swift, J., Chasis, J. A., Mohandas, N., and Discher, D. E. (2013). Lamins regulate cell trafficking and lineage maturation of adult human hematopoietic cells. *Proc. Natl. Acad. Sci. U.S.A.* 110, 18892–18897. doi: 10.1073/pnas.1304996110

Shinoda, T., Nagasaka, A., Inoue, Y., Higuchi, R., Minami, Y., Kato, K., et al. (2018). Elasticity-based boosting of neuroepithelial nucleokinesis via indirect energy transfer from mother to daughter. *PLoS Biol.* 16:e2004426. doi: 10.1371/journal.pbio.2004426

Shu, T., Ayala, R., Nguyen, M. D., Xie, Z., Gleeson, J. G., and Tsai, L. H. (2004). Ndel1 operates in a common pathway with LIS1 and cytoplasmic dynein to regulate cortical neuronal positioning. *Neuron* 44, 263–277. doi: 10.1016/j.neuron.2004.09.030

Silva, C. G., Peyre, E., Adhikari, M. H., Tielens, S., Tanco, S., Van-Damme, P., et al. (2018). Cell-intrinsic control of interneuron migration drives cortical morphogenesis. *Cell* 172, 1063.e19–1078.e19. doi: 10.1016/j.cell.2018.01.031

Silva, C. G., Peyre, E., and Nguyen, L. (2019). Cell migration promotes dynamic cellular interactions to control cerebral cortex morphogenesis. *Nat. Rev. Neurosci.* 20, 318–329. doi: 10.1038/s41583-019-0148-y

Smith, L. R., Cho, S., and Discher, D. E. (2018). Stem cell differentiation is regulated by extracellular matrix mechanics. *Physiology* 33, 16–25. doi: 10.1152/physiol.00026.2017

Solecki, D. J., Trivedi, N., Govek, E.-E., Kerekes, R. A., Gleason, S. S., and Hatten, M. E. (2009). Myosin II motors and F-Actin dynamics drive the coordinated movement of the centrosome and soma during CNS glial-guided neuronal migration. *Neuron* 63, 63–80. doi: 10.1016/j.neuron.2009.05.028

Solovei, I., Wang, A. S., Thanisch, K., Schmidt, C. S., Krebs, S., Zwerger, M., et al. (2013). LBR and lamin A/C sequentially tether peripheral heterochromatin and inversely regulate differentiation. *Cell* 152, 584–598. doi: 10.1016/j.cell.2013.01.009

Sosa, B. A., Kutay, U., and Schwartz, T. U. (2013). Structural insights into LINC complexes. *Curr. Opin. Struct. Biol.* 23, 285–291. doi: 10.1016/j.sbi.2013.03.005

Spear, P. C., and Erickson, C. A. (2012a). Apical movement during interkinetic nuclear migration is a two-step process. *Dev. Biol.* 370, 33–41. doi: 10.1016/j.ydbio.2012.06.031

Spear, P. C., and Erickson, C. A. (2012b). Interkinetic nuclear migration: a mysterious process in search of a function. *Dev. Growth Differ.* 54, 306–316. doi: 10.1111/j.1440-169X.2012.01342.x

Starr, D. A., and Han, M. (2002). Role of ANC-1 in tethering nuclei to the actin cytoskeleton. *Science* 298, 406–409. doi: 10.1126/science.1075119

Stiles, J., and Jernigan, T. L. (2010). The basics of brain development. *Neuropsychol. Rev.* 20, 327–348. doi: 10.1007/s11065-010-9148-4

Stroka, K. M., Jiang, H., Chen, S. H., Tong, Z., Wirtz, D., Sun, S. X., et al. (2014). Water permeation drives tumor cell migration in confined microenvironments. *Cell* 157, 611–623. doi: 10.1016/j.cell.2014.02.052

Sullivan, T., Escalante-Alcalde, D., Bhatt, H., Anver, M., Bhat, N., Nagashima, K., et al. (1999). Loss of A-type lamin expression compromises nuclear envelope integrity leading to muscular dystrophy. *J. Cell Biol.* 147, 913–919. doi: 10.1083/jcb.147.5.913

Sunyer, R., Conte, V., Escribano, J., Elosegui-Artola, A., Labernadie, A., Valon, L., et al. (2016). Collective cell durotaxis emerges from long-range intercellular force transmission. *Science* 6304, 1157–1161. doi: 10.1126/science.aaf7119

Suter, D. M., and Miller, K. E. (2011). The emerging role of forces in axonal elongation. *Prog. Neurobiol.* 94, 91–101. doi: 10.1016/j.pneurobio.2011.04.002

Swift, J., Ivanovska, I. L., Buxboim, A., Harada, T., Dingal, P. C. D. P., Pinter, J., et al. (2013). Nuclear lamin-A scales with tissue stiffness and enhances matrix-directed differentiation. *Science* 341:1240104. doi: 10.1126/science.1240104

Tanaka, T., Serneo, F. F., Higgins, C., Gambello, M. J., Wynshaw-Boris, A., and Gleeson, J. G. (2004). Lis1 and doublecortin function with dynein to mediate coupling of the nucleus to the centrosome in neuronal migration. *J. Cell Biol.* 165, 709–721. doi: 10.1083/jcb.200309025

Thomas, D. G., Yenepalli, A., Denais, C. M., Rape, A., Beach, J. R., Wang, Y., et al. (2015). Non-muscle myosin IIB is critical for nuclear translocation during 3D invasion. *J. Cell Biol.* 210, 583–594. doi: 10.1083/jcb.201502039

Trivedi, N., and Solecki, D. J. (2011). Neuronal migration illuminated: a look under the hood of the living neuron. *Cell Adhes. Migr.* 5, 42–47. doi: 10.4161/cam.5.1.13609

Trivedi, N., Stabley, D. R., Cain, B., Howell, D., Laumonnerie, C., Ramahi, J. S., et al. (2017). Drebrin-mediated microtubule-actomyosin coupling steers cerebellar granule neuron nucleokinesis and migration pathway selection. *Nat. Commun.* 8:14484. doi: 10.1038/ncomms14484

Tsai, J. W., Bremner, K. H., and Vallee, R. B. (2007). Dual subcellular roles for LIS1 and dynein in radial neuronal migration in live brain tissue. *Nat. Neurosci.* 10, 970–979. doi: 10.1038/nn1934

Turgay, Y., Eibauer, M., Goldman, A. E., Shimi, T., Khayat, M., Ben-Harush, K., et al. (2017). The molecular architecture of lamins in somatic cells. *Nature* 543, 261–264. doi: 10.1038/nature21382

Uhler, C., and Shivashankar, G. V. (2017). Regulation of genome organization and gene expression by nuclear mechanotransduction. *Nat. Rev. Mol. Cell Biol.* 18, 717–727. doi: 10.1038/nrm.2017.101

Umeshima, H., Hirano, T., and Kengaku, M. (2007). Microtubule-based nuclear movement occurs independently of centrosome positioning in migrating neurons. *Proc. Natl. Acad. Sci. U.S.A.* 104, 16182–16187. doi: 10.1073/pnas.0708047104

Umeshima, H., Nomura, K., Yoshikawa, S., Hörning, M., Tanaka, M., Sakuma, S., et al. (2019). Local traction force in the proximal leading process triggers nuclear translocation during neuronal migration. *Neurosci. Res.* 142, 38–48. doi: 10.1016/j.neures.2018.04.001

Ungricht, R., and Kutay, U. (2017). Mechanisms and functions of nuclear envelope remodelling. *Nat. Rev. Mol. Cell Biol.* 18, 229–245. doi: 10.1038/nrm.2016.153

Wang, H.-B., Dembo, M., Hanks, S. K., and Wang, Y.-L. (2002). Focal adhesion kinase is involved in mechanosensing during fibroblast migration. *Proc. Natl. Acad. Sci. U.S.A.* 98, 11295–11300. doi: 10.1073/pnas.201201198

Watanabe, Y., Kawaue, T., and Miyata, T. (2018). Differentiating cells mechanically limit the interkinetic nuclear migration of progenitor cells to secure apical cytogenesis. *Development* 145, dev162883. doi: 10.1242/dev.162883

Wolf, K., Te Lindert, M., Krause, M., Alexander, S., Te Riet, J., Willis, A. L., et al. (2013). Physical limits of cell migration: control by ECM space and nuclear deformation and tuning by proteolysis and traction force. *J. Cell Biol.* 201, 1069–1084. doi: 10.1083/jcb.201210152

Wolfenson, H., Yang, B., and Sheetz, M. P. (2018). Steps in Mechanotransduction Pathways that Control Cell Morphology. *Annu. Rev. Physiol.* 81, 585–605. doi: 10.1146/annurev-physiol-021317-121245

Wu, J., Kent, I. A., Shekhar, N., Chancellor, T. J., Mendonca, A., Dickinson, R. B., et al. (2014). Actomyosin pulls to advance the nucleus in a migrating tissue cell. *Biophys. J.* 106, 7–15. doi: 10.1016/j.bpj.2013.11.4489

Wu, Y. K., and Kengaku, M. (2018). Dynamic interaction between microtubules and the nucleus regulates nuclear movement during neuronal migration. *J. Exp. Neurosci.* 12, 0–2. doi: 10.1177/1179069518789151

Wu, Y. K., Umeshima, H., Kurisu, J., and Kengaku, M. (2018). Nesprins and opposing microtubule motors generate a point force that drives directional nuclear motion in migrating neurons. *Development* 145:dev158782. doi: 10.1242/dev.158782

Xia, Y., Ivanovska, I. L., Zhu, K., Smith, L., Irianto, J., Pfeifer, C. R., et al. (2018). Nuclear rupture at sites of high curvature compromises retention of DNA repair factors. *J. Cell Biol.* 217, 3796–3808. doi: 10.1083/jcb.201711161

Yanakieva, I., Erzberger, A., Matejčić, M., Modes, C. D., and Norden, C. (2019). Cell and tissue morphology determine actin-dependent nuclear migration mechanisms in neuroepithelia. *J. Cell Biol.* 218, 3272–3289. doi: 10.1083/jcb.201901077

Yang, B., Wolfenson, H., Chung, V. Y., Nakazawa, N., Liu, S., Hu, J., et al. (2019). Stopping transformed cancer cell growth by rigidity sensing. *Nat. Mater* 19, 239–250. doi: 10.1038/s41563-019-0507-0

Young, S. G., Jung, H. J., Coffinier, C., and Fong, L. G. (2012). Understanding the roles of nuclear A- and B-type lamins in brain development. *J. Biol. Chem.* 287, 16103–16110. doi: 10.1074/jbc.R112.354407

Young, S. G., Jung, H.-J., Lee, J. M., and Fong, L. G. (2014). Nuclear Lamins and Neurobiology. *Mol. Cell. Biol.* 34, 2776–2785. doi: 10.1128/mcb.00486-14

Zhang, X., Lei, K., Yuan, X., Wu, X., Zhuang, Y., Xu, T., et al. (2009). SUN1/2 and Syne/Nesprin-1/2 complexes connect centrosome to the nucleus during neurogenesis and neuronal migration in mice. *Neuron* 64, 173–187. doi: 10.1016/j.neuron.2009.08.018

Zhao, Y., Wang, Y., Sarkar, A., and Wang, X. (2018). Keratocytes generate high integrin tension at the trailing edge to mediate rear de-adhesion during rapid cell migration. *iScience* 9, 502–512. doi: 10.1016/j.isci.2018.11.016

Zhen, Y., Libotte, T., Munck, M., Noegel, A. A., and Korenbaum, E. (2002). NUANCE, a giant protein connecting the nucleus and actin cytoskeleton. *J. Cell Sci.* 115, 3207–3222.

Conflict of Interest: The authors declare that the research was conducted in the absence of any commercial or financial relationships that could be construed as a potential conflict of interest.

Copyright © 2020 Nakazawa and Kengaku. This is an open-access article distributed under the terms of the Creative Commons Attribution License (CC BY). The use, distribution or reproduction in other forums is permitted, provided the original author(s) and the copyright owner(s) are credited and that the original publication in this journal is cited, in accordance with accepted academic practice. No use, distribution or reproduction is permitted which does not comply with these terms.

frontiers in Cell and Developmental Biology

ORIGINAL RESEARCH
published: 17 June 2019
doi: 10.3389/fcell.2019.00106

Vimentin Intermediate Filament Rings Deform the Nucleus During the First Steps of Adhesion

Emmanuel Terriac[1], Susanne Schütz[2] and Franziska Lautenschläger[1,2]**

[1] Leibniz Institute for New Materials, Saarbrücken, Germany, [2] Faculty of Natural Sciences and Technology, Saarland University, Saarbrücken, Germany

During cell spreading, cells undergo many changes to their architecture and their mechanical properties. Vimentin, as an integral part of the cell architecture, and its mechanical stability must adapt to the new state of the cell. This study focuses on the structures formed by vimentin during the first steps of cell adhesion. Very early, ball-like structures, or "knots," are seen and often vimentin filaments emerge in the shape of rings around the nucleus. Although intermediate filaments are not known to be associated to motor proteins to form contractile systems, these rings can nonetheless strongly deform the cell nucleus. In the first 6 to 12 h of adhesion, these vimentin knots and rings disappear, and the intermediate filament network returns to the state seen before detachment of the cells. As these vimentin structures are very transient in the early steps of cell spreading, they have rarely been described in the literature. However, they can also be seen during mitosis, which is an event that involves partial detachment and re-spreading of the cells. Interestingly, the turnover dynamics of vimentin are reduced in both the knots and rings, compared to vimentin in the lamellipodia. It remains to define how the force is transmitted from the ball-like structures to the rings, and to measure the impact of such strong nuclear deformation on gene expression during cell re-spreading and the rearrangement of the vimentin network.

Keywords: vimentin, adhesion, nuclear deformation, ring, cell spreading

OPEN ACCESS

Edited by:
Guillermo Alberto Gomez, University of South Australia, Australia

Reviewed by:
Thomas Fath, Macquarie University, Australia
René-Marc Mège, Centre National de la Recherche Scientifique (CNRS), France

****Correspondence:***
Emmanuel Terriac
emmanuel.terriac@leibniz-inm.de
Franziska Lautenschläger
franziska.lautenschlaeger@leibniz-inm.de

Specialty section:
This article was submitted to Cell Adhesion and Migration, a section of the journal Frontiers in Cell and Developmental Biology

Received: *11 March 2019*
Accepted: *28 May 2019*
Published: *17 June 2019*

Citation:
Terriac E, Schütz S and Lautenschläger F (2019) Vimentin Intermediate Filament Rings Deform the Nucleus During the First Steps of Adhesion. Front. Cell Dev. Biol. 7:106. doi: 10.3389/fcell.2019.00106

INTRODUCTION

During embryogenesis, as also in the more detrimental context of metastasis, cells translocate from their original surrounding or tissue in other tissues (Greenburg and Hay, 1982; Hay, 1995; Davies, 1996; Nieto et al., 2016; Li et al., 2017; Roche, 2018). Upon arrival at their new location, the cells need to anchor to their new environment. During these processes, to correctly migrate, cells detach, by at least partial down-regulation of the expression of E-cadherin, among other factors, and up-regulation of the expression of mesenchymal markers, like N-cadherin and vimentin (Grunert et al., 2003; Christofori, 2006). This is referred to as epithelial-to-mesenchymal transition (Kalluri and Weinberg, 2009; Lamouille et al., 2014). Eventually, the cells will re-spread in a new environment, and will thus undergo the reversed transition called mesenchymal-to-epithelial transition (Davies, 1996). *In vitro* cell migration studies often require full detachment of cultured cells from their

original surface, with these studies then carried out once the cells have re-adhered a new surface. To understand how cells move from one surface, or tissue, to another, an understanding of the mechanisms of cell detachment and cell spreading is crucial.

Several studies have compared cells in adhered and suspended states, and it is clear that the cellular properties are very different. In particular, the mechanical properties of the cells are strongly altered in those two cases (Maloney et al., 2010; Chan et al., 2015). These detachment and spreading transitions whereby cells can adapt to a new state have been studied for many decades (Aoyama and Okada, 1977; Urushihara et al., 1977; Okano et al., 1995; Wakatsuki et al., 2003; Lynch et al., 2013).

Cellular mechanics are mainly governed by the cytoskeleton (Fletcher and Mullins, 2010) through the cytoskeleton fiber types: actin microfilaments, microtubules, and intermediate filaments. Several proteins fall in this last category (Fuchs and Weber, 1994; Herrmann and Aebi, 2016) and it has been shown that different cell types express different intermediate filament proteins, and that failure of correct expression of intermediate filament proteins can lead to several diseases (Danielsson et al., 2018). In the context of epithelial-to-mesenchymal transition, and in the reverse process, the expression for intermediate filaments changes between mainly keratin (epithelial) to mainly vimentin (mesenchymal).

In the present study, we show that during the first hours of adhesion, vimentin forms ball-like structures in close vicinity to the nuclei. These "knot" structures are transient and generally disappear within the first 6 h after re-spreading of the cells. These structures are often associated with vimentin rings around the nuclei, which can also slide along the nuclei. However, most surprisingly, while the non-polar vimentin filaments are not associated with molecular motors, these rings can exert force on the nuclei, and can even cause them to become deformed. We further show that this transient phenomenon can also be observed after re-spreading of mitotic cells.

MATERIALS AND METHODS

Cell Culture

Immortalized retinal pigmented epithelium (hTERT-RPE1) cells were cultured in DMEM/F12 medium (Gibco) with 10% fetal bovine serum (Fisher Scientific), 1% GlutaMAX (Fisher Scientific) and 1% penycilin/streptomycin (Gibco). Human foreskin fibroblasts (HFFs) were cultured with DMEM (Gibco) supplemented in the same manner.

Wild-type hTERT-RPE1 cells were from American Type Culture Collection (ATCC CRL-400). TALEN-edited cell lines included hTERT-RPE1 cells expressing mEmerald-vimentin and mTagRFP-tubulin, and HFFs expressing mEmerald-vimentin, and these were kindly provided by Gaudenz Danuser (UT Southwestern, Dallas, TX, United States). The genome editing has been described previously (Gan et al., 2016; Costigliola et al., 2017). These cell lines express the aforementioned proteins at levels comparable to their respective parental cell lines. The amount of the fluorescent protein, compared to the total amount of protein, was reported to be 4% for mEmerald-vimentin in HFFs, 8 and 5% for mEmerald-vimentin and mTagRFP-tubulin, respectively, in hTERT-RPE1 cells.

Immunostaining

Cells were fixed for 10 min in 4% paraformaldehyde in phosphate-buffered saline (PBS) and were rinsed three times for 5 min each in PBS. The cell membranes were permeabilized for 10 min in a 0.5% Triton X-100 in PBS, followed by three rinsing steps. Before immunostaining, the cells were blocked in 3% bovine serum albumin in PBS solution for 1 h. Vimentin was stained overnight with an Alexa Fluor 647 tagged human anti-vimentin V9 antibody (sc-6260; Santa Cruz) at 0.2 μg/mL in 3% bovine serum albumin in PBS. Actin was stained with fluorescently labeled phalloidin (phalloidin-iFluor 488; ab176753; Abcam) at a dilution of 1:1000, accordingly to the manufacturer protocol. After staining, the cells were rinsed three times in PBS and once in MilliQ water, and then they were mounted on glass slides using Fluoromount-G (Thermo Fisher Scientific), which contained DAPI to counterstain the cell nuclei.

Imaging

Epi-fluorescence images were acquired on different inverted microscopes (Ti-Eclipse; Nikon). The light sources used were either an Intensilight Epi-Fluorescence illuminator (Nikon) or a Sola Light engine (Lumencor). The microscopes were equipped with a temperature controlled (37°C) environmental chamber (Okolab) that provided 5% CO_2 and 100% humidity for the live-cell imaging. Confocal images were acquired on a confocal microscope (LSM 880; Zeiss). For live-cell imaging, the confocal images were acquired on an inverted microscope (Ti-Eclipse; Nikon) equipped with a Yokogawa spinning disk head (CSU-W1; Andor Technology) and a "fluorescence recovery after photobleaching/ photoactivation" (FRAPPA; Andor Technology) module. Live-cell imaging was performed in 23 mm diameter glass-bottomed dishes (World Precision Instruments). When mentioned, the dishes were pre-coated after 30 s of activation with plasma (Harrick PDC 32G), with a 25 μg/mL solution of bovine plasma fibronectin (F1141; Merck) and rinsed three times with PBS before adding cells.

RESULTS

Vimentin Ball-Like Structures and Rings Deform the Cell Nuclei During the First Hours of Adhesion

To investigate the cytoskeleton of single cells during their spreading, we used epithelial-like hTERT-RPE1 cells that were genetically edited to express mEmerald-vimentin and mTagRFP-tubulin (Gan et al., 2016). RPE cells are of epithelial origin, although in culture they show attributes of both epithelial cells, such as collective migration in wound-closure assays (Gan et al., 2016), and mesenchymal cells, such as high levels of vimentin expression (Yang et al., 2018). Of note, they also show higher expression of N-cadherin than E-cadherin (Youn et al., 2006), which is also a marker attributed to mesenchymal phenotypes. As

such, RPE cells are a good model for initiation of mesenchymal-to-epthelial transition, i.e., for cell attachment and spreading to a new surface.

These cells were allowed to spread on glass coverslips, which were incubated overnight in the cell growth medium. They were then fixed at different times after re-adhesion (1, 3, 5, and 24 h). The nuclear staining was added prior to the epi-fluorescence imaging. **Figure 1A** shows representative images of the cells at these times. In these images, large ball-like structures, or knots, can be seen close to the nuclei. In some cases, those structures were accompanied by thin lines of vimentin that span the nuclei, and which were related to nuclear deformation. As an example, **Figure 1A** (zoom) shows a high-magnification image of a cell.

To determine whether these linear structures corresponded to a more complex three-dimensional (3D) assembly, confocal images were obtained (**Figure 1B**). Through to the projections of the 3D images reconstructed at different angles, it could be seen that the thin vimentin lines previously observed corresponded to rings of vimentin around the nucleus. These rings appeared to be under enough tension for local deformation of the nuclei.

We quantified the numbers of cells that had vimentinn rings at 1, 3, 5, and 24 h after re-adhesion (**Figure 1C**). Here, we noted that some cells had several rings, and some of these rings had more of a shape of a shaft around the nuclei, i.e., thick bundles of vimentin filaments, seen in the high-magnification shown in **Figure 1A**, rather than as thin structures. The number of cells with a vimentin ring rapidly decreased during the first hours of spreading, from nearly 40% after 1 h, to around 20% after 5 h (**Figure 1C**). These structures are very rarely seen after 24 h of cell adhesion.

To determine whether these effects were a consequence of the fluorescent tag fused to vimentin and tubulin, we performed immunofluorescence analysis in wild-type RPE1 cells. Here there were also rings, and therefore we concluded that the rings were not artifacts of the genetic editing performed on these cells (**Supplementary Figure S1**). In order to assess the need of vimentin to form the ring structures, we compared cells during adhesion after they were treated for 30 min in suspension with withaferin A, a steroidal lactone that has been shown to destabilize the vimentin filaments network, and is not expected to be lethal at short time scales (Grin et al., 2012). We observed that rings were appearing at a later time in the case of the withaferin A treated cells. We could also see that the appearance of the rings were corresponding to synchronous nuclear deformation (**Supplementary Materials and Methods**, **Supplementary Figure S2**, and **Supplementary Movies S1**, **S2**).

As vimentin intermediate filaments are known to interact with other cytoskeletal components, such as actin (Wiche et al., 1993; Cary et al., 1994; Foisner et al., 1995; Svitkina et al., 1996; Esue et al., 2006) and tubulin (Svitkina et al., 1996; Sakamoto et al., 2013; Gan et al., 2016), we looked for these two proteins in these rings. **Figure 1D** shows representative images of cells with vimentin rings where they were also stained for actin and tubulin. While the rings were seen in the vimentin channels and the nuclei are deformed, there does not appear to be any link with actin. For tubulin, its association with the ring was possible, as seen in the high-magnification panel of **Figure 1A**, but not necessary as seen in **Figure 1D**.

Altogether, these data show that during the first hours of cell adhesion, vimentin intermediate filaments form ball-like structures in close vicinity to the nuclei. Thin vimentin filaments then emerge from these vimentin "knots," and they appear to form rings around the nuclei. These rings appear to deform the nuclei and to create invaginations in the nuclear surface. They also generally appear not to be related to other cytoskeletal structures, as actin is not found in them, and as tubulin is not necessarily present.

Rings Are Transient Structures That Slide Along the Nucleus

As the ball-like structures and rings disappear with time, to better define their dynamics, we carried out time-lapse recordings over several hours of cell spreading. For the rings, it was difficult to establish the timing of their disappearance, especially when several of them could be present within a single cell. **Figure 2A** (extracted from **Supplementary Movie S3**) shows an example of the disappearance of a ring. In this case, the ring started to disappear about 5 h after cell adhesion. At that moment, it slid along the nucleus. Upon reaching the edge of the nucleus, the ring became smaller, and then it fused into the knot from which it had initially emerged. We could also see that the deformation of the nucleus was aligned with the position of the vimentin ring. In the **Supplementary Figure S3**, images of the same sequence than **Figure 2A** are depicted with a smaller time interval and with black and white balance settings chosen in order to saturate the vimentin knot signal to better emphasize the vimentin rings. Arrows are aligned to show that the deformation of the nucleus corresponds to the position of a vimentin ring.

This raised the question of the stability of the knot itself. To quantify this, the images used in the quantification of **Figure 1B** were further analyzed, to determine the proportions of ball-like structures at the four different times. Considering the proportions of cells with a vimentin ring (**Figure 1B**), **Figure 2B** shows a similar decrease in the proportions of these ball-like vimentin knots, compared to the vimentin rings. However, the total proportions for the knots are a lot higher. Indeed, after 1 h of spreading, more than 75% of the cells showed the knot structures. This decreased to roughly 10% after 24 h.

To better quantify the disappearance of the vimentin rings and the vimentin ball-like structures during cell re-attachment, the spreading of the cells was monitored over 60 h. Time-lapse movies were analyzed automatically with FiJi software (Schindelin et al., 2012) by setting a threshold that excluded vimentin as the more diffused network (low homogeneous intensities taken from the last time points), and thus quantified only the (brighter) ball-like structures. In parallel, the numbers of cell nuclei were automatically quantified (according to DAPI staining). In **Figure 2C**, the proportions of the ball-like structures over 60 h are shown.

At the same time, the potential influences of cell-cell adhesion, cell secretion, and cell-substrate affinity were tested, in terms of varying the concentrations of the cells added to the dishes (either

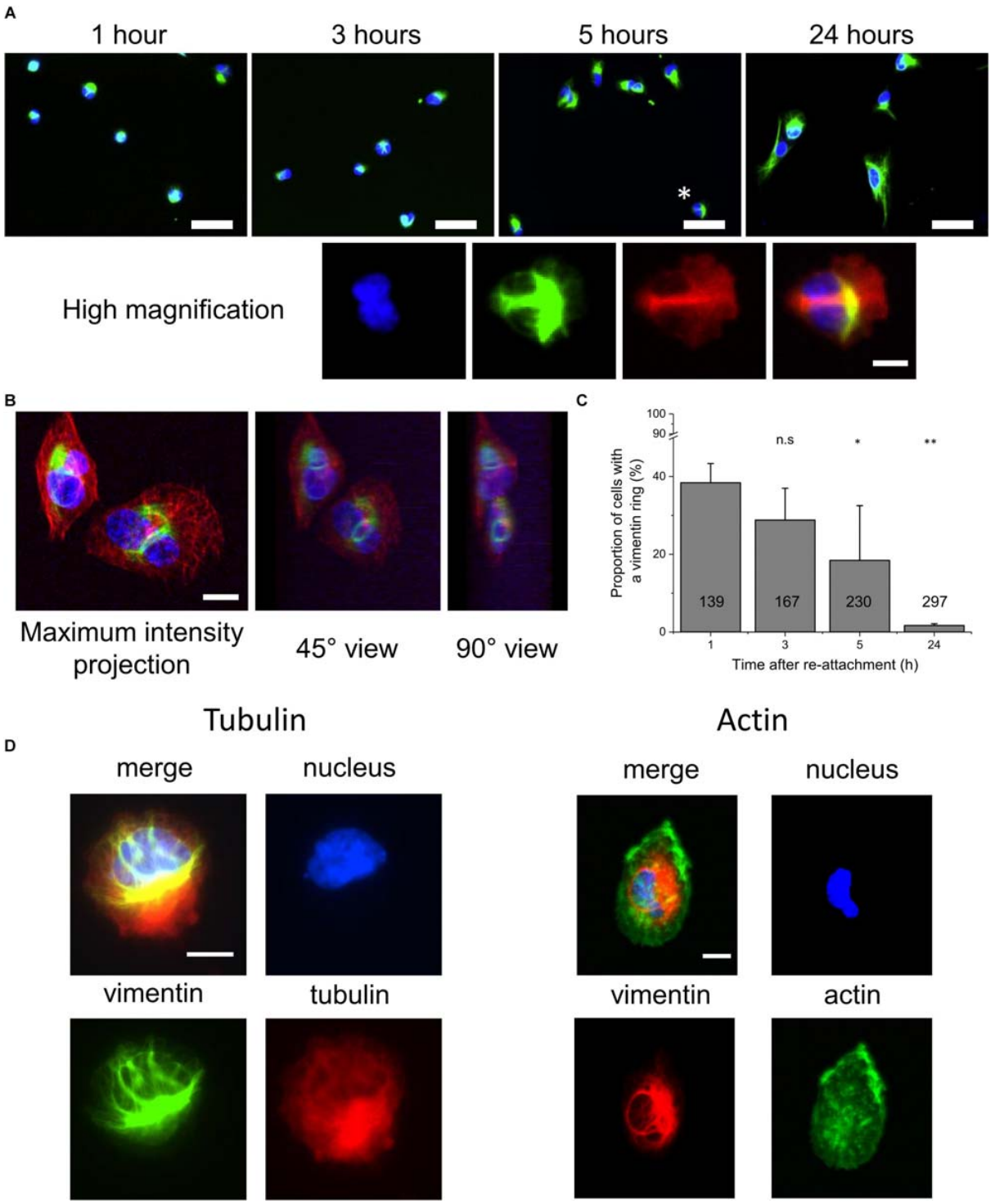

FIGURE 1 | Appearance of vimentin rings around the nuclei during the first hours of cell adhesion and spreading. **(A)** Top: Representative fluorescence images of fixed RPE1 cells after 1, 3, 5, and 24 h of adhesion on medium-incubated glass slides (20× magnification). Bottom: Magnification of the cell indicated with a * above. Green, vimentin; blue, nucleus. Scale bar: 50 μm (top); 10 μm (bottom) **(B)** Representative spinning disk confocal images of a vimentin ring. Left: maximum intensity projection in height image. Middle, right: three-dimension representation of left image at 45° and 90° angles, respectively. Green, Vimentin; red, tubulin; blue, nucleus. Scale bar: 10 μm. **(C)** Quantification of the proportion of cells with vimentin rings, based on fluorescence images of **(A)**. Data are means ± standard deviation; the number in each column corresponds to the total number of cells analyzed; * and ** $p < 0.05$ and $p < 0.01$, respectively, compared to the 1 h condition, one-way ANOVA with Bonferonni's test. **(D)** Representative images of high magnification (100×) fluorescence images of cells after 3 h of adhesion and spreading. Left: Green, vimentin; red, tubulin; blue, nucleus. Right: Red, vimentin; Green, actin; blue, nucleus. Scale bars: 10 μm.

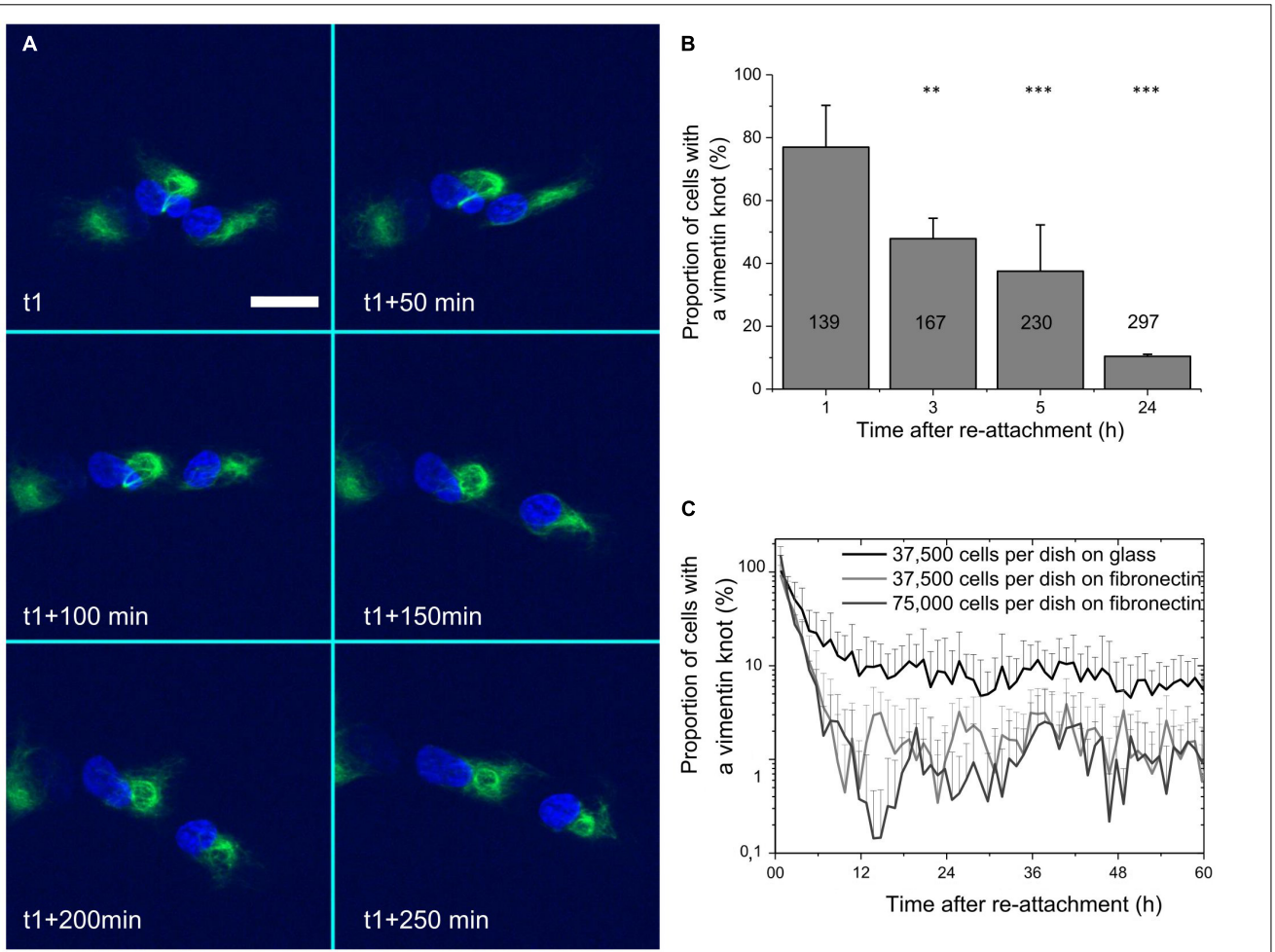

FIGURE 2 | Vimentin rings are transient and are accompanied by vimentin knots. **(A)** Representative images of deformation of a nucleus by a vimentin ring and its recovery after the sliding of the vimentin ring. Spinning disk confocal images were acquired at different times after call adhesion (t1, 400 min). Green, vimentin; blue, nucleus. Scale bar: 20 μm. The full movie is available as **Supplementary Material**. **(B)** Quantification of the proportions of cells with vimentin ball-like structures during cell adhesion and spreading, based on quantification of **Figure 1B**; the number in each column corresponds to the total number of cells analyzed; ** and *** $p < 0.01$ and $p < 0.001$, respectively, compared to the 1 h condition, one-way ANOVA with Bonferroni's test. **(C)** Quantification of proportions of cells with vimentin ball-like structures, over 60 h of cell adhesion and spreading, including different coatings and different cell concentrations. Each time point represents the proportion of knot for a minimum of 125 cells for the 37,500 cells per dish conditions and 250 cells for the 75,00 cells per dish condition.

37,500 or 75,000 cells per 23 mm diameter dish) or the coatings of the dish surface for cell attachment (bare glass, or 25 μg/mL fibronectin pre-coating).

Here, there were strong decreases in the proportions of cells showing the ball-like structures during the first hours of cell spreading. This stabilized between 2 and 10% after 12 h. Over this time, while the number of cells added to the dishes appeared to have little effect, the pre-coating of the dish had an important role. With the uncoated glass dishes, the proportion of cells with vimentin knot structures stabilized to 10% after 12 h, where it then remained for the duration of the experiment. For the fibronectin-coated dishes, the proportion of cells with vimentin knot structures stabilized to the lower level of around 2% after 12 h, and then remained low throughout.

To determine whether these changes in the appearance of vimentin rings and the ball-like vimentin knots are a particular phenotype of the epithelial-like hTERT-RPE1 cell type, this was repeated in HFFs, that were genetically engineered in the same manner as the RPE cells, although only regarding for vimentin (Costigliola et al., 2017). Similar data were obtained (**Supplementary Figure S4**), which thus showed that this phenotype is not cell-type specific.

These data thus demonstrate that during cell attachment and spreading, while a relatively low proportion of cells show the nucleus-deforming rings of vimentin, the majority show the ball-like juxtanuclear vimentin knots. These two structures are not fully independent of each other, as during the sliding of a ring along the nucleus, the ring remains anchored to the ball-like structure it emerged from. Also, these ball-like structures only persist through the first few hours of cell adhesion and spreading, and after roughly 12 h, very few cells still show them. Furthermore, this behavior is not a phenotype specific

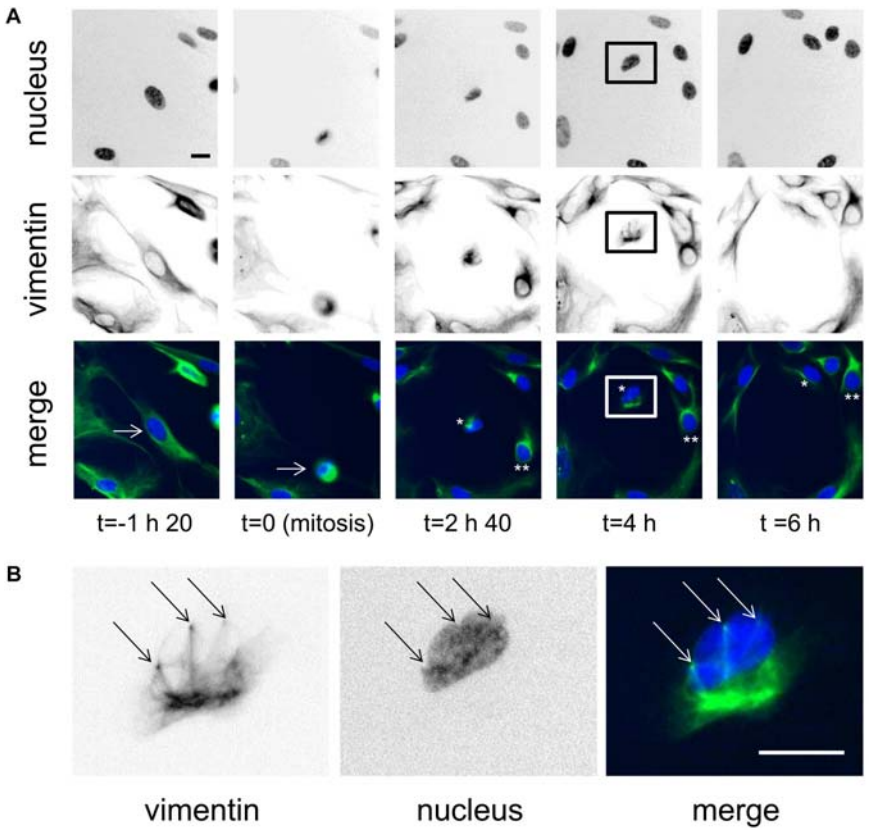

FIGURE 3 | Vimentin knots and rings are observed during mitosis. **(A)** Representative images of a cell dividing over time. Initially, the cell is shown 1 h 40 before cell division, then at cell division, and at three times after cell division. The original cell is indicated by the arrow on the two first panels. The daughter cells are indicated as * and ** in the color-merged views. Scale bar: 20 μm. **(B)** Magnification of the daughter cell [framed in (A)] showing the vimentin rings, (arrows). Scale bar: 10 μm.

being to the RPE cells, and the strength of the adhesion of the cells to different surfaces appears to have a role in the rate of disappearance of these ball-like vimentin knots.

Vimentin Ball-Like Structures and Rings Are Also Observed During Mitosis

During mitosis, cells do not fully detach, but they do 'round up' for the cell division, and during cytokinesis, both of the daughter cells spread back onto the surface. Here, during this re-spreading of the daughter cells after division, it was possible to see the ball-like vimentin knots, and sometimes also the nucleus-deforming vimentin rings (**Figure 3** and **Supplementary Movie S4**). However, these were not always clear in all cells, nor did they necessarily proceed in parallel. Indeed, **Figure 3A**, shows a case of daughter-cell asymmetry over the first 6 h from mitosis. In one daughter-cell, from 2 h 40 min from mitosis (**Figure 3A**, **), the vimentin network was rapidly reformed without any vimentin rings seen, and thus without deforming the nucleus. On the other hand, the second daughter cell, (**Figure 3A**, *, see also higher magnification in **Figure 3B**) showed a vimentin knot structure that was accompanied by nucleus-deforming vimentin rings while it was spreading (4 h after mitosis). This nucleus was seen to be bound by three nucleus-deforming vimentin rings (**Figure 3B**). In this case, the ball-like vimentin knot remained for longer than for the other daughter cell. This thus also shows that the vimentin ball-like knot or the deformation of the nucleus by vimentin rings might delay the reassembly of the vimentin network after cell division.

Vimentin Turnover Is Lower in the Ring Than in the Ball-Like Structure

The dynamics of the vimentin in the ball-like knot and the ring structures, were examined using fluorescence recovery after photobleaching (FRAP) experiments. Initially, the vimentin was bleached in three different regions: the lamellipodium and the juxtanuclear ball and ring (**Figures 4A,B**). Using a high intensity laser for the bleaching phase also allowed monitoring of the recovery of tubulin in the lamellipodium, as a control for recovery. These data were analyzed according to the protocol of Kappel and Eils (Kappel and Eils, 2004) and plotted accordingly (**Figure 4C**). Due to the low number of cases and the lack of a more refined model for the dynamic of vimentin, only the final values of recovery (plateau values at 10 min) were compared.

A recovery of 30% to 35% of the vimentin bleaching in the vimentin ball-like knots and the lamellipodia was seen over the 600 s recording following the bleaching. As a control, the

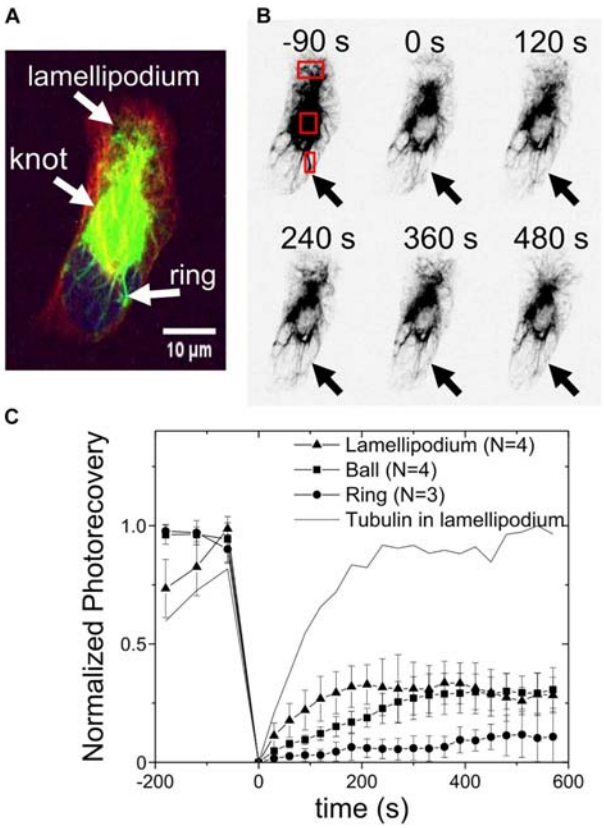

FIGURE 4 | Vimentin dynamics in the knot and ring structures measured by fluorescence recovery after photobleaching. **(A)** Representative image of a cell before photobleaching and the labeling of the three regions of interest: lamellipodium, and vimentin knot and ring. Green, vimentin; red, tubulin; blue, nucleus. **(B)** Fluorescence recovery after photobleaching time-lapse. Red squares: Three regions where photobleaching occurred, and where recovery was measured. Arrows, where the ring was initially. **(C)** Photorecovery curves of vimentin in the lamellipodium (▲), knot (■), and ring (●). Line, example of recovery of tubulin in the lamellipodium (same region), as comparison.

recovery of the bleaching of the microtubules was measured in the same lamellipodial region, which reached 100% over the time of recording. However, only about 10% of the vimentin in the rings was recovered within the same time. At this level of analysis, the vimentin in the knots and lamellipodia appears to be 3–5 fold more dynamic than the vimentin in the ring structures.

DISCUSSION

During the spreading of cells in a new tissue *in vivo* or in a new sample environment *in vitro*, they undergo drastic changes in their architecture, protein expression, and mechanical properties. Cells can adapt to such transitions due to their plasticity. Here, we have looked at the rearrangement of the vimentin intermediate filaments network during cell attachment and spreading as this protein is one contributor to cell mechanics (Wang and Stamenovic, 2000; Mendez et al., 2014).

Prahlad et al. (1998) described the interplay between vimentin filament precursors and microtubules at the cell periphery during the early stages of cell spreading. Furthermore, Lynch et al. (2013) showed that this interaction between vimentin and microtubules was required for spreading of the endoplasm, whereby for correct spreading of the endoplasmic cage, small fragments of vimentin are connected following their transport along microtubules. In both of these studies, the images presented showed a large accumulation of vimentin around the nuclei.

In the present study, we focused on these ball-like structures, or "knots," of vimentin. We detected vimentin rings that spanned from this structure, using confocal microscopy. While no motors are known to act directly on vimentin filaments to provide a contractile system, our data show that these rings can cause deformation of the nuclei of the spreading cells.

These rings are reminiscent of the structures reported by Parysek and Eckert (1984) for spreading neutrophils. They described loose juxtanuclear knots of vimentin from which filaments can radiate. However, they did not further investigate the radiating filaments, which might have also included rings of vimentin. Furthermore, while electron micrographs of spreading cells have shown deformed nuclei, it would have been difficult to attribute this effect specifically to the vimentin rings, particularly as neutrophil nuclei are known to be poly-lobulated (Campbell et al., 1995).

Ring-like structures composed of intermediate filaments and their creation of nuclear invaginations were previously reported by Kamei (1994) in different cancer cell lines, where they were mainly prominent in PaCa cells (i.e., undifferentiated human pancreatic carcinoma cells). However, neither the resilience of the structures nor their temporal relationships to cell adhesion and spreading were touched upon, as the main aspects that we have addressed in the present study. However, this PaCa cell line might represent a specific model for the formation of long lasting vimentin ring structures.

During the spreading of the cells in the present study, the two vimentin structures, as knots and rings, disappeared over time. After 3 h, less than 50% of the cells still showed those structures, and after 12 h, they were almost all gone, for both the hTERT-RPE1 cells and HFFs during cell attachment and spreading on fibronectin-coated glass. This might be the reason why these vimentin ring structures have not been described previously. Indeed, most *in vitro* studies have been actually performed on cells that have been left to adhere for several hours, to give the cells time to adapt to their new environment.

A reversed effect was reported by Hirano et al. (1992). They treated 3T3 fibroblasts with the protein phosphatase inhibitor calyculin A. This led to partial detachment of the cells with the description of ball structures of vimentin that formed around the nuclei and deformed them. In some of their micrographs some vimentin ring-like structures can indeed be recognized. However, their study might be more difficult to interpret, as calyculin A is often use as a vimentin disassembling molecule (Eriksson et al., 2004).

Interestingly, it is possible to see ball-like vimentin structures, and even vimentin rings, in cell that have undergone mitosis. During cell division, the cells partially detach from their substrate

to assemble the mitotic spindle. Once mitosis has occurred, then they re-spread on the surrounding surface. During mitosis, vimentin interacts with the actin cortex via its tail domain, and indeed, selective deletion of amino acids in the tail domain of vimentin has shown to impair cell progression through mitosis (Duarte et al., 2018).

Here, in a daughter cell, we observed the assembly of several vimentin rings that resulted in the deformation of the cell nucleus, which was not seen for the other daughter cell. It has recently been shown that vimentin is involved in asymmetric partitioning of "Juxta nuclear quality control" (JUNQ) inclusion bodies, which are responsible for the degradation of misfolded proteins (Ogrodnik et al., 2014). Our observations are in line with what they reported, although we also show here that similar behavior can be seen outside of the mitosis context.

We also quantified the turn-over of vimentin in these ball-like vimentin knots and rings, and in lamellipodia, using FRAP. Compared to other cytoskeletal fibers, like microtubules, the vimentin filaments are much less dynamic. This is in line with previous reports (Yoon et al., 1998). It is also especially true for formed filaments, which have lower rates of subunit exchange than unit-length filaments (Robert et al., 2015). In the present study, we even show differences in the recovery amount of vimentin along the rings, in the vimentin knots and in the lamellipodia.

It can be hypothesized that the vimentin rings interact with the nuclei, and hence this might slow down the exchange of the vimentin. It has been shown, that nesprin-3 connects both plectin and vimentin to the nuclear envelope in Sertoli cells (Ketema et al., 2013). In the ball-like vimentin structure, the vimentin turn-over also appear to be impaired compared to the lamellipodia as the signal needs more time to reach the final recovery value. These reduced vimentin dynamics might also arise from interactions between vimentin and other cellular proteins: indeed inactive ROCK might represent one such factor (Sin et al., 1998). This interaction has been suggested to be a way for migrating fibroblast to maintain their polarity, by controlling both the stress at the back of the cell and the Rac1-activating vimentin squiggles at the front of the cell (Terriac et al., 2017). This is also not necessarily the only occurrence of interactions between intermediate filaments and the contractile system of cells; another study has indeed shown that keratin K8/K18 can modulate cell stiffness through its interactions with the RhoA-ROCK pathway (Bordeleau et al., 2012).

We hypothesize that interactions between ROCK and vimentin are involved in the observed structures here. During the early stage of cell spreading, cells first down-regulate active ROCK via phosphorylation of p190RhoGAP (Arthur et al., 2000; Huveneers and Danen, 2009). This step is assumed to allow the relief of the stress in the spreading cell. Later on, ROCK becomes active through activation of p190RhoGEF, and can then be used for stress fiber formation, as well as for polarity initiation (Lim et al., 2008). Vimentin, on the other hand, can be phosphorylated at the amino-acid S71 by ROCK, which leads to its own reorganization (Lei et al., 2013; Hyder et al., 2015). We speculate that in our case the disappearance of the vimentin ball-like structures during cell adhesion is mainly due to the activation of ROCK over time. Moreover, integrin signaling is involved in the activation of RhoA during the later stage of cell adhesion (Danen et al., 2002). This is in line with the present study, where we show that on uncoated glass surfaces, the ball-like vimentin knots required more time to disappear.

CONCLUSION

In conclusion, our study shows that during cell adhesion and spreading, vimentin intermediate filaments can assemble into ball-like structures, or knots. These vimentin knots may be reminiscent of the previously vimentin assembled network before cell detachment. During the re-spreading of cells on a new surface, the vimentin knots might be the origin of the vimentin rings that are seen to strongly deform the cell nuclei. The origin of the force that must act on the nuclei during this deformation is for now unclear, as vimentin intermediate filaments are not known to form a contractile system, as does acto-myosin. Thus, at this stage, it would appear that this nucleus deformation is the result of the transmission of force generated during the re-arrangement of the vimentin knots. In the later steps of spreading, the vimentin filaments are reorganized into a flat and more homogeneous network. The implications of such strong deformation of the nuclei also remain unclear. It is known that gene expression can be affected by external forces exerted on the nucleus (Miroshnikova et al., 2017). As such, the strong deformation that we have observed here might have also an impact on gene regulation during cell adhesion and spreading.

DATA AVAILABILITY

All datasets generated for this study are included in the manuscript and/or the **Supplementary Files**.

AUTHOR CONTRIBUTIONS

ET and FL designed the experiments. ET performed the experiments, drafted the figures, and wrote the manuscript. SS helped in the preparation of samples for microscopy. FL revised the manuscript.

FUNDING

We acknowledge financial support from the Sonderforschungbereich SFB 1027 and from the Deutsche Forschungsgemeinschaft.

SUPPLEMENTARY MATERIAL

The Supplementary Material for this article can be found online at: https://www.frontiersin.org/articles/10.3389/fcell.2019.00106/full#supplementary-material

REFERENCES

Aoyama, H., and Okada, T. S. (1977). Mechanisms of cell-to-cell and cell-to-substrate adhesion of human epithelial, chang conjunctiva cells. *Cell Struct. Funct.* 2, 281–288. doi: 10.1247/csf.2.281

Arthur, W. T., Petch, L. A., and Burridge, K. (2000). Integrin engagement suppresses RhoA activity via a c-Src-dependent mechanism. *Curr. Biol.* 10, 719–722.

Bordeleau, F., Myrand Lapierre, M. E., Sheng, Y., and Marceau, N. (2012). Keratin 8/18 regulation of cell stiffness-extracellular matrix interplay through modulation of Rho-mediated actin cytoskeleton dynamics. *PLoS One* 7:e38780. doi: 10.1371/journal.pone.0038780

Campbell, M. S., Lovell, M. A., and Gorbsky, G. J. (1995). Stability of nuclear segments in human neutrophils and evidence against a role for microfilaments or microtubules in their genesis during differentiation of HL60 myelocytes. *J. Leuko. Biol.* 58, 659–666. doi: 10.1002/jlb.58.6.659

Cary, R. B., Klymkowsky, M. W., Evans, R. M., Domingo, A., Dent, J. A., and Backhus, L. E. (1994). Vimentin's tail interacts with actin-containing structures in vivo. *J. Cell Sci.* 107(Pt 6), 1609–1622.

Chan, C. J., Ekpenyong, A. E., Golfier, S., Li, W., Chalut, K. J., Otto, O., et al. (2015). Myosin II activity softens cells in suspension. *Biophys. J.* 108, 1856–1869. doi: 10.1016/j.bpj.2015.03.009

Christofori, G. (2006). New signals from the invasive front. *Nature* 441, 444–450. doi: 10.1038/nature04872

Costigliola, N., Ding, L., Burckhardt, C. J., Han, S. J., Gutierrez, E., Mota, A., et al. (2017). Vimentin fibers orient traction stress. *Proc. Natl. Acad. Sci. U.S.A.* 114, 5195–5200. doi: 10.1073/pnas.1614610114

Danen, E. H., Sonneveld, P., Brakebusch, C., Fassler, R., and Sonnenberg, A. (2002). The fibronectin-binding integrins alpha5beta1 and alphavbeta3 differentially modulate RhoA-GTP loading, organization of cell matrix adhesions, and fibronectin fibrillogenesis. *J. Cell Biol.* 159, 1071–1086. doi: 10.1083/jcb.200205014

Danielsson, F., Peterson, M. K., Caldeira Araujo, H., Lautenschlager, F., and Gad, A. K. B. (2018). Vimentin diversity in health and disease. *Cells* 7:147. doi: 10.3390/cells7100147

Davies, J. A. (1996). Mesenchyme to epithelium transition during development of the mammalian kidney tubule. *Acta Anat.* 156, 187–201.

Duarte, S., Viedma-Poyatos, Á, Navarro-Carrasco, E., Martínez, A. E., Pajares, M. A., and Pérez-Sala, D. (2018). Vimentin filaments interact with the mitotic cortex allowing normal cell division. *bioRxiv* doi: 10.1101/356642

Eriksson, J. E., He, T., Trejo-Skalli, A. V., Harmala-Brasken, A. S., Hellman, J., Chou, Y. H., et al. (2004). Specific in vivo phosphorylation sites determine the assembly dynamics of vimentin intermediate filaments. *J. Cell Sci.* 117(Pt 6), 919–932. doi: 10.1242/jcs.00906

Esue, O., Carson, A. A., Tseng, Y., and Wirtz, D. (2006). A direct interaction between actin and vimentin filaments mediated by the tail domain of vimentin. *J. Biol. Chem.* 281, 30393–30399. doi: 10.1074/jbc.M605452200

Fletcher, D. A., and Mullins, R. D. (2010). Cell mechanics and the cytoskeleton. *Nature* 463, 485–492. doi: 10.1038/nature08908

Foisner, R., Bohn, W., Mannweiler, K., and Wiche, G. (1995). Distribution and ultrastructure of plectin arrays in subclones of rat glioma C6 cells differing in intermediate filament protein (vimentin) expression. *J. Struct. Biol.* 115, 304–317. doi: 10.1006/jsbi.1995.1055

Fuchs, E., and Weber, K. (1994). Intermediate filaments: structure, dynamics, function, and disease. *Annu. Rev. Biochem.* 63, 345–382. doi: 10.1146/annurev.bi.63.070194.002021

Gan, Z., Ding, L., Burckhardt, C. J., Lowery, J., Zaritsky, A., Sitterley, K., et al. (2016). Vimentin intermediate filaments template microtubule networks to enhance persistence in cell polarity and directed migration. *Cell Syst* 3, 252.e258–263.e258. doi: 10.1016/j.cels.2016.08.007

Greenburg, G., and Hay, E. D. (1982). Epithelia suspended in collagen gels can lose polarity and express characteristics of migrating mesenchymal cells. *J. Cell Biol.* 95, 333–339. doi: 10.1083/jcb.95.1.333

Grin, B., Mahammad, S., Wedig, T., Cleland, M. M., Tsai, L., Herrmann, H., et al. (2012). Withaferin a alters intermediate filament organization, cell shape and behavior. *PLoS One* 7:e39065. doi: 10.1371/journal.pone.0039065

Grunert, S., Jechlinger, M., and Beug, H. (2003). Diverse cellular and molecular mechanisms contribute to epithelial plasticity and metastasis. *Nat. Rev. Mol. Cell Biol.* 4, 657–665. doi: 10.1038/nrm1175

Hay, E. D. (1995). An overview of epithelio-mesenchymal transformation. *Acta Anat.* 154, 8–20.

Herrmann, H., and Aebi, U. (2016). Intermediate filaments: structure and assembly. *Cold Spring Harb. Perspect. Biol.* 8:a018242. doi: 10.1101/cshperspect.a018242

Hirano, K., Chartier, L., Taylor, R. G., Allen, R. E., Fusetani, N., Karaki, H., et al. (1992). Changes in the cytoskeleton of 3T3 fibroblasts induced by the phosphatase inhibitor, calyculin-A. *J. Muscle Res. Cell Motil.* 13, 341–353.

Huveneers, S., and Danen, E. H. (2009). Adhesion signaling - crosstalk between integrins, Src and Rho. *J. Cell Sci.* 122(Pt 8), 1059–1069. doi: 10.1242/jcs.039446

Hyder, C. L., Kemppainen, K., Isoniemi, K. O., Imanishi, S. Y., Goto, H., Inagaki, M., et al. (2015). Sphingolipids inhibit vimentin-dependent cell migration. *J. Cell Sci.* 128, 2057–2069. doi: 10.1242/jcs.160341

Kalluri, R., and Weinberg, R. A. (2009). The basics of epithelial-mesenchymal transition. *J. Clin. Invest.* 119, 1420–1428. doi: 10.1172/JCI39104

Kamei, H. (1994). Relationship of nuclear invaginations to perinuclear rings composed of intermediate filaments in MIA PaCa-2 and some other cells. *Cell Struct. Funct.* 19, 123–132. doi: 10.1247/csf.19.123

Kappel, K., and Eils, R. (2004). Fluorescence recovery after phtobleaching with the leica TCS SP2. *Confocal Appl. Lett.* 18, 1–12.

Ketema, M., Kreft, M., Secades, P., Janssen, H., and Sonnenberg, A. (2013). Nesprin-3 connects plectin and vimentin to the nuclear envelope of sertoli cells but is not required for sertoli cell function in spermatogenesis. *Mol. Biol. Cell* 24, 2454–2466. doi: 10.1091/mbc.E13-02-0100

Lamouille, S., Xu, J., and Derynck, R. (2014). Molecular mechanisms of epithelial-mesenchymal transition. *Nat. Rev. Mol. Cell Biol.* 15, 178–196. doi: 10.1038/nrm3758

Lei, S., Tian, Y. P., Xiao, W. D., Li, S., Rao, X. C., Zhang, J. L., et al. (2013). ROCK is involved in vimentin phosphorylation and rearrangement induced by dengue virus. *Cell Biochem. Biophys.* 67, 1333–1342. doi: 10.1007/s12013-013-9665-x

Li, Q., Hutchins, A. P., Chen, Y., Li, S., Shan, Y., Liao, B., et al. (2017). A sequential EMT-MET mechanism drives the differentiation of human embryonic stem cells towards hepatocytes. *Nat. Commun.* 8:15166. doi: 10.1038/ncomms15166

Lim, Y., Lim, S. T., Tomar, A., Gardel, M., Bernard-Trifilo, J. A., Chen, X. L., et al. (2008). PyK2 and FAK connections to p190Rho guanine nucleotide exchange factor regulate RhoA activity, focal adhesion formation, and cell motility. *J. Cell Biol.* 180, 187–203. doi: 10.1083/jcb.200708194

Lynch, C. D., Lazar, A. M., Iskratsch, T., Zhang, X., and Sheetz, M. P. (2013). Endoplasmic spreading requires coalescence of vimentin intermediate filaments at force-bearing adhesions. *Mol. Biol. Cell* 24, 21–30. doi: 10.1091/mbc.E12-05-0377

Maloney, J. M., Nikova, D., Lautenschlager, F., Clarke, E., Langer, R., Guck, J., et al. (2010). Mesenchymal stem cell mechanics from the attached to the suspended state. *Biophys. J.* 99, 2479–2487. doi: 10.1016/j.bpj.2010.08.052

Mendez, M. G., Restle, D., and Janmey, P. A. (2014). Vimentin enhances cell elastic behavior and protects against compressive stress. *Biophys. J.* 107, 314–323. doi: 10.1016/j.bpj.2014.04.050

Miroshnikova, Y. A., Nava, M. M., and Wickstrom, S. A. (2017). Emerging roles of mechanical forces in chromatin regulation. *J. Cell Sci.* 130, 2243–2250. doi: 10.1242/jcs.202192

Nieto, M. A., Huang, R. Y., Jackson, R. A., and Thiery, J. P. (2016). Emt: 2016. *Cell* 166, 21–45. doi: 10.1016/j.cell.2016.06.028

Ogrodnik, M., Salmonowicz, H., Brown, R., Turkowska, J., Sredniawa, W., Pattabiraman, S., et al. (2014). Dynamic JUNQ inclusion bodies are asymmetrically inherited in mammalian cell lines through the asymmetric partitioning of vimentin. *Proc. Natl. Acad. Sci. U.S.A.* 111, 8049–8054. doi: 10.1073/pnas.1324035111

Okano, T., Yamada, N., Okuhara, M., Sakai, H., and Sakurai, Y. (1995). Mechanism of cell detachment from temperature-modulated, hydrophilic-hydrophobic polymer surfaces. *Biomaterials* 16, 297–303. doi: 10.1016/0142-9612(95)93257-E

Parysek, L. M., and Eckert, B. S. (1984). Vimentin filaments in spreading, randomly locomoting, and f-met-leu-phe-treated neutrophils. *Cell Tissue Res.* 235, 575–581.

Prahlad, V., Yoon, M., Moir, R. D., Vale, R. D., and Goldman, R. D. (1998). Rapid movements of vimentin on microtubule tracks: kinesin-dependent assembly of intermediate filament networks. *J. Cell Biol.* 143, 159–170. doi: 10.1083/jcb.143.1.159

Robert, A., Rossow, M. J., Hookway, C., Adam, S. A., and Gelfand, V. I. (2015). Vimentin filament precursors exchange subunits in an ATP-dependent manner. *Proc. Natl. Acad. Sci. U.S.A.* 112, E3505–E3514. doi: 10.1073/pnas.1505303112

Roche, J. (2018). The epithelial-to-mesenchymal transition in cancer. *Cancers* 10:52. doi: 10.3390/cancers10020052

Sakamoto, Y., Boeda, B., and Etienne-Manneville, S. (2013). APC binds intermediate filaments and is required for their reorganization during cell migration. *J. Cell Biol.* 200, 249–258. doi: 10.1083/jcb.201206010

Schindelin, J., Arganda-Carreras, I., Frise, E., Kaynig, V., Longair, M., Pietzsch, T., et al. (2012). Fiji: an open-source platform for biological-image analysis. *Nat. Methods* 9, 676–682. doi: 10.1038/nmeth.2019

Sin, W. C., Chen, X. Q., Leung, T., and Lim, L. (1998). RhoA-binding kinase alpha translocation is facilitated by the collapse of the vimentin intermediate filament network. *Mol. Cell Biol.* 18, 6325–6339. doi: 10.1128/mcb.18.11.6325

Svitkina, T. M., Verkhovsky, A. B., and Borisy, G. G. (1996). Plectin sidearms mediate interaction of intermediate filaments with microtubules and other components of the cytoskeleton. *J. Cell Biol.* 135, 991–1007. doi: 10.1083/jcb.135.4.991

Terriac, E., Coceano, G., Mavajian, Z., Hageman, T. A., Christ, A. F., Testa, I., et al. (2017). Vimentin levels and serine 71 phosphorylation in the control of cell-matrix adhesions, migration speed, and shape of transformed human fibroblasts. *Cells* 6:E2. doi: 10.3390/cells6010002

Urushihara, H., Masamichi, J. U., Okada, T. S., and Takeichi, M. (1977). Calcium-dependent and-independent adhesion of normal and transformed BHK cells. *Cell Struct. Funct.* 2, 289–296. doi: 10.1247/csf.2.289

Wakatsuki, T., Wysolmerski, R. B., and Elson, E. L. (2003). Mechanics of cell spreading: role of myosin II. *J. Cell Sci.* 116(Pt 8), 1617–1625. doi: 10.1242/jcs.00340

Wang, N., and Stamenovic, D. (2000). Contribution of intermediate filaments to cell stiffness, stiffening, and growth. *Am. J. Physiol. Cell Physiol.* 279, C188–C194. doi: 10.1152/ajpcell.2000.279.1.C188

Wiche, G., Gromov, D., Donovan, A., Castanon, M. J., and Fuchs, E. (1993). Expression of plectin mutant cDNA in cultured cells indicates a role of COOH-terminal domain in intermediate filament association. *J. Cell Biol.* 121, 607–619. doi: 10.1083/jcb.121.3.607

Yang, X., Chung, J. Y., Rai, U., and Esumi, N. (2018). Cadherins in the retinal pigment epithelium (RPE) revisited: P-cadherin is the highly dominant cadherin expressed in human and mouse RPE in vivo. *PLoS One* 13:e0191279. doi: 10.1371/journal.pone.0191279

Yoon, M., Moir, R. D., Prahlad, V., and Goldman, R. D. (1998). Motile properties of vimentin intermediate filament networks in living cells. *J. Cell Biol.* 143, 147–157. doi: 10.1083/jcb.143.1.147

Youn, Y. H., Hong, J., and Burke, J. M. (2006). Cell phenotype in normal epithelial cell lines with high endogenous N-cadherin: comparison of RPE to an MDCK subclone. *Invest. Ophthalmol. Vis. Sci.* 47, 2675–2685. doi: 10.1167/iovs.05-1335

Conflict of Interest Statement: The authors declare that the research was conducted in the absence of any commercial or financial relationships that could be construed as a potential conflict of interest.

Copyright © 2019 Terriac, Schütz and Lautenschläger. This is an open-access article distributed under the terms of the Creative Commons Attribution License (CC BY). The use, distribution or reproduction in other forums is permitted, provided the original author(s) and the copyright owner(s) are credited and that the original publication in this journal is cited, in accordance with accepted academic practice. No use, distribution or reproduction is permitted which does not comply with these terms.

frontiers in Cell and Developmental Biology

MINI REVIEW
published: 04 October 2019
doi: 10.3389/fcell.2019.00199

YAP/TAZ Related BioMechano Signal Transduction and Cancer Metastasis

Bridget Martinez[1,2,3,4], Yongchao Yang[5], Donald Mario Robert Harker[3], Charles Farrar[1], Harshini Mukundan[1], Pulak Nath[2] and David Mascareñas[1]*

[1] Engineering Institute, Los Alamos National Laboratory, Los Alamos, NM, United States, [2] Applied Modern Physics, Los Alamos National Laboratory, Los Alamos, NM, United States, [3] Department of Medicine, St. George's University School of Medicine, St. George's, Grenada, [4] Chemistry Division, Physical Chemistry and Applied Spectroscopy, Los Alamos National Laboratory, Los Alamos, NM, United States, [5] Energy and Global Security, Argonne National Laboratory, Lemont, IL, United States

Mechanoreciprocity refers to a cell's ability to maintain tensional homeostasis in response to various types of forces. Physical forces are continually being exerted upon cells of various tissue types, even those considered static, such as the brain. Through mechanoreceptors, cells sense and subsequently respond to these stimuli. These forces and their respective cellular responses are prevalent in regulating everything from embryogenic tissue-specific differentiation, programmed cell death, and disease progression, the last of which being the subject of extensive attention. Abnormal mechanical remodeling of cells can provide clues as to the pathological status of tissues. This becomes particularly important in cancer cells, where cellular stiffness has been recently accepted as a novel biomarker for cancer metastasis. Several studies have also elucidated the importance of cell stiffness in cancer metastasis, with data highlighting that a reversal of tumor stiffness has the capacity to revert the metastatic properties of cancer. In this review, we summarize our current understanding of extracellular matrix (ECM) homeostasis, which plays a prominent role in tissue mechanics. We also describe pathological disruption of the ECM, and the subsequent implications toward cancer and cancer metastasis. In addition, we highlight the most novel approaches toward understanding the mechanisms which generate pathogenic cell stiffness and provide potential new strategies which have the capacity to advance our understanding of one of human-kinds' most clinically significant medical pathologies. These new strategies include video-based techniques for structural dynamics, which have shown great potential for identifying full-field, high-resolution modal properties, in this case, as a novel application.

Keywords: cancer biology, biomarkers, metastasis and actin dynamics, cell rigidity measurement, cell morphodynamics

OPEN ACCESS

Edited by:
Selwin Kaixiang Wu, Harvard Medical School, United States

Reviewed by:
Sandeep Kumar Vishwakarma, Deccan College of Medical Sciences, India
Brian A. Wall, Colgate-Palmolive, United States
Lin Deng, Harvard Medical School, United States

****Correspondence:***
Bridget Martinez
bridgetm@lanl.gov;
bmartinez26@ucmerced.edu

Specialty section:
This article was submitted to Cell Adhesion and Migration, a section of the journal Frontiers in Cell and Developmental Biology

Received: *07 January 2019*
Accepted: *05 September 2019*
Published: *04 October 2019*

Citation:
Martinez B, Yang Y, Harker DMR, Farrar C, Mukundan H, Nath P and Mascareñas D (2019) YAP/TAZ Related BioMechano Signal Transduction and Cancer Metastasis. Front. Cell Dev. Biol. 7:199. doi: 10.3389/fcell.2019.00199

INTRODUCTION

Cancer is defined as a set of diseases in which cells bypass the mechanisms that normally limit their growth and replication capacity (Hanahan and Weinberg, 2000; Brower, 2007). This uncontrolled growth is characterized by overexpression of oncogenes, coupled with the loss of tumor suppressor genes (Hanahan and Weinberg, 2000). Eventually, this uncontrolled replication is followed by the

invasion of nearby or distant tissue (Hanahan and Weinberg, 2000). Metastasis, or the spreading of a secondary cancer *via* the translocation of cancer cells to different parts of the body, is the cause of over 90% of human cancer deaths (Weigelt et al., 2005; Brower, 2007). This stark percentage highlights the importance of understanding the metastatic processes in cancer and the need to explore and elucidate more effective treatment options. These efforts are currently hindered by many factors, one of them being that a tumor's microenvironment imparts anti-cancer drug resistance (Lin et al., 2017), making a tumor's milieu an attractive area of study in the search for novel and unique anti-cancer strategies. Although, several environmental factors have been shown to increase the risk of cancer development (Evanthia et al., 2012; Di Ciaula et al., 2017), it is well known that the human genome plays a crucial role (Thean et al., 2017; Wilson et al., 2017; Gooskens et al., 2018) suggesting that future studies most employ a holistic approach in both the undertaking and subsequent interpretation.

MICROENVIRONMENTS AND MECHANICAL CELL SIGNALING

Over the last 30 years, studies have emerged which highlight the effect of mechanical signals on cell behavior (Dupont et al., 2011; Wei et al., 2015; Lachowski et al., 2017). These signals, which emerge from the cells' microenvironment are influenced by a wide variety of physical forces, including blood flow, gravity, muscle contractions and tissue rigidity (Butcher et al., 2009; Discher et al., 2009; Jaalouk and Lammerding, 2009; Panciera et al., 2017). The prevalence of physical forces, and its implications are observed in a range of fields spanning embryology, physiology as well as pathology. For example, mechanical force has been implicated in directing embryonic development (Farge, 2003; Ruiyi et al., 2006; Page-McCaw et al., 2007; Krieg et al., 2008). Studies show that force is necessary for proper tissue organization. Mesenchymal stem cells differentiate to lineages based on the specific composition of its surrounding matrix (Engler et al., 2006).

EXTRACELLULAR MATRIX COMPOSITION AND CANCER PROGRESSION

It is clear that the ECM balances forces that maintain tissue homeostasis. The ECM is a dynamic, 3-dimensional, non-cellular structure that is constantly undergoing remodeling in response to mechanical and genetic cues (Bateman et al., 2009; **Figure 1**). ECM is composed of over 300 different proteins, all in compositional homeostasis, regulating respective structure and function, the precise configuration of which varies with tissue type (Hynes and Naba, 2012). The ECM comprises both the interstitium, as well as the basement membrane, and in this capacity is poised to be in constant interactions with epithelial cells. These interactions enable signal transduction processes which potentially regulate cell health/survival, apoptosis, migration and cell division among many others functions (Hynes, 2009; Hynes and Naba, 2012; Mushtaq et al., 2018; van Helvert et al., 2018). The main structural component of the ECM are collagens- which provide tensile strength and limit distensibility (Hynes and Naba, 2012). Other components include varying types of proteoglycans and glycoproteins, which include elastin (Hynes and Naba, 2012). Additional noteworthy components of the ECM are lysyl oxidase and hydroxylase (LOX and LOXL) (Kirschmann et al., 2002; Payne et al., 2007; Nilsson et al., 2016; Esposito et al., 2018). These secreted copper-dependent amine oxidases function to cross-link collagen and elastin, enabling them to play key roles in tumor progression and metastasis (Nilsson et al., 2016; Esposito et al., 2018). Indeed, many studies have outlined the effects and mechanism of action of LOX/LOXL in a myriad of oncogenic settings (Palamakumbura et al., 2009; Barker et al., 2012; Cox et al., 2016).

The importance of maintenance of ECM biophysical properties can be extrapolated from studies showing that inappropriate alterations are associated with fibrotic conditions and metastatic cancer. Indeed, it is well recognized that the ECM of a tumor is largely distinct from its counterpart in healthy cells (Aszódi et al., 2006; Cox and Erler, 2011; Sotgia et al., 2012; Leight et al., 2017). Studies which outline how post-translational cross-linking of the ECM in premalignant breast cancer is a necessary step for transformation into a malignant cancer suggest that the ECM's biochemical composition is of paramount importance in cancer progression in this response (Paszek et al., 2005; Levental et al., 2009). This highly impactful data underscores the significance of ECM homeostasis and highlights the necessity to better understand the mechanism(s) that drive ECM remodeling in the context of oncology.

FROM MECHANICAL TO MOLECULAR

The topology and rigidity of the extracellular matrix (ECM) is used as a counterbalancing external force against internal pulling forces (Vogel and Sheetz, 2006). Cell structure appears to be regulated by cycles of mechano-sensing, mechano-transduction and mechano-response; where a local sensing of spatial geometry is translated into biochemical cues which can eventually control cell growth, differentiation, shape changes and cell death as previously mentioned (Vogel and Sheetz, 2006). It is through this mechanism that macroscopic cues reach the microscopic scale, regulating cell fate through the modulation of gene expression.

Thus, it is now well established that mechanical cues comprise an integral part of both normal and abnormal physiology, or pathology (Jaalouk and Lammerding, 2009). However, the mechanism(s) by which such cues are translated into molecular signals which subsequently drive increases in gene expression are unclear. Given that cells can perceive their position and shape by interpreting such mechanical cues, it is not surprising that any missteps in the translation of such signals can also lead to abnormalities such as cancer. Understanding the molecular mechanisms involved in this process can thus provide strategies for the identification and treatment of cancer. The focus of this

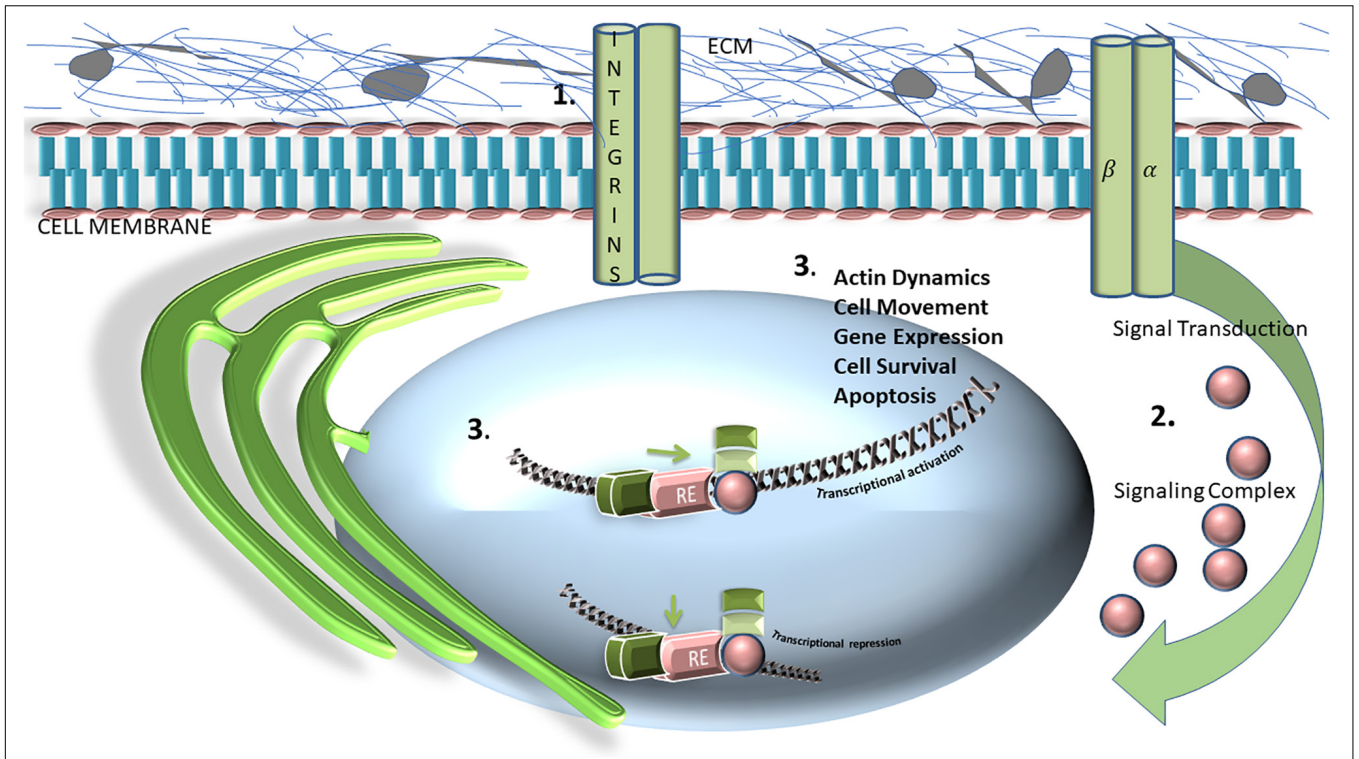

FIGURE 1 | Schematic representation and general overview of extracellular matrix (ECM) matrix and its relationship with transcriptional activation, or repression. Integrins, consisting of, and labeled as alpha and beta subunits, are transmembrane heterodimeric glycoprotein receptors are comprised of an extracellular domain, a transmembrane domain, and a cytoplasmic tail. This schematic represents how the integrin cytoplasmic domains directly associates with various cytoskeletal proteins **(1)** and intracellular signaling molecules **(2)**, which are crucial for modulating fundamental cell processes and functions including cell adhesion, proliferation, migration, and survival **(3)**.

manuscript will be on mechano-transducing transcriptional co-activators, changes in whose expression can potentially mediate the development of cancer.

MECHANO-TRANSDUCING TRANSCRIPTIONAL CO-ACTIVATORS IN CANCER

Yes-associated protein (YAP) and transcriptional co-activator with PDZ binding motif (TAZ), are oncogenic transcriptional co-regulators which are part of the Hippo pathway, and have recently been identified as mechano-transducing transcriptional co-activators (Panciera et al., 2017). YAP/TAZ have been tightly linked to actin cytoskeleton architecture, promoting cancer drug resistance through actin remodeling; by interacting with transcriptional enhancer factor TEF-1, also known as TEA domain family member (TEAD). These transcription factors are able to translate mechanical cues such as ECM rigidity into genomic transcriptional changes which can then promote processes such as stem cell behavior and regeneration (Kim et al., 2016; Panciera et al., 2017). This translational regulation is mediated *via* Rho GTPase activity, making YAP/TAZ necessary for the ECM stiffness-mediated mesenchymal stem cell differentiation described earlier (Deng et al., 2006; Dupont et al., 2011). Mechanical stimuli and tension create force-dependent mechanical restriction, which results in the inhibition of nuclear pores for molecular transport, thereby directly driving YAP nuclear translocation (Elosegui-Artola et al., 2017). YAP and TAZ are thus re-localized into the nucleus in cells that experience enhanced signaling from processes such as cytoskeletal tension, or increased stretch (Elosegui-Artola et al., 2017), resulting in YAP-dependent and TAZ-dependent biological effects, including cell proliferation (Aragona et al., 2013). In addition, results suggest that the restriction of transport/translocation is further regulated *via* the addition of mechanical stability, a property which the transported protein exhibits (Elosegui-Artola et al., 2017). This determines both the active and passive nuclear transport of YAP, as well as other proteins (Elosegui-Artola et al., 2017). YAP and TAZ are thus necessary for uncontrolled cell proliferation, overcoming contact inhibition, and consequently, are very important in cancer development and metastasis (Kanellos et al., 2015; Zanconato et al., 2016). The microenvironment of tumors is known to impart specific mechanical inputs, which are a consequence of aberrant tissue organization, metalloproteinase-mediated ECM remodeling and ECM stiffening (Tang et al., 2013), which in turn induce YAP and TAZ overactivity in cancer cells. ECM remodeling and stiffening are interesting candidates of study in the understanding of YAP- and TAZ-mediated conversion of

benign neoplastic cells into cancer stem cells. Intrinsically, cells appear to be tumor-suppressive, and while remaining in relatively unagitated mechanical conditions, experience low mechanical forces, which leads to low levels of YAP/TAZ. However, in disturbed tissue architecture ECM stiffening induces YAP/TAZ activation/nuclear translocation (Finch-Edmondson and Sudol, 2016; Wang et al., 2016). Recent published studies have validated that active nuclear import indeed controls YAP localization by using AFM as a means for force application on nuclei, results of which suggest that increased active nuclear import is the mediator of YAP nuclear translocation when force is applied both directly as well as indirectly (Elosegui-Artola et al., 2017).

The mechanism linking tissue rigidity and YAP/TAZ-mediated uncontrolled proliferation in tumor cells is not well understood, and offers possible new research targets against epithelial mesenchymal transition (EMT). For example, it is still not clear whether the development of cancer results in mechanical stimuli which induces YAP activity or whether Yap induction contributes to the reorganization, however it is likely that both scenarios are possible, one being driven by genetic predispositions for example, while the other, likely environmental. EMT is a cellular process by which immotile epithelial cells are converted into motile mesenchymal cells via the degradation of the underlying basement membrane. In normal cells, epithelial cells tightly adhere to the basement membrane, which is thus responsible for holding the cells in place (Yang and Weinberg, 2008). The transformation of epithelial cells to motile mesenchymal cells is characterized by the attainment of migratory capacity, invasiveness, resistance to apoptosis and increased ECM production leading to cell rigidity (Kalluri and Weinberg, 2009).

A critical element of EMT is an actin-dependent protrusion of cell pseudopodia; resulting in the destabilization of the actin cytoskeleton, which is a key component of EMT-driven cancer metastasis (Shankar et al., 2010). Known mesenchymal cell markers included FTS binding protein FAP, FSP-1, N-cadherin, vimentin, fibronectin, and β- catenin, among others (Kalluri and Weinberg, 2009; Fernandez-Garcia et al., 2014). Given that YAP is a regulator of these markers, it is not surprising that EMT is promoted by YAP overexpression (Yuan et al., 2016). Recent studies have affirmed that cytoskeleton stability plays an important role in cancer metastasis, given its association with EMT (Sun et al., 2015). Understanding the physical interplay of this intracellular filament network, and its real-time contribution to cancer metastasis is an intriguing therapeutic target against cancer, and the focus of our research. Studies to date have focused on actin cytoskeleton reorganization using live cell imaging and GFP-coronin, as an F-actin reporter (Mun and Jeon, 2012). In a study investigating the relationship of matrix stiffness in EMT, it was found that in genetically engineered pancreatic cancers, fibrotic rigidities promote elements of EMT (Rice et al., 2017). Pancreatic cancer is one of the stiffest of all human solid carcinomas (Rice et al., 2017). Pancreatic ductal adenocarcinoma (PDAC) is an aggressive malignancy characterized by the presence of extensive desmoplasia and myofibroblast-like, high matrix secreting phenotype (Lachowski et al., 2017). Stiffness is also an associated finding in other cancers. For instance, in breast cancer ECM stiffness induces EMT through mechano-transduction, leading to nuclear translocation of YAP and TAZ (Dupont et al., 2011; Wei et al., 2015). In HER2-amplified breast cancer cells, fibronectin, type IV collagen, and matrix rigidity all contribute to drug resistance as tumor microenvironments modulate and dampen the efficacy of targeted anti-cancer therapies (Allen and Louise Jones, 2011; Lin et al., 2017).

BRIDGING THE GAP – NEW METHODS TOWARD UNDERSTANDING THE CELLULAR BIOPHYSICS IN CANCER

There is a need for more sensitive techniques in order to address the gaps in this field; current research aims are to develop and use sensitive image analyses techniques for quantitatively characterizing structural dynamics at the cellular level- specifically, in cells undergoing cancer metastasis. There still exists significant gaps in quantitatively analyzing the data from current techniques, and in using them to verify and validate finite element models describing the mechanics of cells. This is primarily because of the lack of comprehensive techniques to measure the full-field structural stiffness of cells. With its resolution in the order of fractions of a nanometer, atomic force microscopy (AFM) is one of many methods currently being evaluated in order to obtain high-resolution imaging of cell surface topography as it offers the convenience of being able to measure forces and elasticity in fixed and living cells (Naitoh et al., 2010; Garcia and Proksch, 2013). Applications thus far have included the study of cellular events including locomotion, differentiation and aging, physiological activation and electromotility, as well as cell pathology (Lekka et al., 1999; Nagayama et al., 2001; Müller and Dufrêne, 2011). Bimodal force microscopy uses AFM with several eigenmode excitations frequencies which can be detected, allowing the different resonances to act as channels, which can then be used to isolate material properties such as Young's modulus of elasticity (a measure of stiffness) (Rodrìguez and Garcìa, 2004; Proksch, 2006). The detection of the cantilever interaction with the sample is monitored and translated into a three-dimensional image (Mozafari et al., 2005), which can reveal heterogeneities of mechanical properties of both the surface and subsurface of cells (Kuznetsova et al., 2007). The methods so far discussed have allowed us to gain preliminary insight into the contribution of mechanical signals and changes in the development and propagation of cancer. However, even with AFM, there are limitations such as the addition of unwanted background flow modes from piezoelectric shakers (Guan et al., 2017). Additionally, AFM sensitivity significantly decreases when probing properties in a liquid medium, given that frequency modulation and dual-frequency imaging are designed for operation in air (Minary-Jolandan et al., 2012). Recently, this limitation has been averted with a unique technique which images cells using AFM with a long-needle probe using only the tip of the probe as the point of interaction with a liquid medium, and spares the cantilever's high-quality resonant modes by maintaining its

air-functioning quality and providing non-contact viscoelastic imaging of living cells (Guan et al., 2017). AFM interrogation of YAP/TAZ has shown that force application to the nucleus is enough to enable YAP translocation independent of rigidity, focal adhesions, the actin cytoskeleton, and also cell-cell adhesion using a constant force of 1.5 nN to the cell nucleus, using cantilevers with 20-μm spherical tips (Elosegui-Artola et al., 2017). In addition, force application to the nucleus increased the nuclear/cytosolic YAP ratio, and then proceeded to return to baseline levels when the force was withdrawn, suggesting that force disrupts YAP distribution and that the observed equilibrium lasts only while force is being applied (Elosegui-Artola et al., 2017). Additionally, it should be noted that these studies have found that there were no measurable differences in YAP ratios when the probe was used to press outside the nucleus, suggesting that the forces produced by exposure to a stiff environment are exerted through focal adhesions and are thereby able to reach the nucleus (Elosegui-Artola et al., 2017). Lastly, because a force-induced breakage of the nucleocytoplasmic barrier cannot be responsible for such an immediate nuclear export, it rules out the possibility that these translocation are simply due to high nuclear deformations (Elosegui-Artola et al., 2017).

Another interesting non-contact/non-intrusive imaging method currently used for diagnostic purposes is interferometric phase microscopy (IPM), which provides several advantages over AFM (Bishitz et al., 2014). The appeal of IPM is that it captures the entire amplitude and phase data from the optical illumination of the sample, generating an optical thickness fluctuation map, which indicates rigidity strength for every cell in the field of view (Bishitz et al., 2014), with the added benefit of cell to cell comparison. However, even as we circumvent existing limitations and find novel techniques that increase imaging sensitivity, it is imperative to note that we are only beginning to understand the relationship between biophysical properties of cells, and their potential to regulate tumorigenesis and motility (Paszek and Weaver, 2004). There is a need for novel and unique imaging techniques develop that provide verification and validation of finite element models of cellular structure.

AUTHOR CONTRIBUTIONS

BM devised the project, the main conceptual ideas to be explored, and manuscript outline, worked out the technical details of the review, and performed the literature review and data gathering. All authors contributed substantial context addition, editing and revision of all drafts.

FUNDING

BM was supported by a Director's post-doctoral fellowship under the Laboratory Directed Research and Development program of the Los Alamos National Laboratory under project number 20170694PRD4. YY was partially supported by the U.S. Defense Advanced Research Projects Agency (DARPA) "Physics of AI" program.

REFERENCES

Allen, M., and Louise Jones, J. (2011). Jekyll and Hyde: the role of the microenvironment on the progression of cancer. *J. Pathol.* 223, 163–177. doi: 10.1002/path.2803

Aragona, M., Panciera, T., Manfrin, A., Giulitti, S., Michielin, F., Elvassore, N., et al. (2013). A mechanical checkpoint controls multicellular growth through YAP/TAZ regulation by actin-processing factors. *Cell* 154, 1047–1059. doi: 10.1016/j.cell.2013.07.042

Aszódi, A., Legate, K. R., Nakchbandi, I., and Fässler, R. (2006). What mouse mutants teach us about extracellular matrix function. *Annu. Rev. Cell Dev. Biol.* 22, 591–621. doi: 10.1146/annurev.cellbio.22.010305.104258

Barker, H. E., Cox, T. R., and Erler, J. T. (2012). The rationale for targeting the LOX family in cancer. *Nat. Rev. Cancer* 12, 540–552. doi: 10.1038/nrc3319

Bateman, J. F., Boot-Handford, R. P., and Lamandé, S. R. (2009). Genetic diseases of connective tissues: cellular and extracellular effects of ECM mutations. *Nat. Rev. Genet.* 10, 173–183. doi: 10.1038/nrg2520

Bishitz, Y., Gabai, H., Girshovitz, P., and Shaked, N. T. (2014). Optical-mechanical signatures of cancer cells based on fluctuation profiles measured by interferometry. *J. Biophoton.* 7, 624–630. doi: 10.1002/jbio.201300019

Brower, V. (2007). Researchers tackle metastasis, cancer's last frontier. *J. Natl. Cancer Inst.* 99, 109–111. doi: 10.1093/jnci/djk047

Butcher, D. T., Alliston, T., and Weaver, V. M. (2009). A tense situation: forcing tumour progression. *Nat. Rev. Cancer* 9, 108–122. doi: 10.1038/nrc2544

Cox, T. R., and Erler, J. T. (2011). Remodeling and homeostasis of the extracellular matrix: implications for fibrotic diseases and cancer. *Dis. Models Mech.* 4, 165–178. doi: 10.1242/dmm.004077

Cox, T. R., Gartland, A., and Erler, J. T. (2016). Lysyl oxidase, a targetable secreted molecule involved in cancer metastasis. *Cancer Res.* 76, 188–192. doi: 10.1158/0008-5472.CAN-15-2306

Deng, J., Petersen, B. E., Steindler, D. A., Jorgensen, M. L., and Laywell, E. D. (2006). Mesenchymal stem cells spontaneously express neural proteins in culture and are neurogenic after transplantation. *Stem Cells* 24, 1054–1064. doi: 10.1634/stemcells.2005-0370

Di Ciaula, A., Wang, D. Q.-H., Molina-Molina, E., Baccetto, R. L., Calamita, G., Palmieri, V. O., et al. (2017). Bile acids and cancer: direct and environmental-dependent effects. *Ann. Hepatol.* 16, 81–99.

Discher, D. E., Mooney, D. J., and Zandstra, P. W. (2009). Growth factors, matrices, and forces combine and control stem cells. *Science* 324, 1673–1677. doi: 10.1126/science.1171643

Dupont, S., Morsut, L., Aragona, M., Enzo, E., Giulitti, S., Cordenonsi, M., et al. (2011). Role of YAP/TAZ in mechanotransduction. *Nature* 474, 179–183. doi: 10.1038/nature10137

Elosegui-Artola, A., Andreu, I., Beedle, A. E. M., Lezamiz, A., Uroz, M., Kosmalska, A. J., et al. (2017). Force triggers YAP nuclear entry by regulating transport across nuclear pores. *Cell* 171, 1397.e14–1410.e14. doi: 10.1016/j.cell.2017.10.008

Engler, A. J., Sen, S., Sweeney, H. L., and Discher, D. E. (2006). Matrix elasticity directs stem cell lineage specification. *Cell* 126, 677–689. doi: 10.1016/j.cell.2006.06.044

Esposito, P., Estienne, L., Serpieri, N., Ronchi, D., Comi, G. P., Moggio, M., et al. (2018). Rhabdomyolysis-associated acute kidney injury. *Am. J. Kidney Dis.* 71, A12–A14.

Evanthia, D.-K., Charikleia, C., and Evangelos, M. (2012). Phenotypes and enviromental factors: their influence in PCOS. *Curr. Pharmaceut. Design* 18, 270–282. doi: 10.2174/138161212799040457

Farge, E. (2003). Mechanical induction of twist in the *Drosophila* Foregut/Stomodeal Primordium. *Curr. Biol.* 13, 1365–1377. doi: 10.1016/s0960-9822(03)00576-1

Fernandez-Garcia, B., Eiró, N., Marín, L., González-Reyes, S., González, L. O., Lamelas, M. L., et al. (2014). Expression and prognostic significance

of fibronectin and matrix metalloproteases in breast cancer metastasis. *Histopathology* 64, 512–522. doi: 10.1111/his.12300

Finch-Edmondson, M., and Sudol, M. (2016). Framework to function: mechanosensitive regulators of gene transcription. *Cell. Mol. Biol. Lett.* 21:28. doi: 10.1186/s11658-016-0028-7

Garcia, R., and Proksch, R. (2013). Nanomechanical mapping of soft matter by bimodal force microscopy. *Eur. Polym. J.* 49, 1897–1906. doi: 10.1016/j.eurpolymj.2013.03.037

Gooskens, S. L., Klasson, T. D., Gremmels, H., Logister, I., Pieters, R., Perlman, E. J., et al. (2018). TCF21 hypermethylation regulates renal tumor cell clonogenic proliferation and migration. *Mol. Oncol.* 12, 166–179. doi: 10.1002/1878-0261.12149

Guan, D., Charlaix, E., Qi, R. Z., and Tong, P. (2017). Noncontact viscoelastic imaging of living cells using a long-needle atomic force microscope with dual-frequency modulation. *Phys. Rev. Appl.* 8:044010.

Hanahan, D., and Weinberg, R. A. (2000). The hallmarks of cancer. *Cell* 100, 57–70.

Hynes, R. O. (2009). Extracellular matrix: not just pretty fibrils. *Science* 326, 1216–1219. doi: 10.1126/science.1176009

Hynes, R. O., and Naba, A. (2012). Overview of the Matrisome—An inventory of extracellular matrix constituents and functions. *Cold Spring Harb. Perspect. Biol.* 4:a004903. doi: 10.1101/cshperspect.a004903

Jaalouk, D. E., and Lammerding, J. (2009). Mechanotransduction gone awry. *Nat. Rev. Mol. Cell Biol.* 10, 63–73. doi: 10.1038/nrm2597

Kalluri, R., and Weinberg, R. A. (2009). The basics of epithelial-mesenchymal transition. *J. Clin. Investig.* 119, 1420–1428. doi: 10.1172/JCI39104

Kanellos, G., Zhou, J., Patel, H., Ridgway Rachel, A., Huels, D., Gurniak Christine, B., et al. (2015). ADF, and cofilin1 control actin stress fibers, nuclear integrity, and cell survival. *Cell Rep.* 13, 1949–1964. doi: 10.1016/j.celrep.2015.10.056

Kim, M. H., Kim, J., Hong, H., Lee, S. H., Lee, J. K., Jung, E., et al. (2016). Actin remodeling confers BRAF inhibitor resistance to melanoma cells through YAP/TAZ activation. *EMBO J.* 35, 462–478. doi: 10.15252/embj.201592081

Kirschmann, D. A., Seftor, E. A., Fong, S. F. T., Nieva, D. R. C., Sullivan, C. M., Edwards, E. M., et al. (2002). A molecular role for lysyl oxidase in breast cancer invasion. *Cancer Res.* 62, 4478–4483.

Krieg, M., Arboleda-Estudillo, Y., Puech, P. H., Käfer, J., Graner, F., Müller, D. J., et al. (2008). Tensile forces govern germ-layer organization in zebrafish. *Nat. Cell Biol.* 10, 429–436. doi: 10.1038/ncb1705

Kuznetsova, T. G., Starodubtseva, M. N., Yegorenkov, N. I., Chizhik, S. A., and Zhdanov, R. I. (2007). Atomic force microscopy probing of cell elasticity. *Micron* 38, 824–833. doi: 10.1016/j.micron.2007.06.011

Lachowski, D., Cortes, E., Pink, D., Chronopoulos, A., Karim, S. A., Morton, J. P., et al. (2017). Substrate rigidity controls activation and durotaxis in pancreatic stellate cells. *Sci. Rep.* 7:2506. doi: 10.1038/s41598-017-02689-x

Leight, J. L., Drain, A. P., and Weaver, V. M. (2017). Extracellular matrix remodeling and stiffening modulate tumor phenotype and treatment response. *Annu. Rev. Cancer Biol.* 1, 313–334. doi: 10.1146/annurev-cancerbio-050216-034431

Lekka, M., Laidler, P., Gil, D., Lekki, J., Stachura, Z., and Hrynkiewicz, A. Z. (1999). Elasticity of normal and cancerous human bladder cells studied by scanning force microscopy. *Eur. Biophys. J.* 28, 312–316. doi: 10.1007/s002490050213

Levental, K. R., Yu, H., Kass, L., Lakins, J. N., Egeblad, M., Erler, J. T., et al. (2009). Matrix crosslinking forces tumor progression by enhancing integrin signaling. *Cell* 139, 891–906. doi: 10.1016/j.cell.2009.10.027

Lin, C.-H., Jokela, T., Gray, J., and LaBarge, M. A. (2017). Combinatorial microenvironments impose a continuum of cellular responses to a single pathway-targeted anti-cancer compound. *Cell Rep.* 21, 533–545. doi: 10.1016/j.celrep.2017.09.058

Minary-Jolandan, M., Tajik, A., Wang, N., and Yu, M.-F. (2012). Intrinsically high-Q dynamic AFM imaging in liquid with a significantly extended needle tip. *Nanotechnology* 23, 235704–235704. doi: 10.1088/0957-4484/23/23/235704

Mozafari, M. R., Reed, C. J., Rostron, C., and Hasirci, V. (2005). A review of scanning probe microscopy investigations of liposome-DNA complexes. *J. Liposome Res.* 15, 93–107. doi: 10.1081/lpr-200064965

Müller, D. J., and Dufrêne, Y. F. (2011). Atomic force microscopy: a nanoscopic window on the cell surface. *Trends Cell Biol.* 21, 461–469. doi: 10.1016/j.tcb.2011.04.008

Mun, H., and Jeon, T. J. (2012). Regulation of actin cytoskeleton by Rap1 binding to RacGEF1. *Mol. Cells* 34, 71–76. doi: 10.1007/s10059-012-0097-z

Mushtaq, M. U., Papadas, A., Pagenkopf, A., Flietner, E., Morrow, Z., Chaudhary, S. G., et al. (2018). Tumor matrix remodeling and novel immunotherapies: the promise of matrix-derived immune biomarkers. *J. Immunother. Cancer* 6:65. doi: 10.1186/s40425-018-0376-0

Nagayama, M., Haga, H., and Kawabata, K. (2001). Drastic change of local stiffness distribution correlating to cell migration in living fibroblasts. *Cell Motil. Cytoskeleton* 50, 173–179. doi: 10.1002/cm.10008

Naitoh, Y., Ma, Z., Li, Y. J., Kageshima, M., and Sugawara, Y. (2010). Simultaneous observation of surface topography and elasticity at atomic scale by multifrequency frequency modulation atomic force microscopy. *J. Vac. Sci. Technol. B Nanotechnol. Microelectron.* 28, 1210–1214. doi: 10.1116/1.3503611

Nilsson, M., Adamo, H., Bergh, A., and Halin Bergström, S. (2016). Inhibition of lysyl oxidase and lysyl oxidase-like enzymes has tumour-promoting and tumour-suppressing roles in experimental prostate cancer. *Sci. Rep.* 6:19608. doi: 10.1038/srep19608

Page-McCaw, A., Ewald, A. J., and Werb, Z. (2007). Matrix metalloproteinases and the regulation of tissue remodelling. *Nat. Rev. Mol. Cell Biol.* 8, 221–233.

Palamakumbura, A. H., Vora, S. R., Nugent, M. A., Kirsch, K. H., Sonenshein, G. E., and Trackman, P. C. (2009). Lysyl oxidase propeptide inhibits prostate cancer cell growth by mechanisms that target FGF-2-cell binding and signaling. *Oncogene* 28, 3390–3400. doi: 10.1038/onc.2009.203

Panciera, T., Azzolin, L., Cordenonsi, M., and Piccolo, S. (2017). Mechanobiology of YAP and TAZ in physiology and disease. *Nat. Rev. Mol. Cell Biol.* 18, 758–770. doi: 10.1038/nrm.2017.87

Paszek, M. J., and Weaver, V. M. (2004). The tension mounts: mechanics meets morphogenesis and malignancy. *J. Mamm. Gland Biol. Neoplasia* 9, 325–342. doi: 10.1007/s10911-004-1404-x

Paszek, M. J., Zahir, N., Johnson, K. R., Lakins, J. N., Rozenberg, G. I., Gefen, A., et al. (2005). Tensional homeostasis and the malignant phenotype. *Cancer Cell* 8, 241–254. doi: 10.1016/j.ccr.2005.08.010

Payne, S. L., Hendrix, M. J. C., and Kirschmann, D. A. (2007). Paradoxical roles for lysyl oxidases in cancer—A prospect. *J. Cell. Biochem.* 101, 1338–1354. doi: 10.1002/jcb.21371

Proksch, R. (2006). Multifrequency, repulsive-mode amplitude-modulated atomic force microscopy. *Appl. Phys. Lett.* 89:113121. doi: 10.1063/1.2345593

Rice, A. J., Cortes, E., Lachowski, D., Cheung, B. C. H., Karim, S. A., Morton, J. P., et al. (2017). Matrix stiffness induces epithelial-mesenchymal transition and promotes chemoresistance in pancreatic cancer cells. *Oncogenesis* 6:e352. doi: 10.1038/oncsis.2017.54

Rodrìguez, T. R., and Garcìa, R. (2004). Compositional mapping of surfaces in atomic force microscopy by excitation of the second normal mode of the microcantilever. *Appl. Phys. Lett.* 84, 449–451. doi: 10.1063/1.1642273

Ruiyi, R., Martina, N., Emilios, T., Rudi, W., and Karen, S. (2006). Migrating anterior mesoderm cells and intercalating trunk mesoderm cells have distinct responses to Rho and Rac during Xenopus gastrulation. *Dev. Dyn.* 235, 1090–1099. doi: 10.1002/dvdy.20711

Shankar, J., Messenberg, A., Chan, J., Underhill, T. M., Foster, L. J., and Nabi, I. R. (2010). Pseudopodial actin dynamics control epithelial-mesenchymal transition in metastatic cancer cells. *Cancer Res.* 70, 3780–3790. doi: 10.1158/0008-5472.CAN-09-4439

Sotgia, F., Martinez-Outschoorn, U. E., Howell, A., Pestell, R. G., Pavlides, S., and Lisanti, M. P. (2012). Caveolin-1 and cancer metabolism in the tumor microenvironment: markers, models, and mechanisms. *Annu. Rev. Pathol. Mech. Dis.* 7, 423–467. doi: 10.1146/annurev-pathol-011811-120856

Sun, B. O., Fang, Y., Li, Z., Chen, Z., and Xiang, J. (2015). Role of cellular cytoskeleton in epithelial-mesenchymal transition process during cancer progression. *Biomed. Rep.* 3, 603–610. doi: 10.3892/br.2015.494

Tang, Y., Rowe, R. G., Botvinick, E. L., Kurup, A., Putnam, A. J., Seiki, M., et al. (2013). MT1-MMP-dependent control of skeletal stem cell commitment via a β1-integrin/YAP/TAZ signaling axis. *Dev. Cell* 25, 402–416. doi: 10.1016/j.devcel.2013.04.011

Thean, L. F., Low, Y. S., Lo, M., Teo, Y.-Y., Koh, W.-P., Yuan, J.-M., et al. (2017). Genome-wide association study identified copy number variants associated with sporadic colorectal cancer risk. *J. Med. Genet.* 55, 181–188. doi: 10.1136/jmedgenet-2017-104913

van Helvert, S., Storm, C., and Friedl, P. (2018). Mechanoreciprocity in cell migration. *Nat. Cell Biol.* 20, 8–20. doi: 10.1038/s41556-017-0012-0

Vogel, V., and Sheetz, M. (2006). Local force and geometry sensing regulate cell functions. *Nat. Rev. Mol. Cell Biol.* 7, 265–275. doi: 10.1038/nrm1890

Wang, K.-C., Yeh, Y.-T., Nguyen, P., Limqueco, E., Lopez, J., Thorossian, S., et al. (2016). Flow-dependent YAP/TAZ activities regulate endothelial phenotypes and atherosclerosis. *Proc. Natl. Acad. Sci. U.S.A.* 113, 11525–11530. doi: 10.1073/pnas.1613121113

Wei, S. C., Fattet, L., Tsai, J. H., Guo, Y., Pai, V. H., Majeski, H. E., et al. (2015). Matrix stiffness drives Epithelial-Mesenchymal transition and tumour metastasis through a TWIST1-G3BP2 mechanotransduction pathway. *Nat. Cell Biol.* 17, 678–688. doi: 10.1038/ncb3157

Weigelt, B., Peterse, J. L., and van't Veer, L. J. (2005). Breast cancer metastasis: markers and models. *Nat. Rev. Cancer* 5, 591–602. doi: 10.1038/nrc1670

Wilson, C. L., Mann, D. A., and Borthwick, L. A. (2017). Epigenetic reprogramming in liver fibrosis and cancer. *Adv. Drug Deliv. Rev.* 121, 124–132. doi: 10.1016/j.addr.2017.10.011

Yang, J., and Weinberg, R. A. (2008). Epithelial-Mesenchymal transition: at the crossroads of development and tumor metastasis. *Dev. Cell* 14, 818–829. doi: 10.1016/j.devcel.2008.05.009

Yuan, Y., Li, D., Li, H., Wang, L., Tian, G., and Dong, Y. (2016). YAP overexpression promotes the epithelial-mesenchymal transition and chemoresistance in pancreatic cancer cells. *Mol. Med. Rep.* 13, 237–242. doi: 10.3892/mmr.2015.4550

Zanconato, F., Battilana, G., Cordenonsi, M., and Piccolo, S. (2016). YAP/TAZ as therapeutic targets in cancer. *Curr. Opin. Pharmacol.* 29, 26–33. doi: 10.1016/j.coph.2016.05.002

Conflict of Interest: The authors declare that the research was conducted in the absence of any commercial or financial relationships that could be construed as a potential conflict of interest.

Copyright © 2019 Martinez, Yang, Harker, Farrar, Mukundan, Nath and Mascareñas. This is an open-access article distributed under the terms of the Creative Commons Attribution License (CC BY). The use, distribution or reproduction in other forums is permitted, provided the original author(s) and the copyright owner(s) are credited and that the original publication in this journal is cited, in accordance with accepted academic practice. No use, distribution or reproduction is permitted which does not comply with these terms.

frontiers in Cell and Developmental Biology

MINI REVIEW
published: 31 October 2019
doi: 10.3389/fcell.2019.00260

Formation and Function of Mammalian Epithelia: Roles for Mechanosensitive PIEZO1 Ion Channels

Teneale A. Stewart[1,2] *and Felicity M. Davis*[1,2]*

[1] *Faculty of Medicine, Mater Research-The University of Queensland, Brisbane, QLD, Australia,* [2] *Translational Research Institute, Brisbane, QLD, Australia*

Mechanical forces play important roles in shaping mammalian development. In the embryo, cells experience force both during the formation of the mammalian body plan and in the ensuing phase of organogenesis. Physical forces – including fluid flow, compression, radial pressure, contraction, and osmotic pressure – continue to play central roles as organs mature, function, and ultimately dysfunction. Multiple mechanisms exist to receive, transduce, and transmit mechanical forces in mammalian epithelial tissues and to integrate these cues, which can both fluctuate and coincide, with local and systemic chemical signals. Drawing near a decade since the discovery of the bona fide mechanically activated ion channel, PIEZO1, we discuss in this mini-review established and emerging roles for this protein in the form and function of mammalian epithelia.

Keywords: mechanotransduction, PIEZO1, calcium channel, calcium signaling, epithelial biology

OPEN ACCESS

Edited by:
Selwin Kaixiang Wu,
Harvard Medical School,
United States

Reviewed by:
Rodger Liddle,
Duke University, United States
Arthur Beyder,
Mayo Clinic, United States

***Correspondence:**
Felicity M. Davis
f.davis@uq.edu.au

Specialty section:
This article was submitted to Cell Adhesion and Migration, a section of the journal Frontiers in Cell and Developmental Biology

Received: *27 August 2019*
Accepted: *17 October 2019*
Published: *31 October 2019*

Citation:
Stewart TA and Davis FM (2019) Formation and Function of Mammalian Epithelia: Roles for Mechanosensitive PIEZO1 Ion Channels. Front. Cell Dev. Biol. 7:260. doi: 10.3389/fcell.2019.00260

INTRODUCTION

The transformation of a fertilized egg into a multicellular organism in the reproductive tract of female mammals is a complex and multifactorial process that is completed over a period of less than 3 weeks in mice. Visualization of this process (from gastrulation to early organogenesis) *in toto* at single cell resolution has recently been achieved using adaptive light-sheet microscopy (McDole et al., 2018), producing a dynamic map of embryogenesis and the cellular rearrangements that occur as mammalian organs form and take shape. These data reinforce pioneering studies in vertebrate models describing force production and propagation during gastrulation and organogenesis (Lewis, 1947; Beloussov, 1980; Keller et al., 2003; Krieg et al., 2008) and provide compelling visual evidence that mechanisms-of-multicellularity and mechanosensing in mammals are inextricably linked (Nelson et al., 2005; Orr et al., 2006; Miller and Davidson, 2013). The shaping of epithelial tissues is no exception (Behrndt et al., 2012; Guo et al., 2012).

Development of the mammary gland, the namesake epithelial organ of mammals, commences at around E10 in mice with the formation of the mammary lines, which resolve into five pairs of placodes by E11.5 (Cowin and Wysolmerski, 2010). Expansion of the placodes cause these structures to physically bulge above the plane of the surrounding epidermis and ultimately to invaginate into the underlying mesenchyme, creating a series of light bulb-shaped (ball and stick) mammary buds (**Figure 1A**; Watson and Khaled, 2008; Cowin and Wysolmerski, 2010). This early

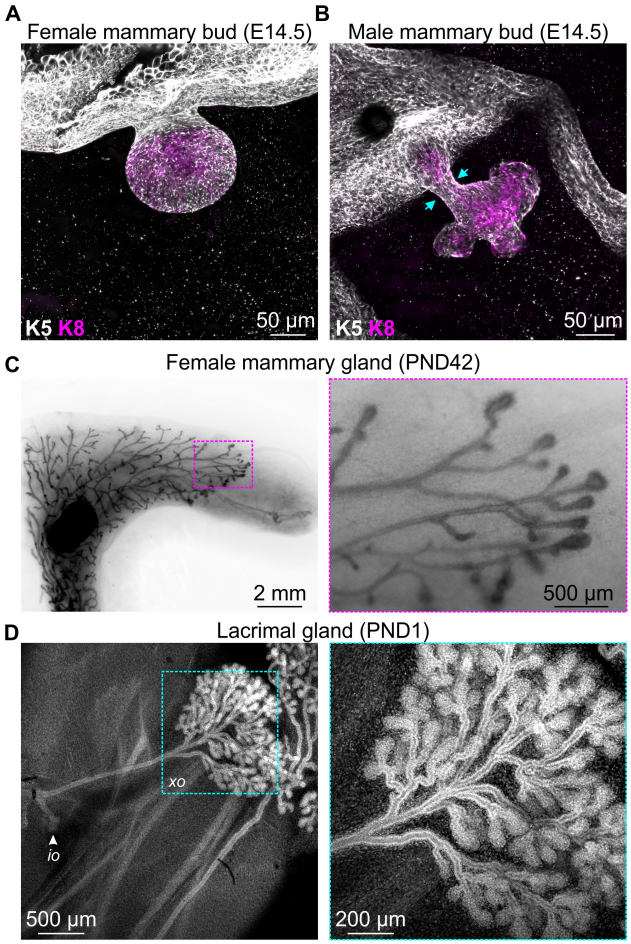

FIGURE 1 | Examples of events that occur in mouse epithelial tissues during development that are associated with extensive cellular rearrangements and morphological changes. 3D confocal imaging of **(A)** female and **(B)** male mouse mammary buds at embryonic day E14.5 immunostained with epithelial cell markers keratin K8 (magenta) and K5 (gray). **(C)** Mammary gland wholemount (methyl green) shows pubertal epithelial branching in the female mouse at postnatal day (PND) 42. Boxed region shows terminal end buds, enlarged in the adjacent sub-panel. **(D)** 3D confocal imaging of mouse lacrimal gland branching at PND1. Cells are stained with DAPI (gray). Arrow indicates the intra-orbital lobe (*io*). Boxed region shows the exorbital lobe (*xo*) and is enlarged in the adjacent sub-panel.

reorganization of mammary stem cells and their progeny also corresponds with the elongation, condensation, and radial rearrangement of surrounding cells to create the primary mesenchyme (Cowin and Wysolmerski, 2010). Of particular interest in the context of mechanobiology, the mesenchyme surrounding the epithelial stalk of male mice condenses to such a degree that it physically amputates the mammary bud from the overlying epidermis (**Figure 1B**; Dunbar et al., 1999; Heuberger et al., 2006), a process that presumably generates considerable compressive forces on epithelial cells. The intact female bud, however, later sprouts to invade the embryonic fat pad, with subsequent rounds of branching morphogenesis occurring both prenatally in the late embryo and postnatally at puberty (**Figure 1C**; Watson and Khaled, 2008). Similar branching morphogenesis is observed in other epithelial tissues including lacrimal gland (**Figure 1D**), salivary gland, kidney, lung, pancreas, and prostate (Iber and Menshykau, 2013). Epithelial branching morphogenesis can involve lateral branching, planar bifurcation, orthogonal bifurcation, and (in some tissues) trifurcation of proliferating epithelial structures, which may be regulated by both local signaling gradients and physical constraints (Iber and Menshykau, 2013). The relative contribution of chemical and mechanical signaling, the interplay and integration of these environmental cues and the potential for pathway compensation, however, remains an area of active investigation. The continued development of genetically engineered mice with targeted disruptions to specific ligand-activated receptors and mechanosensing machinery will complement computational modeling of *in vivo* epithelial branching (Iber and Menshykau, 2013; Hannezo et al., 2017; Menshykau et al., 2019) and continue to shed new light on this important aspect of mammalian morphogenesis.

Once epithelial tissues are formed, they continue to experience mechanical load (Latorre et al., 2018). For example, mechanical forces prevent collapse of the lungs, which are considered a stress-supported structure (Waters et al., 2012). Moreover, epithelial cells in the lung undergo cyclical distension during the process of respiration, which can greatly vary in frequency and amplitude to precisely match physiological demands (Orr et al., 2006). Studies investigating the micromechanics of alveolar distension using real-time optical sectioning microscopy in rats have revealed that increasing the alveolar pressure from 5 cm H_2O to 20 cm H_2O (hyperinflation) increases alveolar diameter on average by 15% (Perlman and Bhattacharya, 2007). Expansion, however, is not uniform and alveolar type 1 cells experience greater load compared to type 2 cells (Perlman and Bhattacharya, 2007). This heterogeneity in the division of strain between neighboring cells is not uncommon in epithelial systems (Latorre et al., 2018). Like the lung, epithelial cells lining the urinary system (Nauli et al., 2003; Araki et al., 2008) as well as epithelial cells of functionally mature mammary gland (Stewart et al., 2019) and pancreas (Mamidi et al., 2018) experience a range of applied and intrinsic forces during normal function – including fluid flow, distension, compression, and contraction – which can both fluctuate and coincide. The magnitude, duration, and pulsatility of each of these forces is also likely to vary within and between tissues. Frictional forces exerted by flowing milk on luminal epithelial cells that line mammary ducts and alveoli, for example, conceivably change with milk composition and volume throughout the stages of lactation (Neville et al., 1991) and, owing to viscosity, are likely to generate distinct mechanical responses when compared to frictional forces exerted on cells lining other fluid transporting structures (Orr et al., 2006; Baeyens and Schwartz, 2016).

Multiple mechanisms exist to sense, transduce, and transmit force in epithelial cells and tissues, including mechanosensitive ion channels (e.g., transient receptor potential channels, the epithelial sodium channel, and PIEZO channels), focal adhesions and cadherin based cell-cell adhesions (Martinac, 2014;

Gomez et al., 2011). It is important to note that these modes of force detection are not mutually exclusive and have been demonstrated to interact (McHugh et al., 2010; Nourse and Pathak, 2017). For example, in endothelial cells, shear force activates calcium entry though PIEZO1 channels, which promotes the proteolytic cleavage of cytoskeletal and focal adhesion proteins (Li et al., 2014).

Due to space constraints, we will limit our discussion in this mini-review to established and emerging roles of the recently identified, mechanically activated ion channel PIEZO1 in the development and physiology of mammalian epithelia. Roles for PIEZO1 in endothelial cells have recently been reviewed (Beech, 2018; Hyman et al., 2017) and will not be discussed further here.

THE MECHANOSENSITIVE ION CHANNEL PIEZO1

PIEZO1 represents one half of the recently identified PIEZO family of mechanically activated ion channels (Coste et al., 2010). Since their discovery, important roles for both PIEZO1 and PIEZO2 have been described in mammals, with major insights gained from the development of conditional gene deletion models (Li et al., 2014; Ranade et al., 2014; Nonomura et al., 2018; Romac et al., 2018; Segel et al., 2019; Solis et al., 2019) and descriptions of hereditary mutations in humans (Zarychanski et al., 2012; Alper, 2017). These include the perception of touch (Murthy et al., 2018; Zhang et al., 2019), red blood cell volume regulation (Zarychanski et al., 2012; Cahalan et al., 2015) and vascular development (Li et al., 2014; Ranade et al., 2014). While both PIEZO1 and PIEZO2 are able to convert physical force into biochemical information, PIEZO2 is largely expressed in cells of neuronal origin, has recently been reviewed in this context (Anderson et al., 2017) and will thus not be discussed further here.

PIEZO1 was discovered in 2010 (Coste et al., 2010). Details of the structure and gating of this channel have only recently started to emerge and have largely been based on studies of mouse PIEZO1 (Ge et al., 2015; Saotome et al., 2018; Wang et al., 2018; Zhao et al., 2018; Lin et al., 2019). While investigations into the specific mechanisms of PIEZO1 gating are ongoing, studies using heterologous expression systems and reconstituted lipid bilayers have confirmed mechanical force as a direct regulator of channel opening (Syeda et al., 2016). A chemical activator of PIEZO1 has also been developed (Syeda et al., 2015), suggesting a complexity in channel gating that is yet to be fully understood. Upon its initial discovery, elevated *Piezo1* transcripts were identified in various mouse epithelial tissues, including bladder, colon, kidney, lung, and skin (Coste et al., 2010). Since then, a number of studies have investigated the physiological roles of PIEZO1 in specific epithelial tissues known to be the subject of mechanical forces (Peyronnet et al., 2013; Miyamoto et al., 2014; Martins et al., 2016; Michishita et al., 2016; Ihara et al., 2018; Romac et al., 2018; Stewart et al., 2019).

Roles for PIEZO1 channels in the morphogenesis and maintenance of epithelial tissues can also be inferred from studies linking this channel to life and death symmetry in healthy epithelia, including human colon epithelia (Eisenhoffer et al., 2012; Gudipaty et al., 2017). These studies have shown that overcrowding-strain in Madin-Darby canine kidney (MDCK) epithelial cell cultures resulted in live cell extrusions, which were blocked by inhibitors of Rho kinase and sphingosine-1 phosphate signaling as well as the non-selective ion channel blocker gadolinium (Gd^{3+}) (Eisenhoffer et al., 2012). Genetic knockdown of *Piezo1* also inhibited homeostatic cell extrusions in the epidermis of developing zebrafish, producing localized epidermal cell masses (Eisenhoffer et al., 2012). This work set the scene for subsequent studies investigating cell extrusion and stretch in the development and homeostasis of other epithelial tissues *in vivo*, including the mammary gland (discussed in further detail below). This same group subsequently demonstrated that epithelial cell stretch at areas of low cell density was also detected and translated by PIEZO1, leading to cell division (Gudipaty et al., 2017). Comprehensive assessment of roles for PIEZO1 in controlled cell death and division in the developing mammalian embryo, however, have been hindered by embryonic lethality in *Piezo1-null* mice by E14.5, an effect that has largely been attributed to impaired vascular development (Li et al., 2014; Ranade et al., 2014). Analysis of epithelial development and branching morphogenesis using conditional *Piezo1* knockout mice will yield important new insights into the role of this channel in the formation of mammalian epithelial tissues.

The following sections of this review will specifically describe physiological roles for PIEZO1 mechanically activated ion channels in three epithelial organ-systems in mammals: the mammary gland, pancreas, and urinary system.

MAMMARY GLAND

As discussed, mammary epithelial cells experience mechanical forces in the embryo and during pubertal ductal morphogenesis. However, epithelial cells in the mammary gland also experience applied and cell-generated forces during lactation – when the mammary gland produces and expels milk to fulfill its sole biological role – and in the phase of post-lactational regression (involution) (Watson and Khaled, 2008; VanHouten et al., 2010; Davis et al., 2015). Shed cells have long been observed in the early phase of mammary gland involution (Watson, 2006). During this period, lactation can be resumed upon re-initiation of infant suckling (Watson and Kreuzaler, 2011). This is an important feature of mammalian biology, as it allows female mammals to continue nursing their offspring after modest periods of absence (e.g., during hunting or foraging). During this time, mammary epithelial cells experience substantial pressure due to milk accumulation in the alveolar lumen (Stewart et al., 2019). The apical extrusion of cells from the alveolar epithelium may help to preserve epithelial barrier integrity during this period of protracted tissue strain (Eisenhoffer et al., 2012). If it is live cells that are extruded from the epithelium during mammary gland involution to subsequently die via anoikis in the alveolar lumen as previously reported (Watson, 2006), this process may be mediated wholly or in-part by PIEZO1 (Eisenhoffer et al., 2012).

To investigate this hypothesis, we recently generated mice with conditional deletion of *Piezo1* in luminal (secretory) mammary epithelial cells (Stewart et al., 2019, pre-print). The number of cleaved caspase 3 (CC3)-positive shed cells during the early phase of involution was not affected in mice with luminal cell *Piezo1* deletion (Stewart et al., 2019). In contrast to previous reports, however, CC3-positive cells were observed in both the alveolar lumen and the alveolar wall in this study, suggesting that, unlike live cell extrusions in other epithelial systems, cell death may precede cell extrusion in the involuting mouse mammary gland (Stewart et al., 2019), making a role for PIEZO1 unlikely.

Milk is ejected upon infant suckling, a response that most likely involves mechanical activation of sensory neurons at the nipple. This results in the release of centrally produced oxytocin into the circulation (Gimpl and Fahrenholz, 2001). Studies performing multi-scale activity imaging on live mammary tissue during lactation have revealed in unprecedented detail oxytocin-mediated, calcium-dependent contractions of alveolar myoepithelial cells (Stevenson et al., 2019, pre-print). These contractions cause alveolar units to eject their supply of milk and ductal myoepithelial contractions help to propel milk toward the nipple (Stevenson et al., 2019). These actomyosin-based contractions cause considerable warping of the ductal and alveolar structures, which may activate mechanosensing proteins. *Piezo1* deletion in luminal epithelial cells, however, has no effect on milk ejection or postnatal pup development (Stewart et al., 2019). These results, again, suggest that PIEZO1 channels either do not have a major role in the physiology of the functionally mature mammary gland or that their role can be compensated for by another pathway. It is interesting to note, however, that whilst suckling of one nipple generates a systemic oxytocin response, milk ejection is principally limited to the physically stimulated nipple. How a localized mechanical stimulus produces systemic release of a ligand to ultimately result in a highly localized response remains an unanswered question in mammalian biology. In any case, milk production, secretion, and coordinated ejection does not appear to depend on luminal cell expression of the mechanically activated ion channel *Piezo1* (Stewart et al., 2019).

PANCREAS

Pancreatic development commences at E9.5 in the mouse, with obvious branching morphogenesis of epithelial buds observed at around E12.5 (Villasenor et al., 2010). As mentioned above, embryonic organogenesis is a dynamic process involving significant cellular rearrangements and cell-cell and cell-extracellular matrix (ECM) interactions (Orr et al., 2006). Using a *Pdx1-Cre;Itgb1*$^{fl/fl}$ knockout mouse model, initiation of branching morphogenesis was shown to rely on β1 integrin-mediated interactions between pancreatic progenitors and localized regions of the ECM (Shih et al., 2016). Further supporting a role for mechanosignaling in pancreas development, are recent findings from Mamidi et al. (2018), who, using embryonic stem cells, identified a distinct role for ECM-integrin α5 interactions in driving ductal lineage specification of bipotent pancreatic progenitors. In addition to cell fate determination, integrin signaling regulates a range of cellular processes important in development, including remodeling of the cytoskeleton, cell adhesion, and migration (reviewed in Bökel and Brown, 2002). Early studies identified a role for *Piezo1* (known as *Fam38A* at the time) in regulating β1 integrin activation and cell adhesion in HeLa cells (McHugh et al., 2010). Since then, the majority of studies of PIEZO1 function have been assessed in the context of externally generated forces; however, recent findings by Pathak and colleagues, using super resolution imaging techniques, identified highly localized PIEZO1-dependent calcium flickers in response to cell generated traction forces (Ellefsen et al., 2019). It would be informative to investigate the impact of targeted *Piezo1* deletion under native conditions and to assess its role in epithelial cell-ECM signaling events in early embryonic development [for a comprehensive review of the relationship between PIEZO1, internally generated forces and the cytoskeleton, see (Nourse and Pathak, 2017)].

The mature exocrine pancreas consists of two main epithelial cell types: pancreatic ductal epithelial cells and acinar cells, with acinar cells representing the predominant cell type (>90%) (Romac et al., 2018; Gál et al., 2019). Unique to the pancreas, is its exquisite sensitivity to touch (Romac et al., 2018). Recently, *Piezo1* expression was confirmed in pancreatic acinar cells, where it has been proposed to mediate touch and pressure sensitivity (Romac et al., 2018). *In vivo* studies performed by Romac et al. (2018) showed that mouse pancreas exposed to the PIEZO1 agonist, Yoda1, exhibited signs of cellular injury similar to that caused by high intraductal pressure. Furthermore, damage caused by high intraductal pressure is reduced in the presence of GsMTx4 as well as by targeted deletion of *Piezo1* in acinar cells (Romac et al., 2018). While levels of *Piezo1* mRNA specifically in pancreatic ductal epithelial cells have not been reported, perfusion of mouse pancreas tissue slices with the bile acid, chenodeoxycholic acid, is associated with transient calcium increases in these cells (Gál et al., 2019). Given its role in the transport of pancreatic secretions and this tissue's sensitivity to physical obstruction and compression (Hegyi and Petersen, 2013; Romac et al., 2018), it would be valuable to know whether PIEZO1 is also active in epithelial cells lining the pancreatic duct.

To date, few studies have assessed the role of PIEZO1 in the pancreas. As mentioned above, the cell-intrinsic forces encountered during its development, combined with its unique pressure sensitivity, makes the pancreas an interesting candidate for future investigations into how the magnitude and nature of mechanical stimulation can influence its normal growth and functioning.

URINARY SYSTEM

Unlike the mammary gland and pancreas, epithelial cells of the urinary system have been the focus of a number of studies investigating physiological roles of PIEZO1 (Peyronnet et al., 2013; Miyamoto et al., 2014; Martins et al., 2016;

Michishita et al., 2016; Ihara et al., 2018). Fluid flow, distension, and contraction are just some examples of the dynamic forces faced by epithelial cells lining the urinary system, which includes the urinary bladder, ureters, and renal pelvis (Andersson and Arner, 2004). Of the epithelial tissues assessed by Coste et al. (2010) mouse *Piezo1* transcript levels were shown to be highly expressed in the bladder, supporting a potential role in mechanosensory processes in tissues of the urinary system. Indeed, an early study assessing PIEZO1 function in cultured proximal convoluted tubule (PCT) cells identified a reduction in endogenous stretch activated channel activity upon siRNA-mediated *Piezo1* knockdown (Peyronnet et al., 2013). Further, this group showed that stretch activated channel activity is reduced upon co-expression of the calcium permeable ion channel, Polycystin-2 (PC2), and *Piezo1*, suggesting a regulatory role of PC2 (Peyronnet et al., 2013). The physiological relevance of this interaction remains unknown; however, it would be interesting to evaluate the expression and activity of PIEZO1 in disease states in which PC2 is mutated, such as autosomal dominant polycystic kidney disease (Mochizuki et al., 1996).

The urothelium, a highly specialized epithelium lining the urinary bladder, ureters, and renal pelvis, plays an important role in sensing and responding to forces generated within the bladder (Mochizuki et al., 2009; Birder, 2011; Negoro et al., 2014). Similar to studies in PCT cells, knockdown of *Piezo1* in primary cultured mouse bladder urothelial cells resulted in a reduced response to mechanical stimuli (Miyamoto et al., 2014). This group also showed a reduction in urothelial cell stretch-mediated adenosine triphosphate (ATP) release as a consequence of either *Piezo1* knockdown or GsMTx4 treatment, illustrating a potential role for PIEZO1 channels in the translation of mechanical force into downstream signaling events in bladder cells. Yet another function of PIEZO1 in epithelia of the urinary tract was recently identified, this time in collecting duct epithelial cells of the kidney (Martins et al., 2016). Using a conditional *Piezo1* knockout model targeted to epithelial cells of the collecting ducts and renal tubules in adult mice, Martins et al. (2016) demonstrated a role for PIEZO1 in the regulation of urine osmolarity post-dehydration or fasting, via an as yet unknown mechanism.

As discussed briefly in the studies presented above, there is mounting evidence for a role for PIEZO1 in the normal functioning of various epithelial cell types of the urinary tract. Currently, the majority of studies assessing PIEZO1 have largely relied on the use of *in vitro* primary and immortalized cell lines. It will be interesting to see whether these phenotypes are reproduced and expounded in the future using targeted knockout animal models.

CONCLUDING REMARKS

In this review, we considered the physical forces that are exerted on epithelial cells as they evolve into complex tissues and perform their basic physiological functions. Applied and cell-generated forces are encountered in a developmental stage- and tissue-specific manner as cells proliferate, reorganize and interact with neighboring cells and their physical environment (Chen, 2008; Latorre et al., 2018). The sheer scale of force experienced (often simultaneously) by cells in multicellular systems is unlikely to be detected, decoded, and transferred by a single protein or family of proteins (Orr et al., 2006), nor do physical forces act in isolation from chemical signaling (Orr et al., 2006; Li et al., 2018; Stewart and Davis, 2019). Whilst our focus in this mini-review has been on PIEZO1, it is important to note that PIEZO1 is only one recently identified piece of a highly complex puzzle. It is also important to note that mechanical tension is not only a feature of normal development and physiology, as discussed here, it is also an integral component of disease signaling. Asthma (Gunst and Tang, 2000; Waters et al., 2012), pulmonary fibrosis (Waters et al., 2012), pancreatitis (Romac et al., 2018), and breast cancer (Li et al., 2015) are all examples of epithelial pathologies that are linked to altered mechanosensing. Lessons learned from epithelial mechanobiology will no doubt provide important new insights into epithelial "mechanopathologies."

ETHICS STATEMENT

Animal experimentation was carried out in accordance with the Australian Code for the Care and Use of Animals for Scientific Purposes and the Queensland Animal Care and Protection Act (2001), with local animal ethics committee approval (The University of Queensland Health Sciences Animal Ethics Committee, The University of Queensland).

AUTHOR CONTRIBUTIONS

TS and FD contributed to the writing and editing of this manuscript.

FUNDING

This work was supported by the National Health and Medical Research Council [1141008 and 1138214 (FD)] and the Mater Foundation (Equity Trustees/AE Hingeley Trust).

REFERENCES

Alper, S. L. (2017). Genetic diseases of PIEZO1 and PIEZO2 dysfunction. *Curr. Top. Membr.* 79, 97–134. doi: 10.1016/bs.ctm.2017.01.001

Anderson, E. O. O., Schneider, E. R. R., and Bagriantsev, S. N. N. (2017). Piezo2 in cutaneous and proprioceptive mechanotransduction in vertebrates. *Curr. Top. Membr.* 79, 197–217. doi: 10.1016/bs.ctm.2016.11.002

Andersson, K.-E., and Arner, A. (2004). Urinary bladder contraction and relaxation: physiology and pathophysiology. *Physiol. Rev.* 84, 935–986. doi: 10.1152/physrev.00038.2003

Araki, I., Du, S., Kobayashi, H., Sawada, N., Mochizuki, T., Zakoji, H., et al. (2008). Roles of mechanosensitive ion channels in bladder sensory transduction and overactive bladder. *Int. J. Urol.* 15, 681–687. doi: 10.1111/j.1442-2042.2008.02052.x

Baeyens, N., and Schwartz, M. A. (2016). Biomechanics of vascular mechanosensation and remodeling. *Mol. Biol. Cell* 27, 7–11. doi: 10.1091/mbc.E14-11-1522

Beech, D. J. (2018). Endothelial Piezo1 channels as sensors of exercise. *J. Physiol.* 596, 979–984. doi: 10.1113/JP274396

Behrndt, M., Salbreux, G., Campinho, P., Hauschild, R., Oswald, F., Roensch, J., et al. (2012). Forces driving epithelial spreading in zebrafish gastrulation. *Science* 338, 257–260. doi: 10.1126/science.1224143

Beloussov, L. V. (1980). The role of tensile fields and contact cell polarization in the morphogenesis of amphibian axial rudiments. *Wilhelm Roux's Arch. Dev. Biol.* 188, 1–7. doi: 10.1007/BF00848603

Birder, L. A. (2011). "Urothelial signaling," in *Urinary Tract. Handbook of Experimental Pharmacology*, Vol. 2011, eds K. E. Andersson, and M. Michel (Berlin: Springer).

Bökel, C., and Brown, N. H. (2002). Integrins in development: moving on, responding to, and sticking to the extracellular matrix. *Dev. Cell.* 3, 311–321.

Cahalan, S. M., Lukacs, V., Ranade, S. S., Chien, S., Bandell, M., and Patapoutian, A. (2015). Piezo1 links mechanical forces to red blood cell volume. *eLife* 4:e07370. doi: 10.7554/eLife.07370

Chen, C. S. (2008). Mechanotransduction – a field pulling together? *J. Cell Sci.* 121, 3285–3292. doi: 10.1242/jcs.023507

Coste, B., Mathur, J., Schmidt, M., Earley, T. J., Ranade, S., Petrus, M. J., et al. (2010). Piezo1 and Piezo2 are essential components of distinct mechanically activated cation channels. *Science* 330, 55–60. doi: 10.1126/science.1193270

Cowin, P., and Wysolmerski, J. (2010). Molecular mechanisms guiding embryonic mammary gland development. *Cold Spring Harb. Perspect. Biol.* 2:a003251. doi: 10.1101/cshperspect.a003251

Davis, F. M., Janoshazi, A., Janardhan, K. S., Steinckwich, N., D'Agostin, D. M., Petranka, J. G., et al. (2015). Essential role of Orai1 store-operated calcium channels in lactation. *Proc. Natl. Acad. Sci. U.S.A.* 112, 5827–5832. doi: 10.1073/pnas.1502264112

Dunbar, M. E., Dann, P. R., Zhang, J.-P., Wysolmerski, J. J., Robinson, G. W., and Hennighausen, L. (1999). Parathyroid hormone-related protein signaling is necessary for sexual dimorphism during embryonic mammary development. *Development* 126, 3485–3493.

Eisenhoffer, G. T., Loftus, P. D., Yoshigi, M., Otsuna, H., Chien, C. B., Morcos, P. A., et al. (2012). Crowding induces live cell extrusion to maintain homeostatic cell numbers in epithelia. *Nature* 484, 546–549. doi: 10.1038/nature10999

Ellefsen, K. L., Holt, J. R., Chang, A. C., Nourse, J. L., Arulmoli, J., Mekhdjian, A. H., et al. (2019). Myosin-II mediated traction forces evoke localized Piezo1-dependent Ca2+ flickers. *Commun. Biol.* 2:298. doi: 10.1038/s42003-019-0514-3

Gál, E., Dolenšek, J., Stožer, A., Pohorec, V., Ébert, A., and Venglovecz, V. (2019). A novel in situ approach to studying pancreatic ducts in mice. *Front. Physiol.* 10:938. doi: 10.3389/fphys.2019.00938

Ge, J., Li, W., Zhao, Q., Li, N., Chen, M., Zhi, P., et al. (2015). Architecture of the mammalian mechanosensitive Piezo1 channel. *Nature* 527, 64–69. doi: 10.1038/nature15247

Gimpl, G., and Fahrenholz, F. (2001). The oxytocin receptor system: structure, function, and regulation. *Physiol. Rev.* 81, 629–683. doi: 10.1152/physrev.2001.81.2.629

Gomez, G. A., McLachlan, R. W., and Yap, A. S. (2011). Productive tension: force-sensing and homeostasis of cell-cell junctions. *Trends Cell Biol.* 21, 499–505. doi: 10.1016/j.tcb.2011.05.006

Gudipaty, S. A., Lindblom, J., Loftus, P. D., Redd, M. J., Edes, K., Davey, C. F., et al. (2017). Mechanical stretch triggers rapid epithelial cell division through Piezo1. *Nature* 543, 118–121. doi: 10.1038/nature21407

Gunst, S. J., and Tang, D. D. (2000). The contractile apparatus and mechanical properties of airway smooth muscle. *Eur. Respir. J.* 15, 600–616. doi: 10.1034/j.1399-3003.2000.15.29.x

Guo, C. L., Ouyang, M., Yu, J. Y., Maslov, J., Price, A., and Shen, C. Y. (2012). Long-range mechanical force enables self-assembly of epithelial tubular patterns. *Proc. Natl. Acad. Sci. U.S.A.* 109, 5576–5582. doi: 10.1073/pnas.1114781109

Hannezo, E., Scheele, C. L. G. J., Moad, M., Drogo, N., Heer, R., Sampogna, R. V., et al. (2017). A unifying theory of branching morphogenesis. *Cell* 171, 242–255. doi: 10.1016/j.cell.2017.08.026

Hegyi, P., and Petersen, O. H. (2013). The exocrine pancreas: the acinar-ductal tango in physiology and pathophysiology. *Rev. Physiol. Biochem. Pharmacol.* 165, 1–30. doi: 10.1007/112_2013_14

Heuberger, B., Fitzka, I., Wasner, G., and Kratochwil, K. (2006). Induction of androgen receptor formation by epithelium-mesenchyme interaction in embryonic mouse mammary gland. *Proc. Natl. Acad. Sci. U.S.A.* 79, 2957–2961. doi: 10.1073/pnas.79.9.2957

Hyman, A. J., Tumova, S., and Beech, D. J. (2017). Piezo1 channels in vascular development and the sensing of shear stress. *Curr. Top. Membr.* 79, 37–57. doi: 10.1016/bs.ctm.2016.11.001

Iber, D., and Menshykau, D. (2013). The control of branching morphogenesis. *Open Biol.* 3:130088. doi: 10.1098/rsob.130088

Ihara, T., Mitsui, T., Nakamura, Y., Kanda, M., Tsuchiya, S., Kira, S., et al. (2018). The oscillation of intracellular Ca2+ influx associated with the circadian expression of Piezo1 and TRPV4 in the bladder urothelium. *Sci. Rep.* 8:5699. doi: 10.1038/s41598-018-23115-w

Keller, R., Davidson, L. A., and Shook, D. R. (2003). How we are shaped: the biomechanics of gastrulation. *Differentiation* 71, 171–205. doi: 10.1046/j.1432-0436.2003.710301.x

Krieg, M., Arboleda-Estudillo, Y., Puech, P. H., Käfer, J., Graner, F., Müller, D. J., et al. (2008). Tensile forces govern germ-layer organization in zebrafish. *Nat. Cell Biol.* 10, 429–436. doi: 10.1038/ncb1705

Latorre, E., Kale, S., Casares, L., Gómez-González, M., Uroz, M., Valon, L., et al. (2018). Active superelasticity in three-dimensional epithelia of controlled shape. *Nature* 563, 203–208. doi: 10.1038/s41586-018-0671-4

Lewis, W. H. (1947). Mechanics of invagination. *Anat. Rec.* 97, 139–156. doi: 10.1002/ar.1090970203

Li, C., Rezania, S., Kammerer, S., Sokolowski, A., Devaney, T., Gorischek, A., et al. (2015). Piezo1 forms mechanosensitive ion channels in the human MCF-7 breast cancer cell line. *Sci. Rep.* 5:8364. doi: 10.1038/srep08364

Li, J., Hou, B., Tumova, S., Muraki, K., Bruns, A., Ludlow, M. J., et al. (2014). Piezo1 integration of vascular architecture with physiological force. *Nature* 515, 279–282. doi: 10.1038/nature13701

Li, J., Wang, Z., Chu, Q., Jiang, K., Li, J., and Tang, N. (2018). The strength of mechanical forces determines the differentiation of alveolar epithelial cells. *Dev. Cell* 44, 297–312. doi: 10.1016/j.devcel.2018.01.008

Lin, Y. C., Guo, Y. R., Miyagi, A., Levring, J., MacKinnon, R., and Scheuring, S. (2019). Force-induced conformational changes in PIEZO1. *Nature* 573, 230–234. doi: 10.1038/s41586-019-1499-2

Mamidi, A., Prawiro, C., Seymour, P. A., de Lichtenberg, K. H., Jackson, A., Serup, P., et al. (2018). Mechanosignalling via integrins directs fate decisions of pancreatic progenitors. *Nature* 564, 114–118. doi: 10.1038/s41586-018-0762-2

Martinac, B. (2014). The ion channels to cytoskeleton connection as potential mechanism of mechanosensitivity. *Biochim. Biophys. Acta Biomembr.* 1838, 682–691. doi: 10.1016/j.bbamem.2013.07.015

Martins, J. R., Penton, D., Peyronnet, R., Arhatte, M., Moro, C., Picard, N., et al. (2016). Piezo1-dependent regulation of urinary osmolarity. *Pflugers Arch. Eur. J. Physiol.* 468, 1197–1206. doi: 10.1007/s00424-016-1811-z

McDole, K., Guignard, L., Amat, F., Berger, A., Malandain, G., Royer, L. A., et al. (2018). In toto imaging and reconstruction of post-implantation mouse development at the single-cell level. *Cell* 175, 859–876. doi: 10.1016/j.cell.2018.09.031

McHugh, B. J., Buttery, R., Lad, Y., Banks, S., Haslett, C., and Sethi, T. (2010). Integrin activation by Fam38A uses a novel mechanism of R-Ras targeting to the endoplasmic reticulum. *J. Cell Sci.* 123, 51–61. doi: 10.1242/jcs.056424

Menshykau, D., Michos, O., Lang, C., Conrad, L., McMahon, A. P., and Iber, D. (2019). Image-based modeling of kidney branching morphogenesis reveals GDNF-RET based Turing-type mechanism and pattern-modulating WNT11 feedback. *Nat. Commun.* 10:239. doi: 10.1038/s41467-018-08212-8

Michishita, M., Yano, K., Tomita, K. I., Matsuzaki, O., and Kasahara, K. I. (2016). Piezo1 expression increases in rat bladder after partial bladder outlet obstruction. *Life Sci.* 166, 1–7. doi: 10.1016/j.lfs.2016.10.017

Miller, C. J., and Davidson, L. A. (2013). The interplay between cell signalling and mechanics in developmental processes. *Nat. Rev. Genet.* 14, 733–744. doi: 10.1038/nrg3513

Miyamoto, T., Mochizuki, T., Nakagomi, H., Kira, S., Watanabe, M., Takayama, Y., et al. (2014). Functional role for Piezo1 in stretch-evoked Ca2+ influx

and ATP release in Urothelial cell cultures. *J. Biol. Chem.* 289, 16565–16575. doi: 10.1074/jbc.M113.528638

Mochizuki, T., Sokabe, T., Araki, I., Fujishita, K., Shibasaki, K., Uchida, K., et al. (2009). The TRPV4 cation channel mediates stretch-evoked Ca2+ influx and ATP release in primary urothelial cell cultures. *J. Biol. Chem.* 284, 21257–21264. doi: 10.1074/jbc.M109.020206

Mochizuki, T., Wu, G., Hayashi, T., Xenophontos, S. L., Veldhuisen, B., Saris, J. J., et al. (1996). PKD2, a gene for polycystic kidney disease that encodes an integral membrane protein. *Science* 272, 1339–1342. doi: 10.1126/science.272.5266.1339

Murthy, S. E., Loud, M. C., Daou, I., Marshall, K. L., Schwaller, F., Kühnemund, J., et al. (2018). The mechanosensitive ion channel Piezo2 mediates sensitivity to mechanical pain in mice. *Sci. Transl. Med.* 10:eaat9897. doi: 10.1126/scitranslmed.aat9897

Nauli, S. M., Alenghat, F. J., Luo, Y., Williams, E., Vassilev, P., Li, X., et al. (2003). Polycystins 1 and 2 mediate mechanosensation in the primary cilium of kidney cells. *Nat. Genet.* 33, 129–137. doi: 10.1038/ng1076

Negoro, H., Urban-Maldonado, M., Liou, L. S., Spray, D. C., Thi, M. M., and Suadicani, S. O. (2014). Pannexin 1 channels play essential roles in urothelial mechanotransduction and intercellular signaling. *PLoS One* 9:e106269. doi: 10.1371/journal.pone.0106269

Nelson, C. M., Jean, R. P., Tan, J. L., Liu, W. F., Sniadecki, N. J., Spector, A. A., et al. (2005). Emergent patterns of growth controlled by multicellular form and mechanics. *Proc. Natl. Acad. Sci. U.S.A.* 102, 11594–11599. doi: 10.1073/pnas.0502575102

Neville, M. C., Allen, J. C., Archer, P. C., Casey, C. E., Seacat, J., Keller, R. P., et al. (1991). Studies in human lactation: milk volume and nutrient composition during weaning and lactogenesis. *Am. J. Clin. Nutr.* 54, 81–92. doi: 10.1093/ajcn/54.1.81

Nonomura, K., Lukacs, V., Sweet, D., Goddard, L., Kanie, A., Whitwam, T., et al. (2018). Mechanically activated ion channel PIEZO1 is required for lymphatic valve formation. *Proc. Natl. Acad. Sci. U.S.A.* 115, 12817–12822. doi: 10.1073/pnas.1817070115

Nourse, J. L., and Pathak, M. M. (2017). How cells channel their stress: interplay between Piezo1 and the cytoskeleton. *Semin. Cell Dev. Biol.* 71, 3–12. doi: 10.1016/j.semcdb.2017.06.018

Orr, A. W., Helmke, B. P., Blackman, B. R., and Schwartz, M. A. (2006). Mechanisms of mechanotransduction. *Dev. Cell* 10, 11–20.

Perlman, C. E., and Bhattacharya, J. (2007). Alveolar expansion imaged by optical sectioning microscopy. *J. Appl. Physiol.* 103, 1037–1044. doi: 10.1152/japplphysiol.00160.2007

Peyronnet, R., Martins, J. R., Duprat, F., Demolombe, S., Arhatte, M., Jodar, M., et al. (2013). Piezo1-dependent stretch-activated channels are inhibited by Polycystin-2 in renal tubular epithelial cells. *EMBO Rep.* 14, 1143–1148. doi: 10.1038/embor.2013.170

Ranade, S. S., Qiu, Z., Woo, S. H., Hur, S. S., Murthy, S. E., Cahalan, S. M., et al. (2014). Piezo1, a mechanically activated ion channel, is required for vascular development in mice. *Proc. Natl. Acad. Sci. U.S.A.* 111, 10347–10352. doi: 10.1073/pnas.1409233111

Romac, J. M. J., Shahid, R. A., Swain, S. M., Vigna, S. R., and Liddle, R. A. (2018). Piezo1 is a mechanically activated ion channel and mediates pressure induced pancreatitis. *Nat. Commun.* 9:1715. doi: 10.1038/s41467-018-04194-9

Saotome, K., Murthy, S. E., Kefauver, J. M., Whitwam, T., Patapoutian, A., and Ward, A. B. (2018). Structure of the mechanically activated ion channel Piezo1. *Nature* 554, 481–486. doi: 10.1038/nature25453

Segel, M., Neumann, B., Hill, M. F. E., Weber, I. P., Viscomi, C., Zhao, C., et al. (2019). Niche stiffness underlies the ageing of central nervous system progenitor cells. *Nature* 573, 130–134. doi: 10.1038/s41586-019-1484-9

Shih, H. P., Panlasigui, D., Cirulli, V., and Sander, M. (2016). ECM signaling regulates collective cellular dynamics to control pancreas branching morphogenesis. *Cell Rep.* 14, 169–179. doi: 10.1016/j.celrep.2015.12.027

Solis, A. G., Bielecki, P., Steach, H. R., Sharma, L., Harman, C. C. D., Yun, S., et al. (2019). Mechanosensation of cyclical force by PIEZO1 is essential for innate immunity. *Nature* 573, 69–74. doi: 10.1038/s41586-019-1485-8

Stevenson, A. J., Vanwalleghem, G., Stewart, T. A., Condon, N. D., Lloyd-Lewis, B., Marino, N., et al. (2019). Multiscale activity imaging in the mammary gland reveals how oxytocin enables lactation. *bioRxiv* [Preprint].

Stewart, T. A., and Davis, F. M. (2019). An element for development: calcium signaling in mammalian reproduction and development. *Biochim. Biophys. Acta Mol. Cell Res.* 1866, 1230–1238. doi: 10.1016/j.bbamcr.2019.02.016

Stewart, T. A., Hughes, K., Stevenson, A. S. J., Marino, N., Ju, A. J. L., Morehead, M., et al. (2019). Mammary mechanobiology: mechanically-activated ion channels in lactation and involution. *bioRxiv* [Preprint].

Syeda, R., Florendo, M. N., Cox, C. D., Kefauver, J. M., Santos, J. S., Martinac, B., et al. (2016). Piezo1 channels are inherently mechanosensitive. *Cell Rep.* 17, 1739–1746. doi: 10.1016/j.celrep.2016.10.033

Syeda, R., Xu, J., Dubin, A. E., Coste, B., Mathur, J., Huynh, T., et al. (2015). Chemical activation of the mechanotransduction channel piezo1. *eLife* 4:e07369.

VanHouten, J., Sullivan, C., Bazinet, C., Ryoo, T., Camp, R., Rimm, D. L., et al. (2010). PMCA2 regulates apoptosis during mammary gland involution and predicts outcome in breast cancer. *Proc. Natl. Acad. Sci. U.S.A.* 107, 11405–11410. doi: 10.1073/pnas.0911186107

Villasenor, A., Chong, D. C., Henkemeyer, M., and Cleaver, O. (2010). Epithelial dynamics of pancreatic branching morphogenesis. *Development* 137, 4295–4305. doi: 10.1242/dev.052993

Wang, Y., Chi, S., Guo, H., Li, G., Wang, L., Zhao, Q., et al. (2018). A lever-like transduction pathway for long-distance chemical- and mechano-gating of the mechanosensitive Piezo1 channel. *Nat. Commun.* 9:1300. doi: 10.1038/s41467-018-03570-9

Waters, C. M., Roan, E., and Navajas, D. (2012). Mechanobiology in lung epithelial cells: measurements, perturbations, and responses. *Compr. Physiol.* 2, 1–29. doi: 10.1002/cphy.c100090

Watson, C. J. (2006). Key stages in mammary gland development Involution: apoptosis and tissue remodelling that convert the mammary gland from milk factory to a quiescent organ. *Breast Cancer Res.* 8:203.

Watson, C. J., and Khaled, W. T. (2008). Mammary development in the embryo and adult: a journey of morphogenesis and commitment. *Development* 135, 995–1003. doi: 10.1242/dev.005439

Watson, C. J., and Kreuzaler, P. A. (2011). Remodeling mechanisms of the mammary gland during involution. *Int. J. Dev. Biol.* 55, 757–762. doi: 10.1387/ijdb.113414cw

Zarychanski, R., Schulz, V. P., Houston, B. L., Maksimova, Y., Houston, D. S., Smith, B., et al. (2012). Mutations in the mechanotransduction protein PIEZO1 are associated with hereditary xerocytosis. *Blood* 120, 1908–1915. doi: 10.1182/blood-2012-04-422253

Zhang, M., Wang, Y., Geng, J., Zhou, S., and Xiao, B. (2019). Mechanically activated piezo channels mediate touch and suppress acute mechanical pain response in mice. *Cell Rep.* 26, 1419.e4–1431.e4. doi: 10.1016/j.celrep.2019.01.056

Zhao, Q., Zhou, H., Chi, S., Wang, Y., Wang, J., Geng, J., et al. (2018). Structure and mechanogating mechanism of the piezo1 channel. *Nature* 554, 487–492. doi: 10.1038/nature25743

Conflict of Interest: The authors declare that the research was conducted in the absence of any commercial or financial relationships that could be construed as a potential conflict of interest.

Copyright © 2019 Stewart and Davis. This is an open-access article distributed under the terms of the Creative Commons Attribution License (CC BY). The use, distribution or reproduction in other forums is permitted, provided the original author(s) and the copyright owner(s) are credited and that the original publication in this journal is cited, in accordance with accepted academic practice. No use, distribution or reproduction is permitted which does not comply with these terms.

Advantages of publishing in Frontiers

OPEN ACCESS
Articles are free to read for greatest visibility and readership

FAST PUBLICATION
Around 90 days from submission to decision

HIGH QUALITY PEER-REVIEW
Rigorous, collaborative, and constructive peer-review

TRANSPARENT PEER-REVIEW
Editors and reviewers acknowledged by name on published articles

Frontiers
Avenue du Tribunal-Fédéral 34
1005 Lausanne | Switzerland

Visit us: www.frontiersin.org
Contact us: frontiersin.org/about/contact

REPRODUCIBILITY OF RESEARCH
Support open data and methods to enhance research reproducibility

DIGITAL PUBLISHING
Articles designed for optimal readership across devices

FOLLOW US
@frontiersin

IMPACT METRICS
Advanced article metrics track visibility across digital media

EXTENSIVE PROMOTION
Marketing and promotion of impactful research

LOOP RESEARCH NETWORK
Our network increases your article's readership